

**Studies directed towards the synthesis,
associated reaction mechanisms and structure
of inositols and their derivatives**

Thesis

Submitted to the

UNIVERSITY OF PUNE

For the degree of

DOCTOR OF PHILOSOPHY

in

CHEMISTRY

By

Chebrolu Murali

Organic Chemistry Division
National Chemical Laboratory
Pune-411008

March 2008

Dedicated to my Parents...

CERTIFICATE

This is to certify that the work incorporated in the thesis entitled “**Studies directed towards the synthesis, associated reaction mechanisms and structure of inositols and their derivatives**” submitted by **Chebrolu Murali** was carried out by him under my supervision at the National Chemical Laboratory, Pune, India. Such materials, obtained from other sources have been duly acknowledged in the thesis.

Date: 18 March 2008

Division of Organic Chemistry

National Chemical Laboratory

Pune-411 008, India

Dr. M. S. SHASHIDHAR

Research Supervisor

DECLARATION

I hereby declare that the thesis entitled “**Studies directed towards the synthesis, associated reaction mechanisms and structure of inositols and their derivatives**” submitted for Ph. D. degree to the University of Pune has not been submitted by me for a degree to any other University.

Date: 18 March 2008

CHEBROLU MURALI

Division of Organic Chemistry

National Chemical Laboratory

Pune-411 008, India

ACKNOWLEDGEMENTS

I would like to express my deep and sincere gratitude to my research supervisor, Dr. M. S. Shashidhar for introducing me to this fascinating field of inositol chemistry. His wide knowledge and logical way of thinking have been of great value for me. His encouragement and personal guidance have provided a good basis for the present thesis.

I wish to express my gratitude to Dr. M. M. Bhadbhade and Dr. Rajesh Gonnade for their constant support, encouragement and timely help in providing the X-ray analysis data.

I would like to thank Dr. Ganesh Pandey (HOD, Organic Chemistry Division), Dr. N. N. Joshi, Dr. C. S. Gopinath, Dr. (Mrs.) V.G. Puranik, Dr. S. P. Chavan, Dr. Pradeep Tripathi, Dr. K. N. Ganesh, Prof. D. D. Dhavale, and Dr. B. G. Hazra for their suggestions, help and encouragement.

I would like to thank central NMR facility research group, especially Dr. P. R. Rajamohan for his help and fruitful discussions. I also thank Dr. Sujatha Biswas, Mrs. Sunitha Sawant, Mrs. Chitra Sanas, Mr. Gaydhankar and Mr. Senthil Kumar for Microanalysis data. I would like to thank Dr. Chirmule, Mrs. Annegiri and all other library staff members for their help.

I am very much indebted to my seniors Dr. Aditya, Dr. Manash, Dr. Devaraj, Shailesh, Dr. Sachin for their timely help, advices and support. I am thankful to my labmates Madhuri, Manoj, Rajendra, Shobhana, Bharat, Alson for maintaining cheerful and amazing atmosphere. I also thank Moreji for his regular help in laboratory maintenance.

I would like to thank Dr. (Mrs.) Vidya Shashidhar and Dr. (Mrs.) Ranjana Bhadbhade for their advices and help.

I am very much thankful my great friends and colleagues Nageswar reddy, Muduru (Raman), Abhijeet, complicated Victor, Sumanth, Kiran, Rajender, Srinivas, Sreedhar reddy, Fresh (Swaroop), Sreedhar reddy (IISER), Indu, Bala, Nookaraju, Raju, Sreedhar, Satti reddy, Venkateshan, Srikanth, Megastar (Suresh), Keshri, Sachin, Biju, Shanbag, Ankur, Vilas, Sreenu, Santosh, Giri, Ravi, Manmath, Sutar, Deepak, Bapu, Neelakant, Sudhir, Prasanna, Ajish and Remo who made cheerful and pleasant atmosphere in and around NCL.

My special thanks to Mr. Khaja Sai and his family members for their help and affection. I would like to extend my special thanks to Thummala, Paramesh, Kumar, Madhu, Sudhakar, Prasad, Krishna, Venu, Hemasundar, Hemanth, Giri and Jayaprakash for their timely help and support.

I would like to express my deep gratitude to my parents, sister (Vani), brother-in-law (Bhaktavatsal), nephew (Praveen), brother (Poornachandra) and his family members for their constant support, love and affection.

I also wish to thank Prof. Subbaraju, Prof. Gunasekhar, Prof. Bhaskar reddy, Prof. Venkat Rao, Prof. (Mrs.) Padmavathi, Dr. Ramakrishna, Dr. Ramusridhar, Dr. Subrahmanyam Dr. Devaraj and Dr. Jayanthi for their sincere advices and help.

I would like to thank many other people in and around NCL who helped me either directly or indirectly during my research career at NCL

Finally, I thank Director, NCL for providing the Infra-structural facilities and CSIR, New Delhi for the award of Research Fellowship.

CONTENTS


Title	Page No.
Abbreviations.	i
Synopsis of the thesis.	iv
List of publications, presentations and posters.	xiii
Chapter 1. A review of the synthetic utility of <i>myo</i>-inositol-1,3,5-orthoesters.	
1.1. Introduction.	1
1.2 Biological relevance of <i>myo</i> -inositol (1.1).	3
1.3. Inositol isomers.	7
1.4. Orthoesters.	8
1.5. Inositol orthoesters: Preparation.	11
1.6. <i>myo</i> -Inositol-1,3,5-orthoformate as a key intermediate for the synthesis of phosphorylated inositol derivatives.	12
1.6.1. Synthesis of inositol mono-phosphates and their analogs.	12
1.6.2. Synthesis of <i>myo</i> -inositol bis-phosphates.	16
1.6.3. Synthesis of <i>myo</i> -inositol tris-phosphates and their analogs	17
1.6.4. Synthesis of <i>myo</i> -inositol tetrakisphosphates.	22
1.6.5. Synthesis of <i>myo</i> -inositol pentakisphosphates	29
1.6.6. Inositol phospholipids	30
1.7. Partially protected inositol derivatives	32
1.8. Reports on the use of inositol orthoesters other than the orthoformate.	42
1.9. Conclusions.	45
1.10. References.	46

Chapter 2. *myo*-Inositol-1,3,5-orthobenzoate as a versatile intermediate for the synthesis of isomeric inositol derivatives.

2.1. Introduction.	54
2.2. Results and discussion.	55
2.2.1. Preparation of the <i>myo</i>-inositol-1, 3, 5-orthobenzoate and its polymorphism.	55
2.2.2 Orthogonally protected <i>myo</i>-inositol derivatives from the orthobenzoate 1.17.	60
2.2.3 Synthesis of Sequoyitol (5-<i>O</i>-methyl-<i>myo</i>-inositol, 2.79).	73
2.2.4 Present work.	74
2.2.5 Synthesis of <i>neo</i>-inositol (1.25).	74
2.2.6 Present work.	79
2.2.7 Synthesis of 5-deoxy-5-<i>myo</i>-inosamine.	82
2.2.8 Present work.	83
2.2.9 Attempted synthesis of 2-<i>neo</i>-inosamine (2.140).	83
2.2.10 De-oxy inositols (Quercitols).	87
2.2.11 <i>neo</i>-quercitol.	87
2.2.12 Di-deoxy inositol or \squareyclohexane tetrol.	89
2.2.13. Present work.	90
2.2.14. <i>neo</i>-quercitol.	92
2.3. Conclusion.	93
2.4 Experimental.	94
2.5 References.	123
2.6 Appendix.	128

Chapter 3. Transesterification reaction of <i>myo</i>-inositol-1,3,5-orthoester derivatives in the solid state: effect of molecular packing in crystals on acyl transfer reactivity.	
3.1. Introduction.	214
3.2. Results and Discussion.	220
3.2.1. Benzoyl Transfer Reaction in crystals.	220
3.2.2. Correlation of Molecular Pre-Organization and intermolecular interactions with Acyl transfer reactivities.	222
3.2.3. Attempted preparation of co-crystals of unsymmetrical dibenzoates of <i>myo</i>-inositol orthoesters leads to a reactive polymorph of racemic 2,4-dibenzoyl-<i>myo</i>-insitol 1,3,5-orthoacetate (3.2).	227
3.2.4. Benzoyl group transfer reactivity in monobenzoates of <i>myo</i>-inositol orthoesters.	239
3.2.5. Correlation of Molecular Pre-Organization and intermolecular interactions with Acyl transfer reactivities.	241
3.3. Conclusions.	247
3.4. Experimental.	248
3.5. References.	264
3.6. Appendix.	269

Abbreviations.

Ac	Acetyl
Ac ₂ O	Acetic anhydride
AIBN	Azobisisobutyronitrile
All	Allyl
Anhy.	Anhydrous
aq.	Aqueous
Bn	Benzyl
BnBr	Benzyl bromide
BOMCl	Benzyloxy methyl chloride
Bt	butyryl
BuLi	Butyl lithium
Bz	Benzoyl
BzCl	Benzoyl chloride
Calcd.	Calculated
Cat.	Catalytic
Conc.	Concentration
CSA	Camphorsulfonic acid
D ₂ O	Deuterium Oxide
DABCO	1,4-diazabicyclo[2.2.2]octane 
DAG	Diacylglycerol
DCM	Dichloromethane
DEAD	Diethyl azo-dicarboxylate
DIAD	Diisopropyl azo-dicarboxylate

DIBAL	Diisobutyl aluminium Hydride
dil.	Dilute
DIPEA/Hunig's base/DIEA	Di-isopropyl ethyl amine
DMAP	<i>N, N</i> -dimethylamino pyridine
DMF	<i>N, N</i> -Dimethylformamide
DMSO	Dimethyl sulfoxide
DPCP	Diphenylchloro phosphate
eq.	Equivalent
Et ₃ N	Triethyl amine
EtOAc	Ethyl acetate
g	Gram
GCMS	Gas chromatography-mass spectrometry
GPI	Glycophosphatidylinositol
h	Hour (s)
Hz	Hertz
<i>i</i> -BuNH ₂	Iso-butyl amine
IDH	<i>myo</i> -Inositol dehydrogenase
IR	Infrared
M.p.	Melting point
Me	Methyl
MeI	Methyl iodide
MeOH	Methanol
mg.	Milli gram
min.	Minute(s)
mL	Milliliter

mmol	Milli molar
NaOMe	Sodium methoxide
NLO	Non Linear Organic
NMR	Nuclear magnetic Resonance
ORTEP	Orthogonal thermal ellipsoid plot
PDC	Pyridinium dichromate
Ph	Phenyl
PI-PLC	Phosphatidylinositol-specific phospholipase C
PMB	para-methoxy benzyl
PMP	para-methoxy phenyl
PNBCl	para-nitro benzoyl chloride
PPTS	Pyridinium para toluene sulfonate
PtdIns	Phosphatidyl inositol
<i>rac</i> -	Racemic
Rf	Retention factor
rt.	Room temperature (23-30 °C)
TBAI	tetra (n-butyl) ammonium iodide
TBDMS	<i>tert</i> -Butyldimethylsilyl
TFA	Trifluoroacetic acid
THF	Tetrahydrofuran
TLC	Thin layer chromatography
TMS	Trimethyl silyl
TsCl	<i>p</i> -Toluene sulfonyl chloride
TsOH	<i>p</i> -Toluene sulfonic acid

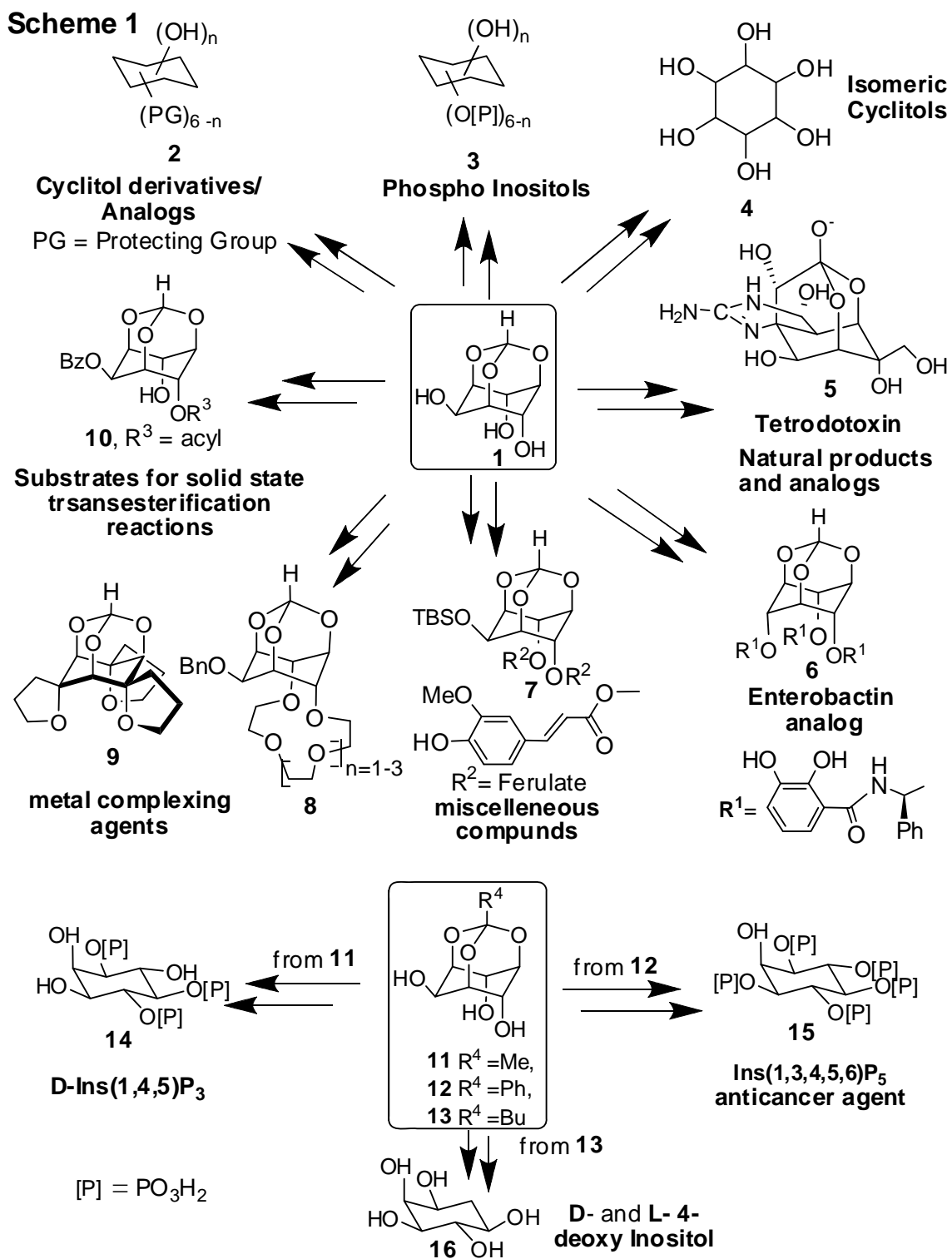
Synopsis of the Thesis

The thesis entitled '**Studies directed towards the synthesis, associated reaction mechanisms and structure of inositols and their derivatives**' consists of three chapters. Chapter 1 is a review on the utility of *myo*-inositol 1,3,5-orthoesters for the synthesis of natural and unnatural inositol derivatives such as phosphoinositols and their analogs, metal complexing agents, etc. Chapter 2 describes the preparation and use of *myo*-inositol 1,3,5-orthobenzoate for the synthesis of isomeric inositol derivatives / analogs. This chapter also describes a new method (discovered during the synthetic studies using *myo*-inositol 1,3,5-orthobenzoate) of de-protection of O-benzyl groups, orthoesters and acetals using Perlman's catalyst. Chapter 3 presents results on the investigation of acyl transfer reactions in crystals of *myo*-inositol orthoacetate and orthobenzoate derivatives and a comparison of these solid state reactions with earlier known systems which underwent acyl transfer reactions in the solid state. Chapters 2 and 3 also have detailed experimental procedures, spectroscopic, crystallographic and analytical data relevant to the new results described in the thesis. Some of the results reported in this thesis are published in (a) Identical Molecular Strings Woven Differently by Intermolecular Interactions in Dimorphs of *myo*-Inositol 1,3,5-Orthobenzoate G. Bhosekar, C. Murali, R. G. Gonnade, M. S. Shashidhar, M. M. Bhabhade, *Cryst.Growth.Des.* **2005**, 5, 1977-1982; (b) Hydroxyl group deprotection reactions with Pd(OH)₂/C: a convenient alternative to hydrogenolysis of benzyl ethers and acid hydrolysis of ketals C. Murali, M. S. Shashidhar, C. S. Gopinath, *Tetrahedron*,

2007, 63, 4149-4155; (c) Investigating Organization of Molecules that Facilitates Intermolecular Acyl Transfer in Crystals: Reactivity and X-ray Structures of *O*-Benzoyl-*myo*inositol 1,3,5-Orthoesters C. Murali, M. S. Shashidhar, R. G. Gonnade, M. M. Bhadbhade, *Eur. J. Org. Chem.* **2007**, 1153–1159.; (d) A convenient method for the preparation D-4-*O* and D-6-*O*-benzyl-*myo*-inositol, precursors for the preparation of enantiomeric *myo*-inositol-1,2,3,4,5-pentakisphosphates. C. Murali, M. S. Shashidhar communicated to *Carbohydr. Res.* **2007**.

Chapter 1. A review of the synthetic utility of *myo*-inositol 1,3,5-orthoesters:

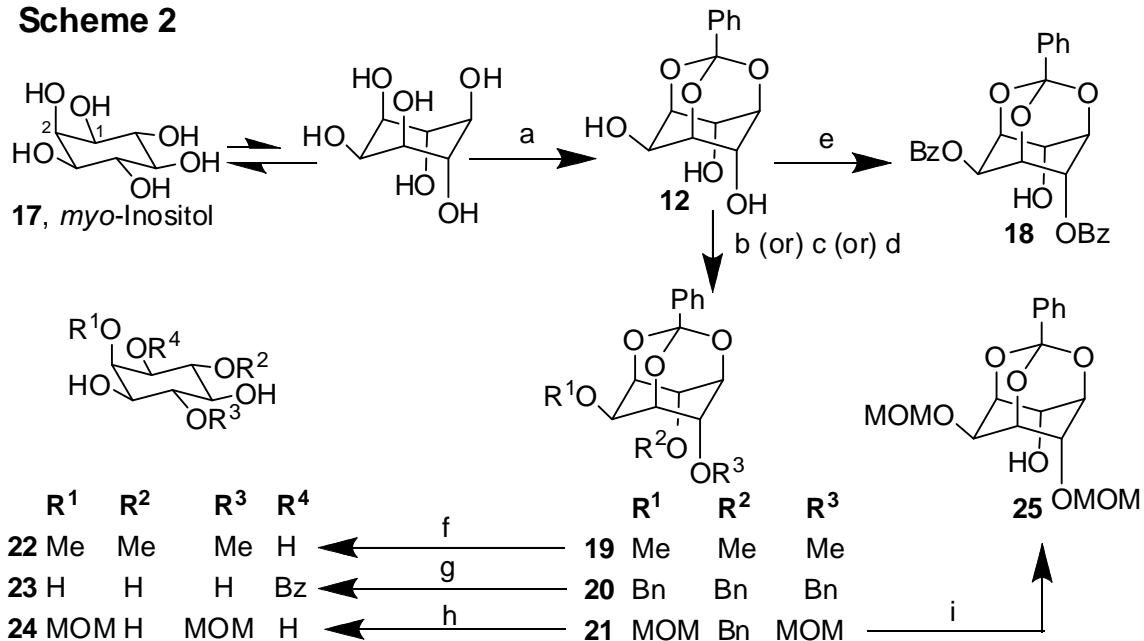
myo-Inositol and its derivatives / analogs have become conspicuous in the literature related to chemistry and biology due to the involvement of phosphoinositols in cellular signal transduction mechanisms¹ and anchoring of certain proteins to cell membranes². The biological implications of the *myo*-inositol cycle are not yet completely understood. Many synthetic methodologies and techniques have been developed in the recent past³ for the synthesis of inositol derivatives useful in studies directed towards understanding all the implications of the *myo*-inositol cycle. Some of these methods have also been used for the synthesis of natural products (other than phosphoinositols) and their analogs. In the last two decades, *myo*-inositol orthoformate⁴ (**1**, Scheme 1) which can be easily obtained in gram quantities, has been frequently used as an intermediate during the synthesis of inositol derivatives. Several other interesting aspects of derivatives of **1**, such as solid state reactivity and metal ion complexation have also been explored. In contrast, reports on the chemistry and utility of other *myo*-inositol orthoesters such as **11-13** are scarce. Hence we have investigated the synthetic utility of *myo*-inositol orthobenzoate; results of this study are described in Chapter 2.



Chapter 2. *myo*-Inositol 1,3,5-orthobenzoate as a versatile intermediate for the synthesis of isomeric inositol derivatives.

myo-Inositol 1,3,5-orthobenzoate (**12**) was prepared from *myo*-inositol (Scheme 2); it exhibited polymorphic behavior on crystallization from different solvents. Several O-protected derivatives of *myo*-inositol 1,3,5-orthobenzoate were prepared (Scheme 2) and converted to isomeric inositol derivatives. During this work, we discovered that (a) the racemic dibenzoate **18** underwent facile transesterification reaction in the solid state (this has been discussed in detail in chapter 3); and (b) O-benzyl groups, orthoesters and acetals can be deprotected to the corresponding alcohols using Pearlman's catalyst [Pd(OH)₂/C] in refluxing methanol. Carboxylic acid esters were stable to this reaction condition.

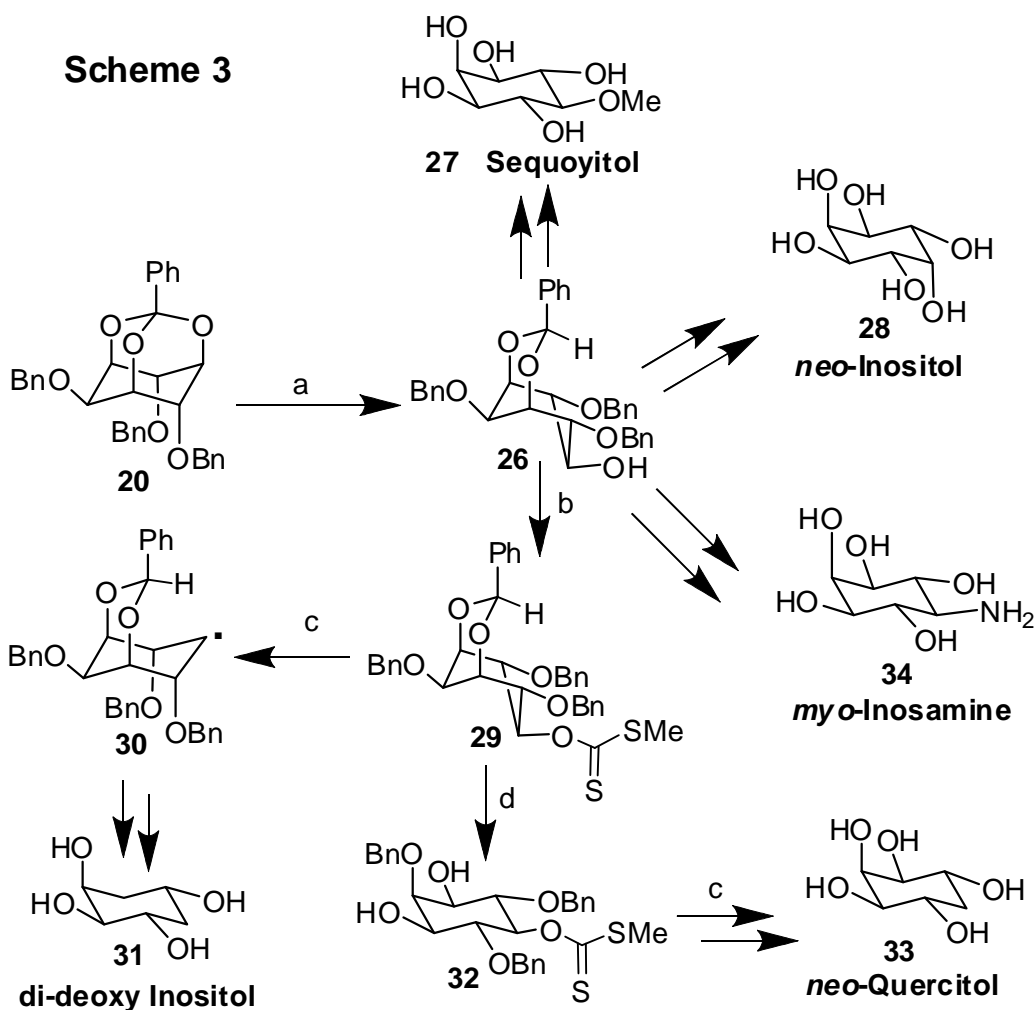
Scheme 2



Reagents and Conditions: (a) PhC(OMe)₃, DMF, TsOH, 140 °C, 93%; (b) DMF, NaH, MeI, rt, 30 min., 97%; (c) DMF, NaH, BnBr, rt, 30 min, 98%; (d)(i) BnBr, NaH, DMF; ii) MOMCl, NaH; (e) 2.2 eq BzCl, Pyr., rt, 18 h, 82%; (f) H₂(55psi), Pd(OH)₂/C, MeOH; (g) Pd(OH)₂/C, MeOH; (h) H₂ (55psi), Pd(OH)₂/C, MeOH; (i) H₂ (55psi), Pd(OH)₂/C, EtOAc, 95%

XPS analysis of the palladium catalyst recovered after the completion of the reaction (cleavage of benzyl ether) showed that Pd(II) had been converted to Pd(0) which

suggested the oxidative cleavage of benzyl ethers by Pd(OH)₂/C. This new method of deprotection was used for the preparation of naturally occurring sequoyitol from *myo*-inositol 1,3,5-orthobenzoate. This method of de-protection of *O*-benzyl groups, orthoesters and acetals has the potential to be useful in the synthesis of different classes of organic compounds since the reaction conditions do not involve strong acids, bases or hydrogenolysis. *myo*-Inositol orthobenzoate was also used for the synthesis of other inositol derivatives as shown in Scheme 3. It is interesting to note that mono- or di-deoxygenation of *myo*-inositol could be carried out using the xanthate **29**.



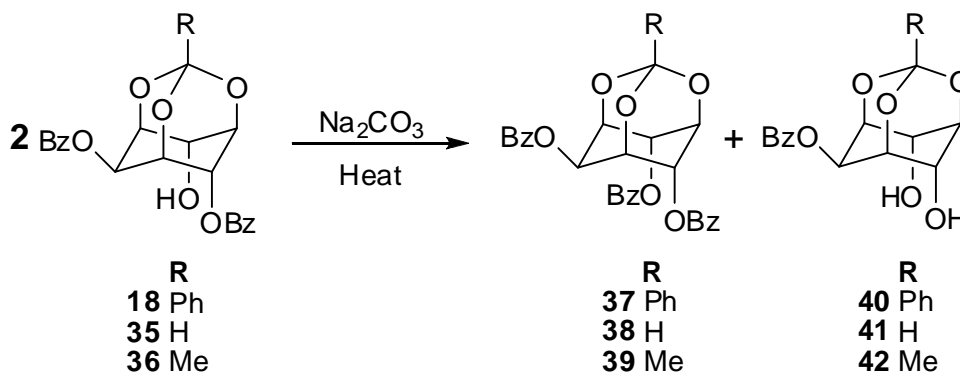
Reagents and conditions: (a) DIBAL-H, DCM, rt, 2 h, 97 %; (b) NaH(5 eq), THF, CS₂ (15 eq), reflux, 1h, Mel (5eq), rt, 16 h, 98 %; (c) Toluene, Bu₃SnH, AIBN, 110°C, 1h; (d) TFA, THF + H₂O, rt, 24h, 96%

The results presented in this chapter clearly show that the orthobenzoate **12** is a potential synthon for the preparation of important isomeric inositol derivatives and has advantages over other *myo*-inositol orthoesters.

Chapter 3. Transesterification reaction of *myo*-inositol 1,3,5-orthoester derivatives in the solid state: effect of molecular packing in crystals on acyl transfer reactivity.

Acyl migration reactions among the hydroxyl groups of inositol derivatives in solution occurs frequently and this has been exploited for the preparation of several inositol derivatives. Most of these acyl migration reactions however result in the formation of a mixture of isomeric hydroxyl esters and consequently result in poor isolated yield of the required *O*-protected inositol derivative. Facile acyl transfer reactions of inositol derivatives (**35** and its co-crystal with **36**) in the solid state (Scheme 4) have earlier been reported from our laboratory.⁵

Scheme 4



Reactions in the solid state are of interest since they often proceed with high regio and stereo specificity. During the course of the work described in the previous chapter we realized that racemic-2,4-di-*O*-benzoyl-*myo*-inositol 1,3,5-orthobenzoate (**18**) undergoes facile transesterification in its crystals (Scheme 4); this reaction was relatively less facile in solution. The results on the investigation of this interesting solid state reaction in *myo*-

inositol orthoester derivatives **18** and one of the polymeric crystals of **36** are presented in this chapter. An attempt has been made to compare the crystal structure and reactivity of the orthobenzoate **18** with other compounds that show similar acyl transfer reactivity in their crystals. This comparison showed that the facility of these transesterification reactions is controlled by molecular packing and crystal lattice interactions as well as the availability of a channel (Figure 1) for the acyl transfer reaction to proceed in a domino fashion.

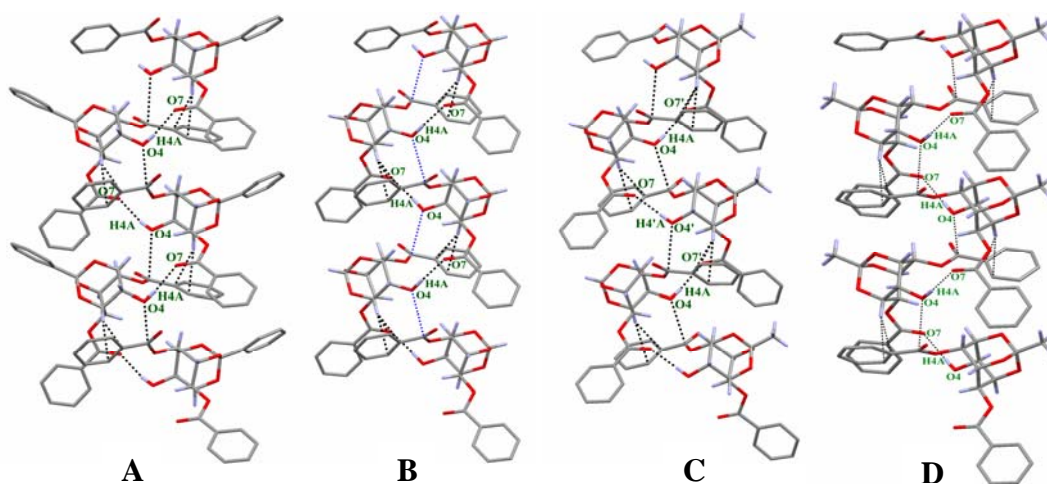
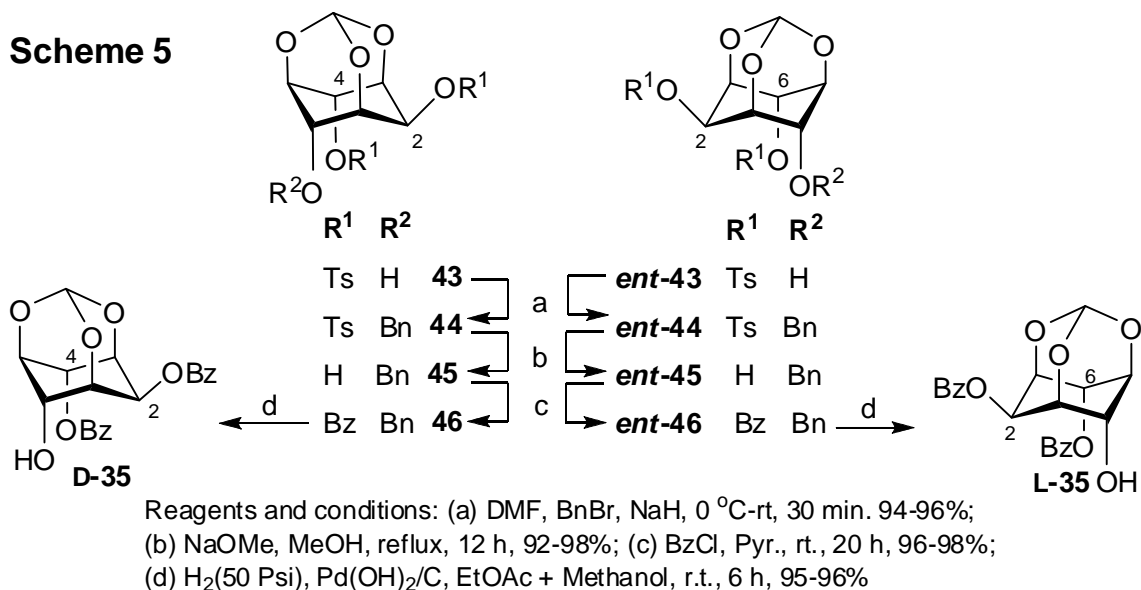
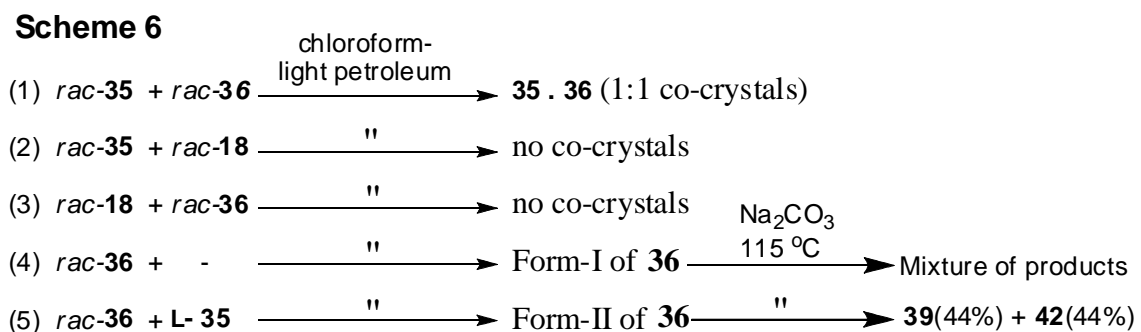


Figure 1. Molecular packing in the crystals of **18** (A), **35** (B) molecular complex **35.36** (C) and Form-II crystals of *rac*- **36**.

We also attempted to grow co-crystals of *myo*-inositol orthoester derivatives **18**, **35**, **36** and **L35** since previous work in our laboratory had shown that acyl transfer reactions could be carried out in co-crystals (**35.36**). Compounds used for such attempts as well as the preparation of enantiomeric orthoformate dibenzoates **D35** and **L35** are shown in Scheme 5. Enantiomeric ditosylates **43** and *ent*-**43** were prepared as reported earlier from our laboratory.⁶



One of these attempts (see (5), Scheme 6) led us to a new polymorph (Form-II) of racemic **36** (Scheme 6). Solid state acyl transfer reactivity in Form-I crystals of racemic **36** had earlier been reported from our laboratory.^{5b}



The Form-II crystals underwent crystal to crystal transformation to Form-I crystals at 145 °C, which indicated that Form I crystals are thermodynamically stable while Form II crystals are meta-stable. Single crystal X-ray diffraction data of Form II crystals suggested assembly of molecules favorable for transesterification reaction in crystals. The crystal structure was found to be isostructural (Figure 1D) with crystals of **18** and **35** which exhibited very good acyl transfer reactivity. As expected from the crystal structure, Form II crystals of racemic **36** underwent facile transesterification reaction (unlike the

polymorph Form-I, reported earlier).^{5b} The results presented in this chapter show that the facility of acyl transfer reaction in crystals can be predicted from their structure.

References:

1. (a) Hinchliffe, K.; Irvine, R. *Nature*, **1997**, *390*, 123.; b) Schmittberger, T.; Waldmann, H., *Synlett*. **1988**, 574.; c) *Phosphoinositides: chemistry, biochemistry and biochemical applications*, Bruzik, K. S. Ed.; ACS symposium series 718. American chemical society, Washington D.C. USA, 1999.
2. Ferguson, M. A. J.; Williams, A. F., *Annu. Rev. Biochem.***1988**, *57*, 285.
3. Sureshan, K. M.; Shashidhar; M. S.; Praveen, T.; Das, T. *Chem. Rev.* **2003**, *103*, 4477.
4. Lee, H. W.; Kishi, Y. *J. Org. Chem.* **1985**, *50*, 4402.
5. (a) Praveen, T; Samanta, U.; Das, T; Shashidhar, M. S.; Chakrabarthy, P; *J. Am. Chem. Soc.* **1998**, *120*, 3842; (b) Sarmah, M. P.; Gonnade, R. G.; Shashidhar, M. S.; Bhadbhade, M. M. *Chem. Eur. J.* **2005**, *11*, 2103.
6. Sarmah, M. P.; Shashidhar, M. S.; Sureshan, K. M.; Gonnade, R. G.; Bhadbhade M. M. *Tetrahedron* **2005**, *61*, 4437.

----X----

Note: Compound numbers in the synopsis are different from those in thesis and references were are given separately for each chapter.

List of Publications.

1. Identical Molecular Strings Woven Differently by Intermolecular Interactions in Dimorphs of *myo*-Inositol-1,3,5-Orthobenzoate G. Bhosekar, **C. Murali**, R. G. Gonnade, M. S. Shashidhar, M. M. Bhabhade, *Cryst. Growth. Des.* **2005**, *5*, 1977-1982.
2. Hydroxyl group deprotection reactions with Pd(OH)₂/C: a convenient alternative to hydrogenolysis of benzyl ethers and acid hydrolysis of ketals **C. Murali**, M. S. Shashidhar, C. S. Gopinath, *Tetrahedron*, **2007**, *63*, 4149-4155.
3. Investigating Organization of Molecules that Facilitates Intermolecular Acyl Transfer in Crystals: Reactivity and X-ray Structures of *O*-Benzoyl-*myo*-inositol-1,3,5-Orthoesters **C. Murali**, M. S. Shashidhar, R. G. Gonnade, M. M. Bhadbhade, *Eur. J. Org. Chem.* **2007**, 1153-1159.
4. Enhancing Intermolecular Benzoyl Transfer Reactivity in Crystals by Nucleating the 'Right' Polymorph Using Optically Pure Enantiomer as an Additive. **C. Murali**, M. S. Shashidhar, R. G. Gonnade, M. M. Bhadbhade *Manuscript to be communicated*
5. *myo*-Inositol-1,3,5-orthobenzoate: A versatile intermediate for the synthesis of *neo*-Quercitol, *neo*-Inositol, 1(3),5-dideoxy-*myo*-Inositol and 5-deoxy-5-amino-*myo*-Inositol. **C. Murali**, M. S. Shashidhar, R. G. Gonnade, M. M. Bhadbhade *Manuscript to be communicated*

Presentations and Posters.

1. Solvent induced polymorphism in *myo*-inositol 1,3,5-orthoesters: X-ray structure of four triols of *myo*-Inositol and their polymorphs. Sarmah, M. P.; **Murali, C.**; Bhosekar, G.; Gonnade, R. G.; Sureshan, K. M.; Shashidhar, M. S.; Bhadbhade,

M. M. Poster presented at the XXXIII National Seminar on Crystallography, Jan. 8-10, 2004; National Chemical Laboratory; Pune- 411 008; Maharashtra, India.

2. *myo*-Inositol 1,3,5-orthobenzoate: A key intermediate for the preparation of inositol derivatives; synthesis of sequoyitol via non-hydrogenolytic cleavage of *O*-benzyl groups with Pd(OH)₂/C. Murali, C. and Shashidhar, M. S. Oral presentation at II Junior NOST (11th-14th October 2006), ICG, Jaipur, Rajasthan, India.

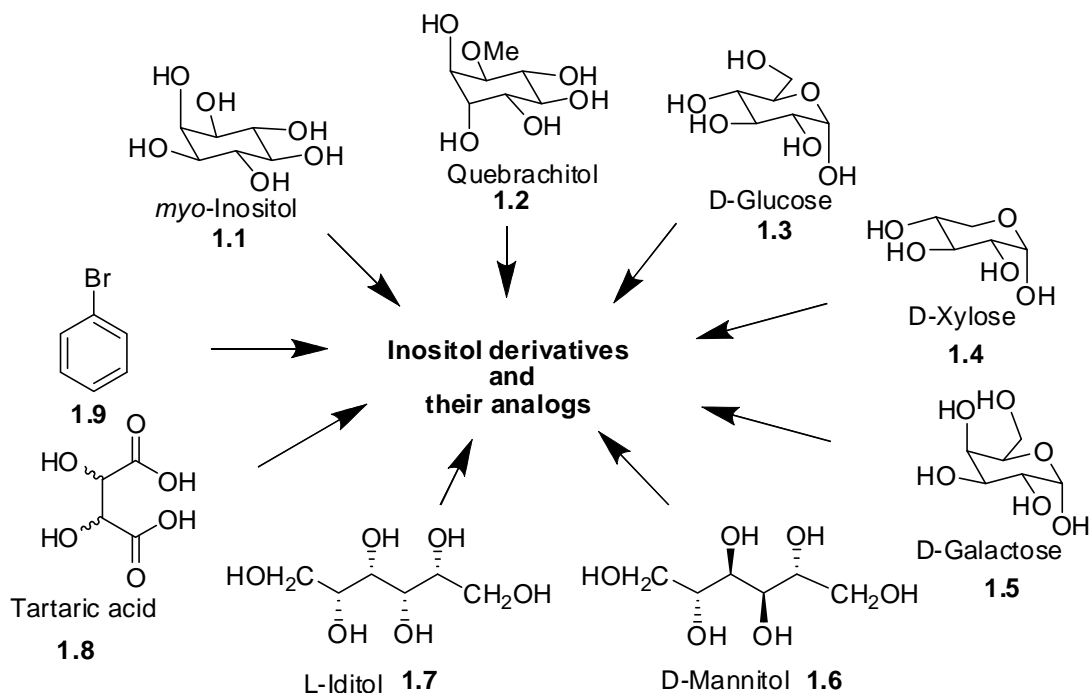
Chapter 1

**A review of the synthetic utility of *myo*-inositol-1,3,5-
orthoesters**

1.1. Introduction.

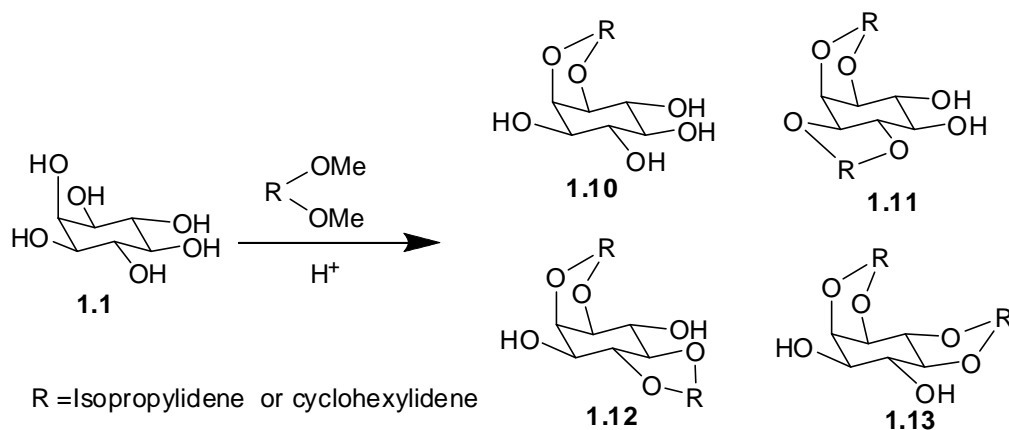
myo-Inositol and its derivatives / analogs have become conspicuous in the literature related to chemistry and biology due to the involvement of phosphoinositols in cellular signal transduction mechanisms¹ and anchoring of certain proteins to cell membranes.² However, the complete biological implications of the *myo*-inositol cycle are not yet clearly understood. Hence, sizeable amounts of inositol phosphates, their derivatives and analogs are required to study and understand the intricate details and implications of the *myo*-inositol cycle. This necessitates the efficient synthesis of naturally occurring phosphoinositols and their synthetic analogs. Consequently, many synthetic methodologies and techniques have been developed in the recent past³ for the synthesis of inositol derivatives useful in the study of the inositol cycle. Some of these methods have also been adopted for the synthesis of natural products (other than inositol derivatives and their analogs).⁴ Derivatives of inositols other than phosphoinositols are also important since several of them occur in nature and are essential constituents of our diet. Amino derivatives of inositols are present in antibiotics⁵ and some of them act as glycosidase inhibitors.⁶

Key intermediates for the synthesis of biologically important derivatives of inositols are the corresponding hydroxyl group protected derivatives. Many of these intermediates have been synthesized from commercially available *myo*-inositol,⁷ naturally occurring quebrachitol,⁸ carbohydrates,⁹ tartaric acid,¹⁰ benzene and its derivatives¹¹ (Scheme 1.1).



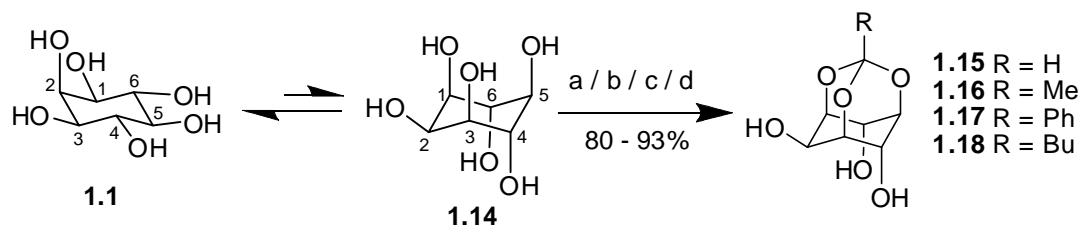
Scheme 1.1

Regioselective protection of *myo*-inositol hydroxyl groups is a difficult task since all the hydroxyl groups are secondary and the reactivity differences between them is subtle. Hence reaction of inositols with most reagents leads to the formation of a mixture of products; formation of acetals (**1.10** - **1.13**) of *myo*-inositol is shown in Scheme 1.2 as an example.



Scheme 1.2

In contrast, reaction of *myo*-inositol with trialkyl-orthoesters results in the formation of *myo*-inositol-1,3,5-orthoester as the sole product in high yield (Scheme 1.3), where in three hydroxyl groups are protected simultaneously.^{7a,7c,12} Incidentally, this also brings about an inversion of the inositol ring; some chemists have used the terms ‘equatorial rich’ and ‘axial rich’¹³ to describe the normal conformation of the *myo*-inositol ring and the inverted conformation of the same ring present in the orthoesters of *myo*-inositol. Furthermore, any one or two hydroxyl groups of inositol orthoesters can be derivatized selectively in high yields.^{3,14} Hence, orthoester derivatives of *myo*-inositol have emerged as useful intermediates for the preparation of many biologically relevant inositol derivatives.



Scheme 1.3: (a) HC(OEt)₃, TsOH, DMSO, 100 °C, 18 h; (b) MeC(OEt)₃, TsOH, DMF, 90-100 °C, 4 h; (c) PhC(OMe)₃, DMF, TsOH, 140°-145 °C; (d) BuC(OMe)₃, CSA, DMSO, 60 °C.

The major portion of this chapter is devoted to review the utility of *myo*-inositol-1,3,5-orthoesters **1.15 - 1.18** for the synthesis of natural and unnatural derivatives or analogs of inositols. However, before going into these details, short notes on the biological relevance of *myo*-inositol derivatives and orthoesters in general, are given.

1.2. Biological relevance of *myo*-inositol (1.1).

Communication between cells and between organelles within a cell (cell signaling) controls the inner workings of organisms, assisting them to survive, respond and adapt to their surroundings.¹⁵ All living cells (plant or animal) receive and transmit signals in many forms continuously. Hence all cells must have the ability to detect the

presence of extracellular molecules and conditions, and must also be able to instigate a range of intracellular responses for their survival. Since different kinds of cell signaling systems are interdependent they must work in concert for the well being of an organism. Knowledge of the mechanism of cell signaling is also important for the understanding of the growth and activity of an aberrant cell or that of a cell that is combating adverse conditions, since impairment of cell signaling systems could lead to diseases. Cells may signal to each other in different ways, often classified depending on the distance between the signaling cell and the target cell. Cell signaling in multicellular organisms often involve chemicals such as hormones and neurotransmitters. Lipophilic hormones such as steroids can pass through the lipid bi-layer of cell membranes and bind to their target receptors within the cell. However, hydrophilic chemical messengers are incapable of crossing cell membranes. Hence in order to deliver their message they bind to specific receptors on the outside of the cell membrane and activate mechanisms that transmit the signal into the cell. This process is known as *transmembrane signaling* or *signal transduction*.^{7b} A schematic diagram of the transmembrane cell signaling is shown in Figure 1.1.

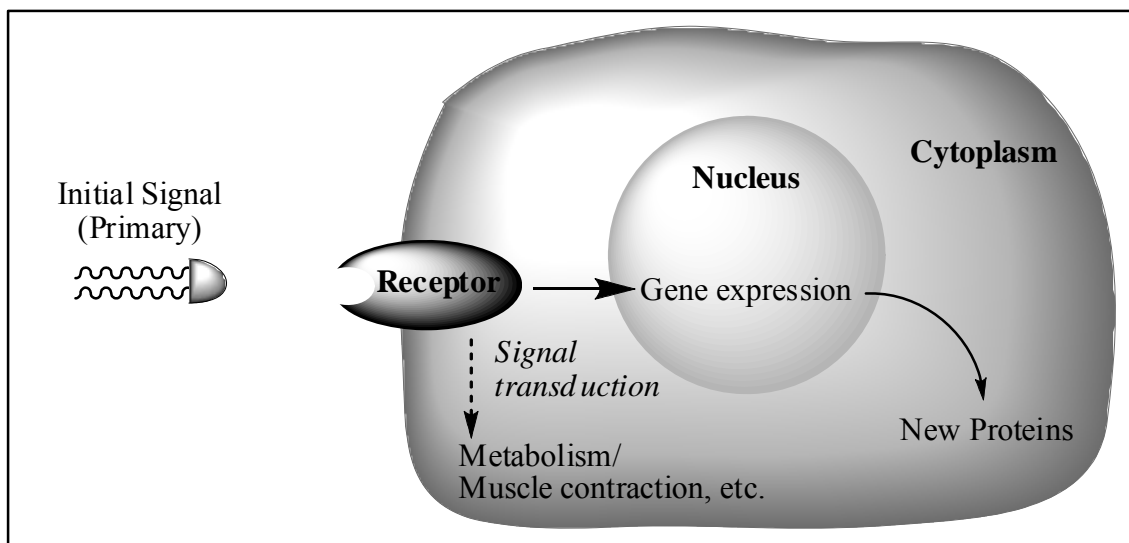
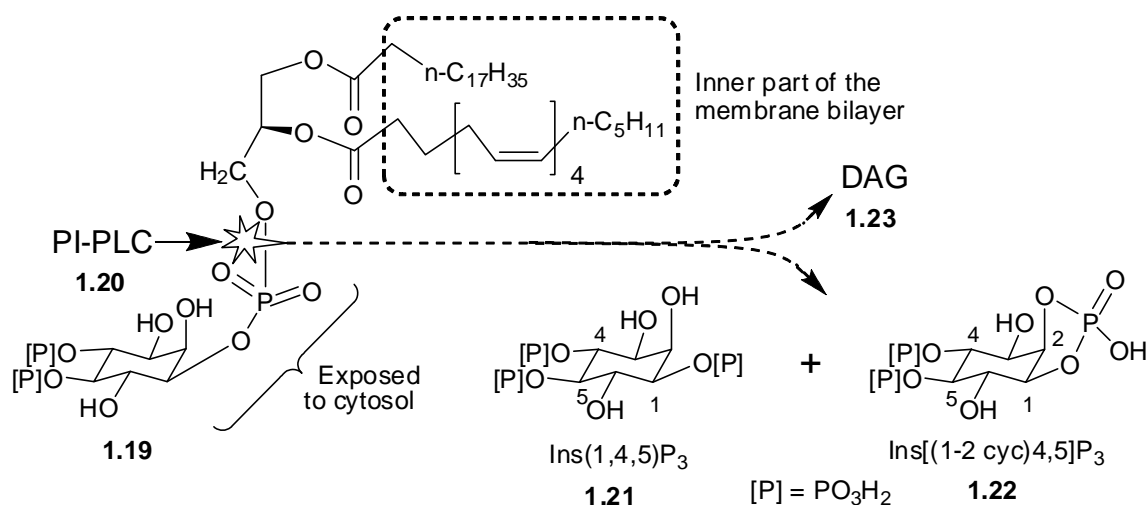


Figure1.1. Transmembrane cell signaling.

After the arrival of a signaling molecule at the cell surface, the events listed below usually follow: (a) perception of the signal by certain proteins referred to as receptors; (b) transmission of the signal by the receptor into the cell; (c) transmission of the ‘message’ to a series of cell signaling components referred to as the signaling cascade; (d) receipt of the message by the final destination in the cell; (e) generation of a response by the cell. *D*-myo-Inositol-1,4,5-trisphosphate [Ins(1,4,5)P₃] functions as a second messenger in signal transduction pathways in eukaryotic cells.¹⁵ The receptor controlled hydrolysis (Scheme 1.4) of the membrane bound lipid, phosphatidylinositol-4,5-bisphosphate [PtdIns(4,5)P₂ - **1.19**] by phosphatidylinositol-specific phospholipase C (PI-PLC - **1.20**) gives Ins(1,4,5)P₃ (**1.21**), *D*-myo-inositol-1,2-cyclic-4,5-trisphosphate [Ins(1-2cyc)4,5)P₃ - **1.22**] and diacylglycerol (DAG, **1.23**).



Scheme 1.4

On cleavage of the phospholipid, hydrophobic DAG (**1.23**) is left in the cell membrane while the hydrophilic inositol phosphates, are released into the cytoplasm. **1.23** activates protein kinase C, while the trisphosphate **1.21** helps in the release of calcium ions from intracellular stores (endoplasmic reticulum). Both **1.21** and **1.23** act as secondary messengers in the target cell.¹⁵ Ins(1,4,5)P₃-induced Ca²⁺ release mediates a variety of cellular responses as diverse as fertilization, cell growth and differentiation,

neuronal signaling, secretion and phototransduction.^{1c} The trisphosphate **1.21** is metabolized eventually to *myo*-inositol *via* a number of phosphorylation and dephosphorylation reactions. *myo*-Inositol is then reused in the biosynthesis of phosphatidylinositol lipids in the endoplasmic reticulum; phospholipids so produced are reincorporated back into the plasma membrane by vesicular transport.¹⁵

myo-Inositol is also a part of the covalent anchors (glycosyl phosphatidylinositols -GPI) that attach certain proteins to cell membranes, for example, variant surface glycoprotein of trypanosomes.¹⁶ A typical structure of a GPI anchor is shown in Figure 1.2; GPI anchors attach proteins to cell membranes *via* a phosphoethanolamine unit linked to a trimannose-glucosamine-inositol backbone and a hydrophobic lipid (DAG) anchors the system to the cell membrane.¹⁷ Lipophosphoglycans and glycoinositol phospholipids, are also thought to play an important role in parasite virulence.^{16b}

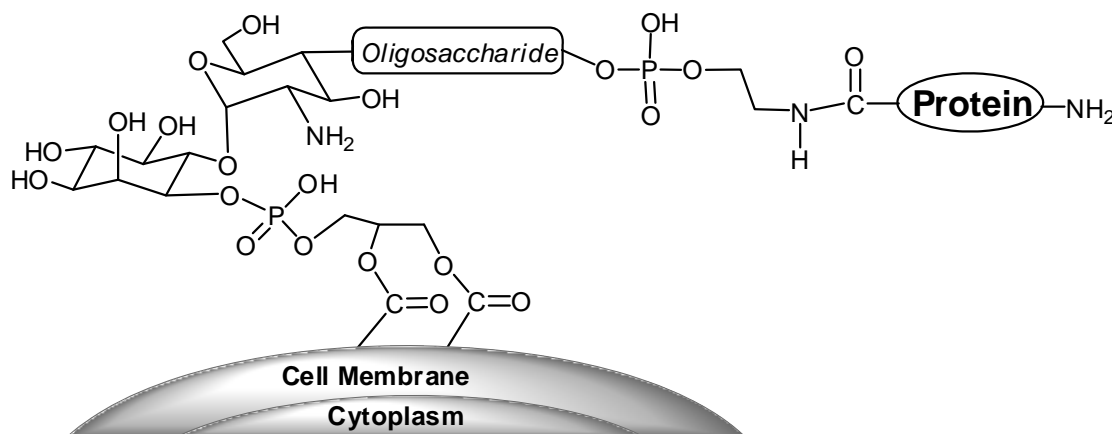


Figure 1.2 Structure of GPI anchor.

Impairment of the *myo*-inositol cycle, which involves several enzymes, could lead to several diseases and hence these pathways in the *myo*-inositol cycle are potential targets for the development of drugs. These developments in biology and medicine revived the chemistry associated with inositols in the past two decades.

1.3. Inositol isomers.

Inositols are cyclohexane hexols; there are eight known isomers, one of them being an enantiomeric pair (D- & L-*chiro*-inositols) making a total of nine distinct stereoisomers (Figure 1.3). Among these nine isomers, *myo*-, *scyllo*-, *cis*-, *neo*- and (D- and L-) *chiro*-inositols or their derivatives occur in nature; *myo*-inositol being the most abundant.¹⁸

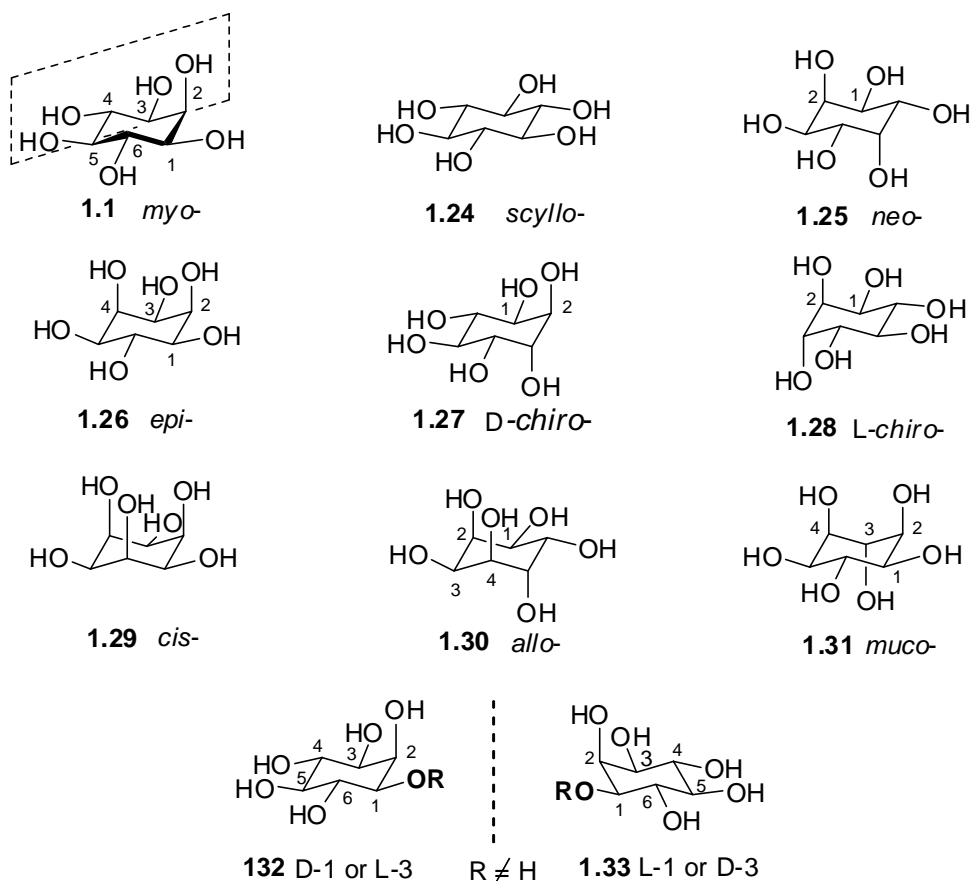


Figure 1.3. Nine isomers of inositol reported in the literature.

myo-Inositol is a *meso* isomer with five equatorial hydroxyl groups and an axial hydroxyl group. There is a plane of symmetry passing through two carbon atoms (as shown in Figure 1.3). The carbon bearing the axial hydroxyl group is designated as C-2 and the other ring carbons can be numbered from C-1 to C-6 starting from a C-1 atom and proceeding around the ring in clockwise (**1.33**) or anticlockwise (**1.32**) fashion.

According to convention,¹⁹ anti-clockwise numbering in an unsymmetrically substituted *myo*-inositol leads to the configurational D-prefix and clockwise numbering gives the substituted *myo*-inositol an L-prefix. An IUPAC nomenclature allowing all biologically relevant compounds to be denoted as D-isomers has also been proposed.²⁰ Although, many of the unsymmetrically substituted *myo*-inositol derivatives reported in this thesis are racemic, for clarity and simplicity they are represented by only one enantiomer in schemes. Optically inactive (*racemic, meso*) synthetic derivatives of inositol (other than phosphates) are numbered without prefixes, while optically active derivatives are numbered with a suitable prefix (**D-**, **L-**, **ent-**, **Dia-** etc).

1.4. Orthoesters.

Orthoesters are acetal-like derivatives of carboxylic acid esters (one carbon atom covalently attached to three alkoxy groups). Some biologically active natural products such as daphnetoxin, resiniferatoxin (RTX), kirkinine, synaptoplep factors,²¹ orthoesterol B²² and Hygromycin B²³ contain the orthoester moiety (Figure 1.4). Xylocensins O (1) and P (2) are a unique class of highly oxidized phragmalins that were isolated from the stem bark of the mangrove plant *X. granatum* and identified as 8,9,30-phragmalin orthoesters.²⁴

Cyclic and acyclic orthoesters have been extensively used for the protection of alcohols as well as carboxylic acids.²⁵ Orthoesters are stable to alkaline conditions and the parent alcohol or the carboxylic acid can be regenerated by the acid hydrolysis of the orthoesters. Alternately, certain orthoesters can also be subjected to reduction reactions to generate ketals and ethers. These reactions provide certain degree of flexibility during the synthesis of complex organic molecules.

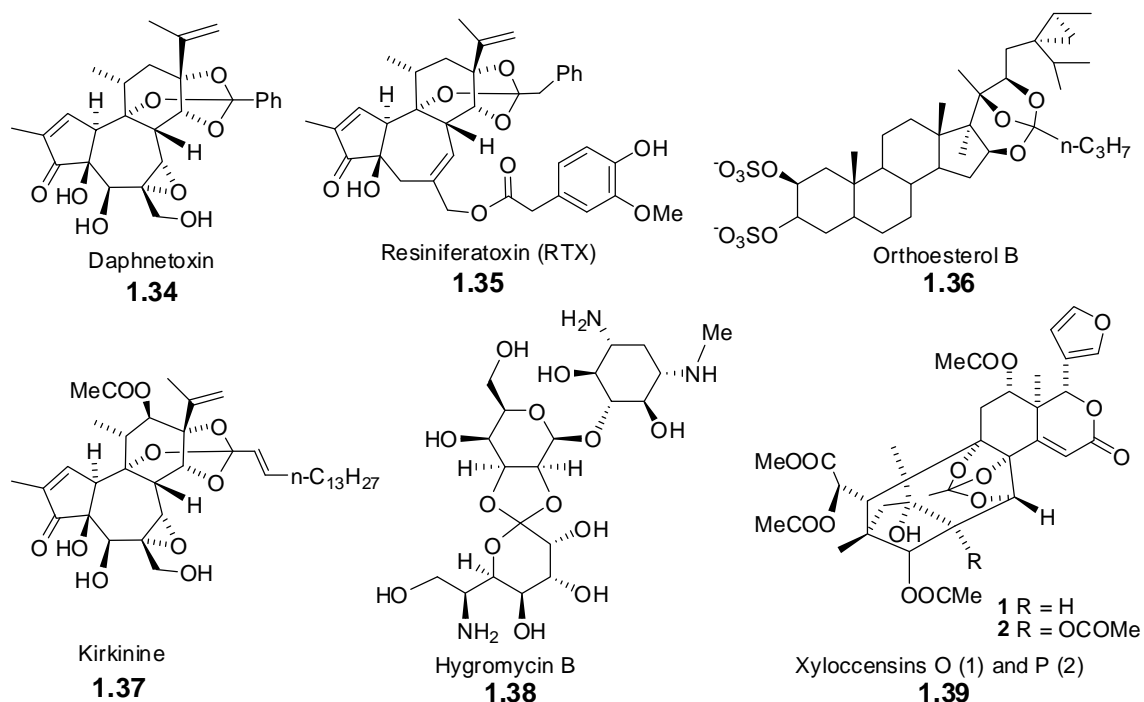
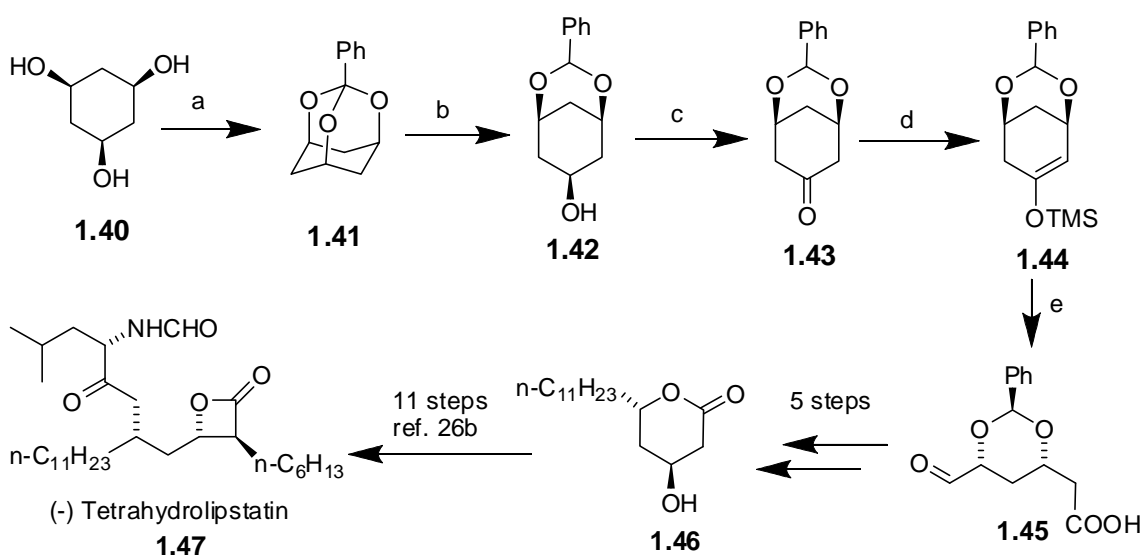
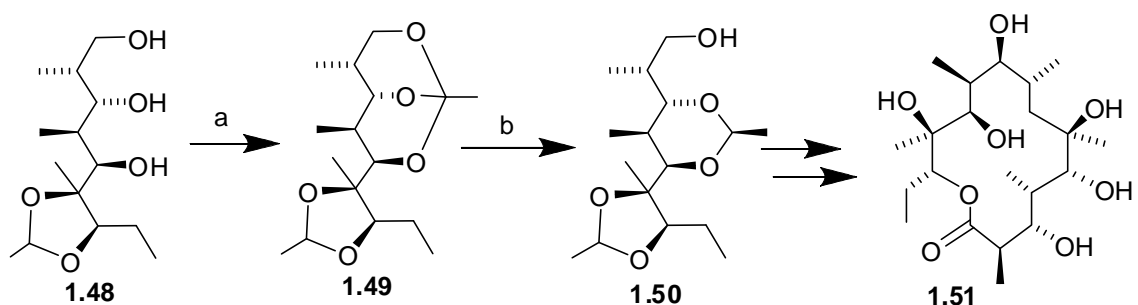


Figure 1.4. Structures of some natural products containing orthoester functionality.

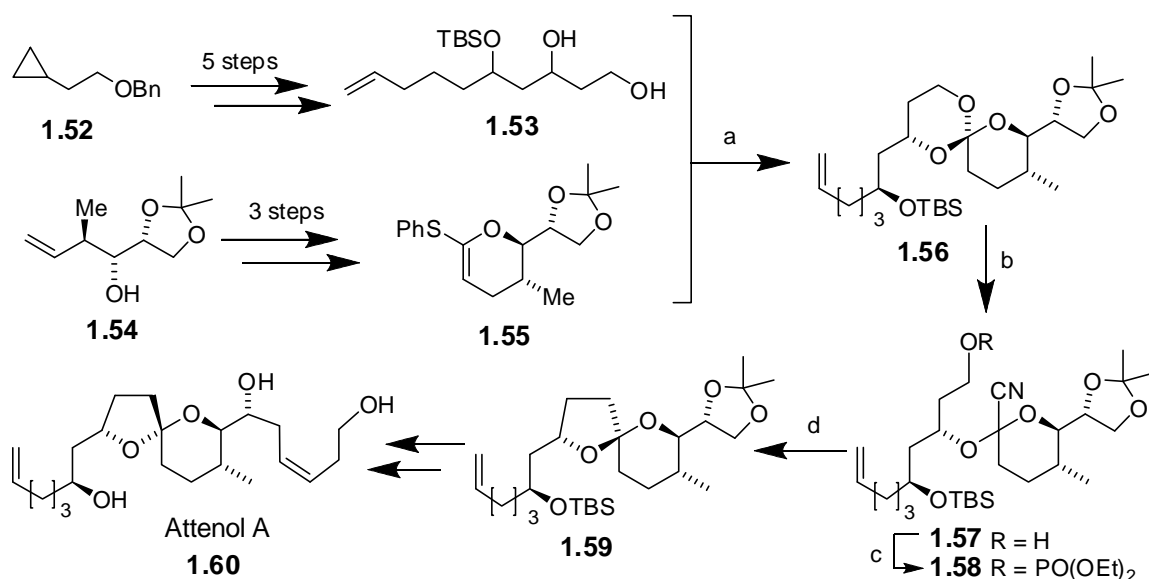
Synthesis of an antiobesity agent, tetrahydrolipstatin **1.47**,²⁶ a natural product, (+)-(9s)-dihydroerythronolide A (**1.51**)²⁷ and a cytotoxic agent attenol A (**1.60**)²⁸ are shown in Schemes **1.5**, **1.6** and **1.7** for illustration.



Scheme 1.5: (a) $\text{PhC}(\text{OEt})_3$, $\text{BF}_3 \cdot \text{OEt}_2$; (b) $\text{BH}_3 \cdot \text{THF}$, HMPA-THF ; (c) periodinane; (d) lithium (S,S')- α,α -dimethylidenebenzylamide, TMSCl ; (e) O_3 , MeOH-DCM , -78°C ; then PPh_3 .



Scheme 1.6: (a) MeC(OEt)₃, PPTS; (b) BH₃, THF.



Scheme 1.7: Synthesis of attenol-A²⁷: (a) CSA; (b) BF₃•Et₂O, TMSCN; (c) (EtO)₂P(O)Cl; (d) lithium di-*t*-butyl biphenylide (LiDBB).

Orthoesters have been used as glycosyl donors in carbohydrate chemistry.^{16c, 29} Formation of glycosidic bonds is of immense importance in the synthesis of complex glycosides and their conjugates, which are being realized to have profound biological implications (Figure 1.5).

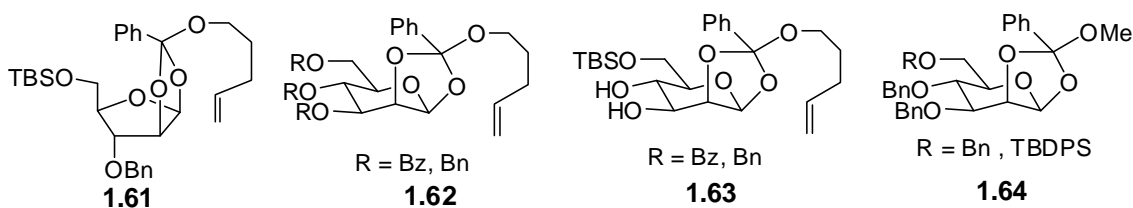
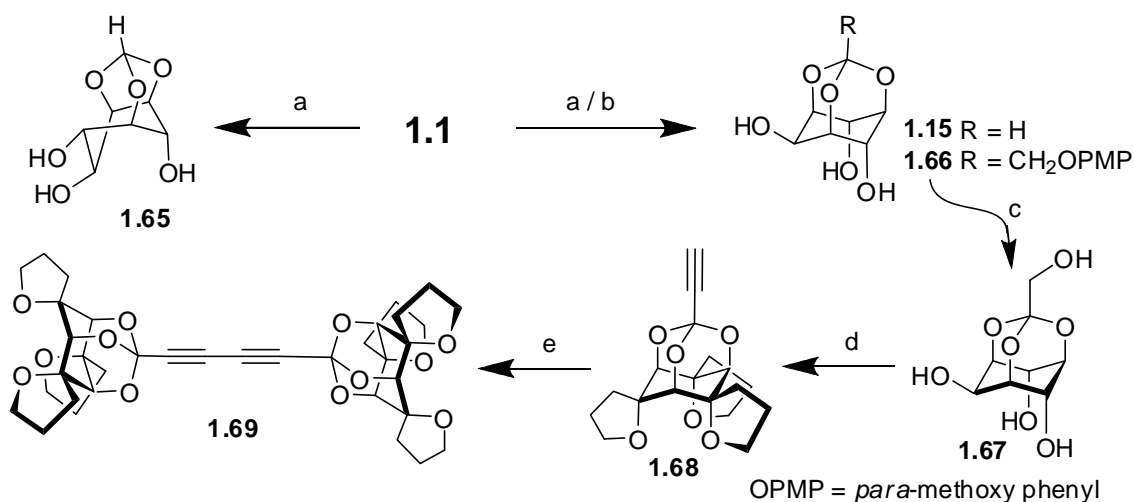


Figure 1.5: Orthoesters used as glycosyl donors.

1.5. Inositol orthoesters: Preparation.

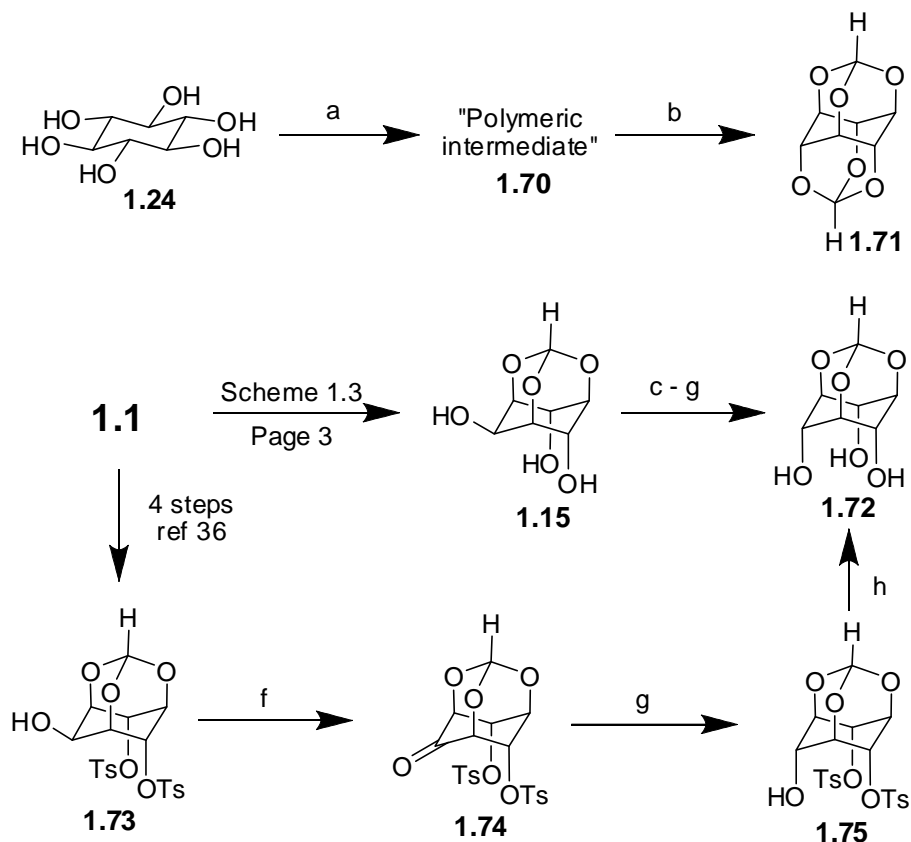
Luk'yanov and Tolkachev³⁰ reported the synthesis of *myo*-inositol mono-orthoformate and assigned the structure **1.65** (Scheme 1.8). However, the structure of the mono-orthoformate was proved to be **1.15** by Lee and Kishi^{7a}. Procedures for the preparation of the orthoacetate **1.16**,^{7c} the orthobutanoate **1.18**^{12a} (Scheme 1.3) and the *para*-methoxy phenoxy-orthoacetate **1.66**³¹ have been published. Although the orthobenzoate is reported in the literature,³² procedure for its preparation was not available. Orthoesters of *myo*-inositol are usually prepared by the reaction of *myo*-inositol with a suitable trimethyl or triethyl orthoester, in DMF or DMSO and the inositol orthoester is isolated by column chromatography. Procedures for the preparation of *myo*-inositol orthoesters, without the involvement of chromatography were also developed later.³³ The PMP orthoester **1.66** has also been converted to other inositol orthoesters such as the acetylene derivative **1.69**³⁴ (Scheme 1.8).



Scheme 1.8: (a) HC(OEt)₃, TsOH, DMSO, 100 °C, 18 h; (b) MeOC₆H₄OCH₂C(OEt)₃, DMF, TsOH, 100 °C, 24 h, 95%; (c) 7 steps as in reference 34 (d) DCM, oxalyl chloride, DMSO, Et₃N; CH₃COC(=N₂)P(O)(OMe)₂, K₂CO₃; (e) CuCl, TMEDA.

The reaction of *scyllo*-inositol **1.24** with triethyl orthoformate in DMSO and other solvents has been investigated.³⁵ The reaction yielded a polymeric intermediate **1.70**

(Scheme 1.9) which on pyrolysis gave hexaoxadiamantane (**1.71**). *scyllo*-Inositol mono-orthoformate **1.72** has been prepared by the inversion of the C2-hydroxyl group (Scheme 1.9) in the orthoformate **1.15**.^{7a, 36}

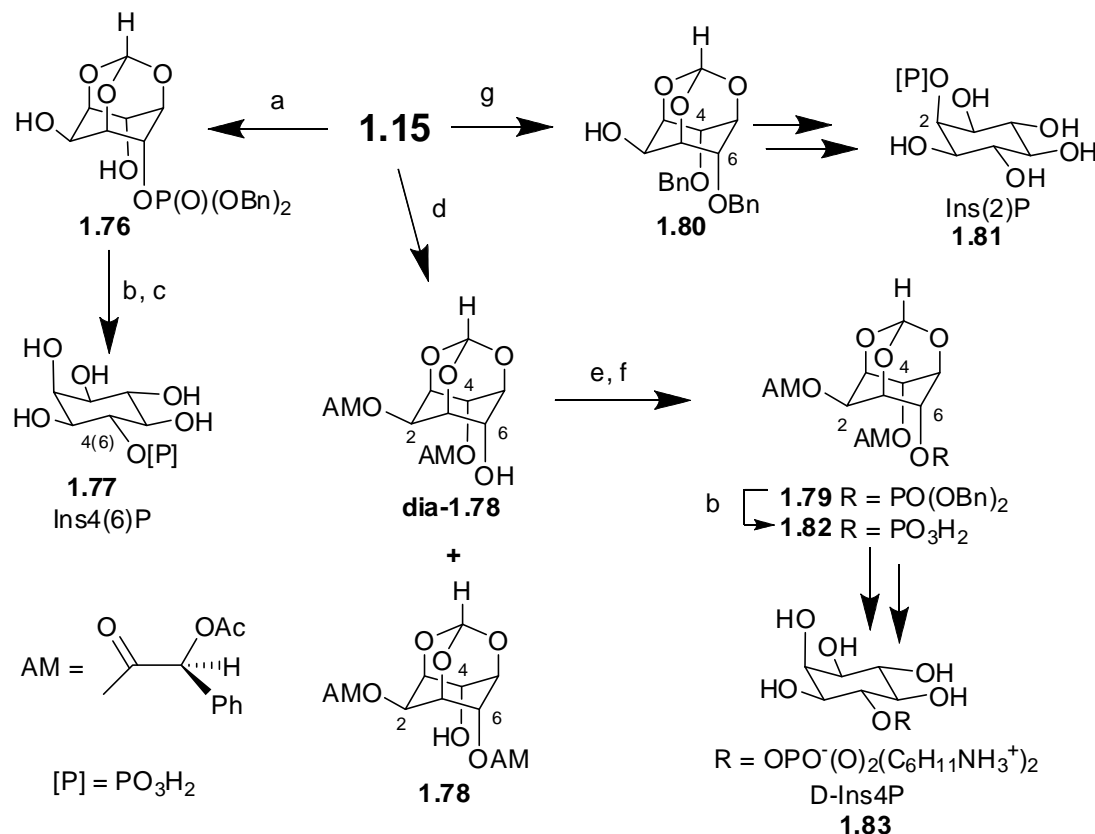


Scheme 1.9: (a) $\text{HC}(\text{OEt})_3$, DMSO, $\text{BF}_3 \cdot \text{OEt}_2$, 150-200 °C; (b) 250-350 °C (c) DMF, TBDMSCl, imidazole; (d) NaH, BnBr, DMF; (e) TBAF, THF; (f) Swern oxidation; (g) NaBH_4 , THF-MeOH; (h) MeOH/ NaOMe.

1.6. *myo*-Inositol-1,3,5-orthoformate as a key intermediate for the synthesis of phosphorylated inositol derivatives.

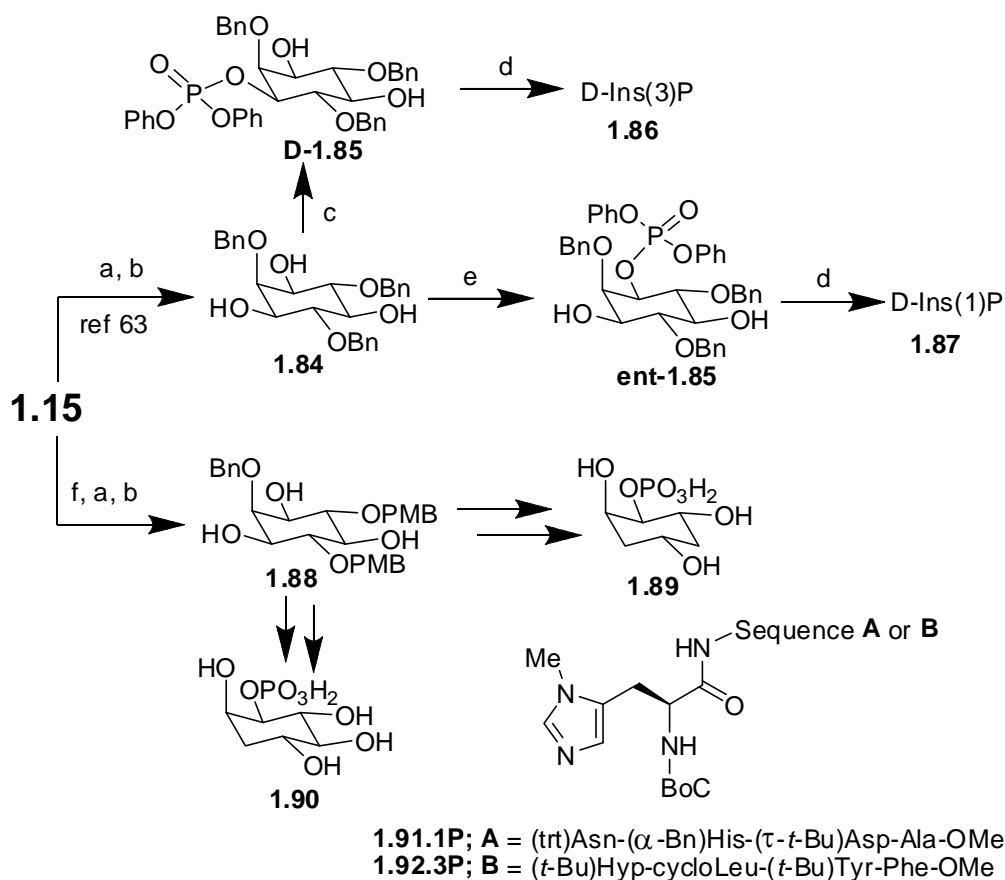
1.6.1. Synthesis of inositol mono-phosphates and their analogs: Racemic *myo*-inositol-4-phosphate (**1.77**)³⁷ and *myo*-inositol-2-phosphate (**1.81**)³⁸ have been prepared from the orthoformate **1.15** (Scheme 1.10). While the racemic 4-phosphate **1.77** can be obtained by the direct phosphorylation of the orthoformate **1.15**, preparation of the 2-

phosphate **1.81** required initial protection of the C4- and C6- hydroxyl groups. *D*-myo-Inositol-4-phosphate (**1.83**) was prepared in four steps from *myo*-inositol³⁹ by initially desymmetrizing the orthoformate as its di-(*S*)-*O*-acetylmandelate esters **1.78** and **dia-1.78**



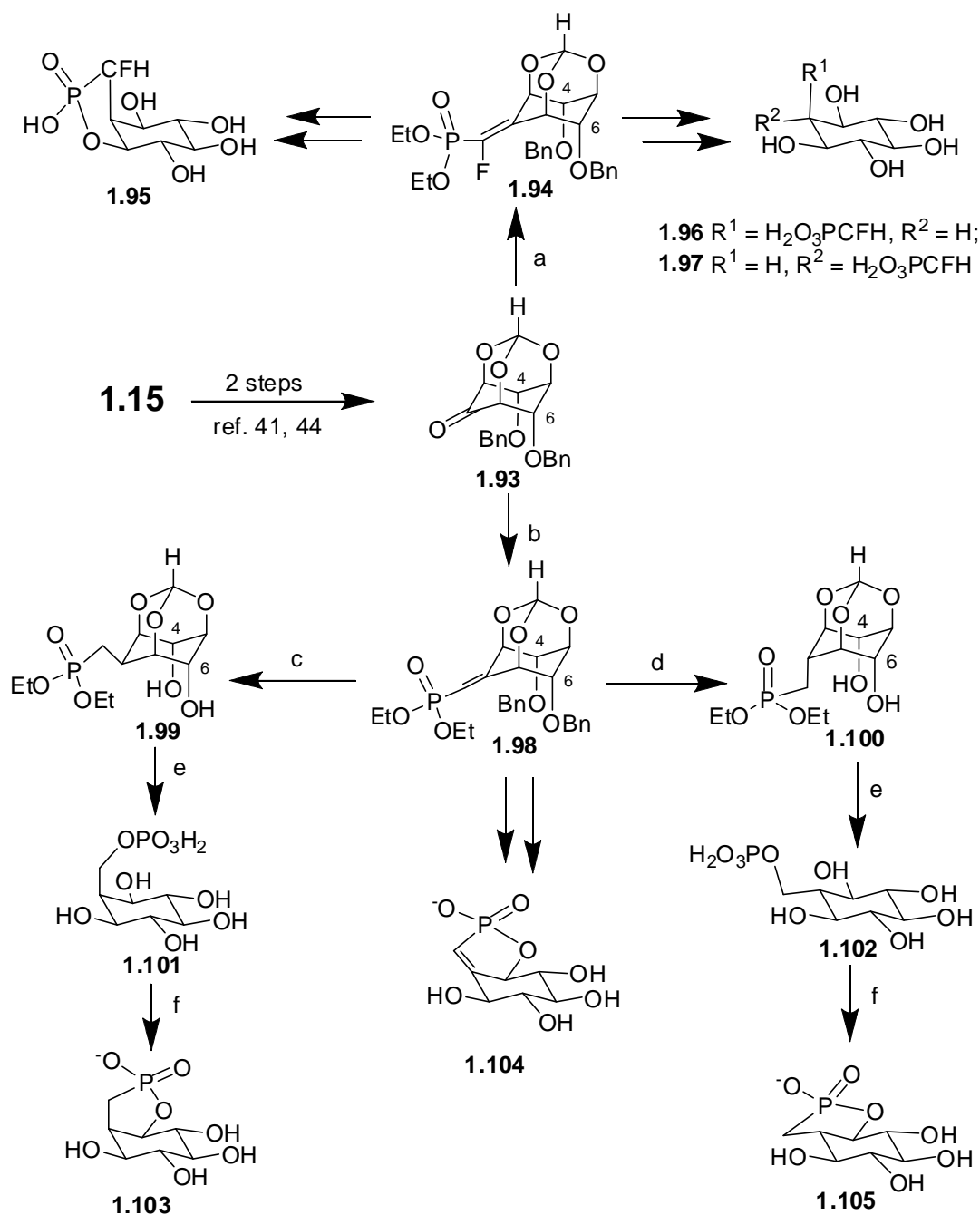
Scheme 1.10: (a) NaH, $[(\text{BnO})_2\text{PO}]_2\text{O}$; (b) Pd-C, H_2 ; (c) 80 % TFA - H_2O ; (d) (*S*)-(+)-*O*-acetylmandeloyl chloride, Py; (e) $(\text{BnO})_2\text{PN}(i\text{-Pr})_2$, tetrazole, DCM; (f) *m*-CPBA, DCM; (g) NaH (2 eq), BnBr (2 eq).

D-myo-Inositol-1-phosphate (**1.87**), *D*-myo-inositol-3-phosphate (**1.86**), *D*-myo-inositol-3-deoxy-1-phosphate (**1.90**) and *D*-myo-inositol-3,5-dideoxy-1-phosphate (**1.89**) were made from the orthoformate **1.15** via the tribenzyl ether **1.84** and the methoxy benzyl ether **1.88** as shown in scheme 1.11.⁴⁰



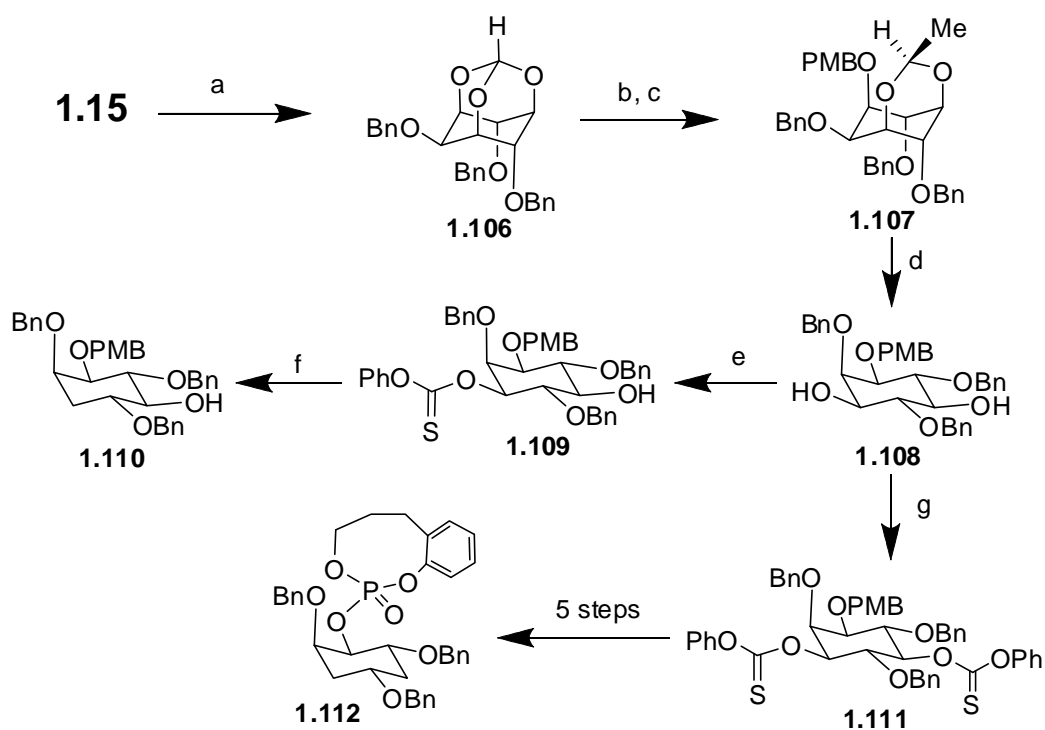
Scheme 1.11: (a) NaH, BnBr, DMF; (b) H^+ / MeOH; (c) peptide **1.92.3P**, DPCP, Et_3N , DCM, 53 %; (d) Li, liquid NH_3 ; (e) peptide **1.91.1P**, DPCP, Et_3N , DCM, 65 %; (f) NaH, PMBCl, DMF.

Fluorophosphonate analogues **1.95-1.97** (Scheme 1.12) and 1,2-cyclic phosphates **1.103-1.105** were synthesized and tested for the inhibition of PI-PLC in order to gain an understanding of the mechanism of action of the PI-PLC family of enzymes. The dibenzyl ketone **1.93** was used as the key intermediate for the preparation of the fluoro phosphonate derivatives **1.95-1.97**.⁴¹ A similar synthetic sequence was used for the preparation of three inositol cyclic phosphonates **1.103-1.105** with varying stereochemistry at the C-2 position of the inositol ring; they were tested as water-soluble inhibitors of PI-PLC.⁴²



Scheme 1.12 : (a) LDA, $[(EtO)_2(O)P]_2CHF$, THF; (b) $CH_2[P(O)(OEt)_2]_2$, LDA, THF; (c) H_2 , 10 % Pd-C, EtOH, 60 °C, 10 h, >90% stereoselectivity; (d) H_2 , Raney Ni, EtOH, 0 °C, 5 h, >95 % stereoselectivity; (e) TFA- H_2O ; (f) DCC, DMF.

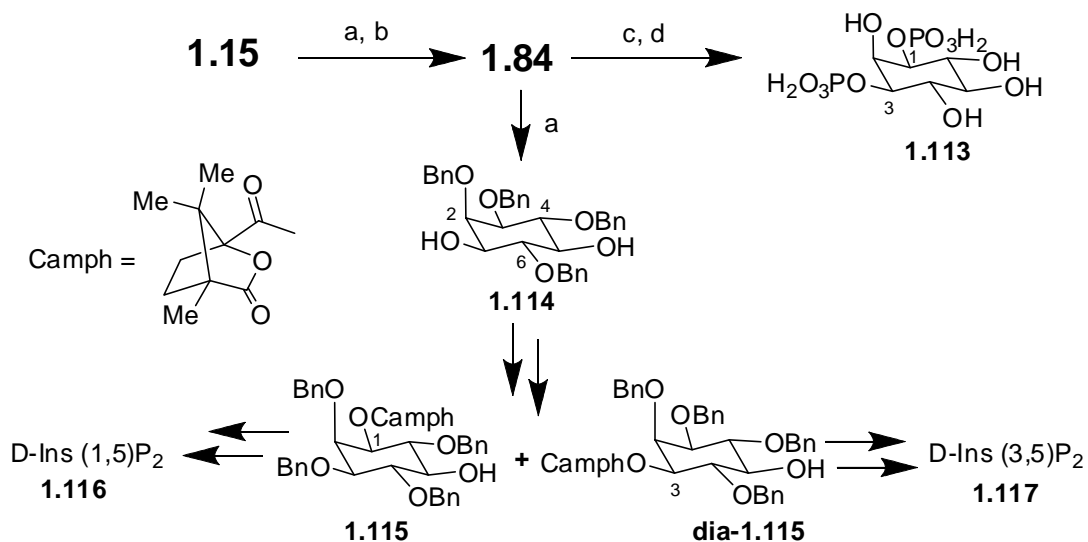
The inositol derivative **1.112** (Scheme 1.13) was prepared from the orthoformate **1.15** and tested as a pro-drug of inositolmonophosphatase ligands.⁴³



Scheme 1.13: (a) NaH, BnBr, DMF; (b) Me₃Al, DCM; (c) NaH, PMBCl, DMF; (d) aq. TFA; (e) PhOCSCl, DMAP, MeCN; (f) Bu₃SnH, AIBN, PhMe; (g) NaH, THF; CS₂; MeI

1.6.2. Synthesis of *myo*-inositol bis-phosphates.

Symmetric *myo*-inositol-1,3-bis phosphate (**1.113**, Scheme 1.14)⁴⁴ and optically active *myo*-inositol-1,5- and 3,5-bisphosphates **1.116** and **1.117**⁴⁵ were synthesized from

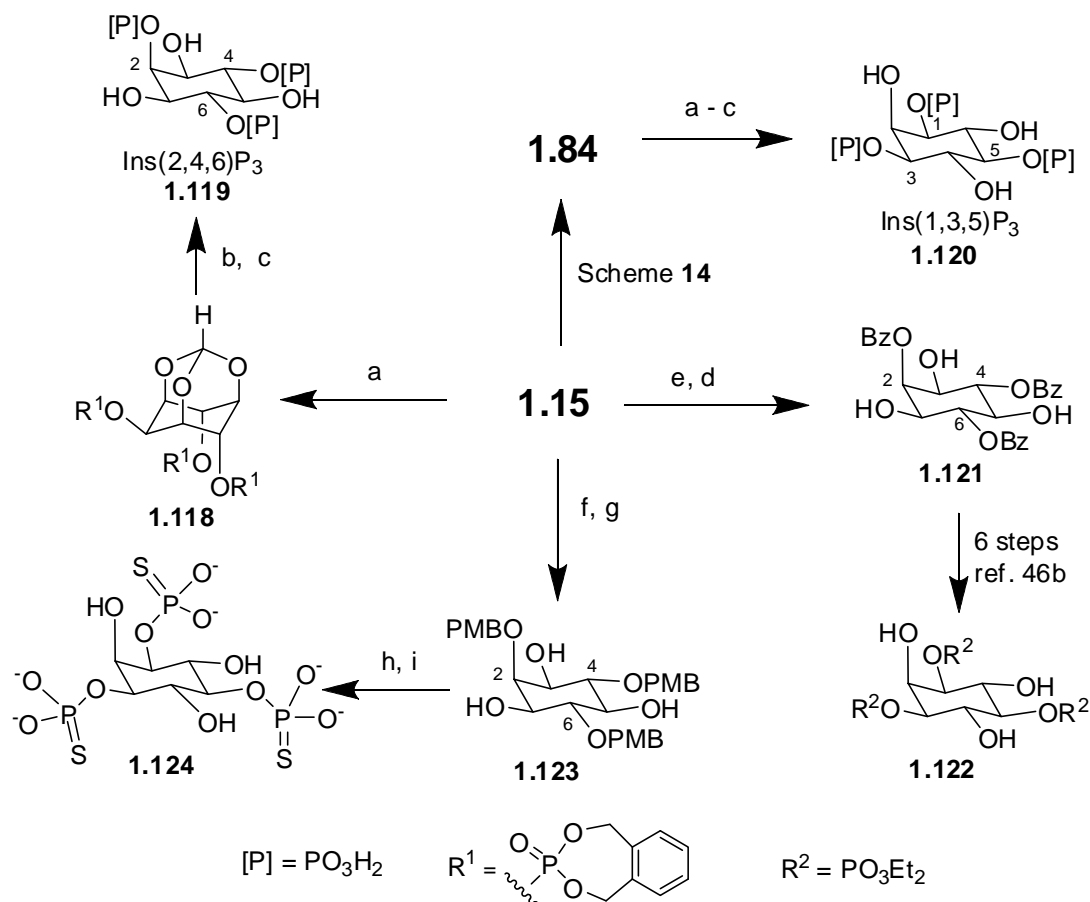


Scheme 1.14: (a) NaH, BnBr; (b) H⁺/MeOH; (c) (PhO)₂POCl, Et₃N; (d) Li-liq.NH₃.

the tribenzyl ether **1.84** (Scheme 1.11) which can readily be prepared from the orthoformate **1.15**.

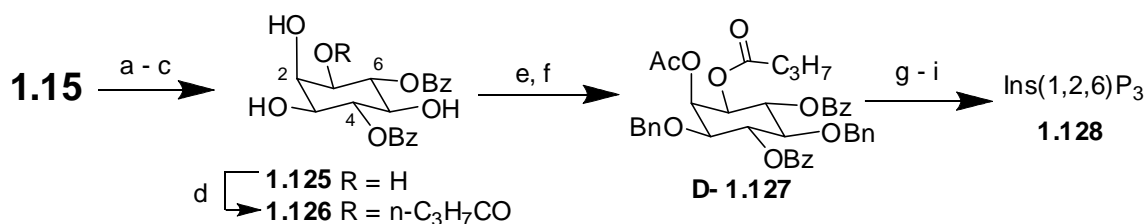
1.6.3. Synthesis of *myo*-inositol tris-phosphates and their analogs.

The orthoformate **1.15** is a precursor for the preparation of the trisphosphate⁴⁶ **1.119** and it serves as a convenient intermediate for the preparation of precursors for *myo*-inositol-1,3,5-trisphosphate (**1.120**)^{46b,47} as well as its analogs **1.122** and **1.124** (Scheme 1.15).⁴⁸ Some of these trisphosphates were investigated for their ability to complex with several metal ions.^{46a} The phosphorothioate analog **1.124** did not mobilize intracellular Ca^{2+} but was a highly potent inhibitor of $\text{Ins}(1,4,5)\text{P}_3$ 5-phosphatase and hence served as a non- Ca^{2+} -mobilizing inhibitor of $\text{Ins}(1,4,5)\text{P}_3$ 5-phosphatase.⁴⁸



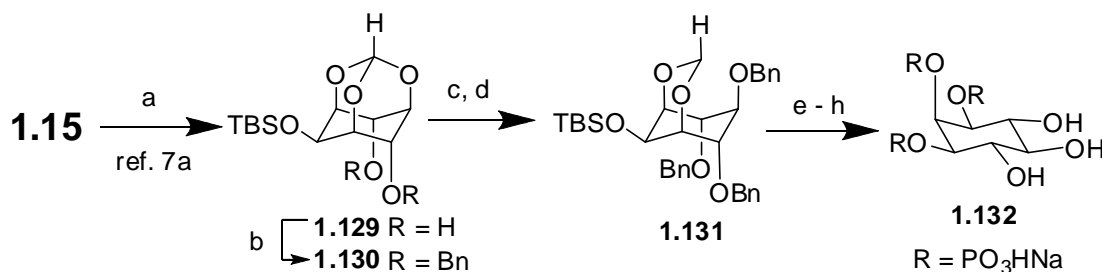
Scheme 1.15: (a) 2-Ethylamino-1,3,2-benzodioxaphosphepane; (b) *m*-CPBA; (c) H_2 , Pd-C; (d) TsOH, MeOH; (e) BzCl, Py; (f) PMBCl, NaH, DMF; (g) 2 M HCl, MeOH (1:20); (h) $(\text{BnO})_2\text{P-N}(i\text{-Pr})_2$, 1*H*-tetrazole, then S8, Py.; (i) Na-liq. NH_3 .

D-*myo*-inositol-1,2,6-trisphosphate [Ins(1,2,6)P₃ or α -trinositol, **1.128**] was prepared⁴⁹ in enantiomerically pure form *via* a facile enzyme assisted route (Scheme 1.16). The key reactions in the synthetic sequence starting from the orthoformate **1.15** involved (a) regioselective acetylation of the triol **1.15**; (b) enantioselective esterification of the dibenzoate **1.125**; (c) the selective acylation of the axial hydroxyl group in **1.126** and (d) the selective, base catalyzed methanolysis of one of the benzoate groups in D-**1.127** followed by phosphorylation and deprotection of benzyl groups gave **1.128**. α -Trinositol (**1.128**) is known to possess a range of pharmacological properties- suppression of inflammation,⁵⁰ prevention of secondary diabetic complications,^{50, 51} antagonist at NP-Y receptors,⁵² influence on cholesterol transport⁵³ and reversing of cadmium induced hypertension.⁵⁴



Scheme 1.16: (a) THF, Vinyl acetate, [LPL]; (b) Py, BzCl, DCM; (c) H⁺ / MeOH; (d) acetone, vinyl butyrate, [LPL]; (e) MeC(OEt)₃, TsOH, THF; (f) Cl₃CCNHOBn, TfOH; (g) K₂CO₃, MeOH; (h) Me₂N-P(OBn)₂, tetrazole; *m*-CPBA, DCM; (i) H₂, Pd(OH)₂-C; EtOH, NaOH; Amberlyst-15.

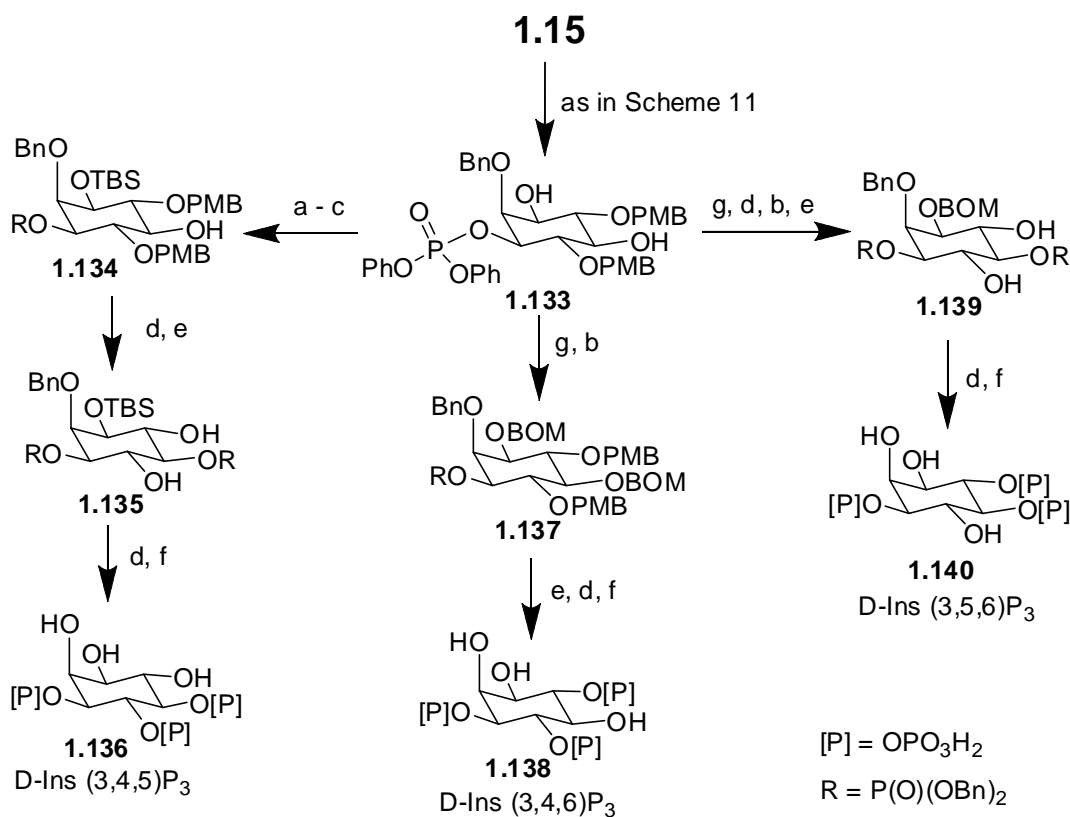
myo-Inositol-1,2,3-trisdihydrogenphosphate (**1.132**) was synthesized from the orthoformate **1.15**;⁵⁵ DIBAL-H reduction of the orthoester moiety in the dibenzyl ether



Scheme 1.17: (a) TBSCl, imidazole, DMF; (b) NaH, BNBr, DMF; (c) DIBAL-H, DCM; (d) BnBr, NaH, *n*-Bu₄NI, DMF; (e) HCl, MeOH; (f) (BnO)₂P-N(*i*-Pr)₂, 1*H*-tetrazole, DCM; (g) *m*-CPBA, DCM; (f) H₂, Pd-C, MeOH; then ion exchange.

1.130 released the C5-hydroxyl group selectively (Scheme 1.17). The trisphosphate **1.132** was obtained from the acetal by deprotection of the C1, C2, and C3- hydroxyl groups followed by phosphorylation.

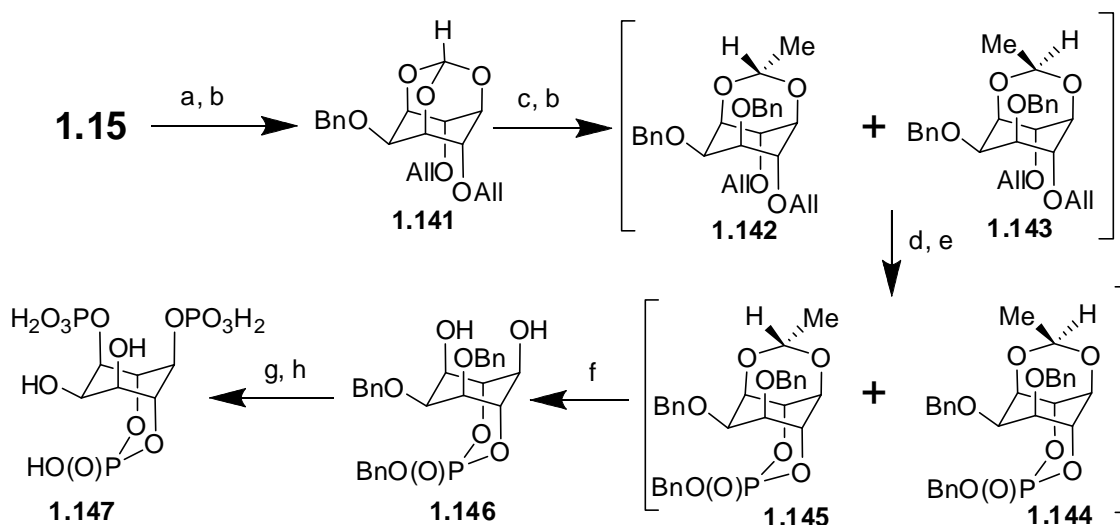
Synthetic routes to several enantiomeric inositol trisphosphates D-Ins(3,4,5)P₃ (**1.136**), D-Ins(3,4,6)P₃ (**1.138**), D-Ins(3,5,6)P₃ (**1.140**) were developed utilizing catalytic enantioselective and site-selective phosphorylation reactions on the triol **1.88** (Scheme 1.11). The common intermediate **1.88** carrying orthogonal protecting groups could be accessed *via* the orthoformate **1.15**.^{40b}



Scheme 1.18: (a) TBSCl, imidazole, DMF; (b) NaH, BnOH; (c) AcCl, MeOH; (d) (*i*-Pr)₂N-P(OBn)₂, dicyanoimidazole, H₂O₂; (e) DDQ, DCM-H₂O; (f) H₂, Pd(OH)₂-C; (g) BOMCl, DIPEA, DMF.

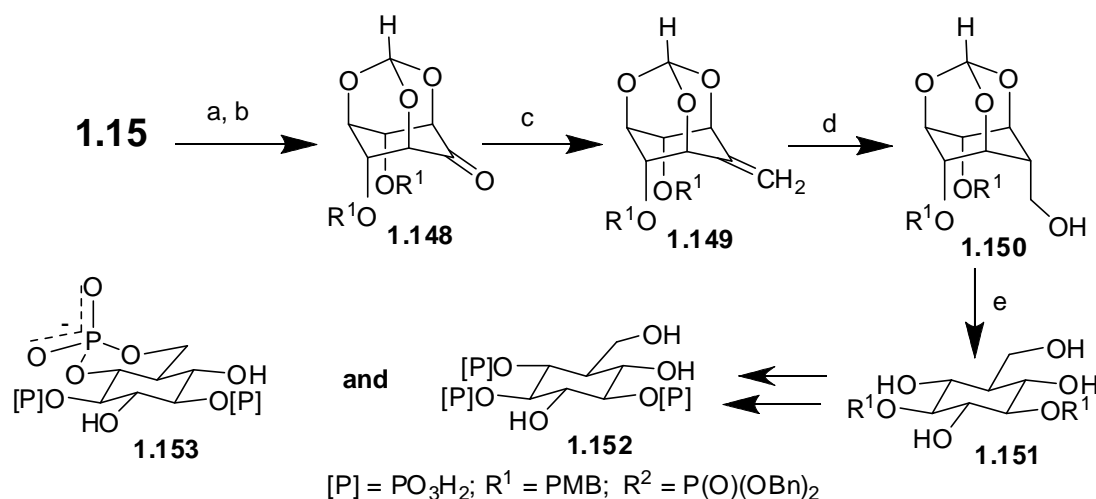
The cyclicphosphate **1.147** has been prepared from the orthoformate **1.15** (Scheme 1.19).⁵⁶ The orthoester moiety in the diallyl ether **1.141** was cleaved using

Trimethyl aluminium to release the C1(3)-hydroxyl group. The diastereomeric mixture of acetals **1.142** and **1.143** served as the key intermediate for the preparation of the cyclic phosphate **1.147**. The trisphosphate **1.147** was used to study the structure activity relationship on the interaction of the second-messenger, D-Ins(1,4,5)P₃ with its receptor.



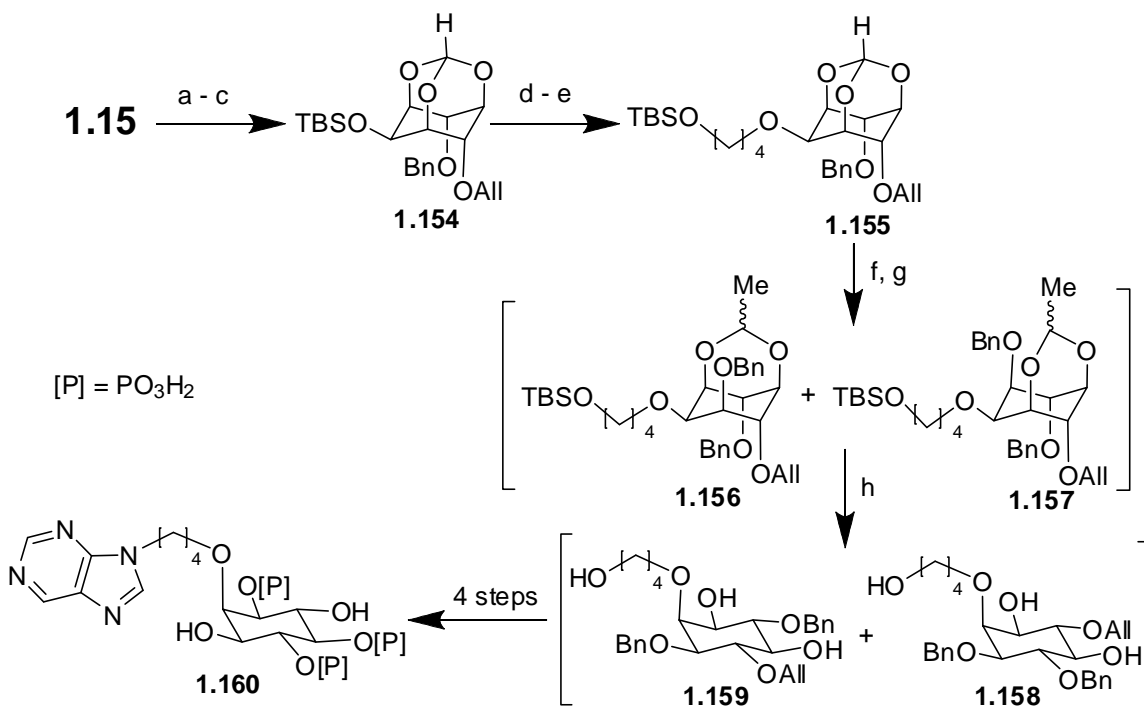
Scheme 1.19: (a) NaH, AlI₃Br, DMF; (b) NaH, BnBr, DMF; (c) Me₃Al, DCM; (d) RhCl(PPh₃)₃, DABCO, then Hg(OAc)₂; (e) (Et₂N)₂POBn, 1*H*-tetrazole, then *m*-CPBA; (f) TFA, THF-EtOH-H₂O; (g) *o*-xylylene *N,N*-diethyl phosphoramidite, 1*H*-tetrazole, then *m*-CPBA; (h) H₂, Pd-C, MeOH.

Conformationally restricted cyclic phosphate, **1.153**, an analogue of the second messenger **1.21**, was prepared⁵⁷ from the protected inosose **1.148** (Scheme 1.20). The inosose **1.148** was obtained from orthoformate **1.15** in two steps; Wittig methylenation followed by hydroboration-oxidation using 9-BBN-H/OH⁻/H₂O₂ gave the axial hydroxymethyl derivative **1.149**. The orthoester **1.149** was converted to the cyclic phosphate **1.153** by a series of protection / deprotection steps followed by phosphorylation. Testing of structurally-modified analogs (such as **1.153**) of biologically active phosphoinositols offers the prospect of pharmacological intervention in the inositol based signaling pathway.



Scheme 1.20: (a) NaH, PMBCl, DMF; (b) Swern oxidation; (c) MePPh₃Br, *t*-BuOK, THF; (d) 9-BBN, OH⁻, H₂O₂, THF; (e) HCl, EtOH.

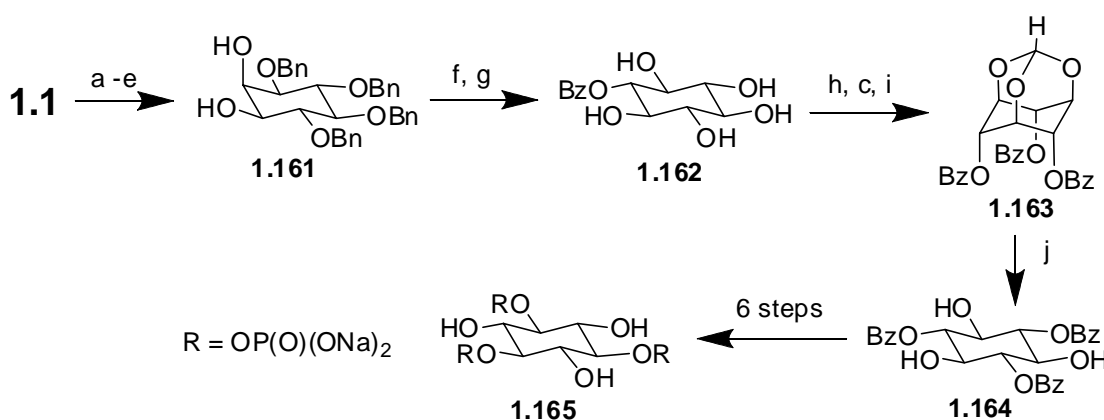
The purinyl derivative racemic **1.160** was synthesized⁵⁸ from the orthoformate **1.15** (Scheme 1.21). Introduction of an alkyl side chain containing the purinyl unit at the



Scheme 1.21: (a) TBSCl, imidazole, DMF; (b) NaH, BnBr, DMF; (c) NaH, AllBr, DMF; (d) TBAF, THF; (e) NaH, 1-*O*-tosyl-4-*O*-TBS butane-1,4-diol; (f) Me₃Al, DCM; (g) NaH, BnBr, DMF; (h) TsOH, MeOH.

2-*O*-position was achieved by the orthogonal protection of the 2, 4 and 6-hydroxyl groups in **1.15**. The purinyl analog **1.160** of Ins(1,4,5)P₃ behaved as a potent full agonist at the Ins(1,4,5) P₃-receptor.

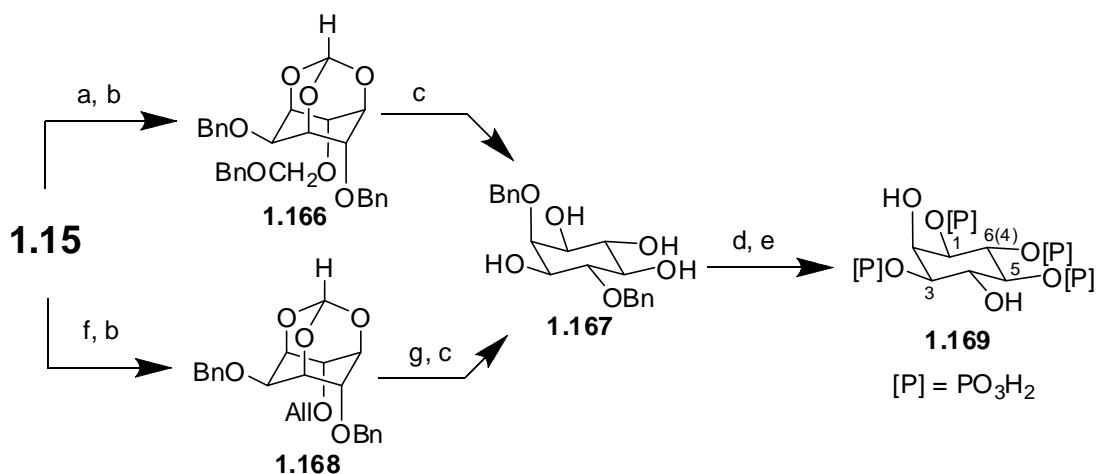
scyllo-Inositol-1,3,5-trisphosphate (**1.165**) was synthesized from *myo*-inositol **1.1**.⁵⁹ The key conversions involved Mitsunobu reaction of the diol **1.161** and protection of the 2,4,6-hydroxyl groups in the monobenzoate **1.162** as the orthoformate (**1.163**, Scheme 1.22).



Scheme 1.22: (a) 2,2-Dimethoxypropane, TsOH; (b) EtOH-ether; (c) Et₃N; (d) NaH, BnBr; (e) aq. AcOH; (f) PPh₃, DEAD, PhCO₂H; (g) H₂, Pd(OH)₂-C; (h) HC(OEt)₃, TsOH; (i) BzCl, Py; (j) TsOH, MeOH.

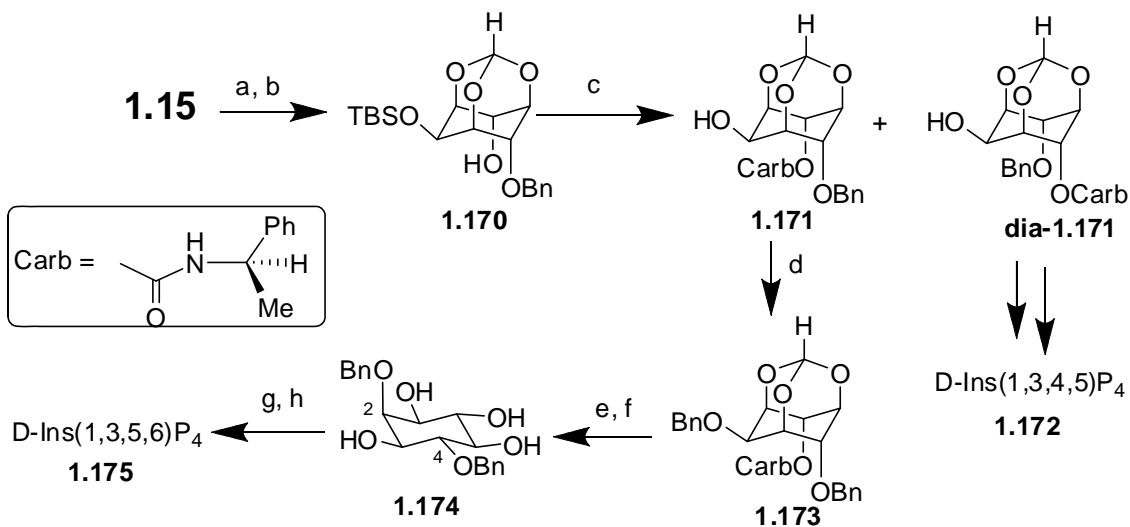
1.6.4. Synthesis of *myo*-inositol tetrakisphosphates.

Synthesis of racemic-*myo*-inositol-1,3,4,5-tetrakisphosphate (**1.169**) was described by two independent groups starting from the orthoformate **1.15**. One of the approaches⁶⁰ (Scheme 1.23) involved the protection of the 4-hydroxyl group in **1.15** as benzyloxymethyl ether while the other³⁷ used an allyl group to protect the same hydroxyl group. In both the reports the key step was a novel, highly regioselective mono-alkylation of one of the axial hydroxyl groups of **1.15**.⁴⁴



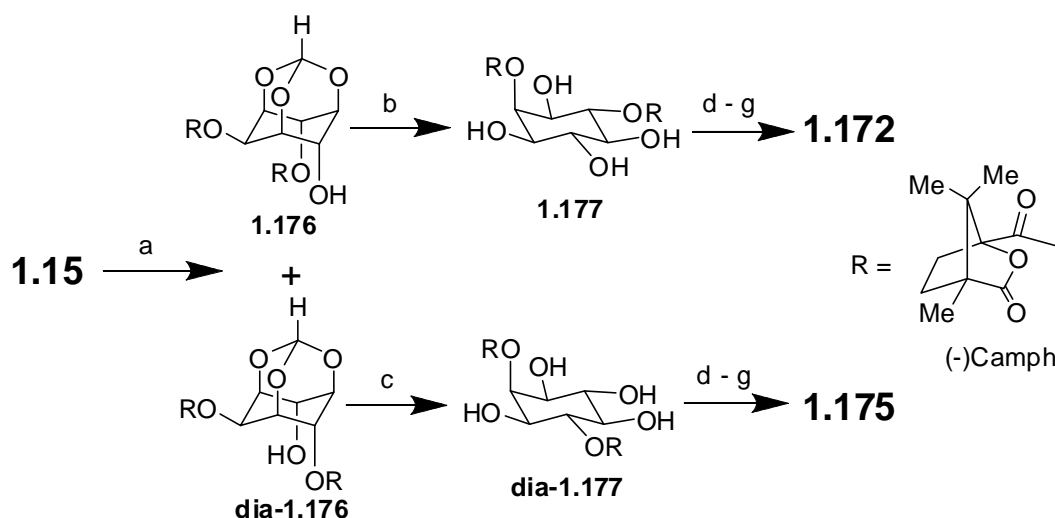
Scheme 1.23: (a) NaH; BnOCH₂Cl, DMF; (b) NaH, BnBr, DMF; (c) HCl-MeOH; (d) [(BnO)₂PO]₂O (TBPP), NaH, DMF; (e) H₂, Pd-C, EtOH; (f) NaH, AllBr, DMF; (g) RhCl(PPh₃)₃, DABCO.

D-Ins(1,3,4,5)P₄ (**1.172**) and D-Ins(1,3,5,6)P₄ (**1.175**) were synthesized^{33a} from *myo*-inositol via the diastereomeric carbamate derivatives **1.171** and **dia-1.171** as shown in the scheme 1.24.



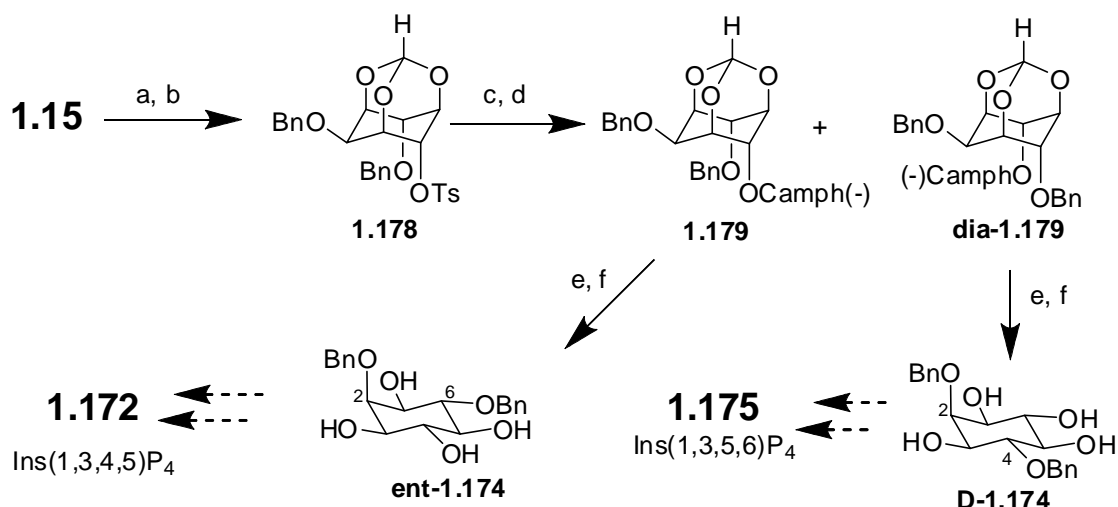
Scheme 1.24: (a) TBSCl, DMF; (b) *t*-BuOK, BnBr, DMF; (c) BuLi, THF, (+)-(*R*)-(1-phenyl ethyl) isocyanate; HCl, MeOH, KH₂PO₄, NaH₂PO₄; (d) BnOC(=NH)CCl₃, TfOH; (e) TFA - H₂O; (f) Na, EtOH; (g) (BnO)₂P-N(*i*-Pr)₂, tetrazole; *m*-CPBA; (h) H₂, Pd-C.

The tetrakisphosphates **1.172** and **1.175** were also prepared⁶¹ via the desymmetrization of the orthoformate **1.15** as its dicamphanate derivative (Scheme 1.25). This method was claimed to be capable of providing D-Ins(1,3,4,5)P₄ (**1.172**) in larger quantities required for crystallographic and NMR studies of its interaction with the rapidly expanding range of Ins(1,3,4,5)P₄-binding proteins.



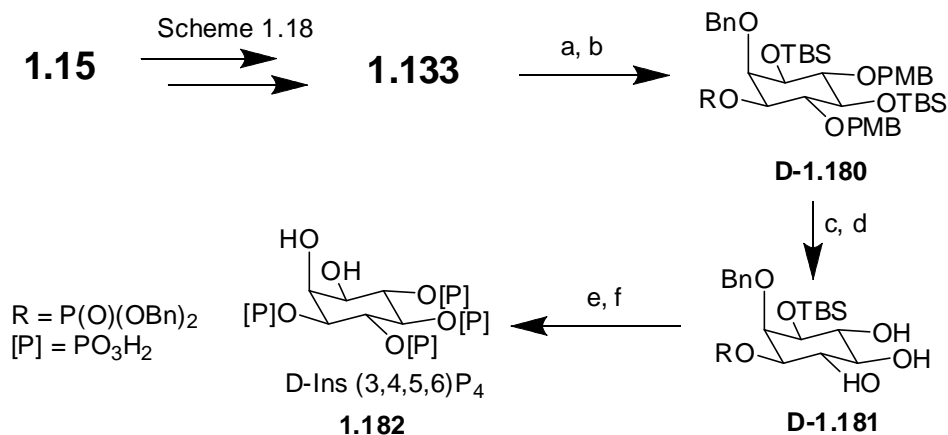
Scheme 1.25: (a) (1*S*)-(-)-camphanoyl chloride, Et₃N, DCM; (b) HCl-MeOH; (c) TFA-H₂O; (d) (BnO)₂P-N(*i*-Pr)₂, 1*H*-tetrazole, DCM; (e) *m*-CPBA, DCM; (f) H₂, Pd-C, MeOH-H₂O; (g) conc: aq NH₃

Precursors for the synthesis of D- and L-*myo*-inositol 1,3,4,5-tetrakisphosphate viz., D-2,4- and D-2,6-di-*O*-benzyl-*myo*-inositols (**1.174** and **ent-1.174**) were prepared⁶² from the orthoformate **1.15** using sulfonate groups for the protection of inositol hydroxyl groups (Scheme 1.26). The regioselectivity of sulfonylation of *myo*-inositol orthoester hydroxyl groups was controlled by the use of different bases to obtain the desired sulfonate. Sulfonylated derivatives of *myo*-inositol orthoesters were stable to conditions of *O*-alkylation but could be cleaved using magnesium / methanol or sodium methoxide in methanol to regenerate the corresponding *myo*-inositol orthoester derivative.



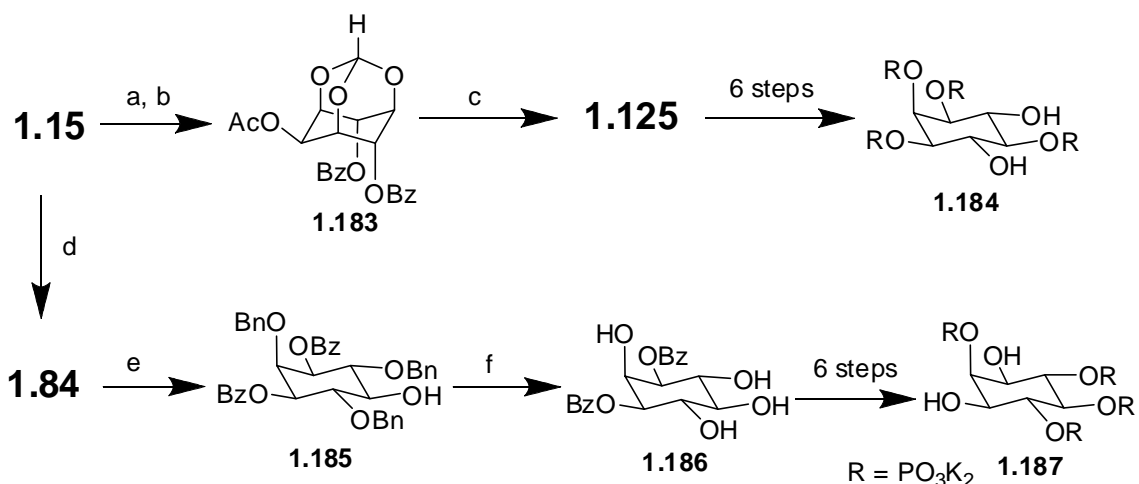
Scheme 1.26: (a) TsCl (1 eq.), Et₃N; (b) NaH, BnBr, DMF; (c) Mg, MeOH; (d) (1*S*)-(-)-camphanoyl chloride, Py, DMAP; (e) NaOMe, MeOH; (f) TFA - H₂O

Enantioselective and site-selective phosphorylation reaction (Scheme 1.18) using a peptide catalyst and further manipulations on the diol **1.133** provided D-Ins (3,4,5,6)P₄ (**1.182**, Scheme 1.27).^{40b}



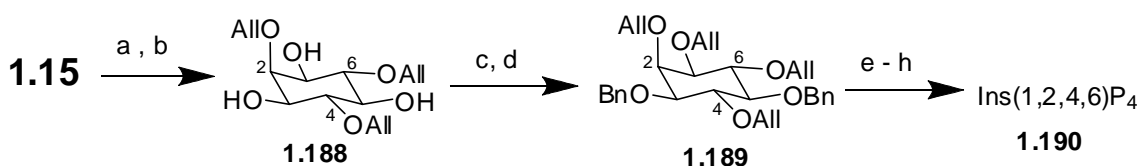
Scheme 1.27: (a) TBSCl, imidazole, DMF; (b) NaH, BnOH; (c) cat. AcCl, MeOH; (d) DDQ, DCM-H₂O; (e) (*i*-Pr)₂N-P(OBn)₂, dicyanoimidazole, H₂O₂; (f) H₂, Pd(OH)₂-C.

The dibenzoates **1.125** and **1.186** obtained from the orthoformate **1.15** were used for the efficient syntheses of Ins(1,2,3,5)P₄ (**1.184**) and Ins(2,4,5,6)P₄ (**1.187**, Scheme 1.28);⁶³ These tetraphosphates were used as inhibitors of I(1,4,5)P₃-3- kinase.



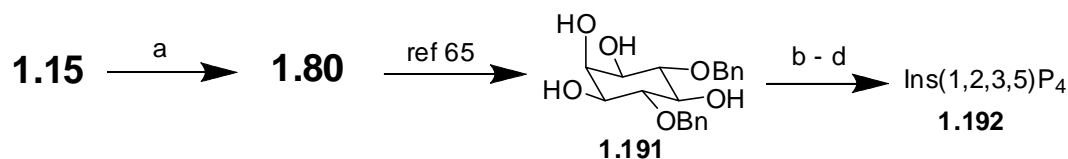
Scheme 1.28: (a) AcCl (1.6 eq.), Py; (b) BzCl (4 eq.); (c) as in Scheme 1.16; (d) Scheme 1.14; (e) BzCl (2.5 eq.), Py., 67%; (f) H₂, Pd(OH)₂-C.

Racemic *myo*-inositol 1,2,4,6-tetrakisphosphate (**1.190**) was synthesized from the orthoformate **1.15** via racemic **1.189**. Benzylation and de-allylation followed by phosphorylation afforded racemic **1.190** (Scheme 1.29). The tetrakisphosphate **1.190** showed no demonstrable agonism or antagonism for Ca²⁺ release in permeabilised hepatocytes.⁶⁴



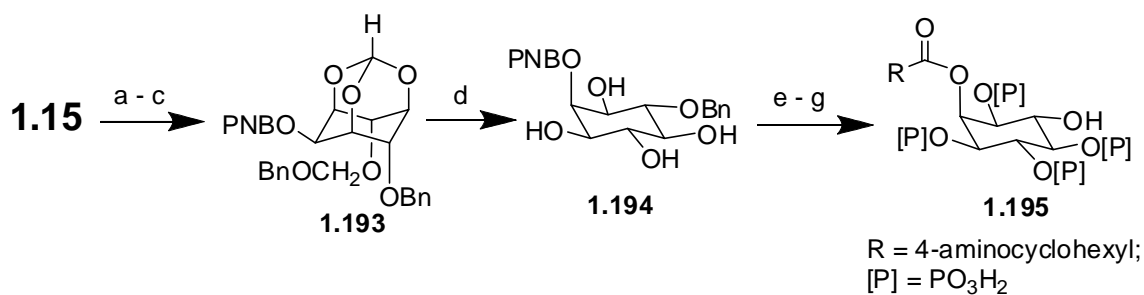
Scheme 1.29: (a) NaH, AllBr, DMF; (b) EtOH-HCl; (c) AllBr, (Bu₄N)₂SO, DCM, aq. NaOH; (d) NaH, BnBr, DMF; (e) Pd-C, TsOH, MeOH-H₂O; (f) (BnO)₂P-N(*i*-Pr)₂, 1*H*-tetrazole, DCM; (g) *m*-CPBA; (h) H₂, Pd-C, MeOH- H₂O.

myo-Inositol-1,2,3,5-tetrakisphosphate (**1.192**) was prepared from the previously mentioned dibenzyl ether **1.80**, obtained in three steps from the orthoformate **1.15** (Scheme 1.30). The tetrakisphosphate **1.192** was tested as an inhibitor of iron-gall-ink corrosion.⁵⁵



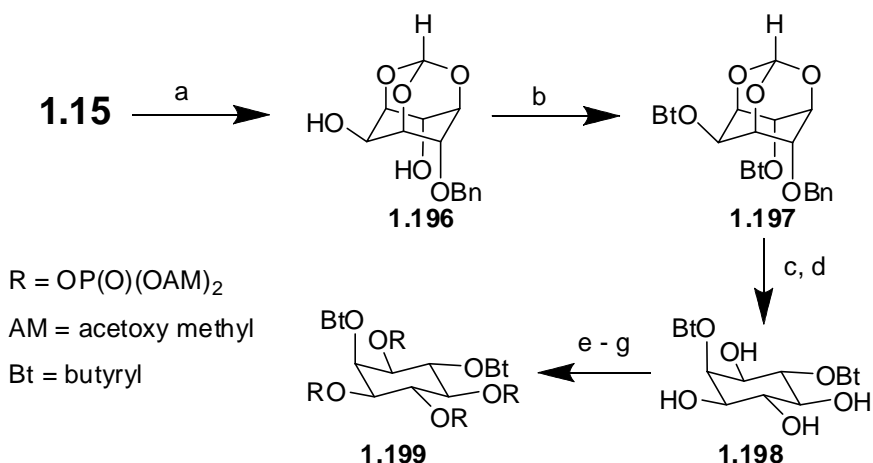
Scheme 1.30: (a) Scheme 1.10, page 13; (b) $(\text{BnO})_2\text{P-N}(i\text{-Pr})_2$, 1*H*-tetrazole, DCM; (c) *m*-CPBA, DCM; (d) H_2 , Pd-C, MeOH- H_2O .

The tetraphosphate derivative **1.195** was synthesized⁶⁶ from the orthoformate **1.15** (Scheme 1.31). The inositol tetrakisphosphate affinity column prepared using **1.195** was found to be effective in isolating the inositol binding proteins from bovine cardiac membranes.



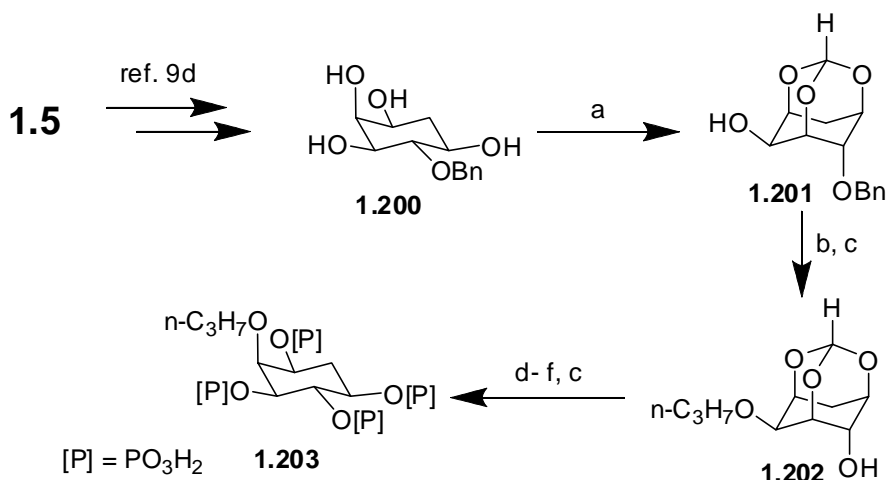
Scheme 1.31: (a) BOMCl, NaH, DMF; (b) PNBCl, Py, DMAP; (c) BnBr, Ag_2O , DMF; (d) HCl-MeOH; (e) *o*-xylylene *N,N*-diethyl phosphoramidite; *m*-CPBA, DCM; (f) H_2 , Pd-C, MeOH- H_2O ; (g) H_2 / RuO_2 .

A membrane-permeant derivative of inositol, racemic **1.199** was synthesized from the dibutyrate **1.197**.⁶⁷ The dibutyrate was obtained by the sequential benzylation and acylation of the orthoformate **1.15** (Scheme 1.32).



Scheme 1.32: (a) BnBr, NaH, DMF; (b) Bt₂O, Py; (c) TFA-H₂O; (d) H₂, Pd-C; (e) Et₂N-P(OBn)₂, tetrazole; AcO₂H; (f) H₂, Pd-C, AcOH; (g) AMBr, DIPEA-MeCN.

Synthesis of the enantiomeric **1.203** (Scheme 1.33) was described,^{68, 9d} starting from D-galactose (**1.5**).

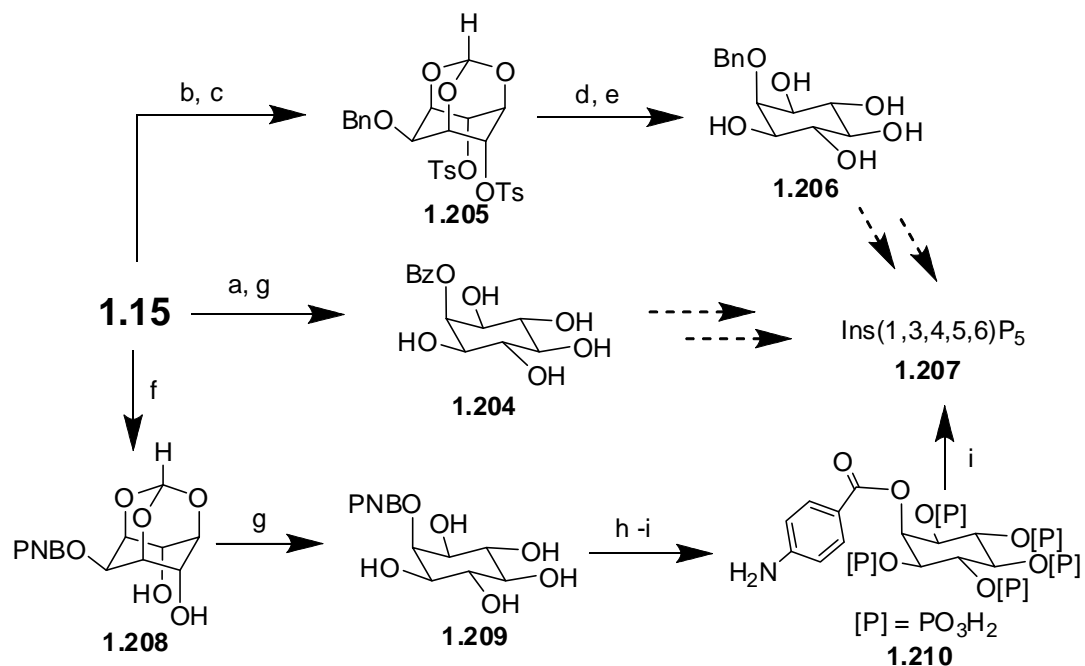


Scheme 1.33: (a) HC(OEt)₃, CSA, DMF; (b) NaH, AllBr, DMF; (c) H₂, Pd-C, EtOH; (d) HCl, MeOH; (e) (*i*-Pr)₂N-P(OBn)₂, 1*H*-tetrazole, (f) *t*-BuOOH.

The three hydroxyl groups in the deoxyinositol derivative **1.200** were protected as the orthoformate (**1.201**). Formation of the *n*-propyl ether followed by deprotection and phosphorylation yielded the tetrakisphosphate **1.203**.

1.6.5. Synthesis of *myo*-inositol pentakisphosphates.

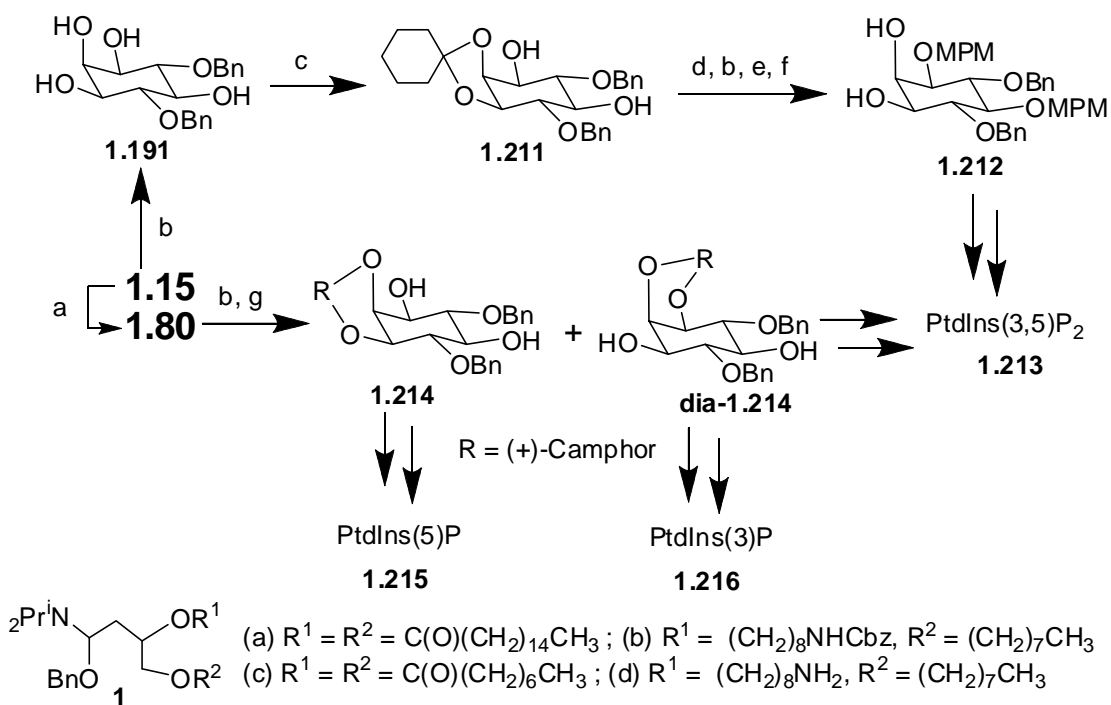
2-*O*-benzoyl-*myo*-inositol (**1.204**) which is a precursor for the preparation of Ins[1,3,4,5,6]P₅ (**1.207**) was obtained from the orthoformate **1.15** by benzylation followed by hydrolysis of the orthoester moiety.⁶⁹ The 2-benzyl ether **1.206**, another precursor for the same pentakisphosphate **1.207** was obtained from the orthoformate **1.15** by using tosylates for the initial protection of the 4- and 6-hydroxyl groups of **1.15**.⁶² Acylation of the C2-hydroxyl group of **1.15** with *p*-nitrobenzoyl chloride provided access to a biologically interesting inositol pentakisphosphate derivative **1.210**. The *p*-aminobenzoate⁶⁶ **1.210** was prepared as a potential ligand for an affinity column to isolate the inositol binding proteins from bovine cardiac membranes (Scheme 1.34).



Scheme 1.34: (a) BzCl, Py; (b) TsCl (2 eq.), NaH or *t*-BuOK (2 eq.); (c) NaH, BnBr; (d) Mg, MeOH; (e) TFA-H₂O; (f) PNBCl, Py; (g) HCl, MeOH; (h) α , α' -diyl-*N,N*-diethyl phosphoramidite, DCM; *m*-CPBA; (i) H₂, Pd-C, MeOH- H₂O.

1.6.6. Inositol phospholipids.

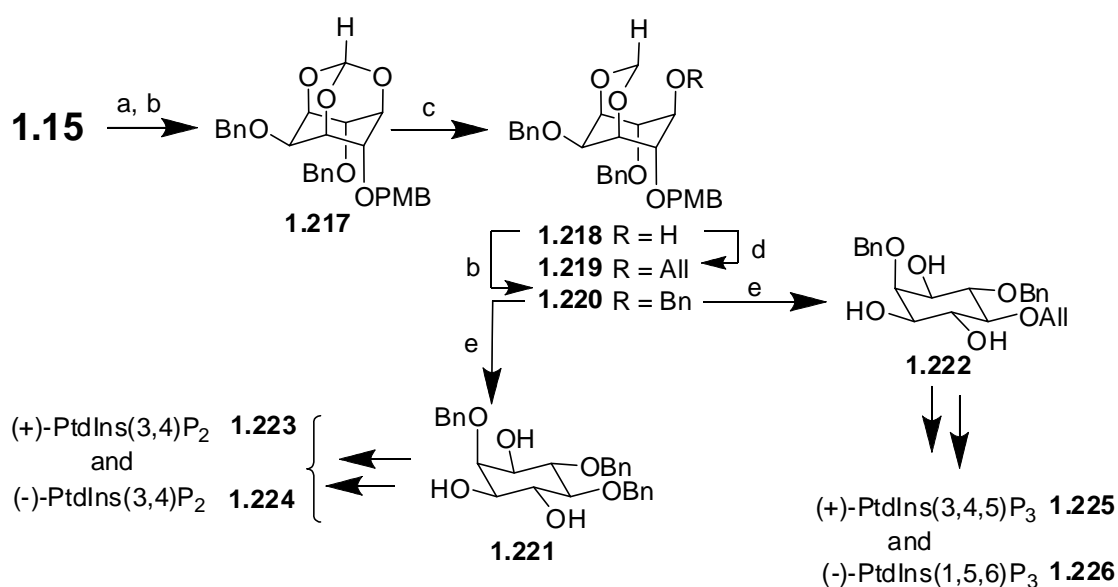
L-Phosphatidyl-D-*myo*-inositol-3,5-bisphosphate [PtdIns(3,5)P₂, **1.213**] has been synthesized from the dibenzyl ether **1.80** which is easily obtainable from the orthoformate **1.15** in two steps. The 1,2-*cis*-diol **1.191** could be selectively protected as cyclohexylidene ketal (**1.211**)⁷⁰ or camphor ketal (**1.214** or **1.215**)⁷¹ since no other vicinal diols are present in the tetrol **1.191** (Scheme 1.35). These ketals were converted to the lipid **1.213** as well as its short chain and cross-linkable aminoether analogues by manipulation of the hydroxyl groups and phosphorylation step, as required.



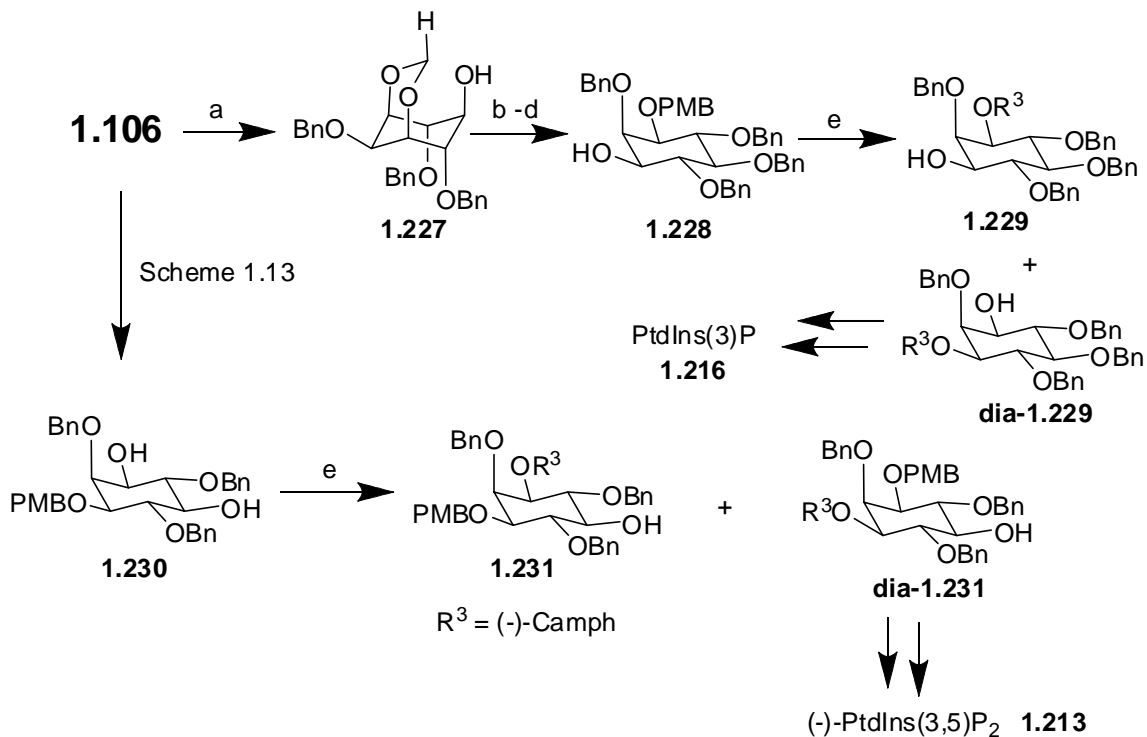
Scheme 1.35: (a) Scheme 1.10, page 13; (b) MeOH-HCl; (c) cyclohexanone, TsOH; (d) MPMCl, NaH; (e) *S*-(-)-camphanic chloride, Et₃N, DCM; (f) MeOH, KOH; (g) (+)-camphor dimethyl ketal, TsOH, DCM.

The D-3-phosphorylated *myo*-inositol phospholipids PtdIns(3)P (**1.216**), PtdIns(3,4)P₂ (**1.223** and **1.224**), PtdIns(3,4,5)P₃ (**1.225**) and PtdIns(3,5)P₂ (**1.213**) were synthesized from the orthoformate **1.15**.⁷² Key transformations in this synthesis included the regioselective cleavage of orthoformate in **1.217** (Scheme 1.36) and **1.106** (Scheme

1.37) with DIBAL-H and a resolution–protection protocol (of **1.221** and **1.222**) using the camphor acetals.



Scheme 1.36: (a) NaH, PMBCl, DMF; (b) NaH, BnBr, DMF; (c) DIBAL-H, DCM-hexane; (d) NaH, AllBr, DMF; (e) HCl-MeOH.

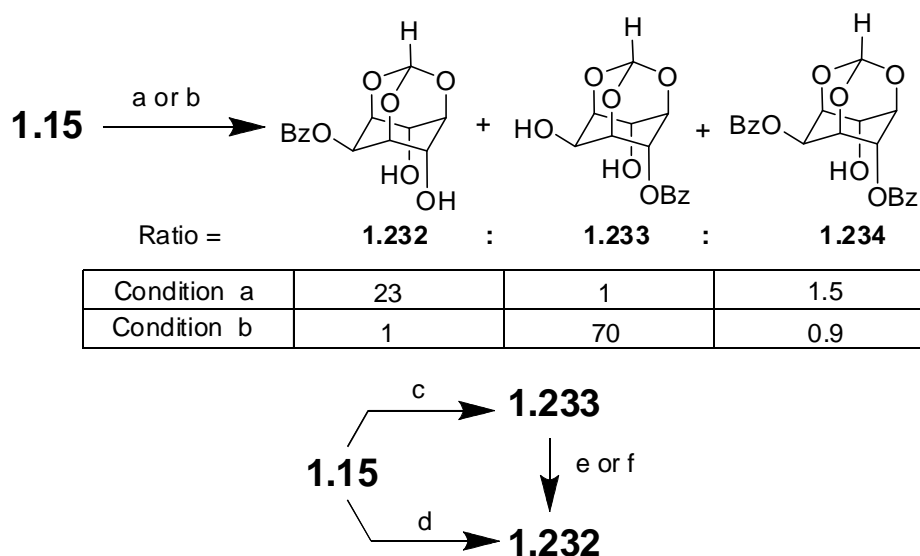


Scheme 1.37: (a) DIBAL-H, DCM; (b) NaH, BnBr, DMF; (c) HCl, MeOH; (d) NaH, PMBCl, THF; (e) (1*S*)-(-)-camphanic chloride, Py, DCM.

1.7. Partially protected inositol derivatives.

There are several reports on the conversion of the orthoformate **1.15** to *O*-protected inositol derivatives, which can be used as intermediates for the preparation of phosphoinositols, their derivatives and analogs. These reports principally deal with the regioselective derivatization of the C2, C4 and the C6 hydroxyl groups of **1.15** or the regioselective cleavage of the orthoformate moiety in tri-*O*-protected derivatives of inositol orthoformate to release any one or two of the C1, C3 and the C5 hydroxyl groups. These reports are grouped below since the protected inositols were not converted to any phosphoinositol or a cyclitol derivative.

Reaction conditions that allow the regioselective monobenzoylation of the orthoformate **1.15** at the equatorial or the axial hydroxyl groups could be arrived at by a detailed study on the benzoylation of **1.15** under a variety of reaction conditions and using different benzoylating agents (Scheme 1.38).⁷³ However, it is not clear whether



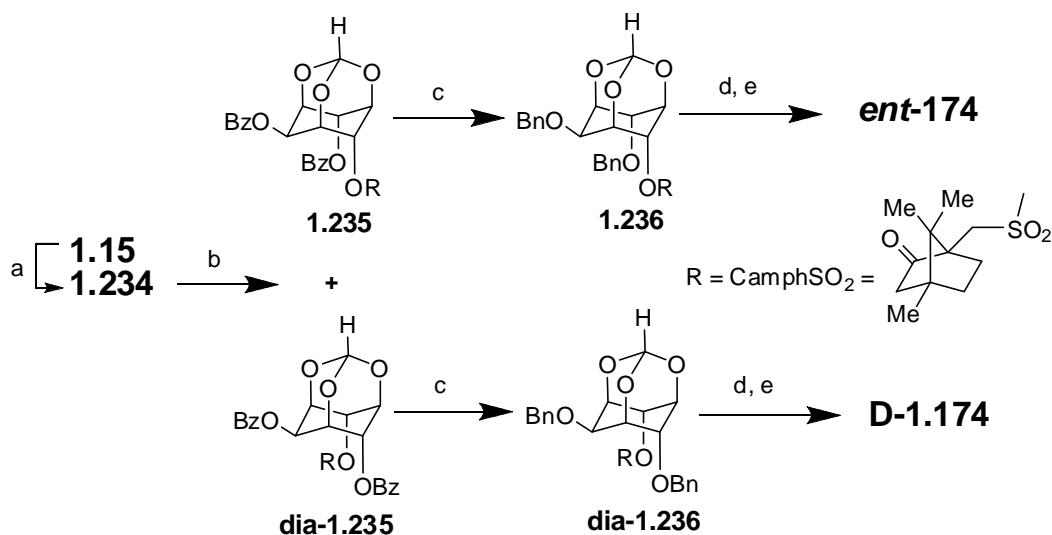
Scheme 1.38: (a) BzCl (0.5 eq), Py; (b) BzCl (0.5 eq), Et₃N; (c) DMF, NaH (1 eq.), PhCOCl; (d) NaH (2 eq.), PhCOCl; (e) DMF, NaH (1 eq.); (f) *t*-BuOK, DMF.

these conditions that allowed the regioselective benzoylation could be extended for the preparation of other esters of **1.15**. Regiospecific *O*-acylation of either the C2- or the C4-

hydroxyl group of **1.15** can be achieved by carrying out the acylation reaction in the presence of excess of sodium hydride or one equivalent of sodium hydride respectively.⁷⁴ Formation of the C2-*O*-acylated derivative is due to the isomerization of the corresponding (initially formed) C4(6)-*O*-acylated derivative in the presence of sodium hydride. Thus regioselectivity of the acylation reaction in the triol **1.15** can be controlled by controlling the amount of sodium hydride in the reaction medium. Although acylation of the orthoformate **1.15** (in the presence of tertiary amines) with two or more equivalents of an acylating agent usually yields a mixture of esters, conditions to obtain the racemic benzoate **1.234** in high yields have been described.⁷⁵ The dibenzoate **1.234** served as a versatile intermediate for the preparation of several protected *myo*-inositol derivatives.⁷⁶

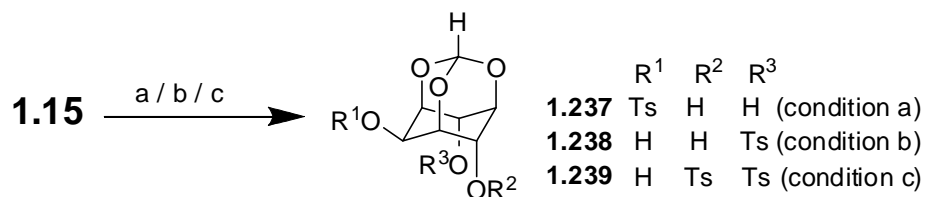
33b

Diastereomeric camphorsulfonates obtained from the racemic dibenzoate **1.234** were separable by column chromatography. D-2,4- and D-2,6-di-*O*-benzyl-*myo*-inositols (**1.174** and **ent-1.174**) could be obtained from the diastereomeric camphor sulfonates in very good yields (Scheme 1.39).⁷⁷



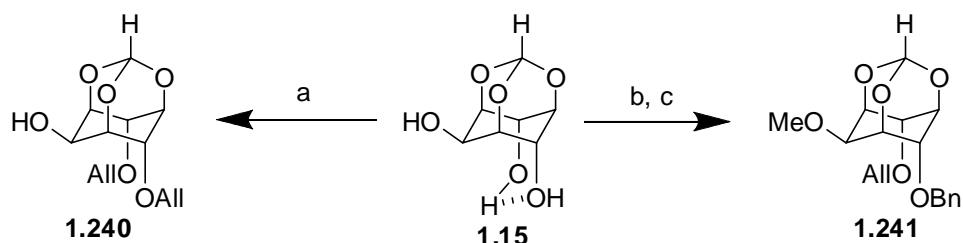
Scheme 1.39: (a) BzCl (2.2 eq), Py; (b) 1*S*-(+)-10-camphorsulphonyl chloride, Py; (c) BnBr, Ag₂O, DMF; (d) NaOMe, MeOH; (e) TFA-H₂O.

Regioselectivity for the sulfonylation of the orthoformate **1.15** with alkyl or aryl sulfonyl chlorides could be controlled by varying the base used (Scheme 1.40).⁷⁸ This methodology was used for the preparation enantiomeric benzyl ethers D-**1.174** and ent-**1.174**⁶² (Scheme 1.26).



Scheme 1.40: (a) TsCl (1eq), Py; (b) TsCl (1 eq), Et₃N; (c) TsCl (2 eq), NaH (2 eq)

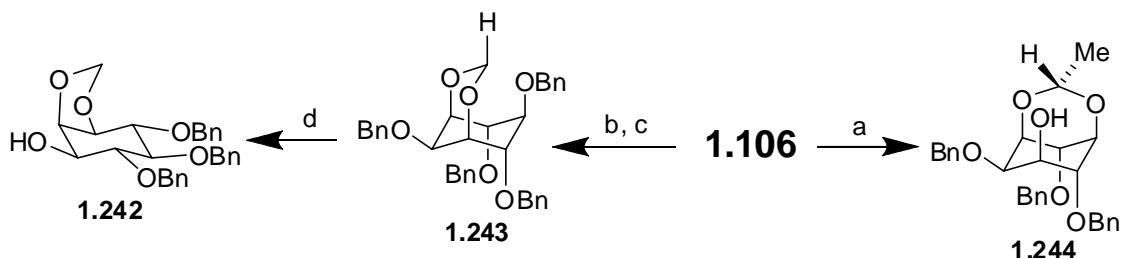
A general method for the preparation of orthogonally protected *myo*-inositol derivatives was developed utilizing the subtle differences in reactivity exhibited by alkali metal alkoxides of the orthoformate **1.15** (Scheme 1.41).¹⁴ Available experimental data suggested that the observed differences in reactivity of alkali metal alkoxides of **1.15** were due to differences in their ability to form chelates (involving the axial and equatorial oxygen atoms of **1.15**) with alkali metal ions.



Scheme 1.41: (a) LiH or BuLi (4 eq), THF-DMF, AllBr (2.3 eq); (b) NaH, BnBr; (c) BuLi (1.1 eq), AllBr (1.2 eq); NaH, MeI.

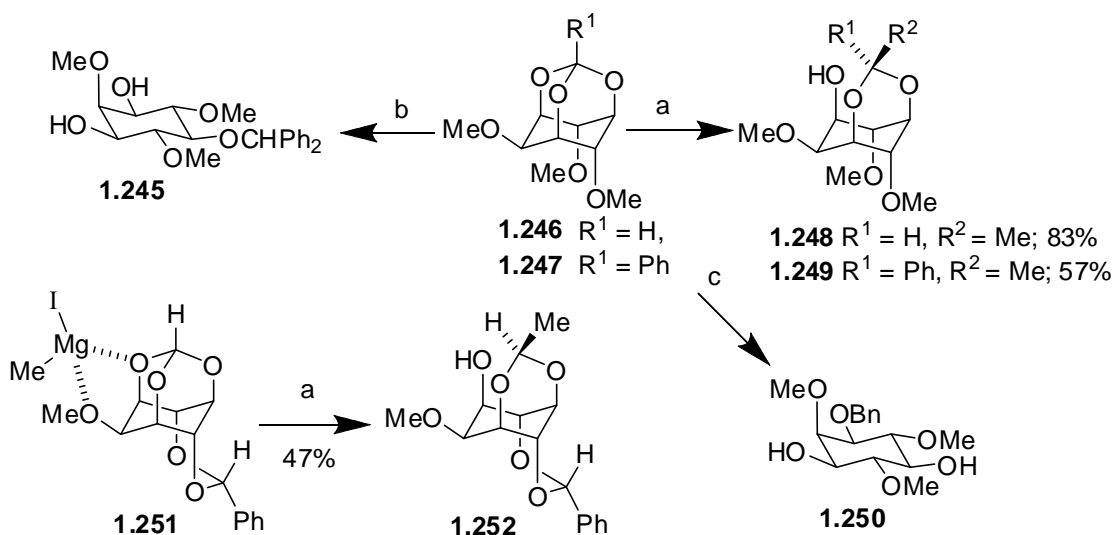
Protected inositol derivatives have also been prepared by the regioselective cleavage of the orthoformate moiety in *O*-protected derivatives of **1.15** as mentioned earlier [See Schemes (pages): 1.13 (16), 1.19 (20), 1.21 (21), 1.36 (31)]. The orthoformate moiety in the tribenzyl ether **1.106** could be cleaved selectively with DIBAL-H to release the C5-hydroxyl group.⁷⁹ The C1-hydroxyl group could be released

selectively in **1.106** by cleavage of the orthoformate using trimethylaluminium (Scheme 1.42). The observed difference in selectivity in the cleavage of the orthoformate by using different reagents was attributed to the bulk of the reagent.



Scheme 1.42: (a) Me_3Al , DCM; (b) DIBAL-H, DCM; (c) NaH, BnBr, rt; (d) TiCl_4 , DCM

Orthoformate moiety in inositol derivatives **1.246**, **1.247** and **1.251** could also be cleaved using Grignard reagents or $\text{LiAlH}_4 / \text{AlCl}_3$, to selectively release one or two hydroxyl groups (Scheme 1.43).³² These results are complimentary to the cleavage of orthoester by DIBAL-H and trimethylaluminium mentioned above.⁷⁹ The regioselectivity for the cleavage of the orthoester **1.251** was rationalized owing to the presence of the



Scheme 1.43: (a) MeMgI ; (b) excess PhMgI , 60%; (c) LAH, AlCl_3 , 49%.

equatorial oxygen at the C2 position which could serve as an auxiliary to form a chelate (as shown in **1.251**) with magnesium.

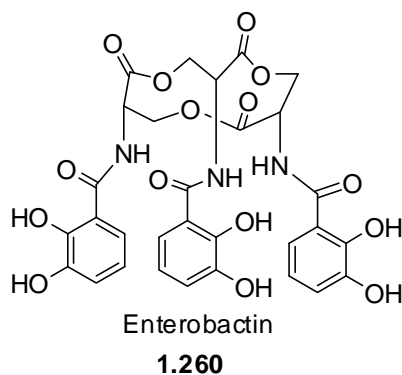
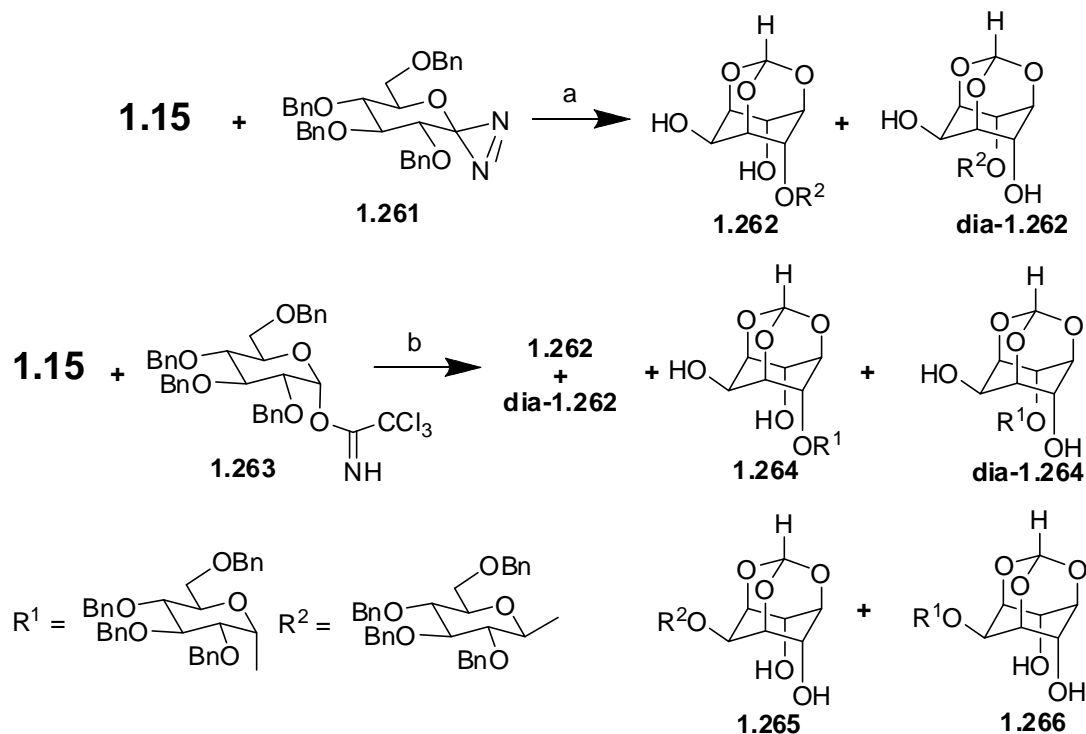


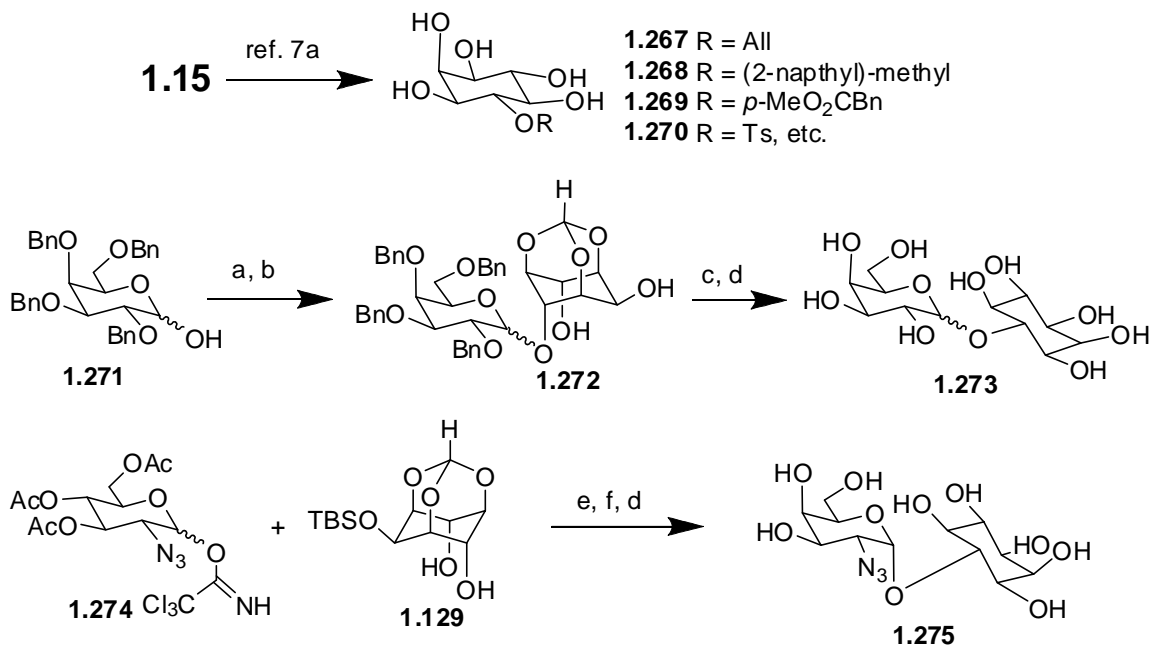
Figure 1.5: Enterobactin

Vasella *et al*⁸⁶ reported the glycosylation reaction of the triol **1.15** with diaziridine **1.261** and the acetamidate **1.263**.

Scheme 1.45: (a) 1,4-dioxane, rt; (b) DCM, BF₃ • Et₂O

Good regioselectivity was observed in the reaction of diaziridine **1.261** which gave 4-*O*-glycosylated products **1.262** and **dia-1.262** in 90% yield where as the reaction of the triol **1.15** with **1.263** gave a mixture of products (Scheme 1.45).

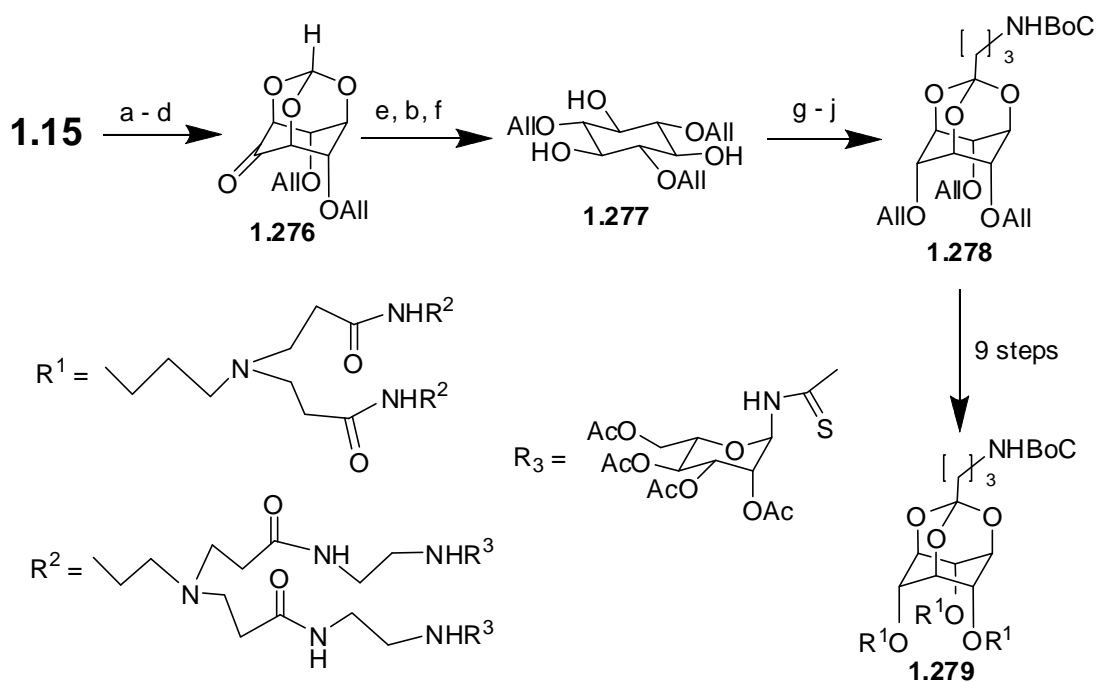
Glycosylation of the orthoformate **1.15** using the Appel–Lee protocol was regioselective for the 4/6-position (Scheme 1.46). Inositol-glycoside conjugates were obtained by removal of the orthoformate group under very mild conditions. These inositol-glycoside conjugates were used as substrates for inositol dehydrogenase from *Bacillus subtilis*.⁸⁷ Active site of the same dehydrogenase was also probed⁸⁸ using a variety of 4-*O*-substituted *myo*-inositol derivatives (such as **1.267** - **1.270**) easily obtainable from **1.15**. X-ray crystallographic analysis of 4-*O*-*p*-toluenesulfonyl-*myo*-inositol (**1.270**) and 4-*O*-(2-naphthyl)-methyl-*myo*-inositol (**1.268**), which is a substrate for IDH, showed a distinct difference in the preferred conformation of the aryl substituent.



Scheme 1.46: (a) PPh₃, CBr₄, DMF-DCM; (b) tetramethylurea, **1.15**; (c) H₂, Pd-C; (d) Dowex (H⁺ form); (e) TMSOTf, DCM; (f) MeONa / MeOH.

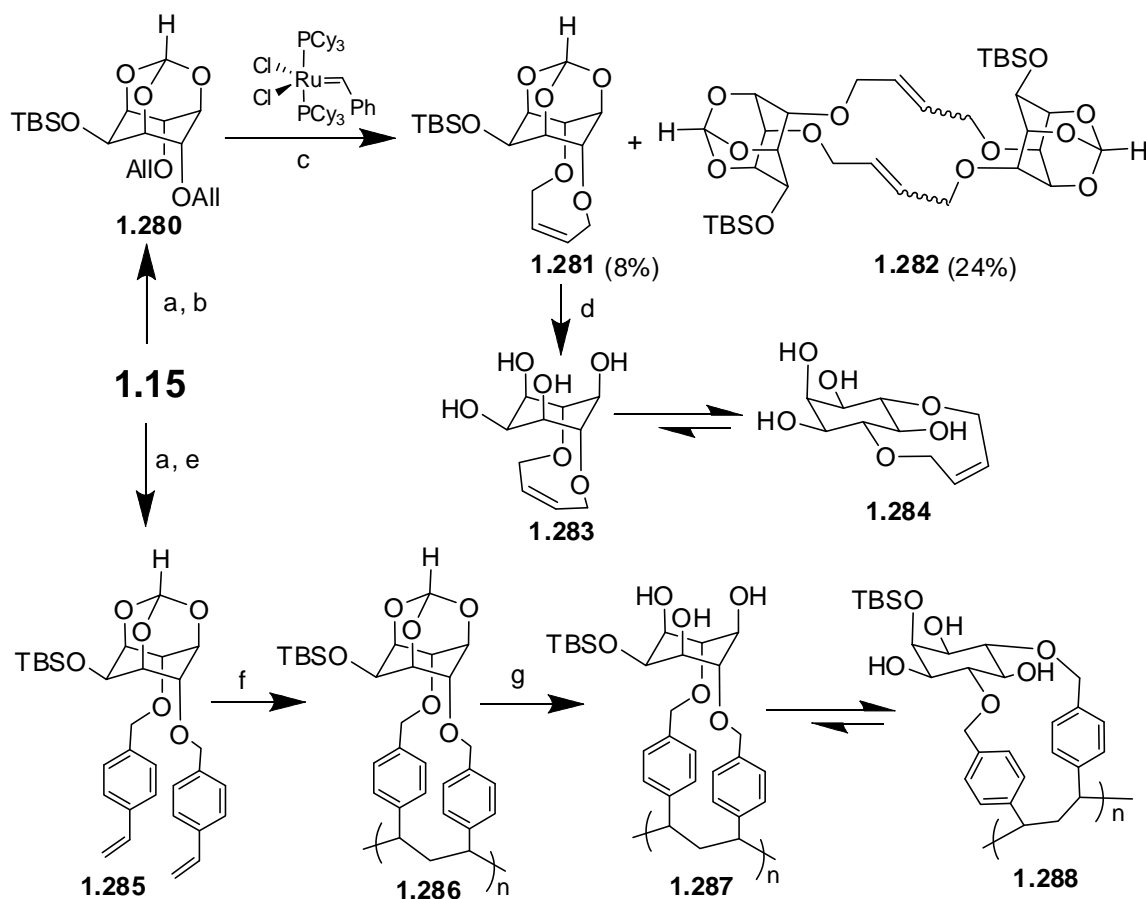
Glycoconjugated dendrimers **1.279** (Scheme 1.47) have been constructed from the orthoformate **1.15** which are potentially useful as glycomimetics for studying multivalency effects in the cell–cell communications by atomic force-field microscopy.⁸⁹

Xanthate esters of **1.15** have served as tools to examine the origin of the β -oxygen effect in the Barton deoxygenation reaction.⁹⁰



Scheme 1.47: (a) TBDMSCl, imidazole, DMF; (b) AllBr, NaH, DMF; (c) *n*-Bu₄NI, THF; (d) PCC, DCM; (e) NaBH₄, MeOH-THF; (f) TsOH, MeOH-EtOAc; (g) trimethyl 4-bromoorthobutyrate, TsOH, Toluene; (h) NaN₃, DMF; (i) PPh₃, H₂O-THF; (j) (Boc)₂O, Et₃N, THF.

The orthoformate **1.15** has been used to prepare inositol cyclopolymer by ring closing metathesis of 4,6-di-*O*-allyl-2-*O*-*t*-butyldimethylsilyl-*myo*-inositol-1,3,5-orthoformate (**1.280**)⁹¹ and construction of rigid polymer by free radical-promoted cyclopolymerization of 4,6-bis(4-vinylbenzyl)-2-*O*-*t*-butyldimethylsilyl-*myo*-inositol-1,3,5-orthoformate (**1.285**)⁹² (Scheme 1.48).



Scheme 1.48: (a) TBDMSCl, lutidine, DMF; (b) AlIBr, NaH, DMF; (c) DCM; (d) TsOH, CHCl₃ - MeOH; (e) 4-vinyl-benzyl chloride, NaH, DMF; (f) AIBN, toluene; (g) TsOH, MeOH-THF.

The orthoformate **1.15** has been used as a platform for the preparation of several metal ion complexing agents^{96b} (**1.289** - **1.291**, Figure 1.6), particularly for the selective complexation of lithium ions.

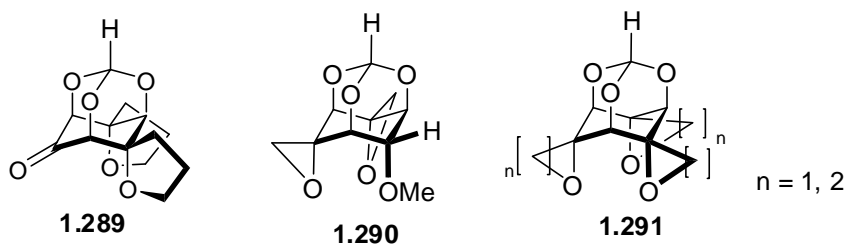


Figure 1.6

The attempts at tuning of metal ion binding ability of neutral complexing agents is because of various applications in areas of chemistry⁹³ biology⁹⁴ and medicine.⁹⁵ A variety of metal ion complexing agents constructed using inositol orthoformate as the platform^{31, 96} are shown in Figure 1.6 and Figure 1.7. High selectivity observed for the binding of many metal ions to these ligands was attributed to the rigid conformation of these ligands due to the presence of the orthoformate moiety. The bifacial ligand **1.69** reacts with one equivalent of LiClO_4 or LiBF_4 to form rod like ionic polymers³⁴ (**1.292**, Figure 1.7).

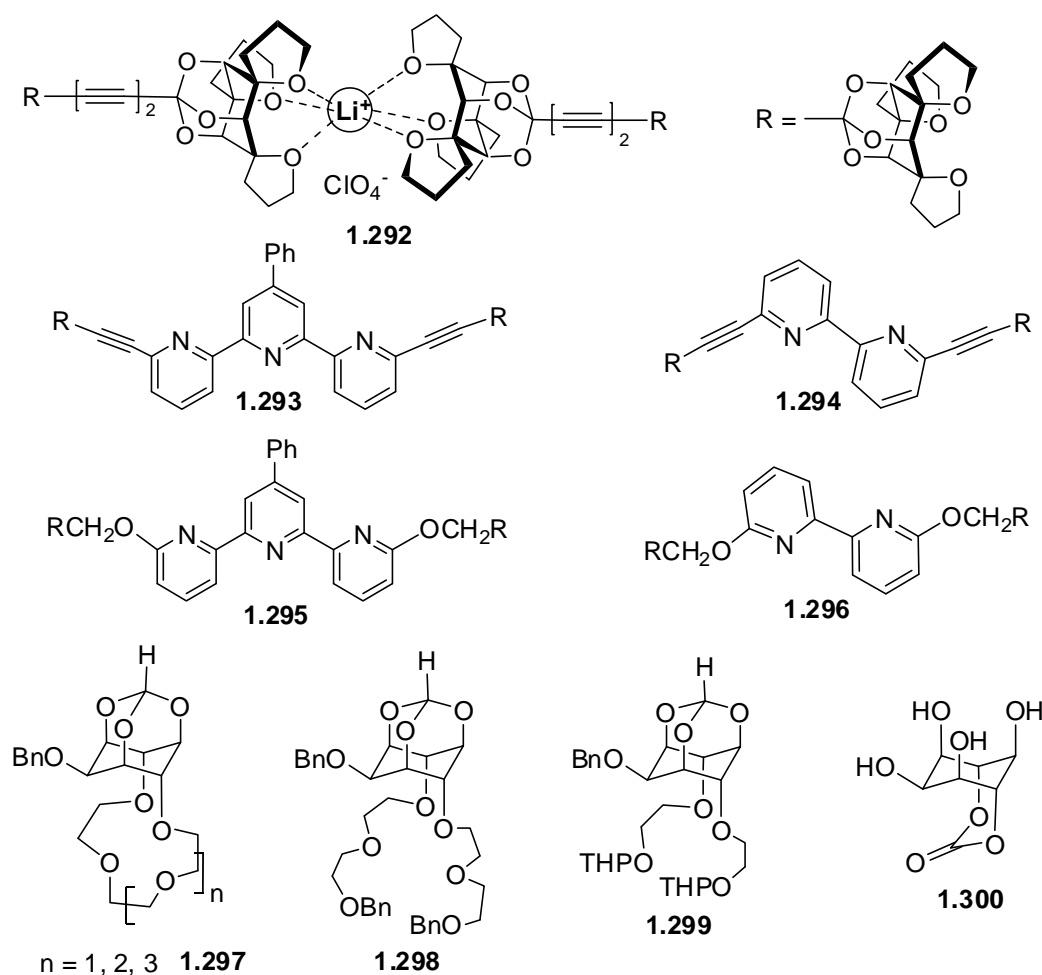


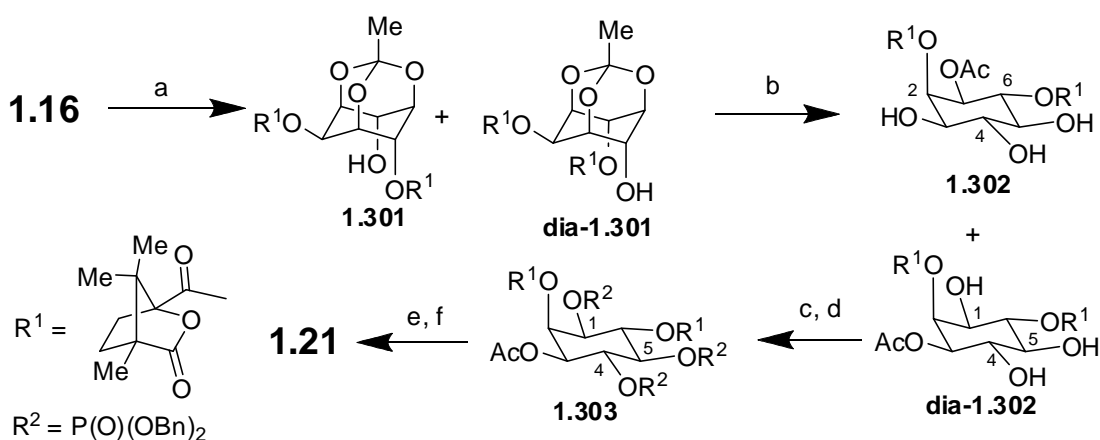
Figure 1.7: Inositol orthoester derived metal ion complexing agents

The bipyridine and terpyridine ligands (**1.293 - 1.296**)⁹⁷ covalently linked *via* acetylenic and alkoxy tethers, to the rigid inositol orthoformate platform provide the possibility of

binding of alkali metal ions and transition-metal ions simultaneously. The results of metal ion binding experiments with inositol derived crown ethers and podands (**1.297** - **1.299**) suggested that relative binding affinity of metal ions to crown ethers can be tuned by varying the relative orientation of the crown ether oxygen atoms.^{96f} *myo*-Inositol 4,6-carbonate (**1.300**) with three *syn*-axial hydroxyl groups was prepared from the orthoformate **1.15**; but its ability to complex with metal ions has not been investigated in detail.⁹⁸

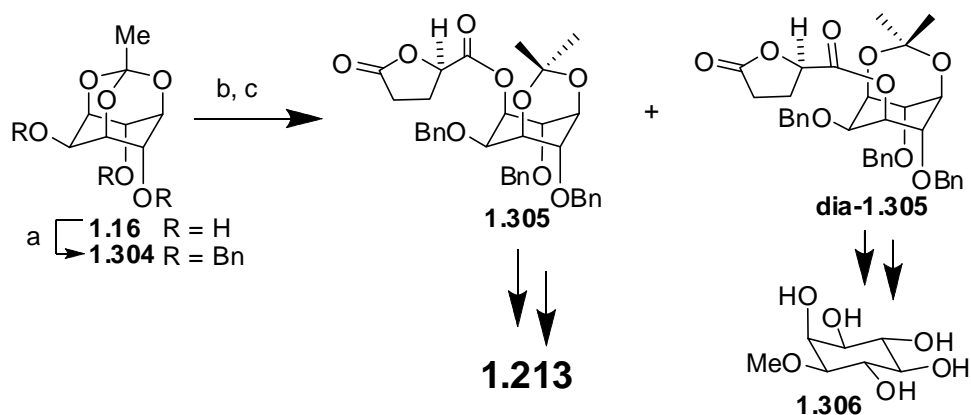
1.8. Reports on the use of inositol orthoesters other than the orthoformate 1.15.

myo-Inositol-1,3,5-orthoacetate **1.16** was converted to D-Ins(1,4,5)P₃ (**1.21**) in five steps *via* desymmetrization of **1.16** followed by hydrolysis to the acetate (Scheme 1.49).^{7c}



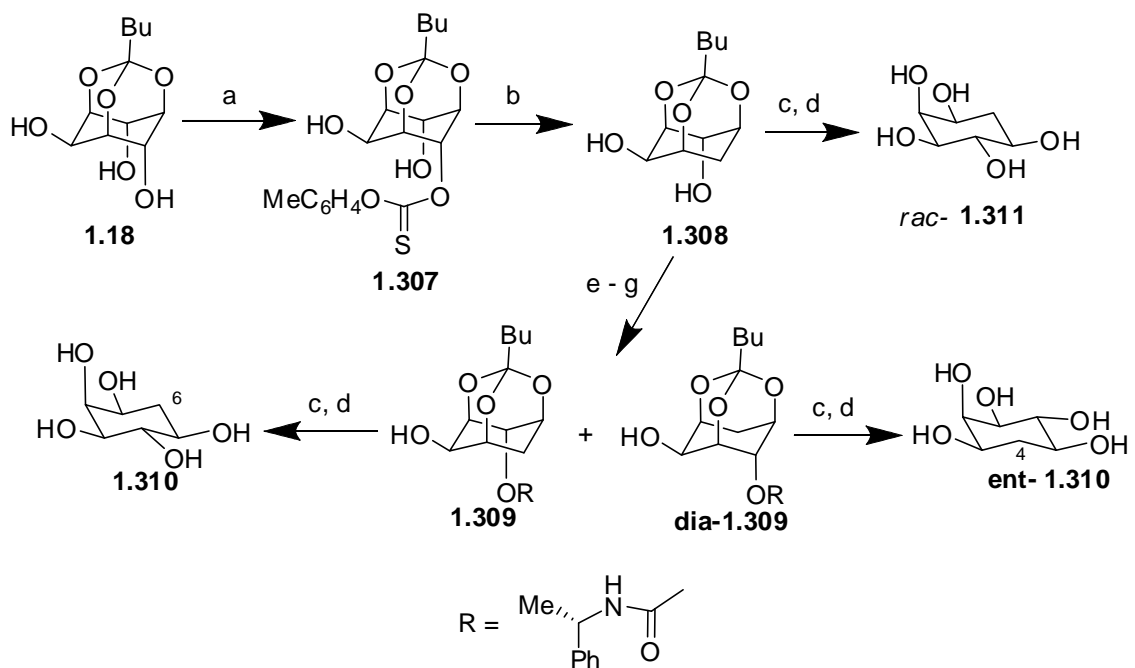
Scheme 1.49: (a) 1*S*-(-)-camphanoyl chloride, Py; (b) TFA-H₂O; (c) (*i*-Pr)₂NP(OBn)₂, 1*H*-tetrazole, DCM; (d) *m*-CPBA, DCM; (e) H₂, Pd-C, MeOH- H₂O; (f) concd. aq. NH₃.

The tribenzyl ethers **1.304** and **dia-1.304** have been used for the synthesis of PtdIns(3,5)P₂ (**1.213**) and (+)-bornisitol (**1.306**)⁹⁹ respectively. The synthetic strategy involved regioselective cleavage of the orthoacetate with trimethylaluminium followed by resolution using (R)-(-)-5-oxo-2-tetrahydrofuran-carboxylate esters (Scheme 1.50).



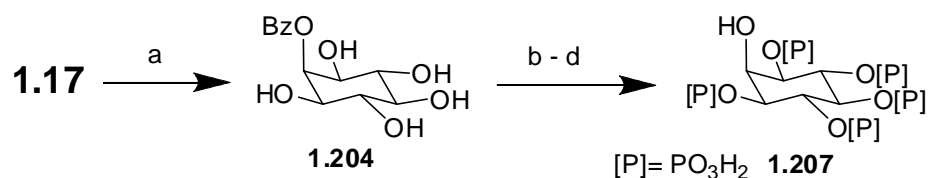
Scheme 1.50: (a) NaH, BnBr, DMF; (b) Me₃Al, DMF; (c) (*R*)-(-)-5-oxo-2-tetrahydrofuran-2-carboxylic acid, DCC, DMAP, DCM.

Enantiomeric mono-deoxy inositols **1.310** and **ent-310** were prepared from *myo*-inositol *via* its 1,3,5-orthobutanoate **1.18**. One of the axial hydroxyl groups was deoxygenated according to Barton's method and the product resolved as diastereomeric carbamates (Scheme 1.51).^{12a}



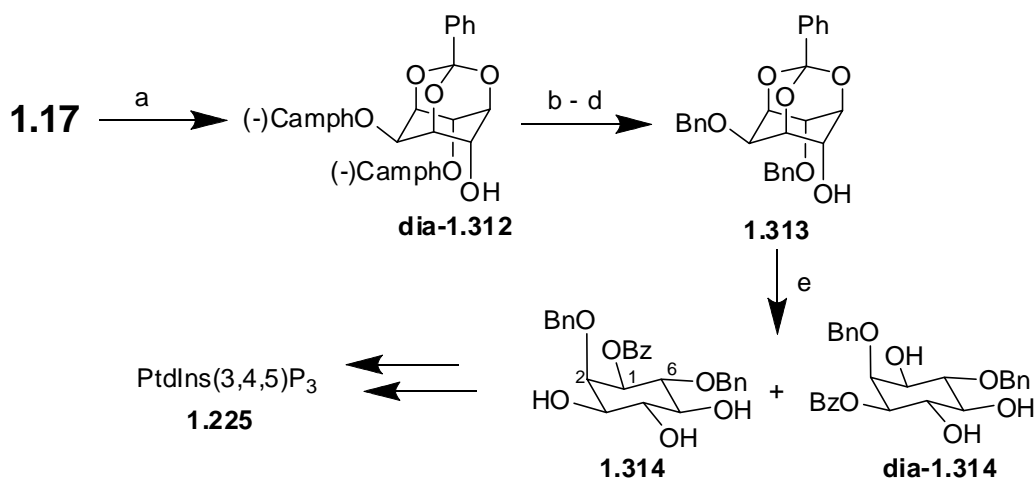
Scheme 1.51: (a) 4-MeC₆H₄OC(=S)Cl, Et₃N, DCM; (b) Bu₃SnH, AIBN, toluene; (c) HCl, MeOH; (d) MeONa, MeOH; (e) TBDMSOTf, 2,6-dimethylpyridine, DCM; (f) (*S*)-phenylethyl isocyanate, DMAP, DCM; (g) LiBHET₃, THF.

Hydrolysis of the orthobenzoate **1.17** in the presence of an acid resulted in the formation of *myo*-inositol 2-benzoate (**1.204**) exclusively. **1.204** is a precursor for the preparation of the anticancer agent Ins(1,3,4,5,6)P₅ (**1.207**, Scheme 1.52).¹⁰⁰



Scheme 1.52: (a) TFA - H₂O; (b) *N,N*-diethyl-1,5-dihydro-2,4,3-benzo-dioxaphosphepin-3-amine, 5-phenyltetrazole; *m*-CPBA, DCM; (c) H₂, Pd(OH)₂-C; (d) conc: aq. NH₃.

Chiral desymmetrization of **1.17** *via* the formation of diastereoisomeric bis[(1*S*)-(-)-camphanate] esters provided convenient access to precursors for the preparation of biologically important inositol phosphates and lipids, and to molecular probes modified at O-1 or O-3 of the inositol ring (Scheme 1.53).¹⁰¹



Scheme 1.53: (a) (1*S*)-(-)-camphanoyl chloride, Et₃N, DCM; (b) 2-methoxypropene, TsOH, THF; (c) LiOH, H₂O, THF; (d) NaH, BnBr, DMF; (e) HCl-EtOH.

1.9. Conclusions.

In the last two decades *myo*-inositol 1,3,5-orthoformate (**1.15**) which can be easily obtained in gram quantities, has been frequently used as an intermediate during the synthesis of inositol derivatives, natural products and their analogs as well as metal ion complexing agents. Some of the crystalline derivatives of the orthoformate are known to exhibit interesting physical and chemical properties (Please see Chapter 3 for details). In contrast, reports on the chemistry and utility of other *myo*-inositol 1,3,5-orthoesters such as **1.16- 1.18** are scarce. Hence we have investigated the synthetic utility of *myo*-inositol 1,3,5-orthobenzoate (**1.17**) for the synthesis of inositol derivatives. During the course of this investigation, we discovered interesting solid state reactivity of *myo*-inositol 1,3,5-orthobenzoate derivatives. Results pertaining to these aspects are described in the subsequent chapters of this thesis.

1.10. References.

1. (a) Hinchliffe, K; Irvine, R. *Nature*, **1997**, 390, 123-124; (b) Schmittberger, T.; Waldmann, H., *Synlett*. **1988**, 574-584; (c) *Phosphoinositides: Chemistry, Biochemistry and Biomedical Applications*; Bruzik, K. S., Ed.; ACS Symposium Series 718; American Chemical Society: Washington, DC, **1999**.
2. Ferguson, M. A. J.; Williams, A. F., *Annu. Rev. Biochem.* **1988**, 57, 285-320
3. Sureshan, K. M.; Shashidhar; M. S.; Praveen, T.; Das, T. *Chem. Rev.* **2003**, 103, 4477-4503 and references cited therein.
4. (a) Gauthier Jr., D. R.; Bender, S. L., *Tetrahedron Lett.* **1996**, 37, 13-16; (b) Sato, K-i.; Akai, S.; Sugita, N.; Ohsawa, T.; Kogure, T.; Shoji, H; Yoshimura, J. *J. Org. Chem.* **2005**, 70, 7496-7504; (c) Li, M.; Wu, A.; Zhou, P. *Tetrahedron Lett.* **2006**, 47, 3707-3710.
5. (a) Walker, J. B. *Appl. Environ. Microbiol.* **2002**, 68, 2404-2410; (b) Busscher, G. F.; Rutjes, F. P. J. T.; van Delft, F. L. *Chem. Rev.* **2005**, 105, 775-791 and references cited therein.
6. Egido-Gabás, M.; Serrano, P.; Casas, J.; Llebaria, A.; Delgado, A. *Org. Biomol. Chem.* **2005**, 3, 1195-1201.
7. (a) Lee, H. W.; Kishi, Y. *J. Org. Chem.* **1985**, 50, 4402-4404; (b) Billington, D. C. *The Inositol Phosphates: Chemical synthesis and biological significance*. VCH, New York, N.Y. 1993; (b) Potter, B. V. L.; Lampe, D. *Angew. Chem. Int. Ed. Engl.* **1995**, 34, 1933-1972; (c) Garrett, S. W.; Liu, C.; Riley, A. M.; Potter, B. V. L. *J. Chem. Soc. Perkin Trans I*, **1998**, 1367-1368; (d) Biomonte, M. A. ; Vasella, A. *Helv. Chim. Acta.* **1998**, 81, 688; (e) M. S. Shashidhar, *ARKIVOC*, **2002** (VII) 63.
8. Chida, N.; Sakata, N.; Murai, K.; Tobe, T.; Nagase, T.; Ogawa, S. *Bull. Chem. Soc. Jpn.* **1998**, 71, 259-272.
9. (a) Chiara, J. L.; Martin-Lomas, M. *Tetrahedron Lett.* **1994**, 35, 2969-2972; (b) Guidot, J. P.; Le Gall, T.; Mioskowski, C. *Tetrahedron Lett.* **1994**, 35, 6671-6672; (c) Prestwich, G. D. *Acc. Chem. Res.* **1996**, 29, 503-513; (d) Dubreuil, D.; Cleophax, J.;

Chapter-1

- Almeida, M. V.; Verre-Sebrie, C.; Liaigre, J.; Vass, G. and Gero, S. D. *Tetrahedron* **1997**, *53*, 16747-16766; (e) Jenkin, D. J.; Potter, B. V. L. *J. Chem. Soc. Perkin Trans. I* **1998**, 41-50; (f) Clive, D. L. J.; He, X.; Poslema, M. H. D.; Mashimbye, M. J. *J. Org. Chem.* **1999**, *64*, 4397-4410.
10. Sawada, T.; Shirai, R.; Iwasaki, S. *Tetrahedron Lett.* **1996**, *37*, 885-886.
11. (a) Mandel, M.; Hudlicky, T. *J. Chem. Soc. Perkin Trans I* **1993**, 741-743; (b) Hudlicky, T. *Chem Rev.* **1996**, *96*, 3-30; (c) Jung, P. M. J.; Motherwell, W. B.; Williams, A. S. *Chem. Commun.* **1997**, 1283-1284; (d) Hudlicky, T.; Restrepo-Sánchez, N.; Kary, P. D.; Jaramillo-Gómez, L.M. *Carbohydr. Res.* **2000**, *324*, 200-203.
12. (a) Biamonte, M. A.; Vasella, A. *Helv. Chim. Acta.* **1998**, *81*, 688-694; (b) Bhosekar, G.; Murali, C.; Gonnade, R. G.; Shashidhar, M. S.; Bhabhade, M. M. *Cryst. Growth. Des.* **2005**, *5*, 1977-1982.
13. Okajima, K.; Mukae, T.; Imagawa, H.; Kawamura, Y.; Nishizawa, M.; Yamada, H. *Tetrahedron* **2005**, *61*, 3497-3506.
14. Devaraj, S.; Shashidhar, M. S.; Dixit, S. S. *Tetrahedron* **2005**, *61*, 529-536.
15. *Cell Signalling*, Hancock, J. T., Oxford University Press, **2005**.
16. (a) Ferguson, M. A. J.; Low, M. G.; Cross, G. A. M. *J. Biol. Chem.* **1985**, *260*, 14547-14555; (b) Thomas, J. R.; Dwek, R. A.; Rademacher, T. W. *Biochemistry*, **1990**, *29*, 5413-5422; (c) Roberts, C.; Madson, R.; Fraser-Reid, B. *J. Am. Chem. Soc.* **1995**, *117*, 1546-1553.
17. Sahai, P.; Vishwakarma, R. A. *J. Chem. Soc. Perkin Trans. I*, **1997**, 1845-1849.
18. Liang, C.; Ewig, C. S.; Stouch, T. R.; Hagler, A. T. *J. Am. Chem. Soc.*, **1994**, *116*, 3904-3911.
19. Parthasarathy, R.; Eisenberg, F. *Biochem. J.* **1986**, *235*, 313-322.
20. Nomenclature committee – IUB, *Biochem. J.* **1989**, *258*, 1-2.
21. Stanoeva, E.; He, W.; De Kimpe, N. *Bioorganic & Medicinal Chemistry* **2005**, *13*, 17-28.

Chapter-1

22. Giner, J-L.; Faraldos, J. A. *J. Org. Chem.* **2002**, *67*, 2717-2720.
23. Pettinger, R. C., Wolfe, R. N., Hoehn, M. M., Marks, P. N., Dailey, W. A., McGuire, J. M. *Antibiotics and Chemotherapy* **1953**, *3*, 1268-1278.
24. Wu, J.; Xiao, G.; Huang, J.; Xiao, Z.; Qi, S.; Li, Q.; Si Zhang, *Org. Lett.* **2004**, *6*, 1841-1844.
25. (a) Greene T. W.; Wuts, P. G. M.; *Protective Groups in Organic Synthesis*, 3 rd ed.; Wiley: New York 1999; (b) Kocienski, P. J. *Protecting Groups*, Georg Thieme: Stuttgart, 1994.
26. (a) Honda, T.; Endo, K.; Ono, S. *Chem. Pharm. Bull.* **2000**, *48*, 1545-1548; (b) Ghosh, A. K.; Liu, C. *Chem. Commun.* **1999**, 1743-1744.
27. Stork, G.; Rychnovsky, S. D. *J. Am. Chem. Soc.* **1987**, *109*, 1565-1567.
28. La Cruz, T. E.; Rychnovsky, S. D. *J. Org. Chem.* **2007**, *72*, 2602-2611.
29. (a) Jayaprakash, K. N.; Lu, J.; Fraser-Reid, B. *Bioorg. Med. Chem. Lett.* **2004**, *14*, 3815-3819; (b) Lu, J.; Fraser-Reid, B. *Org. Lett.* **2004**, *6*, 3051-3054; (c) Cristóbal López, J.; Agocs, A.; Uriel, C.; Gómez, A. M.; Fraser-Reid, B. *Chem. Commun.* **2005**, 5088-5090; (d) Liu, X.; Stocker, B. L.; Seeberger, P. H. *J. Am. Chem. Soc.* **2006**, *128*, 3638-3648; (e) Jayaprakash, K. N.; Chaudhuri, S. R.; Murty, C. V. S. R.; Fraser-Reid, B. *J. Org. Chem.* **2007**, *72*, 5534-5545.
30. Lukyanov, A. V.; Tolkachev, O. N. USSR Patent 184841, 1966; *Chem. Abstr.* **1967**, *66*, 95365.
31. Paquette, L. A.; Tae, J. *J. Am. Chem. Soc.* **2001**, *123*, 4974-4984.
32. Yeh, S-M.; Lee, G. H.; Wang, Y.; Luh, T-Y. *J. Org. Chem.* **1997**, *62*, 8315-8318.
33. (a) Baudin, G.; Glänzer, B. I.; Swaminathan, K. S.; Vasella, A. *Helv. Chim. Acta.* **1988**, *71*, 1367-1378; (b) Praveen, T.; Shashidhar, M. S. *Carbohydr. Res.* **2001**, *330*, 409-411.
34. Paquette, L. A.; Tae, J.; Gallucci, J. C. *Org. Lett.* **2002**, *2*, 143-146.
35. Vogel, B.; Anderson, B. C. Simons, D. M. *J. Org. Chem.* **1969**, *34*, 204-207.
36. Sarmah, M. P.; Shashidhar, M. S. *Carbohydr. Res.* **2003**, *338*, 999-1001.

37. Billington, D. C.; Baker, R. *J. Chem. Soc., Chem. Commun.* **1987**, 1011-1013.
38. Billington, D. C. *Chem. Soc. Rev.* **1989**, *18*, 83-122.
39. Sureshan, K. M.; Watanabe, Y. *Tetrahedron: Asymmetry* **2004**, *15*, 1193-1198.
40. (a) Morgan, A. J.; Wong, Y. K. Roberts, M. F.; Miller, S. J. *J. Am. Chem. Soc.* **2004**, *126*, 15370-15371; (b) Morgan, A. J.; Komiya, S.; Xu, Y.; Miller, S. J. *J. Org. Chem.* **2006**, *71*, 6923- 6931.
41. (a) Campbell, S. A.; Thatcher, C. R. *J. Tetrahedron Lett.* **1991**, *32*, 2207-2210; (b) Vizitiu, D.; Kriste, A. G.; Campbell, A. S.; Thatcher, G. R. *J. J. molecular Recognition* **1996**, *9*, 197-209.
42. Wu, Y.; Zhou, C.; Roberts, M. F. *Biochemistry* **1997**, *36*, 356-363.
43. Schmitt, L.; Spiess, B.; Schlewer, G. *Tetrahedron Lett.* **1998**, *39*, 4817-4820.
44. Billington, D. C.; Baker, R.; Kulagowski, J. J.; Mawer, I. M.; Vacca, J. P.; deSolms, S. J.; Huff, J. R. *J. Chem. Soc. Perkin. Trans. I* **1989**, 1423-1429.
45. Westerduin, P.; Williams, H. A. M.; van Boeckel, C. A. A. *Tetrahedron Lett.* **1990**, *31*, 6915-6918.
46. (a) Mernissi-Arifi, K.; Wehrer, C.; Schlewer, G.; Spiess, B. *Journal of Inorganic Biochemistry* **1994**, *55*, 263-277; (b) Chung, S-K.; Chang, Y-T; Sohn, K-H. *Koroean J. Med Chem.* **1994**, *4*, 57-65.
47. Chung, S-K.; Chang, Y-T.; Sohn, K-H. *Chem. Commun.* **1996**, 163-164.
48. Lampe, D.; Liu, C.; Potter, B. V. L. *J. Med. Chem.* **1994**, *37*, 907-912.
49. Andersch, P.; Schneider, M. P. *Tetrahedron: Asymmetry* **1996**, *7*, 349-352.
50. (a) M. Siren, L. Linnè, L. Persson, A. B. Reitz (Editor), *ACS Symposium Series* **1991**, *463*, 103-110; (b) Blum, C.; Karlsson, S.; Schlewer, G.; Spiess, B.; Rehnberg, N. *Tetrahedron Lett.* **1995**, *36*, 7239-7242.
51. Carrington, A. L.; Calcutt, N. A.; Ettliger, C. B.; Gustafsson, T.; Tomlinson, D. R. *Eur. J. Pharmacol.* **1993**, *237*, 257-263.
52. (a) Schwieler, J. H.; Hjemdahl, P. *J. Cardiovasc. Pharmacol.*, **1993**, *21*, 347-352; (b) Feth, F.; Erdbruegger, W.; Rascher, W.; Michel, M. C. *Life Sci.* **1993**, *52*, 1835-1844;

- (c) Chaudhary, A.; Dormhn, G.; Prestwich, G. D. *Tetrahedron Lett.* **1994**, *35*, 7521-7524 and references cited therein.
53. Wang, W. Q.; Xiang, D.; Gustafson, A. *Pharmacol. Toxicol.* **1993**, *73*, 49-51.
54. Perry, E. F.; Perry, H. M.; Erlanger, M. W.; Gustafsson, T. O. *J. Toxicol. Environ. Health* **1989**, *28*, 151-159.
55. Šala, M.; Kolar, J.; Strlič, M.; Kočevarb, M. *Carbohydr. Res.* **2006**, *341*, 897-902.
56. Ballereau, S.; Poirier, S. N.; Guillemette, G.; Spiess, B.; Schlewer, G. *J. Chem. Soc., Perkin Trans. I*, **1998**, 1859-1864.
57. (a) Riley, A. M.; Potter, B. V. L. *J. Org. Chem.* **1995**, *60*, 4970-4971; (b) Riley, A. M.; Murphy, C. T.; Lindley, C. J.; Westwick, J.; Potter, B. V. L. *Bioorg. & Med. Chem. Lett.* **1996**, *6*, 2197-2200; (c) Riley, A. M.; Guédat, P.; Schlewer, G.; Spiess, B.; Potter, B. V. L. *J. Org. Chem.* **1998**, *63*, 295-305.
58. Moris, M-A.; Caron, A. Z.; Guillemette, G.; Rognan, D.; Schmitt, M.; Schlewer, G. *J. Med. Chem.* **2005**, *48*, 1251-1255.
59. Chung, S-K.; Kwon, Y-U.; Chang, Y-T.; Sohn, K-H.; Shin, J-H.; Park, K-H.; Hong, B-J.; Chung, I-H. *Bioorg. Med. Chem.* **1999**, *7*, 2577-2589.
60. deSolms, S. J.; Vacca, J. P.; Huff, J. R. *Tetrahedron Lett.* **1987**, *28*, 4503-4506.
61. Riley, A. M.; Mahon, M. F.; Potter, B. V. L. *Angew. Chem. Int. Ed. Engl.* **1997**, *36*, 1472-1474.
62. Sureshan, K. M.; Shashidhar, M. S.; Praveen, T.; Gonnade, R. G.; Bhadbhade. M. M. *Carbohydr. Res.* **2002**, *337*, 2399-2410.
63. Chung, S-K.; Chang, Y-T. *Bioorg. Med. Chem. Lett.* **1997**, *7*, 2715-2718.
64. Mills, S. J.; Backers, K.; Erneux, C.; Potter, B. V. L. *Org. Biomol. Chem.* **2003**, *1*, 3546-3556.
65. Laumen, K.; Ghisalba, O. *Biosci. Biotechnol. Biochem.* **1994**, *58*, 2046-2049.
66. Ozaki, S.; Koga, Y.; Ling, L.; Watanabe, Y.; Kimura, Y.; Hirata, M. *Bull. Chem. Soc. Jpn.* **1994**, *67*, 1058-1063.
67. Li, W.; Schultz, C.; Llopis, J. ; Tsien, R. Y. *Tetrahedron* **1997**, *53*, 12017-12040.

Chapter-1

68. Dubreuil, D.; Cleophax, J.; de Almeida, M. V.; Verre-Sebrié, C.; Pipelier, M.; Vass, G.; Gero, S. D. *Tetrahedron* **1999**, *55*, 7573-7582.
69. Chung, S-K.; Chang, Y-T. *Bioorg. Med. Chem. Lett.* **1996**, *6*, 2039-2042.
70. Falck, J. R.; Krishna, U. M.; Capdevila, J. H. *Bioorg. Med. Chem. Lett.* **2000**, *10*, 1711-1713.
71. Falck, J. R. ; Krishna, U. M.; Katipally, K. R.; Capdevila, J. H.; Ulug, E. T. *Tetrahedron Lett.* **2000**, *41*, 4271-4275.
72. (a) Grove, S. J. A. ; Gilbert, I. H. ; Holmes, A. B. ; Painter, G. F. ; Hill, M. L. *Chem. Commun.* **1997**, 1633-1634; (b) Painter, G. F.; Grove, S. J. A.; Gilbert, I. H.; Holmes, A. B.; Raithby, P. R.; Hill, M. L.; Hawkins, P. T.; Stephens, L. R. *J. Chem. Soc., Perkin Trans. 1* **1999**, 923-935.
73. Flores-Mosquera, M.; Martín-Lornas, M.; Chiara, J. L.; *Tetrahedron Lett.* **1998**, *39*, 5085-5088.
74. Sureshan, K. M.; Shashidhar, M. S. *Tetrahedron Lett.* **2000**, *41*, 4185-4188.
75. Das, T.; Shashidhar, M. S. *Tetrahedron Letters* **1994**, *35*, 8053-8056.
76. (a) Das, T.; Shashidhar, M. S. *Carbohydr. Res.* **1998**, *308*, 165-168; (b) Das, T.; Shashidhar, M. S. *Carbohydr. Res.* **1997**, *297*, 243-249.
77. (a) Praveen, T.; Das, T.; Sureshan, K. M.; Shashidhar, M. S.; Samanta, U.; Pal, D.; Chakrabarti, P. *J. Chem. Soc., Perkin Trans. 2*, **2002**, 358-365; (b) Sureshan, K. M.; Das, T.; Shashidhar, M. S.; Gonnade, R. G.; Bhadbhade M. M. *Eur. J. Org. Chem.* **2003**, 1035-1041.
78. Sureshan, K. M.; Shashidhar, M. S. *Tetrahedron Lett.* **2001**, *42*, 3037-3039.
79. Gilbert, I. H.; Holmes, A. B. *Tetrahedron Lett.* **1990**, *31*, 2633-2634; (b) Gilbert, I. H.; Holmes, A. B.; Pestchanker, M. J.; Young, R. C. *Carbohydr. Res.* **1992**, *234*, 117-130.
80. Sarmah, M. P.; Shashidhar, M. S.; Sureshan, K. M.; Gonnade, R. G.; Bhadbhade, M. M. *Tetrahedron* **2005**, *61*, 4437-4446.
81. Chung, S-K.; Kwon, Y-U. *Bioorg. Med. Chem. Lett.* **1999**, *9*, 2135-2140.

Chapter-1

82. Krief, A.; Dumont, W.; Billen, D.; Letesson, J.-J.; Lestrade, P.; Murphy, P. J.; Lacroix, D. *Tetrahedron Lett.* **2004**, *45*, 1461-1463.
83. Hosoda, A.; Ozaki, Y.; Kashiwada, A.; Mutoh, M.; Wakabayashi, K.; Mizuno, K.; Nomura, E.; Taniguchi, H. *Bioorg. Med. Chem.* **2002**, *10*, 1189-1196.
84. Tse, B.; Kishi, Y. *J. Am. Chem. Soc.* **1993**, *115*, 7892-7893.
85. Pollack, J. R.; Neilands, J. B. *Biochem. Biophys. Res. Commun.* **1970**, *38*, 989-992.
86. Uhlmann, P.; Vasella, A. *Helv. Chim. Acta*, **1992**, *75*, 1979-1994.
87. Daniellou, R.; Palmer, D. R. J. *Carbohydr. Res.* **2006**, *341*, 2145-2150.
88. Daniellou, R.; Zheng, H.; Langill, D. M.; Sanders, D. A. R.; Palmer, D. R. J. *Biochemistry* **2007**, *46*, 7469-7477.
89. Lee, N.-Y.; Jang, W.-J.; Yu, S.-H.; Im, J.; Chung, S.-K. *Tetrahedron Lett.* **2005**, *46*, 6063-6066.
90. Crich, D.; Beckwith, A. L. J.; Chen, C.; Yao, Q.; Davison, I. G. E.; Longmore, R. W.; de Parrodi, C. A.; Quintero-Cortes, L.; Sandoval-Ramirez, J. *J. Am. Chem. Soc.* **1995**, *117*, 8757-8768.
91. Kim, T.-H.; Giles, M.; Holmes, A. B. *Chem. Commun.* **2000**, 2421-2422.
92. Kim, T.-H.; Dokolas, P.; Feeder, N.; Giles, M.; Holmes, A. B.; Walther, M. *Chem. Commun.* **2000**, 2419-2420.
93. (a) Jedlinski, Z. *Pure. Appl. Chem.* **1993**, *65*, 483-488; (b) Botti, P.; Ball, H. L.; Rizzi, E.; Lucietto, P.; Pinori, M.; Mascagni, P. *Tetrahedron* **1995**, *51*, 5447-5458; (c) van Nostrum, C. F.; Picken, S. J.; Schouten, A.-J.; Nolte, R. J. M. *J. Am. Chem. Soc.* **1995**, *117*, 9957-9965; (d) *Comprehensive Supramolecular Chemistry Vol. 1, Molecular Recognition: Receptors for Cationic Guests*, Ed. Gokel, G. W. Pergamon Press, New York, N.Y. **1996**; (e) Itoh, T.; Takagi, Y.; Murakami, T.; Hiyama, Y.; Tsukube, H. *J. Org. Chem.* **1996**, *61*, 2158-2163; (f) Shephard, D. S.; Johnson, B. F. G.; Matters, J.; Simon, P. *J. Chem. Soc., Dalton Trans* **1998**, 2289-2292.

Chapter-1

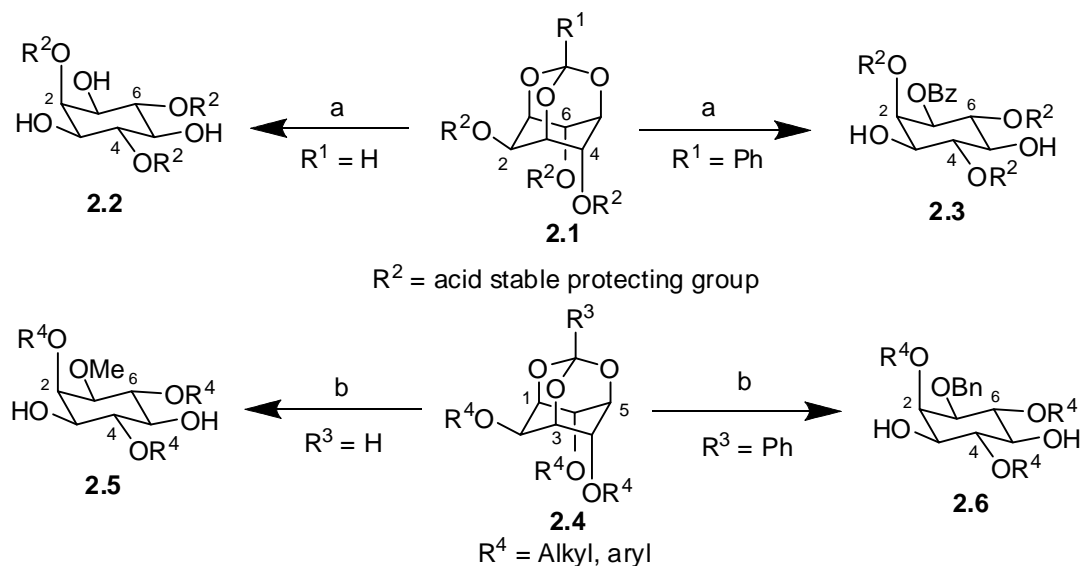
94. (a) Otoda, K.; Kimura, S.; Imanishi, Y. *J. Chem. Soc., Perkin Trans 1* **1993**, 3011-3016. (b) Reetz, M. T.; Huff, J.; Rudolph, J.; Toellner, K.; Deege, A.; Goddard, R. *J. Am. Chem. Soc.* **1994**, *116*, 11588-11589.
95. (a) *Crown Compounds*, Cooper, S. R. Ed. VCH, New York, N. Y. **1992**; (b) Dumont, B.; Joly, J-P.; Chapleur, Y.; Marsura, A. *Bioorg. Med. Chem. Lett.* **1994**, *4*, 1123-1126.
96. (a) Sureshan, K. M.; Shashidhar, M. S.; Varma, A. J. *J. Chem. Soc., Perkin Trans. 2*, **2001**, 2298-2302; (b) Paquette, L. A.; Sup Ra, C.; Gallucci, J. C.; Kang, H-J.; Ohmori, N.; Arrington, M. P.; David, W.; Brodbelt, J. S. *J. Org. Chem.* **2001**, *66*, 8629-8639; (c) Sureshan, K. M.; Shashidhar, M. S.; Varma, A. J. *J. Org. Chem.* **2002**, *67*, 6884-6888; (d) Tae, J.; Rogers, R. D.; Paquette, L. A. *Org. Lett.* **2002**, *2*, 139-142; (e) Paquette, L. A.; Selvaraj, P. R.; Keller, K. M.; Brodbelt, J. S. *Tetrahedron* **2005**, *61*, 231-240; (f) Dixit, S. S.; Shashidhar, M. S. *Tetrahedron* **2008**, *62*, 2160-2171 and references cited therein.
97. Hilmey, D. G.; Paquette, L. A. *J. Org. Chem.* **2004**, *69*, 3262-3270.
98. Angyal, S. J. *Carbohydr. Res.* **2000**, *325*, 313-320.
99. Riley, A. M.; Potter, B. V. L. *Tetrahedron Lett.* **1998**, *39*, 6769-6772.
100. Godage, H. Y.; Riley, A. M.; Woodman, T. J.; Potter, B. V. L. *Chem. Commun.* **2006**, 2989-2991.
101. (a) Riley, A. M.; Godage, H. Y.; Mahonb, M. F. Potter, B. V. L. *Tetrahedron: Asymmetry* **2006**, *17*, 171-174; (b) Sureshan K. M.; Riley, A. M.; Potter, B. V. L. *Tetrahedron Lett.* **2007**, *48*, 1923-1926.

Chapter 2

***myo*-Inositol-1,3,5-orthobenzoate as a versatile intermediate
for the synthesis of isomeric inositol derivatives.**

2.1. Introduction.

In the last two decades *myo*-inositol-1,3,5-orthoesters have been used for the synthesis of several phosphorylated inositols, their analogs, isomeric inositols and their derivatives. As seen in Chapter 1, among the orthoesters of *myo*-inositol (**1.15** - **1.18**), the orthoformate **1.15** has been utilized most, for the synthesis of biologically important inositol derivatives. Although *myo*-inositol orthobenzoate **1.17** was reported in the literature¹ at the time of initiation of the work presented in this thesis, it had not been utilized for the synthesis of any inositol derivative. Also, there was no published procedure for the preparation of the orthobenzoate **1.17**. This was surprising as the orthobenzoate **1.17** presents several synthetic advantages over the orthoformate **1.15** or the orthoacetate **1.16**. For instance, the orthoformate moiety in *myo*-inositol-1,3,5-orthoformate derivatives can only be cleaved with acids (to regenerate C1, C3 and C5 hydroxyl groups), which preclude the use of acid sensitive protecting groups at the C2, C4 and C6-hydroxyl groups (Scheme 2.1). Use of the orthobenzoate for the protection of C1, C3 and C5 hydroxyl groups of *myo*-inositol could allow the use of acid sensitive protecting groups at the C2, C4, C6-hydroxyl groups, as the orthobenzoate can be cleaved by hydrogenolysis to release the C1, C3 and C5 hydroxyl groups (Scheme 2.1). Furthermore, cleavage of the orthoformate with hydride reducing agents in principle, leads to the formation of an inositol - methyl ether which may not be easy to cleave to release the corresponding inositol hydroxyl group; however, the orthobenzoate under similar circumstances yields the corresponding benzyl ether, which can be cleaved by hydrogenolysis to release the inositol hydroxyl group (Scheme 2.1). With these ideas in focus, we undertook the preparation and exploitation of *myo*-inositol-1,3,5-orthobenzoate as an intermediate for the preparation of inositol derivatives and details of this work is reported and discussed in the present chapter.

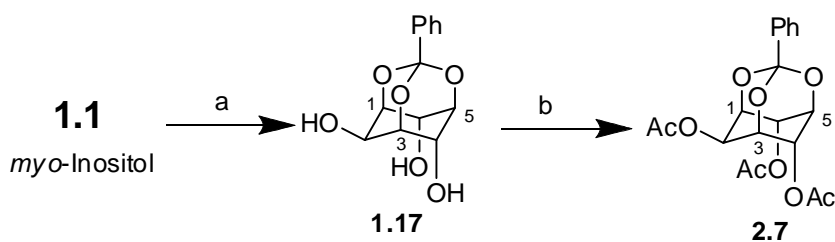


Scheme 2.1: (a) H^+ / H_2O ; (b) > 3 eq DIBAL-H

2.2. Results and discussion.

2.2.1. Preparation of the *myo*-inositol-1, 3, 5-orthobenzoate and its polymorphism.

myo-Inositol-1,3,5-orthobenzoate (**1.17**) was prepared from *myo*-inositol (**1.1**) (Scheme 1.3, Chapter 1, page 3) adopting the procedure reported² for the preparation of the corresponding orthoformate and the orthoacetate. The high yield (90–93%) could be consistently reproduced on several grams scale.



Scheme 2.2: (a) Scheme: 1.3, Chapter 1, page 3; (b) Ac_2O , Py, rt.

The orthobenzoate **1.17** exhibited polymorphic behavior depending upon the solvent and time allowed for crystallization. Crystallization from various solvents was attempted due to the contemporary interest in polymorphic behavior of molecular solids. In particular, *myo*-inositol derivatives are known to frequently exist in polymorphic and

pseudopolymorphic forms.³ Crystallization of the triol **1.17** from methanol, ethanol, water, 2-propanol, dichloromethane, acetone, tetrahydrofuran, nitromethane and triethylamine produced long plate like crystals (Form I, monoclinic $P2_1/n$, Figure 2.1A) while crystallization from ethyl acetate, dioxane and acetonitrile yielded square plate-like crystals (Form II, monoclinic $P2_1/c$, Figure 2.1B). The crystals of Form II could also be obtained by cooling a saturated hot methanol solution of the triol **1.17** to room temperature (~2 h, Figure 2.1C). The fact that Form II crystals could be obtained by rapid crystallization from methanol solution showed that these are kinetic crystals while Form I crystals are thermodynamic.^{3a}

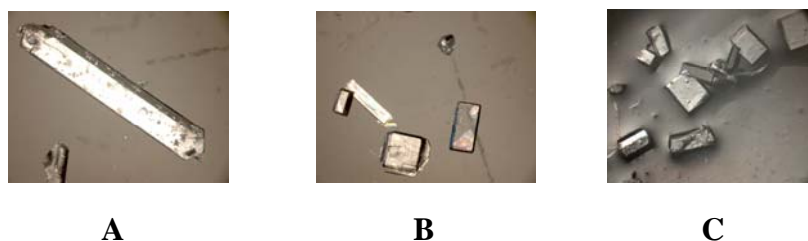


Figure 2.1: Images of the crystals of orthobenzoate **1.17**; A, from methanol; B, from ethyl acetate; C, by cooling a saturated hot methanol solution of the orthobenzoate **1.17**.

Although, melting points (209-211 °C) of the two polymorphs were quite similar, DTA / TGA curves (see Appendix, page 142) showed small but significant differences in the endotherms before the melting of the crystals began, indicating considerable structural differences between the two crystal forms.

Crystal structures of Forms I and II crystals showed very similar conformation of the individual molecules, although free rotations are possible for the phenyl ring and for the three O–H groups (Figure 2.2). The similarity in O–H group orientation could be because of two intra-molecular O–H \cdots O hydrogen bonds O6–H6A \cdots O4 and O2–H2A \cdots O3; the former is somewhat stronger than the latter (Table 2.1) as expected.

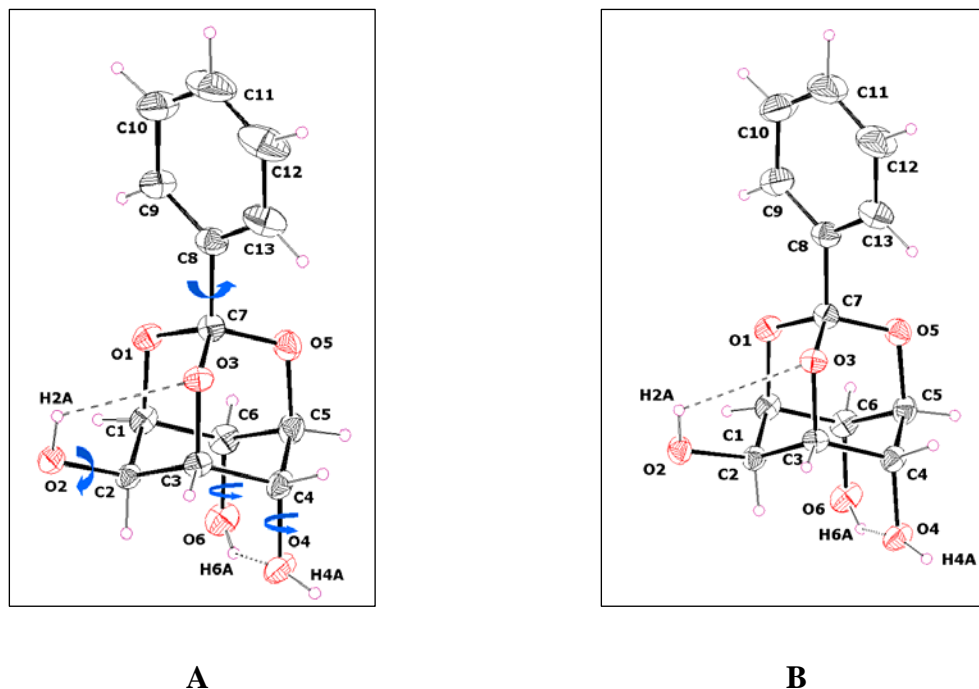


Figure 2.2: ORTEP view of molecule in (A) Form I crystals of **1.17** (B) Form II crystals of **1.17**. Blue arrows indicate possible free rotations; dotted lines (···) indicate intramolecular hydrogen bonds. Ellipsoids are shown at 30% probability level.

Table 2.1: Geometrical parameters for the O–H···O hydrogen bonds in crystals of **1.17**

	D–H···A	D–H (Å)	H···A (Å)	D···A (Å)	D–H···A (°)
Form I	O(4)–H(4A)···O(2) ^a	0.84(3)	1.88(3)	2.712(2)	172(2)
	O(2)–H(2A)···O(6) ^b	0.84(2)	2.03(2)	2.755(2)	144(2)
	O(6)–H(6A)···O(4) ^c	0.82(3)	1.97(3)	2.691(2)	146(2)
	O(2)–H(2A)···O(3) ^c	0.84(2)	2.41(2)	2.851(2)	113.0(18)
Form II	O(4)–H(4A)···O(2) ^d	0.86(2)	1.93(2)	2.779(2)	166.8(18)
	O(2)–H(2A)···O(6) ^e	0.849(19)	2.006(19)	2.802(1)	155.7(18)
	O(6)–H(6A)···O(4) ^c	0.85(2)	2.03(2)	2.762(1)	143.9(18)
	O(2)–H(2A)···O(3) ^c	0.849(19)	2.539(19)	2.940(1)	110.0(15)
	O(6)–H(6A)···O(2) ^f	0.85(2)	2.62(2)	3.098(2)	116.5(16)

Symmetry code: (a) $x, y, z+1$, (b) $x-1, y, z-1$, (c) x, y, z ; (d) $x, y-1, z$, (e) $x, -y+3/2, z+1/2$, (f) $-x, y-1/2, -z+1/2$.

Another common significant feature observed in both the crystal structures was linking of the molecules *via* the strongest intermolecular hydrogen bond O4–H4A···O2 resulting in a one-dimensional H-bonded polymer (Figure 2.3).

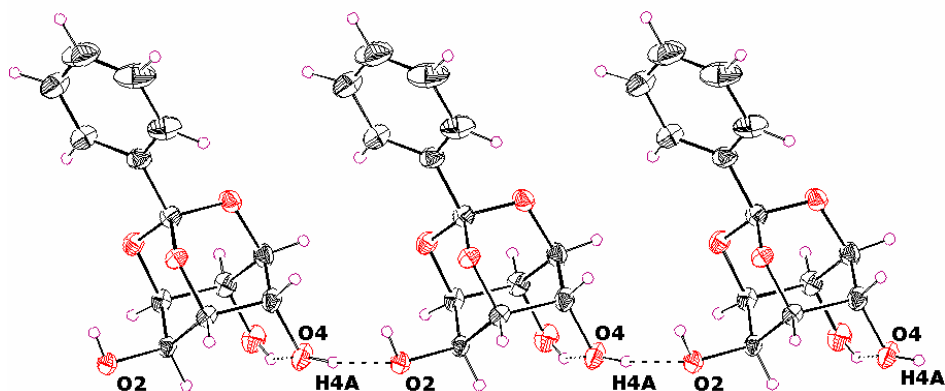


Figure 2.3: Intermolecular O4–H4A···O2 hydrogen bonded molecular string in Form I crystals of **1.17**. Intermolecular hydrogen bonding in Form II crystals of **1.17** is similar to that shown for Form I crystals.

Detailed examination of the crystal structure of the two polymorphs showed that O–H···O linked one-dimensional isostructural molecular strings in the two forms weave differently by weak intermolecular interactions to produce the dimorphs. Striking difference was seen in the ‘zipping’ of molecular layers *via* phenyl···phenyl contacts; thermodynamic crystals of Form I utilize a well-recognized ‘edge-to-face’ herringbone pattern⁴ making C–H··· π interactions (Figure 2.4). The atom H11 does not point to the center of the ring but makes closer contacts with the three edge atoms C10, C11 and C12 and the angle between the two phenyl rings is 85.11(8)°.

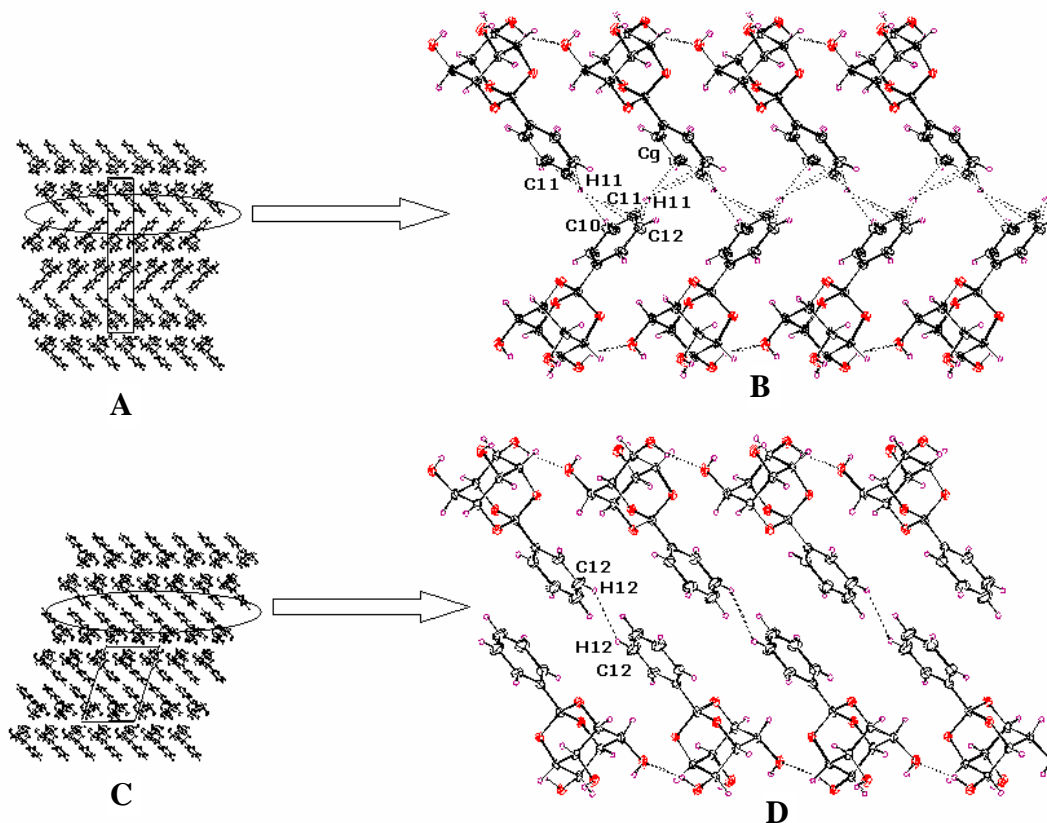


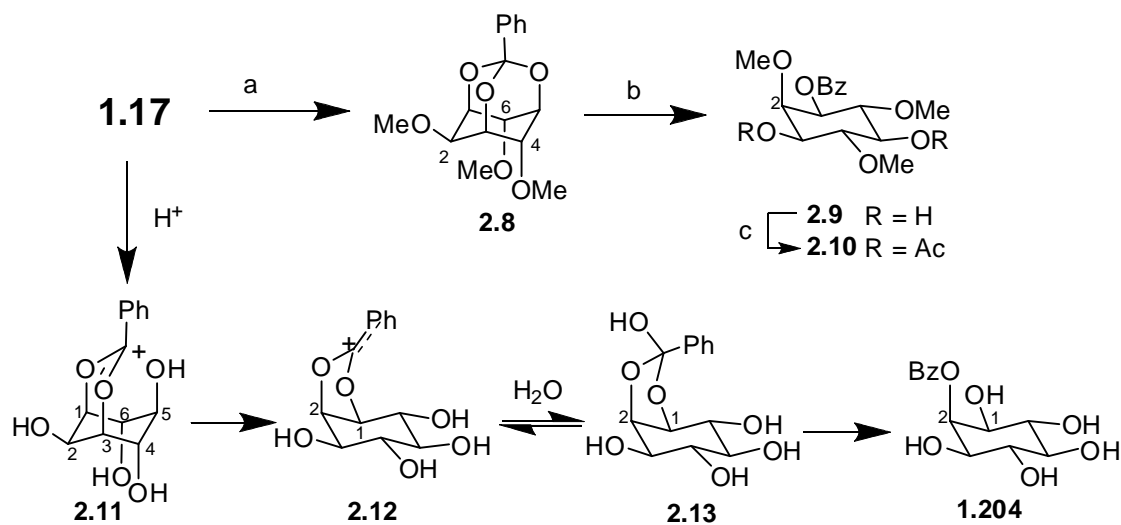
Figure 2.4: Packing of molecules showing Ph...Ph interactions in crystals of **1.17**: (A, B) edge-to-face organization in Form I with C11-H11... π interactions; (C, D) edge-to-edge organization of aromatic rings in Form II with C12-H12...H12-C12 short contacts.

In sharp contrast, parallel phenyl rings across center of symmetry are zipped by short C-H...H-C contacts ($H\cdots H = 2.35 \text{ \AA}$) in Form II crystals (Figure 2.4D). Surprisingly, there are no significant $\pi\cdots\pi$ or C-H... π interactions between the phenyl rings from different layers (the distances between neighboring phenyl rings are $> 6 \text{ \AA}$ and the angle along the row is $42.61(6)^\circ$). Therefore, the cohesion of 2D-layers along a-axis in Form II crystals seems to be only *via* short H...H contacts. The short H...H contacts investigated in metal hydrides and also in some organic molecules has been seen as a new type of attractive interaction.⁵ The H...H contact in Form II crystals is just at the boundary of the sum of the van der Waals radii (2.35 \AA) and any conclusion based on this

alone could be fortuitous. However, packing mode of aromatic rings observed in Form II crystals could imply a weak adhesive interaction and deserves some attention. The Ph...Ph contacts in Form II crystals are expected to be of interest from experimental and theoretical points of view,⁶ since interactions between aromatic rings are important due to their role in the stability of biological macromolecules such as DNA,⁷ proteins⁸ and also in drug-receptor interactions.^{4b}

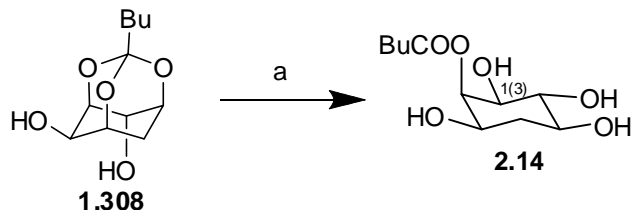
2.2.2. Orthogonally protected *myo*-inositol derivatives from the orthobenzoate **1.17**.

The orthobenzoate **1.17** is stable under basic conditions and can be hydrolyzed to release the C1(3) and C5-hydroxyl groups, in the presence of an acid. For instance, the acid catalyzed hydrolysis of the trimethyl ether **2.8** resulted in the formation of the 1-benzoate **2.9** (Scheme 2.3). Hydrolysis of the orthobenzoate triol **1.17** on the other hand yielded the 2-benzoate **1.204** exclusively.⁹ While our work was in progress, Potter and co-workers⁹ reported the synthesis of the *myo*-inositol-1,3,4,5,6-pentakisphosphate **1.207** from the 2-benzoate **1.204** (Scheme 1.52, Chapter 1). They also investigated the mechanism of hydrolysis of the orthobenzoate **1.17** to yield the 2-benzoate **1.204** exclusively.



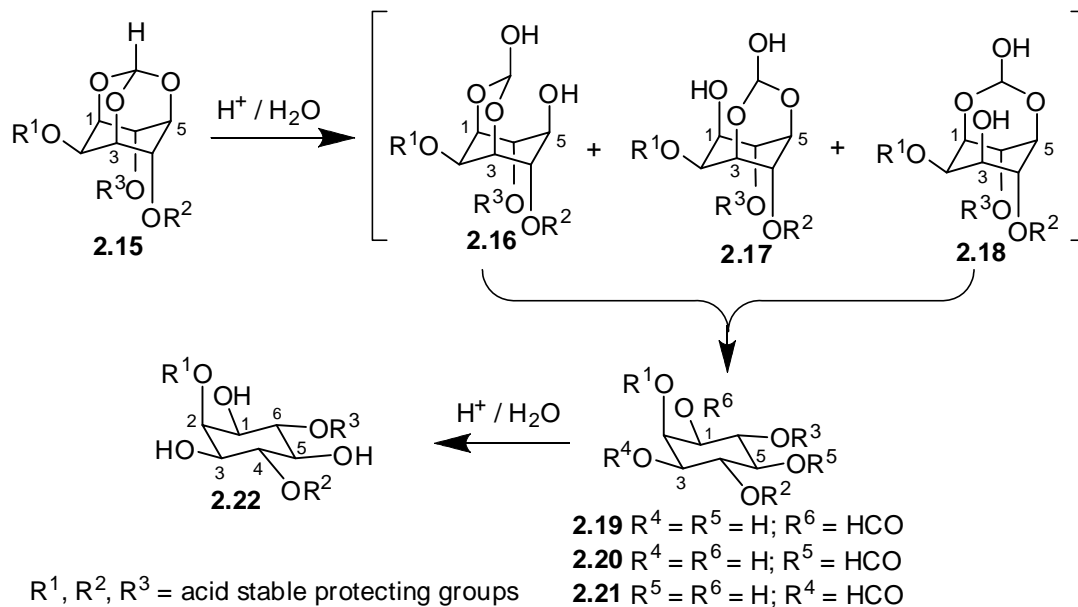
Scheme 2.3: hydrolysis of orthobenzoate **1.17** and its derivative **2.8**; (a) NaH, DMF, MeI, rt, 45 min.; (b) AcCl, MeOH, DCM, rt, 54 h; (c) Ac₂O, Py, rt, 7 h.

Similar pattern for the hydrolysis of other orthoesters **dia-1.301** (Scheme 1.49, Chapter 1, page 42) and orthobutanoate **1.308** (Scheme 2.4) has been reported earlier.^{10, 2b}



Scheme 2.4: (a) H^+ / H_2O

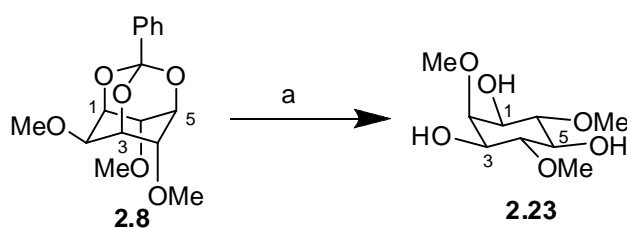
Hydrolysis of the orthoformate (**2.15**) is a special case, since the unstable C1- (**2.19**) or C3- (**2.21**) or C-5 (**2.20**) formate ester formed undergoes further hydrolysis to the corresponding *myo*-inositol derivative **2.22**.



Scheme 2.5: Possible intermediates formed during the hydrolysis of the orthoformate **2.15** to afford the corresponding triol **2.22**.

The acid catalyzed deprotection of *myo*-inositol-1,3,5-orthoesters is not a convenient method during the synthesis of inositol derivatives since it does not allow the use of acid sensitive protecting groups at the three hydroxyl groups of the orthoester.

Unlike the *myo*-inositol orthoesters derived from aliphatic acids, the orthobenzoate can be cleaved under catalytic hydrogenolysis conditions. This is illustrated with the hydrogenolysis of 2,4,6-tri-*O*-methyl-*myo*-inositol-1,3,5-ortho-benzoate (**2.8**), in the presence of Pearlmann's catalyst to give the corresponding triol **2.23** in good yield (Scheme 2.6).

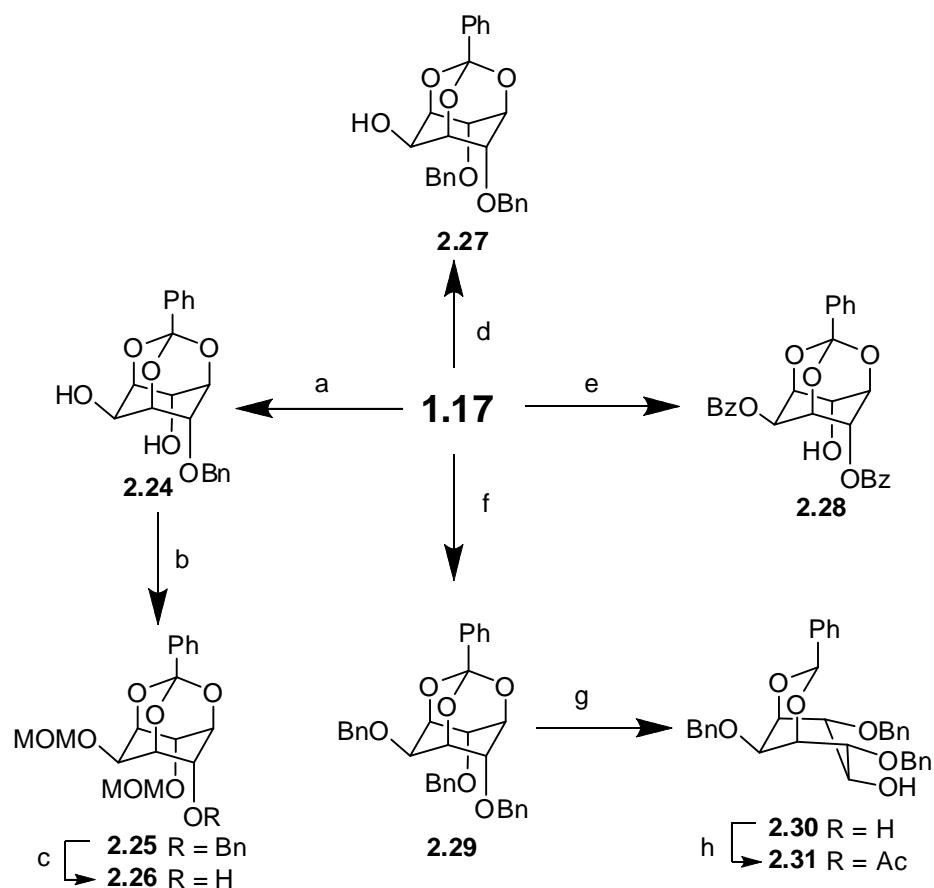


Scheme 2.6: (a) H₂ (55 Psi), Pd(OH)₂-C, MeOH, rt, 6 h, 99%

Orthobenzoate moiety in **2.8** can also be cleaved by Birch reduction to form the corresponding triol (**2.23**) in good yield (see Experimental, page 97).

The relative reactivity of the three hydroxyl groups of the orthobenzoate **1.17** is expected to be similar to that of other orthoesters **1.15**, **1.16** of *myo*-inositol, due to intramolecular hydrogen bonding between the C4 and C6-hydroxyl groups.¹¹ Earlier work in our laboratory¹² and elsewhere¹³ had shown that the three hydroxyl groups of the orthoformate **1.15** can be selectively derivatized under different reaction conditions and using different reagents. Accordingly, several derivatives of the orthobenzoate shown in Scheme 2.7 could be prepared and utilized for the preparation of various inositol derivatives.

Benzoylation of the orthobenzoate could be controlled to obtain the *racemic*-2,4-dibenzoate **2.28** in very good yield, as in the case of the corresponding orthoformate **1.234**.¹⁴ Such derivatives are versatile intermediates for the preparation of phosphoinositols.¹⁵ The dibenzoate **2.28** exhibited interesting benzoyl transfer reactivity in the crystalline state and results pertaining to this are discussed in detail in the next chapter.



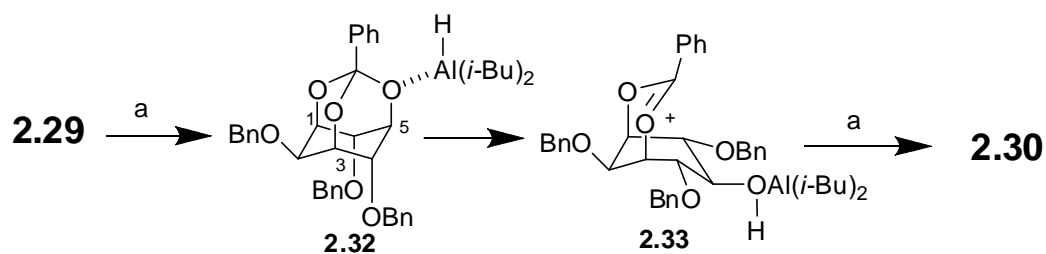
Scheme 2.7: (a) NaH, BnBr (1eq), DMF, rt, 30 min; (b) NaH, MOMCl, rt, 12 h; (c) H₂ (55psi), Pd(OH)₂-C, EtOAc, 95%; (d) LiH, DMF, BnBr, rt, 83%; (e) BzCl, Py, rt, 18 h, 82%; (f) NaH, BnBr (excess), DMF, rt; (g) DIBAL-H, DCM, 0 °C-rt, 2 h, 97%; (h) Ac₂O, Py, rt, 4 h, 96 %.

The di-*O*-benzyl ether **2.27** could be obtained in excess of 83% yield by the benzylation of the orthobenzoate **1.17** using lithium hydride and benzyl bromide in DMF. Use of sodium hydride for the benzylation of *myo*-inositol-1,3,5-orthoesters is known to result in a mixture of isomeric benzyl ethers and we had shown earlier¹² that the *O*-alkylation of the orthoformate **1.15** in the presence of lithium hydride yields the corresponding 4,6-diether **1.80** exclusively. The symmetric dibenzyl ether **2.27** is also a potential intermediate for the preparation of *myo*- as well as *scyllo*-inositol derivatives.^{2a}

Benzylation of orthobenzoate **1.17** with excess of sodium hydride and benzyl bromide gave the tribenzyl ether **2.29** in excellent yield. The tribenzyl ether **2.29** when subjected to reduction with DIBAL-H (2.0-2.2 eq.) underwent partial cleavage of the orthoester moiety to selectively release the hydroxyl group at the C5-position.¹⁷ The benzylidene derivative **2.30** was used for the synthesis of several inositol derivatives *viz.*, sequoyitol, *neo*-inositol (**1.25**), *neo*-quercitol, 5-deoxy-5-amino-*myo*-inositol and 1(3), 5-di-deoxy-*myo*-inositol (see pages 74, 80, 83, 91, 93).

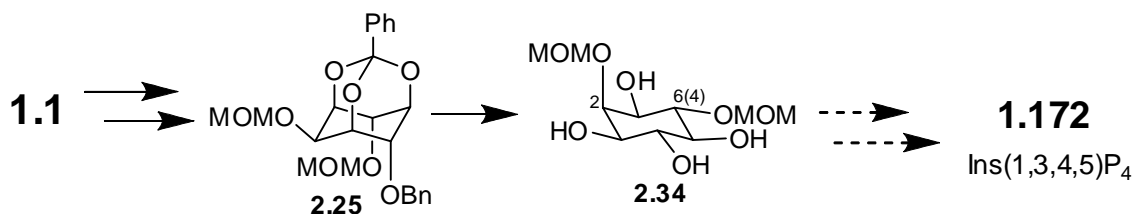
The benzylidene derivative **2.30** was also characterized as its acetate **2.31**. Good crystals of the benzylidene derivative **2.30** as well as its acetate **2.31**, suitable for single crystal X-ray crystallography could be obtained by crystallization from dichloromethane and ethyl acetate respectively. The X-ray crystal structures clearly showed that the *myo*-inositol ring adopts a boat conformation in these derivatives, in their crystals (see Appendix; ORTEP diagrams, pages 134, 135). It is not clear whether the benzylidene derivative exists in the same conformation in solution. But, most of the literature reports dealing with similar acetal derivatives of *myo*-inositol depict the molecule, showing the inositol ring in the chair conformation (see structures of **1.131**, **1.218-1.220**, **1.227**, **1.243** in Chapter 1).^{17, 18} Although we have not determined the conformation of the cyclohexane ring (chair and boat) in *myo*- and *neo*-inositol derivatives (alcohols, triflates and azide etc. mentioned in this chapter) containing the 1,3-acetal moiety in solution, the structures depicted in schemes are based on the single crystal X-ray analysis of these derivatives.

The observed regioselectivity for the cleavage of *myo*-inositol-1,3,5-orthoesters by DIBAL-H was attributed¹⁷ to the bulk of the reducing agent which probably coordinates to the more accessible C5-oxygen atom rather than to C1- and C3- oxygen atoms and cleaves the C5O-CPh bond as shown in the in Scheme 2.8. The oxacarbenium ion **2.33** formed is reduced by DIBAL-H to afford the free alcohol.



Scheme 2.8: A mechanism for the cleavage of orthobenzoate in **2.29** with DIBAL-H; (a) DIBAL-H

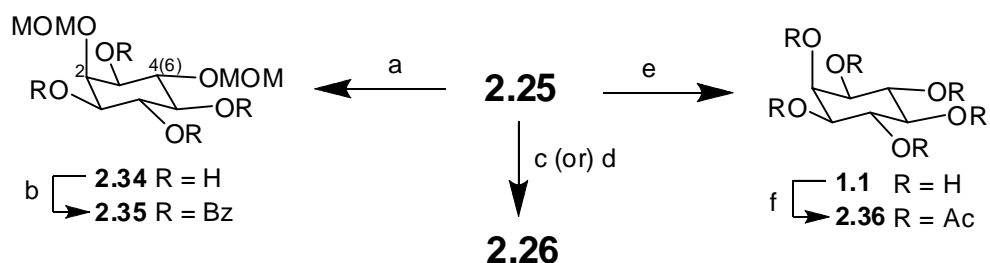
The dimethoxymethyl ether **2.25** was prepared by the regioselective *O*-benzylation¹³ of the orthobenzoate **1.17** using sodium hydride and one equivalent of benzyl bromide followed by reaction with excess of methoxymethyl chloride. Such orthogonally protected derivatives are useful for the synthesis of phosphatidylinositol polyphosphates.¹⁹ We attempted to prepare 2,6-di-*O*-methoxymethyl-*myo*-inositol (**2.34**) by hydrogenolysis of the benzyl ether **2.25**, as the di-methoxymethyl ether **2.34** could serve as a precursor for the preparation of *myo*-inositol-1,3,4,5-tetrakisphosphate (**1.172**).



Scheme 2.9: An intended route for the synthesis of *rac*-2, 4-di-*O*-methoxymethyl-*myo*-inositol (**2.34**).

During our attempts to prepare the di-methoxymethyl ether **2.34** (involving the use of Pearlman's catalyst [Pd(OH)₂-C] in methanol), we observed the unusual cleavage of *O*-benzyl groups, orthoesters and acetals to the corresponding alcohols (in the absence of hydrogen-see next page). The product of hydrogenolysis of the methoxymethyl ether **2.25** in the presence of Pd(OH)₂-C was dependent on both the amount of the catalyst used and the solvent used for the reaction. Selective cleavage of only the benzyl ether (to obtain the orthobenzoate **2.26**) or cleavage of the benzyl ether as well as the

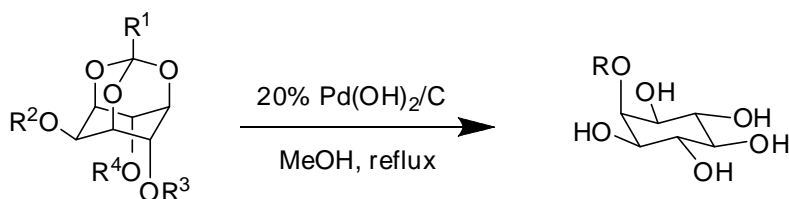
orthobenzoate (to obtain di-*O*-methoxymethyl-*myo*-inositol **2.34**) or complete cleavage of all the protecting groups (to obtain inositol, isolated as its hexa acetate **2.36**) could be achieved by varying the conditions of the hydrogenolysis reaction and the amount of Pd(OH)₂-C used.



Scheme 2.10: (a) H₂ (55psi), 0.2 eq. Pd(OH)₂-C, MeOH, rt, 13 h, 93%; (b) BzCl, Py, rt. - h; (c) H₂ (55psi), 0.16 eq. Pd(OH)₂-C, EtOAc, 95%; (d) 0.8eq Pd(OH)₂-C, MeOH, rt, 7d; (e) H₂ (55psi), 0.8eq. Pd(OH)₂-C, MeOH, 13 h; (f) Ac₂O, Py, rt, 40 h, 96%

Since we observed the cleavage of methoxymethyl ethers under hydrogenolysis conditions, we wondered whether this was due to the complexation of palladium with the substrate which could aid the cleavage of the methoxymethyl ethers. Inositols and their derivatives are known to form complexes with metal ions in solution as well as in the solid state.²⁰ Hence we treated the orthobenzoate derivative **2.25** with Pd(OH)₂-C in ethyl acetate or methanol at ambient as well as reflux temperatures (in the absence of hydrogen). This was also to see if the methoxymethyl ethers were cleaved prior to or subsequent to the cleavage of the orthobenzoate in the hydrogenolysis reactions mentioned above (Scheme 2.10). Reaction of the orthobenzoate derivative **2.25** with Pd(OH)₂-C in methanol unexpectedly resulted in the cleavage of the benzyl ether alone (to give **2.26**). Since the reactions of the orthobenzoate **2.25** in the presence of Pd(OH)₂-C gave unexpected results, we investigated in detail, the reaction of *myo*-inositol-1,3,5-orthoesters **1.15-1.17**, **1.106**, **2.24** and **2.29** with Pd(OH)₂-C under non-hydrogenolytic conditions (Table 2.2).

Table 2.2. Non-hydrogenolytic cleavage of benzyl ethers and orthoesters with Pd(OH)₂-C.



Entry		Substrate				Reaction time	Product	Yield %
		R ¹	R ²	R ³	R ⁴			
1	1.17	Ph	H	H	H	9 h	1.204 , Bz	94
2	2.24	Ph	H	H	Bn	12 h	1.204 , Bz	92
3	2.29	Ph	Bn	Bn	Bn	40 h	1.204 , Bz	84
4	1.16	Me	H	H	H	52 h	2.37 , Ac ^a	93
5	1.15	H	H	H	H	32 h	1.1 , H	96
6	1.106	H	Bn	Bn	Bn	72 h	1.1 , H	96

^a mixture of isomeric mono acetates

These reactions clearly showed that benzyl ethers are cleaved by Pd(OH)₂-C in refluxing methanol and that the orthoester moiety underwent solvolysis to give the corresponding ester. The orthobenzoate **1.17** and its benzyl ethers gave 2-benzoate **1.204** on refluxing with Pd(OH)₂-C in methanol while the orthoacetate **1.16** gave a mixture of mono-acetates due to migration of the acetyl group in the initially formed *myo*-inositol-2-acetate. The orthoformate **1.15** and its tribenzyl ether **1.106** gave *myo*-inositol (**1.1**) as the product since the formate ester (of inositol) initially formed undergoes solvolysis with ease (see Scheme 2.5). *myo*-Inositol-1,3,5-orthoesters are known^{2b, 10} to give the

corresponding *myo*-inositol monoester derivative on acid hydrolysis. (Schemes 2.3 and 2.4, pages 60, 61).

In order to get a clue on the mechanism of cleavage of benzyl ethers by Pd(OH)₂-C and to check the generality of the reaction, we subjected the racemic 1,2:4,5-diisopropylidene-*myo*-inositol (**2.38**) and its di-benzyl ether (**2.39**), as well as cyclohexyl benzyl ether (**2.42**) to reaction with Pd(OH)₂-C under a variety of conditions (Scheme 2.11 and Table 2.3).

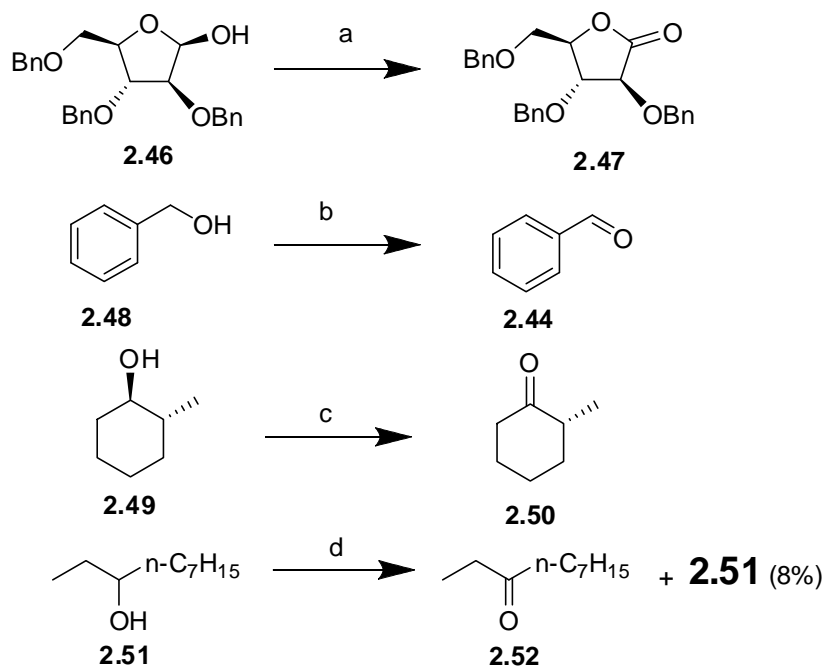


Scheme 2.11: (a) 20% Pd(OH)₂-C, MeOH, reflux, 8 - 22 h

Pd(OH)₂-C in methanol de-protected the diisopropylidene derivative **2.38** completely to give *myo*-inositol (**1.1**). GC-MS analysis (see Appendix, page 142) of the reaction mixture during the cleavage of the ketal **2.38** showed the presence of acetone and 2,2-dimethoxy propane (**2.41**) which indicated that the ketal was cleaved by hydrolysis as well as methanolysis.

Cyclohexanol (**2.43**) was obtained in good yield by the reaction of its benzyl ether **2.42** with Pd(OH)₂-C in methanol (Table 2.3). Ethyl acetate or THF could also be used as solvent for the cleavage of cyclohexyl benzyl ether (**2.42**), but the reaction times were longer. Cyclohexyl benzyl ether (**2.42**) could also be cleaved by palladium acetate, although relatively slowly as compared to Pd(OH)₂-C. ¹H NMR spectra of the mixture of products (see Appendix, page 174) formed on the cleavage of benzyl ethers **2.42** and **1.106** with Pd(OH)₂-C in methanol showed the presence of benzaldehyde (**2.44**) and methyl benzoate (**2.45**), which suggested the oxidative cleavage of benzyl ethers and ruled out their cleavage by transfer hydrogenation (scheme 2.12).²¹

Instances of oxidative cleavage of ethers²² and palladium catalyzed oxidation reactions²³ have been reported earlier (Scheme 2.13).



Scheme 2.13: (a) Pd(OAc)₂, PPh₃, 4-bromodiphenyl, K₂CO₃, THF, 100%; (b) 5% Pd(OAc)₂, O₂, 20% Py, toluene, 80 °C, 2 h, 95%; (c) 3 mol% Pd(OAc)₂, 6 mol% Et₃N, rt, O₂, 12 h, 98%; (d) 10% Pd/C (10 wt %), D₂O, H₂, 160 °C, 24 h, 70%

In order to confirm the oxidative cleavage of benzyl ethers by Pd(OH)₂-C, we carried out a control reaction using Pd(0)-C (obtained from Aldrich Chemical Company as well as Lancaster Synthesis). Unexpectedly, benzyl ether **2.42** was cleaved by these samples of 'Pd(0)-C' in the absence of hydrogen. We suspected this to be due to the presence of Pd(II) species in (supposedly) 'Pd(0)-C' samples that we used and recorded their X-ray photoelectron spectra (XPS).

A comparison of the XPS (Figure 2.5) of the Pd 3d core level of Pd(OH)₂-C (curve 1), 'Pd(0)-C' (curve 2) and the spent Pd(OH)₂-C recovered after the cleavage of benzyl ether (curve 3) clearly showed (i) that the spent palladium recovered after the

reaction did not contain Pd(II) species; (ii) the presence of considerable amount of Pd(II) species in the sample of 'Pd(0)-C' that we used for control experiments.

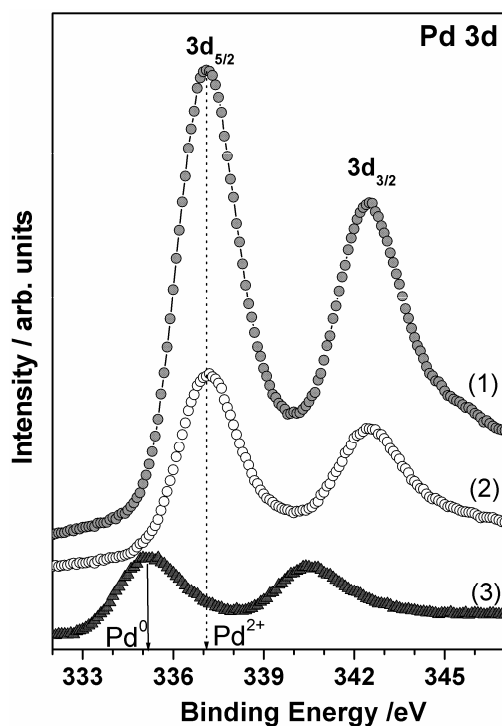
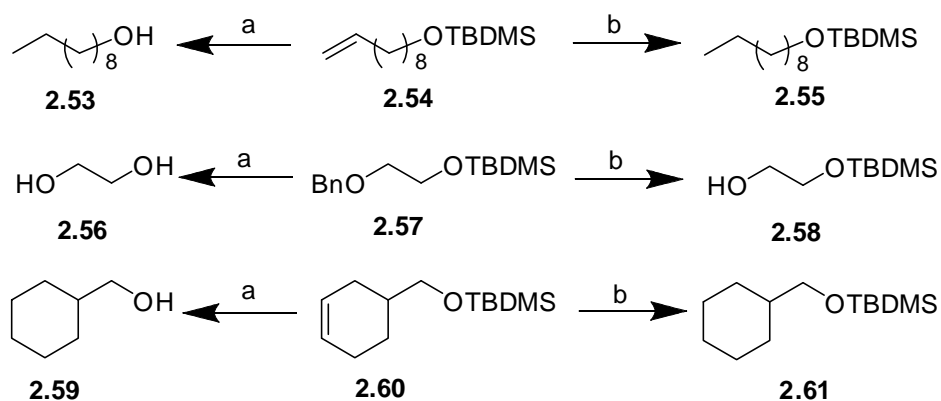


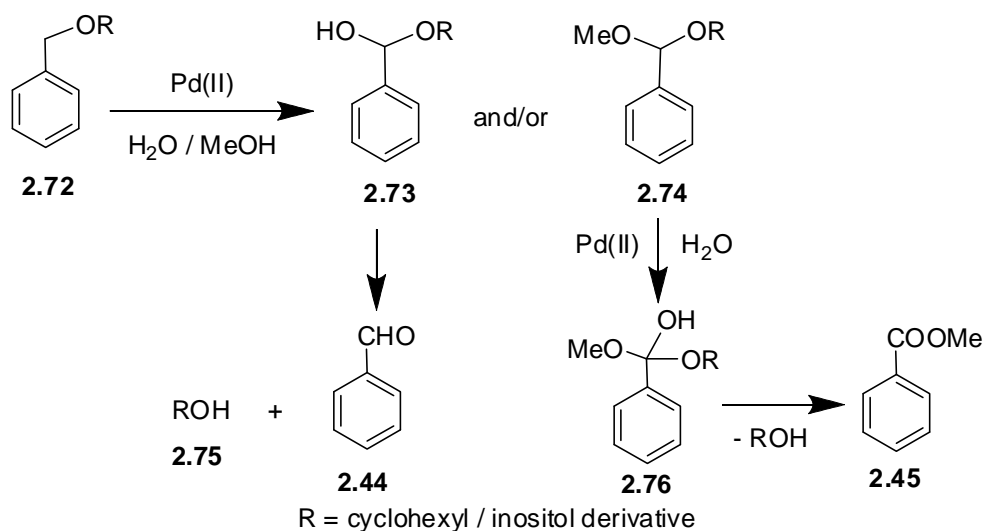
Figure 2.5: Comparison XPS spectra of palladium catalysts, see text for details.

Pd(0) is known to undergo oxidation to Pd(II) on storage and exposing to air.²⁴ Unexpected reactivity patterns of Pd-C during hydroxyl group deprotection have earlier been recorded in the literature (Scheme 2.14).²⁵



Scheme 2.14: (a) 10% Pd-C, H₂, MeOH, 24 h, 73-80%; (b) 10% Pd(en)₂-C, H₂, MeOH, 92-100%

realized during our experiments and supported by the XPS spectra of the catalyst, see Figure 2.5). Based on these results and our own results in the present thesis, it can be postulated that the cleavage of benzyl ethers by Pd(II) species proceeds through benzylidene acetal and / or the corresponding orthoester (Scheme 2.17). We have postulated this pathway for the cleavage of benzyl ethers since the products formed include benzaldehyde as well as methyl benzoate. However, the formation of methyl benzoate can also be explained based on the aerial oxidation of benzaldehyde formed to methyl benzoate. Hence arrival at an unambiguous mechanism for cleavage of benzyl ethers by Pd(OH)₂-C requires further studies.

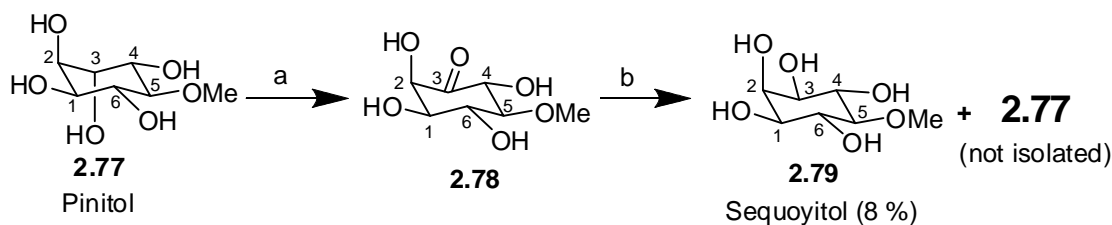


Scheme 2.17: Plausible mechanisms for the cleavage of benzyl ethers by Pd(OH)₂-C

2.2.3. Synthesis of Sequoyitol (5-O-methyl-*myo*-inositol, 2.79).

Sequoyitol was first isolated from the cold water extract of the heartwood of redwood (*Sequoia sempervirens*) and identified as the optically inactive mono-methyl ether of *myo*-inositol.²⁷ Sequoyitol is also found in heartwood of sugarpine,²⁸ soyabean,²⁹ carob pods³⁰ *Amentotaxus yunnanensis*³¹ *Melicope micrococca*³² *Aristolochia arcuata*³³ etc. Sequoyitol was used in the biological experiments to check inhibitory activity in phosphoinositide pathway.³⁴ Sequoyitol (2.79) has been synthesized from pinitol (2.77)³⁵

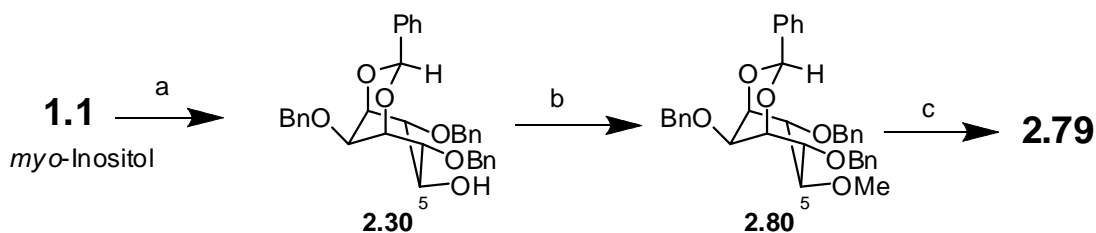
by aerial oxidation in the presence of platinum followed by reduction using sodium amalgam, in an overall yield of 8% (Scheme 2.18).



Scheme 2.18: (a) O₂, Pt, 85-90 °C, 4 h; (b) Na (Hg), glacial AcOH

2.2.4. Present work.

Sequoyitol was prepared from *myo*-inositol (5 steps) in an overall yield of 81%. Methylation of the alcohol **2.30** followed by deprotection of all the hydroxyl groups with Pearlman's catalyst gave sequoyitol.

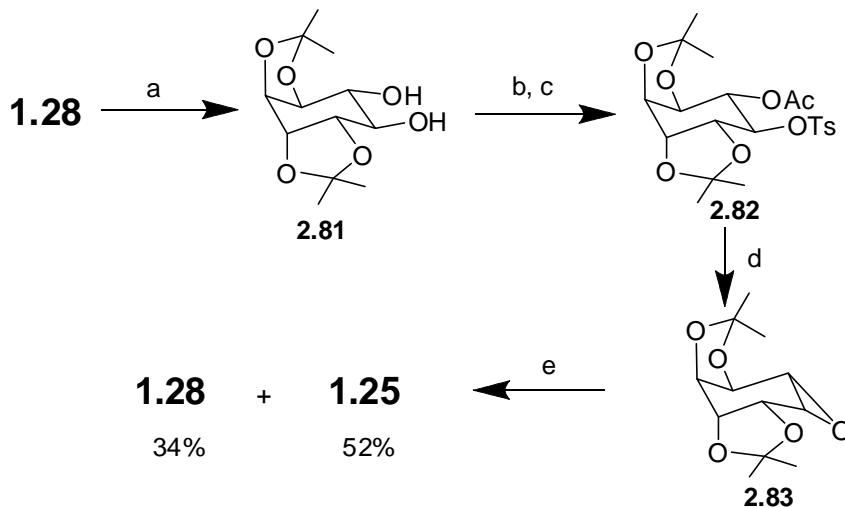


Scheme 2.19: (a) 3 steps, Schemes 2.2 and 2.7; (b) NaH, MeI, DMF, rt, 1 h, 98%; (c) Pd(OH)₂-C, MeOH, reflux, 20 h, 94%

2.2.5. Synthesis of *neo*-inositol (1.25):

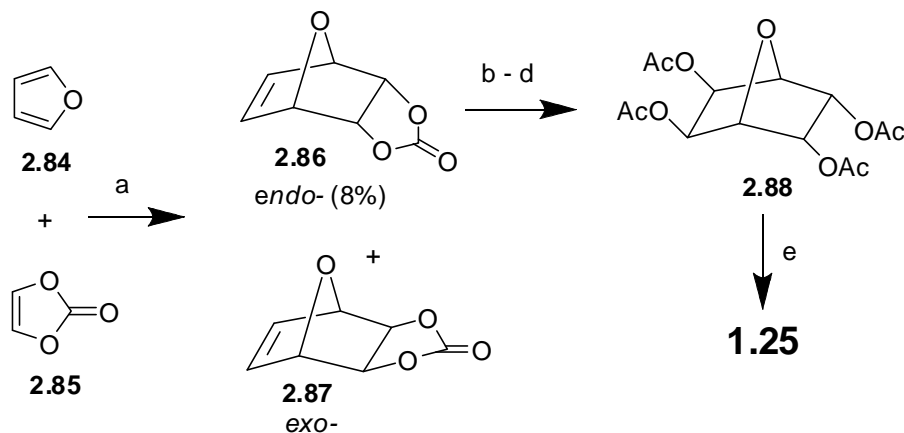
neo-Inositol (**1.25**) has been isolated from calf brain³⁶ and identified as its trimethyl silyl ether and as its acetate ester by GC-MS. *neo*-Inositol also occurs in plants such as *Croton celtidifolius*.³⁷ L-*neo*-Inositol-1-phosphate is present in the brain, heart, kidney, testis, and spleen of rats³⁶ and higher phosphates *viz.*, *neo*-inositol hexakisphosphate, 2-diphospho-*neo*-inositol pentakisphosphate, and 2,5-bisdiphospho-*neo*-inositol tetrakisphosphate are present in trophozoites of the parasitic amoeba, *Entamoeba histolytica*.³⁸ *neo*-Inositol hexakis- and pentakis- phosphates were detected in the soil samples collected from Australia, Canada, England, Scotland, USA.³⁹

In 1955, Angyal and Matheson described an optically inactive inositol obtained from 1,2:5,6-di-*O*-isopropylidene-*L*-chiro-inositol in an overall yield of 4% and named it as ‘*neo*-inositol’ (Scheme 2.20)⁴⁰



Scheme 2.20: (a) ZnCl_2 , AcOH, dry acetone, 43%; (b) TsCl; (c) Ac_2O ; 25% (2 steps); (d) NaOMe, 72%; (e) H_2SO_4 ; total yield = 4%, from *L*-chiro-inositol

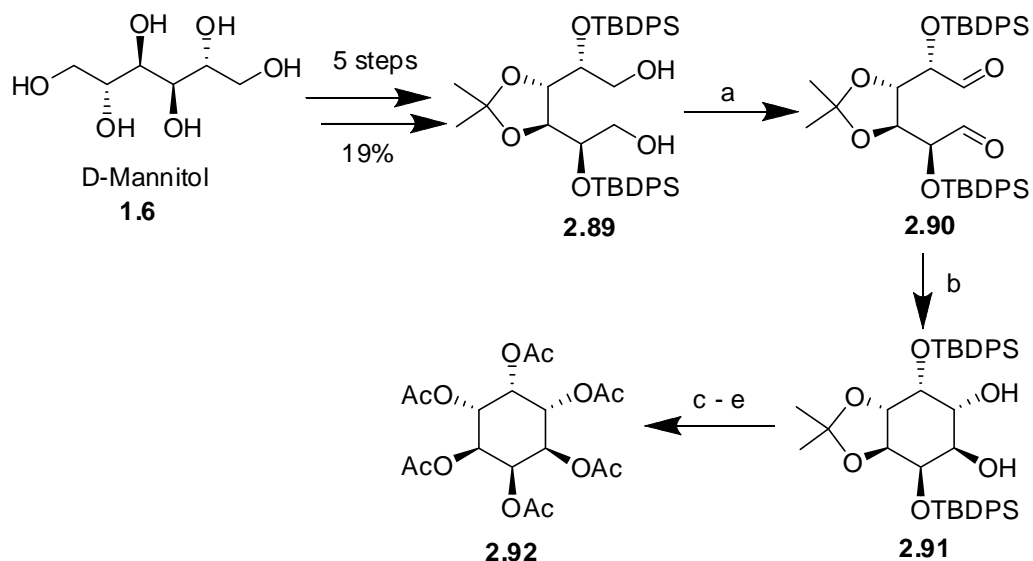
neo-Inositol (1.25) was prepared from the *endo*- adduct 2.86 of the Diels-Alder reaction between vinylene carbonate (2.85) and furan (2.84). The carbonate 2.86 was dihydroxylated with osmium tetroxide and



Scheme 2.21: (a) 120 °C, 12 h; (b) OsO_4 ; (c) NaOH; (d) Ac_2O , Py; (e) AcOH- H_2O - H_2SO_4 .

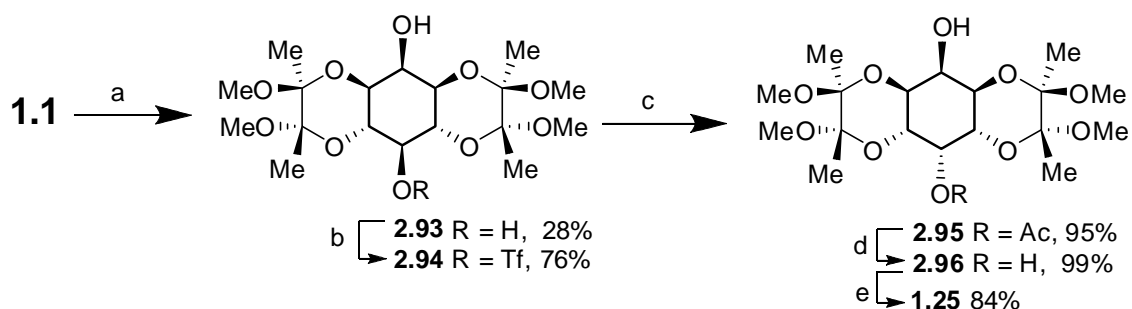
acetylated to afford the tetraacetate **2.88**. Treatment of **2.88** with acetic acid and sulfuric acid in water yielded *neo*-inositol (**1.25**) in an overall yield of ~1%. (Scheme 2.21).⁴¹

Fernández-Mayoralas *et. al.* reported a 10 step synthesis of *neo*-inositol hexaacetate (**2.92**) from D-mannitol (**1.6**) in an overall yield of 7 %.⁴² The key step involved the samarium iodide mediated cyclization of the dialdehyde **2.90**.



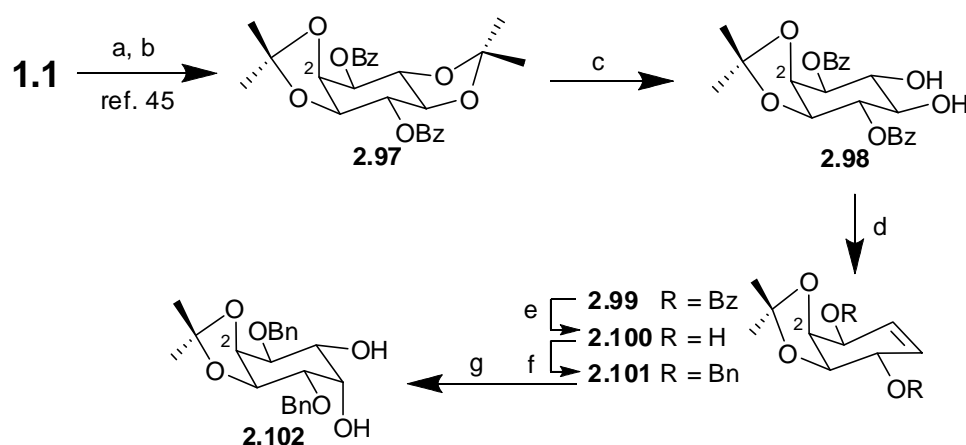
Scheme 2.22: (a) Swern oxidation; (b) SmI₂, *t*-BuOH, THF, – 60 °C, 85% (2 steps); (c) TFA-MeOH; (d) TBAF, THF; (e) Ac₂O, Py, 41% (3 steps)

Potter *et al*⁴³ reported the synthesis of *neo*-inositol (**1.25**) starting from *myo*-inositol (**1.1**) as shown in Scheme 2.23. The 1,3,4,6-hydroxyl groups in **1.1** were protected as the symmetrical bis(butane-2,3-diacetal). Inversion of the 5-hydroxyl group in the diol **2.93** was achieved *via* the triflate **2.94** by treatment with aqueous dimethyl acetamide. Deprotection of acetals afforded *neo*-inositol (**1.25**) in an overall yield of 17 % in 5 steps.



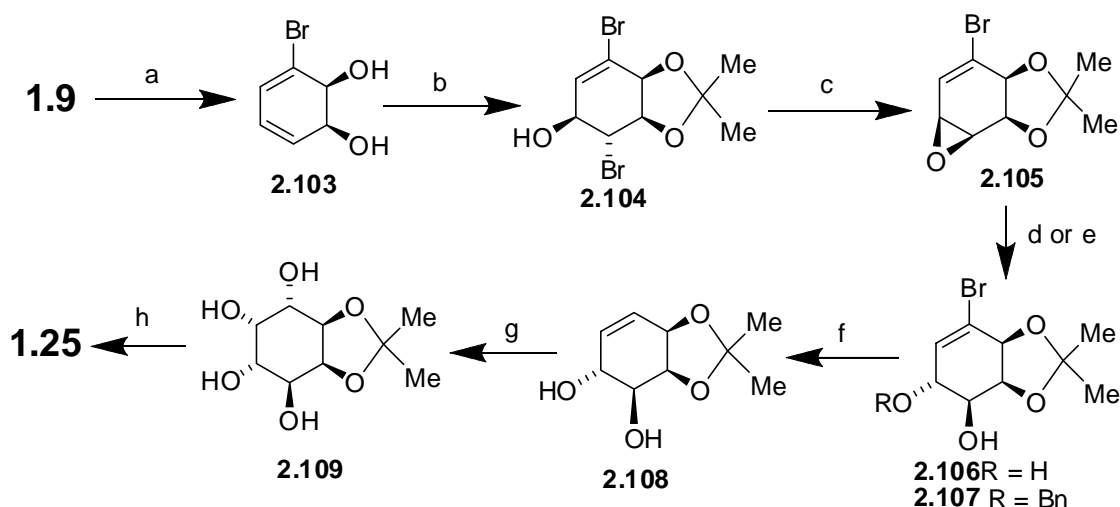
Scheme 2.23: (a) Butanedione, MeOH, HC(OMe)₃, (±)-CSA, reflux; (b) Tf₂O, Py, DCM, -78 °C - rt; (c) dimethylacetamide-H₂O (50:1), 50 °C; (d) NaOMe, MeOH, reflux; (e) AcOH-H₂O (4:1), reflux.

Chung and Kwon⁴⁴ prepared a *neo*-inositol derivative **2.102** in an overall yield of 14% from *myo*-inositol (**1.1**) via the conduritol **2.99** (Scheme 2.24).



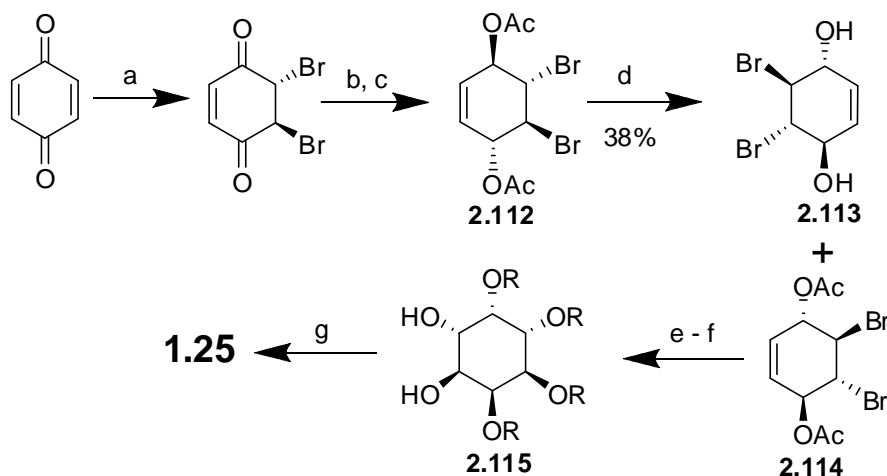
Scheme 2.24: (a) 2,2-mimethoxy propane, DMF, TsOH; (b) BzCl, Py, 26%; (c) AcCl (cat.), DCM-MeOH, 75%; (d) PPh₃, imidazole, I₂, toluene, reflux, 77%; (e) NaOMe, MeOH, reflux; (f) BnBr, NaH, DMF, 90-95%; (g) OsO₄, NMO, aq. acetone (95%)

Biotransformation of bromobenzene to the corresponding cyclohexadiene-*cis*-diol in 99% ee by treatment with *Escherichia coli* JM109 (which expresses both toluene dioxygenase and dihydrocatechol dehydrogenase) formed the key step in the synthesis of *neo*-inositol by Hudlicky *et al.*⁴⁶ Subsequent debromination of **2.106** and dihydroxylation of the diene moiety followed by deprotection of the vicinal diols afforded *neo*-inositol in an overall yield of 17% in 7 steps (Scheme 2.25).



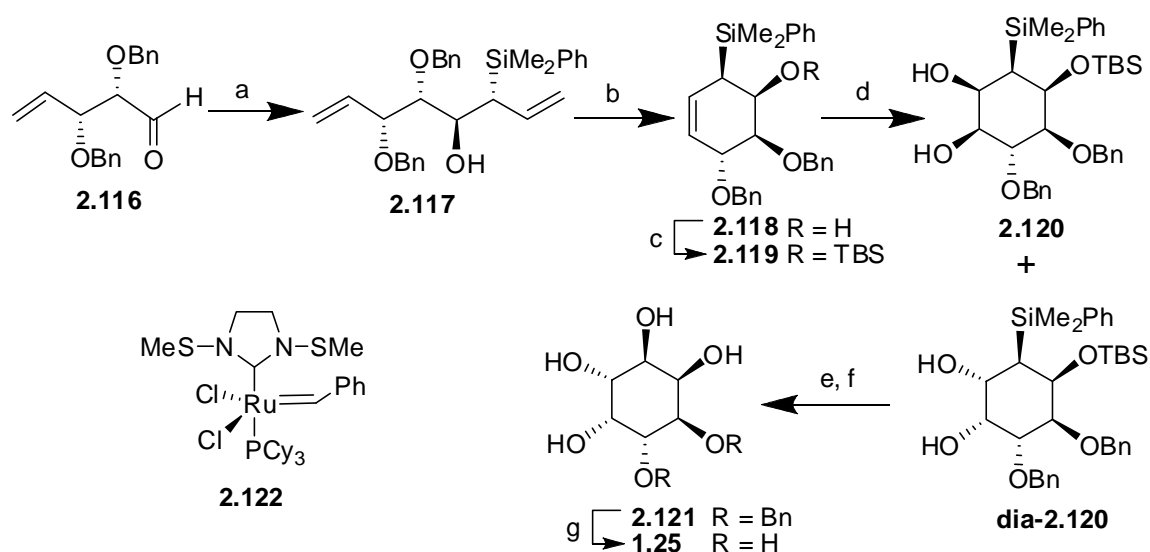
Scheme 2.25: (a) Toluene dioxygenase; (b) dimethoxypropane, TsOH, acetone; 1,3-dibromo-5,5-dimethylhydantoin, H₂O, acetone; (c) 10 % aq. KOH, DME, 5 h, rt; (d) aq. KOH, reflux (to obtain **2.106**); (e) BF₃, BnOH (**2.107**); (f) Bu₃SnH, AIBN, benzene, reflux, 18 h; (g) OsO₄, NMO, *t*-BuOH, acetone-H₂O; (h) concd. HCl, MeOH, 48 h.

Altenbach *et. al.* obtained *neo*-inositol **1.25** from benzoquinone (**2.110**) in an overall yield of 10 % in seven steps.⁴⁷ Enantiopure dibromodiacetate **2.113** was obtained by enzymatic resolution by pig pancreas lipase [PPL] in a phosphate buffer. The dibromoacetate **2.113** was converted into *neo*-inositol **1.25** by epoxidation followed by hydrolysis (Scheme 2.26).



Scheme 2.26: (a) Br₂, CHCl₃, 0 °C; (b) NaBH₄•Et₂O, rt; (c) Ac₂O, Py, 12 h; (d) PPL, phosphate buffer (pH 7), 4 d (38% each); (e) NaOAc, AcOH, 10 d, 130 °C then Ac₂O, DCM, DMAP; (f) Tf₂O, H₂O₂, DCM, NaHCO₃; (g) NaOMe, MeOH, H⁺-Dowex 50-X.

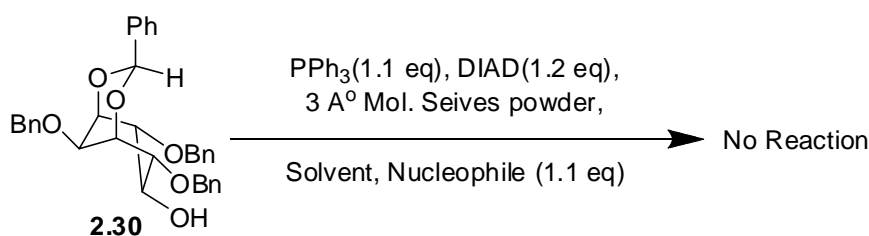
Ring-closing metathesis of the diene **2.117** resulted in the formation of the conduritol **2.118** which was converted to *neo*-inositol in four steps.⁴⁸ The diene **2.117** was obtained by stereoselective γ -allylboration of the aldehyde **2.116** with a chiral γ -silylallylborane. Dihydroxylation of the alkene **2.119** gave a mixture of diastereomeric inositol derivatives **2.120** and **dia-2.120** which were separated and **dia-2.120** was converted to *neo*-inositol **1.25** in an overall yield of 8 %.



Scheme 2.27: (a) $\text{Me}_2\text{PhSiCH}=\text{CHCH}_2\text{B}(\text{Ipc})_2$, from (+)- Ipc_2BOMe 40% (79%, 1:1 dr), (b) **2.122**, 80 °C, toluene, 2 h, 87 %, (c) TBSOTf, 99%; (d) $\text{K}_2\text{OsO}_4 \cdot \text{H}_2\text{O}$ $\text{K}_3\text{Fe}(\text{CN})_6$, K_2CO_3 , MeSO_2NH_2 , quinuclidine; (e) HF-Py, 70%; (f) $\text{Hg}(\text{OAc})_2$, AcOOH, AcOH, 51%; (g) H_2 , Pd-C, 99%

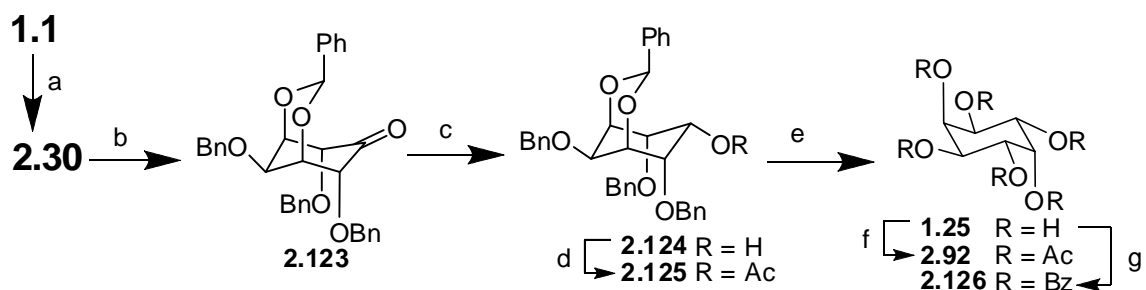
2.2.6. Present work.

Our initial attempts for the inversion of alcohol at the 5-position in the bicyclic derivative **2.31** by Mitsunobu reaction⁴⁹ under different reaction conditions failed and in most of the cases the substrate was recovered (Table 2.4).

Table 2.4: Attempted Mitsunobu reaction on alcohol **2.30**

SL. No.	Solvent	Nucleophile	temperature / reaction time
1	Benzene	AcOH	rt (6 h) and 75 °C (6 h)
2	THF	AcOH	rt (6 h) and reflux (6 h)
3	THF	PhCOOH	— reflux (6 h)

Hence we switched over to oxidation followed by hydride reduction to cause the inversion of the C5-hydroxyl group in **2.30**. Swern oxidation of the C-5 hydroxyl group in **2.30** to obtain the corresponding ketone **2.123** did not give consistent yields, perhaps due to the concomitant de-protection of the acid sensitive benzylidene acetal. Use of pyridinium dichromate for the same reaction afforded the ketone in good yield and the crude product was pure enough to be used in the next step.



Scheme 2.28: (a) 3 steps, Schemes 2.2 and 2.7; (b) PDC (1.5 eq), molecular sieves (3Å), DCM, rt, 22 h; (c) THF-MeOH, NaBH₄, rt, 1 h, 94% (2 steps); (d) Ac₂O, Py, rt, 4 h, 89%; (e) EtOH, Pd(OH)₂-C, H₂ (50 Psi), 6 h, 82% (total yield 68% from *myo*-inositol); (f) excess Ac₂O, Py, rt, 40 h, 96%; (g) BzCl, Py, rt, 56 h, 93%.

The pure ketone **2.123** could be obtained by crystallization of the crude product from dry methanol at low temperature (0 °C). Single crystal X-ray analysis of the ketone (good crystals were obtained from DCM-light petroleum by diffusion method) showed

that the inositol ring is slightly distorted from the chair form (see ORTEP diagram, Appendix, page 136).

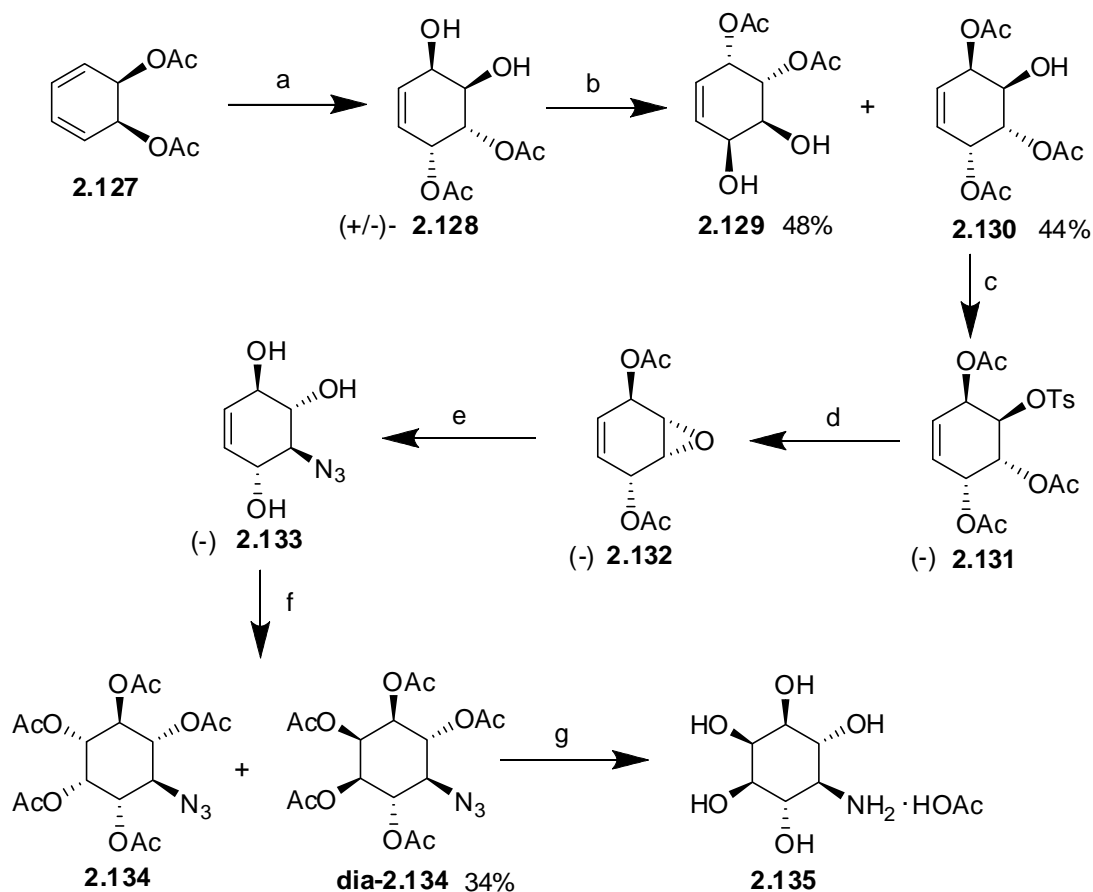
Reduction of the ketone **2.123** with sodium borohydride in a mixture of THF and methanol resulted in the exclusive formation of the C5-alcohol with *neo*-configuration, in 94% yield (for two steps). The exclusive formation of the alcohol with *neo*-configuration is perhaps due to the bulk of the diaxial-dibenzyl ether groups (at C4- and C6-positions) which prevent the attack by the borohydride on one face of the ketone **2.123**. It is interesting to note that the alcohol **2.124** formed crystals with the inclusion of DCM in its crystal lattice (see packing diagram of **2.124**, Appendix, page 137). Deprotection of the benzylidene acetal and three *O*-benzyl groups by catalytic hydrogenolysis in the presence of Pearlmann's catalyst afforded *neo*-inositol which was also characterized as its hexa acetate (**2.92**) as well as hexa benzoate (**2.126**). Thus, we prepared *neo*-inositol in an overall yield of 68 % starting from *myo*-inositol. Table 2.5 shows a comparison of the present work with the literature reports.

Table 2.5. Synthesis of *neo*-inositol (**1.25**); comparison with methods reported in the literature.

SL. No.	Starting material	No. of steps	Yield %	Product	Ref.
1	2.84 and 2.85	3	1	<i>neo</i> -Inositol (1.25)	41
2	D-Mannitol (1.6)	10	7	<i>neo</i> -Inositol hexaacetate (2.92)	42
3	<i>myo</i> -Inositol (1.1)	5	17	<i>neo</i> -Inositol (1.25)	43
4	<i>myo</i> -Inositol (1.1)	6	14	2.102	44
5	Bromobenzene (1.9)	7	17	<i>neo</i> -Inositol (1.25)	46
6	<i>p</i> -Benzoquinone (2.110)	6	10	<i>neo</i> -Inositol (1.25)	47
7	Aldehyde 2.116	7	8	<i>neo</i> -Inositol (1.25)	48
8	<i>myo</i> -Inositol (1.1)	6	68	<i>neo</i> -Inositol (1.25)	Present work

2.2.7. Synthesis of 5-deoxy-5-*myo*-inosamine.

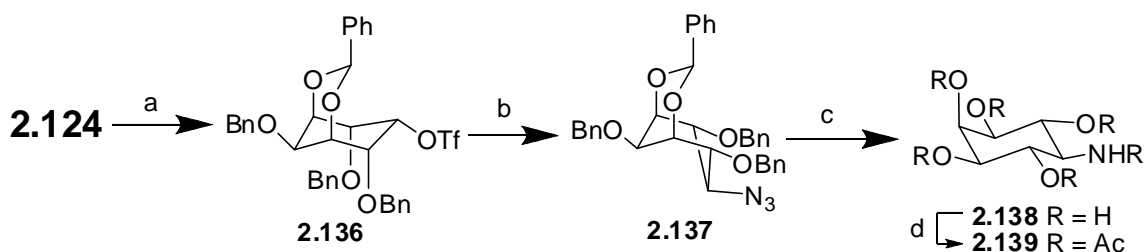
A survey of the literature showed that there is only one report on the synthesis of 5-deoxy-5-*myo*-inosamine acetic acid salt (**2.135**). The inosamine derivative **2.135** was synthesized (Scheme 2.29) from *cis*-1,2-diacetoxycyclohexa-3,5-diene (**2.127**) in an overall yield of 7% (7 steps).⁵⁰ Interest in the preparation of various aminocyclitols is perhaps because they are known to act as glycosidase inhibitors.⁵¹



Scheme 2.29: (a) NMO, OsO₄, DCM, 83%; (b) lipase from *Mucor miehei*, vinyl acetate in *t*-butyl methyl ether; (c) TsCl, Py, 94 %; (d) KOH, MeOH, 2 h, rt, Ac₂O, Py, 84%; (e) NaN₃, NH₄Cl, DMF; NH₄OH, MeOH, 78 %; (f) a) OsO₄, NMMO; Ac₂O, Py; (g) H₂, Pd-C; NH₄OH, MeOH (9:1), 98%.

2.2.8. Present work.

myo-Inosamine **2.138** was prepared from the protected *neo*-alcohol **2.136** (Scheme 2.30). Conversion of the *neo*-alcohol triflate **2.136** to the corresponding *myo*-azide **2.137** proceeded smoothly at room temperature (12 h). The azide **2.137** formed inclusion complex with DCM when crystallized from DCM-light petroleum by diffusion method in a closed container (see packing diagram of **2.137**, page 141). Reduction of the azide **2.137** as well as deprotection of the hydroxyl groups was achieved by hydrogenation in the presence of Pearlmann's catalyst. The crude 5-deoxy-5-*myo*-inosamine (**2.138**) obtained was isolated and characterized as its hexa acetate (**2.139**) in a good overall yield of 55 % (for 7 steps).



Scheme 2.30: (a) TiF_4 , Py, $-42\text{ }^\circ\text{C}$ -rt, 91% (b) NaN_3 , DMF, rt, 12 h, 88%; (c) H_2 (50 Psi), $\text{Pd}(\text{OH})_2\text{-C}$, TFA-EtOH, rt, 44 h; (d) Ac_2O , dry Py, rt, 40 h, 83% (two steps).

2.2.9. Attempted synthesis of 2-*neo*-inosamine (**2.140**).

2-*neo*-inosamine (**2.140**) was isolated by hydrolysis of an antibiotic ‘Hygromycin A’ (Figure 2.8, **2.141**, an inhibitor of bacterial ribosomal peptidyl transferase) produced by *Streptomyces hygroscopicus*⁵²

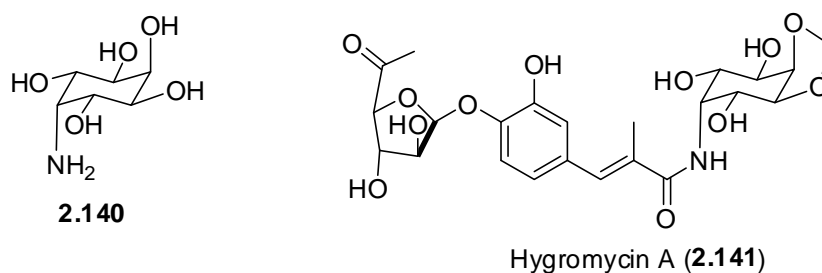
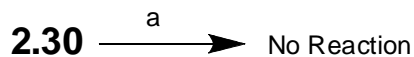


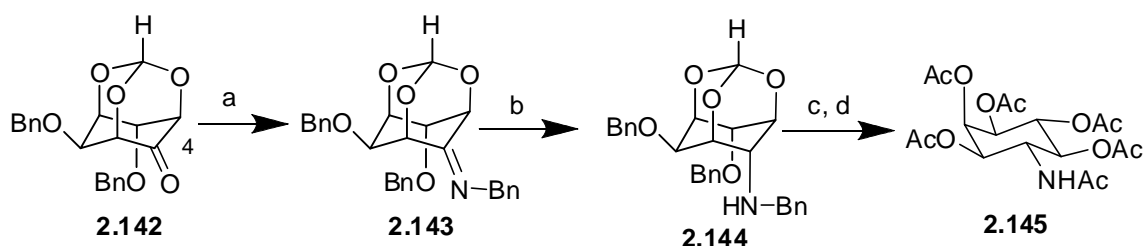
Figure 2.8: 2-*neo*-inosamine (**2.140**) and Hygromycin A (**2.141**).

However there is no reported synthesis of 2-*neo*-inosamine **2.140**. We attempted to prepare 2-*neo*-inosamine by Mitsunobu reaction of the *myo*-inositol derivative **2.30** (Scheme 2.31). However, in all the attempts, the starting alcohol was recovered.



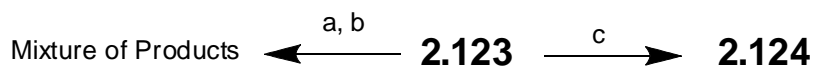
Scheme 2.31: PPh₃ (1.1 eq), DIAD (1.2 eq), 3 Å Mol. Sieves (powder, 2g / 1 mmol), THF, BnNH₂ (1.1 eq), rt, 2 days, reflux, 2 days.

We then attempted to prepare 2-*neo*-inosamine by the reductive amination of the ketone **2.123** used for the preparation of *neo*-inositol. This method (reductive amination of inosose) had earlier been used in our laboratory for the preparation of an inosamine (**2.145**), starting from *myo*-inositol-1,3,5-orthoformate (**1.15**).⁵³



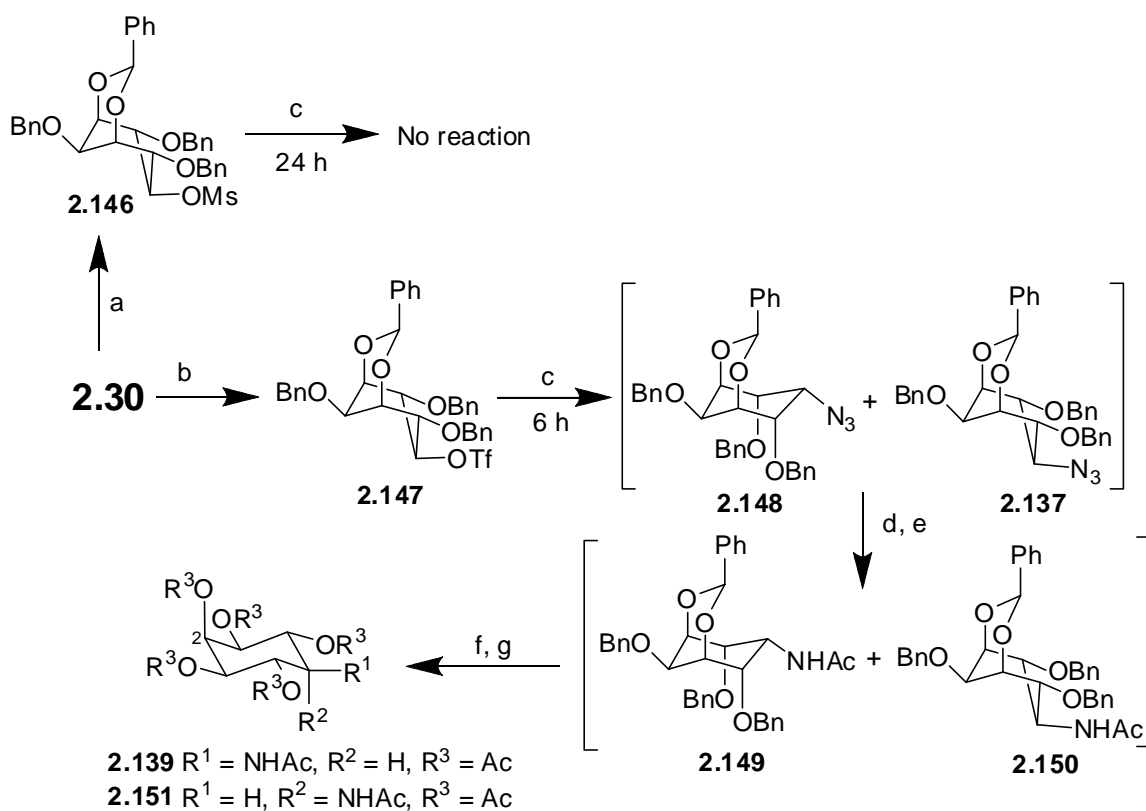
Scheme 2.32: (a) BnNH₂, MeOH, 50 °C, 3 h; (b) NaBH₃CN, rt, 1 h, 89%; (c) Pd(OH)₂-C, TFA-MeOH, H₂ (60 psi), rt, 8 h; (d) Ac₂O, Py, DMAP, rt, 12 h, 82%

Reductive amination of the ketone **2.123** with benzylamine and sodiumcyanoborohydride in methanol resulted in the formation of a mixture of several products as revealed by the ¹H-NMR spectrum of the corresponding acetates. No attempt was made to separate these products. When the reductive amination was carried out at low temperature (−41 °C), *neo*-alcohol **2.124** was obtained as the only product (Scheme 2.33).



Scheme 2.33: (a) BnNH₂, MeOH, rt, or reflux, 30 min.; (b) NaCNBH₃, rt, 1 h; (c) BnNH₂, NaCNBH₃, MeOH, −42 °C, 92 %.

We then attempted to prepare the desired inosamine **2.140** via the corresponding azide **2.148**. Attempted nucleophilic displacement reaction of the mesylate **2.146** with sodium azide was unsuccessful and the starting material was recovered. We then carried out substitution reaction on the triflate **2.147** with sodium azide in DMF at 100 °C. The ^1H and ^{13}C NMR spectra (see appendix, page 196) of the product suggested the presence of a mixture of azides. Lowering of the reaction temperature to 50 °C (30 h) also resulted in a mixture of azides while no reaction was observed at ambient temperature.



Scheme 2.34: (a) MsCl, Py, rt, 7 h; (b) TiF_2O , dry Py-dry DCM, rt, 2 h, 88%; (c) NaN_3 , DMF, 100 °C, 91%; (d) PPh_3 , THF, H_2O ; (e) Ac_2O , Py, rt, 6 h, 84% (2 steps); (f) H_2 (50 Psi), $\text{Pd}(\text{OH})_2\text{-C}$, EtOH, rt, 32 h; (g) Ac_2O , Py, rt, 45 h, 82%.

A comparison of the ^1H NMR spectrum of the mixture of azides with that of the bicyclic azide with the *myo*-configuration **2.137** (Scheme 2.30), showed that the *myo*-azide **2.137** was present in the mixture of azides. The ratio of the two diastereomeric azides (*neo* : *myo*) was estimated to be 1 : 0.46. It is interesting to see that the bicyclic

neo-triflate **2.136** undergoes clean S_N2 displacement reaction with sodium azide to give the *myo*-azide **2.137** exclusively, while the *myo*-triflate **2.147** under similar reaction conditions gives a mixture of *myo*- and the *neo*-azides.

From the result of the displacement reaction of the *neo*-triflate **2.136** with sodium azide, it appears there is enough room for the azide ion to attack the C5-carbon in an S_N2 fashion to yield the azide **2.137** with the *myo*-configuration. But in the reaction of the *myo*-triflate **2.147**, perhaps there is not enough room for the azide to attack the C5-carbon in an S_N2 fashion and hence the reaction proceeds by both S_N1 and S_N2 mechanism resulting in a mixture of products. Also, it is likely that the C4- and C6-oxygen atoms stabilize the carbonium ion formed at C-5 of **2.147** which makes the S_N1 path more facile (in the reaction of *myo*-triflate). While during the reaction of the *neo*-triflate since the C4- and C6-oxygen atoms are axial, they cannot stabilize the carbonium ion which makes the S_N2 path more facile. However, further work is essential to understand the reason for the observed difference in reactivity of the triflates **2.136** and **2.147** towards substitution by the azide ion.

Prior to obtaining the *myo*-azide **2.137** (Section 2.2.8), we were not sure whether the signals at δ 5.78 and 5.59 (page 196) due to the acetal hydrogen arose due to the presence of isomeric azides (mixture of **2.137** and **2.148** or **2.152** and **2.153**, Figure 2.9).

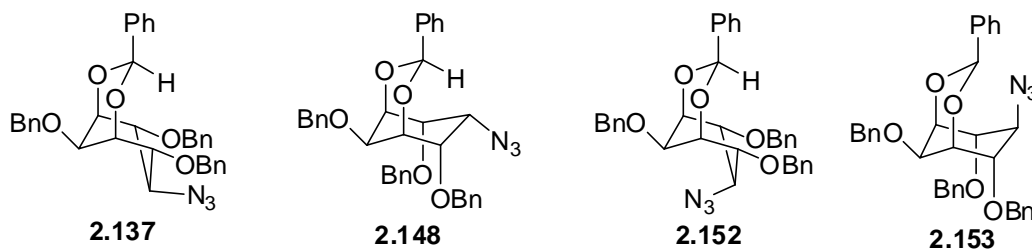


Figure 2.9.

Hence the mixture of azides **2.137** and **2.148** obtained as mentioned above was reduced to the corresponding amines with triphenylphosphine and water in THF and the amines obtained acetylated to afford the corresponding amides **2.149** and **2.150**. The

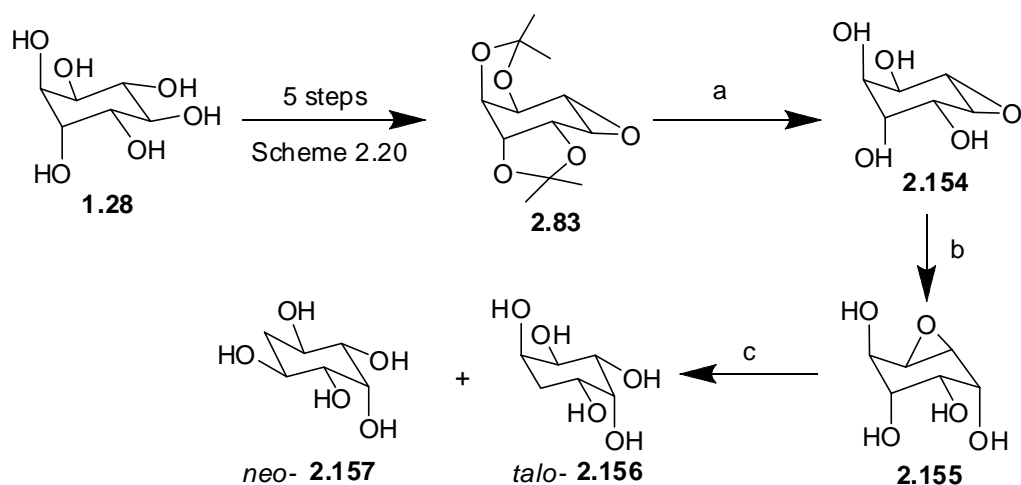
acetamides so obtained were subjected to hydrogenolysis in the presence of Pearlmann's catalyst and the resulting pentol was acetylated in pyridine to obtain hexaacetates **2.139** and **2.151**. The ^1H NMR spectra of the mixture of acetamides **2.149** and **2.150** (see Appendix, Page 197) as well as the hexaacetates **2.139** and **2.151** (see Appendix, Page 198) revealed the presence of isomeric inosamine derivatives (Scheme 2.34). This mixture of products could not be separated by chromatography.

2.2.10. De-oxy inositols (Quercitols).

Cyclohexane pentols or mono-deoxy inositols are called using a generic term, 'Quercitols'. Among the sixteen stereoisomers reported in the literature,⁵⁴ (+)-*proto*-, (-)-*proto*- and (-)-*vibo*- quercitols occur in nature.⁵⁵ The biological activity shown by some of these quercitols against glycosidases led to an interest in the synthesis of natural and unnatural quercitols as well as their derivatives / analogs.

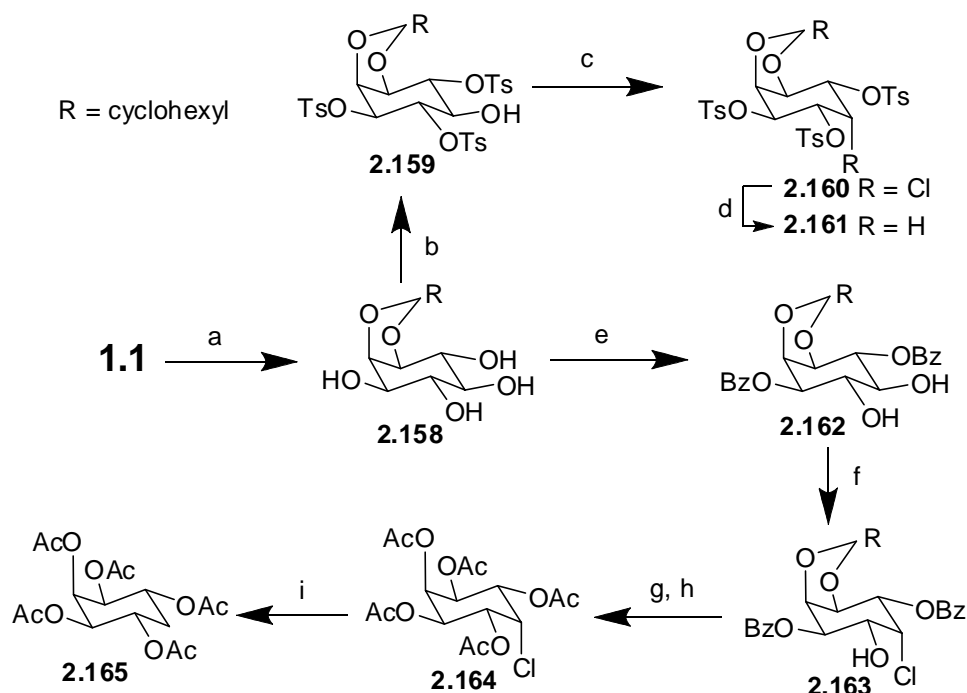
2.2.11. *neo*-quercitol.

neo-Quercitol (**2.157**) was formed in trace amount during the synthesis of *talo*-quercitol (Scheme 2.35) from the *neo*-epoxide **2.156**.⁵⁴



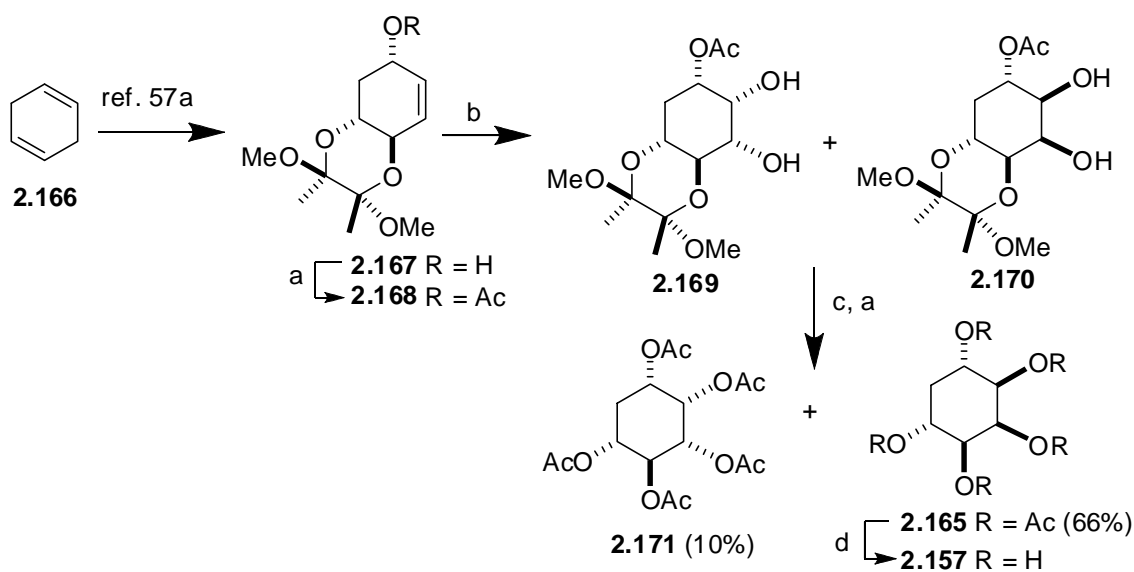
Scheme 2.35: (a) 50% AcOH, 100 °C, 30 min.; (b) aq. Ba(OH)₂, rt; (c) H₂, Raney Ni.

Ogawa et al⁵⁶ reported the synthesis of *neo*-quercitol hexa acetate (**2.165**) from *myo*-inositol in an overall yield of < 1%.



Scheme 2.36: (a) Cyclohexanone, benzene, TsOH; (b) TsCl, Py; (c) SO₂Cl₂, Py, 76 %; (d) Bu₃SnH, toluene, 55 %; (e) 1eq BzCl, Py, -5 °C - 0 °C, overnight, 4 %; (f) SO₂Cl₂, Py, 62 %; (g) H⁺-H₂O; (h) Ac₂O, Py, 87 %; (i) Bu₃SnH, AIBN, toluene, 77 %.

Shih *et. al.* reported the synthesis of *neo*-quercitol (**2.157**) from 1,4- cyclohexadiene (**2.166**) in an overall yield of 27 % (Scheme 2.37).⁵⁷



Scheme 2.37: (a) Ac₂O, Py; (b) 1.5 eq. KMnO₄, 1.5 eq. MgSO₄, EtOH, H₂O, rt; (c) 80 % aq. TFA; (d) 7 N NH₃ - MeOH, 88 %.

2.2.12. Di-deoxy inositol or cyclohexane tetrol.

Synthesis of a few racemic-di-deoxy *myo*-inositols (or cyclohexane tetrols, **2.172-2.174**) have been reported in the literature.⁵⁸

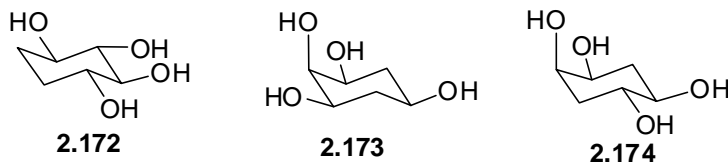
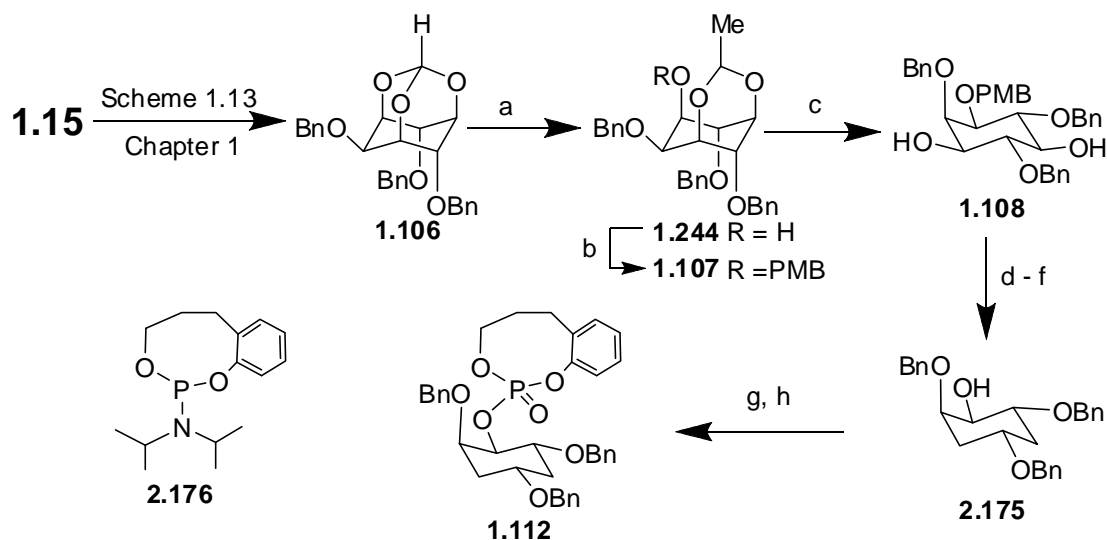


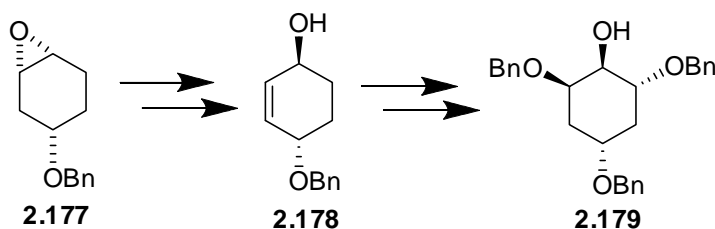
Figure 2.10

Schlewer *et. al.*⁵⁹ reported the synthesis of 3, 5-dideoxy mono phosphorylated *myo*-inositol (**1.112**) in an overall yield of 20 % (10 steps) from *myo*-inositol (Scheme 2.38) and used it as an inhibitor of *myo*-inositol monophosphatase. There is no report on the synthesis of 1(3), 5-dideoxy-*myo*-inositol (**2.184**) so far. Although its 2,4,6-tri-*O*-benzyl ether **2.175** is reported, its preparation and characterization data are not published.⁵⁹



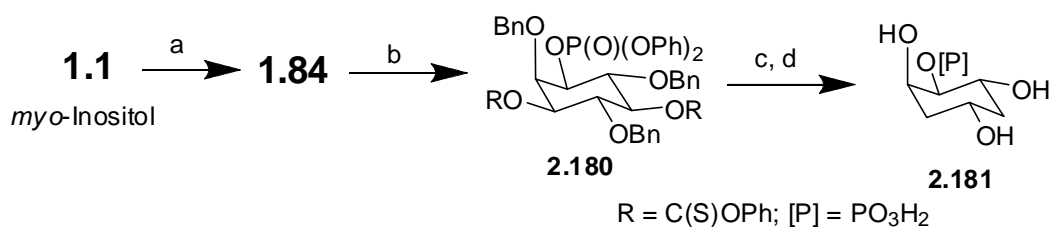
Scheme 2.38: (a) Me_3Al (8 eq.), DCM, 0 °C (3 h) - rt (4 h), 87%; (b) NaH (3 eq.), PMBCl (2 eq.), DMF, rt 4 h, 98%; (c) TFA, EtOH- H_2O , reflux, 2 h, 93%; (d) NaH, THF, CS_2 , MeI, 15 h, 91%; (e) Bu_3SnH , AIBN, Toluene, reflux, 6 h, 68%; (f) HCl (3 N), MeOH, reflux, 30 min., 93%; (g) **2.176**, 1*H*-tetrazole, DCM, rt; (h) *m*-CPBA, DCM, rt, 15 min, 70%.

Optically active tribenzyl ether of 3,5-dideoxy-*myo*-inositol **2.179** was obtained from the cyclohexane epoxide **2.177** (Scheme 2.39).⁶⁰



Scheme 2.39

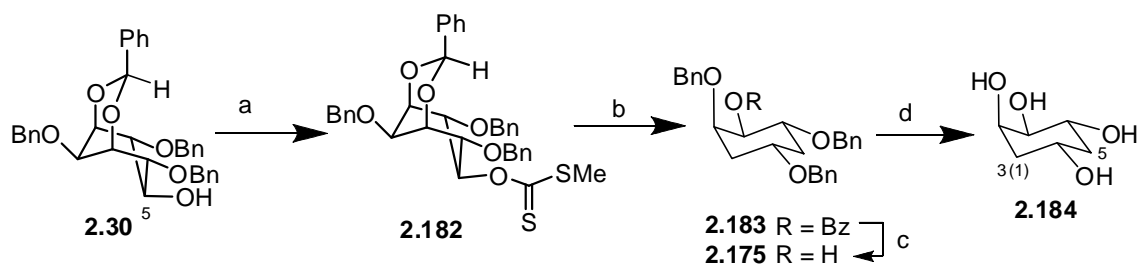
Miller *et. al.*⁶¹ reported the synthesis of dideoxy inositol phosphate (**2.181**) in an overall yield of 14 % from *myo*-inositol. This phosphate was used to test the role of hydroxyl groups in binding of the substrate with mammalian IMPase. The hydroxyl group at 1-position was selectively (> 98% ee) phosphorylated using a peptide catalyst⁶² in good yield as shown in scheme 2.40.



Scheme 2.40: (a) Scheme 1.11, page 14, Chapter 1; (b) CIP(S)OPh, Py, DMAP, DCM, 48 h; (c) Bu₃SnH, AIBN, toluene, reflux; (d) Li, Liq. NH₃.

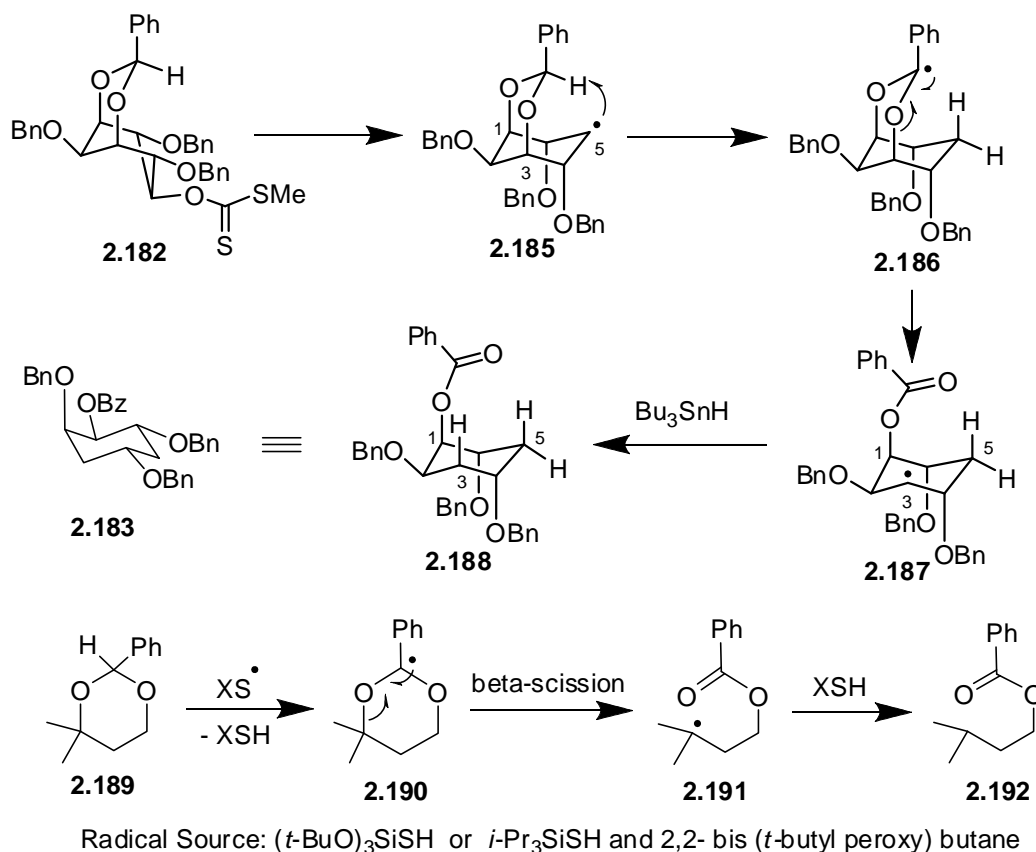
2.2.13. Present work.

We planned to prepare quercitols by the deoxygenation of suitably protected inositol derivatives. The alcohol **2.30** (Scheme 2.41) was converted to the corresponding xanthate (**2.182**) by reaction with carbon disulphide and methyl iodide in the presence of sodium hydride. The de-oxygenation was carried out under Barton reaction condition in toluene at 100 °C. Unexpectedly, the product obtained was 1(3),5-dideoxy inositol **2.183** instead of the C5-deoxygenated inositol derivative. The benzoate was deprotected completely to obtain the tetrol **2.184**.



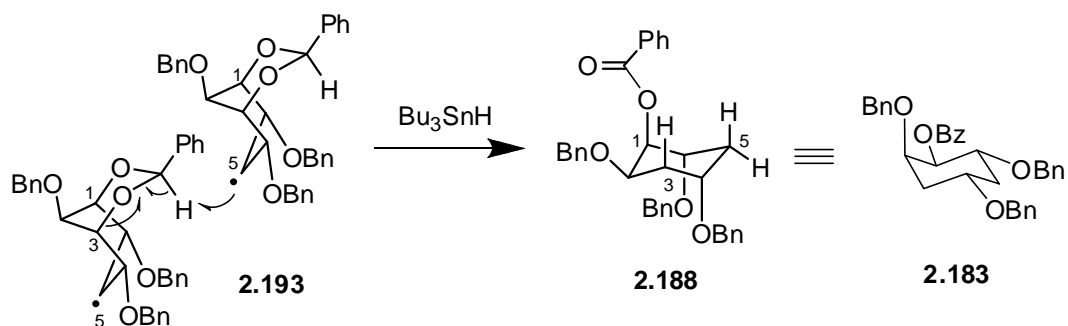
Scheme 2.41: (a) NaH (5 eq), THF, CS₂ (15 eq), reflux, 1 h, MeI (5eq), rt, 16 h, 98 %; (b) toluene, Bu₃SnH, AIBN, 100 °C, 1 h, 91 %; (c) *i*-BuNH₂, MeOH, rt, 12 h, 93%; (d) H₂ (55psi), Pd(OH)₂-C, EtOH, rt, 4 h, 84%.

The formation of the dideoxygenated product **2.183** and conversion of the benzylidene acetal to benzoate can be rationalized as shown in the scheme 2.42. Radical initiated cleavage of benzylidene acetals of 1,3-diols leading to the formation of benzoates has earlier been reported (scheme 2.42).⁶³



Scheme 2.42: Intramolecular hydrogen abstraction in benzylidene acetals.

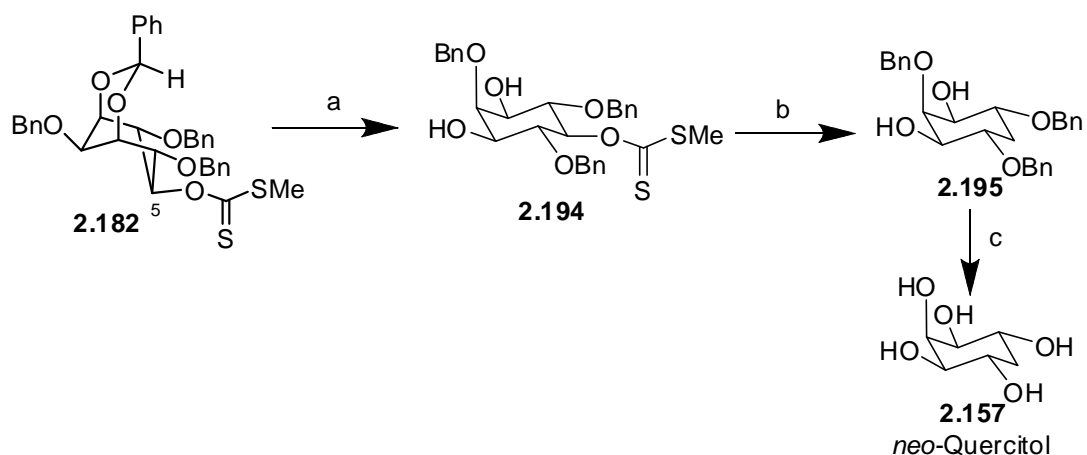
Although cleavage of the benzylidene acetal **2.185** via an intramolecular hydrogen abstraction is shown in the scheme 2.42, other routes shown in the scheme 2.43 are in principle possible. Formation of the benzylidene radical by Bu_3Sn radical (formed in the presence of AIBN) can be ruled out since the alcohol **2.30** was stable to the reaction conditions whereas deoxygenation occurred in the xanthate **2.182**. Further work is essential to rule out or rule in the intermolecular hydrogen abstraction pathway for the cleavage of the benzylidene acetal **2.193** shown in Scheme 2.43.



Scheme 2.43: Intermolecular H-abstraction by the radical.

2.2.14. *neo*-quercitol.

De-oxygenation of only the C5-oxygen could be achieved by first hydrolyzing the benzylidene acetal in **2.182** to obtain the corresponding xanthate diol **2.194** and subjecting the resulting xanthate to Barton de-oxygenation conditions. The benzyl ethers in the deoxy-derivative **2.195** were cleaved by hydrogenolysis to obtain *neo*-quercitol (**2.157**, Scheme 2.44). Hence dideoxylation or mono deoxygenation in the xanthate **2.182** can be achieved by carrying out the deoxygenation reaction prior to or subsequent to the hydrolysis of the benzylidene acetal respectively. *neo*-Quercitol was made in an overall yield of 67 % in 7 steps from *myo*-inositol. The yield in earlier reports did not exceed 27%.



Scheme 2.44: (a) TFA, THF-H₂O, rt, 24 h, 96 % (b) toluene, Bu₃SnH, AIBN, 100 °C, 1 h, 93 %; (c) H₂ (50psi), Pd(OH)₂-C, EtOH, rt, 6 h, 88 %.

2.3 Conclusion.

We have discovered a new method for the cleavage of benzyl ethers and acetals. This method of cleavage could have applications in the synthesis of inositol-derived end-products wherein other functional groups present in the required products do not allow reductive cleavage of benzyl ethers and acid catalyzed hydrolysis of acetals and orthoesters. The results presented in this chapter clearly show that *myo*-inositol-1,3,5-orthoester is a potential synthon for the preparation of isomeric inositol derivatives and has advantages over other protected derivatives of *myo*-inositol. The synthetic schemes reported in this chapter can also be tailored for the preparation of several phosphorylated as well as inositol ring modified derivatives.

2.4. Experimental.

General: All the solvents were purified according to the literature procedures⁶⁴ before use. 60 % dispersion of sodium hydride in mineral oil was used for *O*-alkylation reactions. All air or moisture sensitive reactions were conducted under argon or nitrogen atmosphere. All the palladium compounds used were obtained from Aldrich chemical Co. or Lancaster Synthesis. Thin layer chromatography was performed on E. Merck pre-coated 60 F₂₅₄ plates and the spots were rendered visible either by shining UV light or by charring the plates with concd. H₂SO₄. Column chromatographic separations and flash column chromatographic separations were carried out on silica gel 60-120 mesh and 230-400 mesh respectively, with solvent system as mentioned in experimental procedures. The compounds previously reported in the literature were characterized by comparison of their melting points and / or ¹H NMR spectra with reported data. IR spectra were recorded either in CHCl₃ solution or in Nujol or as thin film (neat) on a Shimadzu FTIR-8400 spectrophotometer. NMR spectra were recorded on Bruker AV200 spectrometer in deuterated solvents as mentioned in the experimental. Microanalytical data were obtained using a Carlo-Erba CHNS-0 EA 1108 elemental analyzer. All the melting points were recorded on a Büchi B-540 electro-thermal melting point apparatus. Yields refer to chromatographically and spectroscopically pure compounds. All the asymmetrically substituted *myo*-inositol derivatives reported are racemic; however, only one of the enantiomers shown in all the schemes. Triethylamine treated silicagel indicates that the silicagel was treated with Et₃N in light petroleum and the solvents were removed under reduced pressure. Work up of the residue / reaction mixture indicates washing of organic layer successively with water, 2% dil. HCl solution (when acid sensitive groups are not present), water, saturated sodium bicarbonate solution and water followed by brine.

Compounds **1.15**,^{2a} **1.16**,^{2b} **1.106**,¹³ **2.38**,^{45,71} **2.39**⁷⁰ were prepared as reported in the literature.

myo-inositol-1,3,5-orthobenzoate (1.17): *myo*-Inositol (**1.1**) (9.072 g, 50.40 mmol), trimethyl orthobenzoate (19.04 mL, 110.87 mmol) and *p*-toluenesulfonic acid (2.5 g, 14.51 mmol) in dry DMF (80 mL) were heated at 145-150 °C for 3.5 h. The clear solution obtained was allowed to cool to room temperature and triethylamine (2.02 mL) was added. The reaction mixture was concentrated under reduced pressure. The gummy residue obtained was purified by flash column chromatography to afford orthobenzoate **1.17** as a white solid. (eluent: 60% ethyl acetate - petroleum ether); yield: 12.45 g (93%).

Data for **1.17**:

Mp. = 210-211 °C; **IR** (nujol) ν : 3200-3450 cm^{-1} ; **¹H NMR** [200 MHz, (CD₃)₂SO] δ 7.51-7.67 (m, 2H), 7.30-7.45 (m, 3H), 5.57 (d, 2 \times OH, J = 6.2 Hz), 5.41 (d, 1 \times OH, J = 6.4 Hz), 4.37-4.53 (m, 2H), 4.16-4.31 (m, 3H), 4.12 (dt, 1H, Ins H, J = 6.2 Hz, 1.8 Hz) ppm; **¹³C NMR** [75.5 MHz, (CD₃)₂SO] δ 138.1 (C_{arom}), 129.3 (C_{arom}), 127.8 (C_{arom}), 125.8 (C_{arom}), 106.8 (PhCO₃), 76.1 (Ins C), 70.3 (Ins C), 67.6 (Ins C), 58.2 (Ins C) ppm; **Elemental analysis** calcd. for C₁₃H₁₄O₆: C, 58.64; H, 5.30. Found: C, 58.27; H, 5.33%.

2,4,6-tri-*O*-acetyl-*myo*-inositol-1,3,5-orthobenzoate (2.7): To an ice cooled solution of triol **1.17** (0.055g, 0.207 mmol) in dry pyridine (2 mL), acetic anhydride (0.2 mL, 2.12 mmol) was added and stirred at ambient temperature for 3 h. The solvent was removed under reduced pressure and the residue obtained was worked up with ethylacetate and dried over anhydrous sodium sulfate. The crude product was purified by column chromatography with 30 % ethylacetate in light petroleum as eluent to afford the triacetate **2.7** as a white solid (0.071 g, 87 %)

Data for **2.7**

Mp. = 168-171 °C; **IR** (CHCl₃) ν = 1751 cm^{-1} ; **¹H NMR** (CDCl₃, 500 MHz): δ 7.63-7.68 (m, 2H, Ar H), 7.33-7.39 (m, 3H, Ar H), 5.63 (t, 2H, Ins H, J = 3.2 Hz), 5.22-5.26 (m, 1H, Ins H), 4.70-4.74 (m, 1H, Ins H), 4.50-4.56 (m, 2H, Ins H), 2.19 (s, 3H, CH₃), 2.12 (s, 6H, 2 \times CH₃) ppm; **¹³C NMR** (CDCl₃, 125.7 MHz): δ 170.5 (C=O), 169.1 (C=O),

136.2 (C_{arom}), 129.7 (C_{arom}), 128.0 (C_{arom}), 125.3 (C_{arom}), 107.83 (PhCO₃), 70.4 (Ins C), 67.7 (Ins C), 67.1 (Ins C), 62.3 (Ins C), 20.9 (CH₃), 20.6 (CH₃) ppm; **Elemental analysis** calcd. for C₁₉H₂₀O₉: C, 58.16; H, 5.10; Found: C, 58.30; H, 4.95 %.

2,4,6-tri-O-methyl-myo-inositol-1,3,5-orthobenzoate (2.8): Sodium hydride (0.8 g, 20.0 mmol) was added to a cooled (0 °C) solution of **1.17**⁶⁵ (1.331 g, 5.0 mmol) in dry DMF (20 mL) and stirred for 15 min. Methyl iodide (1.86 mL, 29.88 mmol) was added to the stirred solution and stirring was continued for 45 min. Solvents were removed under reduced pressure and the crude reaction mixture was worked up with ethyl acetate. The gummy residue obtained was purified by column chromatography (eluent: 20% ethylacetate in petroleum ether) to obtain **2.8**¹ (1.514 g, 98%) as a white solid.

Data for **2.8**

Mp. = 121-123 °C; **¹H NMR** (CDCl₃, 500 MHz): δ 7.62-7.68 (m, 2H, Ar H), 7.31-7.36 (m, 3H, Ar H), 4.55-4.60 (m, 3H, Ins H), 4.28 (t, 2H, *J* = 4 Hz, Ins H), 3.68 (m, 1H, Ins H), 3.54 (s, 3H, CH₃), 3.50 (s, 6H, 2 × CH₃); **¹³C NMR** (CDCl₃, 125.8 MHz): δ 137.0 (C_{arom}), 129.3 (C_{arom}), 127.9 (C_{arom}), 125.3 (C_{arom}), 107.8 (PhCO₃), 76.0 (Ins C), 70.7 (Ins C), 68.4 (Ins C), 68.3 (Ins C), 57.8 (CH₃), 56.8 (CH₃) ppm; **Elemental analysis** calcd. for C₁₆H₂₀O₆: C, 62.33; H, 6.49. Found: C, 62.36; H, 6.76 %.

2,4,6-tri-O-Methyl-myo-inositol (2.23): A solution of **2.8** (0.309 g, 1.0 mmol) in methanol (5 mL) was hydrogenolyzed in the presence of 20% Pd(OH)₂-C (0.112 g, 0.16 mmol) at 55 psi. After 5 h, the reaction mixture was filtered over a short bed of Celite and Celite washed with methanol (10 mL). The combined methanol solution was evaporated under reduced pressure to obtain **2.23** as a white solid (0.22 g, 99%).

Data for **2.23**

Mp. = 192-193°C; **IR** (nujol): ν 3150-3550 cm⁻¹; **¹H NMR** (D₂O, 200 MHz): δ 3.65-3.71 (m, 1H, Ins H), 3.59-3.64 (m, 2H, Ins H), 3.58 (s, 3H, CH₃), 3.56 (s, 6H, 2 × CH₃), 3.19-3.43 (m, 3H) ppm; **¹³C NMR** (50.3 MHz, 0.75 mL D₂O + 0.03 mL CH₃OH): δ 83.5,

83.4, 73.8, 71.6, 62.8, 60.7 ppm; **Elemental analysis** calcd. for C₉H₁₈O₆: C, 48.64; H, 8.16. Found: C, 48.43; H, 8.24 %.

Birch reduction of 2,4,6-tri-*O*-methyl-*myo*-inositol-1,3,5-orthobenzoate (2.8): A mixture of orthobenzoate **2.8** (1.542 g, 5.0 mmol) and *tert*-butyl alcohol (0.53 mL, 5.54 mmol) in dry THF (7 mL) was taken in a clean and dry 250 mL three neck round bottomed flask. Ammonia (120 mL) was collected into the flask at -78 °C. Freshly cut sodium (0.46 g, 20 mmol) was added to the stirred solution and the reaction mixture turned to blue color. Stirring was continued for 3 h and the reaction mixture was quenched with solid ammonium chloride (5 g). Ammonia was allowed to evaporate at rt and the crude compound was extracted with methanol and purified by column chromatography with ethyl acetate-light petroleum (3:1) as eluent to afford trimethyl triol **2.23** as a white solid (0.951 g, 86%), Mp. = 188-191 °C.

Hydrolysis of 2,4,6-tri-*O*-methyl-*myo*-inositol-1,3,5-orthobenzoate (2.8): To a solution of orthobenzoate **2.8** (0.308 g, 0.99 mmol) in methanol (0.16 mL) and DCM (4 mL), acetyl chloride (0.29 mL, 4.08 mmol) was added at 0 °C and allowed to warm to rt. Water (0.2 mL) was added to the reaction mixture and stirred at rt for 54 h. The solvents were removed under reduced pressure and the diol **2.9** (0.345 g) obtained was acetylated with acetic anhydride (0.5 mL, 5.3 mmol) in dry pyridine (3 mL) at rt for 7 h. The solvents were removed under reduced pressure and the residue was worked up with ethylacetate. The crude product was purified by column chromatography using 40% ethyl acetate in light petroleum to afford the diacetate **2.10** (0.371 g, 90 %) as a white solid.

Data for **2.10**

Mp. = 163-166 °C; **IR** (CHCl₃): ν 1732, 1747, 1753 cm⁻¹; **¹H NMR** (CDCl₃, 300 MHz): δ 8.05-8.13 (m, 2H, Ar H), 7.40-7.65 (m, 3H, Ar H), 5.03-5.18 (m, 2H, Ins H), 4.87-4.99 (dd, 1H, Ins H, J = 2.17, 10.25 Hz), 3.51 (s, 3H, CH₃), 3.45 (s, 3H, CH₃), 3.44 (s, 3H, CH₃), 2.15 (s, CH₃), 2.14 (s, CH₃) ppm; **¹³C NMR** (CDCl₃, 50.3 MHz): δ 169.6 (C=O),

169.5 (C=O), 165.1 (C=O), 133.1 (C_{arom}), 129.4 (C_{arom}), 129.3 (C_{arom}), 128.3 (C_{arom}), 78.5 (Ins C), 78.3 (Ins C), 77.9 (Ins C), 73.1 (Ins C), 72.4 (Ins C), 61.4 (CH₃), 60.0 (CH₃), 59.8 (CH₃), 20.7 (CH₃) ppm; **Elemental analysis** calcd. for C₂₀H₂₆O₉: C, 58.53; H, 6.38. Found: C, 58.45; H, 6.38 %.

Racemic-2,4-di-O-methoxymethyl-6-O-benzyl-myo-inositol-1,3,5-orthobenzoate

(2.25): Sodium hydride (0.252 g, 6.30 mmol) was added to a cooled (0 °C) solution of triol **1.17** (1.598 g, 6.0 mmol) in dry DMF (24 mL) and stirred for 15 min. Benzyl bromide (0.71 mL, 6.0 mmol) was added to this solution and stirring was continued for 1 h at rt. To the same reaction mixture, sodium hydride (0.72 g, 18.0 mmol) was added at ice cold temperature and stirring was continued for 15 min. Methoxymethyl chloride (1.36 mL, 18.0 mmol) was then added and stirring was continued for 12 h.⁶⁶ Solvents were then removed under reduced pressure and the residue was worked up with ethyl acetate. The crude product was purified by flash column chromatography (eluent: 15% ethyl acetate in petroleum ether) to obtain **2.25** as a white solid (2.366 g, 89%).

Data for **2.25**

Mp. = 80-82 °C; **¹H NMR** (CDCl₃, 200 MHz): δ 7.60-7.70 (m, 2H, Ar H), 7.27-7.42 (m, 8H, Ar H), 4.69-4.87 (m, 5H), 4.41-4.66 (m, 6H), 4.24 (t, 1H, Ins H, *J* = 1.5Hz), 3.45 (s, 3H, CH₃), 3.42 (s, 3H, CH₃) ppm; **¹³C NMR** (CDCl₃, 50.3 MHz): δ 137.5 (C_{arom}), 137.0 (C_{arom}), 129.1 (C_{arom}), 128.2 (C_{arom}), 127.7 (C_{arom}), 127.5 (C_{arom}), 125.2 (C_{arom}), 107.6 (PhCO₃), 96.7 (CH₂), 95.5 (CH₂), 73.5 (Ins C), 73.3 (Ins C), 73.1 (Ins C), 72.4 (Ins C), 71.4 (CH₂), 69.1 (Ins C), 65.3 (Ins C), 55.6 (CH₃), 55.3 (CH₃) ppm; **Elemental analysis** calcd. for C₂₄H₂₈O₈: C, 64.85; H, 6.35. Found: C, 64.95; H, 6.31 %.

Hydrogenolysis of racemic-2,4-di-O-methoxymethyl-6-O-benzyl-myo-inositol-1,3,5-orthobenzoate (2.25): Method A: The benzyl ether **2.25** (0.222 g, 0.50 mmol) was hydrogenolyzed in ethylacetate (2.5 mL), in the presence of 20% Pd(OH)₂-C (0.06 g) at 55 psi. After 2 h, the reaction mixture was filtered over a short bed of Celite and the

solvent was concentrated. The crude product was purified by column chromatography using 15% ethyl acetate in light petroleum to obtain **2.26** as a gum (0.172 g, 97%).

Data for **2.26**

IR (nujol): ν 3350 - 3600 cm^{-1} ; **$^1\text{H NMR}$** (CDCl_3 , 200 MHz): δ 7.60-7.72 (m, 2H, Ar H), 7.30-7.42 (m, 3H, Ar H), 4.88 (s, 2H, CH_2), 4.79 (q, 2H, CH_2 , $J = 6.8$ Hz), 4.58-4.72 (m, 3H, Ins H), 4.50-4.56 (m, 1H, Ins H), 4.39-4.47 (m, 1H, Ins H), 4.19 (t, 1H, Ins H, $J = 1.8$ Hz), 3.54 (d, 1H, OH, $J = 9.6$ Hz), 3.47 (s, 3H, CH_3), 3.46 (s, 3H, CH_3) ppm; **$^{13}\text{C NMR}$** (CDCl_3 , 50.32 MHz): δ 136.7 (C_{arom}), 129.4 (C_{arom}), 127.9 (C_{arom}), 125.3 (C_{arom}), 107.2 (PhCO_3), 97.5 (CH_2), 95.3 (CH_2), 74.2 (Ins C), 72.5 (Ins C), 69.1 (Ins C), 67.9 (Ins C), 64.2 (Ins C), 56.4 (CH_3), 55.6 (CH_3) ppm; **Elemental analysis** calcd. for $\text{C}_{17}\text{H}_{22}\text{O}_8$: C, 57.62; H, 6.26. Found: C, 57.44; H, 5.95 %.

Method B: The compound **2.25** (0.51 g, 1.15 mmol) was hydrogenolyzed in methanol (6 mL), in the presence of 20% $\text{Pd}(\text{OH})_2\text{-C}$ (0.161 g) at 55 psi at rt. After 13 h, the reaction mixture was filtered over a short bed of Celite and Celite was washed with methanol (10 mL). The combined methanol solution was evaporated under reduced pressure and the gummy residue obtained was purified by flash column chromatography (eluent: 10 % methanol in ethyl acetate) to obtain the tetrol **2.34** as a white solid (0.285 g, 93 %).

Data for **2.34**

Mp. = 117-118 $^\circ\text{C}$; **IR** (nujol) ν : 3200 - 3500 cm^{-1} ; **$^1\text{H NMR}$** (Acetone- d_6 , 200 MHz): δ 4.74 - 4.86 (m, 4H, $2 \times \text{CH}_2$), 3.97 (t, 1H, Ins H, $J = 2$ Hz), 3.52-3.70 (m, 3H, Ins H), 3.43-3.46 (m, 1H, Ins H), 3.41 (s, 3H, CH_3), 3.40 (s, 3H, CH_3), 3.20-3.35 (m, 1H), 2.09 (s, 4H, $4 \times \text{OH}$) ppm; **$^{13}\text{C NMR}$** (Acetone- d_6 , 50.3 MHz): δ 98.7 (CH_2), 98.3 (CH_2), 82.0 (Ins C), 81.4 (Ins C), 74.9 (Ins C), 73.9 (Ins C), 71.8 (Ins C), 71.4 (Ins C), 55.83 (CH_3), 55.78 (CH_3) ppm; **Elemental analysis** calcd. for $\text{C}_{10}\text{H}_{20}\text{O}_8$: C, 44.77; H, 7.51. Found: C, 44.42; H, 7.27 %.

Method C: Hydrogenolysis of the compound **2.25** (0.51 g, 1.15 mmol) using excess of 20% Pd(OH)₂-C (0.64 g) as above gave **1.1** (0.204 g), which was characterized as its hexa-acetate **2.36**: the crude **1.1** was suspended in pyridine (6 mL) and acetic anhydride (1.95 mL, 20.667 mmol) was added at 0 °C and stirring was continued for 40 h at rt. The solvents were removed under reduced pressure and the residue was worked with dichloromethane. The crude product was purified by column chromatography afforded **2.36** as a white solid (0.469 g, 96%), **Mp.** = 210-212 °C (Lit.⁶⁷ **Mp.** = 211-212 °C).

Reaction of racemic 2,4-di-O-methoxymethyl-6-O-benzyl-myoinositol-1,3,5-orthobenzoate (2.25) with 20% Pd(OH)₂-C in methanol: A mixture of racemic **2.25** (0.222 g, 0.50 mmol) in methanol (3 mL) and 20% Pd(OH)₂-C (0.281 g) was stirred at rt for 7 d. The reaction mixture was filtered over a short bed of Celite and Celite was washed with methanol (10 mL). The combined methanol solution was evaporated under reduced pressure. The crude product was purified by column chromatography (eluent: 40% ethylacetate in petroleum ether) to obtain racemic **2.26** as a gum (0.17 g, 96%). This reaction could be carried out in shorter time (32 h) in refluxing methanol to afford racemic **2.26** (0.172 g, 97%).

Racemic-1,3,5,6-tetra-O-benzoyl-2,4-di-O-methoxymethyl-myoinositol (2.35): To an ice cooled solution of tetrol **2.34** (0.033 g, 0.123 mmol) in dry pyridine (1.5 mL), benzoyl chloride (0.14 mL, 1.21 mmol) and DMAP (5 mg) were added and stirred at ambient temperature for 40 h. Solvents were removed under reduced pressure and the residue was worked up with dichloromethane. The crude product was purified by column chromatography using 10% ethyl acetate in light petroleum to obtain tetrabenzoate **2.35** as a white solid (0.079 g, 94%).

Data for **2.35**

Mp. = 212-214 °C; **IR** (CHCl₃): ν 1730 cm⁻¹; **¹H NMR** (CDCl₃, 200 MHz): δ 7.8-8.14 (m, 8H, Ar H), 7.28-7.62 (m, 12H, Ar H), 6.22 (t, 1H, Ins H, *J* = 10.5), 5.76 (t, 1H, Ins H,

$J = 9.4$), 5.38-5.52 (m, 2H, Ins H), 4.54-4.82 (m, 6H, 2 Ins H, $2 \times \text{CH}_2$), 3.18 (s, 3H, CH_3), 3.00 (s, 3H, CH_3) ppm; ^{13}C NMR (CDCl_3 , 50.3 MHz): δ 165.8 (C=O), 165.44 (C=O), 165.39 (C=O), 165.2 (C=O), 133.4 (C_{arom}), 133.3 (C_{arom}), 133.2 (C_{arom}), 133.1 (C_{arom}), 129.7 (C_{arom}), 129.6 (C_{arom}), 129.3 (C_{arom}), 129.0 (C_{arom}), 128.9 (C_{arom}), 128.5 (C_{arom}), 128.3 (C_{arom}), 128.2 (C_{arom}), 97.8 (CH_2), 75.9 (Ins C), 74.1 (Ins C), 73.0 (Ins C), 72.5 (Ins C), 71.7 (Ins C), 70.3 (Ins C), 56.1 (CH_3) ppm; **Elemental analysis** calcd. for $\text{C}_{36}\text{H}_{36}\text{O}_{12}$: C, 66.66; H, 5.3. Found: C, 66.74; H, 5.14 %.

Reaction of *myo*-inositol-1,3,5-orthobenzoate (1.17) with $\text{Pd}(\text{OH})_2\text{-C}$ in methanol: A mixture of orthobenzoate triol **1.17** (0.133 g, 0.50 mmol) in methanol (3 mL) and 20% $\text{Pd}(\text{OH})_2\text{-C}$ (0.281 g) were stirred at rt for 8 days. The reaction mixture was filtered over a short bed of Celite and Celite washed with methanol (10 mL). The combined methanol solution was evaporated under reduced pressure. The residue obtained was purified by column chromatography (eluent: 10% methanol in ethylacetate) to obtain **1.204** as a white solid (0.132 g, 93%). **Mp.** = 236-239 °C (Lit.⁶⁸ Mp. 240-242 °C). Refluxing a solution of triol **1.17** (0.267 g, 1.0 mmol) in methanol (5 mL) in the presence of 20% $\text{Pd}(\text{OH})_2\text{-C}$ (0.562 g) for 9 h also afforded **1.204** (0.266 g, 94%).

Racemic-4-*O*-benzyl-*myo*-inositol-1,3,5-orthobenzoate (2.24): Sodium hydride (0.168 g, 4.2 mmol) was added to a cooled (0 °C) solution of the triol **1.17** (1.065 g, 4.0 mmol) in dry DMF (16 mL) and stirred for 15 min. To this solution, benzyl bromide (0.5 mL, 4.2 mmol) was added and stirring continued for 30 min at rt. Solvents were removed under reduced pressure and the residue was worked up with ethyl acetate. The gummy product obtained was purified by column chromatography (eluent: 40% ethylacetate in petroleum ether) to obtain the monobenzyl ether **2.24** as a white solid (1.363 g, 96%).

Data for **2.24**

Mp. = 86-88 °C; **IR** (CHCl_3): ν 3300-3600 cm^{-1} ; ^1H NMR (CDCl_3 , 200 MHz): δ 7.54-7.68 (m, 2H, Ar H), 7.25-7.49 (m, 8H, Ar H), 4.69 (q, 2H, CH_2 , $J = 12$ Hz), 4.50-4.62 (m,

2H, Ins H), 4.35-4.46 (m, 3H, Ins H), 4.15 (d, 1H, Ins H, $J = 10$ Hz), 3.75 (d, 1H, OH, $J = 10$ Hz), 3.23 (d, 1H, OH, $J = 11$ Hz) ppm; ^{13}C NMR (CDCl_3 , 50.3 MHz): δ 136.5 (C_{arom}), 135.8 (C_{arom}), 129.4 (C_{arom}), 128.6 (C_{arom}), 128.5 (C_{arom}), 127.8 (C_{arom}), 125.1 (C_{arom}), 107.1 (PhCO_3), 75.8 (Ins C), 73.7 (Ins C), 73.3 (Ins C), 72.6 (CH_2), 68.0 (Ins C), 67.5 (Ins C), 59.5 (Ins C) ppm; **Elemental analysis** calcd. for $\text{C}_{20}\text{H}_{20}\text{O}_6$: C, 67.40; H, 5.66. Found: C, 67.10; H, 5.72 %.

Reaction of racemic 4-*O*-benzyl-*myo*-inositol-1,3,5-orthobenzoate (2.24) with $\text{Pd}(\text{OH})_2\text{-C}$ in methanol: A mixture of the monobenzyl ether **2.24** (0.267 g, 0.75 mmol) in methanol (4 mL) and 20% $\text{Pd}(\text{OH})_2\text{-C}$ (0.420 g) were stirred at rt for 6 d. The reaction mixture was filtered over a short bed of Celite and Celite washed with methanol (10 mL). The combined methanol solution was evaporated under reduced pressure and the residue obtained was purified by column chromatography (eluent: 10% methanol in ethylacetate) to obtain **1.204** as a white solid (0.196 g, 92%); **Mp.** = 236-239 °C. When the above reaction of the monobenzyl ether **2.24** (0.179 g, 0.50 mmol) with 20% $\text{Pd}(\text{OH})_2\text{-C}$ (0.281g) was carried out in refluxing methanol (3.5 mL), the reaction was completed in 12 h to afford **1.204** (0.133 g, 93 %).

2,4,6-tri-*O*-benzyl-*myo*-inositol-1,3,5-orthobenzoate (2.29): Sodium hydride (1.92 g, 48.0 mmol) was added to an ice cooled (0 °C) solution of triol **1.17** (3.195 g, 12.0 mmol) in dry DMF (60 mL) and stirred for 15 min. To this solution, benzyl bromide (7.1 mL, 60.0 mmol) was added and stirred for 1 h at ambient temperature. The solvents were removed under reduced pressure and the residue was worked up with ethyl acetate. The crude product obtained was purified by column chromatography (eluent: 10% ethylacetate in petroleum ether) to obtain **2.29** as a white solid (6.288g, 98 %).

Data for **2.29**

Mp. = 83-85 °C (crystals obtained from ethylacetate and light petroleum at ~ 0 °C); ^1H NMR (CDCl_3 , 200 MHz): δ 7.60-7.71 (m, 2H, Ar H), 7.15-7.50 (m, 18H, Ar H), 4.37-

4.80 (m, 11H, 5 × Ins H, 3 × CH₂), 4.11 (t, 1H, Ins H, $J = 2$ Hz) ppm; ¹³C NMR (CDCl₃, 50.3 MHz): δ 137.9 (C_{arom}), 137.5 (C_{arom}), 137.1 (C_{arom}), 129.2 (C_{arom}), 128.2 (C_{arom}), 127.9 (C_{arom}), 127.7 (C_{arom}), 127.6 (C_{arom}), 127.4 (C_{arom}), 125.3 (C_{arom}), 107.7 (PhCO₃), 73.9 (Ins C), 71.7 (Ins C), 71.4 (CH₂), 71.0 (CH₂), 68.8 (Ins C), 66.0 (Ins C) ppm; **Elemental analysis** calcd. for C₃₄H₃₂O₆: C, 76.10; H, 6.00. Found: C, 75.76; H, 6.36 %.

4,6-di-*O*-benzyl-*myo*-inositol-1,3,5-orthobenzoate (2.27): LiH (0.134 g, 16.86 mmol) was added to triol **1.17** (1.064 g, 4.0 mmol) in dry DMF (15 mL) and stirred at rt for 1 h. Benzyl bromide (1.05 mL, 8.83 mmol) in dry DMF (5 mL) was added to the stirred solution drop wise and stirring continued for 12 h. The reaction mixture was quenched with ice cold water and worked up with dichloromethane. The crude product was purified by column chromatography with 30% ethylacetate in light petroleum to afford the dibenzyl ether **2.27** as a white solid (1.488 g, 83 %).

Data for **2.27**

Mp. = 65-67 °C; ¹H NMR (CDCl₃, 200 MHz): δ 7.56-7.69 (m, 2H, Ar H), 7.26-7.44 (m, 13H, Ar H), 4.67 (ABq, 4H, 2 × CH₂, $J = 11.5$ Hz), 4.54-4.58 (m, 1H, Ins H), 4.50 (t, 2H, Ins H, $J = 3.8$ Hz), 4.38-4.46 (m, 2H, Ins H), 4.20-4.33 (m, 1H, Ins H), 3.08 (d, 1H, OH, $J = 9.9$ Hz) ppm.

Reaction of 2,4,6-tri-*O*-benzyl-*myo*-inositol-1,3,5-orthobenzoate (2.29) with Pd(OH)₂-C in methanol: A solution of **2.29** (0.268 g, 0.50 mmol) in methanol (3 mL) and 20% Pd(OH)₂-C (0.526 g, 0.75 mmol) were refluxed for 40 h. The reaction mixture was filtered over a short bed of Celite and Celite washed with methanol (10 mL). The combined methanol solution was evaporated under reduced pressure and the residue obtained was purified by column chromatography (eluent: 10% methanol in ethylacetate) to obtain **1.204** as a white solid (0.121 g, 84%) **Mp.** = 235-238 °C (Lit.⁶⁸ Mp. 240-242 °C).

Reaction of *myo*-inositol-1,3,5-orthoacetate (1.16) with Pd(OH)₂-C in methanol: A solution of the triol **1.16**^{2b} (0.204 g, 1.0 mmol) in methanol (5 mL) and 20% Pd(OH)₂-C (0.562 g) were refluxed for 52 h. The reaction mixture was filtered over a short bed of Celite and Celite washed with methanol (10 mL). The combined methanol solution was evaporated under reduced pressure and the residue obtained was chromatographed (eluent: 10% methanol in ethylacetate) to obtain a mixture of *myo*-inositol monoacetates **2.37** (0.206 g, 93%) as revealed by the ¹H NMR spectrum; no attempt was made to separate them.

Reaction of *myo*-inositol-1,3,5-orthoformate (1.15) with Pd(OH)₂-C in methanol: A solution of the triol **1.15**^{2a} (0.19 g, 1.0 mmol) in methanol (5 mL) and 20% Pd(OH)₂-C (0.562 g) were refluxed for 32 h. The reaction mixture was diluted with distilled water (10 mL) and the catalyst was removed by filtration using a Whatman filter paper. The solvents were removed under reduced pressure and the residue obtained was acetylated with acetic anhydride (1.9 mL, 20.14 mmol) in dry pyridine (5 mL) for 40 h at rt. The solvents were removed under reduced pressure and worked up with dichloromethane. The crude product was purified by column chromatography (eluent: 35% ethyl acetate in petroleum ether) gave the hexa-acetate **2.36** as a white solid (0.41 g, 96%), **Mp.** = 210-212 °C (Lit.⁶⁷ Mp. 211-212 °C).

Reaction of 2,4,6-tri-*O*-benzyl-*myo*-inositol-1,3,5-orthoformate (1.106) with Pd(OH)₂-C in methanol: A solution of **1.106**¹³ (0.231 g, 0.50 mmol) in methanol (3 mL) and 20% Pd(OH)₂-C (0.528 g, 0.75 mmol) were refluxed for 72 h. The reaction mixture was diluted with distilled water (10 mL) and the catalyst was removed by filtration using a short bed of Celite and Celite washed with distilled water (10 mL). The solvents were removed under reduced pressure to obtain **1.1** as a white solid (0.087g, 96 %), **Mp.** = 221-223 °C (Lit.⁶⁹ Mp = 224-225 °C).

Reaction of racemic-1,2:4,5-di-isopropylidene-3,6-di-*O*-benzyl-*myo*-inositol (2.39) with Pd(OH)₂-C in methanol: A mixture of **2.39**⁷⁰ (0.049 g, 0.11 mmol) and 20% Pd(OH)₂-C (0.078 g, 0.11 mmol) in methanol (1 mL) was refluxed for 22 h. The reaction mixture was diluted with water (2 mL) and filtered over a short bed of Celite and Celite washed with water (5 mL). The solvents were evaporated under reduced pressure to obtain **1.1** as a white solid (0.019 g, 95 %).

Reaction of racemic-1,2 : 4,5-di-isopropylidene-*myo*-inositol (2.38) with Pd(OH)₂-C in methanol: A mixture of **2.38**^{45, 71} (0.065 g, 0.25 mmol) and 20% Pd(OH)₂-C (0.175 g, 0.25 mmol) in methanol (3 mL) was refluxed for 8 h, when TLC analysis of the reaction mixture showed the absence of ketal **2.38**. The ketal **2.38** was added (0.065 g for every 8 h) to the same reaction mixture and the refluxing was continued. This addition of **2.38** was repeated ten times at the end of which the reaction mixture was diluted with distilled water (5 mL) and the catalyst was filtered using a short bed of Celite. The solvents were removed under reduced pressure to obtain **1.1** as a white solid (0.436 g, 97 %); **Mp.** = 223-224 °C.

Cyclohexyl benzyl ether (2.42): Sodium hydride (0.48g, 12.0 mmol) was added to a solution of cyclohexanol (**2.43**, 1.004 g, 10.02 mmol) in dry THF (20 mL) at 0 °C and stirring was continued for 1 h. Benzyl bromide (2.05 g, 1.43 mL, 12.02 mmol) was added to the solution and stirred for 4 h. The solvent was removed under reduced pressure and worked up with chloroform. The crude product obtained was purified by column chromatography using 10% ethyl acetate in petroleum ether as eluent to obtain **2.42** as a thick liquid (1.78 g, 93%).

Data for **2.42**

¹H NMR (200 MHz, CDCl₃) = δ 7.23-7.38 (m, 5H, Ar H), 4.54 (s, 2H, CH₂), 3.25-3.44 (m, 1H, CH), 1.89-2.04 (m, 2H, CH₂), 1.65-1.83 (m, 2H, CH₂), 1.15-1.56 (m, 6H, 3 × CH₂) ppm; ¹³C NMR (CDCl₃, 50.3 MHz): δ 139.3 (C_{arom}), 128.2 (C_{arom}), 127.4 (C_{arom}),

127.2 (C_{arom}), 76.8 (CH), 69.6 (CH_2), 32.2 (CH_2), 25.8 (CH_2), 24.0 (CH_2) ppm;

Elemental analysis calcd. for $\text{C}_{13}\text{H}_{18}\text{O}$: C, 82.06; H, 9.53. Found: C, 81.95; H, 9.80 %.

Reaction of cyclohexyl benzyl ether (2.42) with 20% $\text{Pd}(\text{OH})_2\text{-C}$ in methanol : A mixture of benzyl ether **2.42** (0.195 g, 1.03 mmol) and 20% $\text{Pd}(\text{OH})_2\text{-C}$ (0.359 g, 0.51 mmol) in methanol (5 mmol) was refluxed for 10 h under argon atmosphere. The reaction mixture was allowed to cool to room temperature and the catalyst was filtered using a short bed of Celite. The catalyst was washed with methanol (2×5 mL) and the crude product obtained was purified by column chromatography (10% ethyl acetate in petroleum ether) to obtain cyclohexanol (**2.43**) as a colourless liquid (0.086 g, 84%).

Reaction of cyclohexyl benzyl ether (2.42) with $\text{Pd}(\text{OAc})_2$ in methanol: A mixture of benzyl ether **2.42** (0.048 g, 0.25 mmol) and $\text{Pd}(\text{OAc})_2$ (0.028 g, 0.13 mmol) in methanol (5 mL) was refluxed for 40 h. The product (cyclohexanol, **2.43**) (19, 0.021 g, 83%) was isolated as above.

1,3-*O*-benzylidene-2,4,6-tri-*O*-benzyl-myco-inositol (2.30): 1 M solution of DIBAL- H^{17} in toluene (4 mL, 4.0 mmol) was added drop wise over a period of 15 min. to a solution of **2.29** (1.073 g, 2.0 mmol) in dry dichloromethane (16 mL) at 0 °C and stirred at ambient for 2 h. The reaction mixture was poured into a rapidly stirred solution of saturated aq. Na / K tartrate (10 mL) and ammonium chloride (10 mL) and stirred for 12 h. The mixture was extracted with ethylacetate (2×100 mL) and usual workup followed by column chromatography (ethylacetate : dichloromethane : petroleum ether = 1 : 1 : 8) afforded **2.30** (1.05 g, 97 %) as a gummy compound which was converted to solid upon cooling.

Data for **2.30**

Mp. = 102-104 °C (crystallized from a solution of dichloromethane and light petroleum ether cooled to 0 °C); **IR** (neat) $\nu = 3452$ cm^{-1} ; **$^1\text{H NMR}$** (CDCl_3 , 200 MHz): δ 7.49-7.61

(m, 2H, Ar H), 7.27-7.46 (m, 18H, Ar H), 5.72 (s, 1H, PhHCO₂), 4.72 (s, 2H, CH₂), 4.70 (AB q, 2 × CH₂, *J* = 11.8 Hz), 4.41 (d, 2H, Ins H, *J* = 2 Hz), 3.95-4.07 (m, 2H, Ins H), 3.74-3.87 (m, 1H, Ins H), 3.62 (t, 1H, Ins H, *J* = 2.4 Hz), 2.50 (d, 1H, OH, *J* = 2.7 Hz) ppm; ¹³C NMR (CDCl₃, 50.3 MHz): δ 137.9 (C_{arom}), 137.8 (C_{arom}), 137.3 (C_{arom}), 129.3 (C_{arom}), 128.4 (C_{arom}), 128.3 (C_{arom}), 128.2 (C_{arom}), 127.9 (C_{arom}), 127.8 (C_{arom}), 127.6 (C_{arom}), 126.5 (C_{arom}), 92.7 (PhHCO₂), 81.5 (Ins C), 73.5 (Ins C), 73.4 (Ins C), 71.6 (CH₂), 70.6 (CH₂), 68.1 (Ins C) ppm; **Elemental analysis** calcd. for C₃₄H₃₄O₆: C, 75.82; H, 6.36. Found: C, 75.80; H, 6.40 %.

1,3-*O*-benzylidene-2,4,6-tri-*O*-benzyl-5-*O*-acetyl-*myo*-inositol (2.31): Ac₂O (0.36 mL, 3.82 mmol) was added to an ice cooled solution of alcohol **2.30** (0.512 g, 0.95 mmol) in dry pyridine (5 mL) and stirring continued for 4 h at ambient temperature. Solvent was removed under reduced pressure and the gummy residue obtained was worked up with ethylacetate followed by drying over anhy. sodiumsulfate. The crude product was purified by column chromatography with 15 % ethyl acetate in light petroleum to afford acetate **2.31** as a white solid (0.535 g, 96 %).

Data for **2.31**

Mp. = 126-127 C (crystallized from ethylacetate and light petroleum); **IR** (CHCl₃) *ν* = 1747 cm⁻¹; ¹H NMR (CDCl₃, 500 MHz): δ 7.50-7.57 (m, 2H, Ar H), 7.26-7.48 (m, 18 H, Ar H), 5.74 (s, 1H, PhCHO₂), 5.19 (t, 1H, Ins H, *J* = 5.2 Hz), 4.65-4.77 (m, 4H, 2 × CH₂), 4.38-4.53 (m, 4H, 1 × CH₂), 2 × Ins H), 3.97 (d, 2 H, Ins H, *J* = 4.0 Hz), 3.76 (t, 1H, Ins H, *J* = 3.8 Hz), 1.98 (s, 1H, CH₃) ppm; ¹³C NMR (CDCl₃, 125 MHz): δ 169.5 (C=O), 137.9 (C_{arom}), 137.7 (C_{arom}), 137.1 (C_{arom}), 129.2 (C_{arom}), 128.3 (C_{arom}), 128.25 (C_{arom}), 128.19 (C_{arom}), 127.84 (C_{arom}), 127.80 (C_{arom}), 127.61 (C_{arom}), 127.58 (C_{arom}), 126.4 (C_{arom}), 92.71 (PhHCO₂), 78.9 (Ins C), 73.31 (Ins C), 73.25 (Ins C), 70.9 (CH₂), 70.7 (CH₂), 68.0 (Ins C), 20.9 (CH₃) ppm; **Elemental analysis** calcd. for C₃₆H₃₆O₇: C, 74.46; H, 6.25; Found: C, 74.22; H, 6.12 %.

1,3-O-benzylidene-2,4,6-tri-O-benzyl-5-O-methyl-myoinositol (2.80): Sodium hydride (0.040 g, 0.10 mmol) was added to a solution of **2.30** (0.480 g, 0.89 mmol) in dry DMF (3 mL) and stirred for 30 min. The mixture was cooled to 0 °C and methyl iodide (0.08 mL, 1.28 mmol) was added drop wise and the mixture stirred for 1 h at rt. The reaction mixture was concentrated under reduced pressure and worked up with chloroform. Column chromatography (10% ethylacetate in petroleum ether) of the residue obtained after evaporation of chloroform afforded the methyl ether of **2.80** as a solid (0.481g, 98%).

¹H NMR (CDCl₃, 200 MHz): δ 7.50-7.55 (m, 2H, Ar H), 7.25-7.47 (m, 18H, Ar H), 5.74 (s, 1H, PhHCO₂), 4.71 (s, 2H, CH₂), 4.67 (ABq, 4H, 2 × CH₂, *J* = 11.6 Hz), 4.37 (d, 2H, Ins H, *J* = 2 Hz), 4.02 (d, 2H, Ins H, *J* = 7 Hz), 3.63-6.56 (m, 4H, Ins H, CH₃), 3.44 (t, 1H, Ins H, *J* = 7 Hz) ppm; **¹³C NMR** (CDCl₃, 50.3 MHz): δ 138.0 (C_{arom}), 137.8 (C_{arom}), 137.5 (C_{arom}), 129.2 (C_{arom}), 128.3 (C_{arom}), 128.2 (C_{arom}), 127.7 (C_{arom}), 127.6 (C_{arom}), 126.4 (C_{arom}), 92.8 (PhHCO₂), 83.5 (Ins C), 82.3 (Ins C), 73.2 (Ins C), 71.4 (CH₂), 70.6 (CH₂), 68.2 (Ins C), 59.7 (CH₃) ppm; **Elemental analysis** calcd. for C₃₅H₃₆O₆: C, 76.06; H, 6.56; Found: C, 76.21; H, 6.43 %.

5-O-Methyl-myoinositol (Sequoyitol, 2.79): A mixture of the methyl ether of **2.80** (0.280 g, 0.53 mmol) obtained above and 20% Pd(OH)₂-C (0.0554 g, 0.79 mmol) in methanol (5 mL) was refluxed in argon atmosphere for 20 h. The reaction mixture was allowed to cool to rt and diluted with 3 mL of water. The catalyst was filtered using a short bed of Celite and Celite washed with water (2 × 3 mL). The crude product obtained by evaporation of the filtrate, was dissolved in methanol and water mixture (3:1) and cooled in a freezer to obtain colorless crystals of **2.79** (0.096 g, 94%, two crops).

Data for **2.79**

Mp. = 237-239 °C (Lit.⁷² Mp. = 238-239 °C); **¹H NMR** (D₂O, 500 MHz): δ 4.05 (t, 1H, Ins H, *J* = 3 Hz), 3.71 (t, 2H, Ins H, *J* = 10 Hz), 3.60 (s, 3H, CH₃), 3.55 (dd, 2H, Ins H, *J*

= 3 Hz, 10 Hz), 3.07 (t, 1H, Ins H, $J = 10$ Hz); ^{13}C NMR (50.3 MHz, 0.75 mL D_2O + 0.03 mL methanol): δ 84.8 (Ins C), 72.6 (Ins C), 72.3 (Ins C), 71.7 (Ins C), 60.2 (CH_3) ppm.

1,3-*O*-benzylidene-2,4,6-tri-*O*-benzyl-5-*myo*-inosose (2.123): Method A: To a cooled (-78 °C) solution of oxalyl chloride (0.567 g, 4.47 mmol) in dry dichloromethane (12 mL), a solution of dry dimethyl sulfoxide (0.627 g, 8.03 mmol) in dry dichloromethane (8 mL) was added drop-wise and the reaction mixture was stirred for 15 min. A solution of the alcohol **2.30** (2.154g, 4 mmol) in dry dichloromethane (12 mL) was added drop-wise and stirring was continued for 1 h. Dry triethylamine (2.262 g, 22.3 mmol) was then added to the reaction mixture and allowed to warm to room temperature slowly. The reaction mixture was worked up with dichloromethane and dried over anhydrous sodium sulfate. The solvent was removed under reduced pressure and the crude product was purified by column chromatography using triethylamine treated silicagel (eluent: 10 % ethyl acetate in light petroleum) to afford the ketone **2.123** as a white solid (1.684g, 78%).

Data for **2.123**

Mp. = 107-110 °C; **IR** (CHCl_3) $\nu = 1717$ cm^{-1} ; **^1H NMR** (CDCl_3 , 200 MHz): δ 7.40-7.52 (m, 2H, Ar H), 7.17-7.39 (m, 18H, Ar H), 5.67 (s, 1H, PhCHO_2), 4.65-4.80 (m, 4H, $2 \times \text{CH}_2$), 4.45-4.62 (m, 4H, CH_2), 4.25 (t, 1H, Ins H, $J = 2.1$ Hz), 4.17 (d, 2H, Ins H, $J = 4$ Hz) ppm; **^{13}C NMR** (CDCl_3 , 50.3 MHz): δ 200.9 (C=O), 137.8 (C_{arom}), 137.7 (C_{arom}), 136.5 (C_{arom}), 129.4 (C_{arom}), 128.4 (C_{arom}), 128.3 (C_{arom}), 128.2 (C_{arom}), 128.0 (C_{arom}), 127.8 (C_{arom}), 127.6 (C_{arom}), 126.2 (C_{arom}), 93.8 (PhCHO_2), 79.2 (Ins C), 73.6 (Ins C), 71.8 (CH_2), 70.9 (CH_2), 66.4 (Ins C) ppm; **Elemental analysis** calcd. for $\text{C}_{34}\text{H}_{32}\text{O}_6$: C, 76.1; H, 6.01; Found: C, 76.34; H, 5.96 %.

Method B: A mixture of the alcohol **2.30** (2.69 g, 5 mmol), PDC (2.818 g, 7.5 mmol) and 3Å molecular sieves (powder, 5 g) in dry dichloromethane (10 mL) was stirred at rt. for

22 h. Celite (10 g) was added to the stirred reaction mixture and the solvent evaporated under reduced pressure to obtain a free flowing solid. The solid was packed over a short column of Celite and eluted with dry diethyl ether (3×150 mL). The combined organic portions were concentrated under reduced pressure to obtain the crude ketone **2.123** (2.71 g). The ketone was reduced with sodium borohydride in the next step. Crystals of the pure ketone **2.123** could be obtained by crystallization either from methanol or from DCM - light petroleum mixture at low temperature (~ 0 °C); **Mp.** = 106-108 °C

1,3-O-benzylidene-2,4,6-tri-O-benzyl-neo-inositol (2.124): The crude ketone **2.123** (2.71 g) was dissolved in THF (5 mL) and diluted with methanol (20 mL) and cooled to 0 °C. To this solution, sodium borohydride (0.57 g, 15.07 mmol) was added in one lot and stirred for 1 h at ambient temperature. TLC analysis of the reaction mixture showed the absence of the starting material. The solvents were removed under reduced pressure and the gummy residue obtained was worked up dichloromethane. The combined organic extracts were concentrated to obtain a gummy residue which was purified by column chromatography [eluent = ethyl acetate : dichloromethane : light petroleum (1:1:8)] to afford the alcohol **2.124** as a white solid (2.52 g, 94%).

Data for **2.124**

Mp. = 98-102 °C; **IR** (CHCl_3) $\nu = 3332\text{-}3593$ cm^{-1} ; **$^1\text{H NMR}$** (CDCl_3 , 200 MHz): δ 7.47-7.59 (m, 2H, Ar H), 7.16-7.44 (m, 18H, Ar H), 5.81 (s, 1H, PhCHO_2), 4.55-4.76 (m, 6H, $3 \times \text{CH}_2$), 4.27-4.49 (m, 3H, Ins H), 4.04-4.13 (m, 3H, Ins H), 3.22 (d, 1H, OH, $J = 11.0$ Hz) ppm; **$^{13}\text{C NMR}$** (CDCl_3 , 50.3 MHz): δ 139.5 (C_{arom}), 138.2 (C_{arom}), 137.7 (C_{arom}), 129.3 (C_{arom}), 128.4 (C_{arom}), 128.3 (C_{arom}), 127.82 (C_{arom}), 127.79 (C_{arom}), 127.6 (C_{arom}), 127.53 (C_{arom}), 126.9 (C_{arom}), 126.5 (C_{arom}), 95.4 (PhCHO_2), 78.7 (Ins C), 73.9 (CH_2), 71.0 (Ins C), 70.4 (CH_2), 67.7 (Ins C), 65.4 (Ins C) ppm; **Elemental analysis** calcd. for $\text{C}_{34}\text{H}_{34}\text{O}_6$: C, 75.82; H, 6.36; Found: C, 75.84; H, 6.49 %.

1,3-O-benzylidene-2,4,6-tri-O-benzyl-5-O-acetyl-neo-inositol(2.125): Acetic anhydride (0.216 g, 2.12 mmol) was added drop-wise to an ice cooled solution of the alcohol **2.124** (0.115 g, 0.21 mmol) in dry pyridine (2 mL) and stirred at ambient temperature for 4 h. The solvent was removed under reduced pressure and the crude reaction mixture was worked up with ethyl acetate and dried over anhydrous sodium sulphate. The solvents were removed under reduced pressure to obtain a gummy residue which was purified by column chromatography (eluent: 15% ethyl acetate in light petroleum) to afford the acetate **2.125** as a white solid (0.111g, 89%).

Data for **2.125**

Mp. = 119-120 °C (crystals obtained from dichloromethane light petroleum mixture);

IR (CHCl₃) (ν) = 1742 cm⁻¹; **¹H NMR** (CDCl₃, 200 MHz): δ 7.48-7.59 (m, 2 H, Ar H), 7.25-7.44 (m, 18 H, Ar H), 5.87 (s, 1 H, PhCHO₂), 5.60 (t, 1 H, Ins H, *J* = 5.0 Hz), 4.63 (s, 2H, CH₂), 4.65 (ABq, 4 H, 2 × CH₂), 4.31-4.41 (m, 1 H, Ins H), 4.15-4.25 (m, 3 H, Ins H), 2.05 (s, 3 H, CH₃) ppm; **¹³C NMR** (CDCl₃, 50.3 MHz): δ 170.3 (C=O), 139.3 (C_{arom}), 138.1 (C_{arom}), 137.7 (C_{arom}), 129.2 (C_{arom}), 128.4 (C_{arom}), 128.3 (C_{arom}), 127.9 (C_{arom}), 127.83 (C_{arom}), 127.8 (C_{arom}), 127.6 (C_{arom}), 126.6 (C_{arom}), 94.6 (PhCHO₂), 76.4 (Ins C), 73.3 (CH₂), 71.9 (Ins C), 70.5 (CH₂), 68.9 (Ins C), 66.3 (Ins C), 20.9 (CH₃) ppm; **Elemental analysis** calcd. for C₃₆H₃₆O₇: C, 74.46; H, 6.25; Found: C, 74.60; H, 6.24 %.

neo-Inositol (1.25): The *neo*-alcohol **2.124** (2.3 g, 4.27 mmol) was dissolved in ethanol (15 mL) in a hydrogenation flask and 20% Pd(OH)₂-C (0.16 g) was added to the solution. The contents were hydrogenolyzed on Parr hydrogenator for 36 h at rt. The catalyst was allowed to settle and the supernatant liquid was removed using a pipette. The catalyst was repeatedly washed with warm (50 °C) distilled water (6 × 100 mL). The combined washings were filtered through a short column of Celite. The filtrate was evaporated under reduced pressure to get an off white solid which was washed with hot ethyl acetate

to afford *neo*-inositol (**1.25**) as a colorless solid (0.636 g, 83 %). **Mp.** = 305-310 °C (Lit.⁴⁰ Mp = 315 °C).

***neo*-Inositol hexa acetate (2.92):** *neo*-inositol **1.25** (0.05 g, 0.28 mmol) was suspended in dry pyridine (6 mL) and cooled to 0 °C. Acetic anhydride (0.47 mL, 4.98 mmol) was added drop wise to the solution and stirring continued at ambient temperature until the reaction mixture turned to a clear solution (~40 h). The solvents were removed under reduced pressure and the residue obtained was worked up with dichloromethane followed by drying over anhy. sodiumsulphate. The solvent was removed under reduced pressure and the crude product was purified by column chromatography (eluent: 5% ethyl acetate in dichloromethane) to afford *neo*-inositol hexaacetate (**2.92**) as a white solid (0.115 g, 96 %). **Mp.** = 255-258 °C (Lit.⁷³ Mp. = 257-259 °C).

***neo*-Inositol hexa benzoate (2.126):** *neo*-inositol **1.25** (0.03 g, 0.17 mmol) was suspended in dry pyridine (2 mL) and cooled to 0 °C. Benzoyl chloride (0.6 mL, 5.17 mmol) was added drop-wise to the solution and stirring continued at ambient temperature for 56 h. Excess of benzoyl chloride was quenched with ice cold water and the solvent removed under reduced pressure. The gummy residue was worked up with dichloromethane followed by drying over anhy. sodiumsulphate. The crude product was purified by column chromatography to afford *neo*-inositol hexabenzoate **2.126** as a white solid (0.125 g, 93%).

Data for **2.126**

Mp. = 287-290 °C; **IR** (CHCl₃) ν = 1732 cm⁻¹; **¹H NMR** (CDCl₃, 200 MHz): δ 8.07-8.20 (m, 4H, Ar H), 7.78-7.92 (m, 8H, Ar H), 7.39-7.74 (m, 10H, Ar H), 7.20-7.35 (m, 8H, Ar H), 6.44 (s, 2H, Ins H), 6.20 (s, 4H, Ins H) ppm; **¹³C NMR** (CDCl₃, 100.6 MHz): δ 165.35 (C=O), 165.33 (C=O), 133.7 (C_{arom}), 133.4 (C_{arom}), 129.9 (C_{arom}), 129.7 (C_{arom}),

129.0 (C_{arom}), 128.8 (C_{arom}), 128.7 (C_{arom}), 128.3 (C_{arom}), 69.1 (Ins C), 68.7 (Ins C) ppm;

Elemental analysis calcd. for $C_{48}H_{36}O_{12}$: C, 71.64; H, 4.51; Found: C, 71.44; H, 4.86 %.

Amination of inosose 2.123 with amine: To a solution of the ketone **2.123** (0.27 g, 0.56 mmol) in dry methanol (5 mL), benzyl amine (0.177 g, 1.65 mmol) was added and stirred at rt for 30 min. TLC analysis of the reaction mixture showed the absence of starting material. Sodium cyanoborohydride (0.105 g, 1.67 mmol) was added to the reaction mixture at 0 °C and stirring continued for 1 h at ambient temperature. The reaction mixture was quenched with saturated ammonium chloride solution and worked up with dichloromethane followed by drying over anhy. sodiumsulphate. Solvents were removed under reduced pressure and co-evaporated with dry toluene to obtain a gummy compound which was subjected to acetylation with acetic anhydride (1 mL) in dry pyridine (5 mL) for 20 h at rt. Solvents were removed under reduced pressure and the residue was worked up in dichloromethane. The crude product was purified by column chromatography (eluent: 20% ethyl acetate in light petroleum) to afford a mixture of acetamides.

When the reductive amination of the ketone **2.123** (0.54 g, 1 mmol) was carried out with benzyl amine (0.324 g, 2.024 mmol) and sodium cyanoborohydride (0.2 g, 3.2 mmol) at low temperature (−41 °C) the corresponding *neo*-alcohol **2.124** (0.478 g, 88%) with *neo*-configuration was obtained. **Mp.** = 96-100 °C.

1,3-*O*-Benzylidene-2,4,6-tri-*O*-benzyl-5-*O*-trifluoromethane sulfonyl-*neo*-inositol (2.136): Triflic anhydride (0.63 mL, 3.75 mmol) was added drop-wise to a cooled (− 41 °C) solution of the *neo*-alcohol **2.125** (1.347 g, 2.5 mmol) in dry pyridine (5 mL) and dry dichloromethane (5 mL) over a period of 15 min. The temperature of the reaction mixture was allowed raise to rt and stirring was continued for 2 h. Solvents were removed under reduced pressure and the crude reaction mixture was worked up with dichloromethane followed by drying over anhy. sodiumsulphate. The crude product was purified by

column chromatography over triethylamine treated silicagel (eluent: 10% ethyl acetate in light petroleum) to afford the triflate ester **2.136** as a gummy residue (1.529 g, 91%).

Data for **2.136**

¹H NMR (CDCl₃, 200 MHz): δ 7.46-7.55 (m, 2H, Ar H), 7.23-7.41 (m, 18 H, Ar H), 5.74 (s, 1H, PhCHO₂), 5.55 (t, 1H, Ins H, *J* = 4.7 Hz), 4.68 (AB q, 2 × CH₂, *J* = 11.9 Hz), 4.52 (s, 2H, CH₂), 4.33-4.42 (m, 2H, Ins H), 4.22-4.32 (m, 2H, Ins H), 4.19 (t, 1H, Ins H, *J* = 2.1 Hz); **¹³C NMR** (CDCl₃, 100.6 MHz): 139.3, 137.6, 136.9, 129.2, 128.5, 128.3, 128.1, 127.9, 127.8, 127.7, 126.3, 94.5 (PhCHO₂), 82.6 (Ins C), 76.7 (Ins C), 73.6 (CH₂), 71.4 (Ins C), 70.7 (CH₂), 65.8 (Ins C) ppm; **Elemental analysis** calcd. for C₃₅H₃₃O₈SF₃: C, 62.68; H, 4.96; Found: C, 62.68; H, 5.12 %.

1,3-*O*-Benzylidene-2,4,6-tri-*O*-benzyl-5-deoxy-5-azido-*myo*-inositol (2.137): A mixture of the triflate ester **2.136** (1.462 g, 2.18 mmol) and sodium azide (0.85 g, 13.1 mmol) in dry DMF (8 mL) was stirred at rt for 12 h under argon atmosphere. TLC analysis of the reaction mixture showed the complete consumption of the triflate ester **2.136**. The solvent was removed under reduced pressure and the residue obtained was worked up with ethylacetate followed by drying over anhydrous sodium sulphate. The crude product was purified by column chromatography (eluent: 10% ethyl acetate in light petroleum) to afford the *myo*-azide **2.137** as a white solid (1.08 g, 88 %).

Data for **2.137**

Mp. = 90-93 °C; **IR** (CHCl₃) ν = 2106 cm⁻¹; **¹H NMR** (CDCl₃, 200 MHz): δ 7.47-7.56 (m, 2H, Ar H), 7.26-7.46 (m, 18H, Ar H), 5.59 (s, 1H, PhCO₂), 4.72 (s, 2H, PhCH₂), 4.67 (Abq, 4H, 2 × PhCH₂), 4.40 (d, 2H, *J* = 2.4 Hz, Ins H), 3.93 (d, 2H, *J* = 9.3 Hz, Ins H), 3.53-3.62 (m, 2H, Ins H) ppm; **¹³C NMR** (CDCl₃, 50.3 MHz): δ 137.6 (C_{arom}), 136.7 (C_{arom}), 129.4 (C_{arom}), 128.5 (C_{arom}), 128.4 (C_{arom}), 128.1 (C_{arom}), 127.8 (C_{arom}), 127.7 (C_{arom}), 126.4 (C_{arom}), 92.7 (PhCHO₂), 80.2 (Ins C), 73.0 (Ins C), 71.7 (CH₂), 70.8 (CH₂), 68.1 (Ins C), 65.0 (Ins C) ppm; **Elemental analysis** calcd. for C₃₄H₃₃N₃O₅: C, 72.45; H, 5.90, N, 7.46; Found: C, 72.30; H, 5.77, N, 7.35%.

1,2,3,4,6-penta-*O*-acetyl-5-deoxy-5-acetylamino-*myo*-inositol (2.139): The azide **2.137** (0.64 g, 1.1 mmol) was hydrogenolyzed in the presence of 20% Pd(OH)₂-C (0.045 g) in ethanol (4 mL) and acetic acid (2 mL) at rt for 44 h at 50 psi. TLC analysis of the reaction mixture showed the absence of the azide. Catalyst was filtered by using a short bed of Celite and the catalyst was washed with water (2 × 10 mL). The combined filtrate and washings were evaporated under reduced pressure and the residue was co-evaporated with dry toluene (2 × 5 mL) to obtain the crude product (0.262 g) as an off white solid. The crude product was acetylated with acetic anhydride (2.0 mL) in dry pyridine (5 mL), at ambient temperature for 40 h. The crude reaction mixture was worked up with dichloromethane and purified by column chromatography (eluent = 1:1 dichloromethane: ethylacetate) to obtain 5-deoxy-5-acetylamino-*myo*-inositol-pentaacetate **2.139** as a white solid (0.409 g, 83% for two steps).

Data for **2.139**

Mp. = 264-270 °C; **IR** (CHCl₃) ν = 3385, 1751, 1690, 1686 cm⁻¹; **¹H NMR** (CDCl₃, 200 MHz): δ 5.63 (t, 1H, J = 2.8 Hz, Ins H), 5.55 (d, 1H, J = 9.8 Hz, NH), 5.07-5.36 (m, 4H, Ins H), 4.23-4.44 (m, 1H, Ins H), 2.19 (s, 3H, CH₃), 2.04 (s, 6H, 2 × CH₃), 2.00 (s, 6H, 2 × CH₃), 1.91 (s, 3H, CH₃) ppm; **¹³C NMR** (CDCl₃, 50.3 MHz): δ 170.9 (C=O), 170.1 (C=O), 169.5 (C=O), 169.2 (C=O), 69.6 (Ins C), 68.8 (Ins C), 68.3 (Ins C), 51.7 (Ins CH-NH), 22.9 (CH₃), 20.6 (CH₃), 20.5(CH₃), 20.4 (CH₃) ppm; **Elemental analysis** calcd. for C₁₈H₂₅NO₁₁: C, 50.12; H, 5.84, N, 3.25; Found: C, 49.9; H, 6.0, N, 3.2 %

1,3-*O*-Benzylidene-2,4,6-tri-*O*-benzyl-5-*O*-methane sulfonyl-*myo*-inositol (2.146): Methane sulfonyl chloride (0.84 mL, 10.85 mmol) was added to an ice cooled solution of the alcohol **2.30** (2.16 g, 4.01 mmol) in dry pyridine (20 mL) drop wise over a period of 30 min. and stirring was continued for 7 h at ambient temperature. The reaction mixture was diluted with methanol (10 mL) and solvents were removed under reduced pressure.

The residue obtained was worked up with ethylacetate and dried over anhy. sodiumsulfate. The crude product was purified by column chromatography with 15 % ethylacetate in light petroleum as an eluent to afford mesylate **2.146** as a gummy compound (2.275g, 92%).

Data for **2.146**

¹H NMR (CDCl₃, 200 MHz): δ 7.48-7.57 (m, 2H, Ar H), 7.29-7.46 (m, 18H, Ar H), 5.70 (s, 1H, PhCHO₂), 4.68-4.81 (m, 5H), 4.41-4.63 (m, 4H), 4.17 (d, 2H, Ins H, *J* = 8.6 Hz), 3.64 (t, 1H, Ins H, *J* = 2.4 Hz), 2.92 (s, 3H, CH₃) ppm; **¹³C NMR** (CDCl₃, 50.3 MHz): δ 137.42 (C_{arom}), 137.39 (C_{arom}), 136.3 (C_{arom}), 129.5 (C_{arom}), 128.5 (C_{arom}), 128.4 (C_{arom}), 128.2 (C_{arom}), 127.9 (C_{arom}), 127.7 (C_{arom}), 126.4 (C_{arom}), 92.9 (PhCHO₂), 82.6 (Ins C), 79.1 (Ins C), 73.1 (Ins C), 71.5 (CH₂), 71.0 (CH₂), 67.7 (Ins C), 38.9 (CH₃) ppm.

1,3-*O*-Benzylidene-2,4,6-tri-*O*-benzyl-5-*O*-trifluoromethane sulfonyl-*myo*-inositol (2.147): Triflic anhydride (1.0 mL, 5.94 mmol) was added drop-wise to a cooled (– 41 °C) solution of the alcohol **2.30** (2.154 g, 4 mmol) in dry pyridine (8 mL) and dry dichloromethane (8 mL) over a period of 10 min. The cooling bath was removed and stirring was continued at ambient temperature for 2 h. Solvents were removed under reduced pressure and the residue was worked up with dichloromethane and dried over anhy. sodiumsulphate. The solvent was removed under reduced pressure and the crude product was purified by column chromatography (eluent: 10% ethyl acetate in light petroleum) to afford the triflate ester **2.147** as a white solid (2.351 g, 88%).

Data for **2.147**

Mp. = 81-83 °C; **¹H NMR** (CDCl₃, 200 MHz): δ 7.49-7.60 (m, 2 H, Ar H), 7.28-7.47 (m, 18 H, Ar H), 5.71 (s, 1 H, PhCHO₂), 4.94 (t, 1 H, Ins H, *J* = 8.7 Hz), 4.69 (s, 2 H, CH₂), 4.65 (AB q, 4 H, 2 × CH₂, *J* = 11.1 Hz), 4.46 (d, 2 H, Ins H, *J* = 2.3 Hz), 4.23 (d, 2 H, Ins H, *J* = 8.7 Hz), 3.59 (t, 1 H, Ins H, *J* = 2.3 Hz) ppm; **¹³C NMR** (CD₂Cl₂, 100.6 MHz): 138.1, 136.7, 129.9, 128.9, 128.84, 128.73, 128.65, 128.34, 128.17, 126.8, 93.2

(PhCHO₂), 88.3 (Ins C), 78.8 (Ins C), 73.7 (Ins C), 72.3 (CH₂), 71.6 (CH₂), 68.3 (Ins C) ppm; **Elemental analysis** calcd. for C₃₅H₃₃O₈SF₃: C, 62.68; H, 4.96; Found: C, 62.51; H, 5.00 %.

Reaction of *myo*-triflate ester **2.147 with sodium azide:**

A mixture of the triflate ester **2.147** (2.02 g, 3 mmol), sodium azide (1.175 g, 18.1 mmol) in dry DMF (20 mL) was heated at 100 °C for 8 h under argon atmosphere. TLC analysis of the reaction mixture showed the complete consumption of the triflate ester. The reaction mixture was cooled to rt and the solvent was removed under reduced pressure. The residue was worked up with ethyl acetate and dried over anhy. sodiumsulphate. The solvent was removed and the crude product was purified by column chromatography (eluent: 10% ethyl acetate in light petroleum) to afford a mixture of azides **2.148**, **2.137** (as revealed by ¹H NMR spectroscopy, Appendix, page 196) a white solid (1.545 g, 91 %); **IR** (CHCl₃) $\nu = 2110 \text{ cm}^{-1}$; **Elemental analysis** calcd. for C₃₄H₃₃N₃O₅: C, 72.45; H, 5.9; N, 7.45; Found: C, 72.12; H, 5.68, N, 7.07 %.

Reduction of the mixture of azides (2.148**, **2.137**):**

The mixture of azides **2.148** and **2.137** (0.706 g, 1.25 mmol) obtained in the previous step was reduced to amine with triphenylphosphine (0.5 g, 1.91 mmol) and water (0.5 mL) in THF (8 mL) by heating at 65 °C for 15 h. TLC analysis of the reaction mixture showed the absence of the starting material. The reaction mixture was cooled to rt and the solvents were removed under reduced pressure and the residue was co-evaporated with dry toluene (2 × 10 mL). The crude product (1.106 g) obtained was acetylated with acetic anhydride (1.0 mL) in dry pyridine (7 mL) at ambient temperature for 6 h. The reaction mixture was concentrated under reduced pressure and the residue was worked up with ethyl acetate. The crude product obtained on evaporation of the solvent was purified by column chromatography (eluent: 40% ethyl acetate in light petroleum) to afford a mixture

of acetamides **2.149** and **2.150** as white solid (0.61 g, 84%) as revealed by ¹H NMR spectroscopy, Appendix, page 197)

Hydrogenolysis of the mixture of acetamides 2.149 and 2.150: The mixture of acetamides **2.149** and **2.150** (0.583 g) obtained in the previous step was hydrogenolyzed in the presence of 10% Pd-C (0.034 g) in ethanol (6 mL) at 50 psi for 32 h. The reaction mixture was diluted with water (5 mL) and the catalyst was filtered using a short bed of Celite; the catalyst was washed with ethanol-water mixture (1:1, 2 × 10 mL). The combined filtrate and washings were concentrated under reduced pressure and the residue obtained was co-evaporated with dry toluene (2 × 5 mL) to afford the crude compound as an off-white solid. The crude residue (0.206 g) was acetylated with acetic anhydride (1.9 mL) in dry pyridine (6 mL) at rt for 45 h. The solvents were evaporated under reduced pressure and the residue was worked up with dichloromethane and dried over anhy. sodiumsulphate. The crude product obtained on evaporation of the solvent was purified by column chromatography (eluent: 40% ethylacetate in dichloromethane) to afford a mixture hexaacetates **2.139**, **2.151** (as revealed by ¹H NMR spectroscopy, see Appendix, page 198) as a white solid (0.355 g, 82 %).

1,3-O-Benzylidene-2,4,6-tri-O-benzyl-5-O-(methyl-thio) thiocarbonyl-*myo*-inositol (2.182): To a cooled (0 °C) solution of the alcohol **2.30** (2.774 g, 5.15 mmol) in dry THF (25 mL), NaH (1.03 g, 25.75 mmol) was added and stirred at ambient temperature for 30 min. Carbon disulfide (4.68 mL, 77.8 mmol) was added to the reaction mixture and refluxed for 1 h. The reaction mixture was allowed to cool to rt and methyl iodide (1.6 mL, 25.701 mmol) was added and stirred for 16 h at rt. The reaction mixture was diluted with ethanol (6 mL), water (12 mL) and extracted with ethylacetate (200 mL) by washing with saturated ammonium chloride solution, brine followed by drying over anhy. sodium sulfate. The gummy residue obtained after evaporation of the solvent was purified by

column chromatography (eluent: 15% ethylacetate in light petroleum) to obtain the xanthate **2.182** as a white solid (3.118 g, 96 %).

Data for **2.182**

Mp. = 112-114 °C; **IR** (CHCl₃) ν = 1215, 1062 cm⁻¹; **¹H NMR** (CDCl₃, 200 MHz): δ 7.50-7.58 (m, 2H, Ar H), 7.16-7.48 (m, 18 H, Ar H), 6.27 (t, 1H, Ins H, J = 7.2 Hz), 5.81 (s, 1H, PhCHO₂), 4.73 (s, 2H, CH₂), 4.63 (ABq, 4H, 2 \times CH₂, J = 12.1 Hz), 4.45 (d, 2H, InsH, J = 2.3 Hz), 4.13 (d, 2H, Ins H, J = 7.2 Hz), 3.83 (t, 1H, Ins H, J = 2.3 Hz), 2.56 (s, 3H, CH₃) ppm; **¹³C NMR** (CDCl₃, 50.3 MHz): δ 215.4 (C=S), 138.0 (C_{arom}), 137.8 (C_{arom}), 136.9 (C_{arom}), 129.3 (C_{arom}), 128.4 (C_{arom}), 128.3 (C_{arom}), 127.9 (C_{arom}), 127.69 (C_{arom}), 127.65 (C_{arom}), 126.5 (C_{arom}), 92.9 (PHCO₂), 81.8 (Ins C), 79.1 (Ins C), 73.4 (Ins C), 71.5 (CH₂), 70.8 (CH₂), 68.1 (Ins C), 19.2 (CH₃) ppm; **Elemental analysis** calcd. for C₃₆H₃₆O₆S₂: C, 68.77; H, 5.77; Found: C, 69.04; H, 5.63 %.

Racemic-1-O-benzoyl-2,4,6-tri-O-benzyl-3,5-dideoxy-myo-inositol (2.183): To a solution of the xanthate **2.182** (3.11 g, 4.95 mmol) in dry toluene (40 mL), tri-*n*-butyl tin hydride (5.735 g, 19.7 mmol) and AIBN (0.1 g) was added and heated at 100 °C for 1 h. The solvents were removed under reduced pressure to obtain a gummy residue which was purified by column chromatography (eluent: 10 % ethyl acetate in light petroleum) to obtain dideoxy inositol derivative **2.183** as a gum (2.35 g, 91 %).

Data for **2.183**.

IR (CHCl₃) ν = 1720 cm⁻¹; **¹H NMR** (CDCl₃, 200 MHz): δ 8.01-8.12 (m, 2H, Ar H), 7.13-7.66 (m, 18H, Ar H), 5.14 (dd, 1H, Ins H, J = 9.5, 2.9 Hz), 4.45-4.76 (m, 6H, 3 \times CH₂), 3.97-4.17 (m, 2H, Ins H), 3.71-3.95 (m, 1H, Ins H), 2.48-2.64 (m, 1H, CH₂), 2.27-2.46 (m, 1H, CH₂), 1.48-1.71 (m, 2H, CH₂) ppm; **¹³C NMR** (CDCl₃, 50.3 MHz): δ 166.0 (C=O), 138.49 (C_{arom}), 138.46 (C_{arom}), 138.3 (C_{arom}), 133.0 (C_{arom}), 130.2 (C_{arom}), 129.71 (C_{arom}), 128.36 (C_{arom}), 128.32 (C_{arom}), 128.21 (C_{arom}), 128.19 (C_{arom}), 127.59 (C_{arom}),

127.56 (C_{arom}), 127.5 (C_{arom}), 127.4 (C_{arom}), 77.4 (Ins C), 74.3 (Ins C), 74.0 (Ins C), 72.1 (PhCH₂), 71.9 (PhCH₂), 71.4 (Ins C), 70.6 (PhCH₂), 36.0 (Ins CH₂), 34.3 (Ins CH₂) ppm.

Elemental analysis calcd. for C₃₄H₃₄O₅: C, 78.14; H, 6.56; Found: C, 78.28; H, 6.54 %

Racemic-1,5-dideoxy-2,4,6-tri-O-benzyl-myoinositol (2.175): A mixture of the dideoxy mono benzoate **2.183** (2.34 g, 4.48 mmol), *iso*-butylamine (11 mL) and methanol (20 mL) was refluxed for 12 h. Solvents were removed under reduced pressure and the residue obtained was purified by column chromatography (eluent: 10 % ethyl acetate in light petroleum) to afford dideoxy inositol **2.175** as a white solid (1.736 g, 93%).

Data for **2.175**.

Mp. = 54-57 °C; **IR** (CHCl₃) ν = 3276-3616 cm⁻¹; **¹H NMR** (CDCl₃, 200 MHz): δ 7.25-7.42 (m, 15H, Ar H), 4.35-4.75 (m, 6H, 3 × PhCH₂), 3.88-4.02 (m, 1H, Ins H), 3.50-3.84 (m, 3H, Ins H), 2.44-2.69 (m, 3H, 2 × OH, 1 × CH₂), 2.26-2.43 (m, 1H, Ins CH₂), 1.29-1.51 (m, 2H, Ins CH₂) ppm; **¹³C NMR** (CDCl₃, 50.3 MHz): δ 138.42 (C_{arom}), 138.39 (C_{arom}), 138.22 (C_{arom}), 128.2 (C_{arom}), 127.55 (C_{arom}), 127.47 (C_{arom}), 127.43 (C_{arom}), 76.7 (Ins C), 76.1 (Ins C), 75.3 (Ins C), 71.8 (PhCH₂), 71.4 (PhCH₂), 70.4 (PhCH₂), 35.2 (Ins CH₂), 33.7 (Ins CH₂) ppm; **Elemental analysis** calcd. for C₂₇H₃₀O₄: C, 77.48; H, 7.23; Found: C, 77.44; H, 7.23 %.

Racemic-1, 5-dideoxy-myoinositol (2.184): The tribenzyl ether **2.175** (0.8 g, 1.9 mmol) was hydrogenolyzed in ethanol (6 mL) in the presence of Pd(OH)₂-C at 50 psi for 4 h on a Parr shaker. The catalyst was filtered using a short bed of Celite and the catalyst was washed with ethanol (2 × 25 mL). The combined ethanol solution was evaporated under reduced pressure to obtain off white solid which was dissolved in hot ethanol and allowed to cool to rt. Cooling the solution to 0 °C afforded the crystalline tetrol **2.184** (0.238 g, 84%).

Data for **2.184**

Mp. = 154-157 °C (crystals from ethanol); **IR** (nujol) ν = 3090-3520 cm^{-1} ; **^1H NMR** (D_2O , 200 MHz): δ 3.89-4.16 (m, 2H, Ins H), 3.67-3.84 (m, 1H, Ins H), 3.41 (dd, 1H, J = 9.6, 3.3 Hz, Ins H), 1.96-2.32 (m, 2H, CH_2), 1.24-1.60 (m, 2H, CH_2) ppm; **^{13}C NMR** [D_2O (0.6 mL) + MeOH (0.02 mL), 50.3 MHz]: δ 75.9 (CHOH), 69.5 (CHOH), 68.2 (CHOH), 64.6 (CHOH), 41.1 (CH_2), 39.1 (CH_2) ppm; **Elemental analysis** calcd. for $\text{C}_6\text{H}_{12}\text{O}_4$: C, 48.64; H, 8.16; Found: C, 48.78; H, 7.94 %.

2,4,6-tri-*O*-Benzyl-5-*O*-(methyl-thio) thiocarbonyl-*myo*-inositol (2.194): A mixture of the xanthate **2.182** (1.26 g, 2.0 mmol), TFA (1 mL) and THF-water mixture (10 mL + 0.5 mL) was stirred at rt for 24 h. The solvents were removed under reduced pressure and the residue was co-evaporated with dry toluene (2×10 mL) to afford a gummy residue which was purified by column chromatography [eluent = ethyl acetate and light petroleum mixture (1 : 3)] to afford the xanthate diol **2.194** as a colorless gummy compound (1.04 g, 96 %).

Data for **2.194**

IR (CHCl_3) ν = 3323-3580, 1211, 1059 cm^{-1} ; **^1H NMR** (CDCl_3 , 200 MHz): δ 7.27-7.46 (m, 15H, Ar H), 6.17 (t, 1H, Ins H, J = 9.5 Hz), 4.82 (s, 2H, CH_2) 4.68 (ABq, 4H, J = 11 Hz, $2 \times \text{CH}_2$), 4.01 (t, 1H, Ins H, J = 2.6 Hz), 3.94 (t, 2H, Ins H, J = 9.6 Hz), 3.58-3.74 (m, 2H, Ins H), 2.61 (s, 3H, CH_3), 3.41 (d, 2H, 2 OH, J = 5.5 Hz) ppm; **^{13}C NMR** (CDCl_3 , 50.3 MHz): δ 215.8 (C=S), 138.4 (C_{arom}), 137.8 (C_{arom}), 128.4 (C_{arom}), 128.2 (C_{arom}), 127.9 (C_{arom}), 127.8 (C_{arom}), 83.7 (Ins C), 80.0 (Ins C), 78.6 (Ins C), 75.3 (CH_2), 75.0 (CH_2), 72.0 (Ins C), 19.4 (CH_3) ppm; **Elemental analysis** calcd. for $\text{C}_{29}\text{H}_{32}\text{O}_6 \text{S}_2$: C, 64.42; H, 5.96; Found: C, 64.58; H, 5.62 %.

2,4,6-tri-*O*-Benzyl-5-deoxy-*myo*-inositol or 1,3,5-tri-*O*-Benzyl-2-deoxy-*neo*-inositol (2.195): A mixture of the xanthate diol **2.194** (1.0 g, 1.85 mmol), tri-*n*-butyltin hydride (2.153 g, 7.4 mmol) and AIBN (0.04 g) and dry toluene (15 mL) was heated at 100 °C for

1 h. The solvents were removed under reduced pressure and the residue obtained was purified by column chromatography [eluent: ethyl acetate and light petroleum mixture, (1:3)] to afford **2.195** (0.747 g, 93 %) as a colorless gummy compound.

Data for **2.195**

IR (CHCl₃) ν = 3200-3650 cm⁻¹; **¹H NMR** (CDCl₃, 200 MHz): δ 7.26-7.45 (m, 15 H, Ar H), 4.84 (s, 2 H, PhCH₂), 4.62 (ABq, 4H, 2 \times PhCH₂, J = 11.5 Hz), 4.07 (t, 1H, J = 2.4 Hz, Ins H), 3.55-3.78 (m, 4H, Ins H), 2.30-2.69 (m, 3H, 1 \times Ins H, 2 \times OH), 1.19-1.40 (m, 1H, Ins H) ppm; **¹³C NMR** (CDCl₃, 50.3 MHz): δ 138.7 (C_{arom}), 138.2 (C_{arom}), 128.4 (C_{arom}), 128.3 (C_{arom}), 127.7 (C_{arom}), 127.6 (C_{arom}), 79.3 (Ins C), 76.6 (Ins C), 75.1 (PhCH₂), 74.7 (Ins C), 71.7 (PhCH₂), 31.1 (Ins CH₂) ppm; **Elemental analysis** calcd. for C₂₇H₃₀O₅: C, 74.63; H, 6.96; Found: C, 74.60; H, 6.62 %.

2-deoxy-neo-inositol or neo-Quercitol (2.157): The tribenzyl ether **2.195** (0.732 g, 1.69 mmol) was hydrogenolyzed in the presence of Pd(OH)₂-C (0.03 g) in ethanol (8 mL) at 50 psi for 6 h. The catalyst was allowed to settle and the supernatant liquid was removed using a pipette. The catalyst was repeatedly washed with warm (50 °C) aqueous ethanol (1:1, 3 \times 150 mL). Combined washings were filtered over a short column of Celite. The filtrate was evaporated under reduced pressure to obtain a white solid which was crystallized from hot methanol to afford *neo*-quercitol **2.157** colorless crystals (0.245 g, 88 %). **Mp.** = 235-238 °C (Lit.^{57b} Mp. = 237-241 °C).

2.5. References.

1. Yeh, S-M.; Lee, G. H.; Wang, Y.; Luh, T-Y. *J. Org. Chem.* **1997**, *62*, 8315-8318.
2. (a) Lee, H. W.; Kishi, Y. *J. Org. Chem.* **1985**, *50*, 4402- 4404; (b) Garrett, S. W.; Liu, C.; Riley, A. M.; Potter, B. V. L. *J. Chem. Soc., Perkin Trans. 1*, **1998**, 1367-1368.
3. (a) Gonnade, R. G.; Bhadbhade, M. M.; Shashidhar, M. S. *Chem. Commun.* **2004**, 2530-2531; (b) Gonnade, R. G.; Bhadbhade, M. M.; Shashidhar, M. S.; Sanki, A. K. *Chem. Commun.* **2005**, 5870-5872; (c) Manoj, K.; Gonnade, R.G.; Bhadbhade, M. M.; Shashidhar, M. S. *Crystal Growth & Design* **2006**, *6*, 1485-1492.
4. (a) Cox, E. G.; Cruickshank, D. W. J.; Smith, J. A. S. *Proc. R. Soc. London* **1958**, *247*, 1-21; (b) Jennings, W. B.; Farrell, B. M.; Malone, J. F. *Acc. Chem. Res.* **2001**, *34*, 885-894; (c) Mayer, E. A.; Castellano, R. K.; Diederich, F. *Angew. Chem. Int. Ed. Engl.* **2003**, *42*, 1210-1240.
5. (a) Crabtree, R. H.; Siegbahn, P. E. M.; O. Eisenstein, O.; Rheingold, A. L.; Koetzle, T. F. *Acc. Chem. Res.* **1996**, *29*, 348-354; (b) Crabtree, R. H. *Science* **1998**, *282*, 2000-2001; (c) Custelcean, R.; Jackson, J. E. *Chem. Rev.* **2001**, *101*, 1963-1980; (d) Robertson, K. N.; Knop, O.; Cameron, T. S. *Can. J. Chem.* **2003**, *81*, 727-743; (e) Wang, C-C.; Tang, T-H.; Wu, L-C.; Wang, Y. *Acta Crystallogr.* **2004**, *A60*, 488-493.
6. Koch, U.; Egert, E. *J. Comput. Chem.* **1995**, *16*, 937-944.
7. Saenger, W. *Principles of Nucleic Acid Structures*, Springer-Verlag: New York, 1984.
8. Burley, S. K.; Petsko, G. A. *Adv. Protein Chem.* **1988**, *39*, 125-189.
9. Godage, H. Y.; Riley, A. M.; Woodman, T. J.; Potter, B. V. L. *Chem. Commun.*, **2006**, 2989-2991.
10. Biamonte, M. A.; Vasella, A. *Helv. Chim. Acta.* **1998**, *81*, 688-694.
11. Uhlmann, P.; Vasella, A. *Helv. Chim. Acta.* **1992**, *75*, 1979-1994.
12. Devaraj, S.; Shashidhar, M. S.; Dixit, S. S. *Tetrahedron* **2005**, *61*, 529-536.

Chapter-2

13. Billington, D. C.; Baker, R.; Kulagowski, J. J.; Mawer, I. M.; Vacca, J. P.; deSolms, S. J.; Huff, J. R. *J. Chem. Soc. Perkin. Trans. I* **1989**, 1423-1429.
14. Benerjee, T.; Srikantiah, S. M. *Tetrahedron Lett.* **1994**, 35, 8053-8056.
15. (a) Das, T.; Shashidhar, M. S. *Carbohydr. Res.* **1997**, 297, 243-249; (b) Praveen, T.; Shashidhar, M. S. *Carbohydr. Res.* **2001**, 330, 409-411.
16. (a) Laumen, K.; Ghisalba, O. *Biosci. Biotech. Biochem.* **1994**, 58, 2046-2049.
17. Gilbert, I. H.; Holmes A. B.; Pestchanker, M. J.; Young, R. C. *Carbohydr. Res.* **1992**, 234, 117-130.
18. (a) Gilbert, I. H.; Holmes, A. B. *Tetrahedron Lett.* **1990**, 31, 2633-2634; (b) Grove, S. J. A. ; Gilbert, I. H. ; Holmes, A. B. ; Painter, G. F. ; Hill, M. L. *Chem. Commun.* **1997**, 1633-1634.; (c) Painter, G. F.; Grove, S. J. A.; Gilbert, I. H.; Holmes, A. B.; Raithby, P. R.; Hill, M. L.; Hawkins, P. T.; Stephens, L. R. *J. Chem. Soc., Perkin Trans. I*, **1999**, 923-935.
19. Bruzik, K. S.; Tsai, M. D. *J. Am. Chem. Soc.* **1992**, 114, 6361-6374.
20. (a) Dixit, S. S.; Shashidhar, M. S.; Devaraj, S. *Tetrahedron*, **2006**, 62, 4360-4363 and references cited therein; (b) Dixit, S. S.; Shashidhar, M. S. *Tetrahedron*, **2008**, 64, 2160-2171.
21. (a) Brieger, G.; Nestrick, T. J. *Chem. Rev.* **1974**, 74, 567-580; (b) Johnstone, R. A. W.; Wilby, A. H.; Entwistle, I. D. *Chem. Rev.* **1985**, 85, 129-170.
22. (a) Greene T. W.; Wuts, P. G. M.; *Protective Groups in Organic Synthesis*, 3 rd ed.; Wiley: New York 1999.
23. (a) Tsuji, J. *Synthesis*, **1984**, 369; (b) Steinhoff, B. A.; Stahl, S. S. *Org. Lett.* **2002**, 4, 4179-4181; (c) Bessmertnykh, A.; Hénin, F.; Muzart, J. *Carbohydr. Res.* **2004**, 339, 1377-1380; (d) Schultz, M. J.; Hamilton, S. S.; Jensen, D. R.; Sigman, M. S. *J. Org. Chem.* **2005**, 70, 3343-3352.
24. Ketteler, G.; Ogletree, G. F.; Bhuhm, F.; Liu, H.; Hebenstreit, E. L.; Salmemn, M. *J. Am. Chem. Soc.* **2005**, 127, 18269-18273. and references cited therein.
25. Ikawa, T.; Sajiki, H.; Hirota, K. *Tetrahedron* **2004**, 60, 6189-6195 and references cited therein.

Chapter-2

26. del Carmen, M.; Martin-Lomas, M. *Tetrahedron Lett.* **1986**, 27, 2497-2500.
27. Sherrard, E. C.; Kurth, E. F. *J. Am. Chem. Soc.* **1929**, 51, 3139-3141.
28. Ballou, C. E.; Anderson, A. B. *J. Am. Chem. Soc.* **1953**, 75, 648-650.
29. (a) Phillips, D. V.; Dougherty, D. E.; Smith, A. E. *J. Agric. Food. Chem.* **1982**, 30, 456-458; (b) Binder, R. G.; Haddon, W. F. *J. Agric. Food. Chem.* **1984**, 32, 685-687.
30. Baumgartner, S.; Genner-Ritzmann, R.; Amadó, R.; Neukom, H. *J. Agric. Food. Chem.* **1986**, 34, 827-829.
31. Li, S-H.; Zhang, H-J.; Niu, X-M.; Yao, P.; Sun, H-D.; Fong, H. H. S. *J. Nat. Prod.* **2003**, 66, 1002-1005.
32. Sultana, N.; Hartley, T. G.; Waterman, P. G. *Phytochemistry* **1999**, 50, 1249-1253
33. Francisco, M. C.; Nasser, A. L. M.; Lopes, L. M. X. *Phytochemistry* **2003**, 62, 1265-1270.
34. McPhee, F.; Downes, C. P.; Lowe, G. *Biochem. J.* **1991**, 277, 407-412.
35. Anderson, L.; DeLuca, E. S.; Bieder, A.; Post, G. G. *J. Am. Chem. Soc.* **1957**, 79, 1171-1174 .
36. Sherman, W. R.; Goodwin, S. L.; Gunnell, K. D. *Biochemistry* **1971**, 10, 3491-3499.
37. Mukherjee, R.; Axt, E. M. *Phytochem.* **1984**, 23, 2682-2684.
38. Martin, J-B.; Laussmann, T.; Bakker-Grunwald, T.; Vogel, G.; Klein, G. *J. Biol. Chem.* **2000**, 275, 10134-10140.
39. Turner, B.L.; Papházy, M.J.; Haygarth, P.M.; McKelvie, I.D. *Philos. Trans. R. Soc. Lond. B* **2002**, 357, 449-469 and references cited there in.
40. Angyal, S. J.; Matheson, N. K. *J. Am. Chem. Soc.*, **1955**, 77, 4343-4346 and references cited therein.
41. Kowarski, C. R.; Sarel, S. *J. Org. Chem.* **1973**, 38, 117-119.
42. Carpintero, M.; Fernández-Mayoralas, A.; Jaramillo, C. *J. Org. Chem.* **1997**, 62, 1916-1917.
43. Riley, A. M.; Jenkins, D. J.; Potter, B. V. L. *Carbohydr. Res.* **1998**, 314, 277-281.

Chapter-2

44. Chung, S-K.; Kwon, Y-U. *Bioorg. Med. Chem. Lett.* **1999**, 9, 2135-2140.
45. Gigg, J.; Gigg, R.; Payne, S.; Conant, R. *Carbohydr. Res.* **1985**, 142, 132-134.
46. Hudlicky, T.; Restrepo-Sánchez, N.; Kary, P. D.; Jaramillo-Gómez, L. M. *Carbohydr. Res.* **2000**, 324, 200-203.
47. Podeschwa, M.; Plettenburg, O.; vom Brocke, J.; Block, O.; Adelt, S.; Altenbach, H-J. *Eur. J. Org. Chem.* **2003**, 1958-1972 and references cited there in.
48. Heo, J-N.; Holson, E. B.; Roush, W.R. *Org. Lett.* **2003**, 5, 1697-1700.
49. Mitsunobu, O. *Synthesis* **1981**, 1-28.
50. Sanfilippo, C.; Patti, A.; Piattelli, M.; Nicolosi, G. *Tetrahedron: Asymmetry* **1998**, 9, 2808-2817 and references therein.
51. Legler, G. *Adv. Carbohydr. Chem. Biochem.* **1990**, 48, 319-384.
52. (a) Patrik, J. B.; Williams, R. P.; Waller, C. W.; Hutchings, B. L. *J. Am. Chem. Soc.* **1956**, 78, 2652; (b) Habib, El-S. E.; Scarsdale, J. N.; Reynolds, K. A. *Antimicrob. Agents Chemother.* **2003**, 47, 2065-2071 and references cited therein.
53. M. P. Sarmah, Ph.D. thesis, 2005, University of Pune.
54. McCasland, G. E.; Furuta, S.; Johnson, L. F.; Shoolery, J. N. *J. Am. Chem. Soc.* **1961**, 83, 2335-2343.
55. Maras, A.; Secen, H.; Sütbeyaz, Y.; Balci, M. *J. Org. Chem.* **1998**, 63, 2039-2041 and references cited therein.
56. Ogawa, S.; Hongo, Y.; Fujimori, H.; Iwata, K.; Kasuga, A; Suami, T. *Bull. Chem. Soc. Jpn.* **1978**, 51, 2957-2963 and references therein.
57. (a) Kee, A.; O'Brien, P.; Pilgram, C. D.; Watson, S. T. *Chem. Commun.* **2000**, 1521-1522 and references cited therein; (b) Shih, T-L.; Lin, Y-L. Kuo, W-S. *Tetrahedron* **2005**, 61, 1919-1924.
58. (a) McCasland, G. E.; Horswill, E. C. *J. Am. Chem. Soc.* **1953**, 75, 4020-4026; (b) McCasland, G. E.; Horswill, E. C. *J. Am. Chem. Soc.* **1954**, 76, 2373-2379.
59. Schmidtt, L.; Spiess, B.; Schlewer, G. *Tetrahedron Lett.* **1998**, 39, 4817-4820.
60. Baker, R.; Carrick, C.; Leeson, P. D.; Lennon, I. C.; Liverton, N. J. *J. Chem. Soc. Chem. Commun.* **1991**, 298-300.

Chapter-2

61. Morgan, A. J.; Wang, Y. K.; Roberts, M. F.; Miller, S. J. *J. Amer. Chem. Soc.* **2004**, *126*, 15370-15371.
62. Xu, Y.; Sculimbrene, B. R.; Miller, S. J. *J. Org. Chem.* **2006**, *71*, 4919-4928.
63. Dang, H-S.; Roberts, B. P.; Sekhon, J.; Smits, T. M. *Org. Biol. Chem.* **2003**, *1*, 1330-1341.
64. *Purification of Laboratory Chemicals*, Perrin, D. D.; Armarego, W. L. F. 2nd edition, Pergamon Press, Oxford, UK, 1988.
65. Bhosekar, G.; Murali, C.; Gonnade, R. G.; Shashidhar, M. S.; Bhadbhade, M. M. *Cryst. Growth. Des.* **2005**, *5*, 1977-1982.
66. Kluge, A. F.; Untch, K. G.; Fried, J. H. *J. Am. Chem. Soc.* **1972**, *94*, 7827-7832.
67. Dasgupta, F.; Singh, P. P.; Srivastava, H. C. *Carbohydr. Res.* **1980**, *80*, 346-349.
68. Chung S.-K.; Chang Y.-T. *Bioorg. Med. Chem.* **1996**, *6*, 2039-2042.
69. Anderson, R. C.; Wallis, E. S. *J. Am. Chem. Soc.* **1948**, *70*, 2931-2935.
70. Chung, S-K.; Ryu, Y. *Carbohydr. Res.* **1994**, *258*, 145-167.
71. Khersonsky, S. M.; Chang, Y.-T. *Carbohydr. Res.* **2002**, *337*, 75-79.
72. Mukherjee, R.; De Medeiros, C. L. C. *Phytochem.* **1998**, *27*, 279-281.
73. Tschamber, T.; Backenstrass, F.; Fritz, H.; Streith, J. *Helv. Chim. Acta* **1992**, *75*, 1052-1060.

2.6. Appendix.**2.6.1. Appendix Index.**

Sl. No.	Spectrum / Diagram / Table / Compound No.	Page No.
1.	ORTEP and crystal data table of 2.7	131
2.	ORTEP and crystal data table of 2.8	132
3.	ORTEP and crystal data table of 2.29	133
4.	ORTEP and crystal data table of 2.30	134
5.	ORTEP and crystal data table of 2.31	135
6.	ORTEP and crystal data table of 2.123	136
7.	ORTEP, packing diagram and crystal data table of 2.124	137
8.	ORTEP and crystal data table of 2.125	138
9.	ORTEP and crystal data table of 2.126	139
10.	ORTEP and crystal data table of 2.182	140
11.	ORTEP, packing diagram and crystal data table of 2.137	141
12.	GC-MS analysis of the reaction mixture of 2.38 (Scheme 2.11)	142
13.	¹ H NMR and ¹ H NMR- D ₂ O exchange spectra of 1.17	143
14.	¹³ C NMR and DEPT spectra of 1.17	144
15.	IR spectrum of 1.17	145
16.	¹ H NMR spectrum of 2.7	145
17.	¹³ C NMR and DEPT spectra of 2.7	146
18.	IR spectrum of 2.7	147
19.	¹ H NMR spectrum of 2.8	147
20.	¹³ C NMR and DEPT spectra of 2.8	148
21.	IR spectrum of 2.8	149
22.	¹ H NMR spectrum of 2.10	149
23.	¹³ C NMR and DEPT spectra of 2.10	150
24.	IR spectrum of 2.10	151
25.	¹ H NMR spectrum of 2.23	151
26.	¹³ C NMR and DEPT spectra of 2.23	152
27.	IR spectrum of 2.23	153
28.	¹ H NMR spectrum of 2.24	153
29.	¹ H NMR- D ₂ O exchange and ¹³ C NMR spectra of 2.24	154
30.	DEPT and IR spectra of 2.24	155
31.	¹ H and ¹³ C NMR spectra of 2.25	156
32.	DEPT and IR spectra of 2.25	157

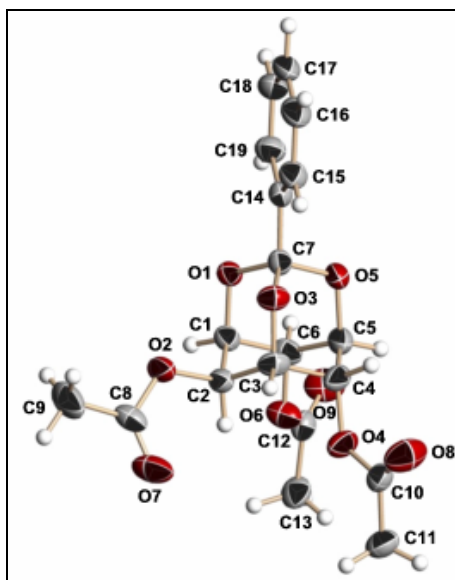
Chapter-2

33	¹ H NMR and ¹ H NMR- D ₂ O exchange spectra of 2.26	158
34	¹³ C NMR and DEPT spectra of 2.26	159
35	IR spectrum of 2.26	160
36	¹ H NMR spectrum of 2.27	160
37	¹ H NMR- D ₂ O exchange spectrum of 2.27	161
38	¹ H NMR spectrum of 2.29	161
39	¹³ C NMR and DEPT spectra of 2.29	162
40	IR spectrum of 2.29	163
41	¹ H NMR spectrum of 2.30	163
42	¹ H NMR- D ₂ O exchange and ¹³ C NMR spectra of 2.30	164
43	DEPT and IR spectra of 2.30	165
44	¹ H and ¹³ C NMR spectra of 2.31	166
45	DEPT and IR spectra of 2.31	167
46	¹ H NMR and ¹ H NMR- D ₂ O exchange spectra of 2.34	168
47	¹³ C NMR and DEPT spectra of 2.34	169
48	IR spectrum of 2.34	170
49	¹ H NMR spectrum of 2.35	170
50	¹³ C NMR and DEPT spectra of 2.35	171
51	IR spectrum of 2.35	172
52	¹ H NMR spectrum of 2.42	172
53	¹³ C NMR and DEPT spectra of 2.42	173
54	¹ H NMR spectrum of reaction mixture of 2.42 (entry 2, table 2.3)	174
55	¹ H NMR spectrum of reaction mixture of 1.106 (entry 6, table 2.2)	174
56	¹ H and ¹³ C NMR spectra of 2.80	175
57	DEPT and IR spectra of 2.80	176
58	¹ H and ¹³ C NMR spectra of 2.123	177
59	DEPT and IR spectra of 2.123	178
60	¹ H NMR and ¹ H NMR- D ₂ O exchange spectra of 2.124	179
61	¹³ C NMR and DEPT spectra of 2.124	180
62	IR spectrum of 2.124	181
63	¹ H NMR spectrum of 2.125	181
64	¹³ C NMR and DEPT spectra of 2.125	182
65	IR spectrum of 2.125	183
66	¹ H NMR spectrum of 2.126	183
67	¹³ C NMR and DEPT spectra of 2.126	184
68	IR spectrum of 2.126	185

Chapter-2

69	¹ H NMR spectrum of 2.136	185
70	¹³ C NMR and DEPT spectra of 2.136	186
71	IR spectrum of 2.136	187
72	¹ H NMR spectrum of 2.137	187
73	¹³ C NMR and DEPT spectra of 2.137	188
74	IR spectrum of 2.137	189
75	¹ H NMR spectrum of 2.139	189
76	¹ H NMR- D ₂ O exchange and ¹³ C NMR spectra of 2.139	190
77	DEPT and IR spectra of 2.139	191
78	¹ H and ¹³ C NMR spectra of 2.146	192
79	DEPT and IR spectra of 2.146	193
80	¹ H and ¹³ C NMR spectra of 2.147	194
81	DEPT and IR spectra of 2.147	195
82	¹ H and ¹³ C NMR spectra of mixture of azides 2.148 and 2.137	196
83	DEPT spectrum of mixture of azides 2.148 and 2.137	197
84	¹ H NMR spectrum of mixture of acetamides 2.149 and 2.150	197
85	¹ H NMR spectrum of mixture of hexaacetates 2.139 and 2.151	198
86	¹ H NMR spectrum of 2.182	198
87	¹³ C NMR and DEPT spectra of 2.182	199
88	IR spectrum of 2.182	200
89	¹ H NMR spectrum of 2.183	200
90	¹³ C NMR and DEPT spectra of 2.183	201
91	IR spectrum of 2.183	202
92	¹ H NMR spectrum of 2.175	202
93	¹ H NMR- D ₂ O exchange and ¹³ C NMR spectra of 2.175	203
94	DEPT and IR spectra of 2.175	204
95	¹ H and ¹³ C NMR spectra of 2.184	205
96	DEPT and IR spectra of 2.184	206
97	¹ H NMR and ¹ H NMR- D ₂ O exchange spectra of 2.194	207
98	¹³ C NMR and DEPT spectra of 2.194	208
99	IR spectrum of 2.194	209
100	¹ H NMR spectrum of 2.195	209
101	¹ H NMR- D ₂ O exchange and ¹³ C NMR spectra of 2.195	210
102	DEPT and IR spectra of 2.195	211
103	Crystal data table of Form-I and Form-II of 1.17	212
104	TGA / DTA of Form I crystals of the orthobenzoate 1.17	213

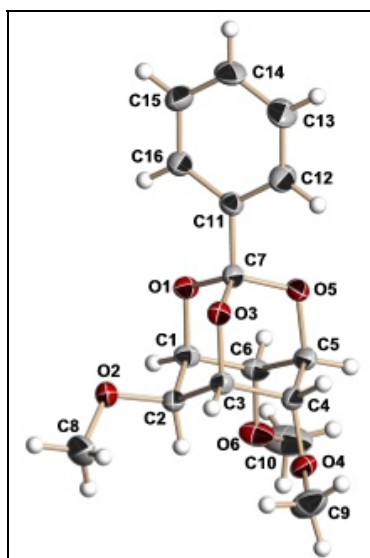
Chapter-2



ORTEP diagram of **2.7**

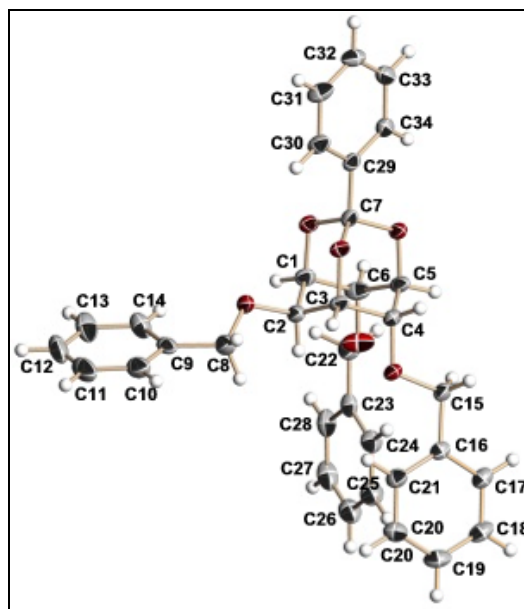
Crystal data table of **2.7**

Identification code	2.7 (crystals from CHCl ₃ -light petroleum)
Empirical formula	C ₁₉ H ₂₀ O ₉
Formula weight	392.35
Temperature	297(2) K
Wavelength	0.71073 Å
Crystal system, space group	Triclinic, P-1
Unit cell dimensions	a = 8.029(4) Å α = 93.700(8)° b = 8.781(4) Å β = 104.715(8)° c = 14.465(7) Å γ = 104.563(8)°
Volume	945.6(8) Å ³
Z, Calculated density	2, 1.378 Mg/m ³
Absorption coefficient	0.111 mm ⁻¹
F(000)	412
Crystal size	0.47 × 0.23 × 0.10 mm
θ range for data collection	1.47 to 25.00 °
Limiting indices	-9 ≤ h ≤ 9, -10 ≤ k ≤ 10, -17 ≤ l ≤ 17
Reflections collected / unique	8977 / 3331 [R(int) = 0.0263]
Completeness to θ = 25.00	99.7 %
Absorption correction	Semi-empirical from equivalents
Max. and min. transmission	0.9890 and 0.9498
Refinement method	Full-matrix least-squares on F ²
Data / restraints / parameters	3331 / 0 / 256
Goodness-of-fit on F ²	1.023
Final R indices [I > 2σ (I)]	R1 = 0.0630, wR2 = 0.1603
R indices (all data)	R1 = 0.0713, wR2 = 0.1673
Largest diff. peak and hole (ρ _{max} & ρ _{min})	0.452 and -0.284 e.Å ⁻³

ORTEP diagram of **2.8**Crystal data table of **2.8**

Identification code	2.8 (crystals from DCM-light petroleum)
Empirical formula	C ₁₆ H ₂₀ O ₆
Formula weight	308.32
Temperature	297(2) K
Wavelength	0.71073 Å
Crystal system, space group	Monoclinic, P 2 ₁ /c
Unit cell dimensions	a = 20.130(5) Å α = 90° b = 12.225(3) Å β = 91.303(4)° c = 12.654(3) Å γ = 90°
Volume	3113.1(13) Å ³
Z, Calculated density	8, 1.316 Mg/m ³
Absorption coefficient	0.101 mm ⁻¹
F(000)	1312
Crystal size	0.26 x 0.12 x 0.10 mm
θ range for data collection	1.95 to 25.00°
Limiting indices	-23 ≤ h ≤ 23, -14 ≤ k ≤ 14, -15 ≤ l ≤ 14
Reflections collected / unique	21890 / 5476 [R(int) = 0.0297]
Completeness to θ = 25.00	99.9 %
Absorption correction	Semi-empirical from equivalents
Max. and min. transmission	0.9900 and 0.9743
Refinement method	Full-matrix least-squares on F ²
Data / restraints / parameters	5476 / 0 / 403
Goodness-of-fit on F ²	1.116
Final R indices [I > 2σ (I)]	R1 = 0.0633, wR2 = 0.1508
R indices (all data)	R1 = 0.0751, wR2 = 0.1581
Largest diff. peak and hole (ρ _{max} & ρ _{min})	0.236 and -0.234 e.Å ⁻³

Chapter-2

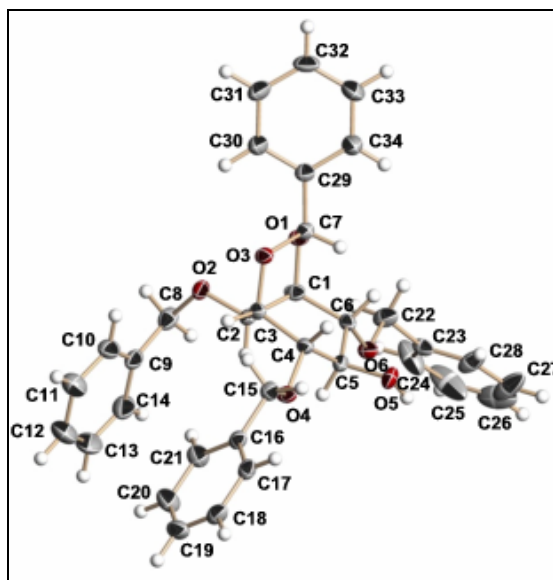


ORTEP diagram of **2.29**

Crystal data table of **2.29**

Identification code	2.29 (crystals from EtOAc-light petroleum)
Empirical formula	C ₃₄ H ₃₂ O ₆
Formula weight	536.60
Temperature	133(2) K
Wavelength	0.71073 Å
Crystal system, space group	Monoclinic, P 21/c
Unit cell dimensions	a = 12.0073(9) Å α = 90° b = 18.6909(14) Å β = 90.8990(10)° c = 12.1567(9) Å γ = 90°
Volume	2728.0(4) Å ³
Z, Calculated density	4, 1.307 Mg/m ³
Absorption coefficient	0.089 mm ⁻¹
F(000)	1136
Crystal size	0.56 x 0.18 x 0.15 mm
θ range for data collection	2.00 to 26.00°
Limiting indices	-14 ≤ h ≤ 14, -23 ≤ k ≤ 14, -14 ≤ l ≤ 14
Reflections collected / unique	14661 / 5336 [R(int) = 0.0248]
Completeness to θ = 25.00	99.5 %
Absorption correction	Semi-empirical from equivalents
Max. and min. transmission	0.9868 and 0.9519
Refinement method	Full-matrix least-squares on F ²
Data / restraints / parameters	5336 / 0 / 361
Goodness-of-fit on F ²	1.048
Final R indices [I > 2σ (I)]	R1 = 0.0397, wR2 = 0.0994
R indices (all data)	R1 = 0.0466, wR2 = 0.1037
Largest diff. peak and hole (ρ _{max} & ρ _{min})	0.552 and -0.409 e.Å ⁻³

Chapter-2

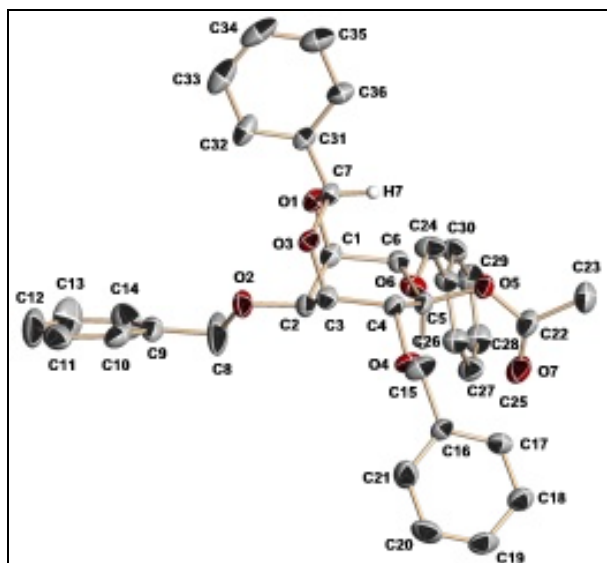


ORTEP diagram of **2.30**

Crystal data table of **2.30**

Identification code	2.30 (crystals from DCM-light petroleum)
Empirical formula	$C_{34} H_{34} O_6$
Formula weight	538.61
Temperature	133(2) K
Wavelength	0.71073 Å
Crystal system, space group	Monoclinic, P21/n
Unit cell dimensions	a = 19.0061(12) Å $\alpha = 90^\circ$ b = 7.3448(5) Å $\beta = 92.8170(10)^\circ$ c = 20.7414(13) Å $\gamma = 90^\circ$
Volume	2891.9(3) Å ³
Z, Calculated density	4, 1.237 Mg/m ³
Absorption coefficient	0.084 mm ⁻¹
F(000)	1144
Crystal size	0.55 x 0.15 x 0.14 mm
θ range for data collection	1.42 to 26.00°
Limiting indices	-20 ≤ h ≤ 23, -8 ≤ k ≤ 8, -25 ≤ l ≤ 24
Reflections collected / unique	15158 / 5617 [R(int) = 0.0192]
Completeness to $\theta = 25.00$	99.2 %
Absorption correction	Semi-empirical from equivalents
Max. and min. transmission	0.9883 and 0.9553
Refinement method	Full-matrix least-squares on F ²
Data / restraints / parameters	5617 / 114 / 508
Goodness-of-fit on F ²	1.041
Final R indices [I > 2 σ (I)]	R1 = 0.0475, wR2 = 0.1090
R indices (all data)	R1 = 0.0545, wR2 = 0.1136
Largest diff. peak and hole (ρ_{\max} & ρ_{\min})	0.280 and -0.209 e.Å ⁻³

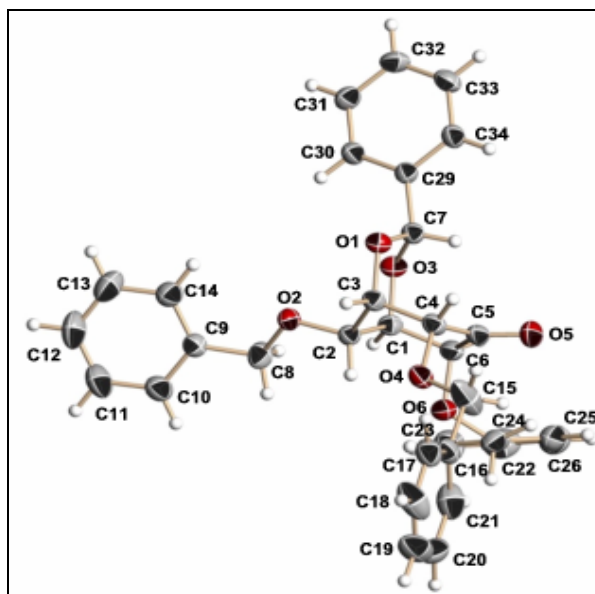
Chapter-2



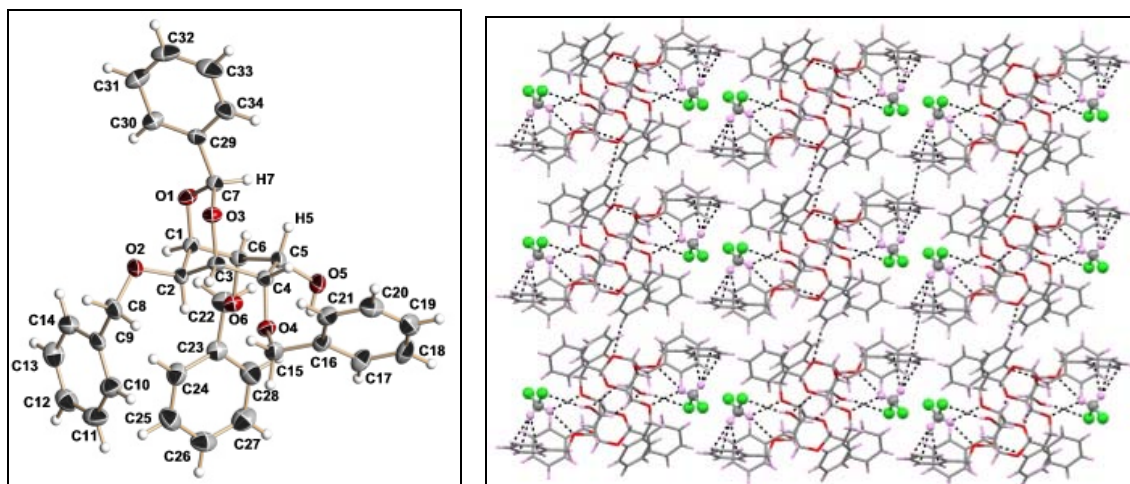
ORTEP diagram of **2.31** (Hydrogen atoms are not shown for clarity)

Crystal data table of **2.31**

Identification code	2.31 crystals from EtOAc-light petroleum
Empirical formula	C ₃₆ H ₃₆ O ₇
Formula weight	580.65
Temperature	297(2) K
Wavelength	0.71073 Å
Crystal system, space group	Monoclinic, Pc
Unit cell dimensions	a = 9.624(5) Å α = 90° b = 18.190(9) Å β = 99.041(12)° c = 9.159(5) Å γ = 90°
Volume	1583.5(14) Å ³
Z, Calculated density	2, 1.218 Mg/m ³
Absorption coefficient	0.084 mm ⁻¹
F(000)	616
Crystal size	0.43 x 0.10 x 0.07 mm
θ range for data collection	2.24 to 24.99°
Limiting indices	-11 ≤ h ≤ 11, -21 ≤ k ≤ 20, -10 ≤ l ≤ 10
Reflections collected / unique	11341 / 5429 [R(int) = 0.0508]
Completeness to θ = 25.00	99.7 %
Absorption correction	Semi-empirical from equivalents
Max. and min. transmission	0.9942 and 0.9648
Refinement method	Full-matrix least-squares on F ²
Data / restraints / parameters	5429 / 2 / 389
Goodness-of-fit on F ²	0.985
Final R indices [I > 2σ (I)]	R1 = 0.0589, wR2 = 0.0883
R indices (all data)	R1 = 0.1384, wR2 = 0.1123
Largest diff. peak and hole (ρ _{max} & ρ _{min})	0.157 and -0.152 e.Å ⁻³

ORTEP diagram of **2.123**Crystal data table of **2.123**

Identification code	2.123 (crystals from DCM-light petroleum)
Empirical formula	C ₃₄ H ₃₂ O ₆
Formula weight	536.60
Temperature	297(2) K
Wavelength	0.71073 Å
Crystal system, space group	Monoclinic, C2/c
Unit cell dimensions	a = 25.703(2) Å α = 90° b = 9.8125(9) Å β = 107.934(2)° c = 23.494(2) Å γ = 90°
Volume	5637.5(9) Å ³
Z, Calculated density	8, 1.264 Mg/m ³
Absorption coefficient	0.086 mm ⁻¹
F(000)	2272
Crystal size	1.06 x 0.18 x 0.14 mm
θ range for data collection	2.06 to 25.00°
Limiting indices	-30 ≤ h ≤ 29, -11 ≤ k ≤ 11, -27 ≤ l ≤ 27
Reflections collected / unique	19882 / 4966 [R(int) = 0.0269]
Completeness to θ = 25.00	100.0 %
Absorption correction	Semi-empirical from equivalents
Max. and min. transmission	0.9881 and 0.9144
Refinement method	Full-matrix least-squares on F ²
Data / restraints / parameters	4966 / 0 / 361
Goodness-of-fit on F ²	1.024
Final R indices [I > 2σ (I)]	R1 = 0.0463, wR2 = 0.1163
R indices (all data)	R1 = 0.0636, wR2 = 0.1282
Largest diff. peak and hole (ρ _{max} & ρ _{min})	0.233 and -0.220 e.Å ⁻³

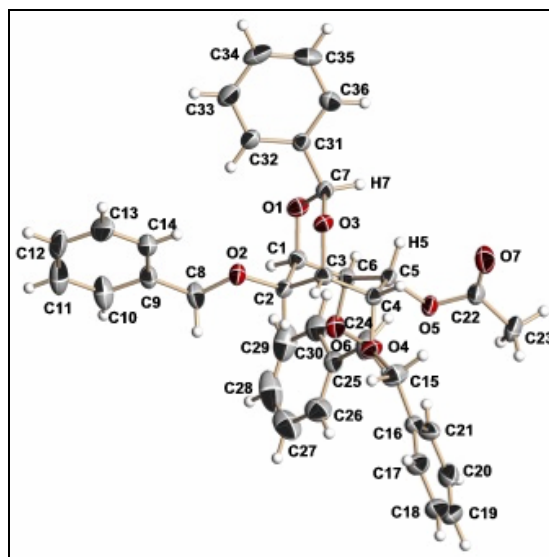


ORTEP diagram and packing of molecules with the inclusion of DCM in **2.124**

Crystal data table of **2.124**

Identification code	2.124 (crystals from DCM-light petroleum)
Empirical formula	C ₃₅ H ₃₆ Cl ₂ O ₆
Formula weight	623.54
Temperature	297(2) K
Wavelength	0.71073 Å
Crystal system, space group	Triclinic, P-1
Unit cell dimensions	a = 9.6485(11) Å α = 91.389(2)° b = 11.7692(13) Å β = 90.479(2)° c = 14.8045(16) Å γ = 107.542(2)°
Volume	1602.3(3) Å ³
Z, Calculated density	2, 1.292 Mg/m ³
Absorption coefficient	0.247 mm ⁻¹
F(000)	656
Crystal size	0.84 x 0.19 x 0.14 mm
θ range for data collection	2.25 to 25.00°
Limiting indices	-11 ≤ h ≤ 11, -13 ≤ k ≤ 13, -17 ≤ l ≤ 17
Reflections collected / unique	15627 / 5626 [R(int) = 0.0223]
Completeness to θ = 25.00	99.7 %
Absorption correction	Semi-empirical from equivalents
Max. and min. transmission	0.9663 and 0.8196
Refinement method	Full-matrix least-squares on F ²
Data / restraints / parameters	5626 / 0 / 389
Goodness-of-fit on F ²	1.049
Final R indices [I > 2σ (I)]	R1 = 0.0457, wR2 = 0.1024
R indices (all data)	R1 = 0.0599, wR2 = 0.1111
Largest diff. peak and hole (ρ _{max} & ρ _{min})	0.261 and -0.197 e. Å ⁻³

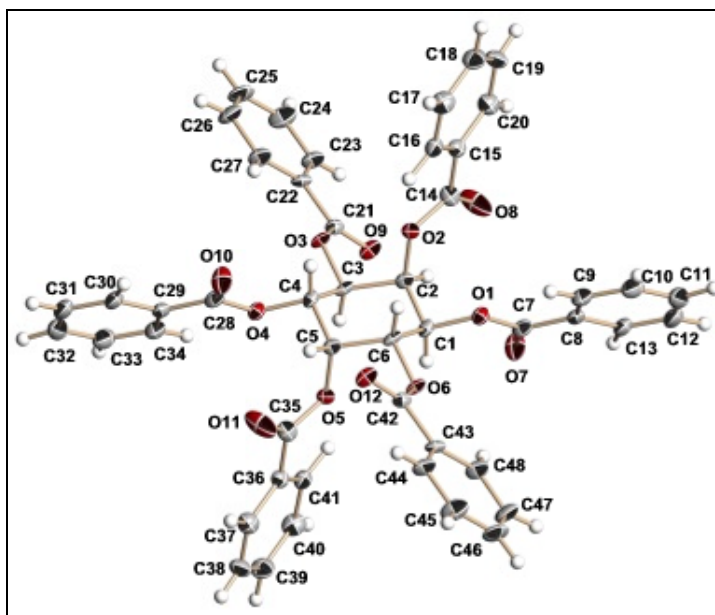
Chapter-2



ORTEP diagram of **2.125**

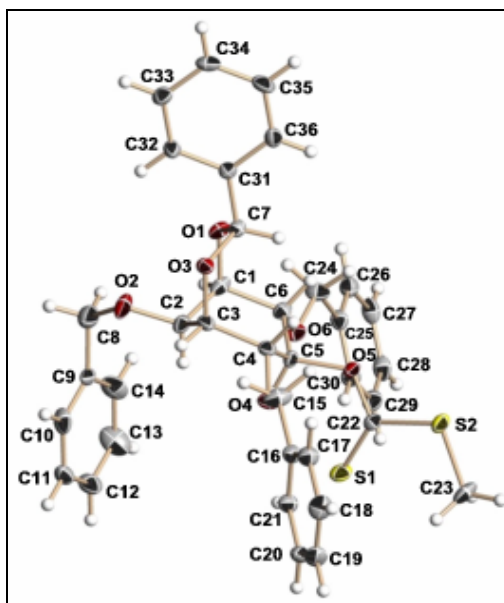
Crystal data table of **2.125**

Identification code	2.125 (crystals from DCM-light petroleum)
Empirical formula	C ₃₆ H ₃₆ O ₇
Formula weight	580.65
Temperature	297(2) K
Wavelength	0.71073 Å
Crystal system, space group	Monoclinic, P2(1)/c
Unit cell dimensions	a = 12.797(6) Å α = 90° b = 21.398(10) Å β = 102.246(11)° c = 11.467(5) Å γ = 90°
Volume	3069(3) Å ³
Z, Calculated density	4, 1.257 Mg/m ³
Absorption coefficient	0.087 mm ⁻¹
F(000)	1232
Crystal size	0.76 x 0.06 x 0.02 mm
θ range for data collection	2.37 to 25.00°
Limiting indices	-15 ≤ h ≤ 15, -25 ≤ k ≤ 25, -13 ≤ l ≤ 13
Reflections collected / unique	29092 / 5400 [R(int) = 0.1492]
Completeness to θ = 25.00	99.9 %
Absorption correction	Semi-empirical from equivalents
Max. and min. transmission	0.9987 and 0.9371
Refinement method	Full-matrix least-squares on F ²
Data / restraints / parameters	5400 / 0 / 390
Goodness-of-fit on F ²	1.022
Final R indices [I > 2σ (I)]	R1 = 0.0785, wR2 = 0.1336
R indices (all data)	R1 = 0.1726, wR2 = 0.1671
Extinction coefficient	0.0078(9)
Largest diff. peak and hole (ρ _{max} & ρ _{min})	0.174 and -0.170 e. Å ⁻³

ORTEP diagram of *neo*-inositol-hexabenzate (**2.126**)Crystal data table of **2.126**

Identification code	2.126 (crystals from CHCl ₃ -light petroleum)
Empirical formula	C ₄₈ H ₃₆ O ₁₂
Formula weight	804.77
Temperature	133(2) K
Wavelength	0.71073 Å
Crystal system, space group	Monoclinic, P 21/c
Unit cell dimensions	a = 12.897(3) Å α = 90° b = 6.5969(15) Å β = 118.285(8)° c = 27.217(5) Å γ = 90°
Volume	2039.1(8) Å ³
Z, Calculated density	2, 1.311 Mg/m ³
Absorption coefficient	0.095 mm ⁻¹
F(000)	840
Crystal size	0.28 x 0.12 x 0.09 mm
θ range for data collection	1.70 to 25.00°
Limiting indices	-14 ≤ h ≤ 15, -7 ≤ k ≤ 7, -32 ≤ l ≤ 32
Reflections collected / unique	9311 / 3570 [R(int) = 0.0502]
Completeness to θ = 25.00	99.7 %
Absorption correction	Semi-empirical from equivalents
Max. and min. transmission	0.9915 and 0.9740
Refinement method	Full-matrix least-squares on F ²
Data / restraints / parameters	3570 / 0 / 343
Goodness-of-fit on F ²	1.251
Final R indices [I > 2σ (I)]	R1 = 0.0813, wR2 = 0.1749
R indices (all data)	R1 = 0.1004, wR2 = 0.1837
Largest diff. peak and hole (ρ _{max} & ρ _{min})	0.470 and -0.269 e.Å ⁻³

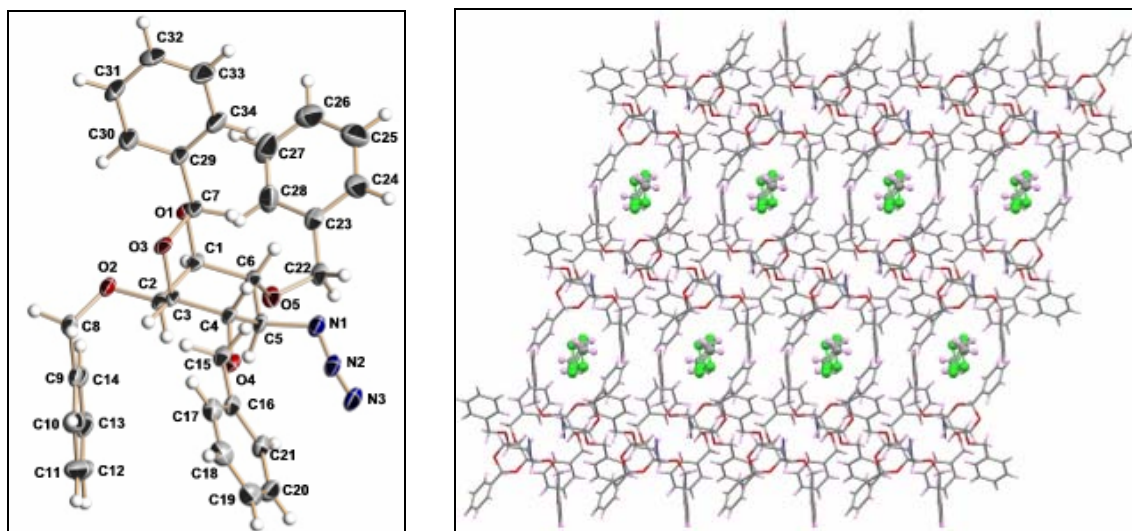
Chapter-2



ORTEP diagram of xanthate **2.182**

Crystal data table of **2.182**

Identification code	2.182 (crystals from DCM-light petroleum)
Empirical formula	C ₃₆ H ₃₆ O ₆ S ₂
Formula weight	628.77
Temperature	133(2) K
Wavelength	0.71073 Å
Crystal system, space group	Triclinic, P-1
Unit cell dimensions	a = 10.1862(9) Å α = 67.4530(10)° b = 13.0607(11) Å β = 80.7270(10)° c = 13.5161(11) Å γ = 70.6430(10)°
Volume	1565.7(2) Å ³
Z, Calculated density	2, 1.334 Mg/m ³
Absorption coefficient	0.217 mm ⁻¹
F(000)	664
Crystal size	0.66 x 0.08 x 0.06 mm
θ range for data collection	1.93 to 25.00°
Limiting indices	-12 ≤ h ≤ 12, -15 ≤ k ≤ 15, -16 ≤ l ≤ 16
Reflections collected / unique	13590 / 5487 [R(int) = 0.0298]
Completeness to θ = 25.00	99.6 %
Absorption correction	Semi-empirical from equivalents
Max. and min. transmission	0.9871 and 0.8703
Refinement method	Full-matrix least-squares on F ²
Data / restraints / parameters	5487 / 0 / 416
Goodness-of-fit on F ²	1.092
Final R indices [I > 2σ (I)]	R1 = 0.0526, wR2 = 0.1090
R indices (all data)	R1 = 0.0653, wR2 = 0.1147
Largest diff. peak and hole (ρ _{max} & ρ _{min})	0.370 and -0.212 e. Å ⁻³



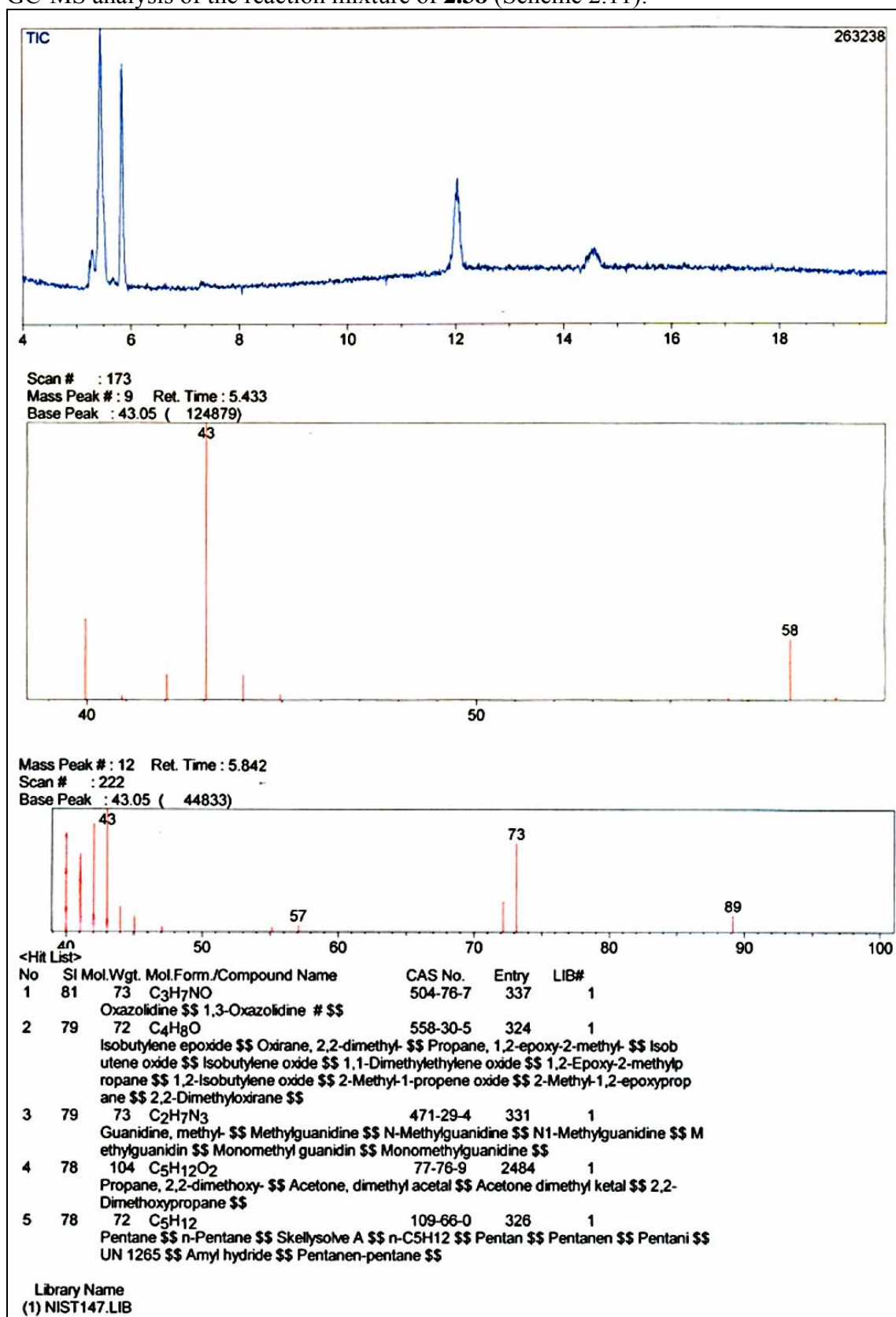
ORTEP diagram and packing of molecules with the inclusion of DCM in azide **2.137**

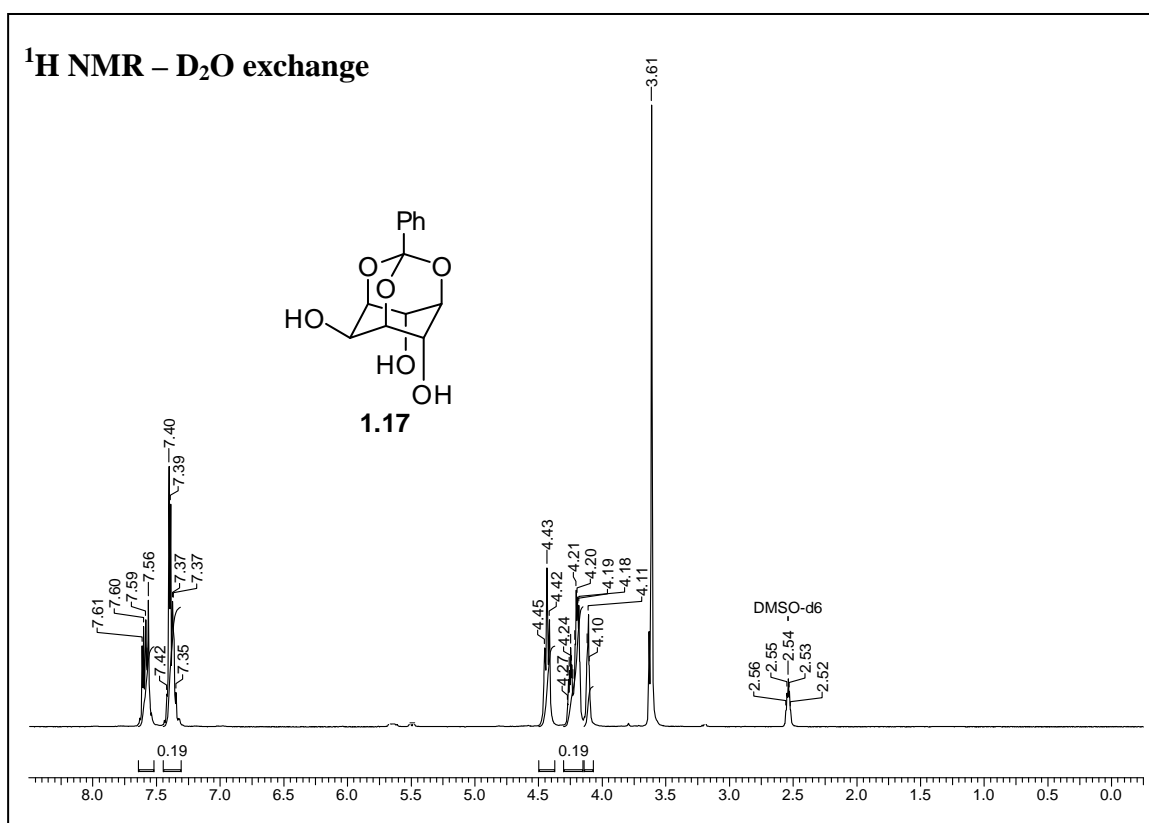
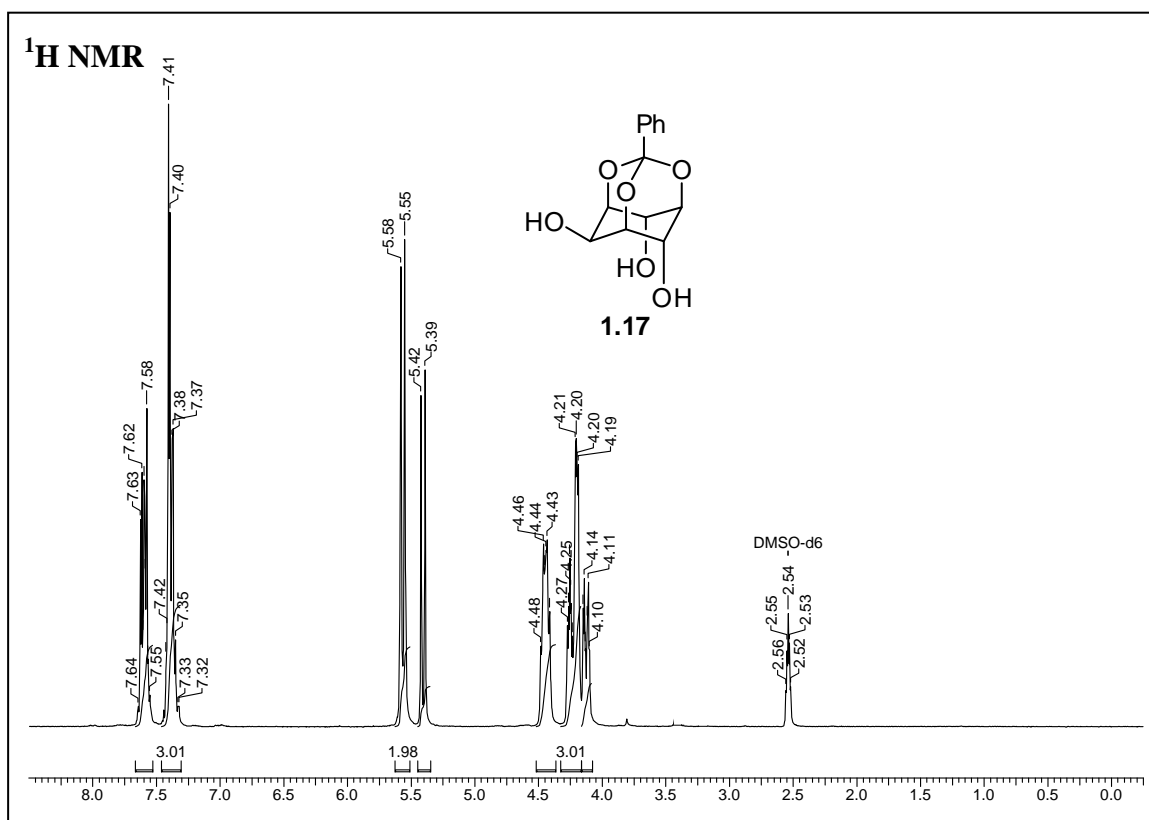
Crystal data table of **2.137**

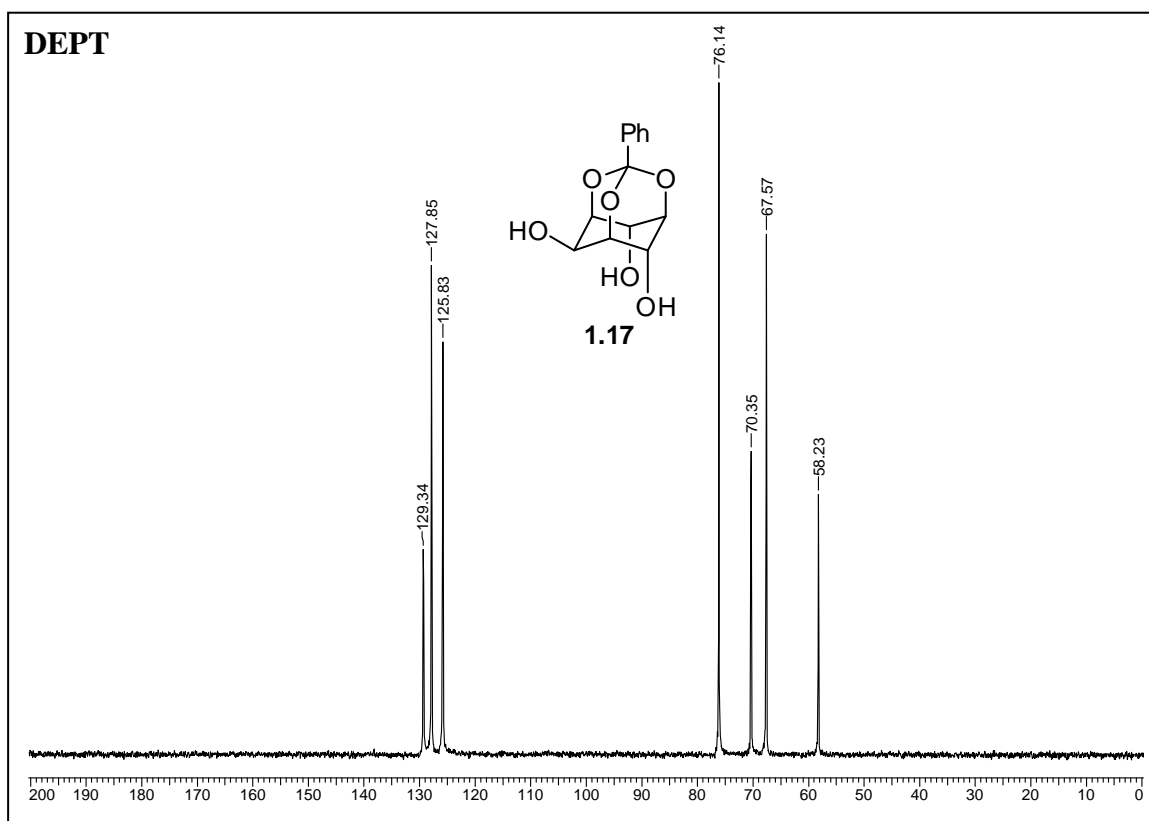
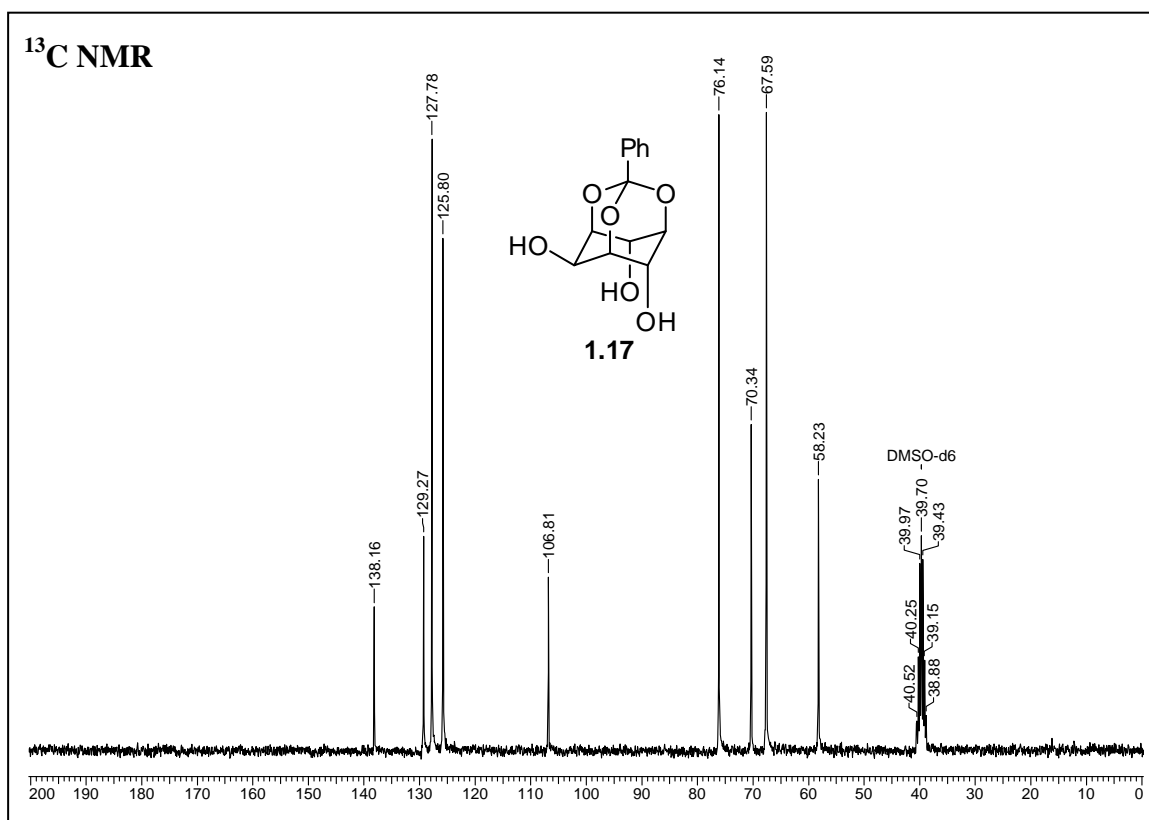
Identification code	2.137 (crystals from DCM-light petroleum)
Empirical formula	C ₃₅ H ₃₅ Cl ₂ N ₃ O ₅
Formula weight	648.56
Temperature	133(2) K
Wavelength	0.71073 Å
Crystal system, space group	Triclinic, P-1
Unit cell dimensions	a = 10.512(4) Å α = 108.742(5)° b = 11.823(4) Å β = 90.330(5)° c = 14.923(5) Å γ = 114.203(5)°
Volume	1581.6(9) Å ³
Z, Calculated density	2, 1.362 Mg/m ³
Absorption coefficient	0.253 mm ⁻¹
F(000)	680
Crystal size	0.71 x 0.52 x 0.14 mm
θ range for data collection	1.46 to 25.00°
Limiting indices	-12 ≤ h ≤ 12, -14 ≤ k ≤ 14, -17 ≤ l ≤ 17
Reflections collected / unique	22142 / 5543 [R(int) = 0.0535]
Completeness to θ = 25.00	99.4 %
Absorption correction	Semi-empirical from equivalents
Max. and min. transmission	0.9654 and 0.8407
Refinement method	Full-matrix least-squares on F ²
Data / restraints / parameters	5543 / 0 / 433
Goodness-of-fit on F ²	1.042
Final R indices [I > 2σ (I)]	R1 = 0.0800, wR2 = 0.2191
R indices (all data)	R1 = 0.0876, wR2 = 0.2312
Largest diff. peak and hole (ρ _{max} & ρ _{min})	0.832 and -0.758 e. Å ⁻³

Chapter-2

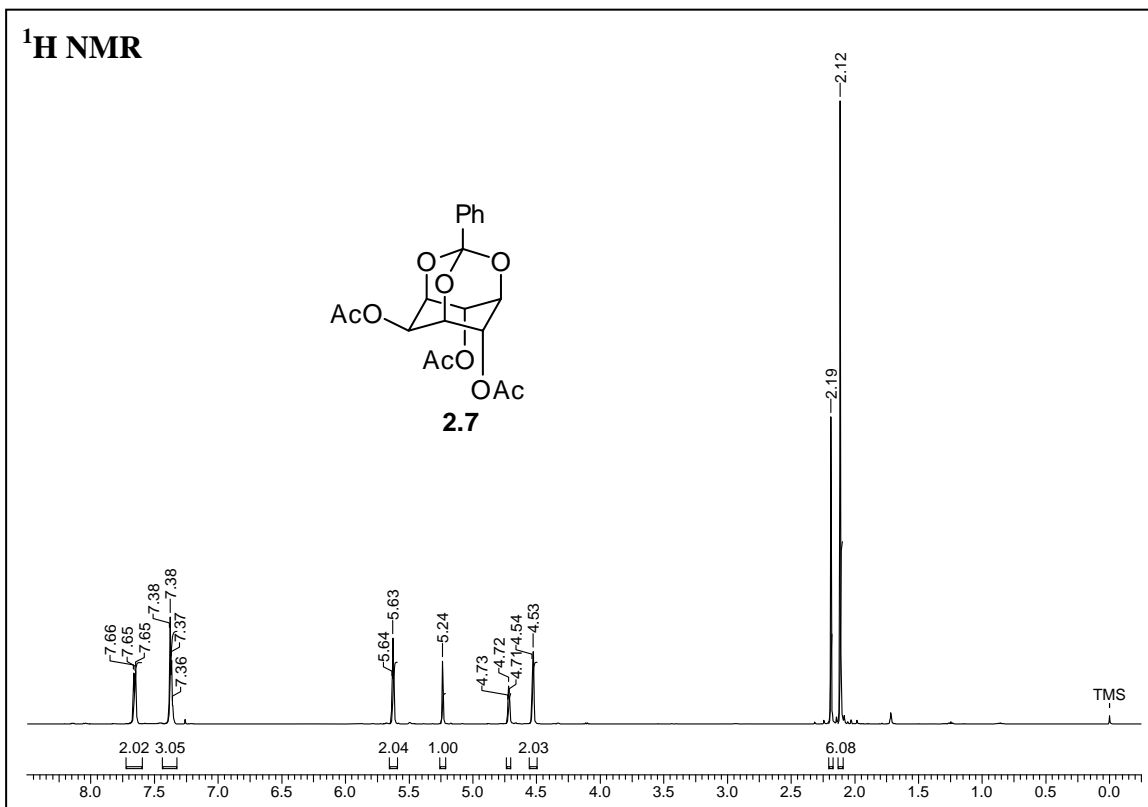
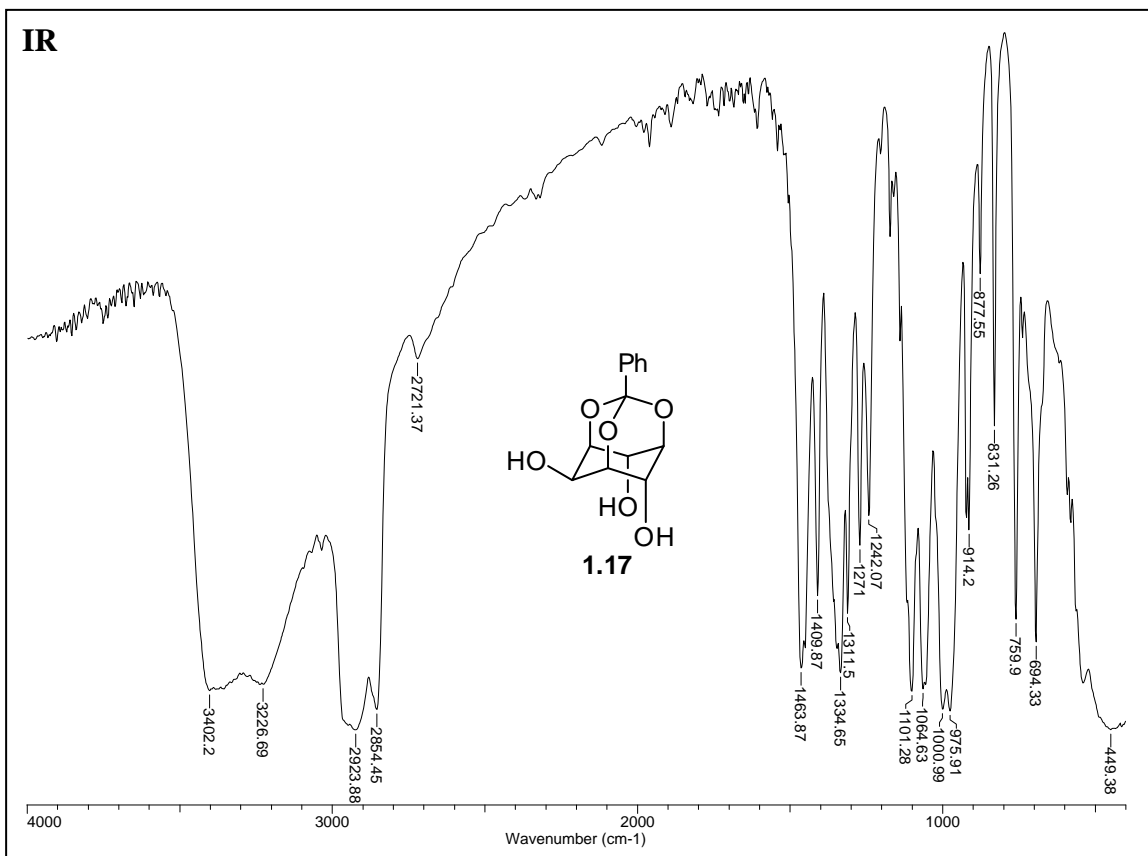
GC-MS analysis of the reaction mixture of **2.38** (Scheme 2.11):



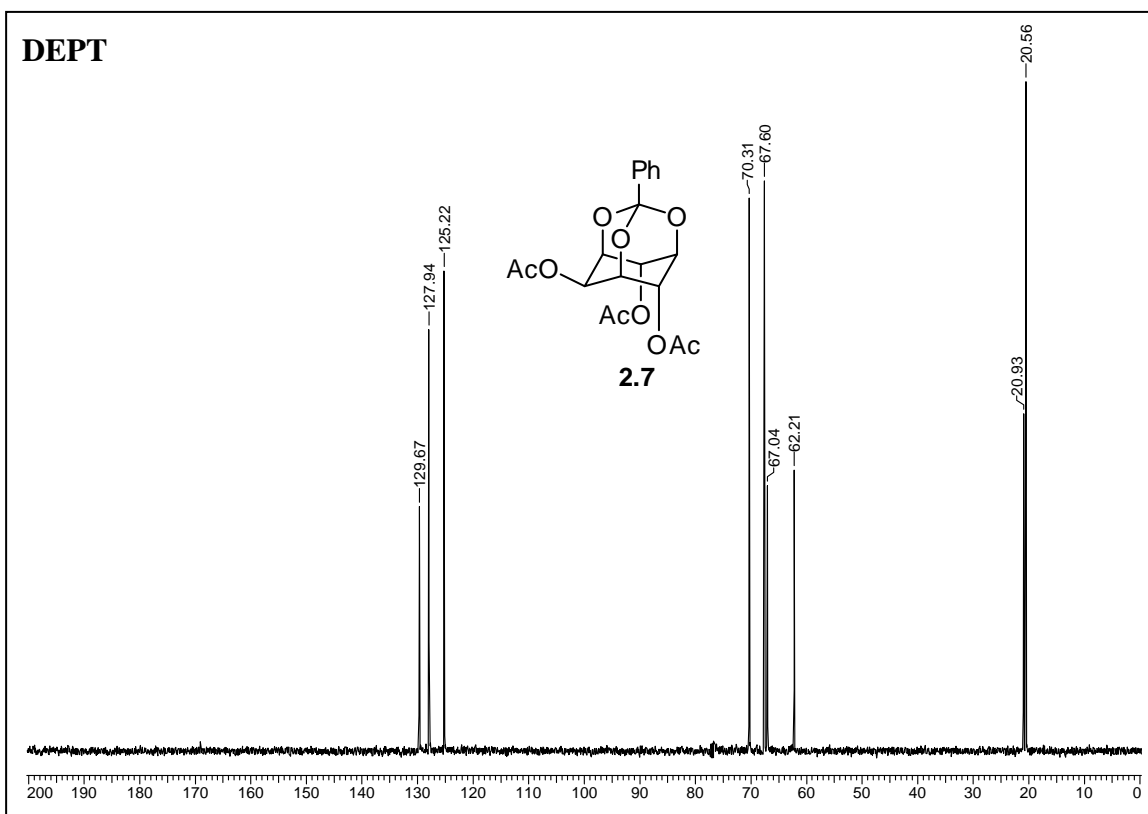
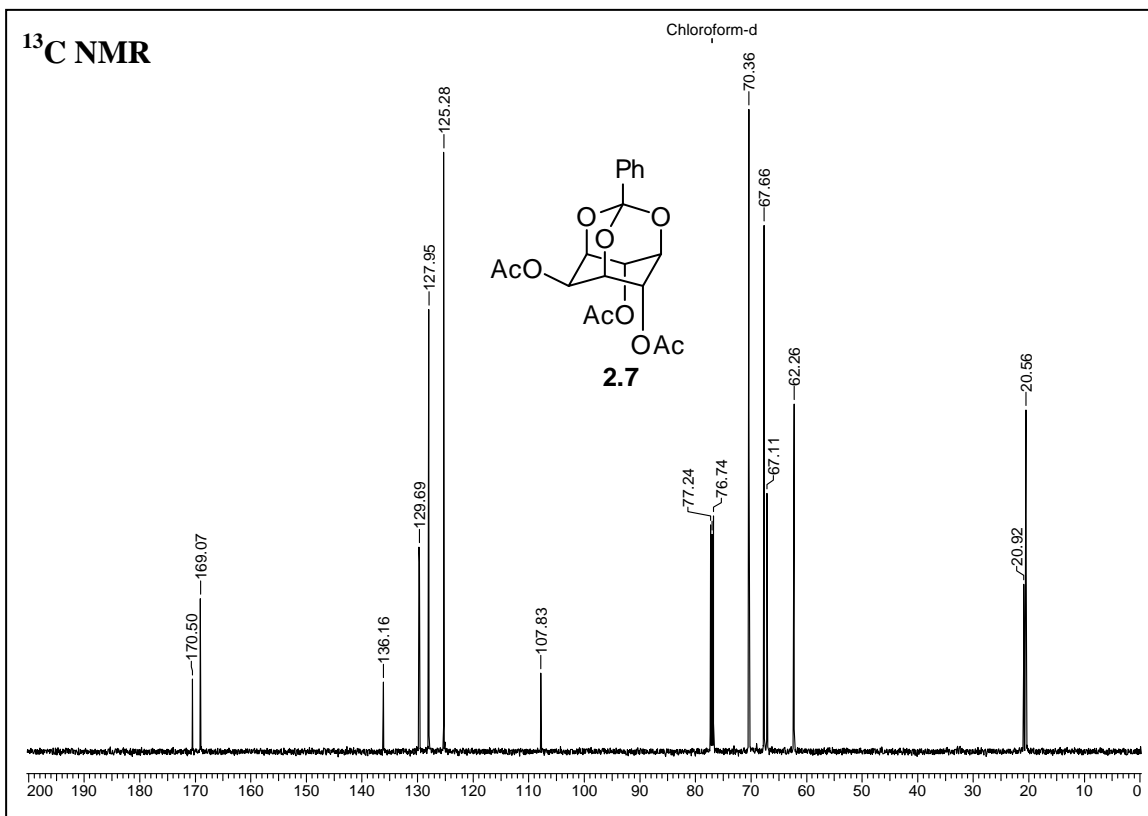




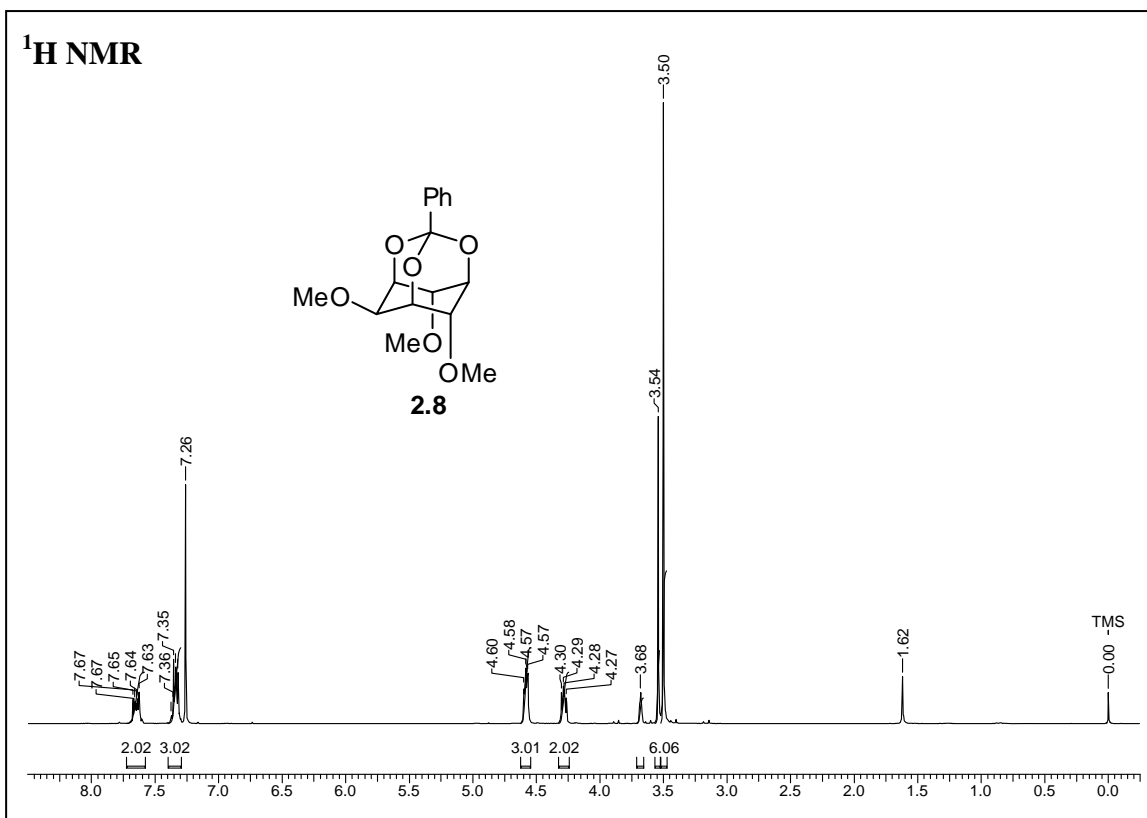
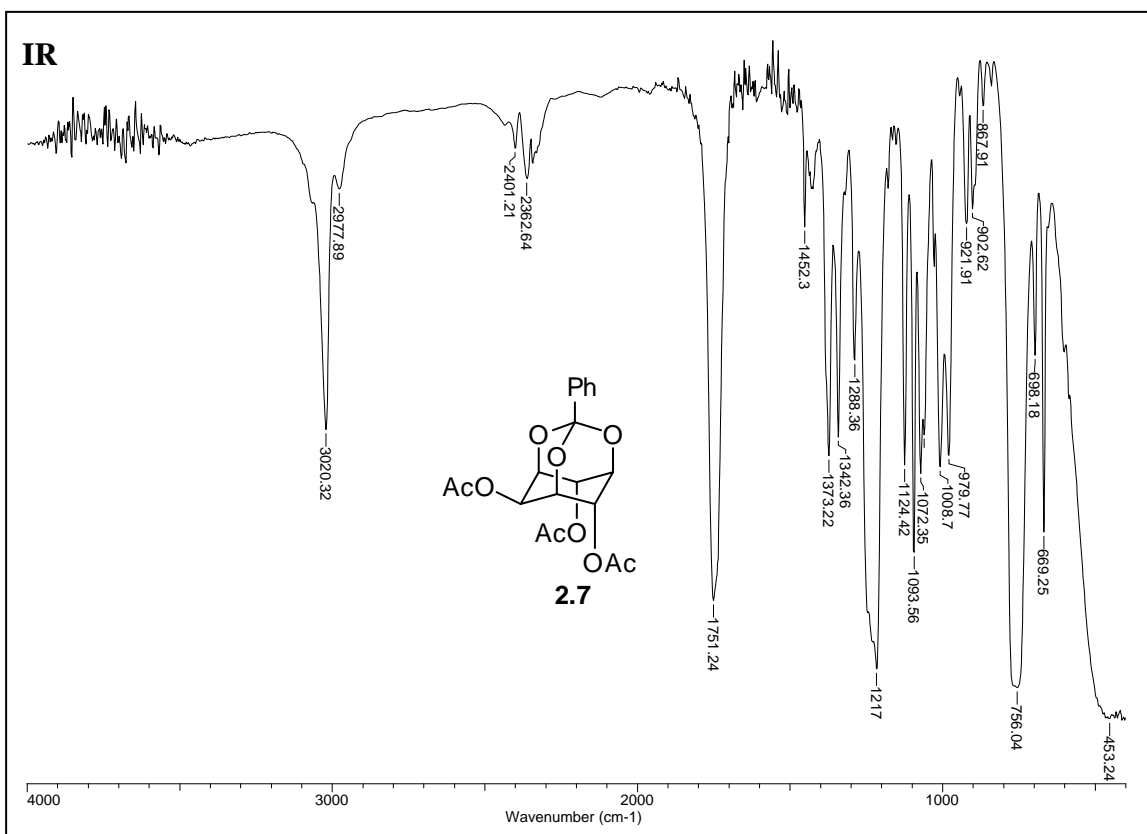
Chapter 2

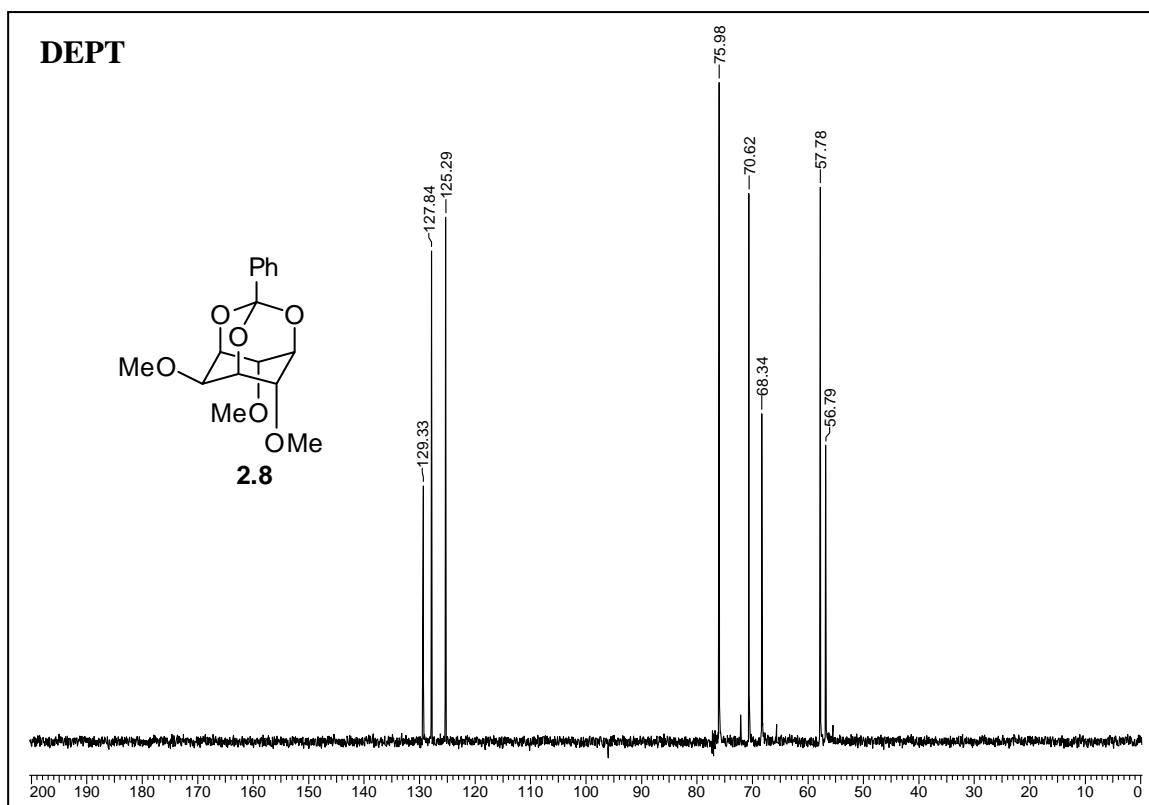
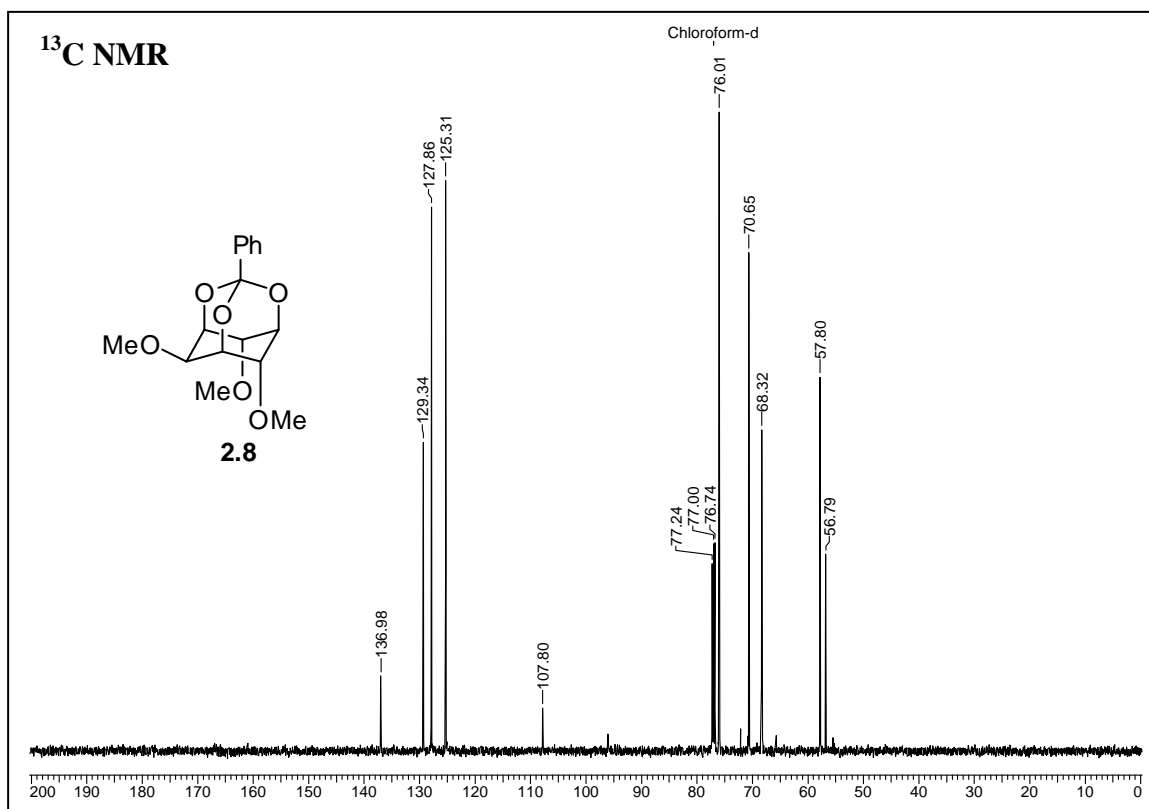


Chapter 2

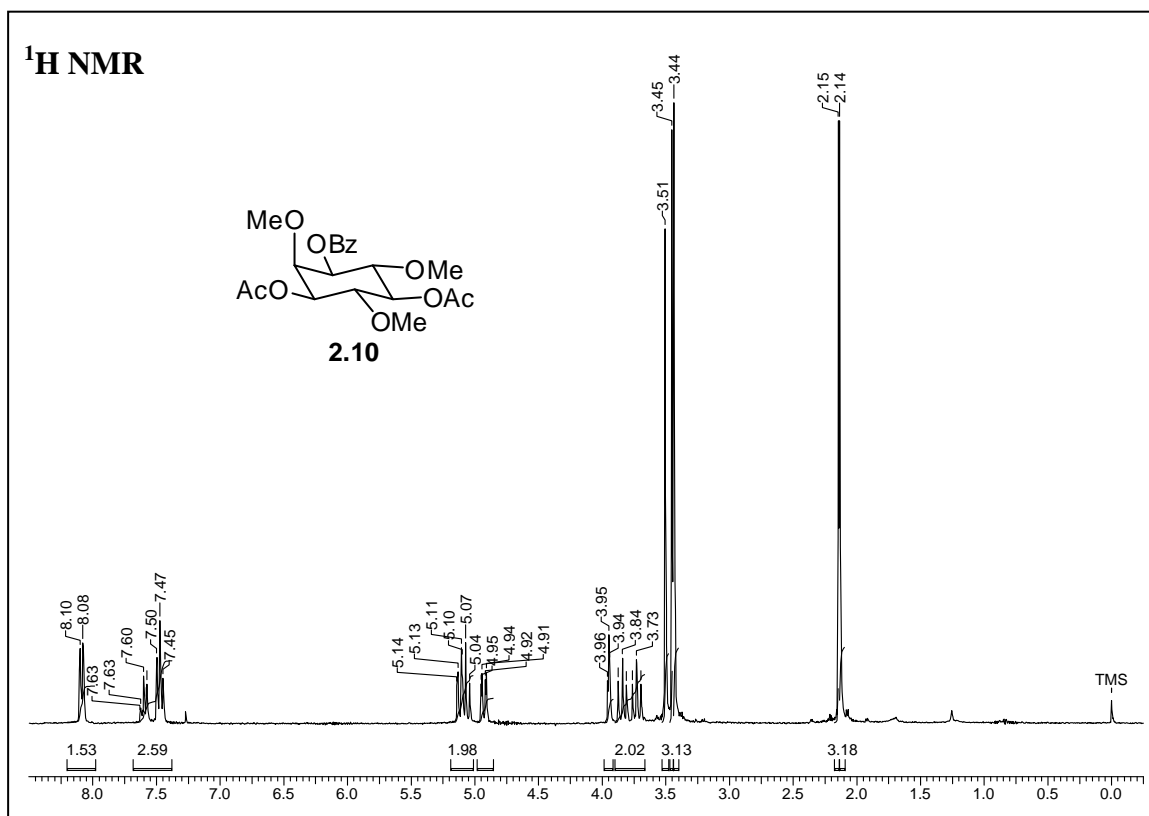
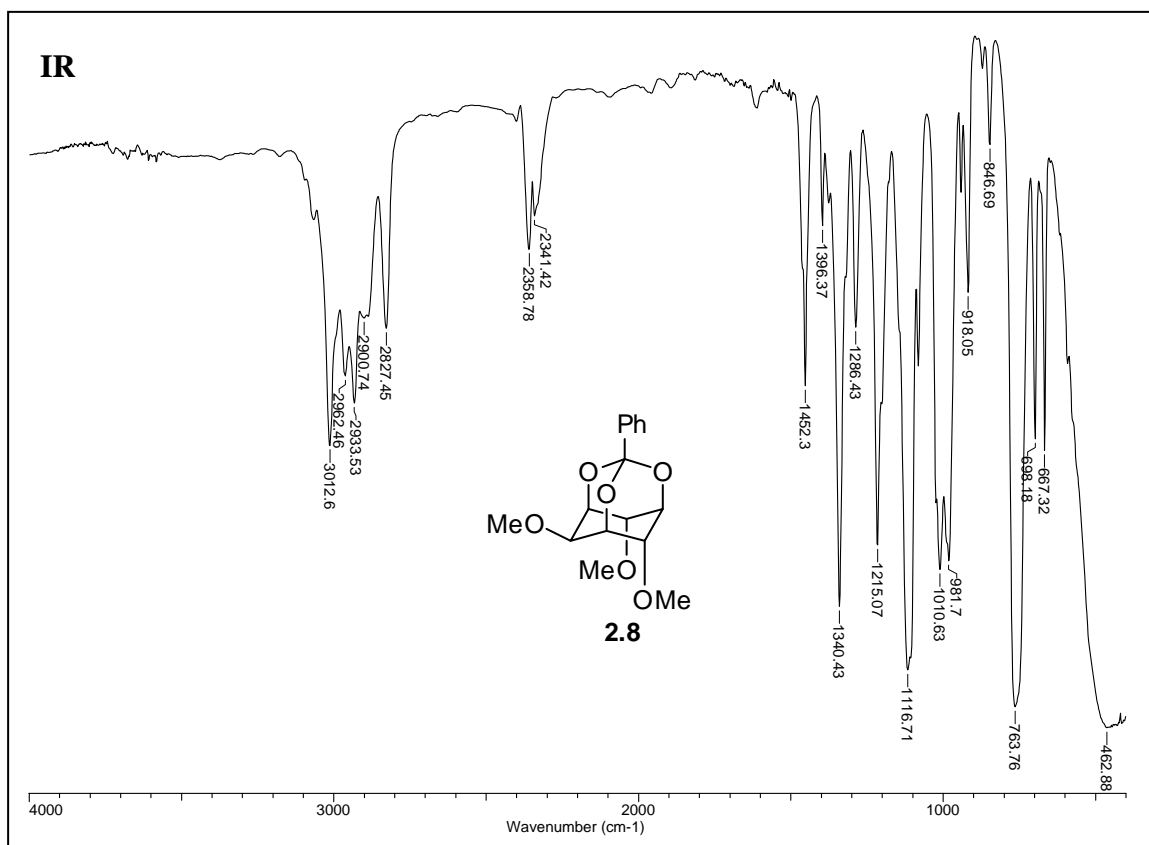


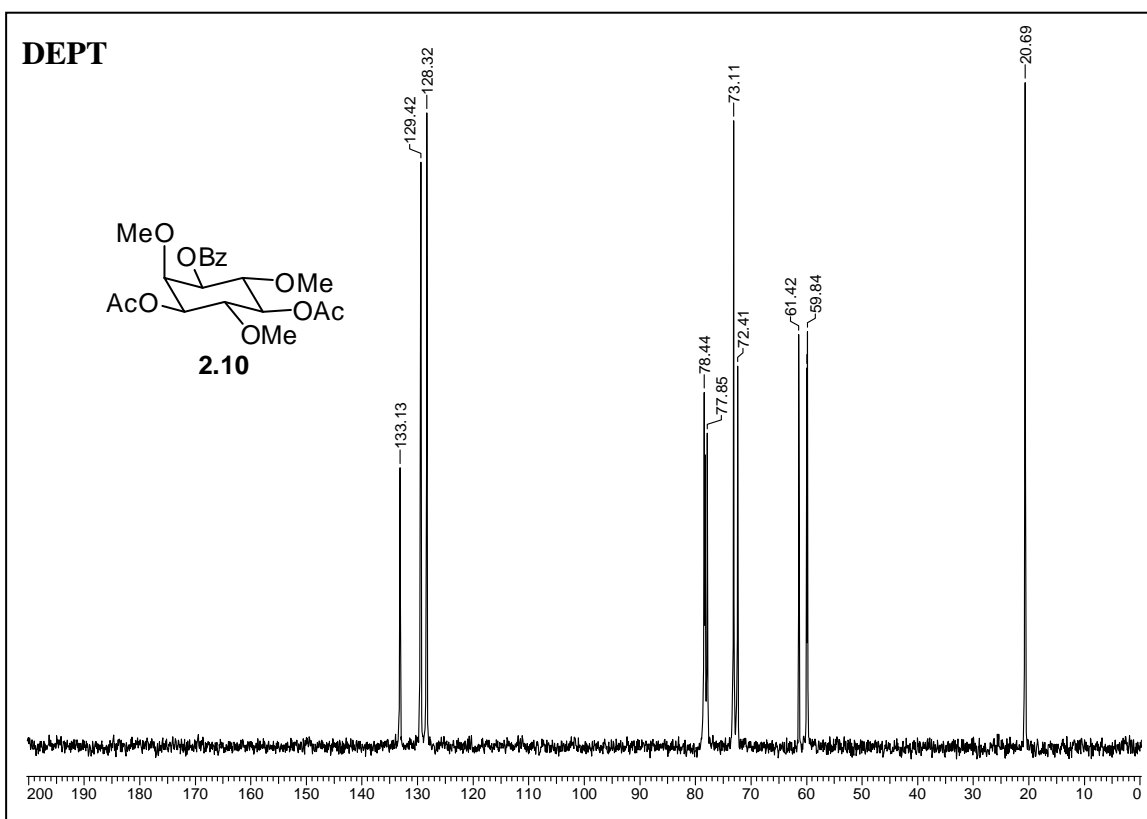
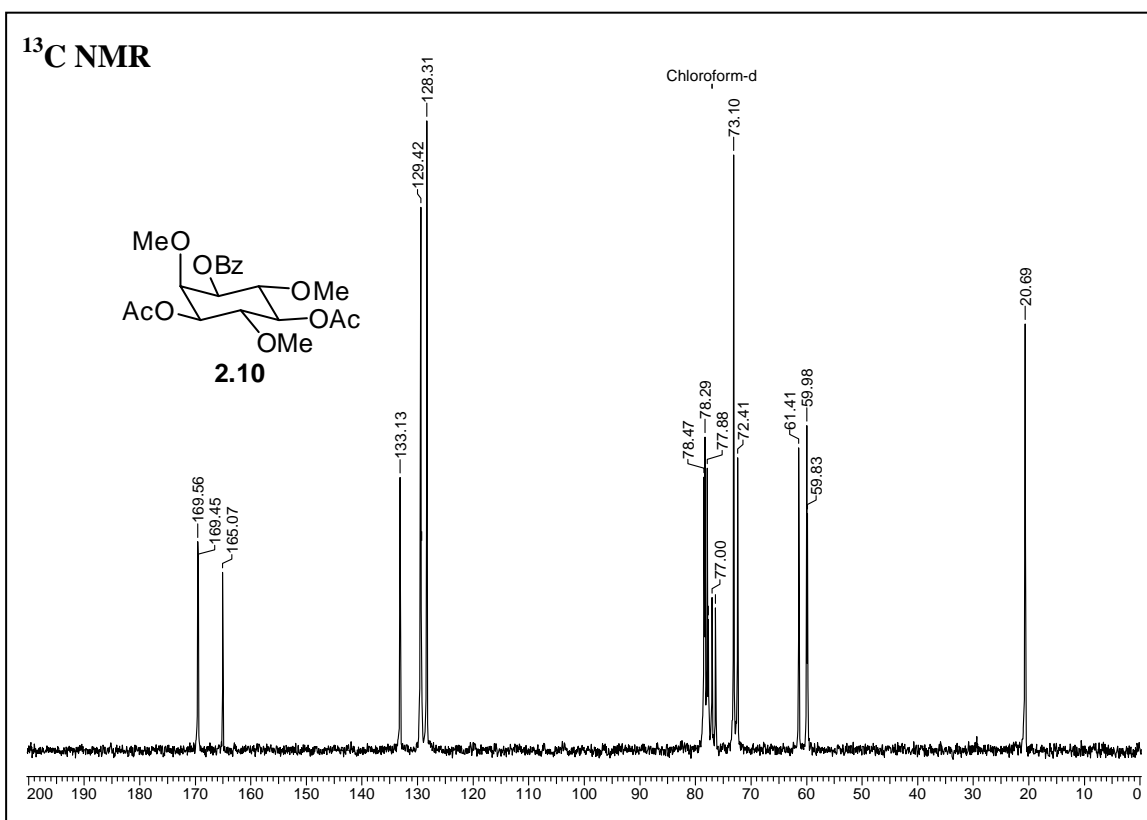
Chapter 2

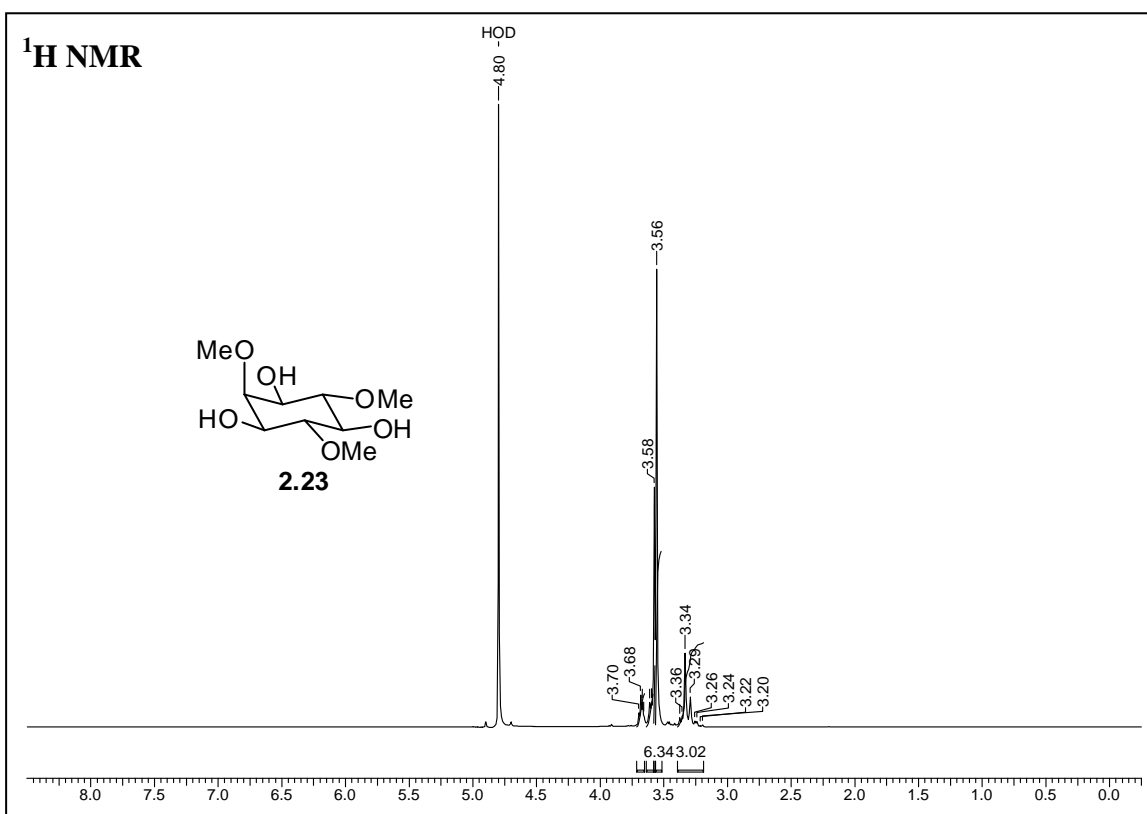
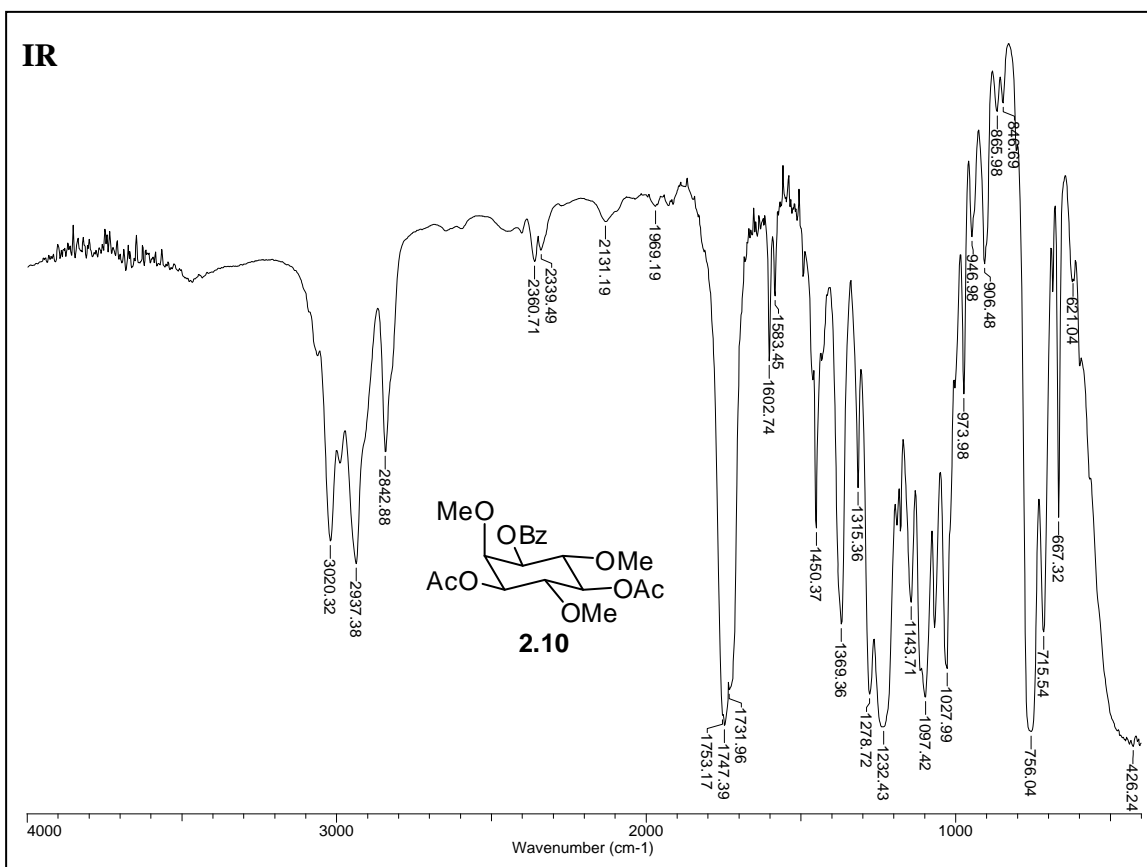


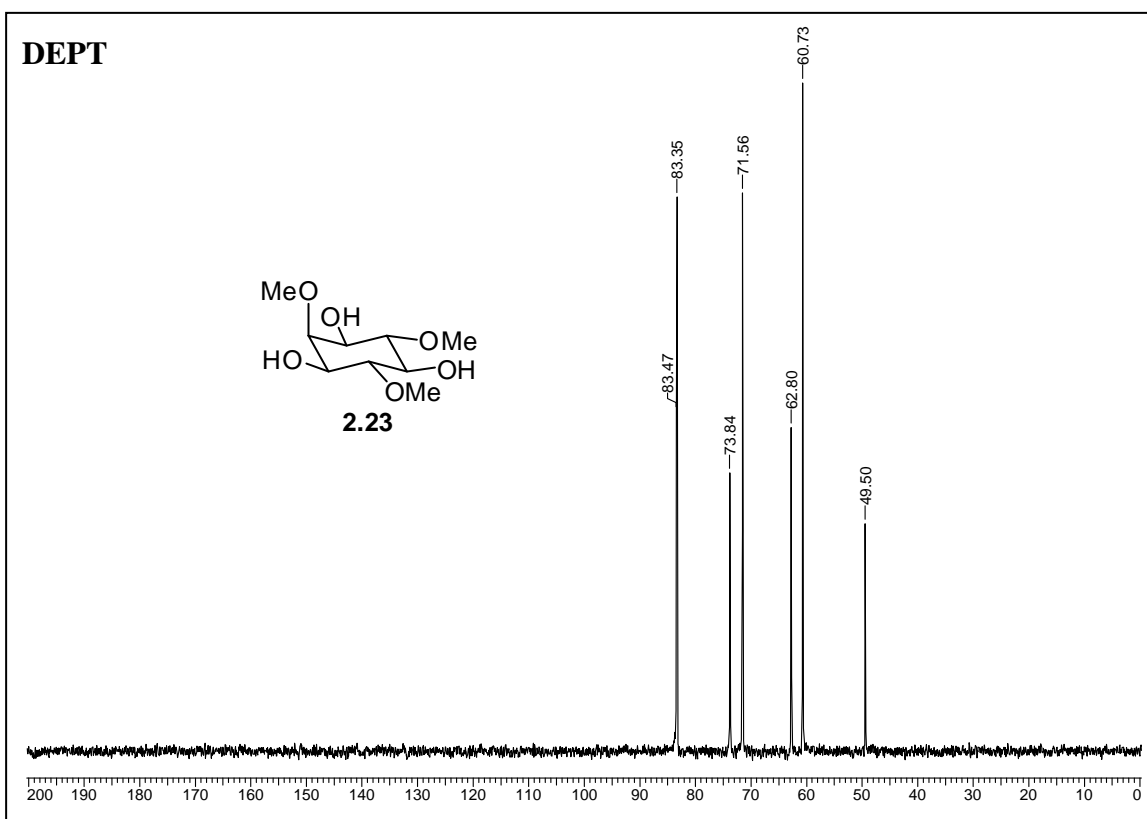
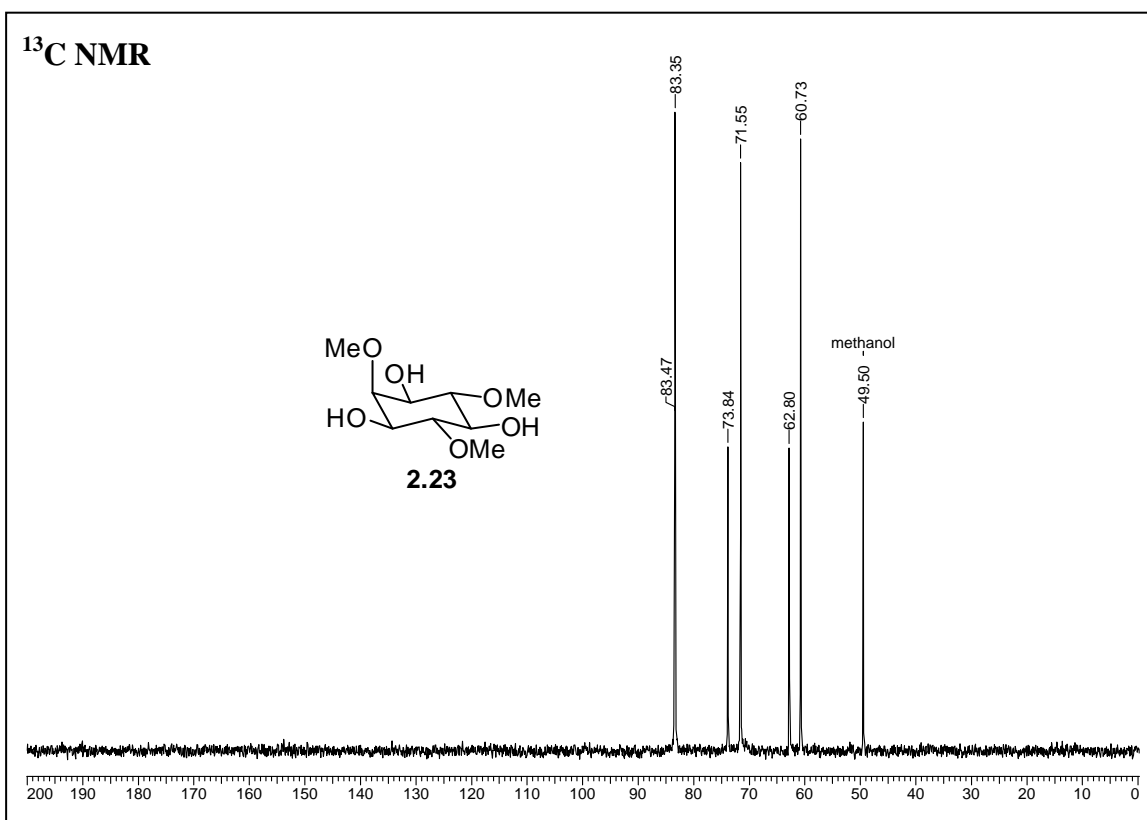


Chapter 2

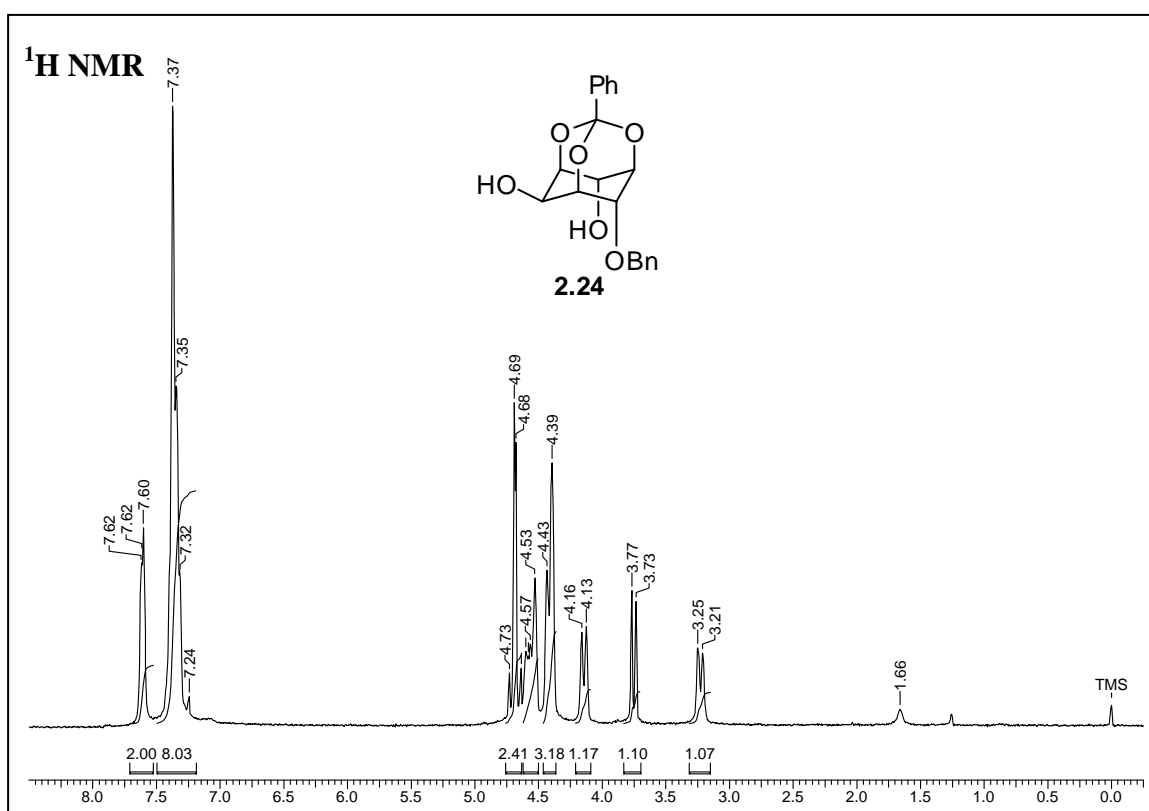
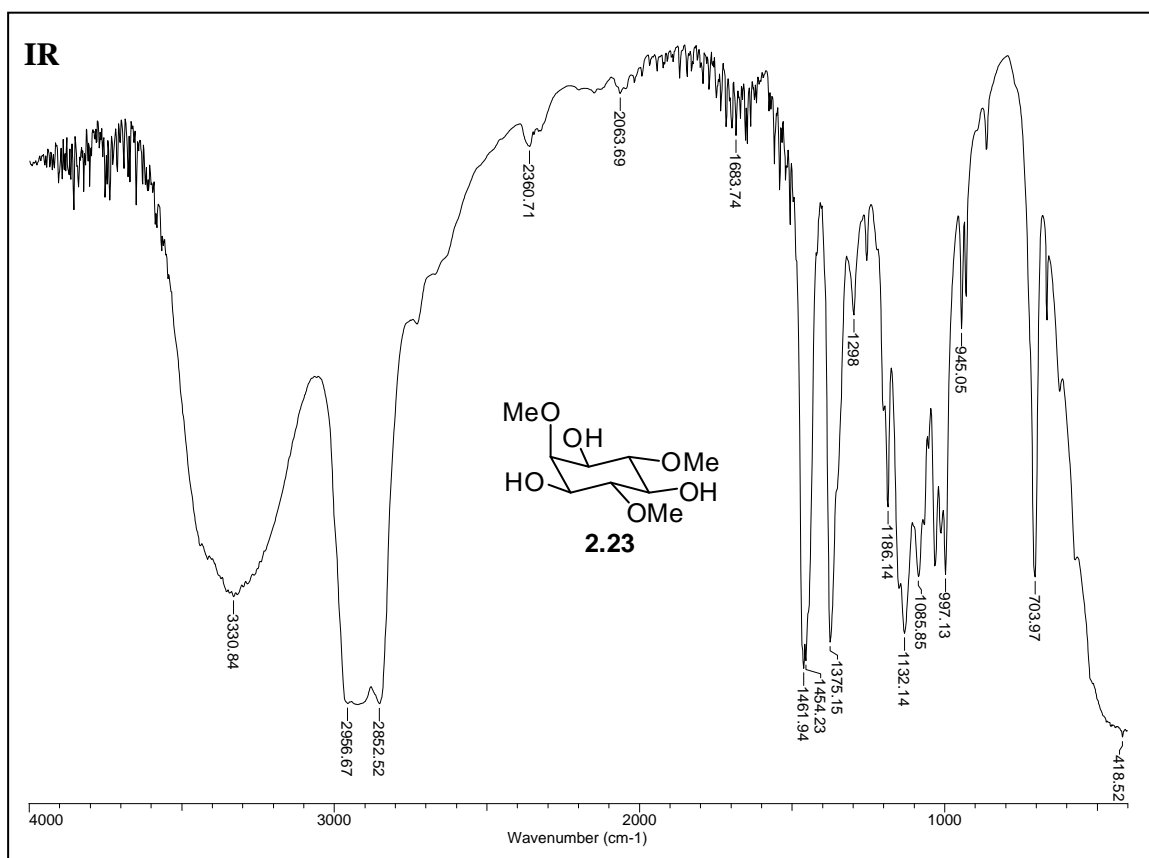


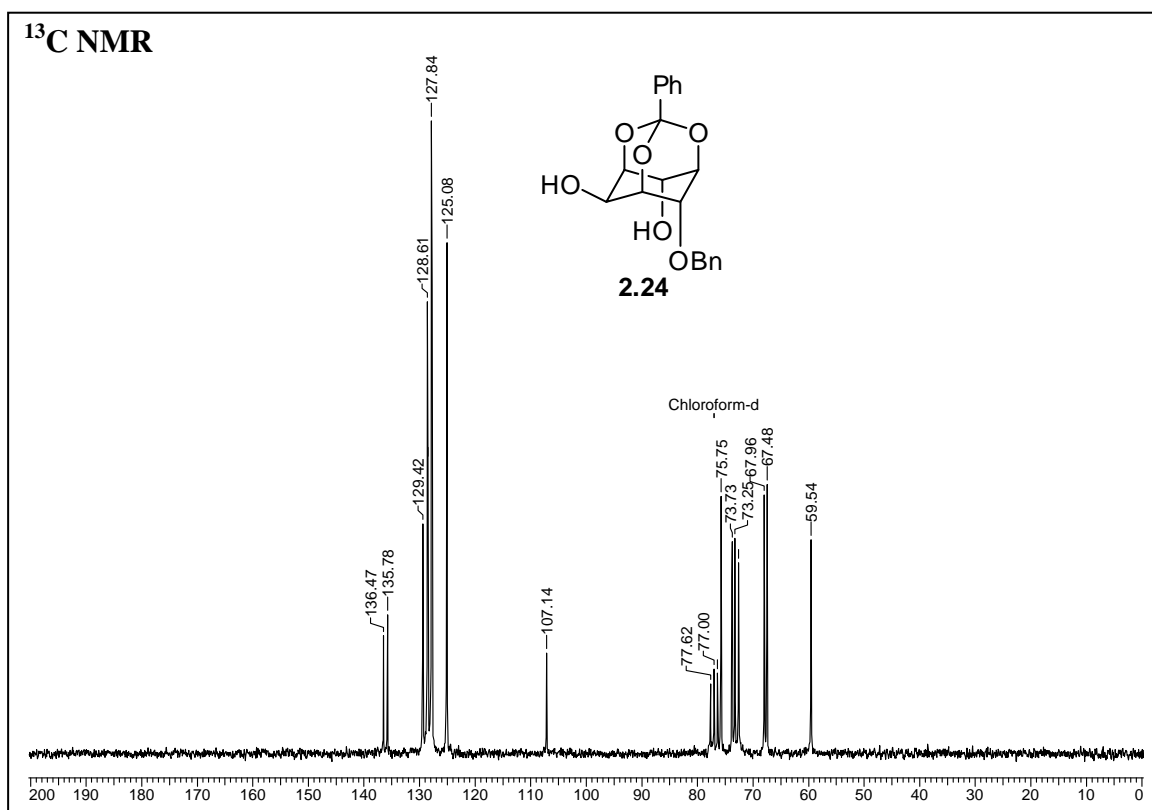
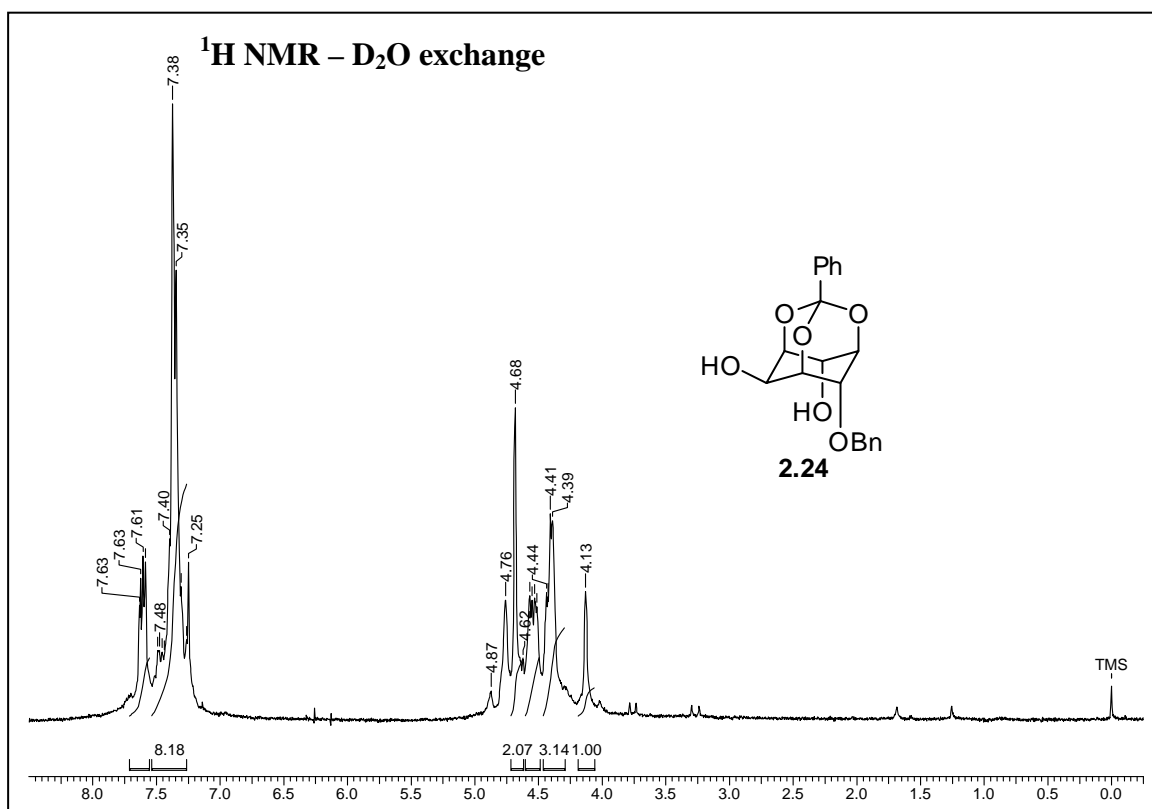


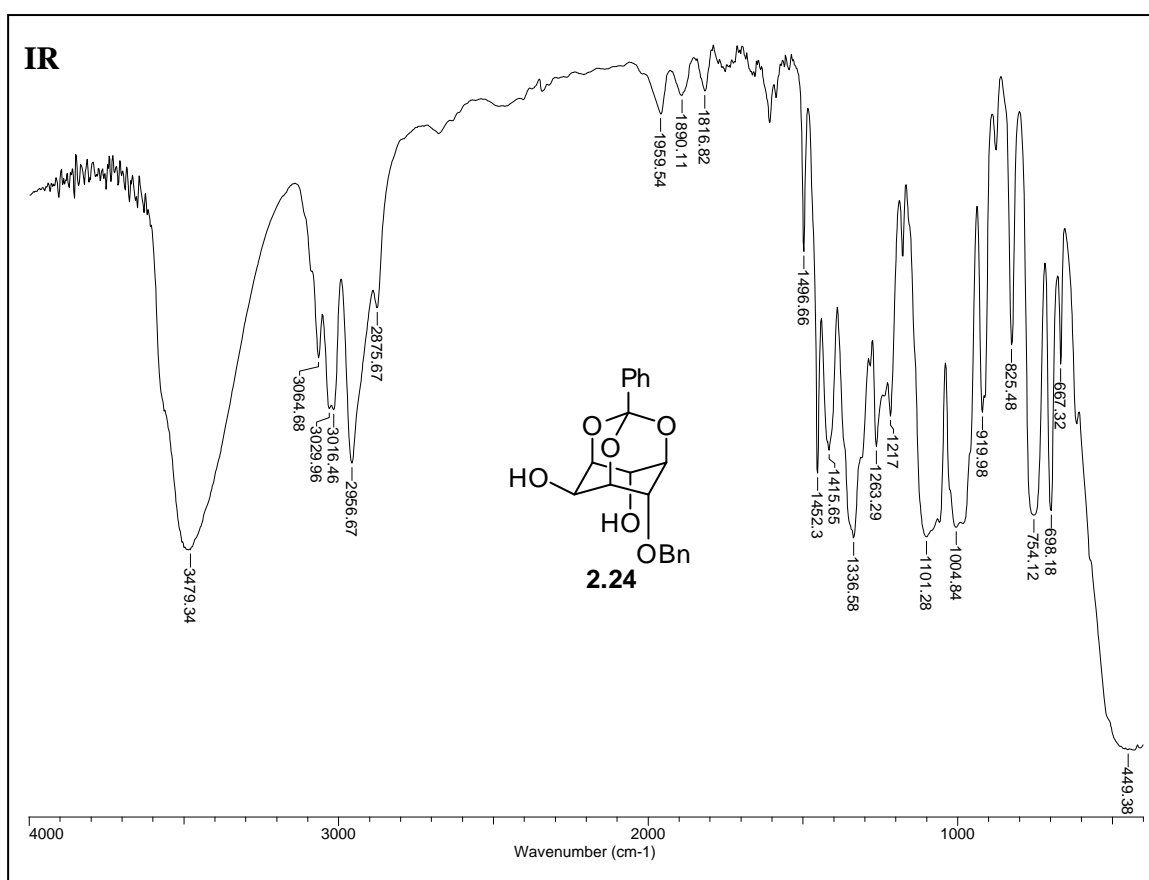
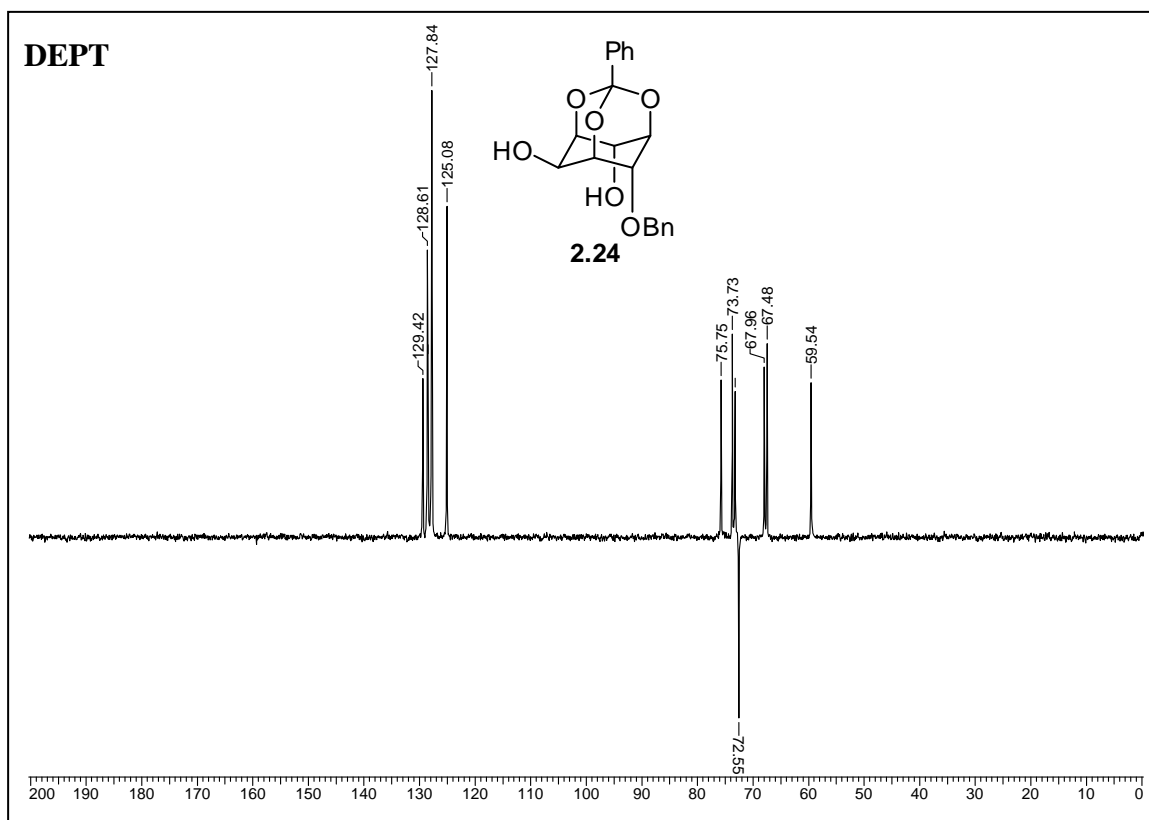




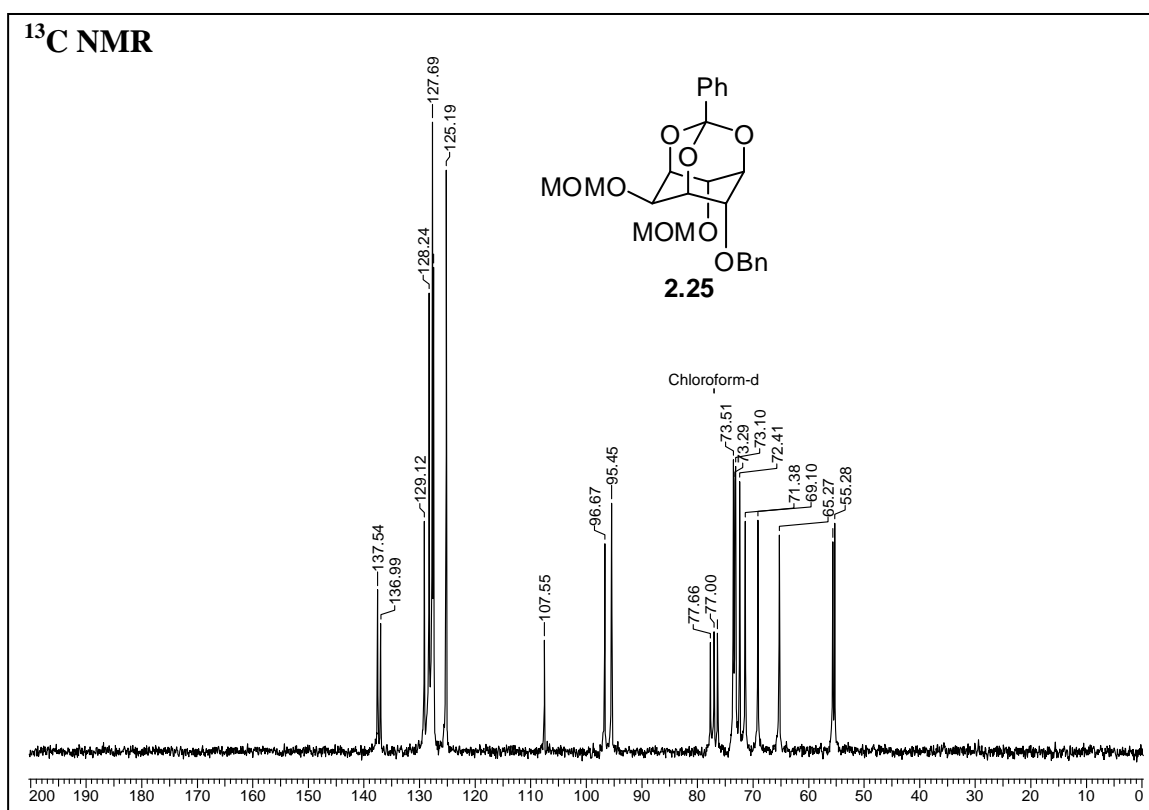
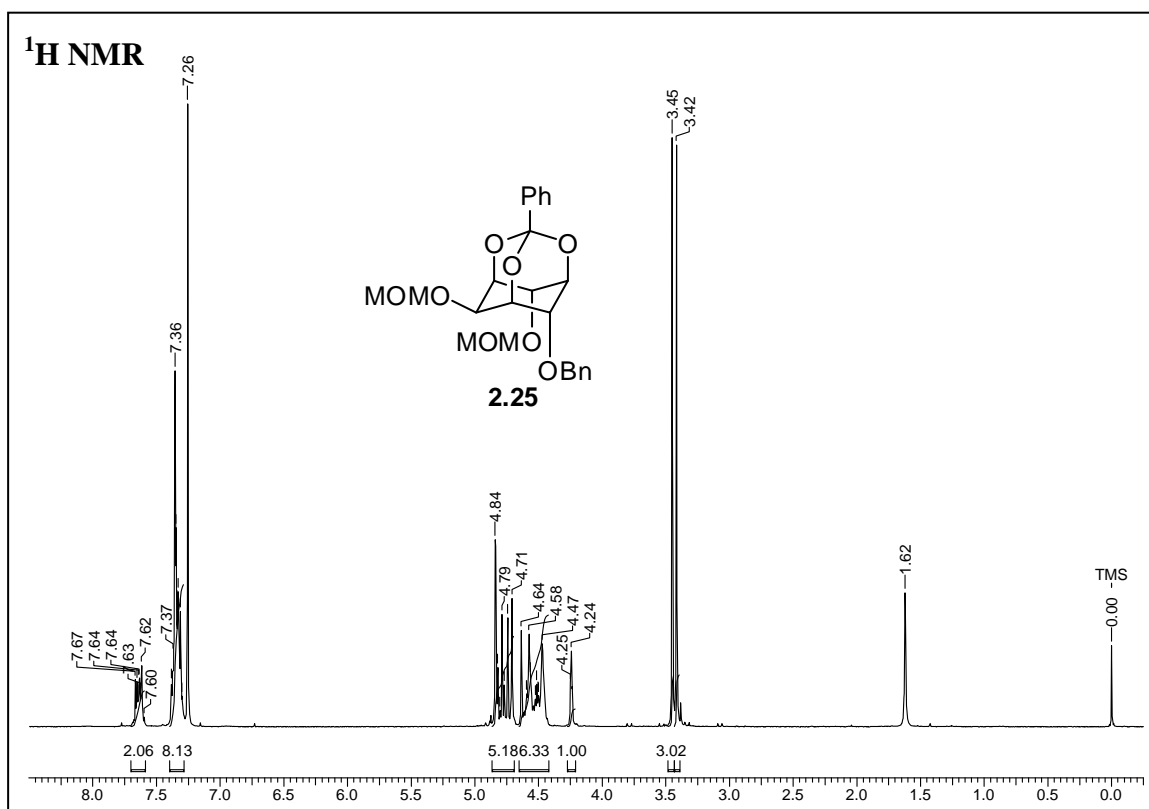
Chapter 2

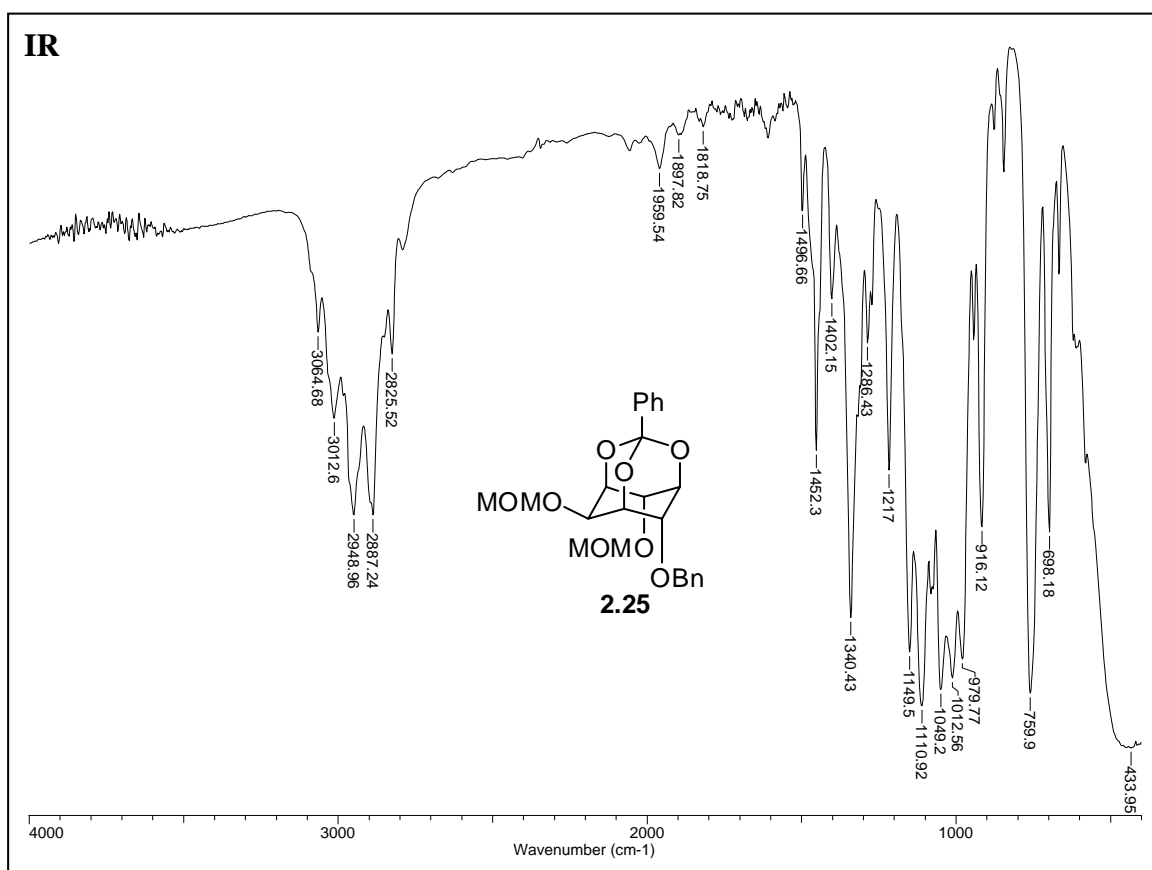
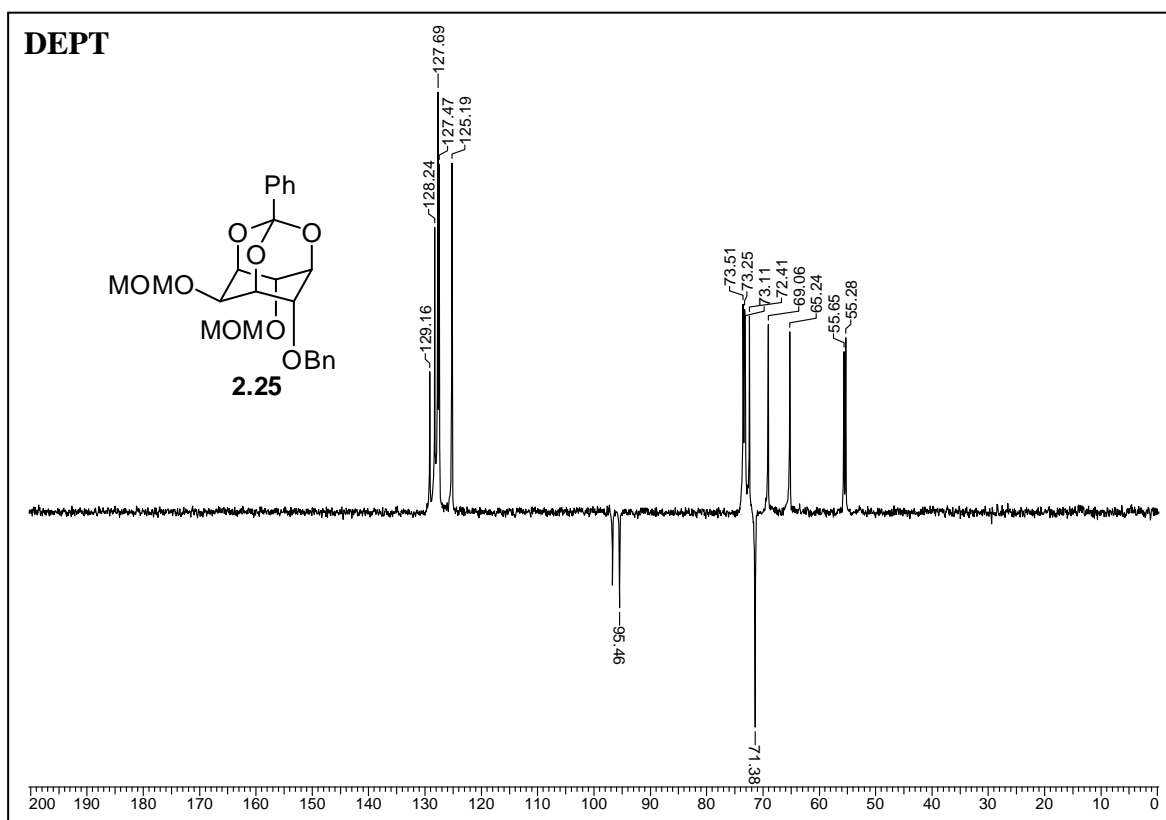


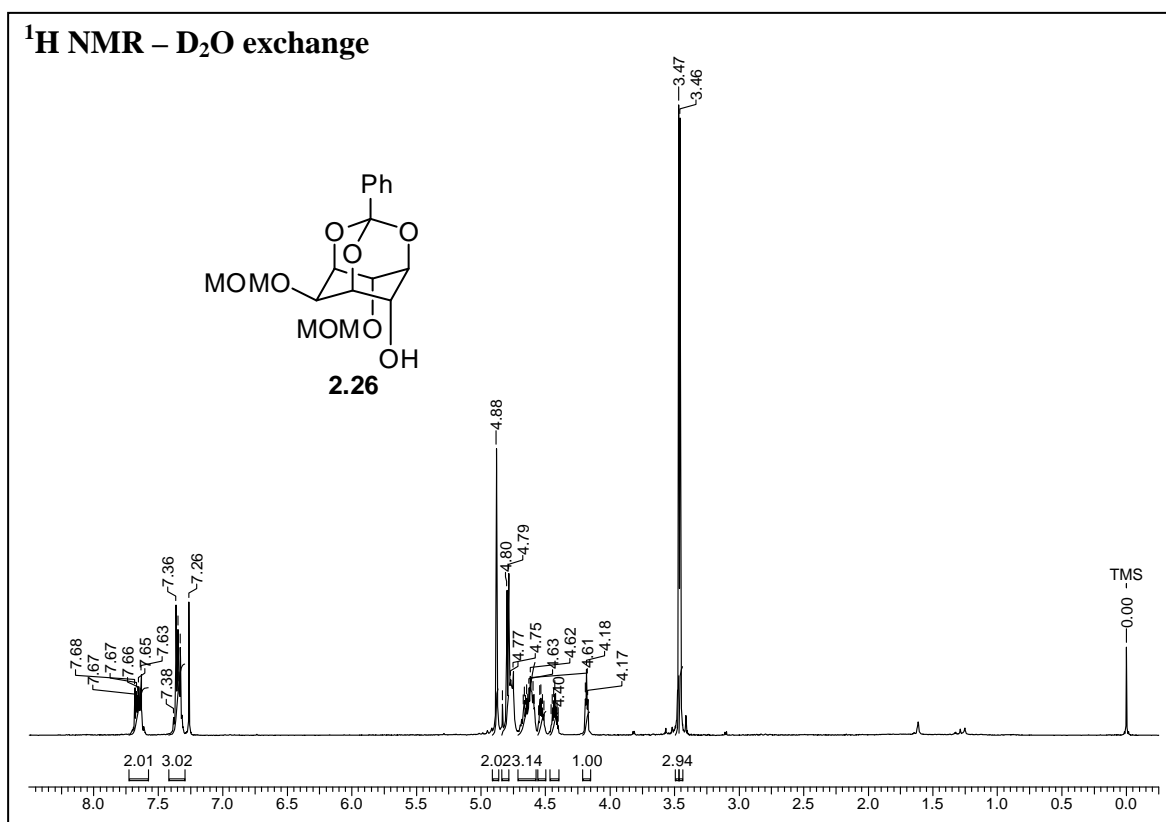
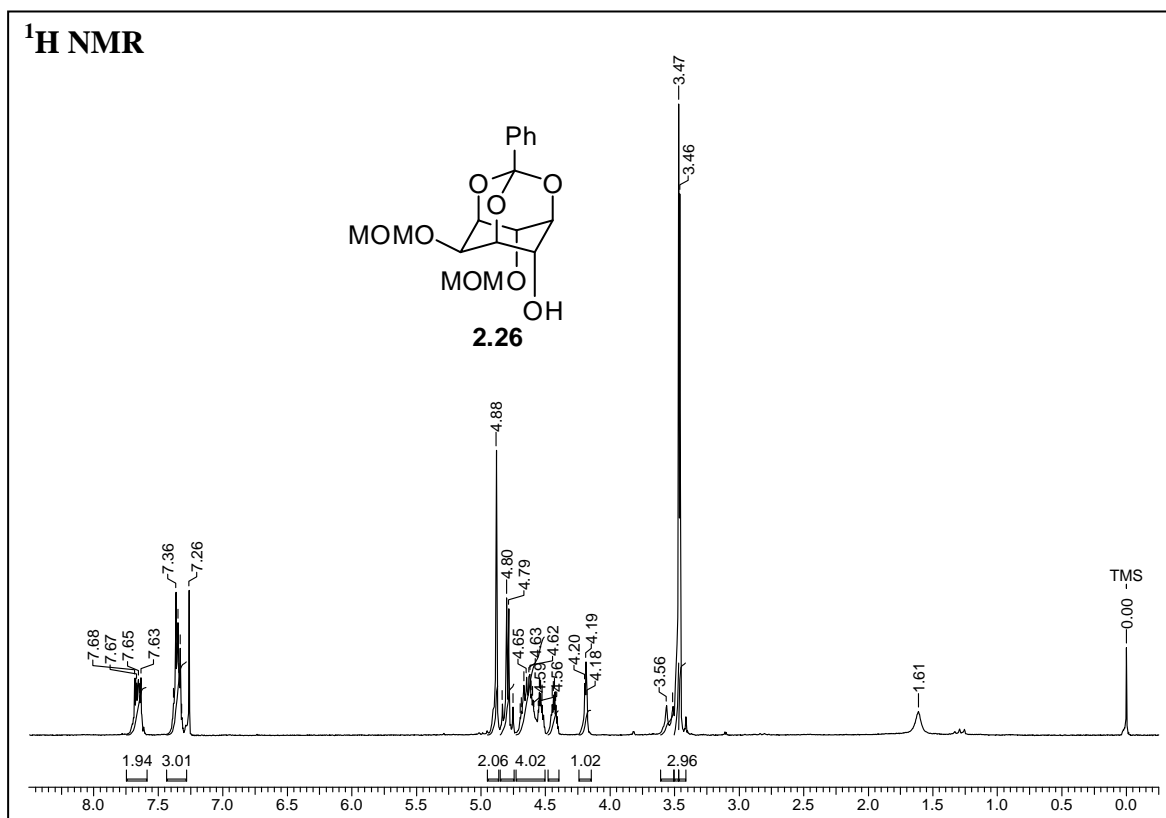


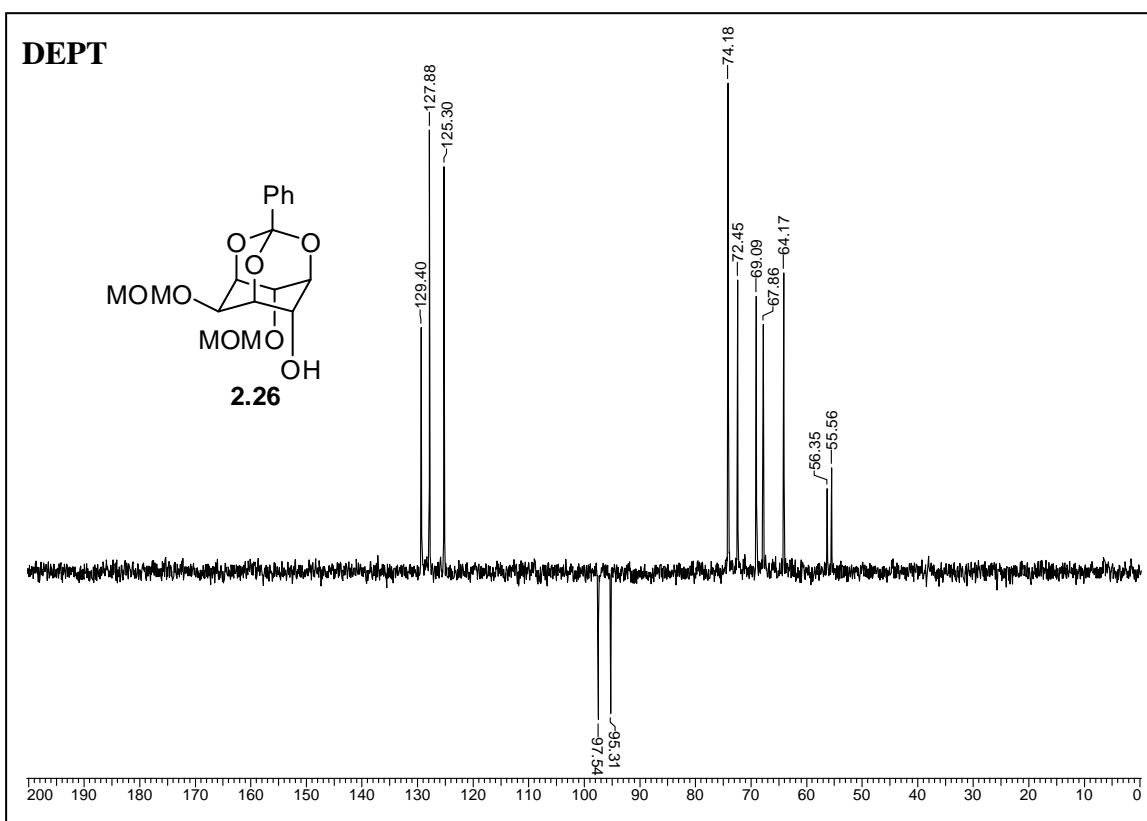
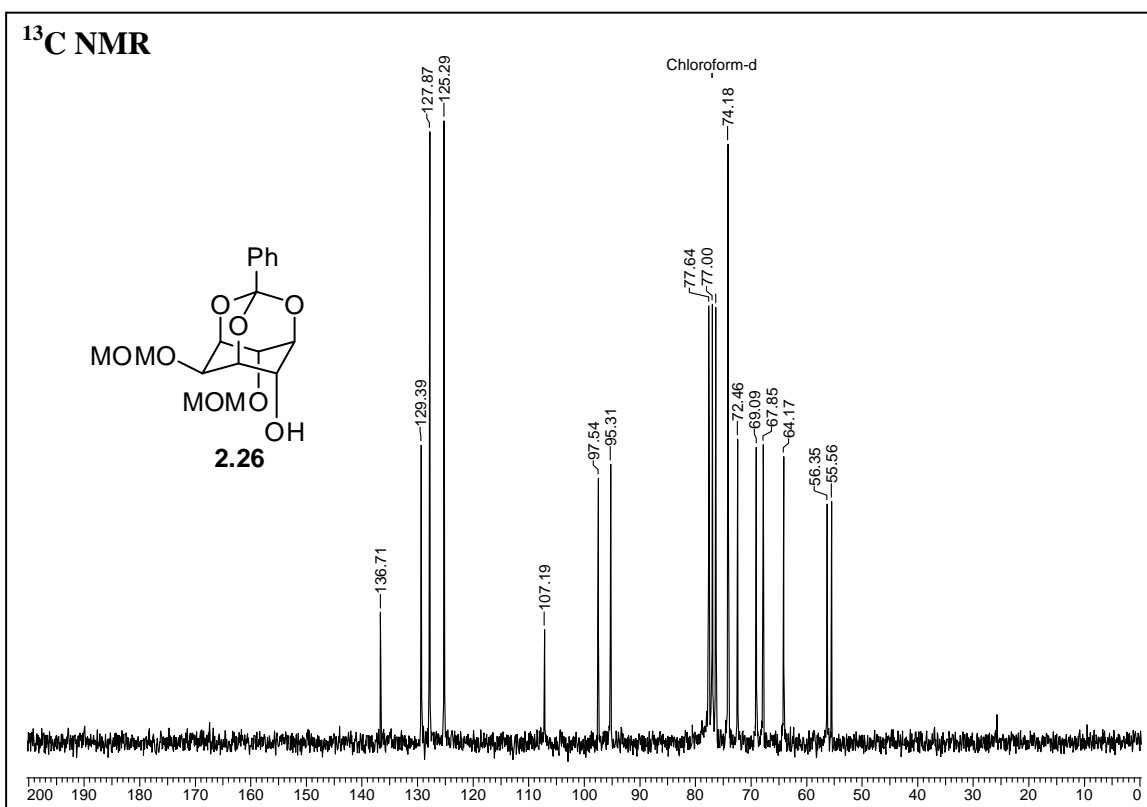


Chapter 2

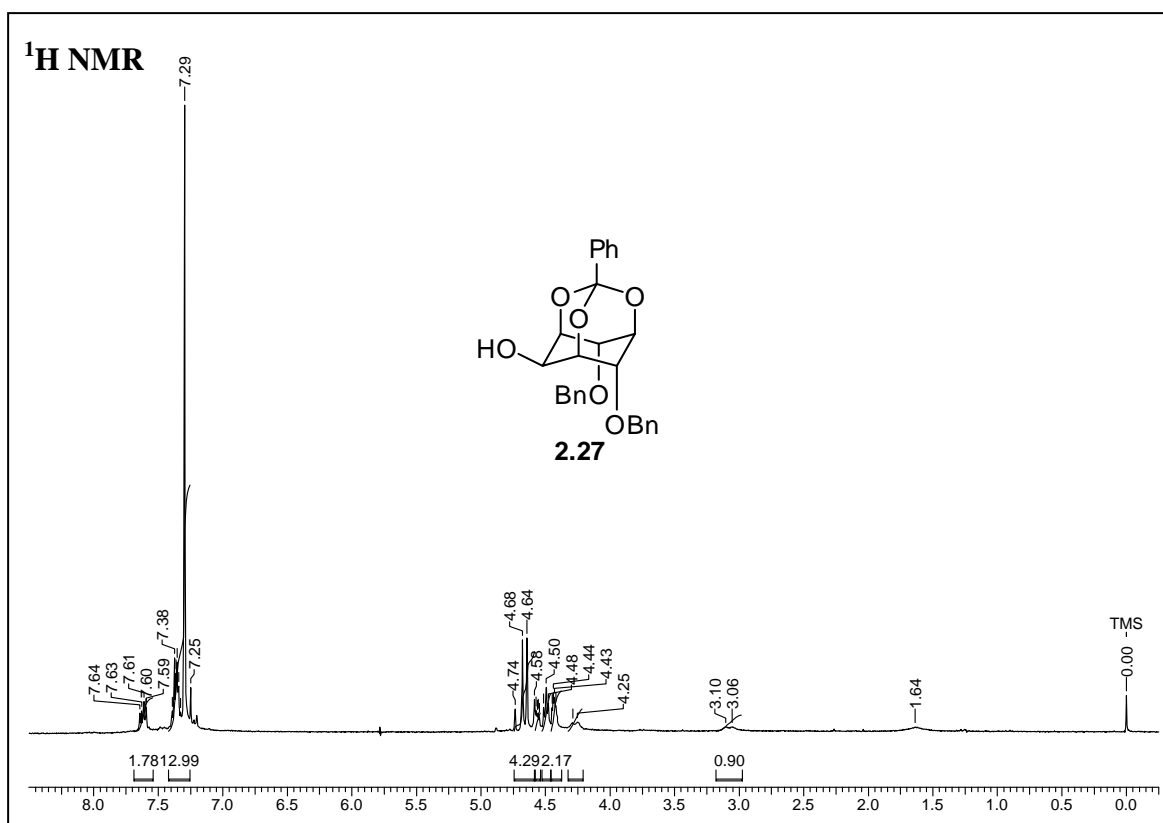
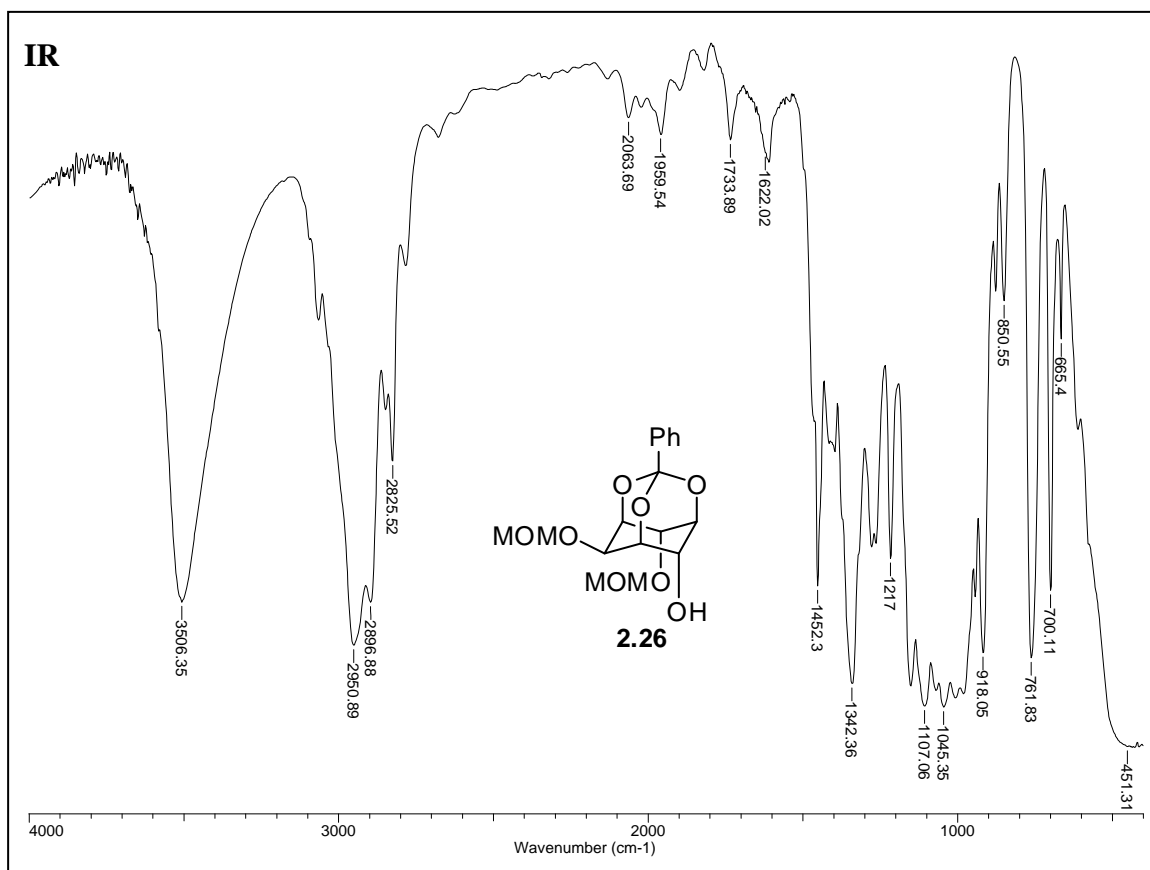


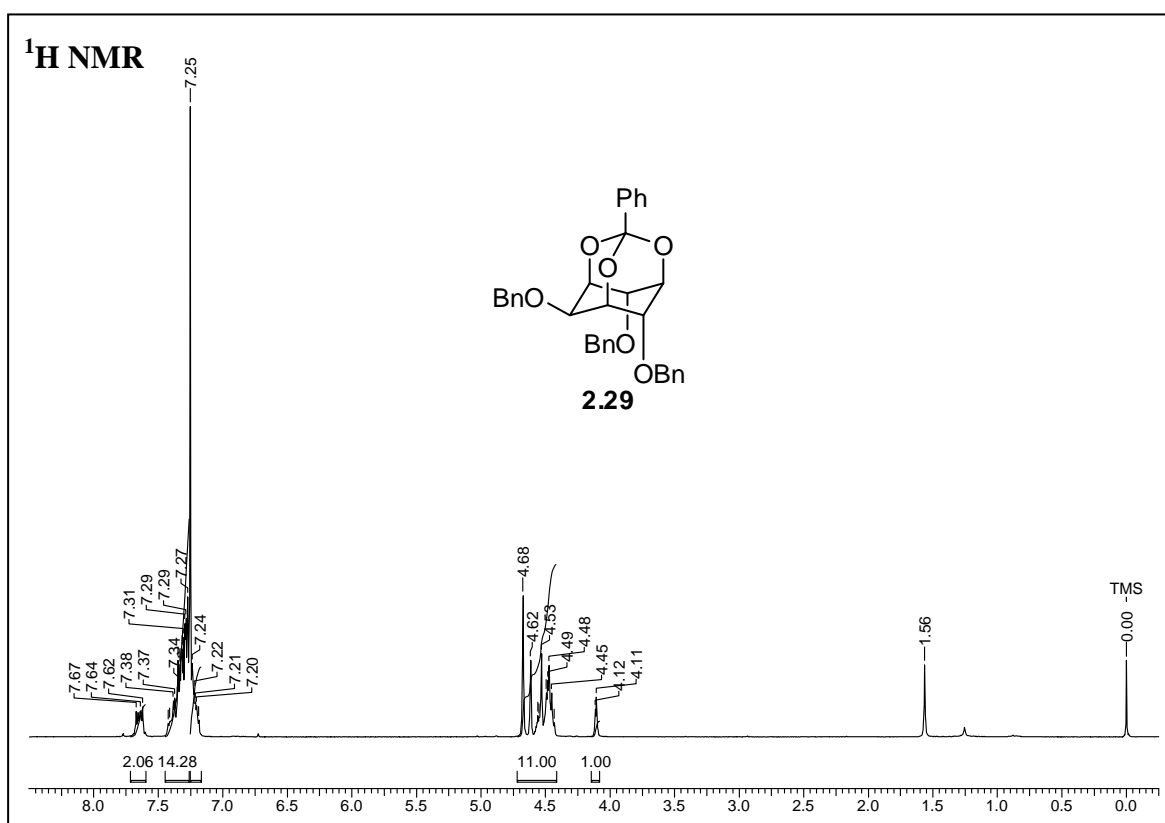
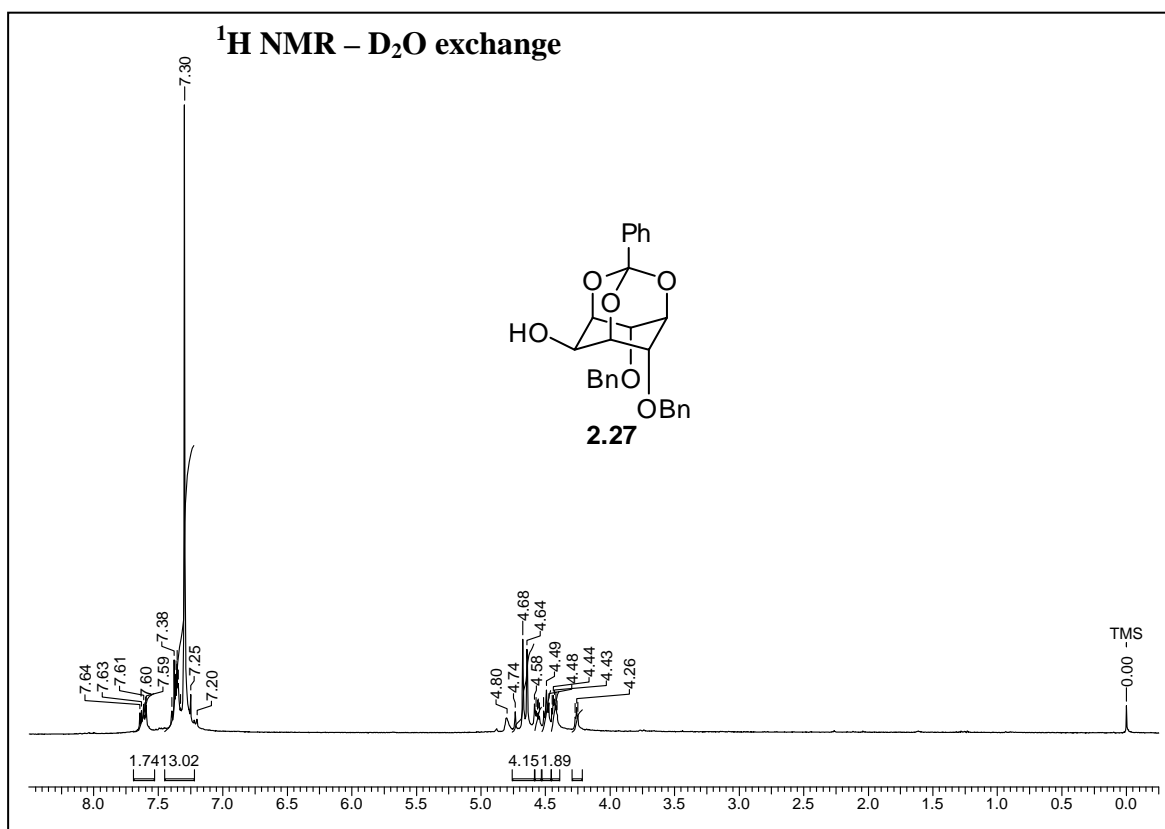


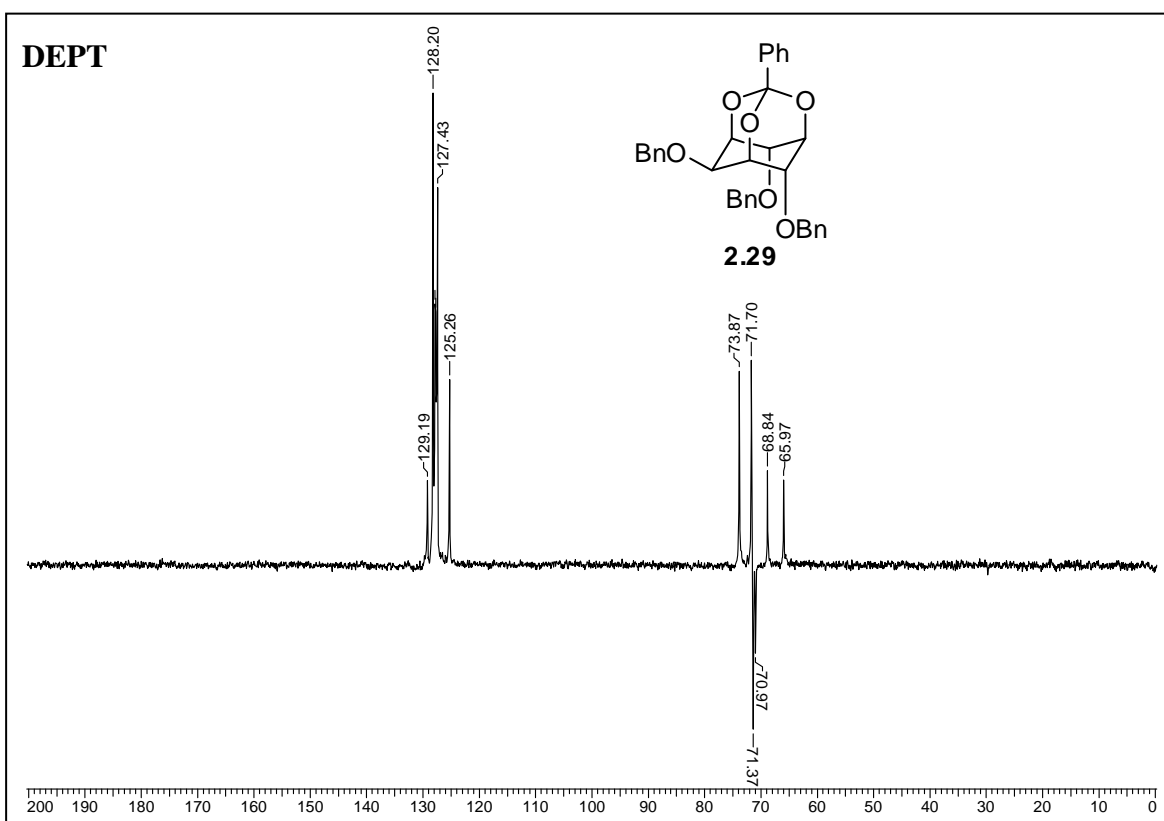
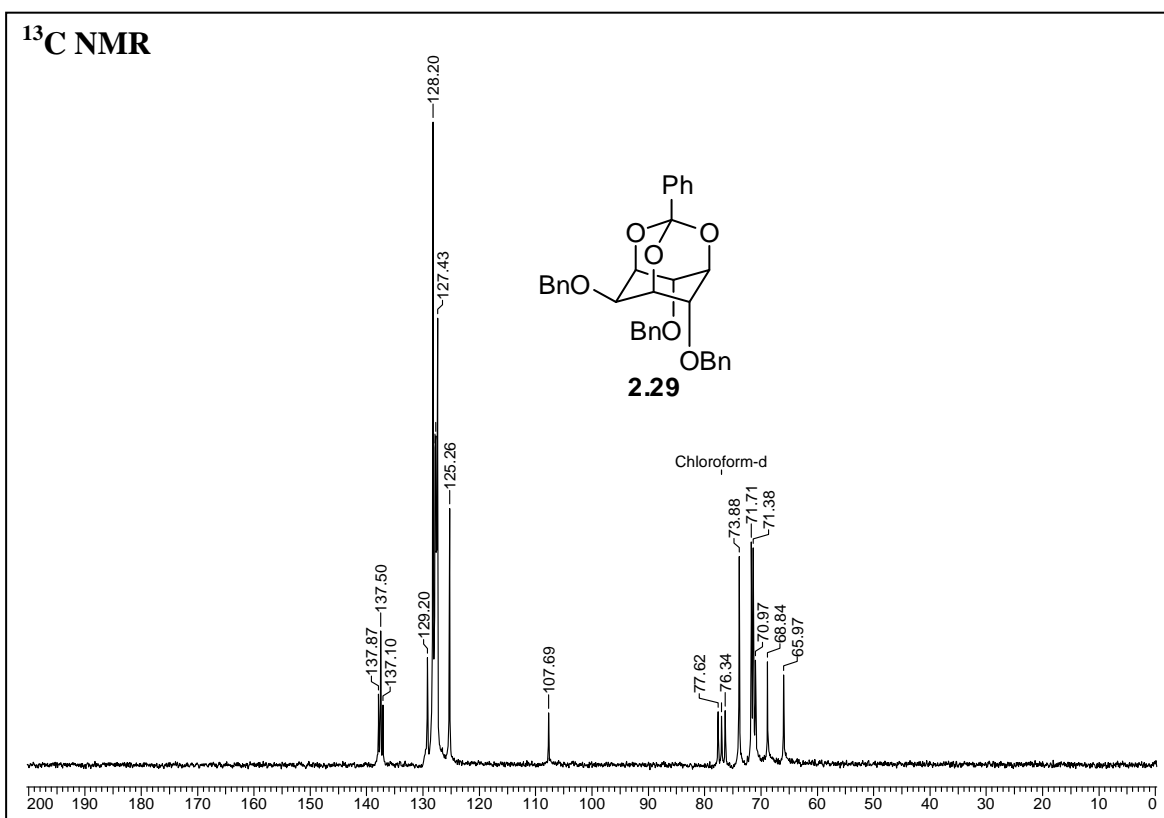




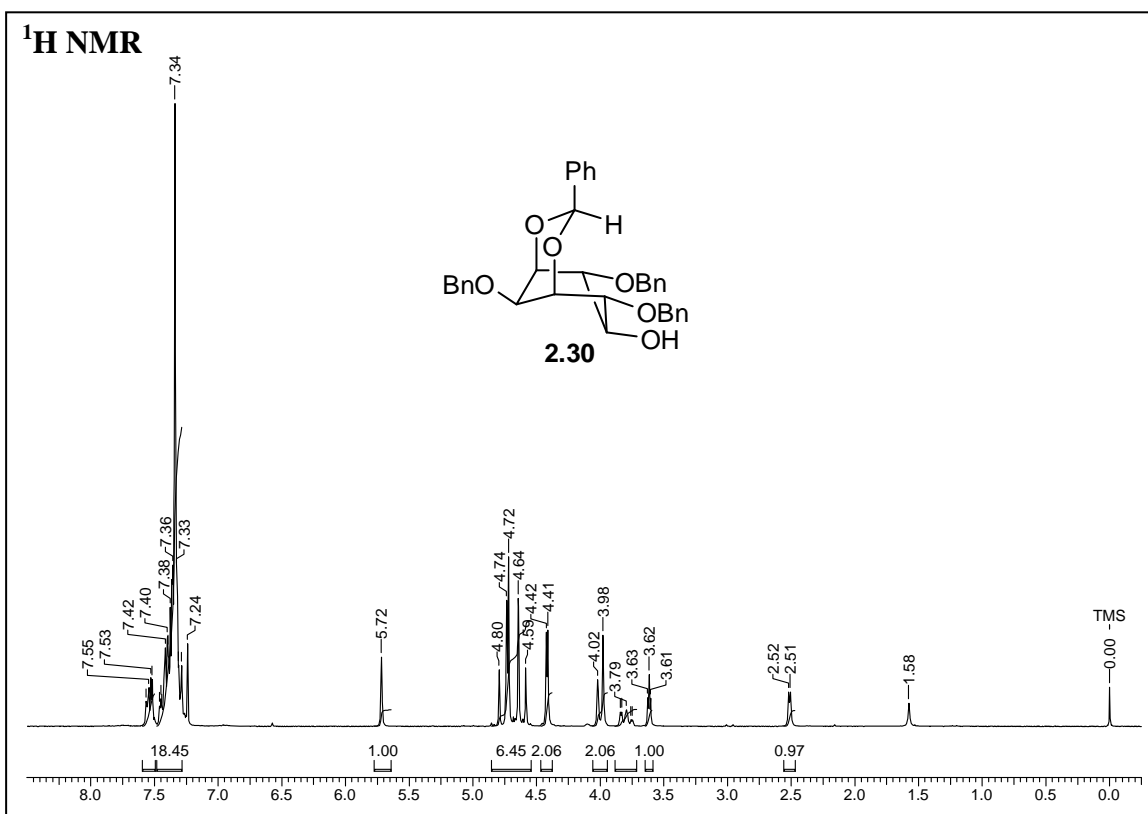
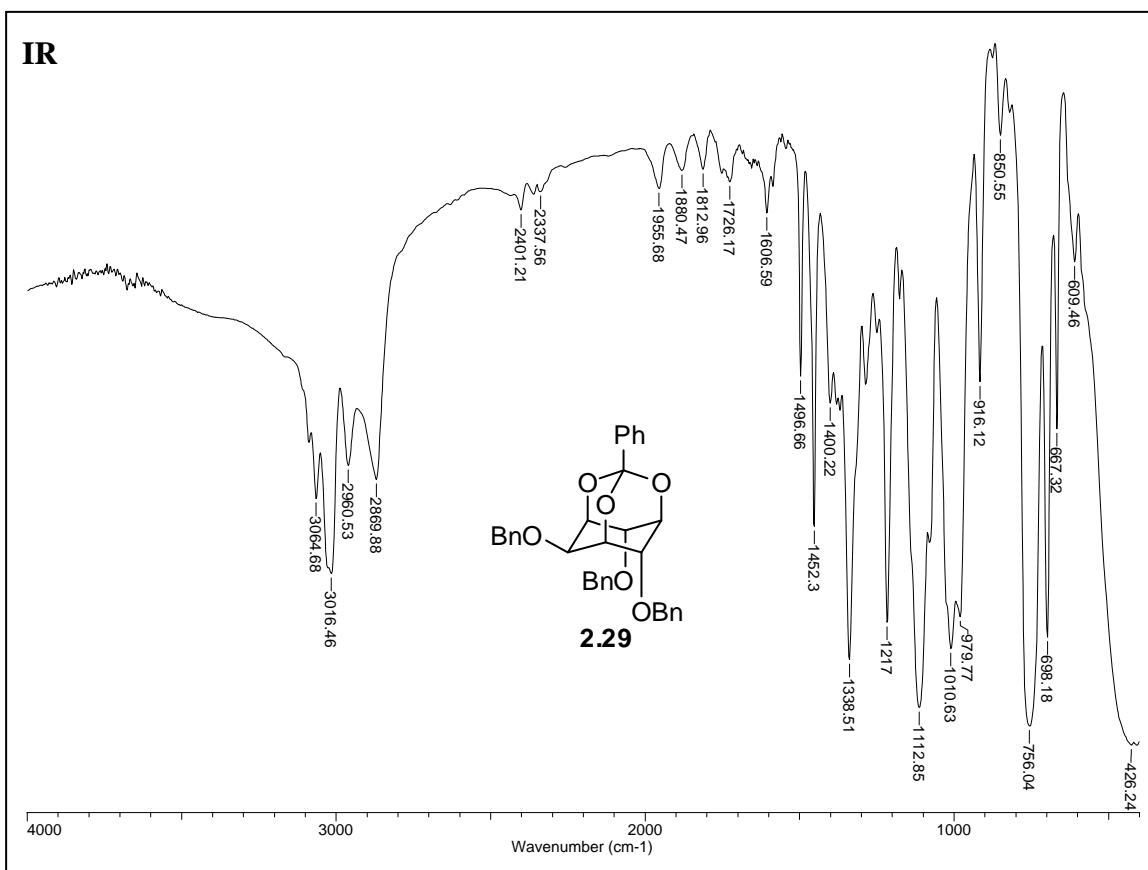
Chapter 2

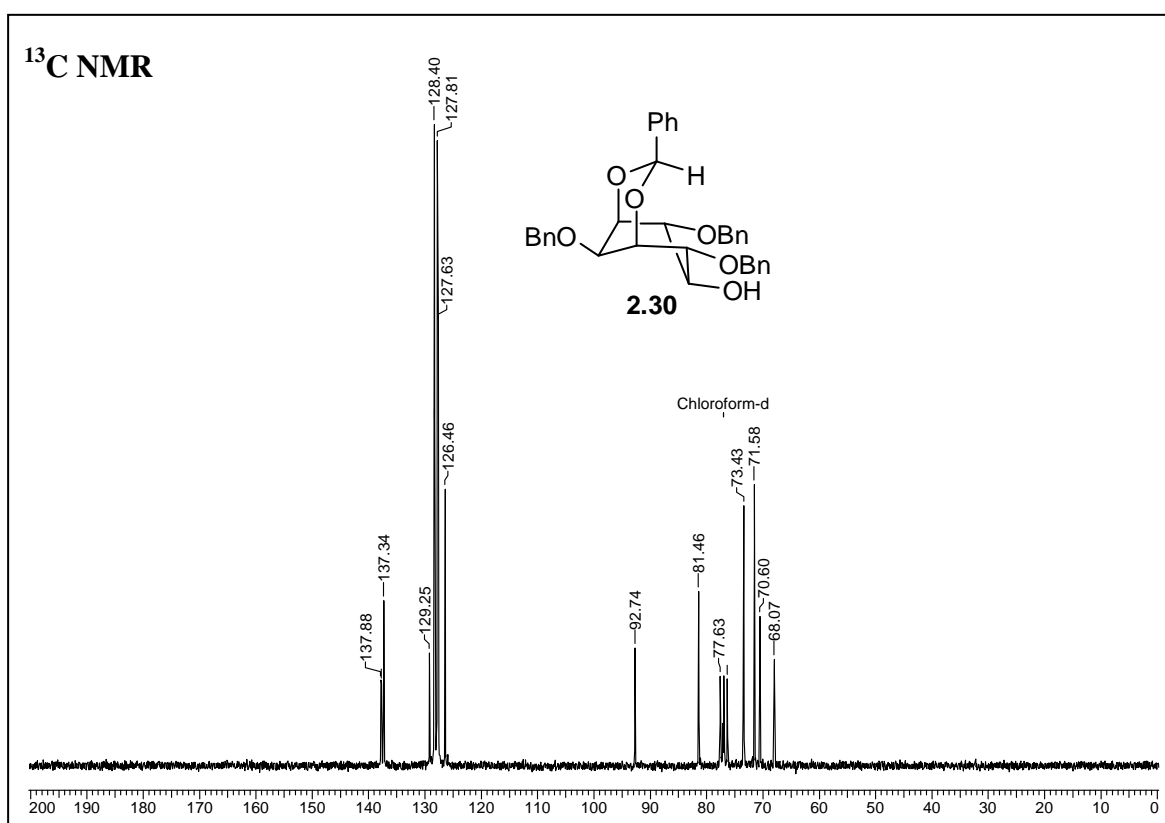
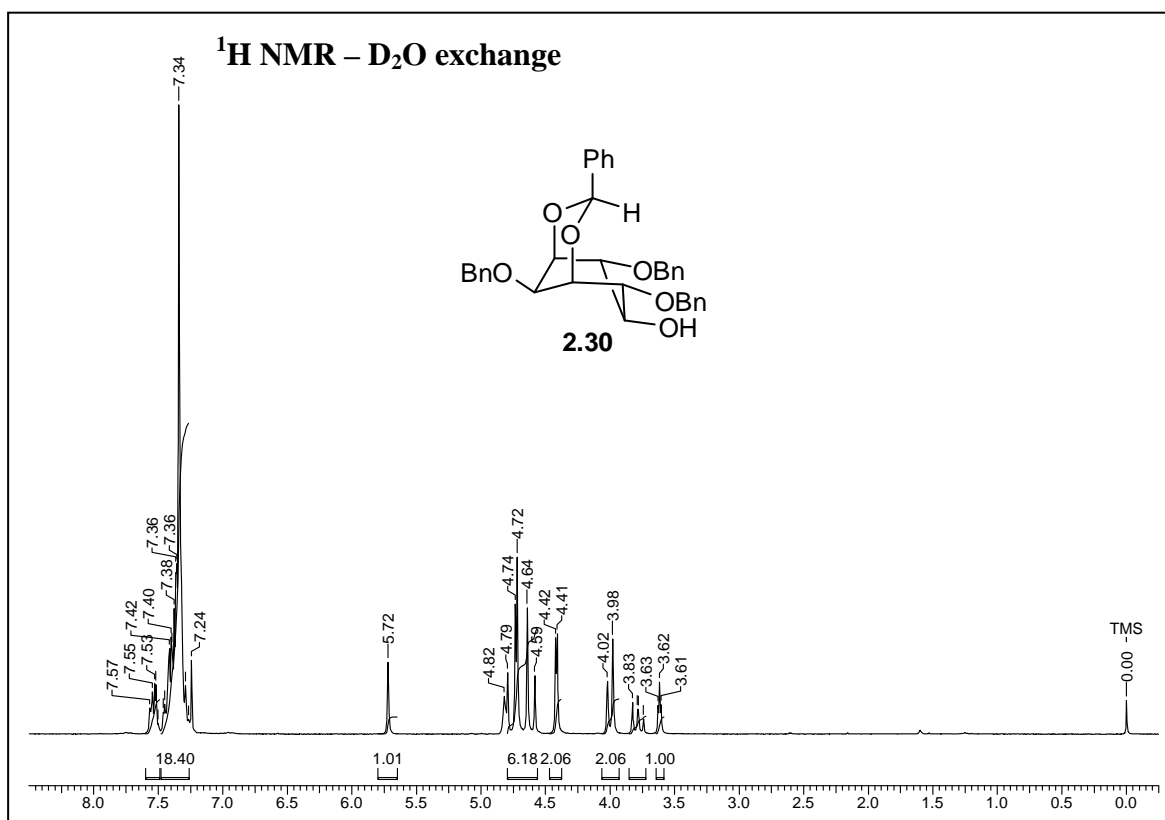


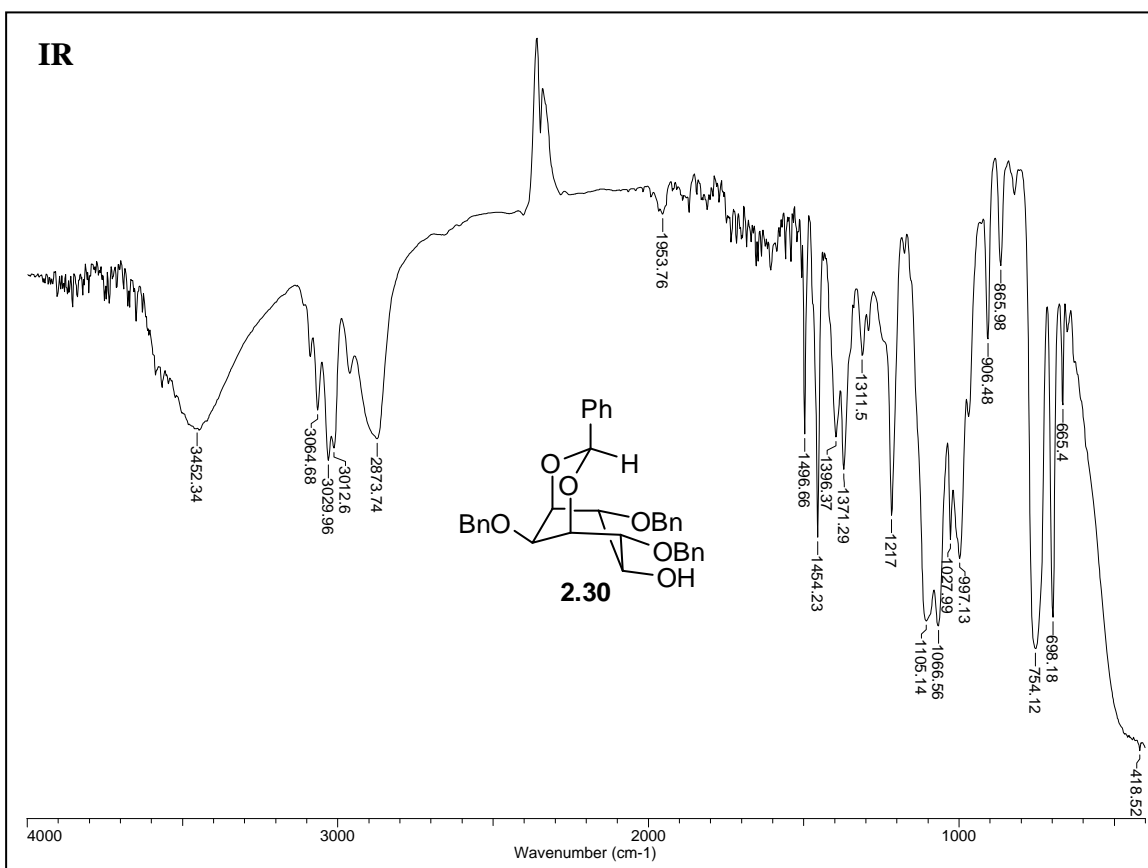
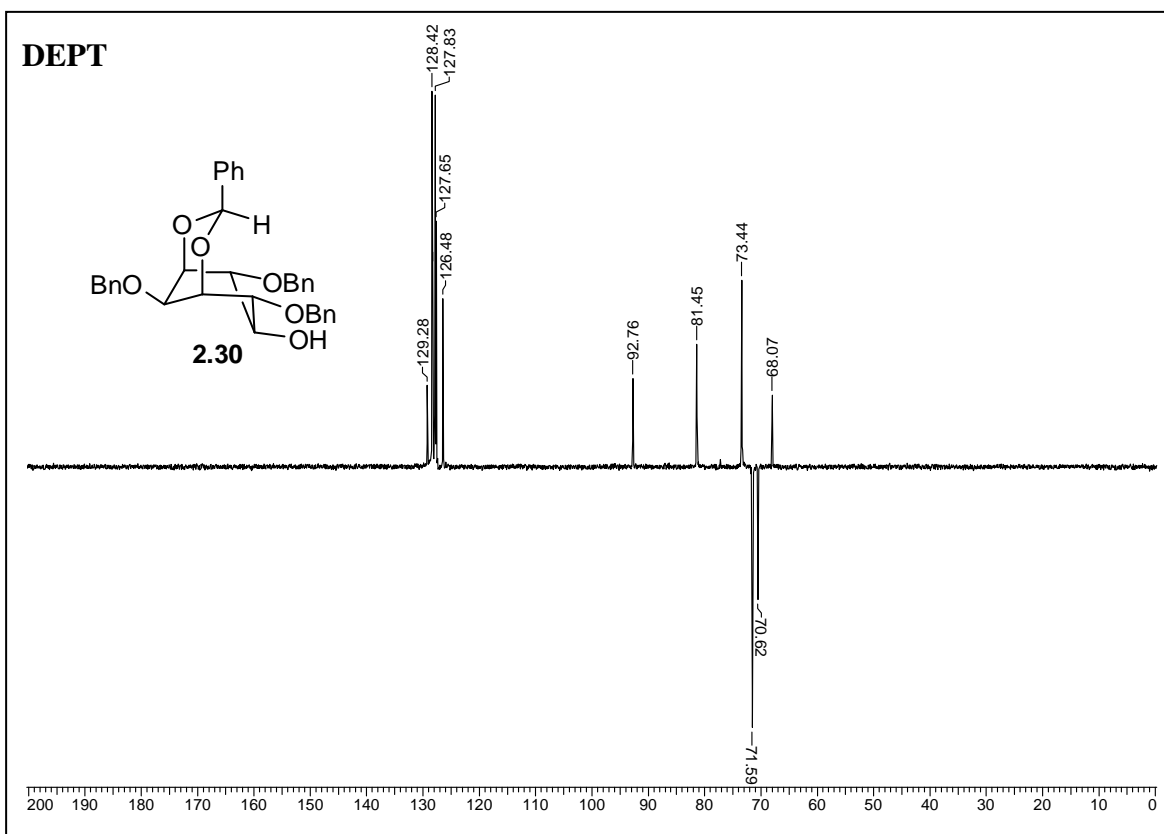


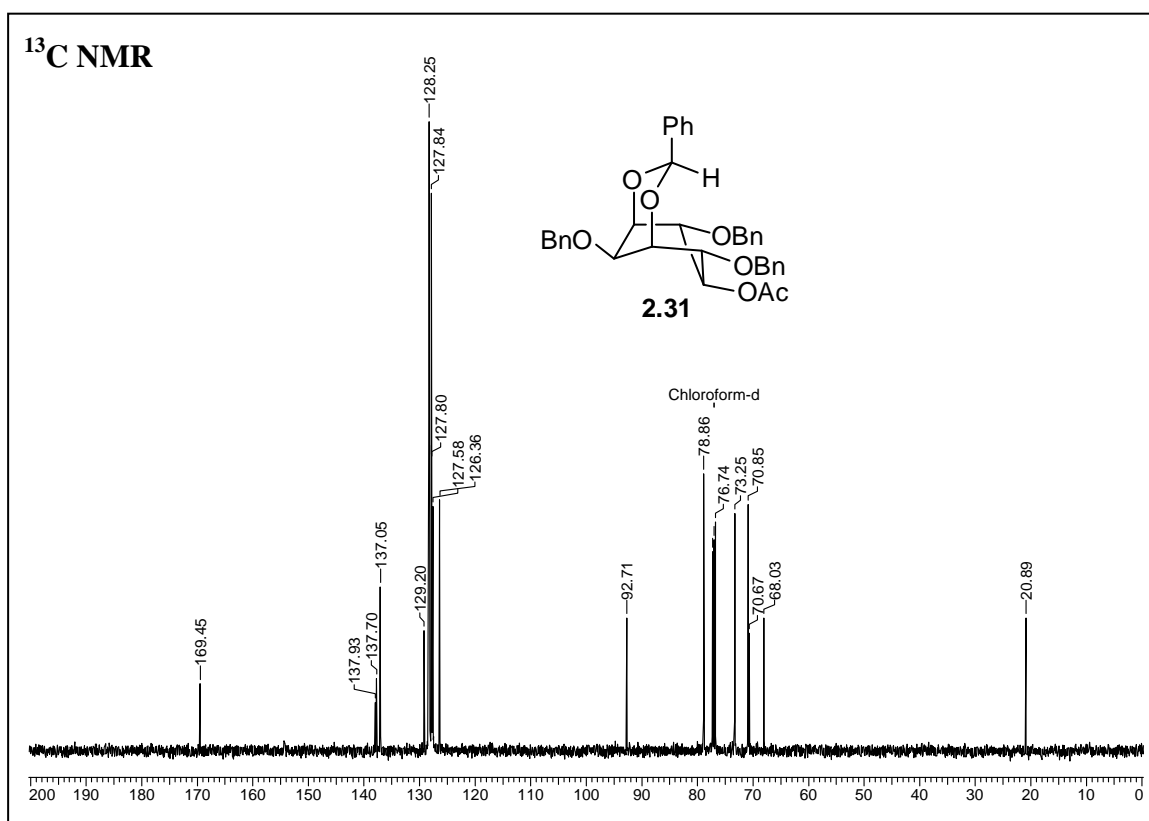
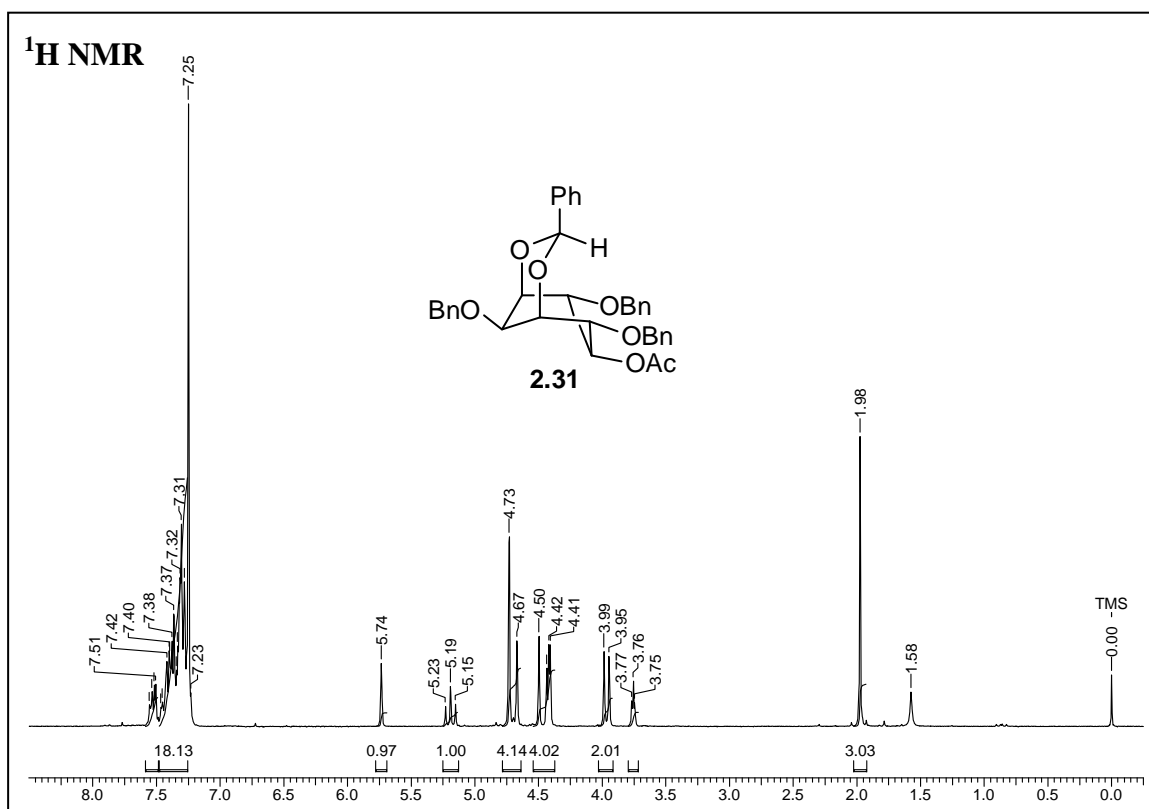


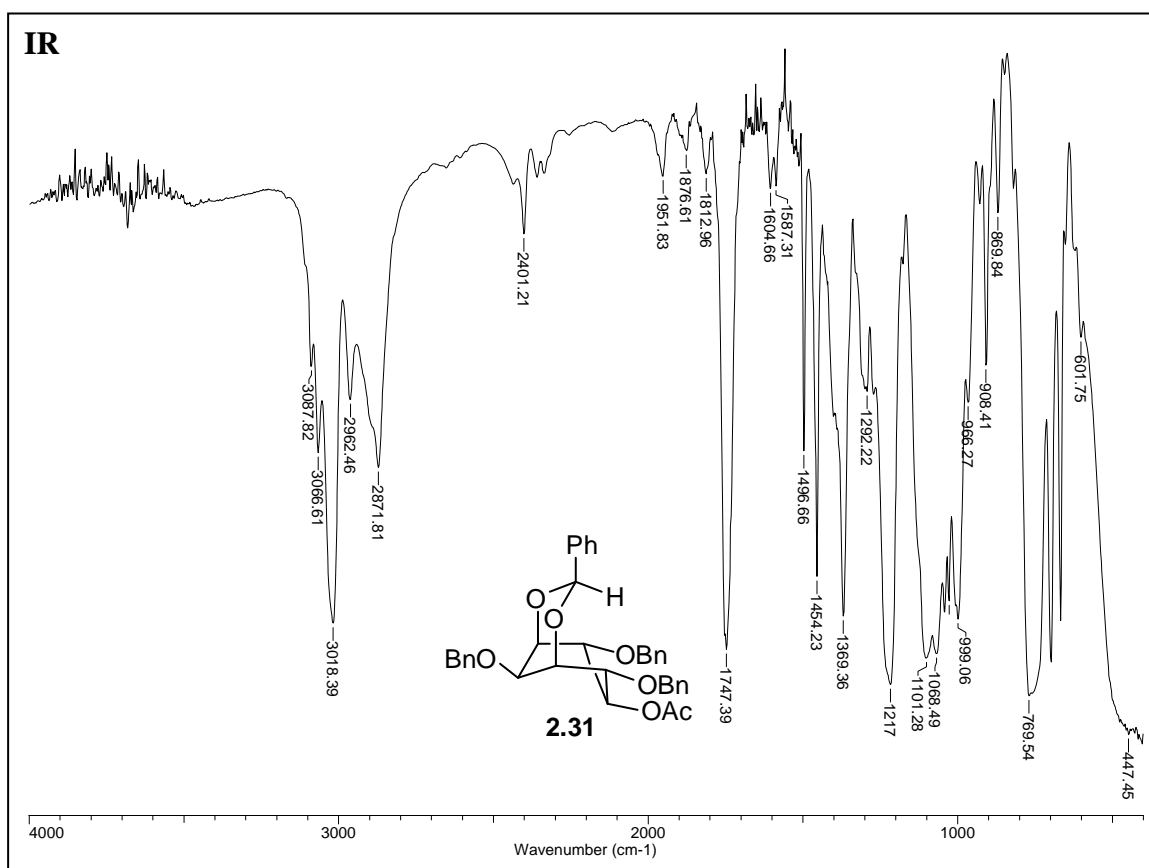
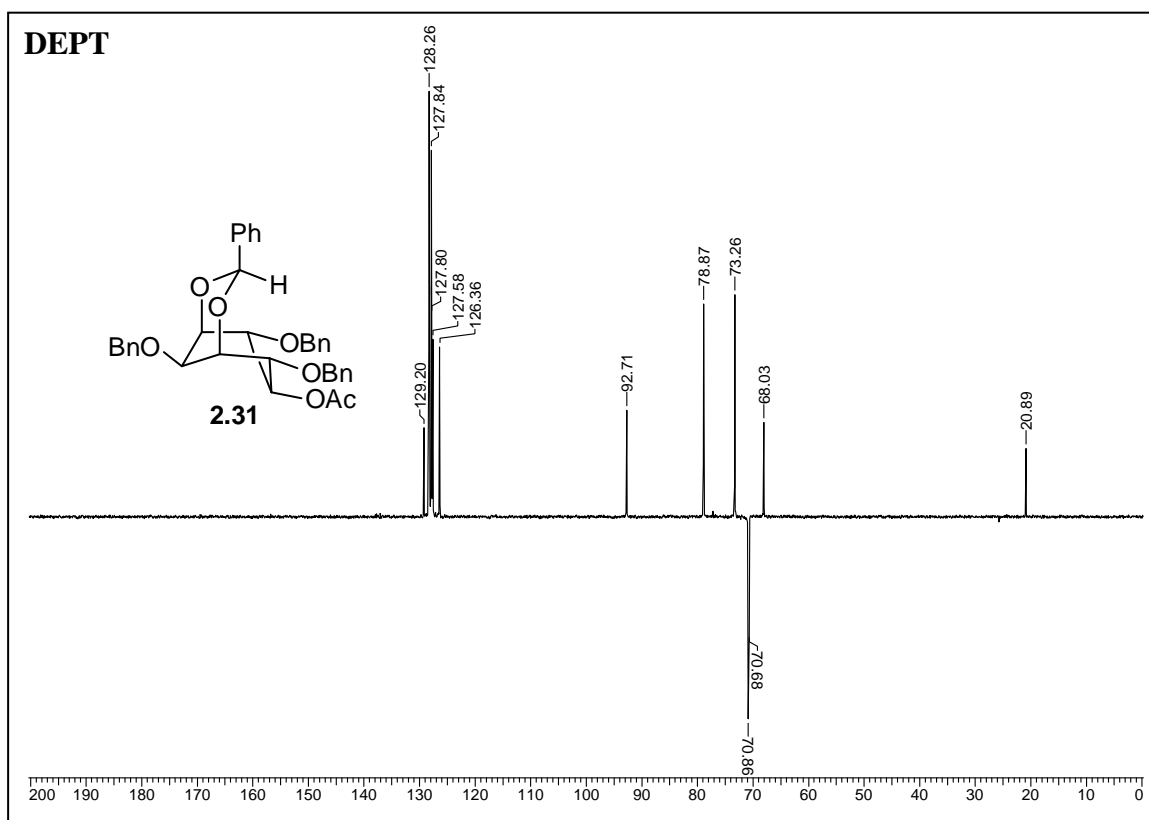
Chapter 2

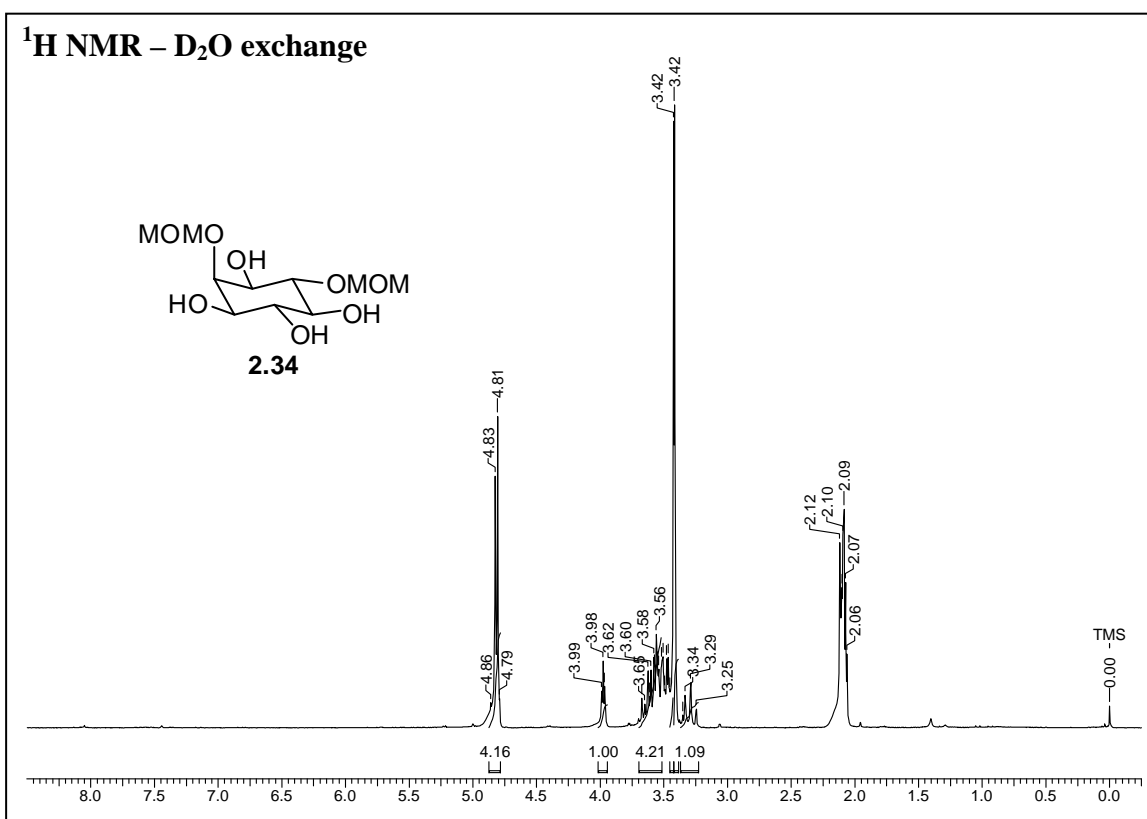
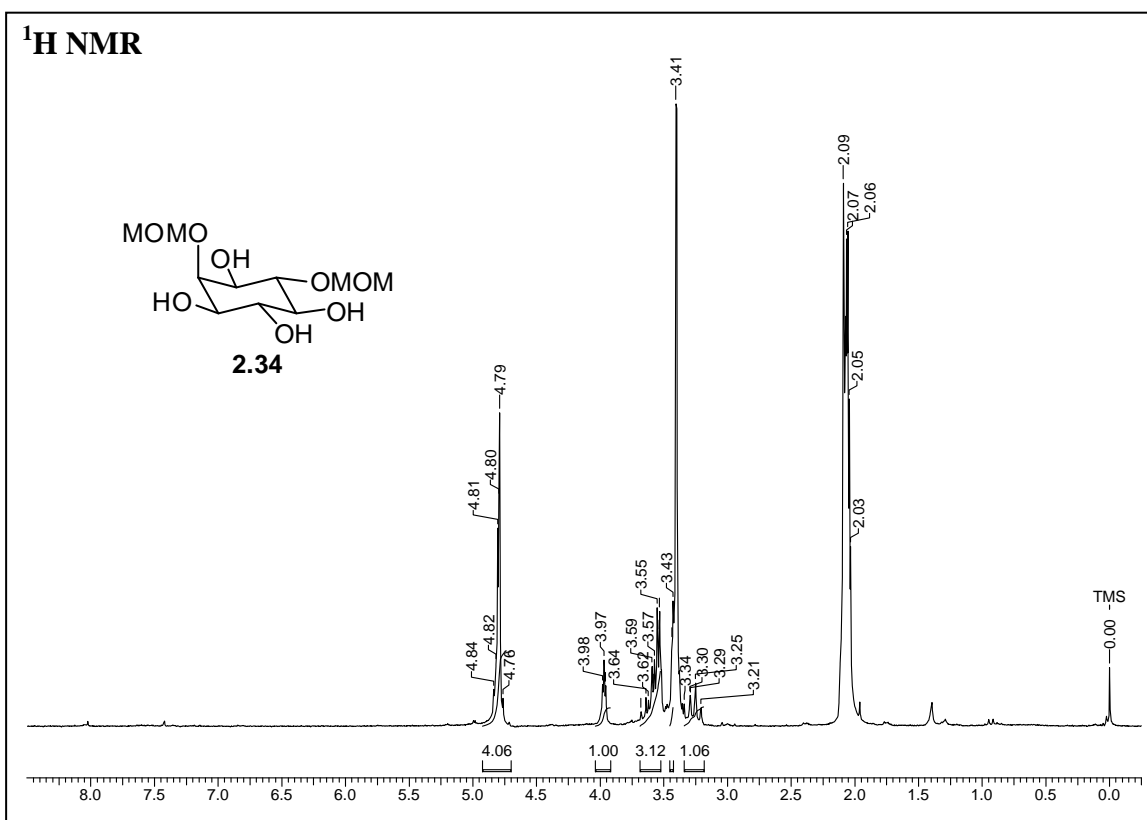


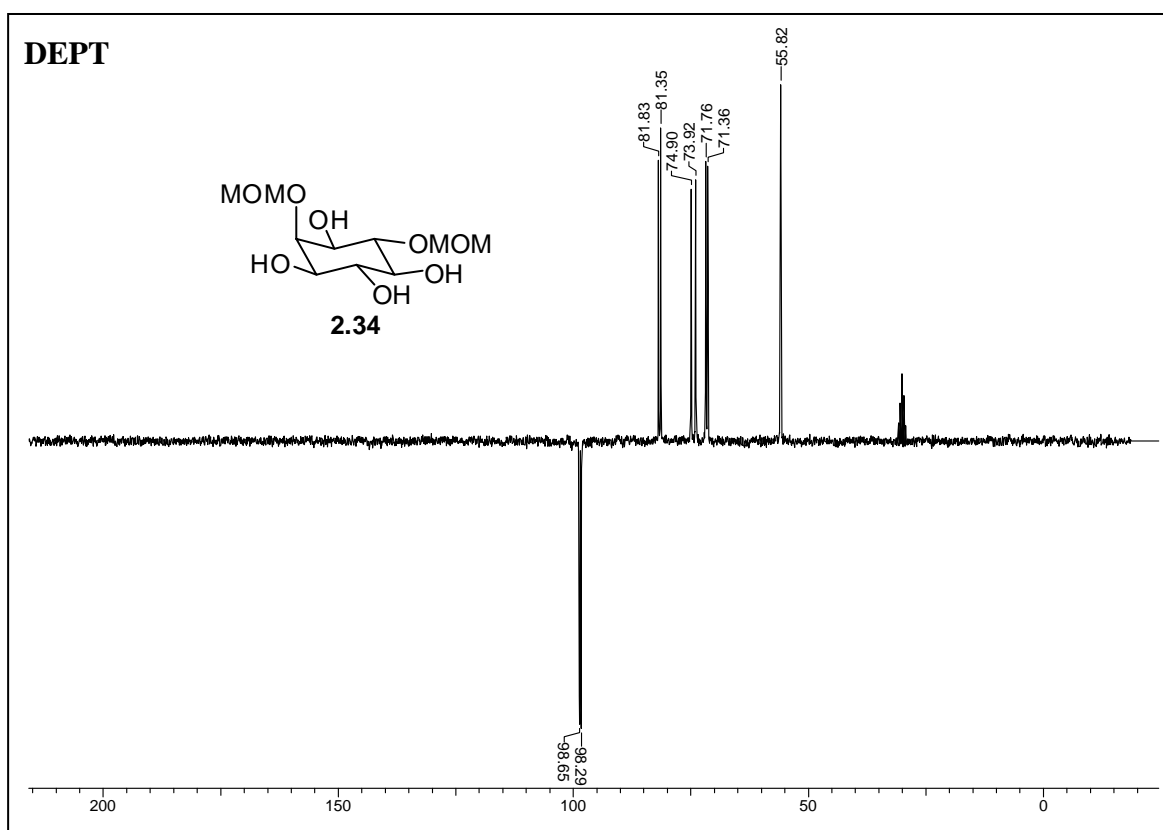
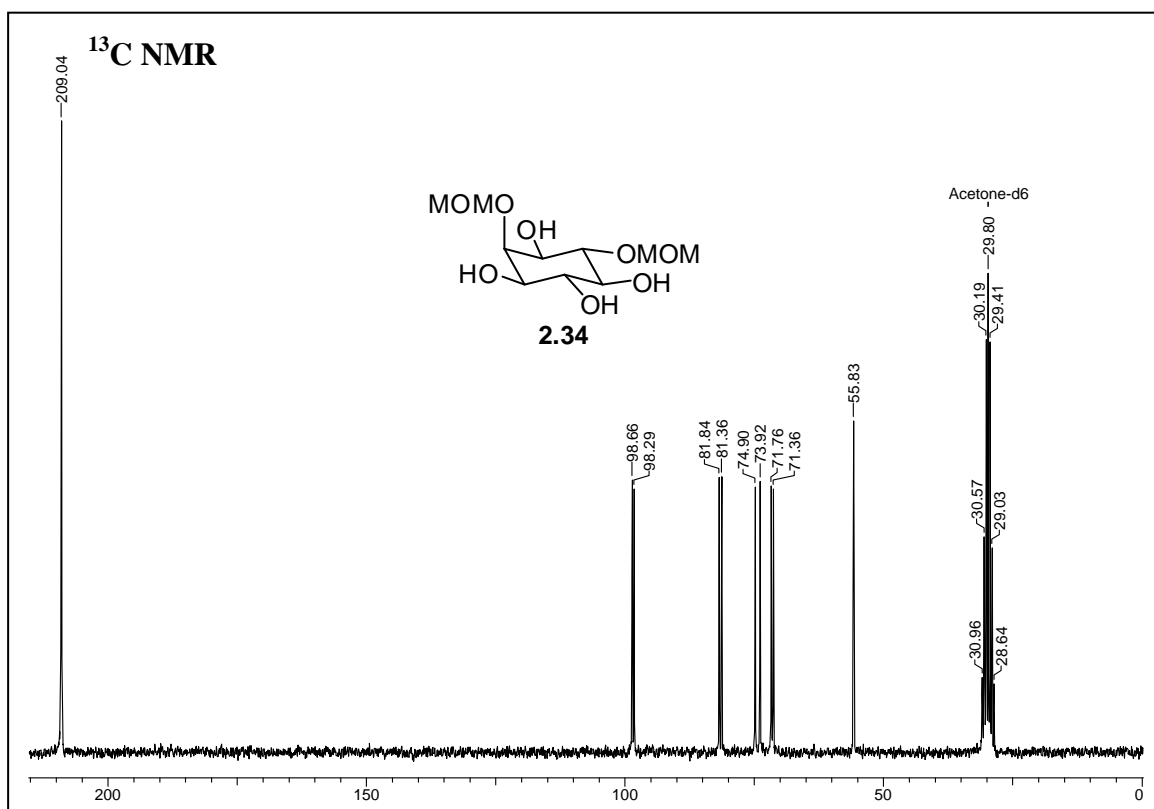


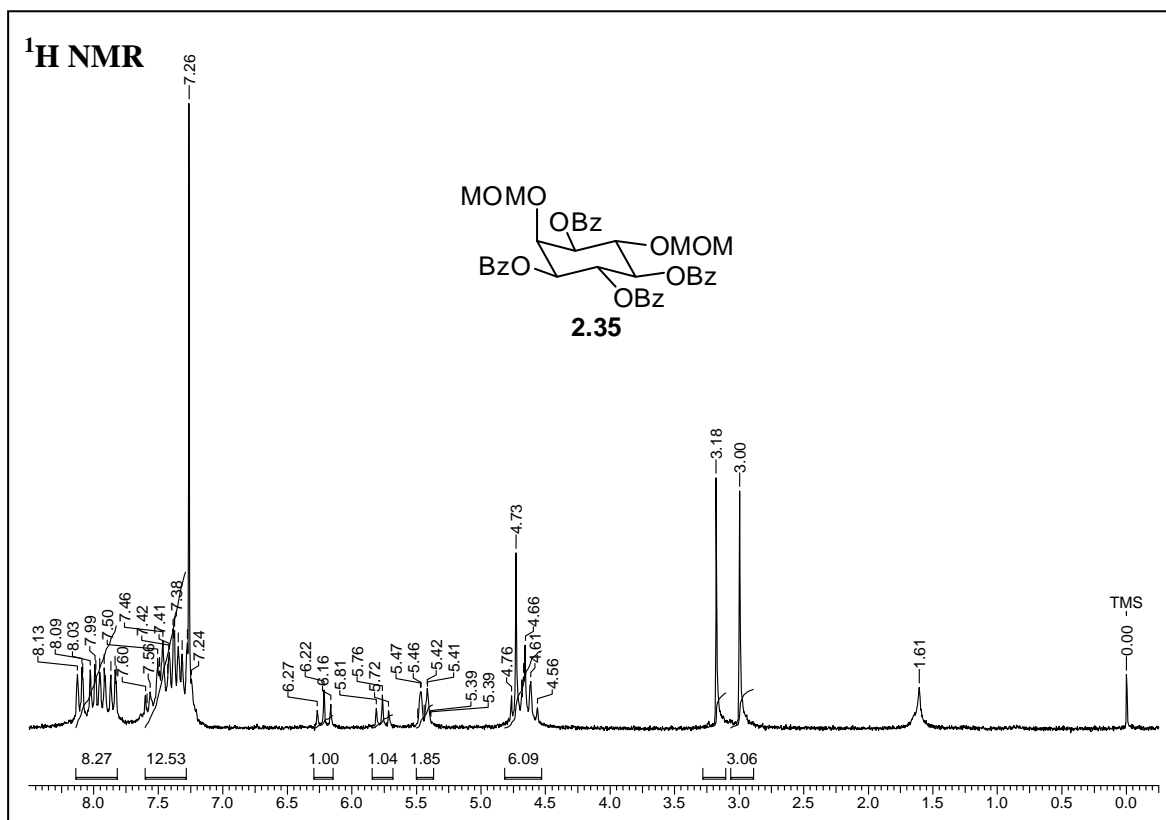
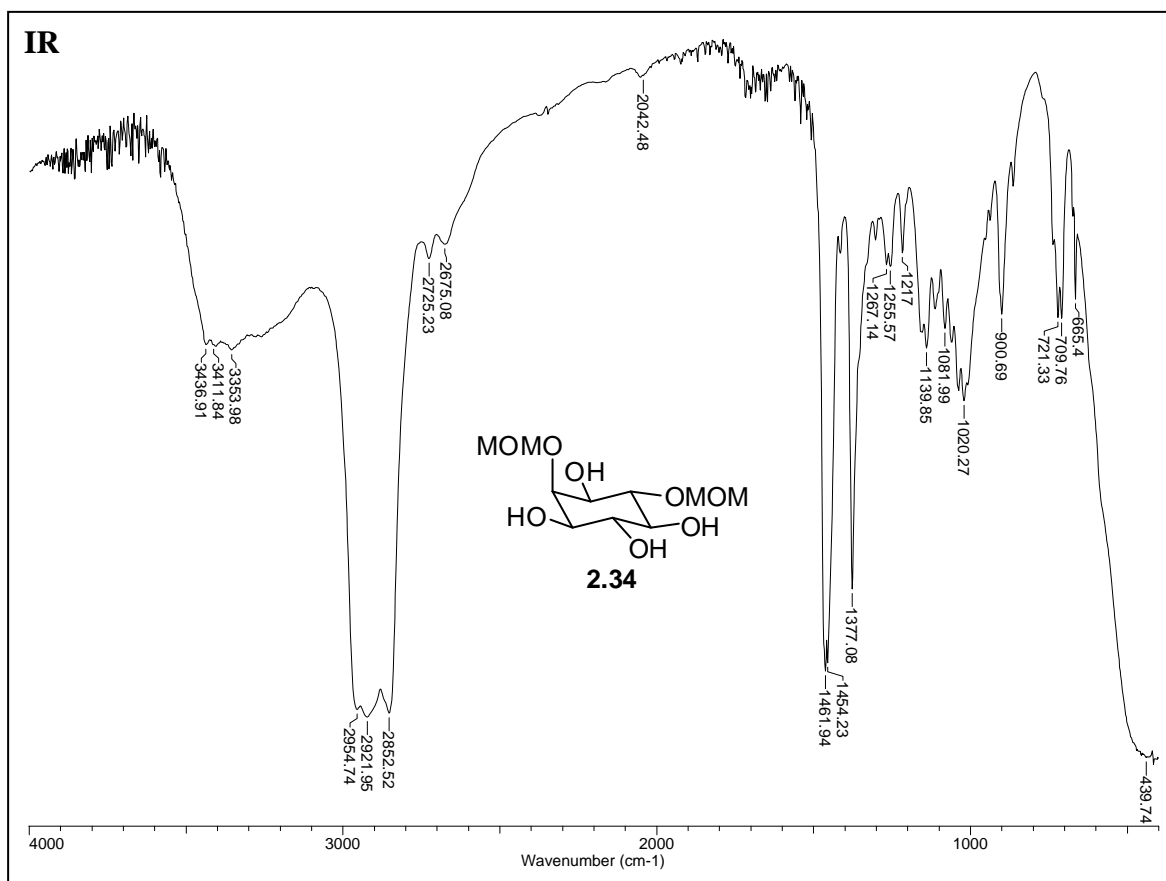


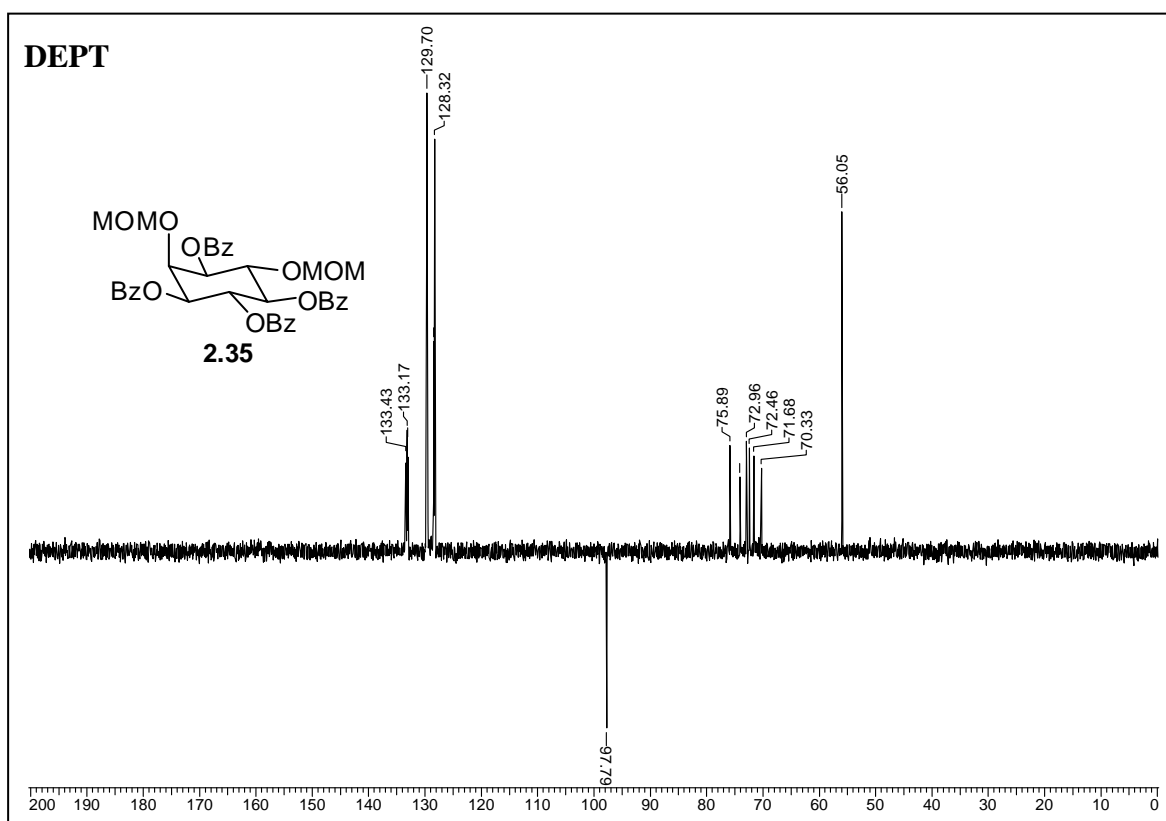
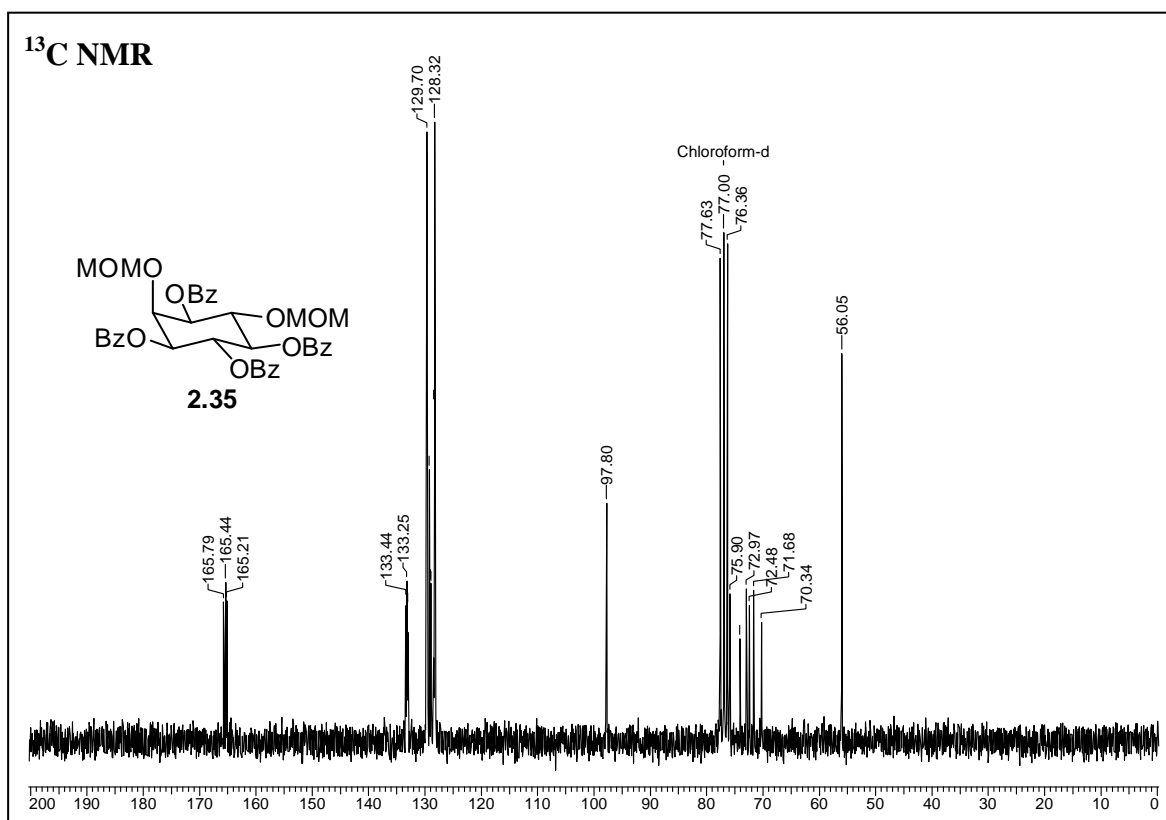




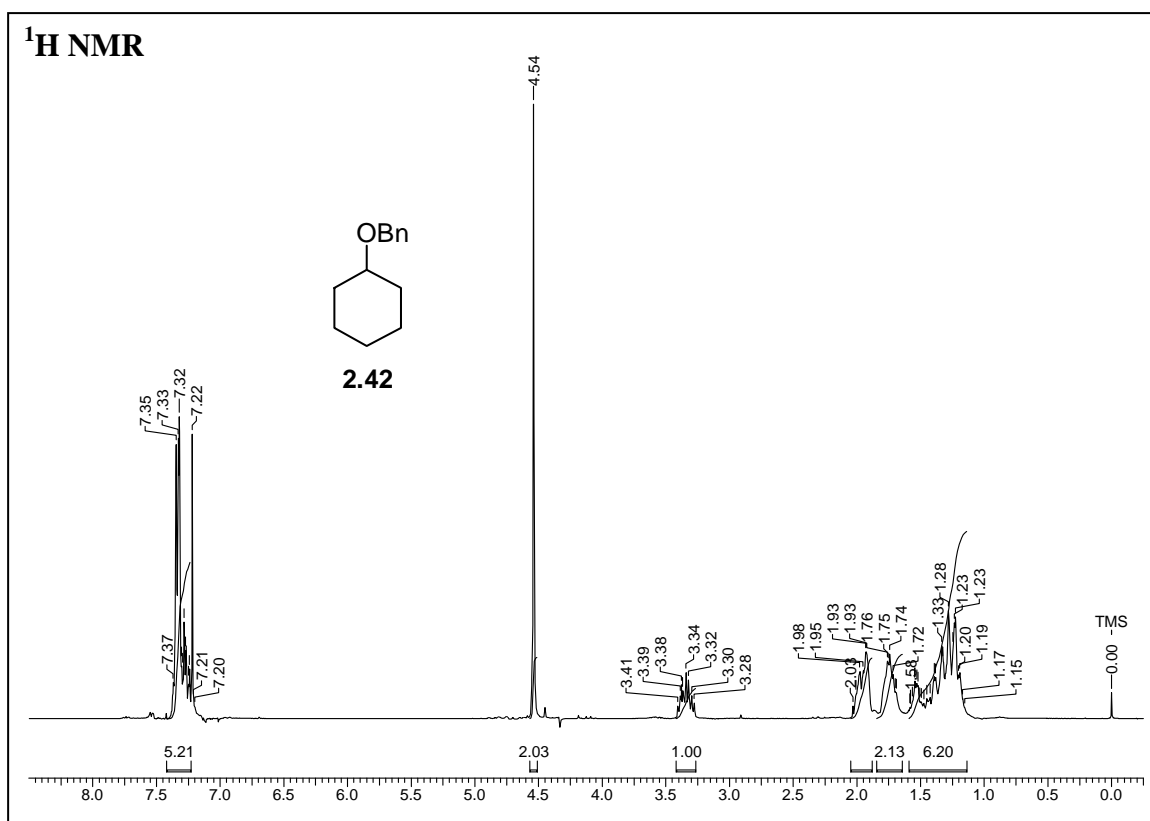
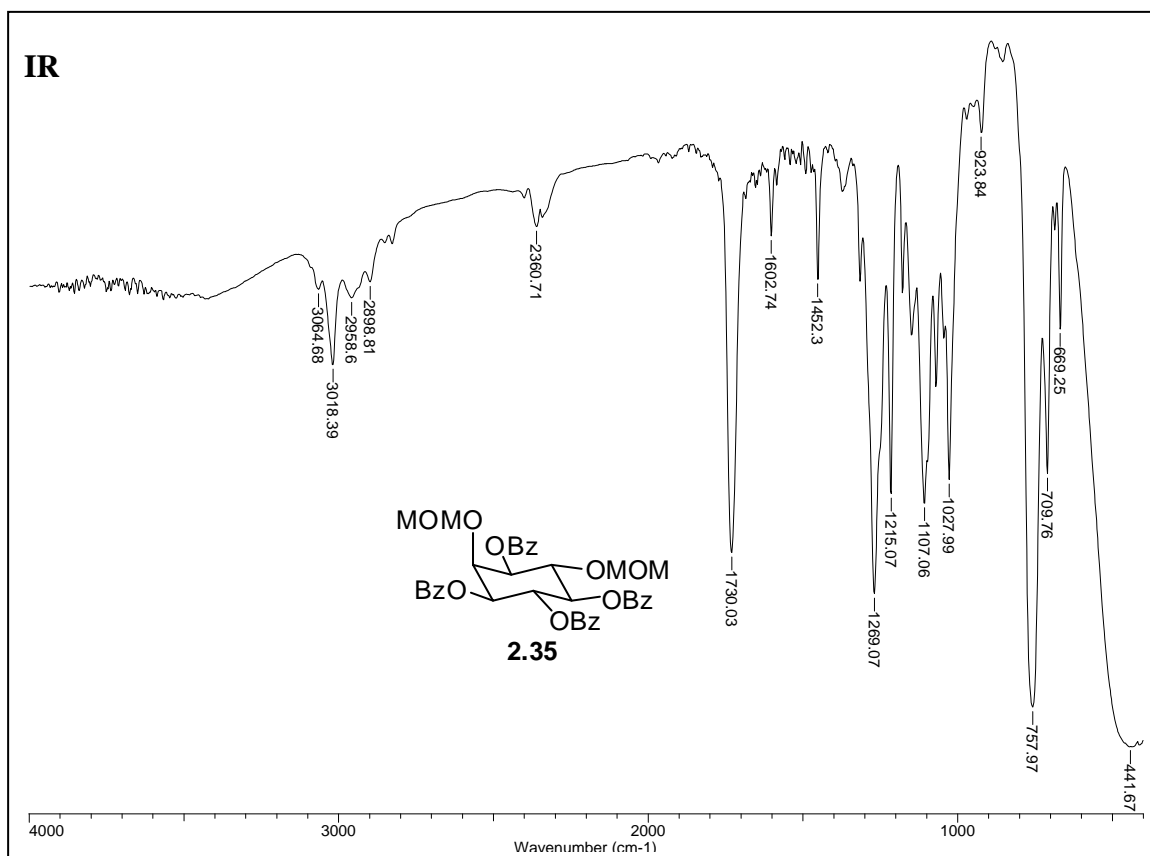


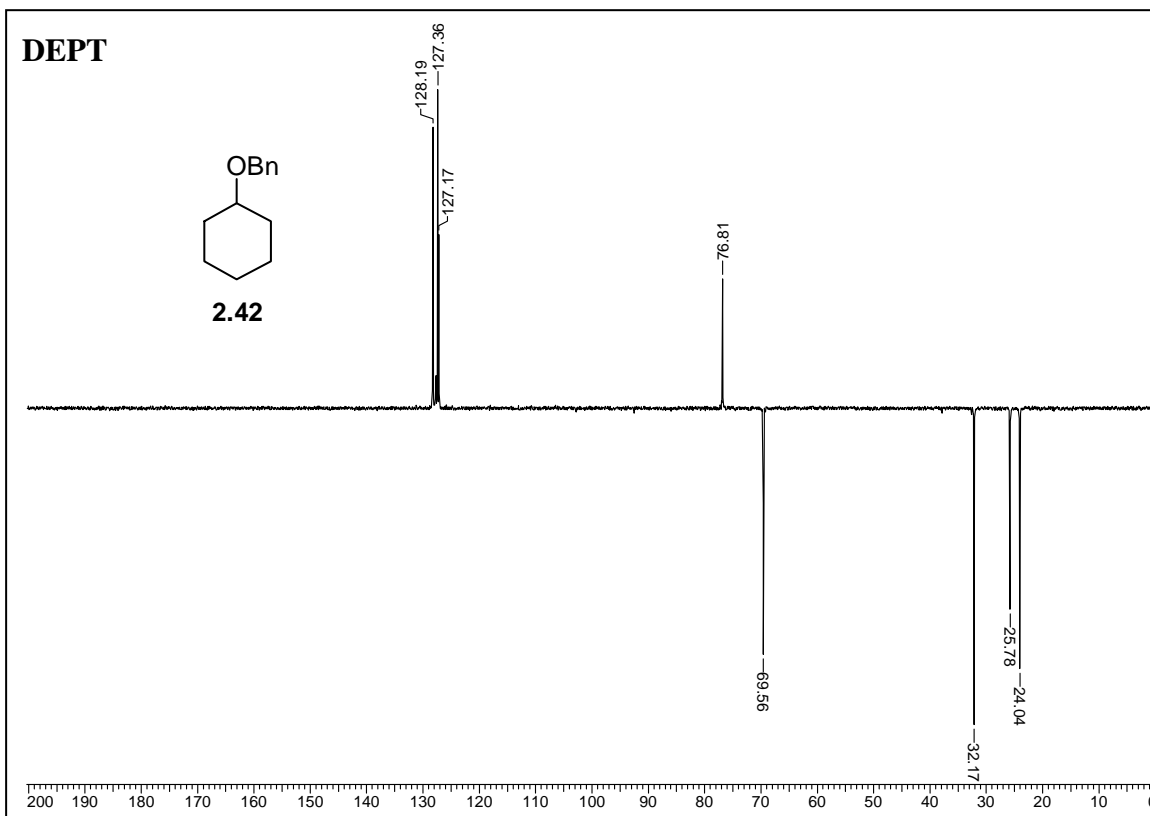
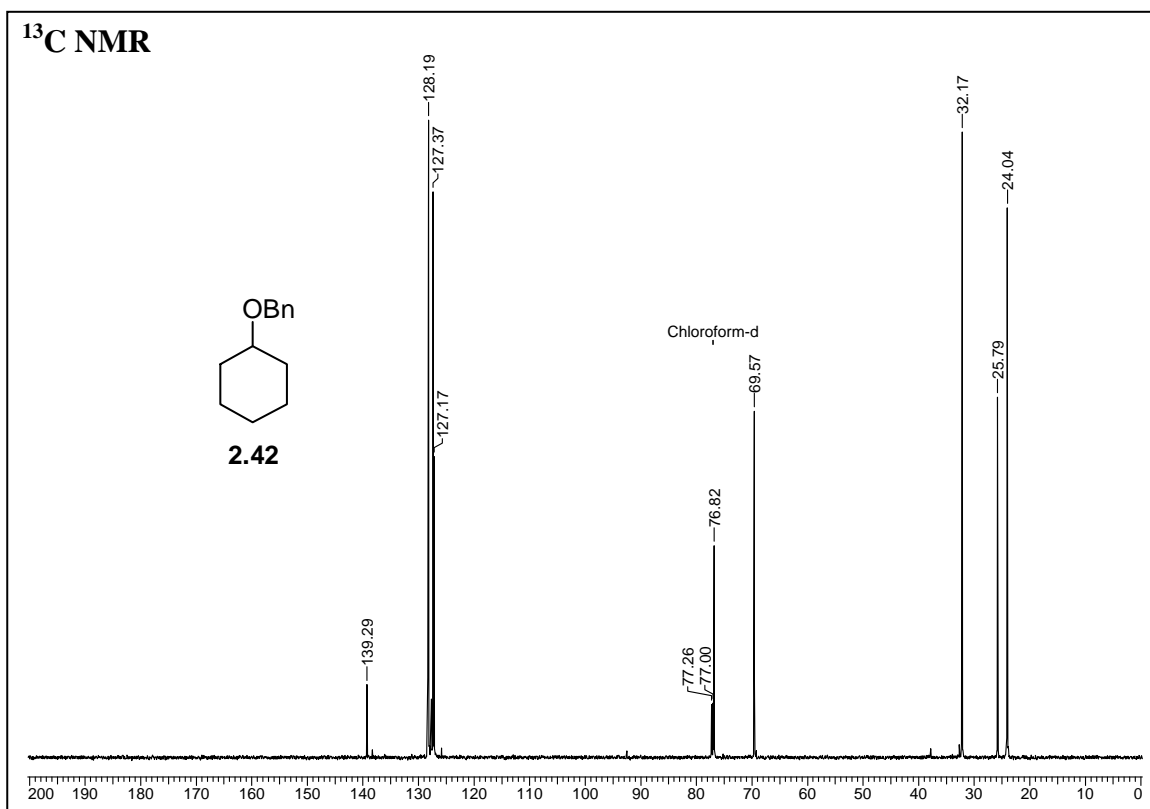


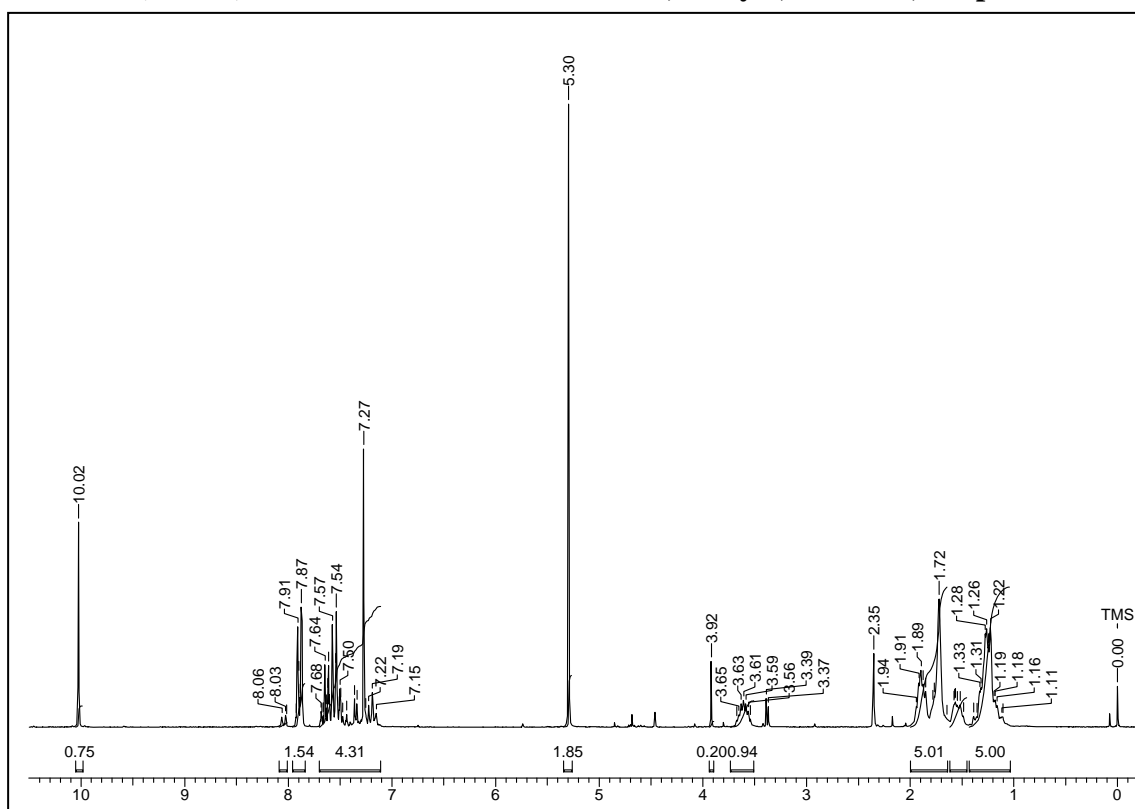
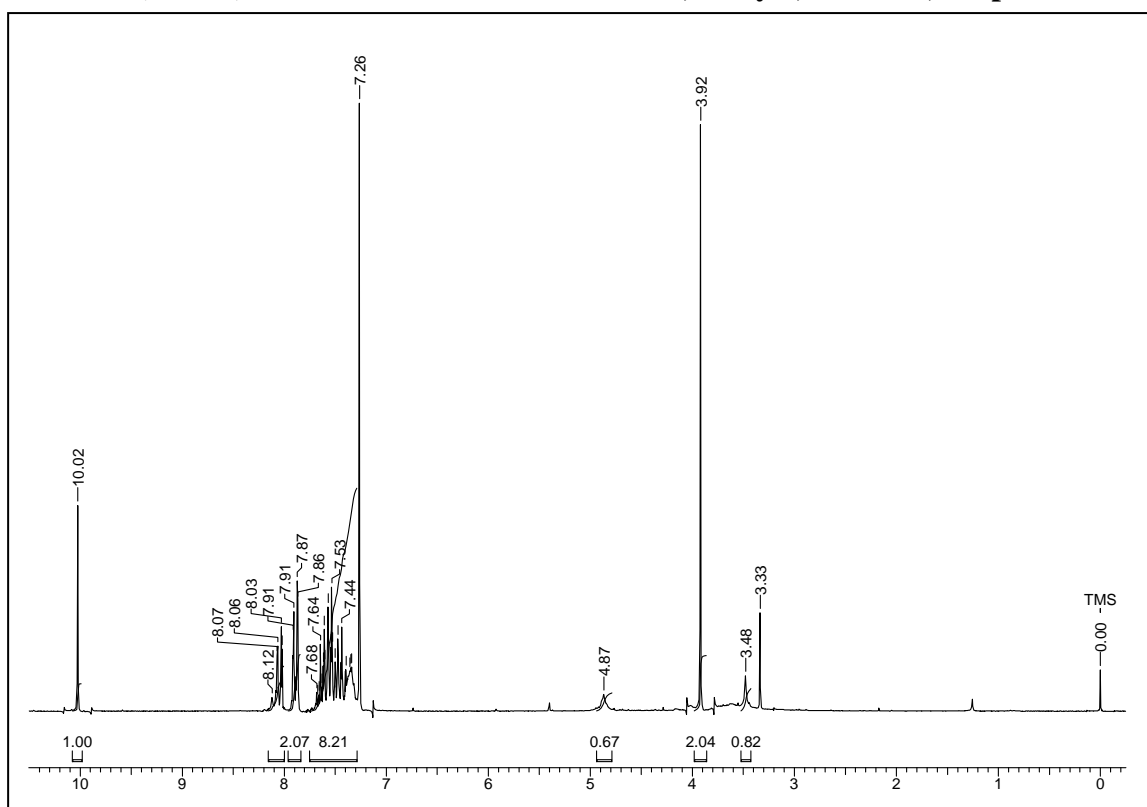




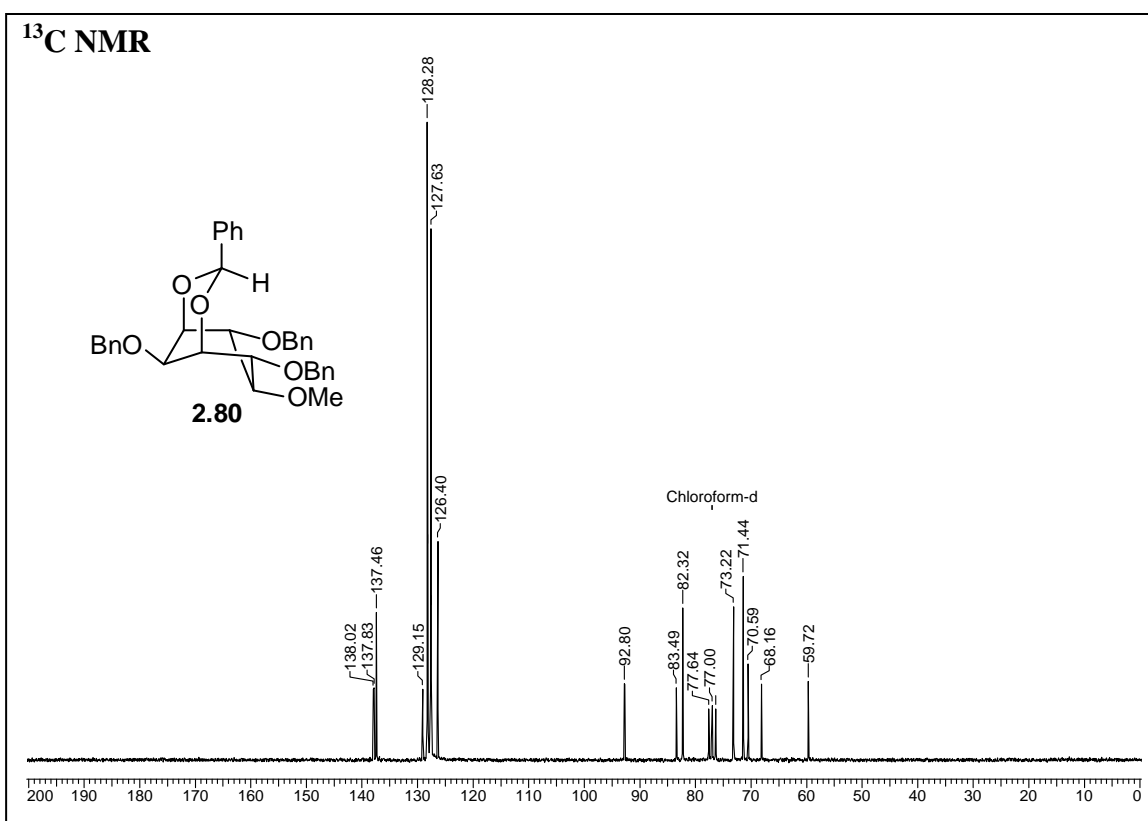
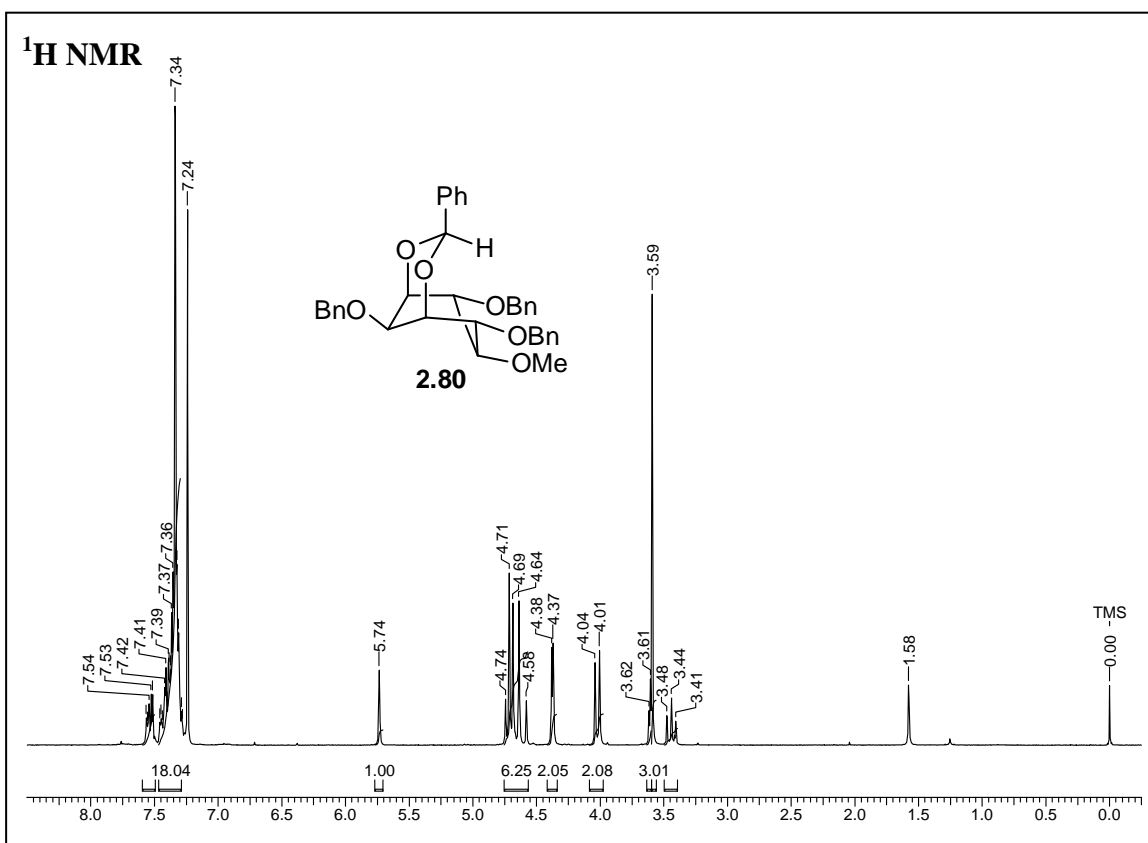
Chapter 2



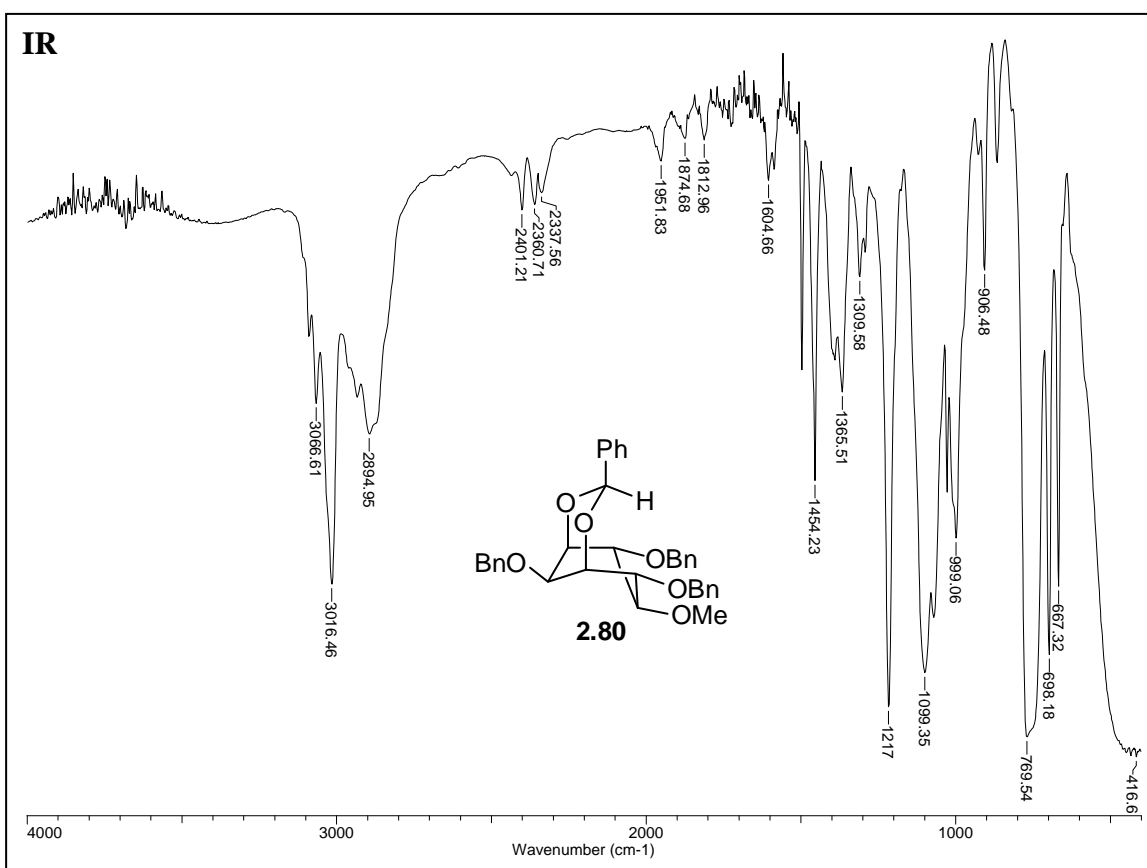
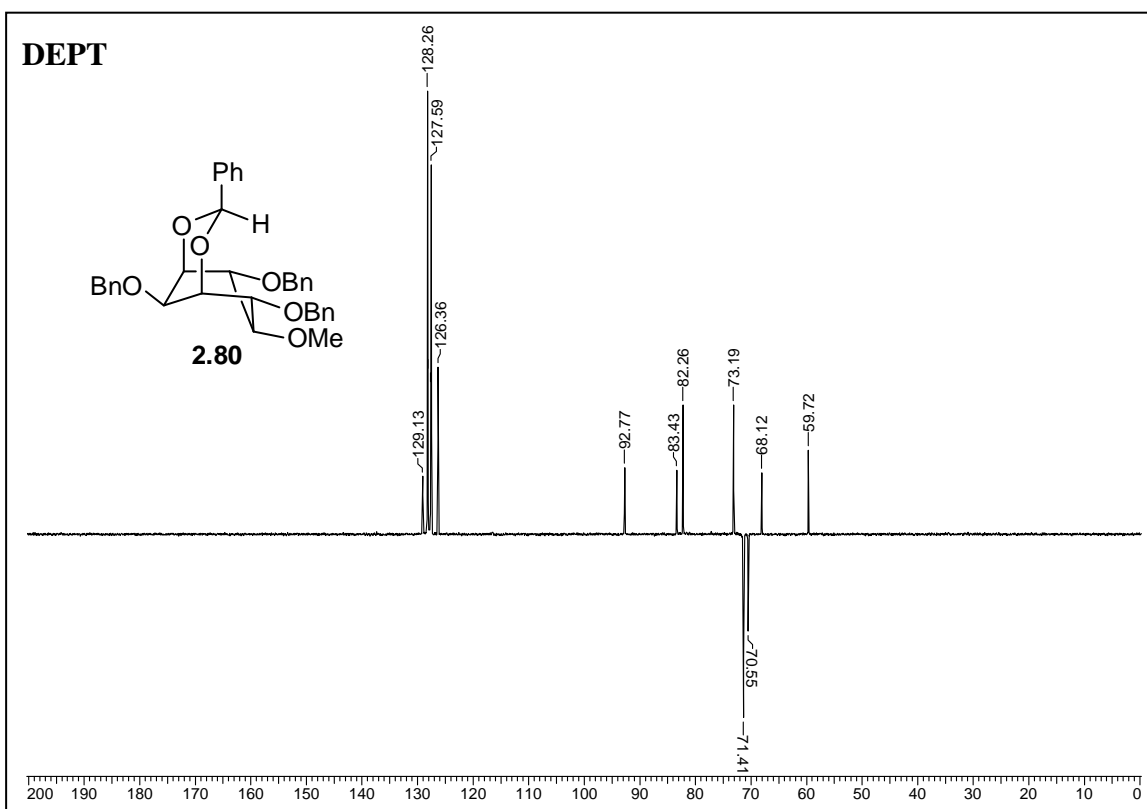


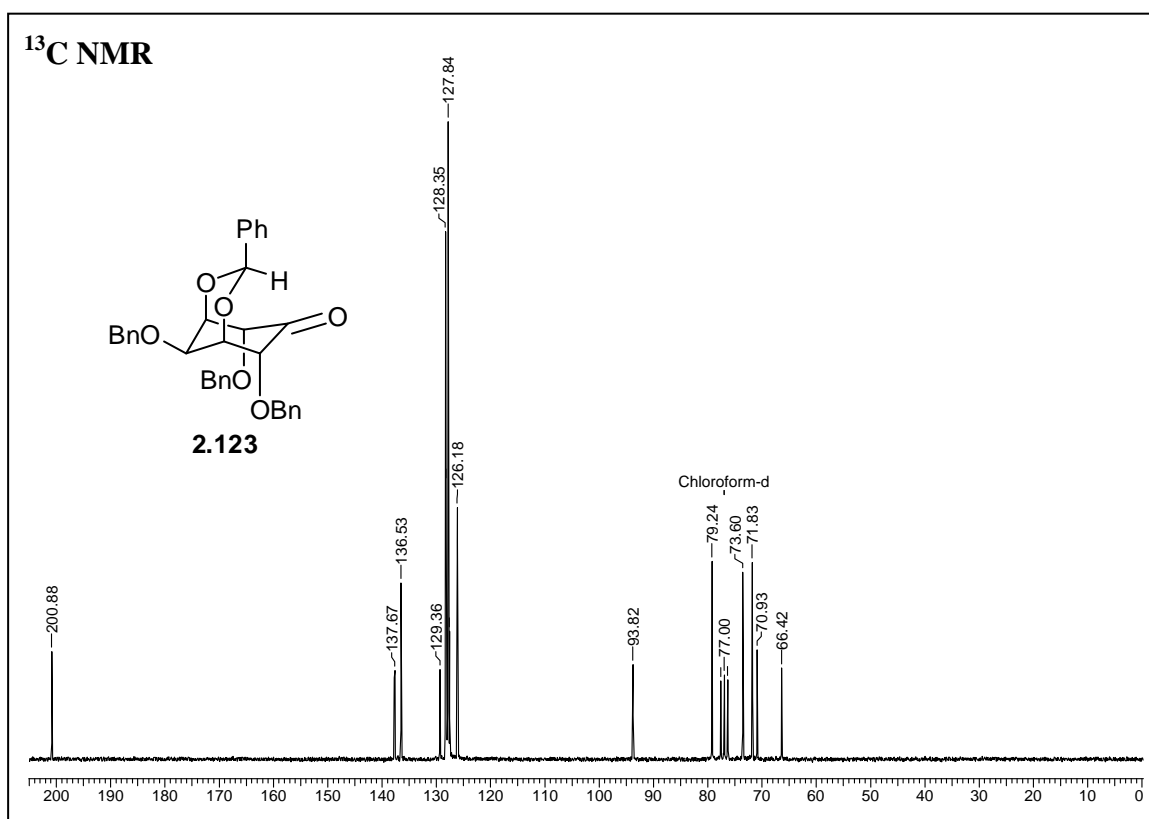
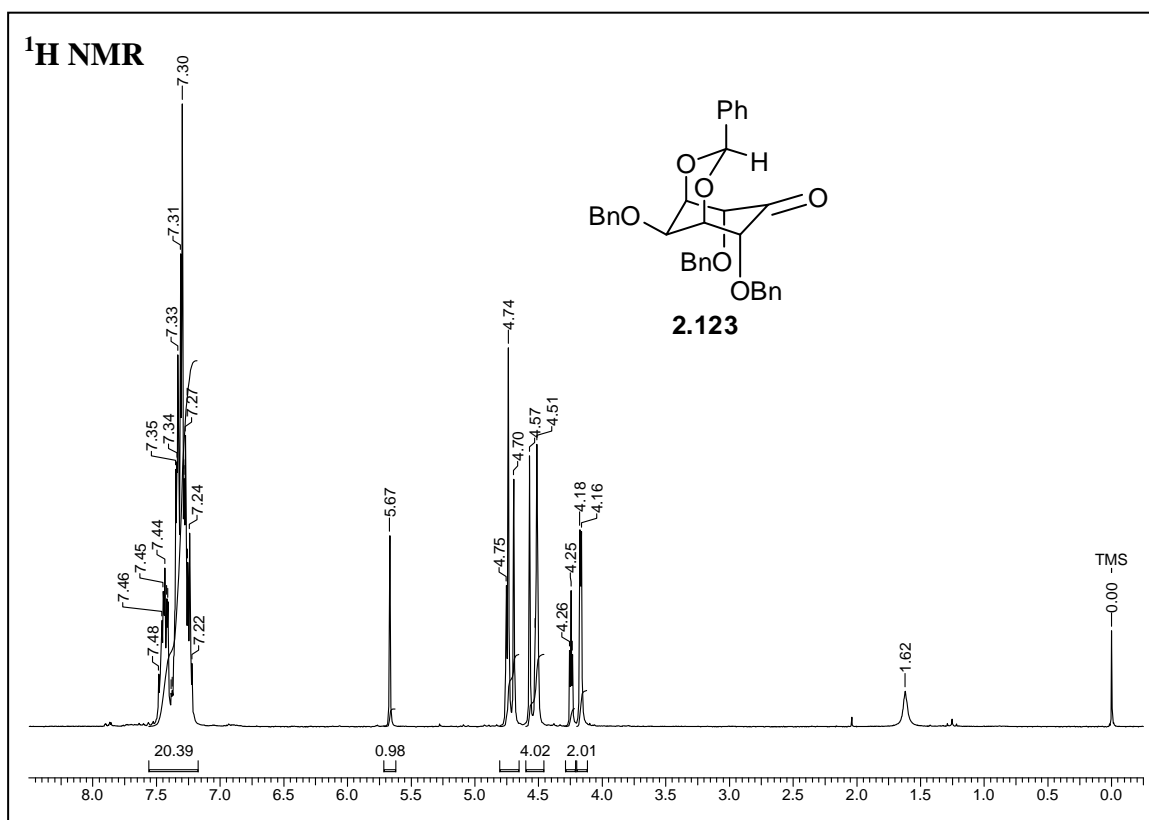
^1H NMR (CDCl_3) of the reaction mixture of 2.42, entry 2, table 2.3, chapter 2 **^1H NMR (CDCl_3) of the reaction mixture of 1.106, entry 6, table 2.2, chapter 2**

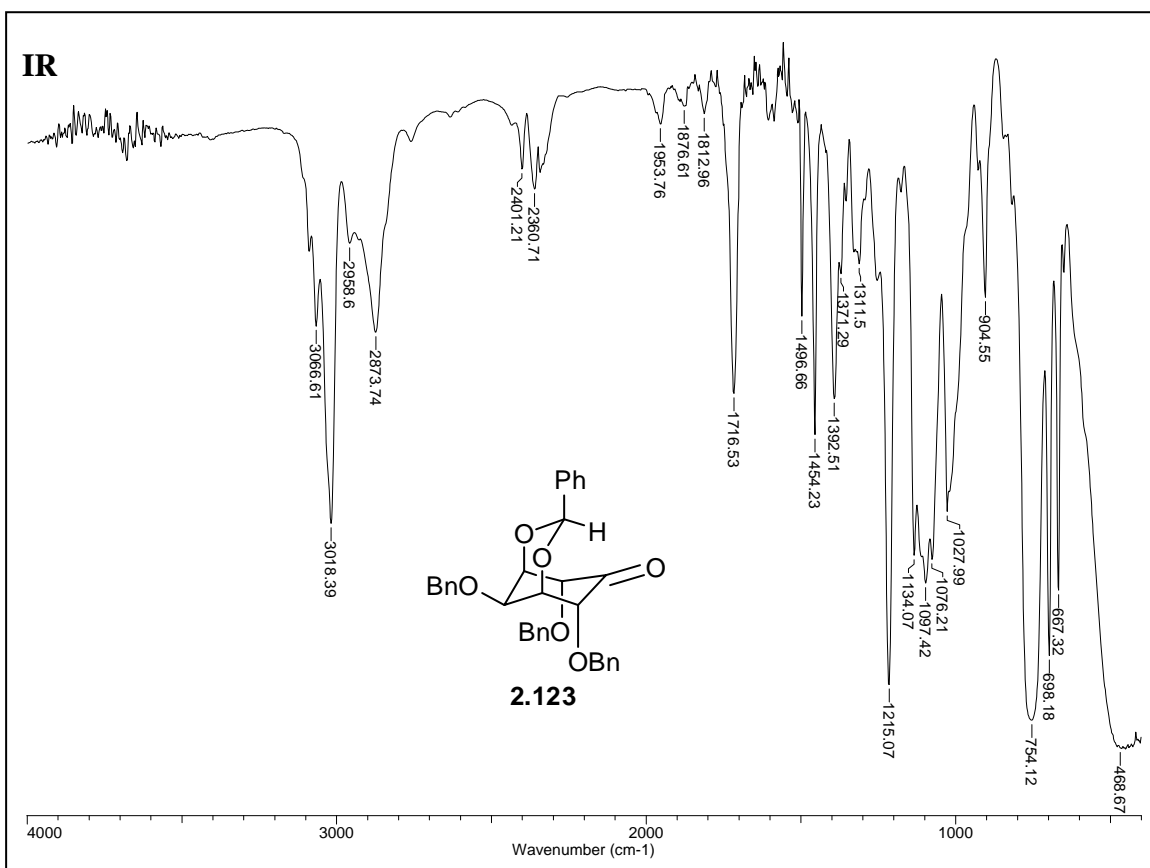
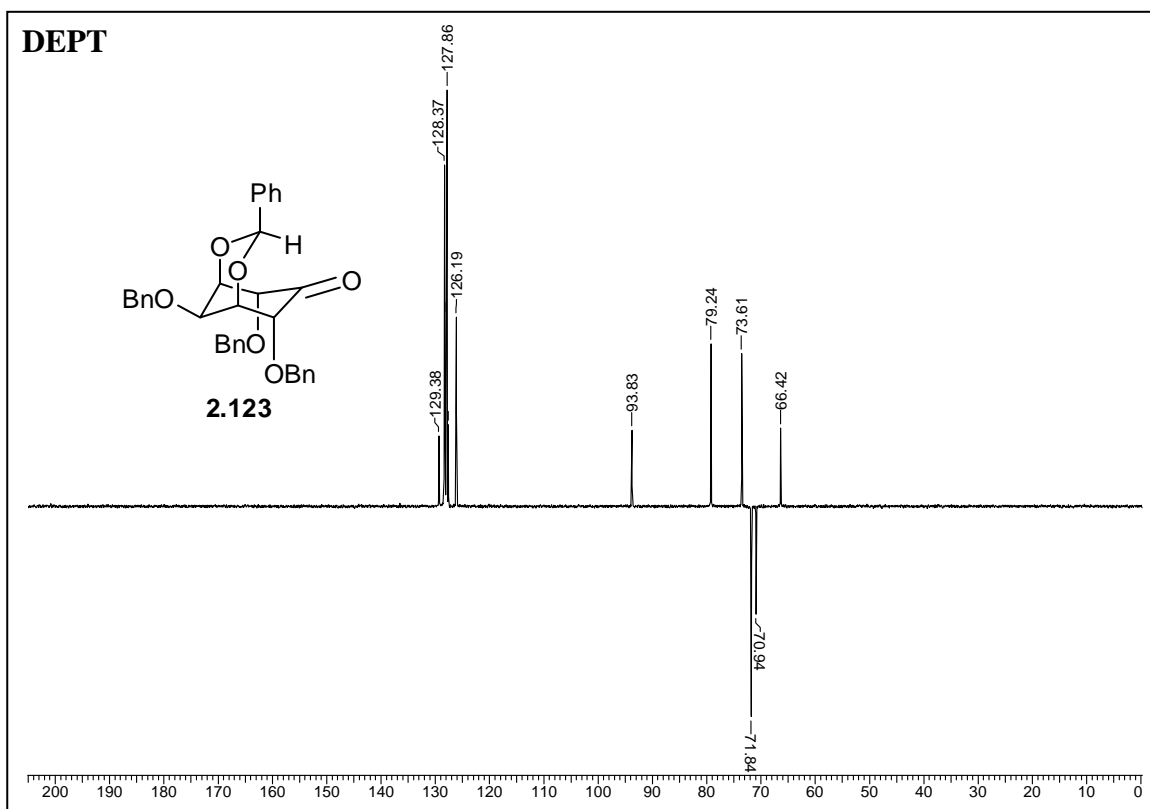
Chapter 2

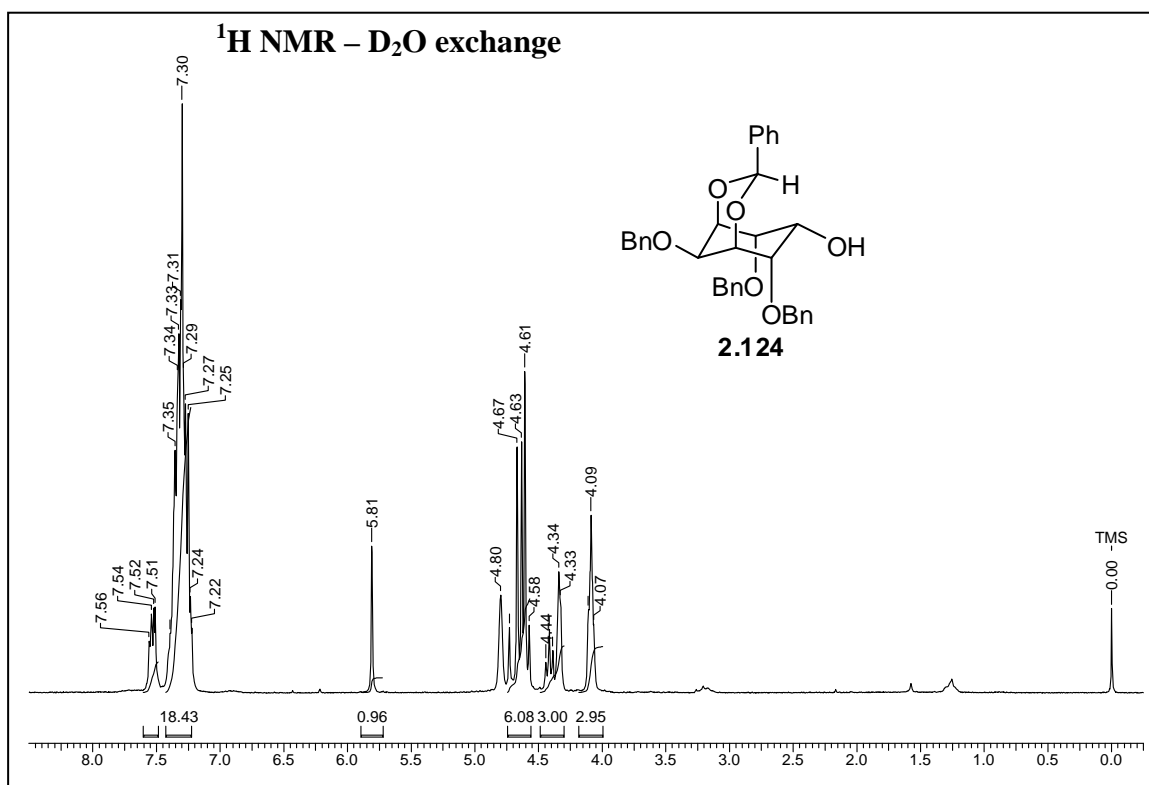
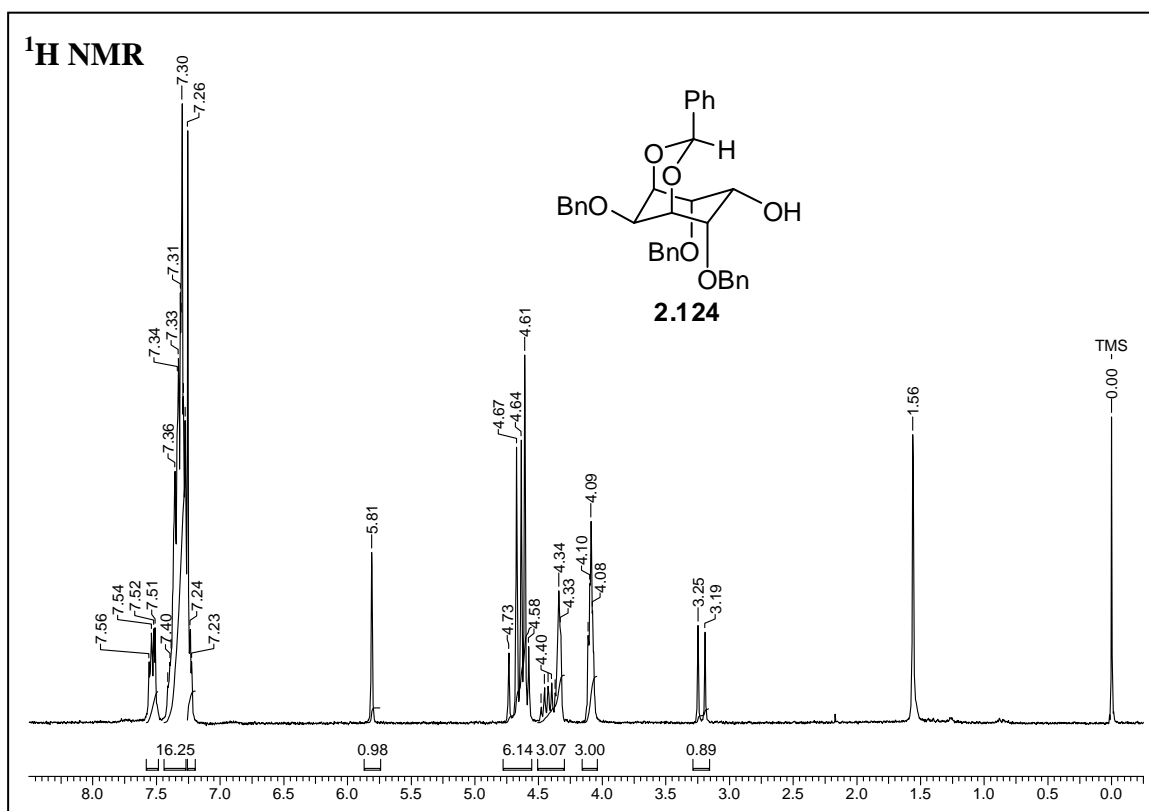


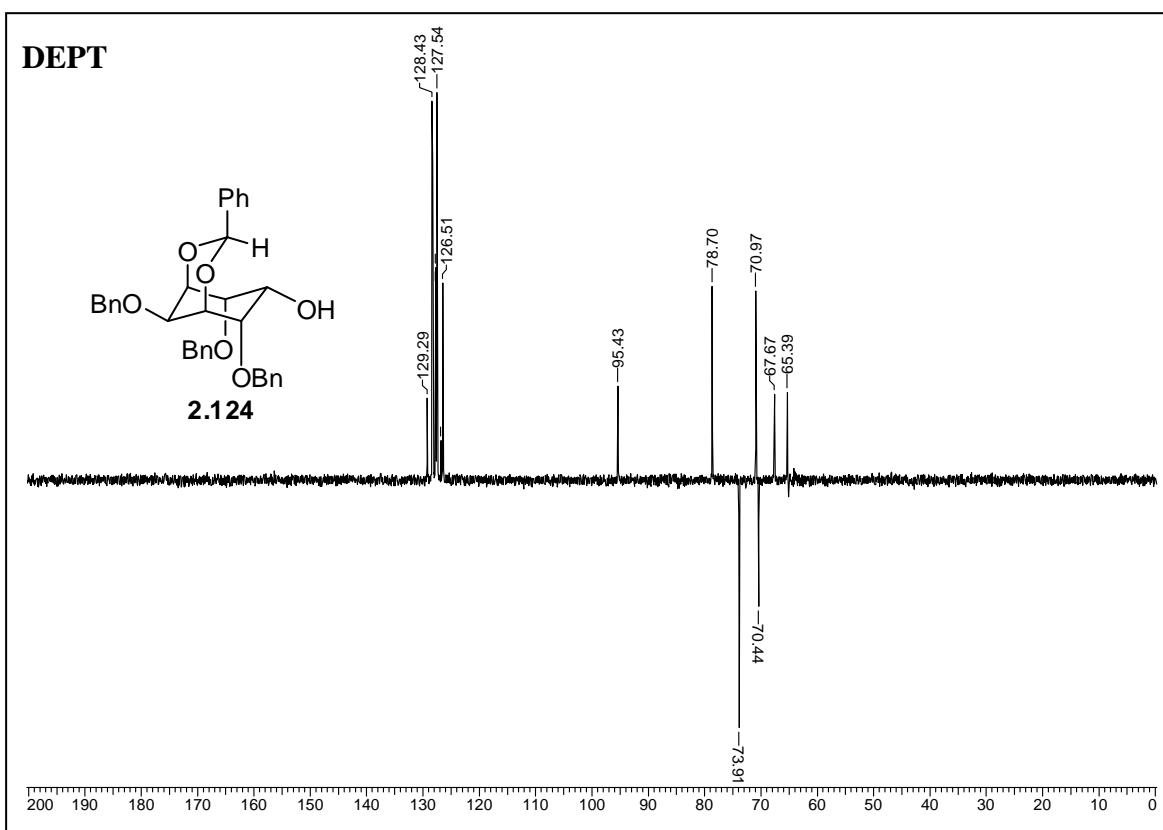
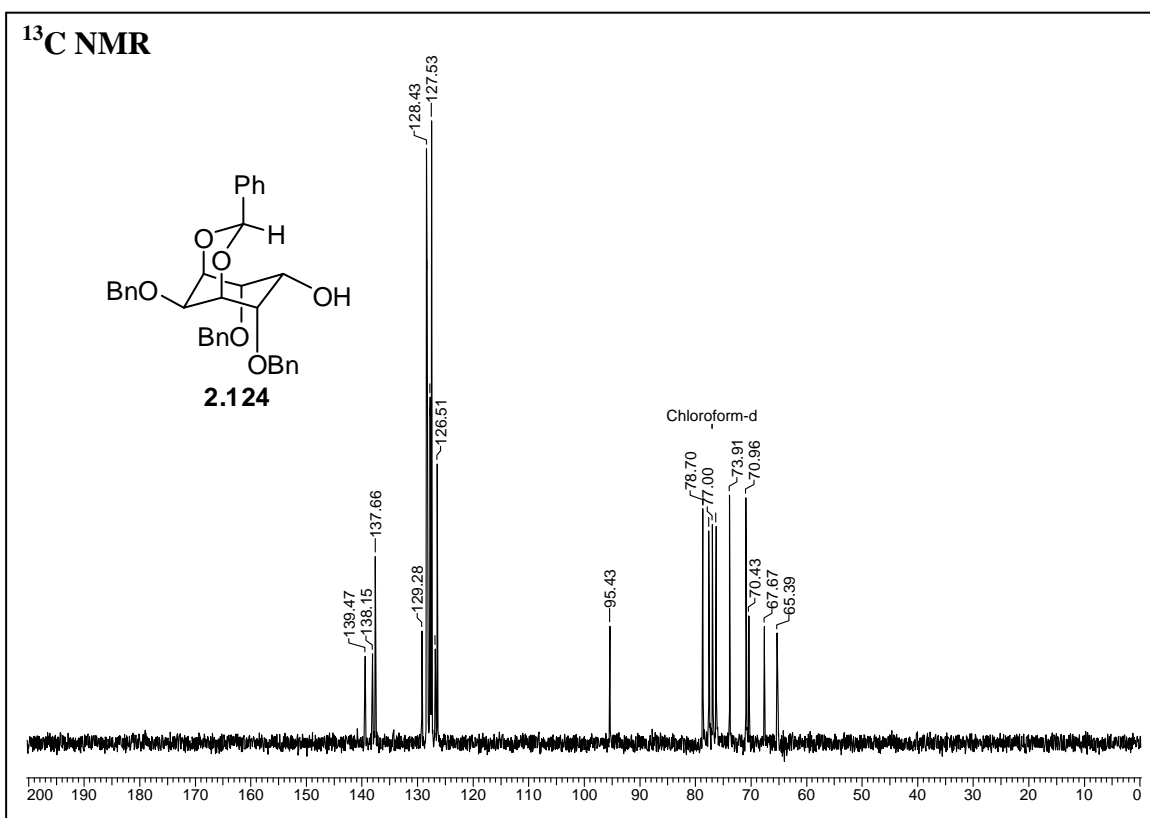
Chapter 2

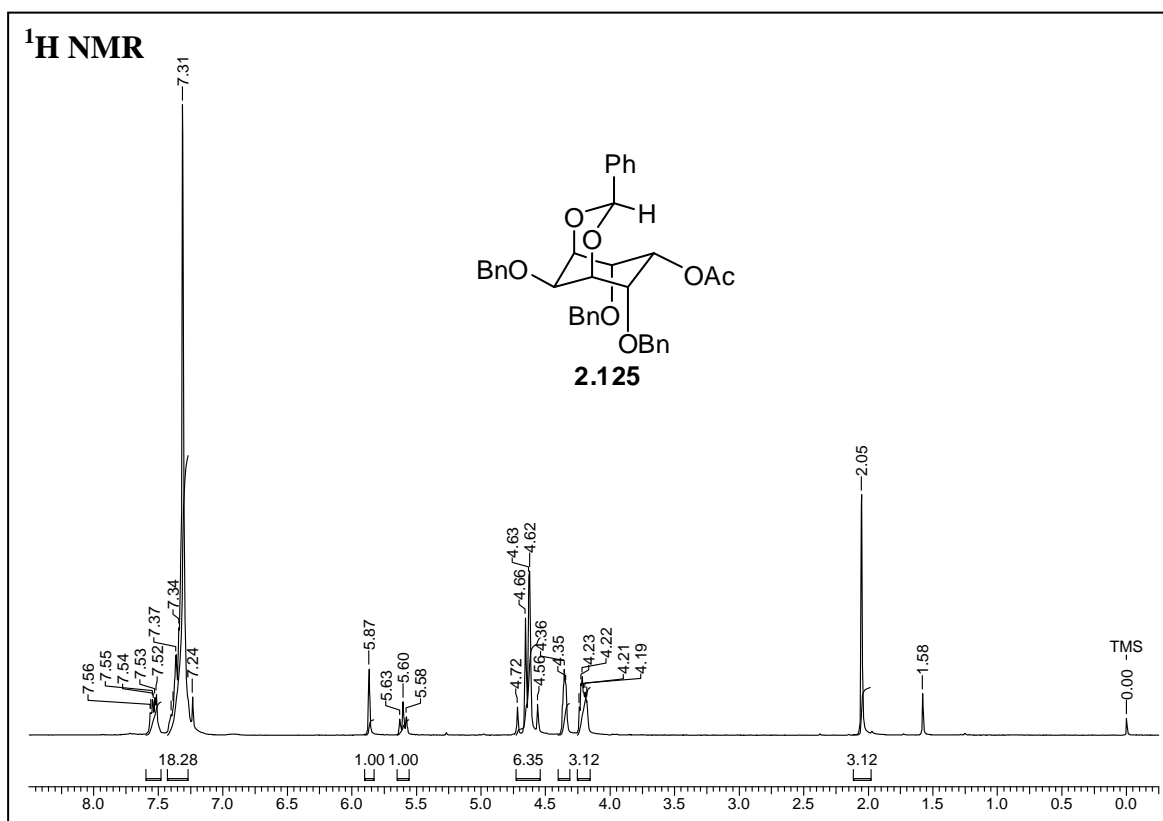
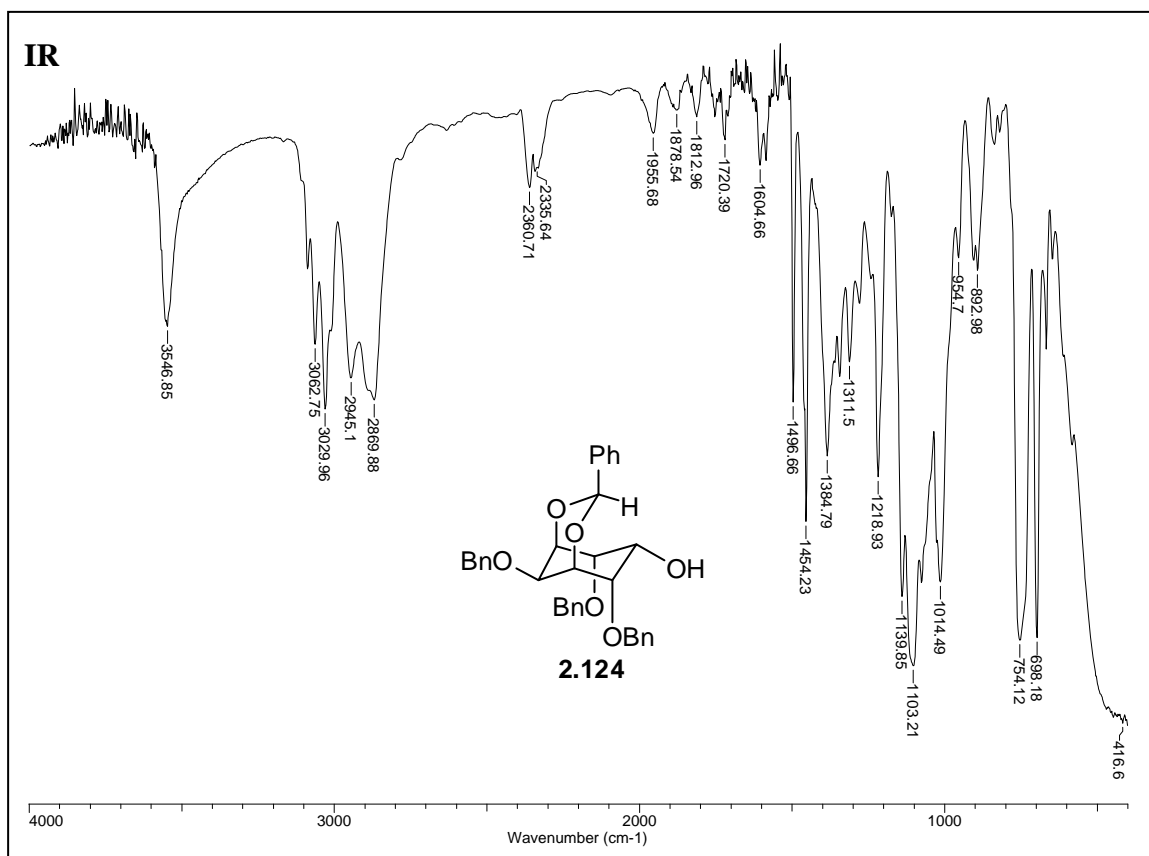


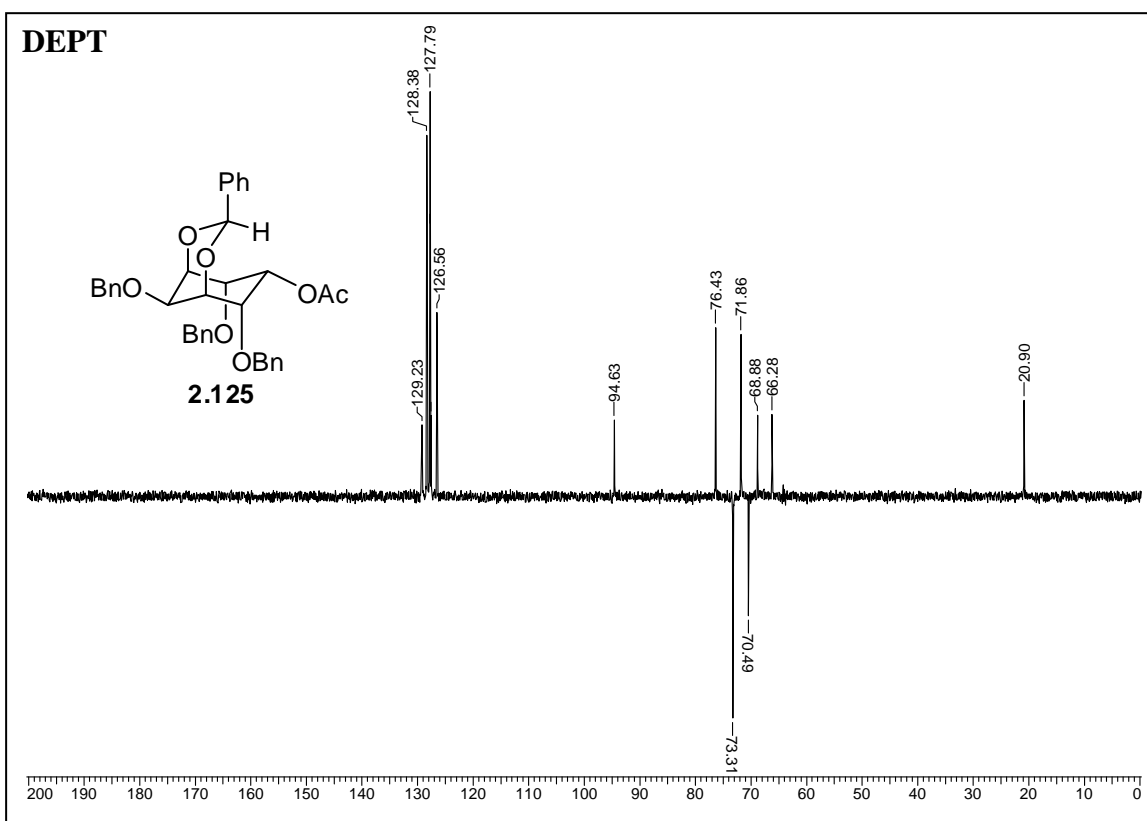
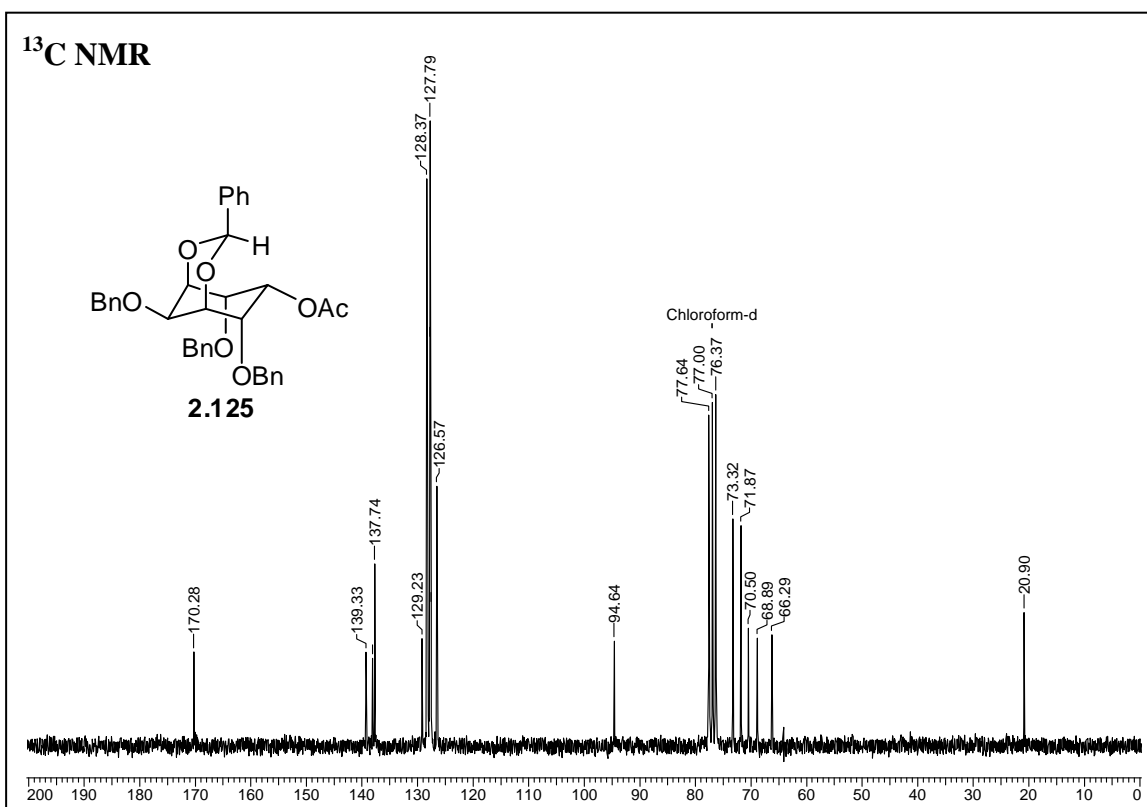




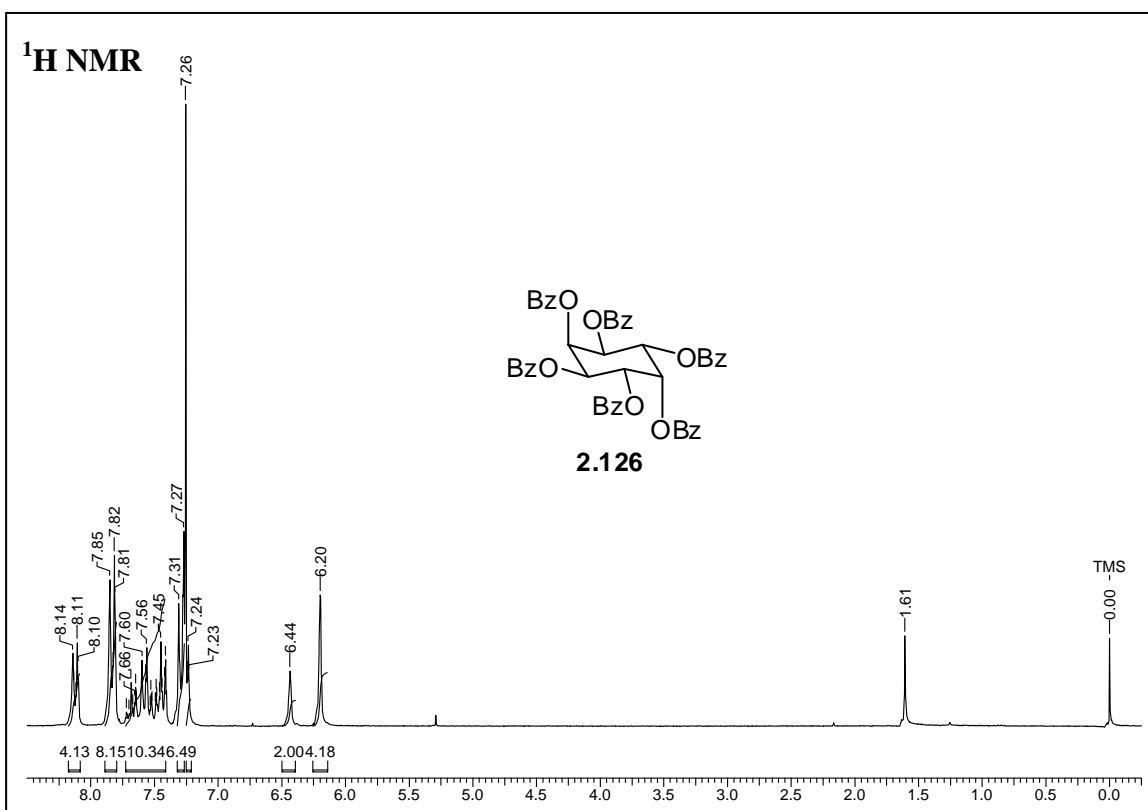
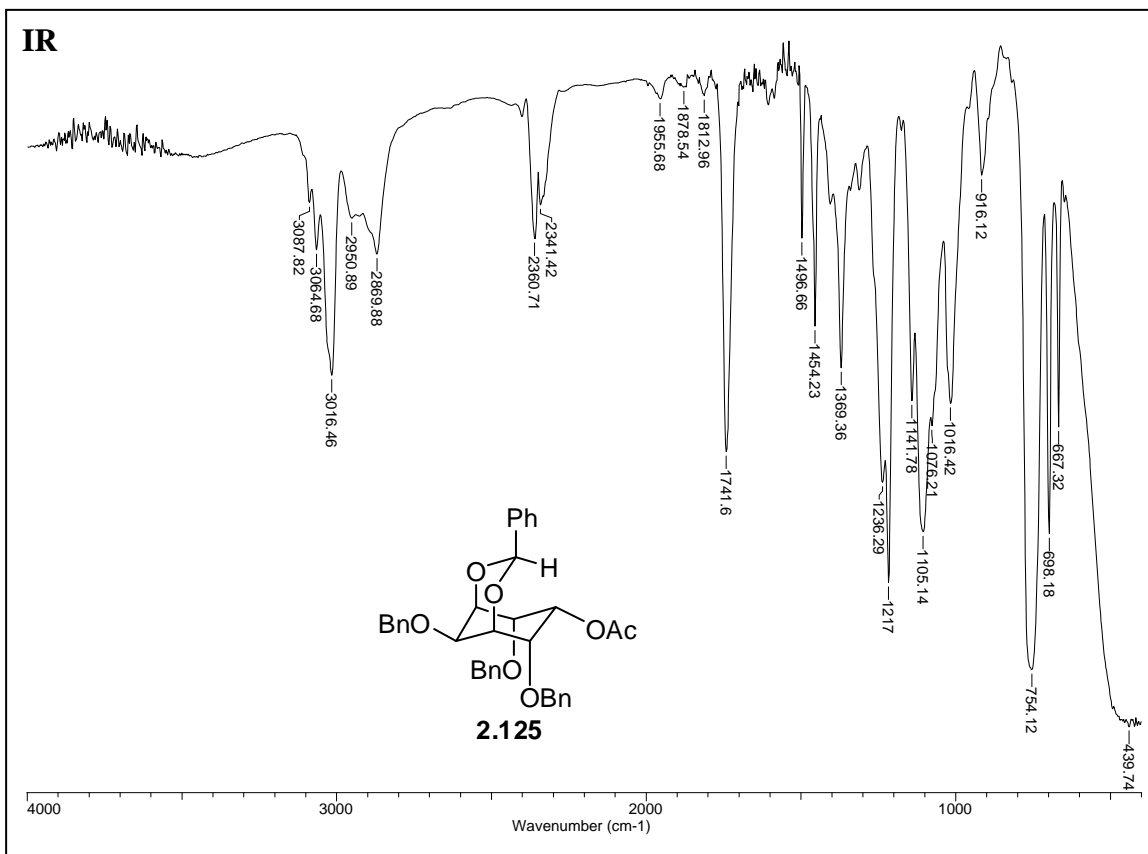


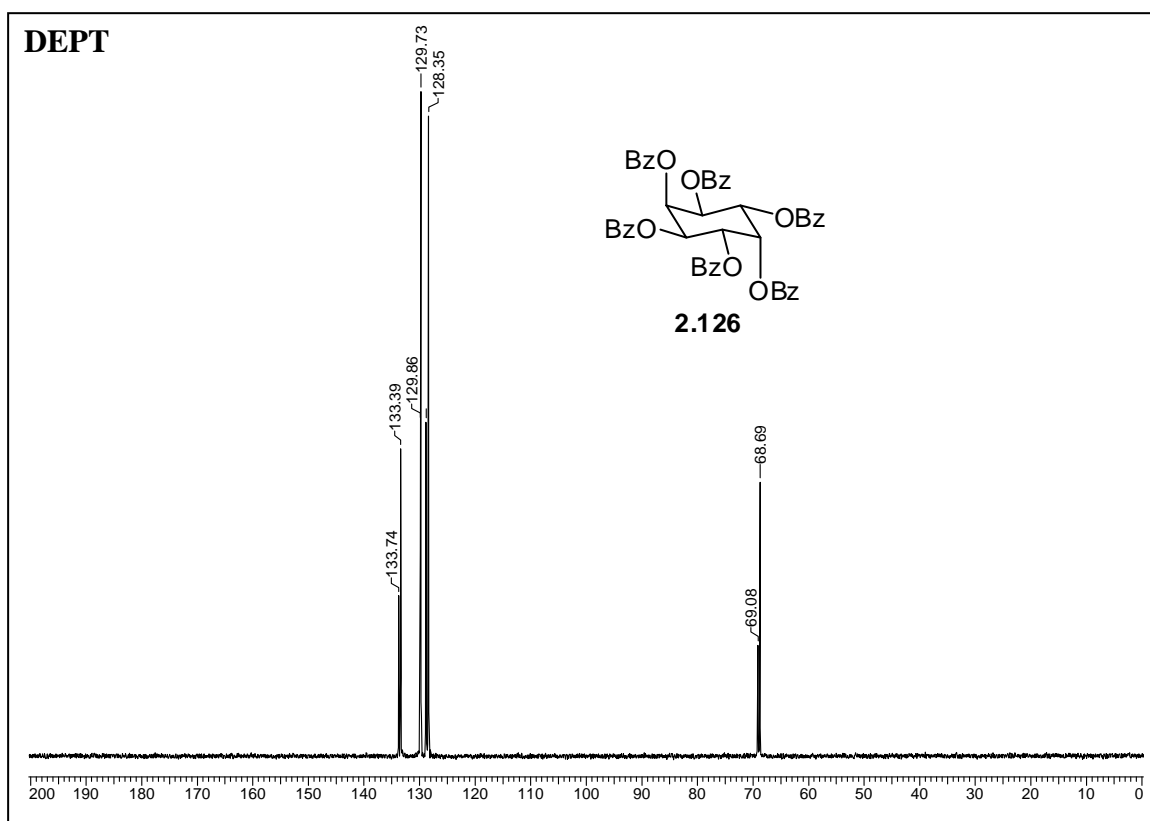
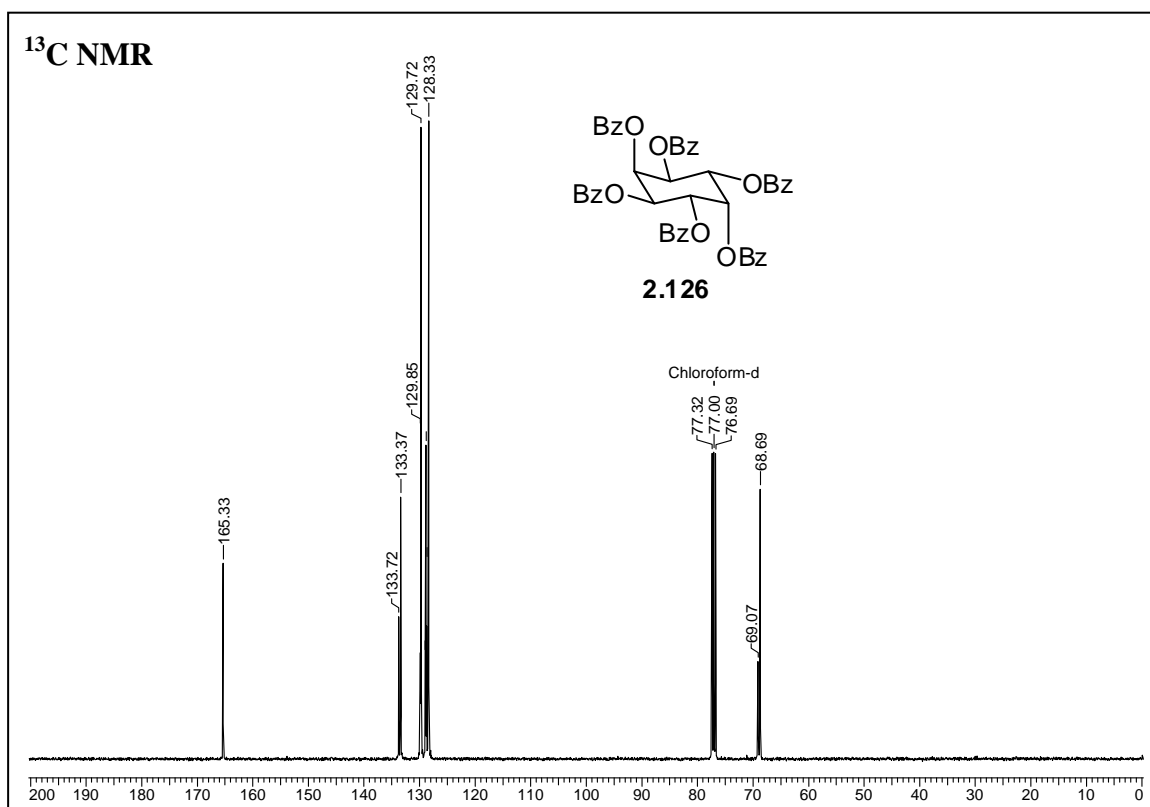


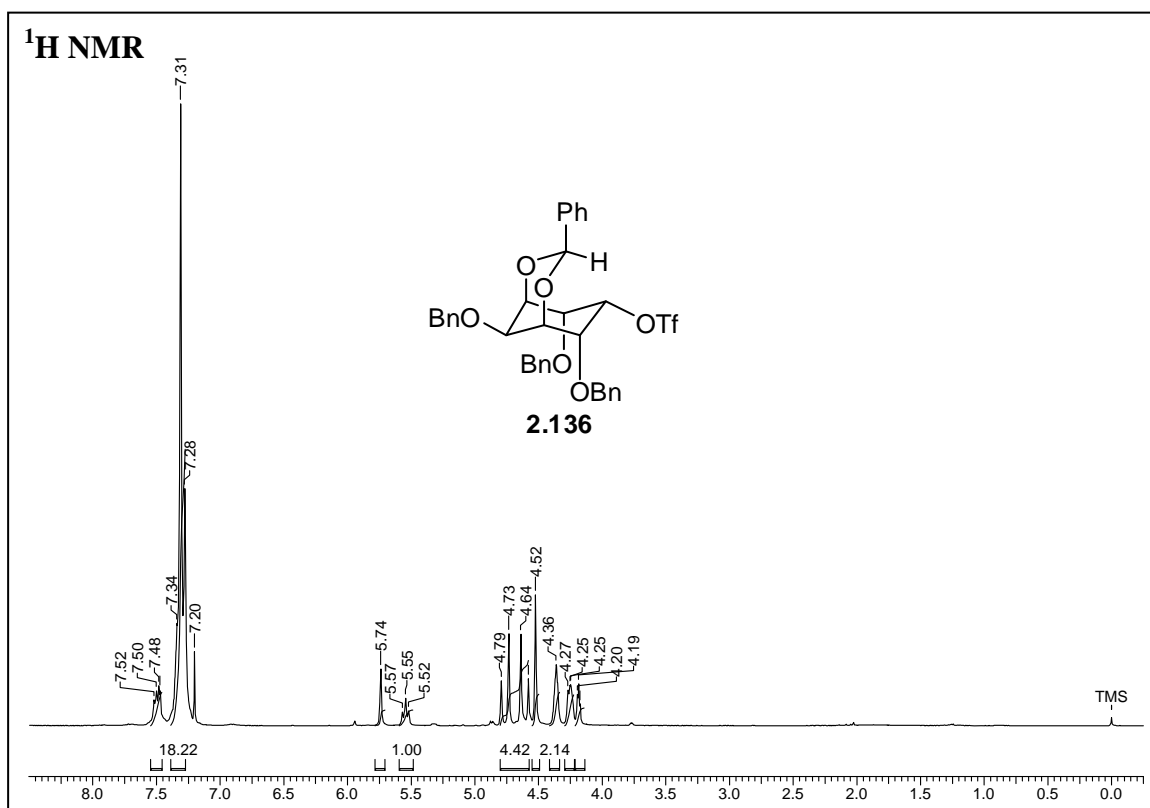
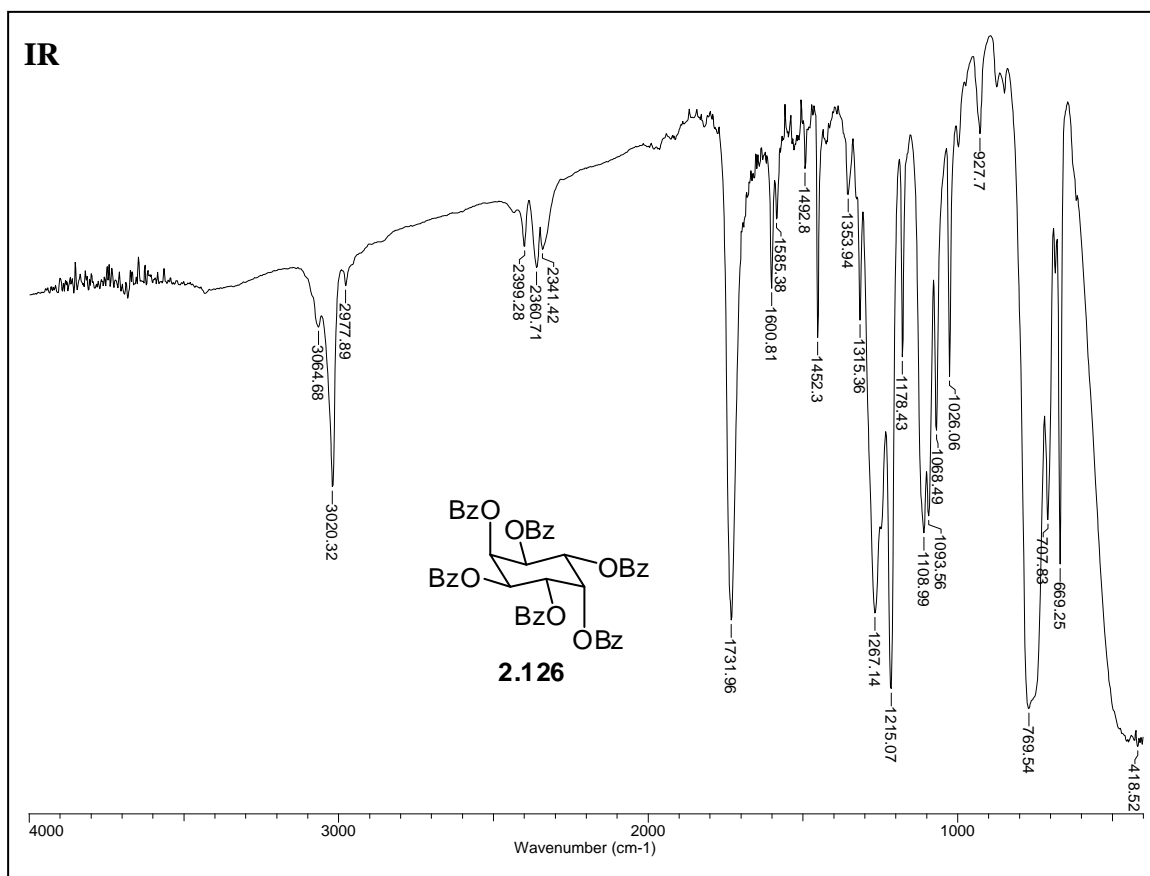


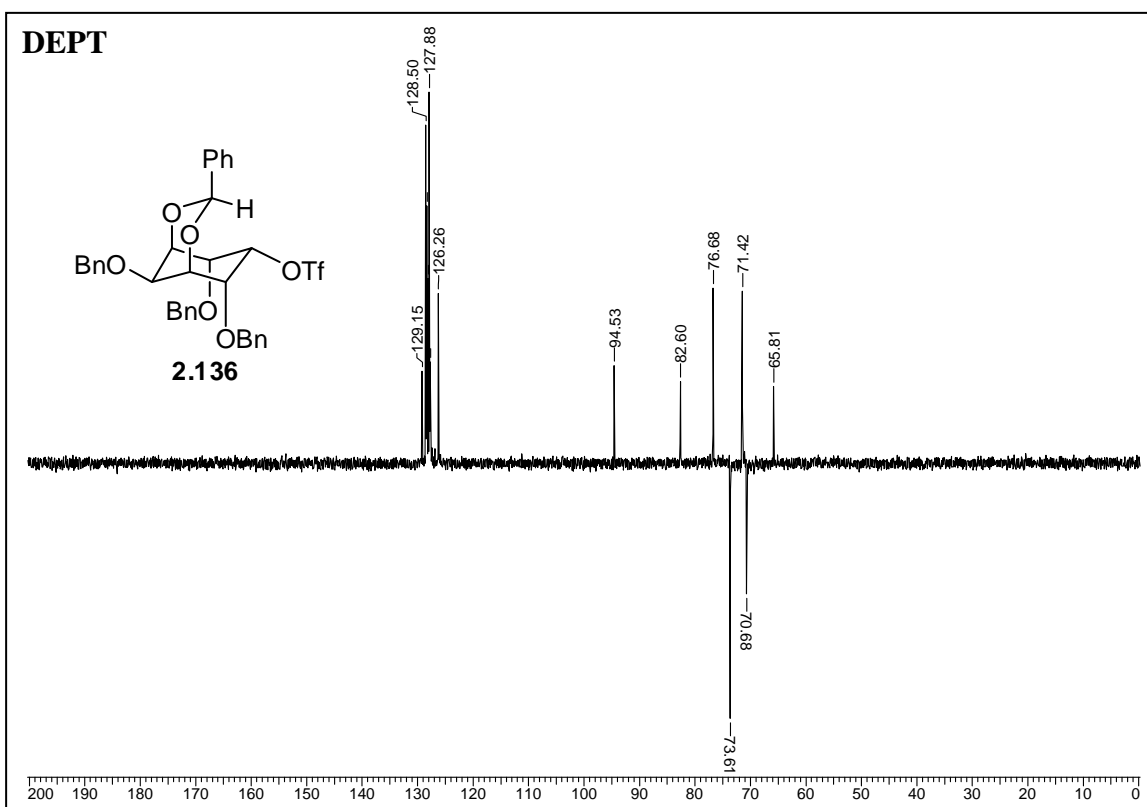
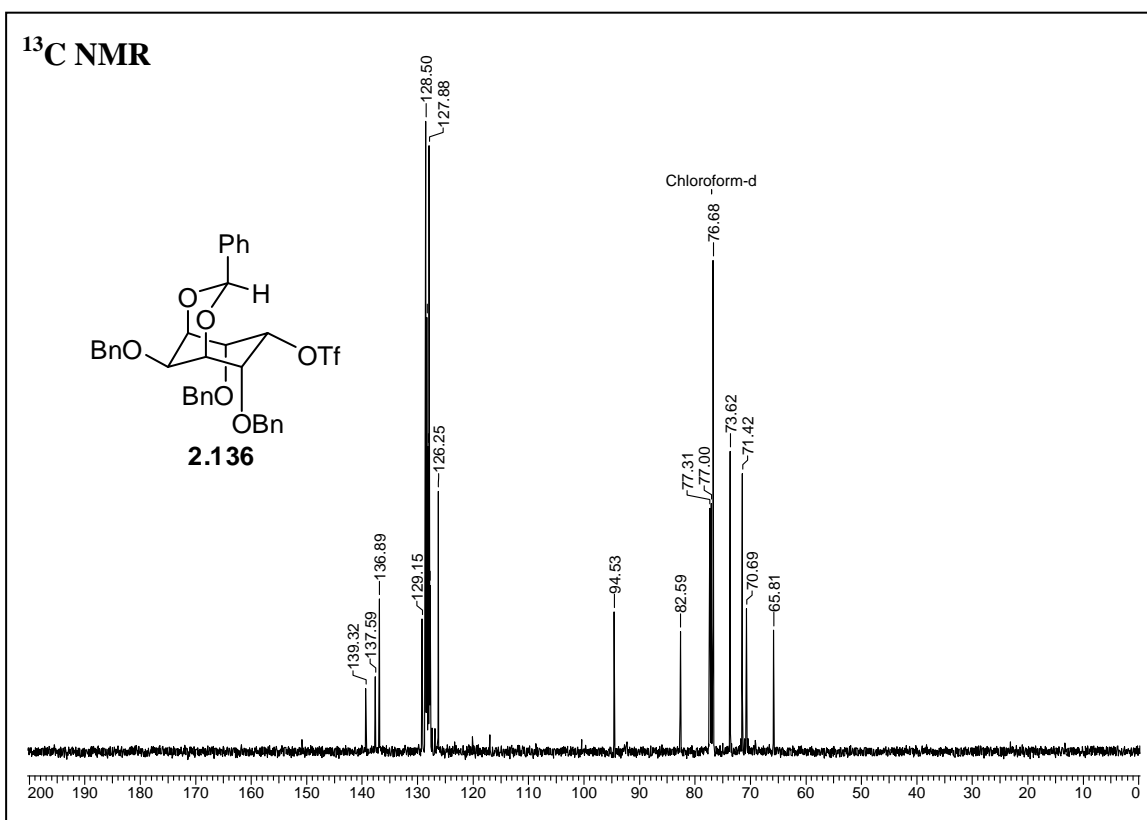


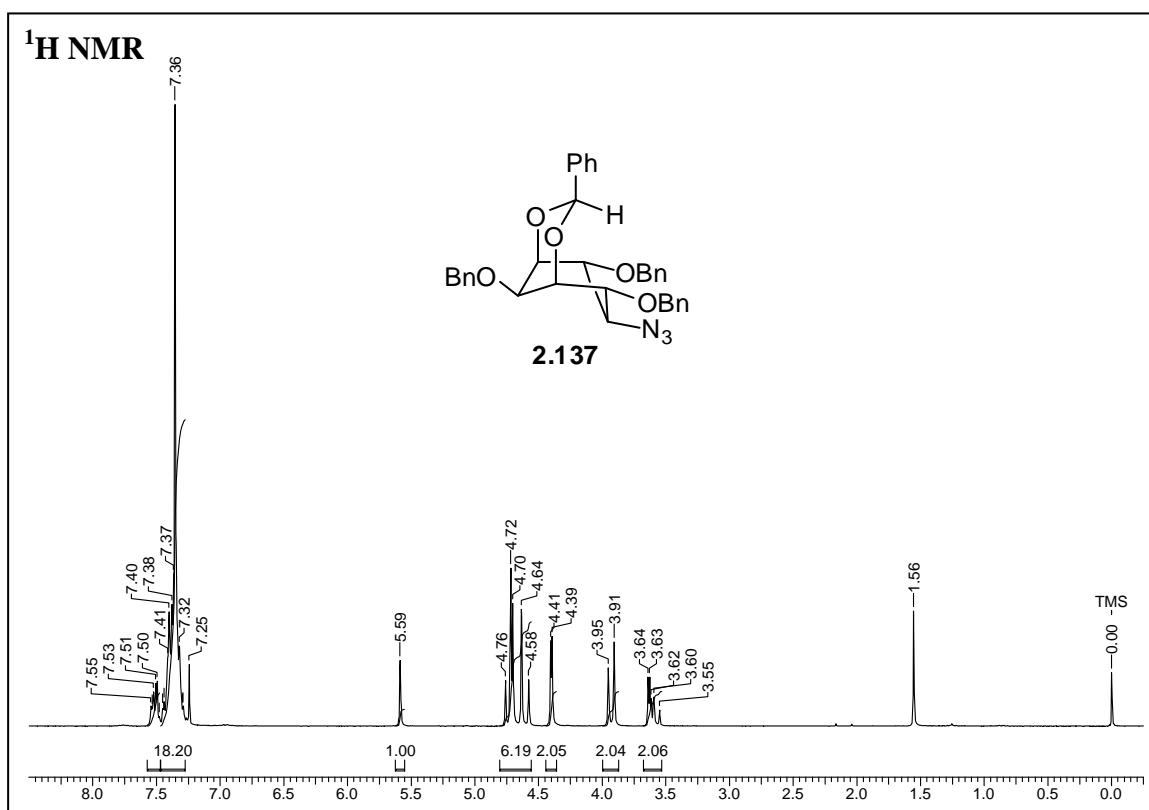
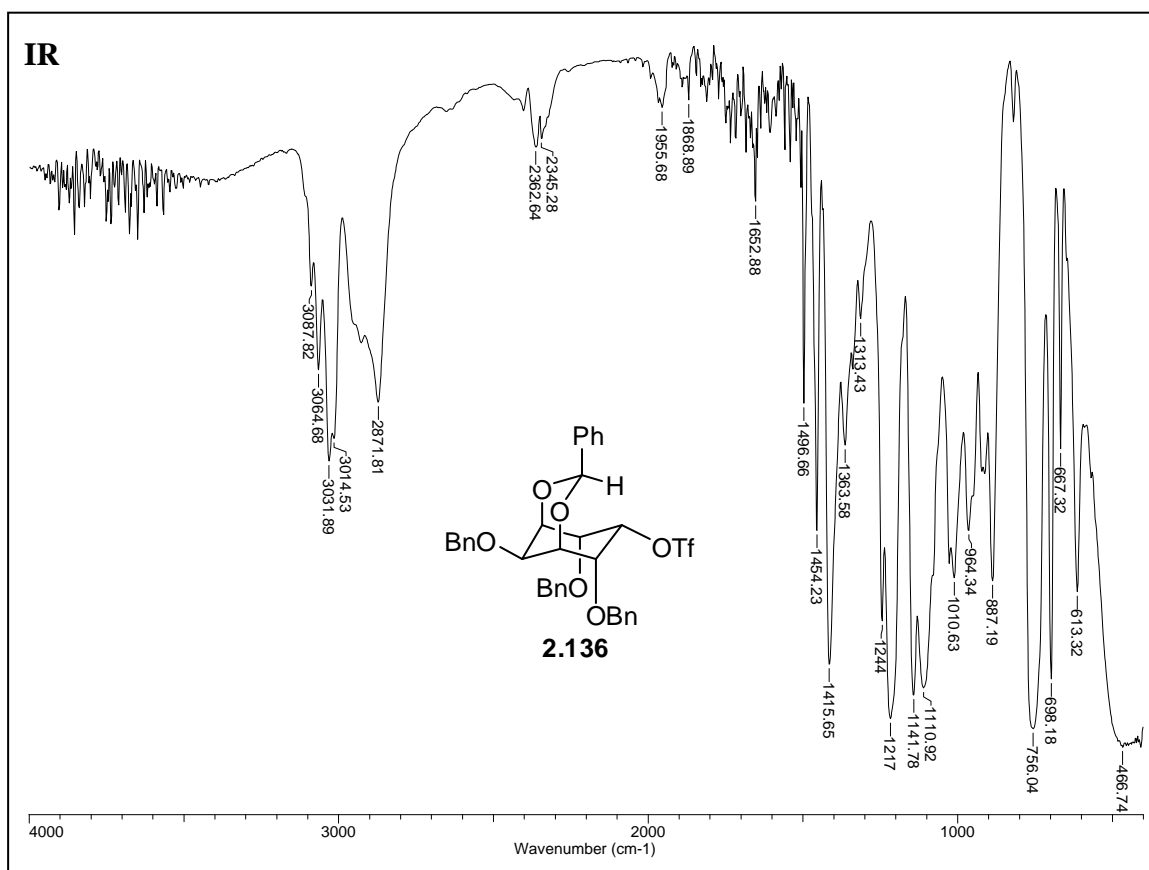
Chapter 2

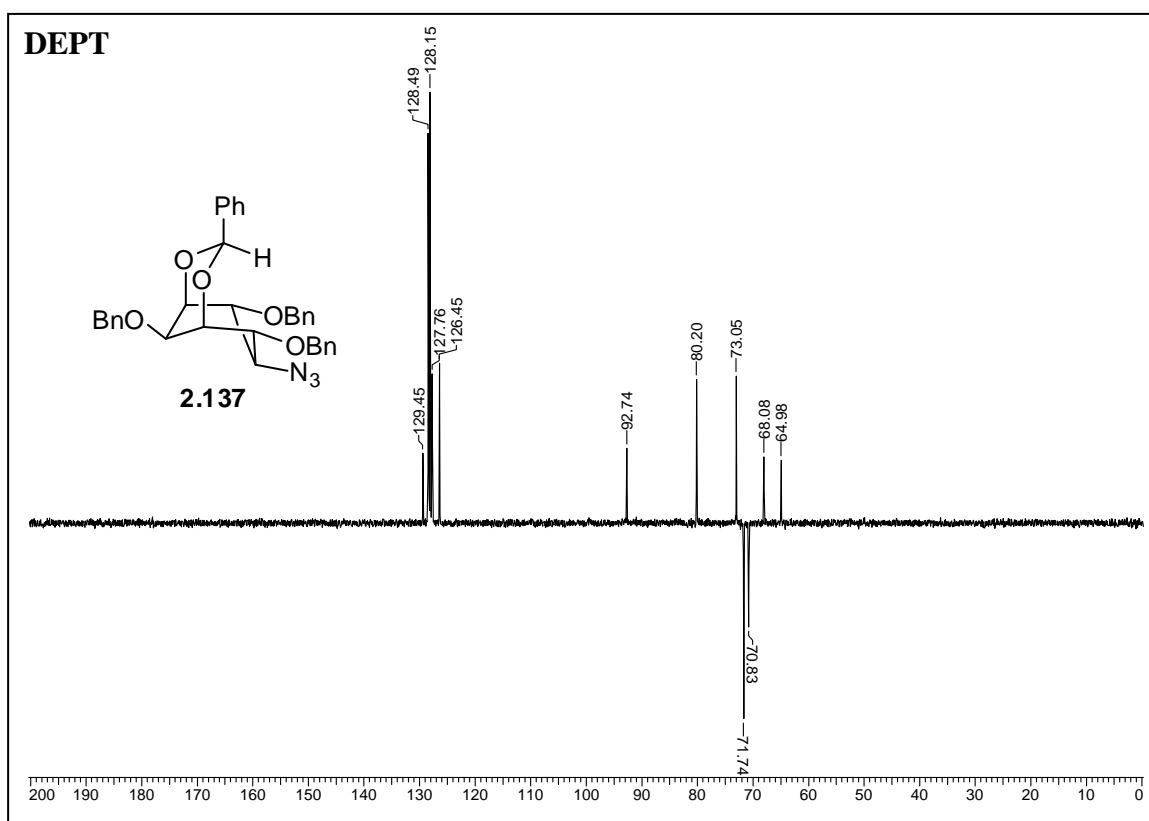
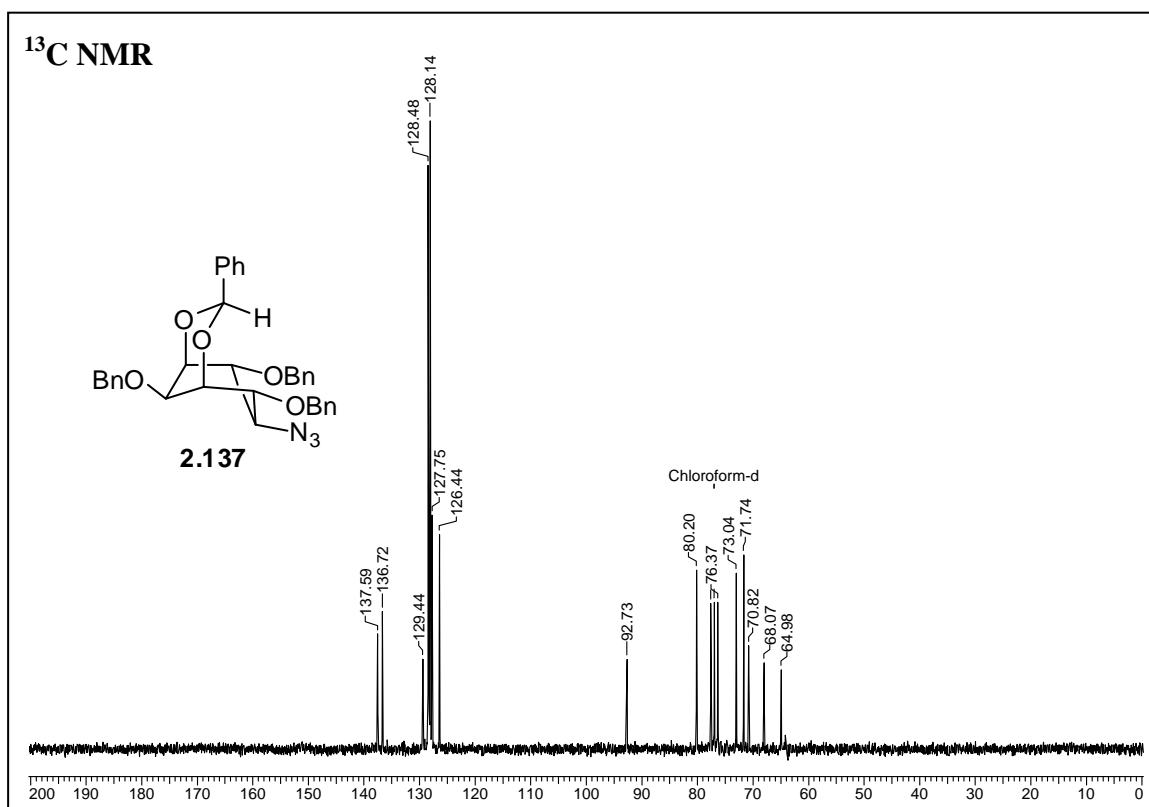


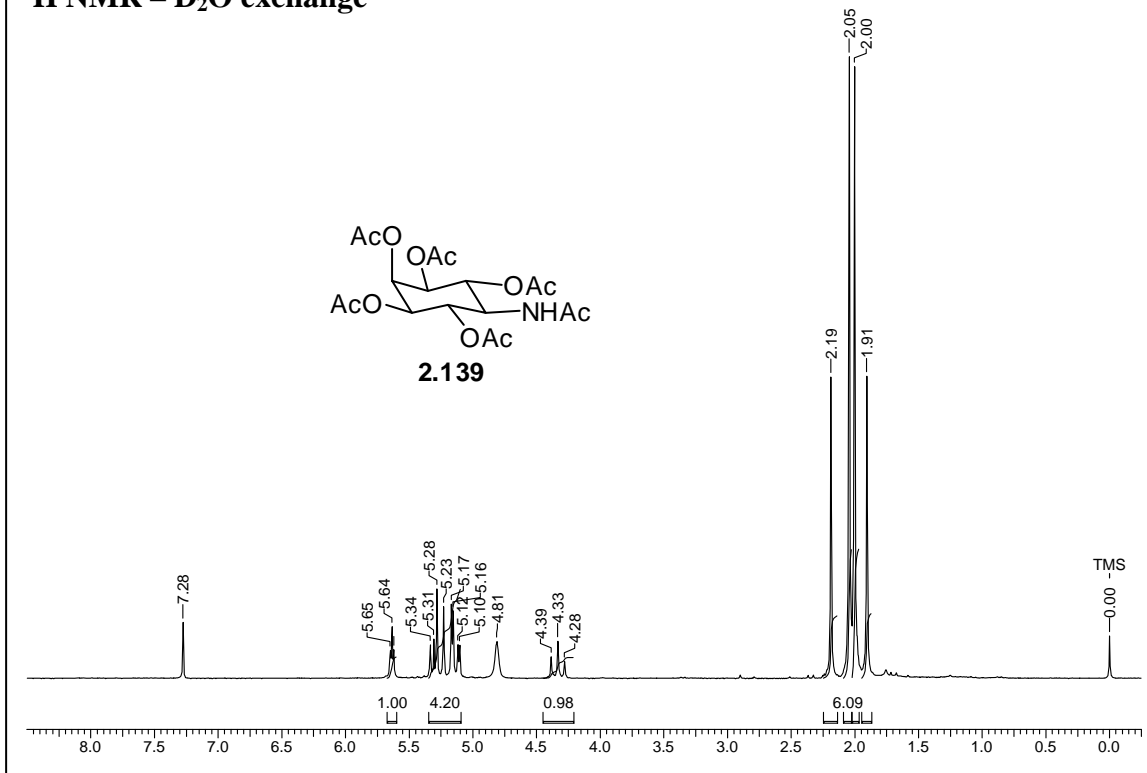
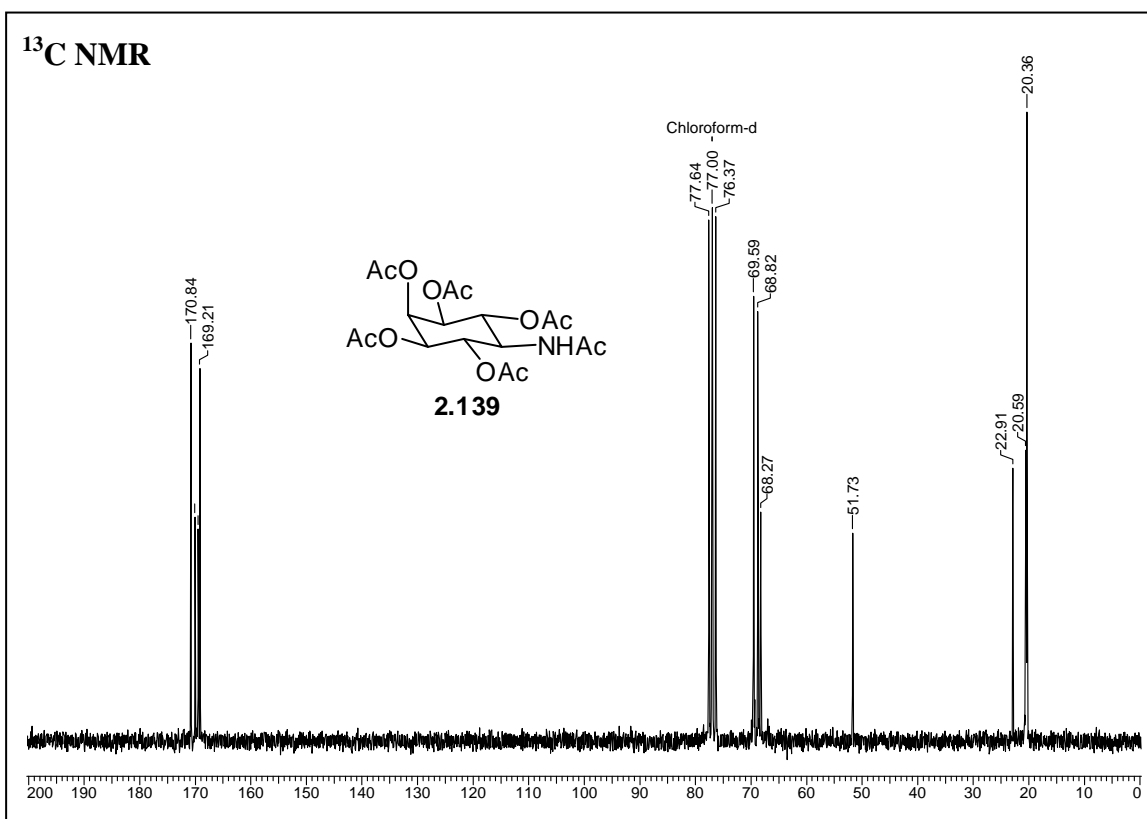


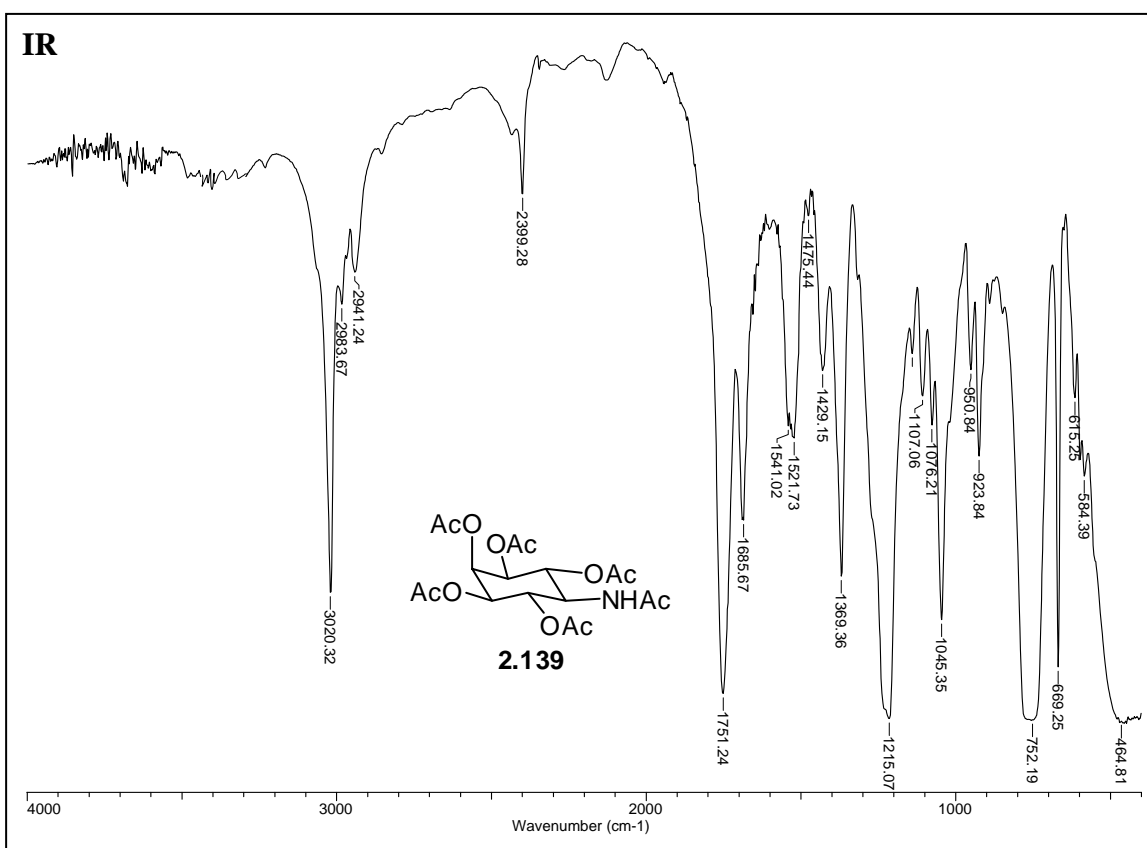
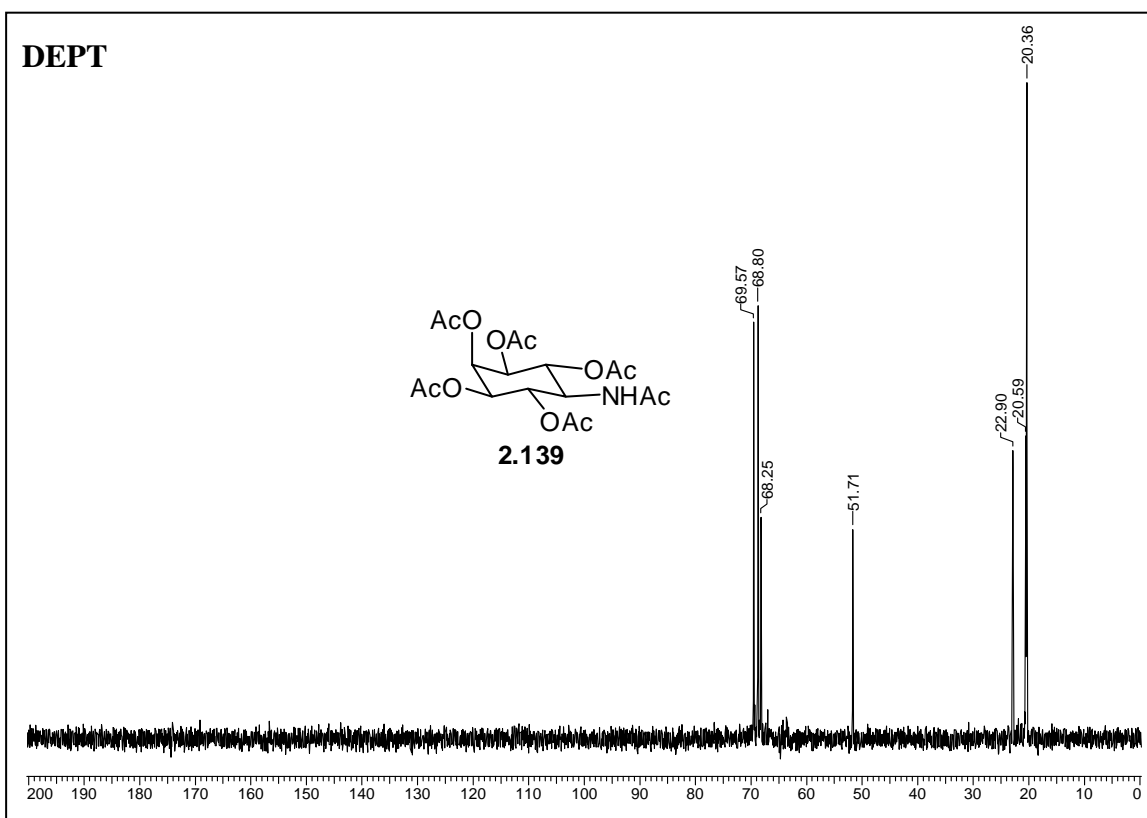




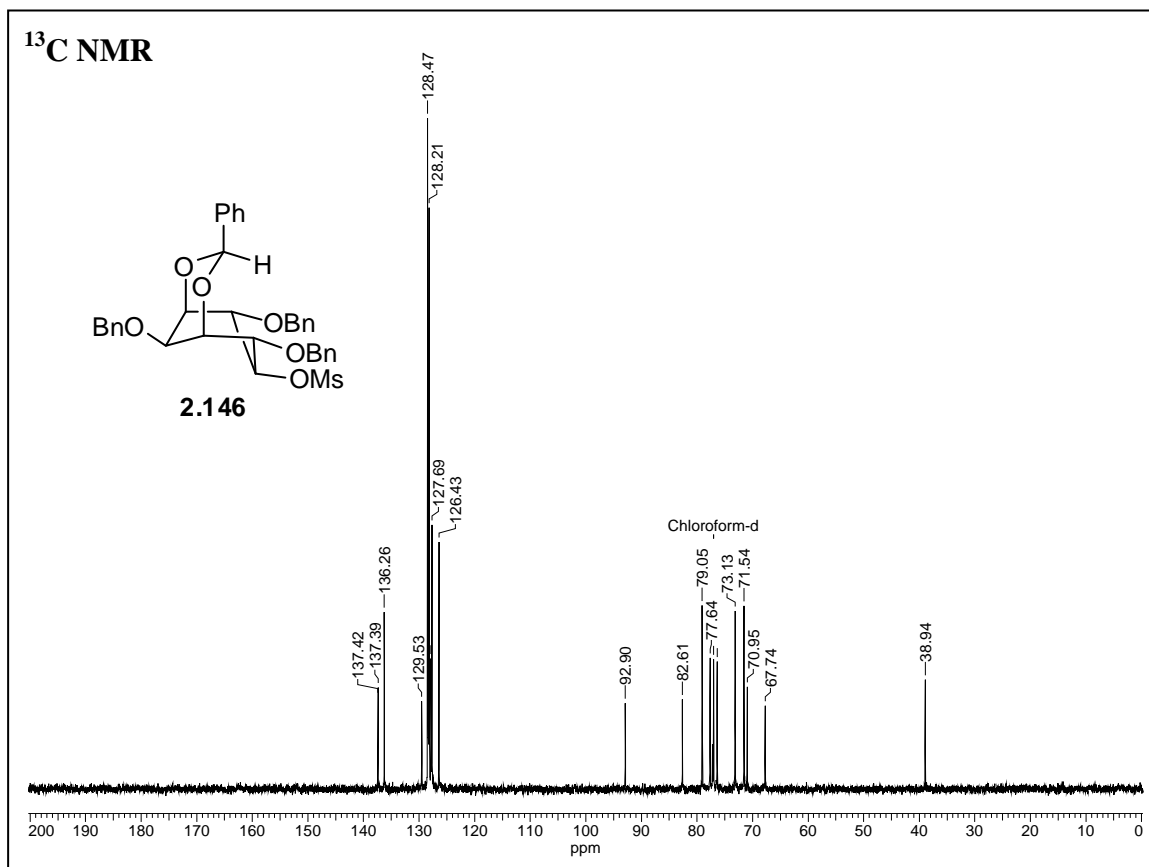
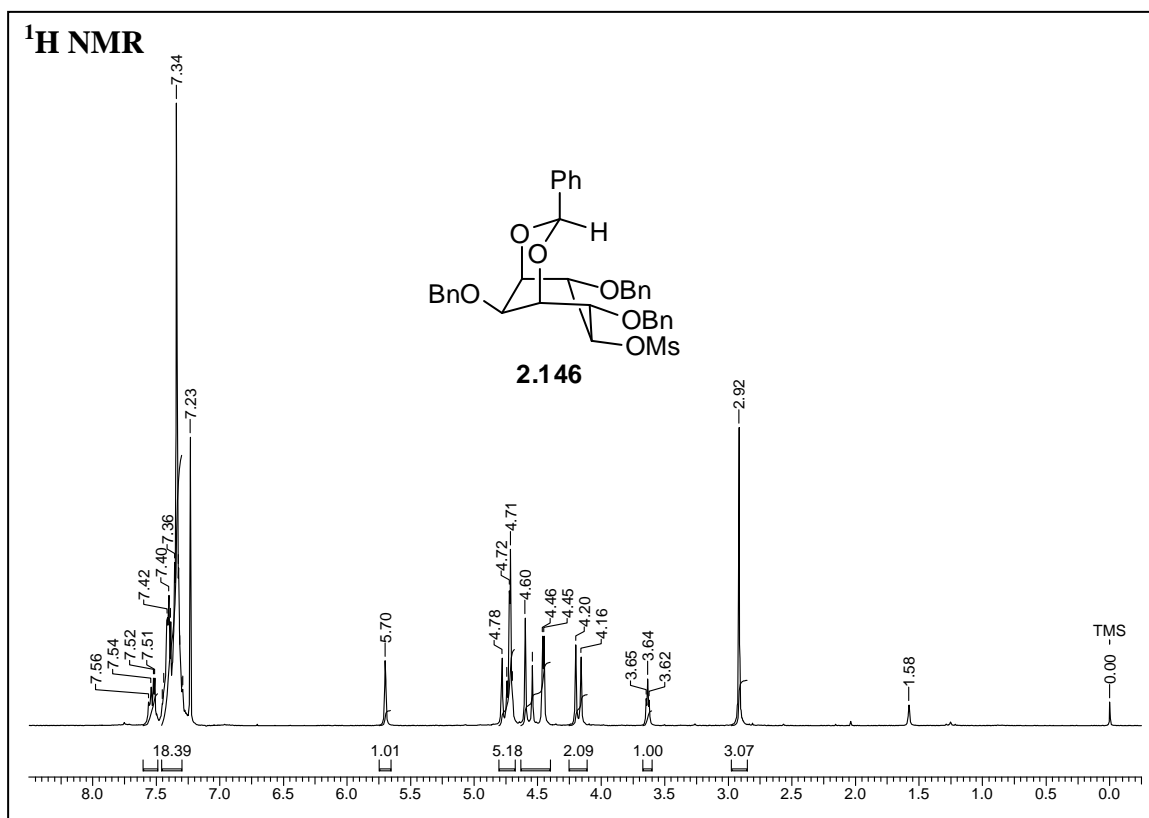


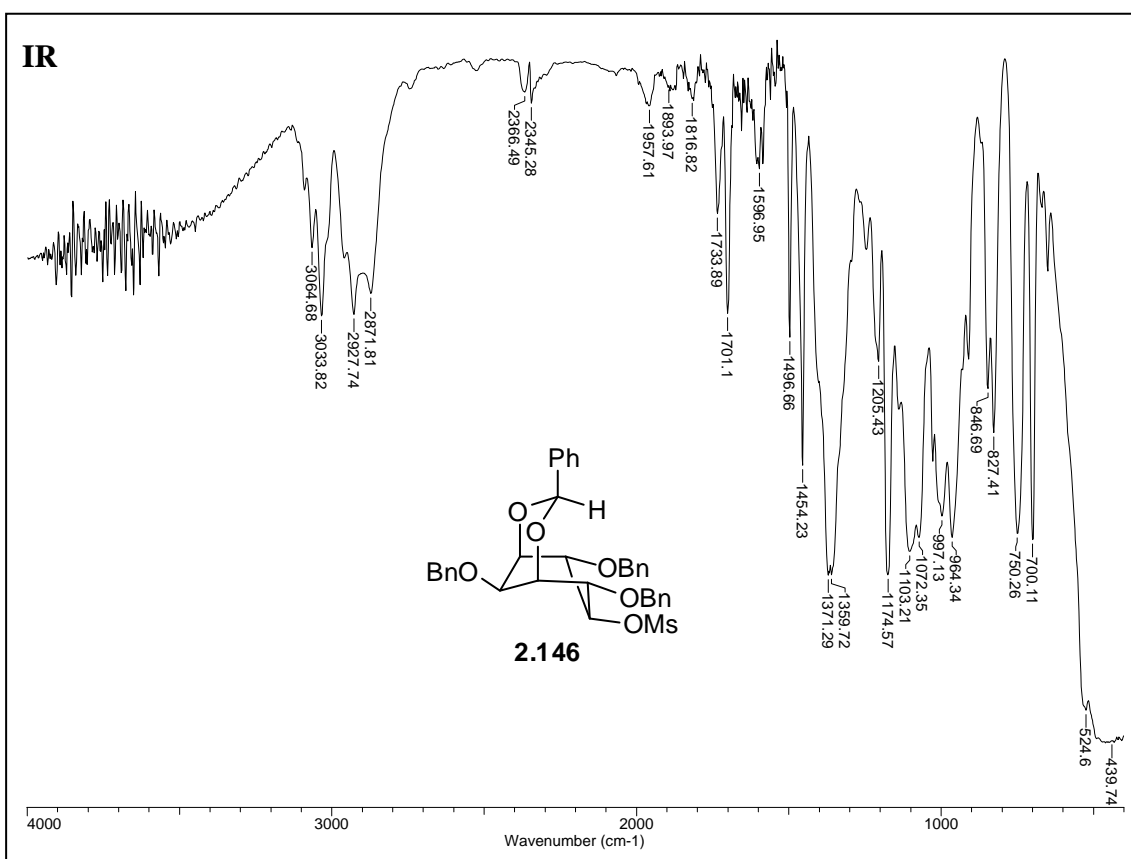
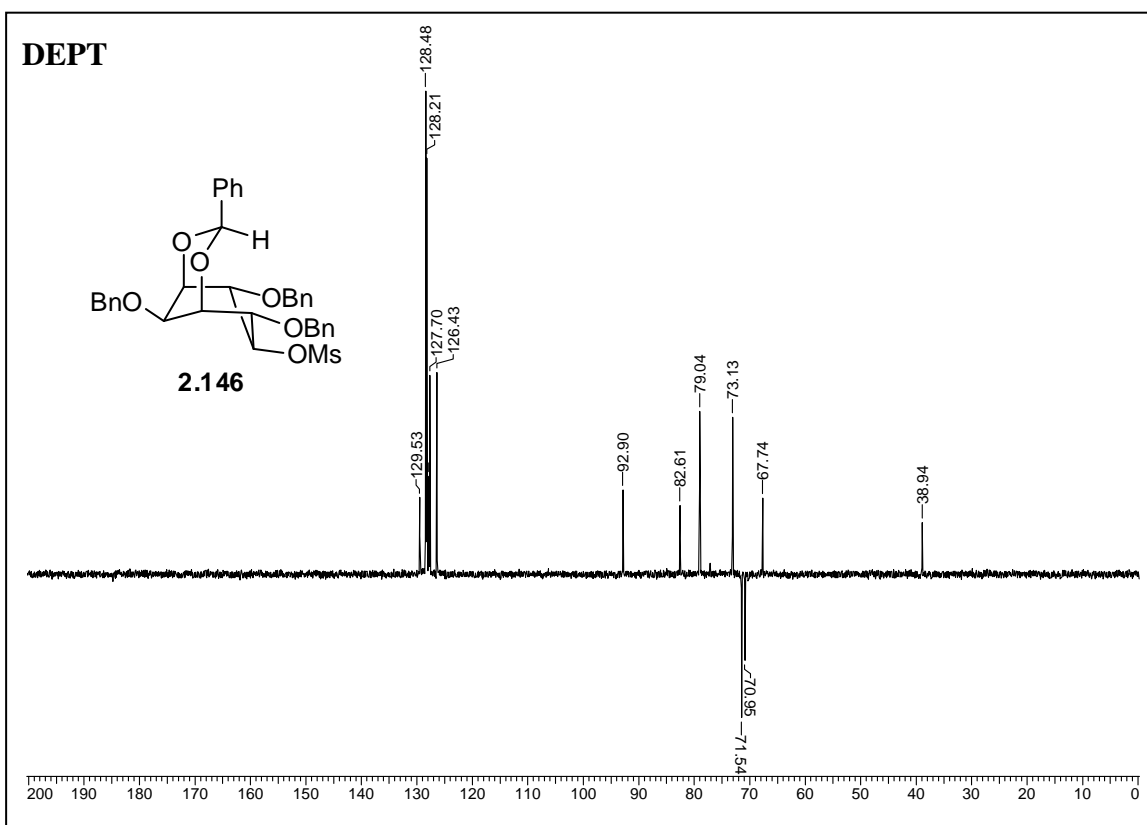


^1H NMR – D_2O exchange **^{13}C NMR**

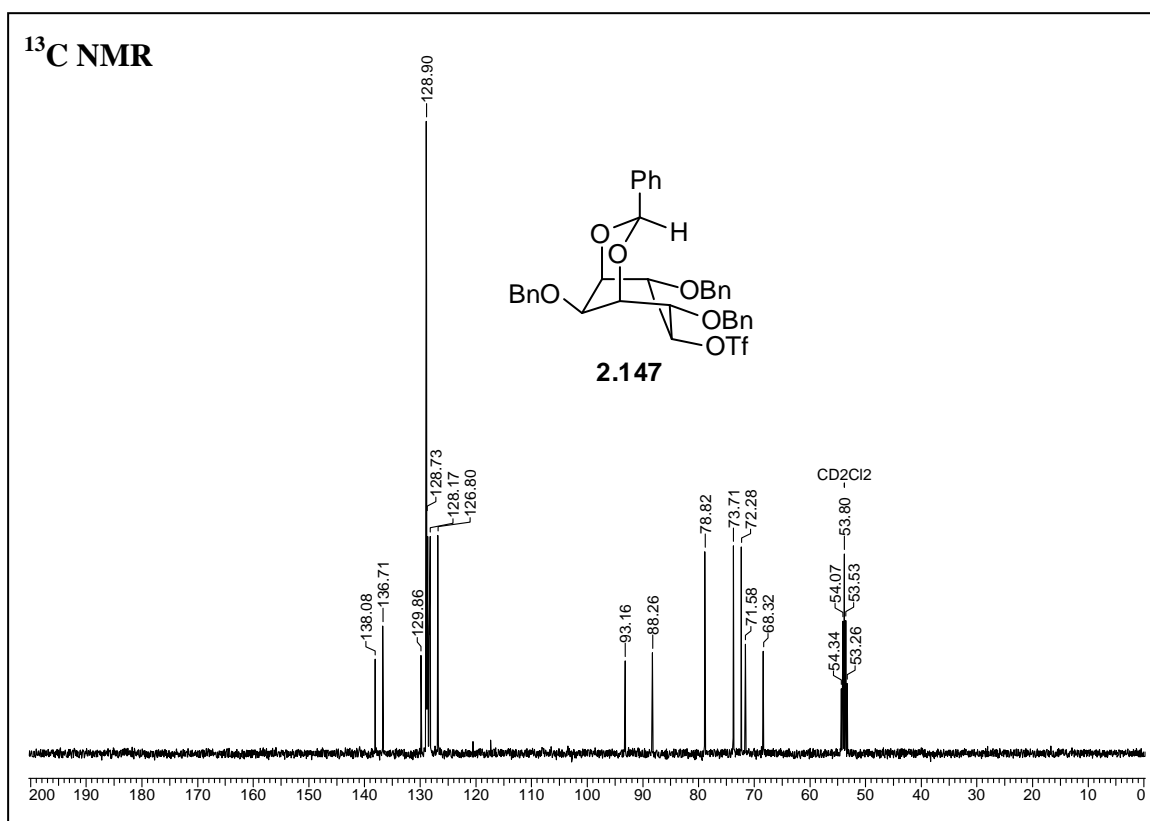
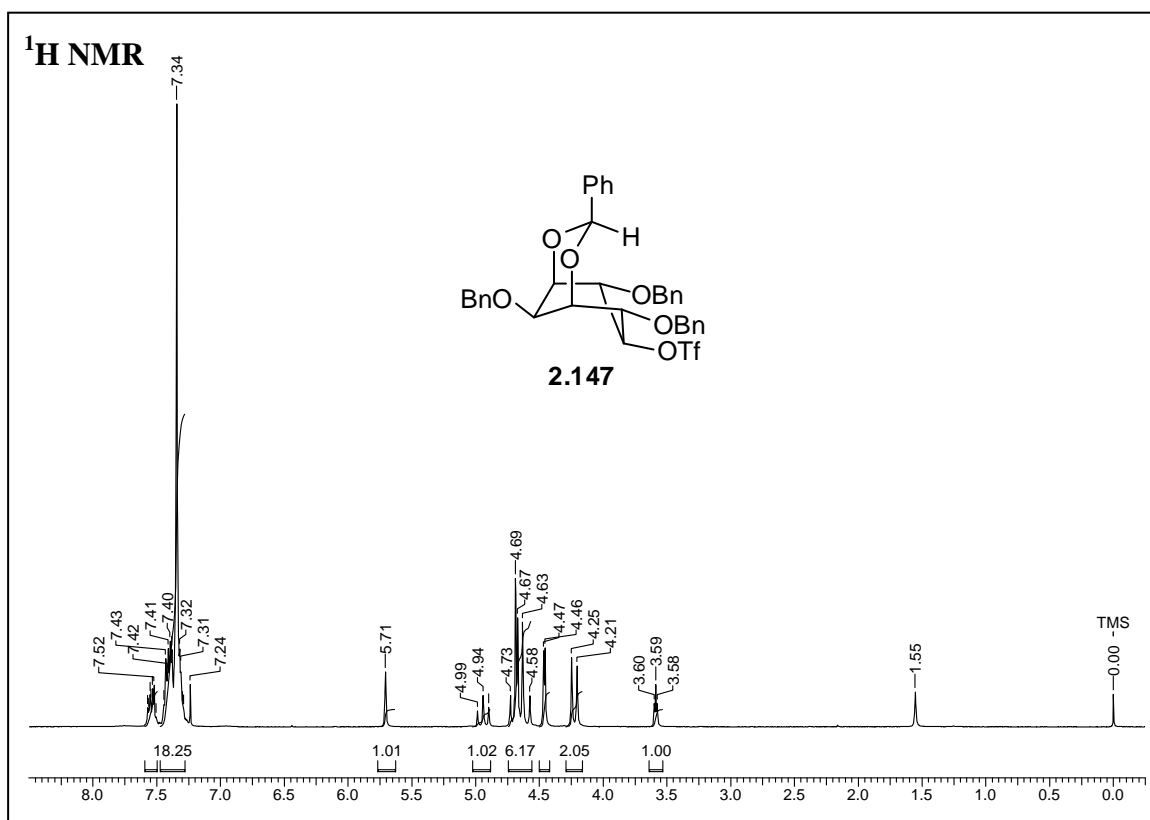


Chapter 2





Chapter 2



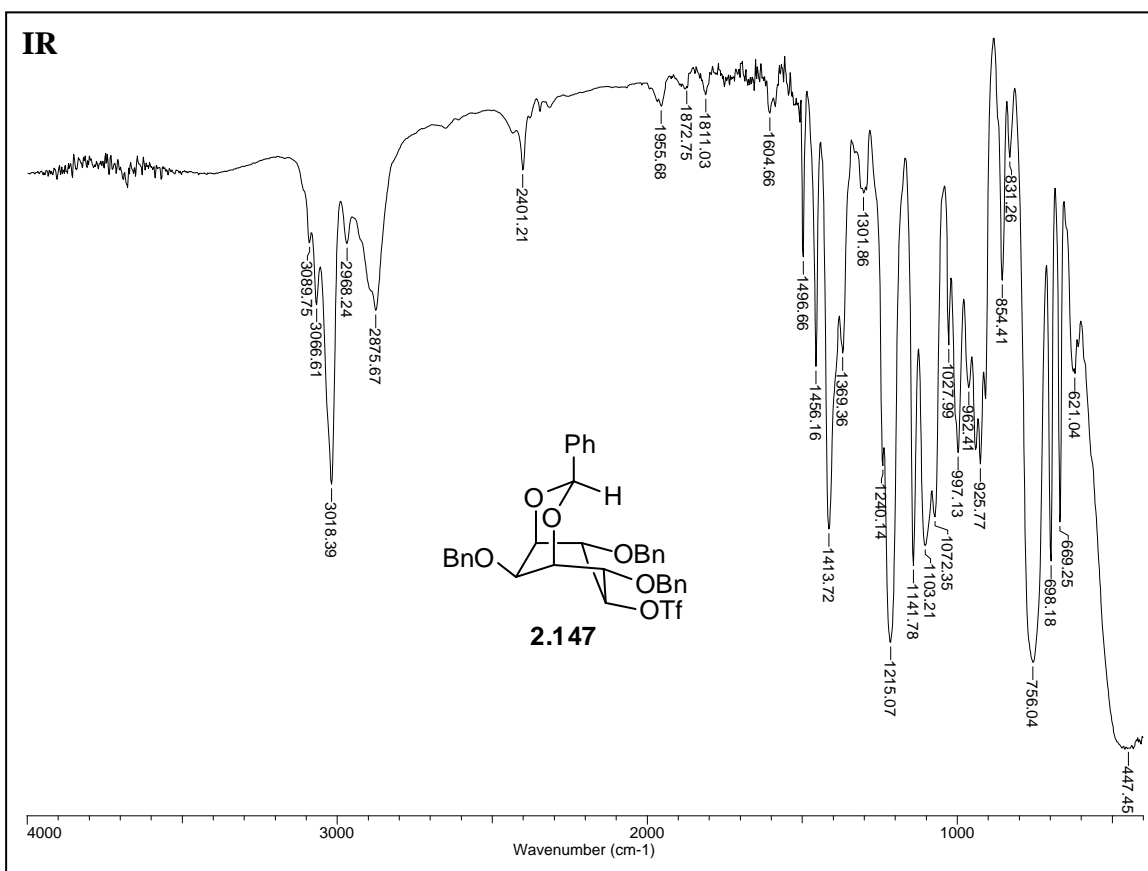
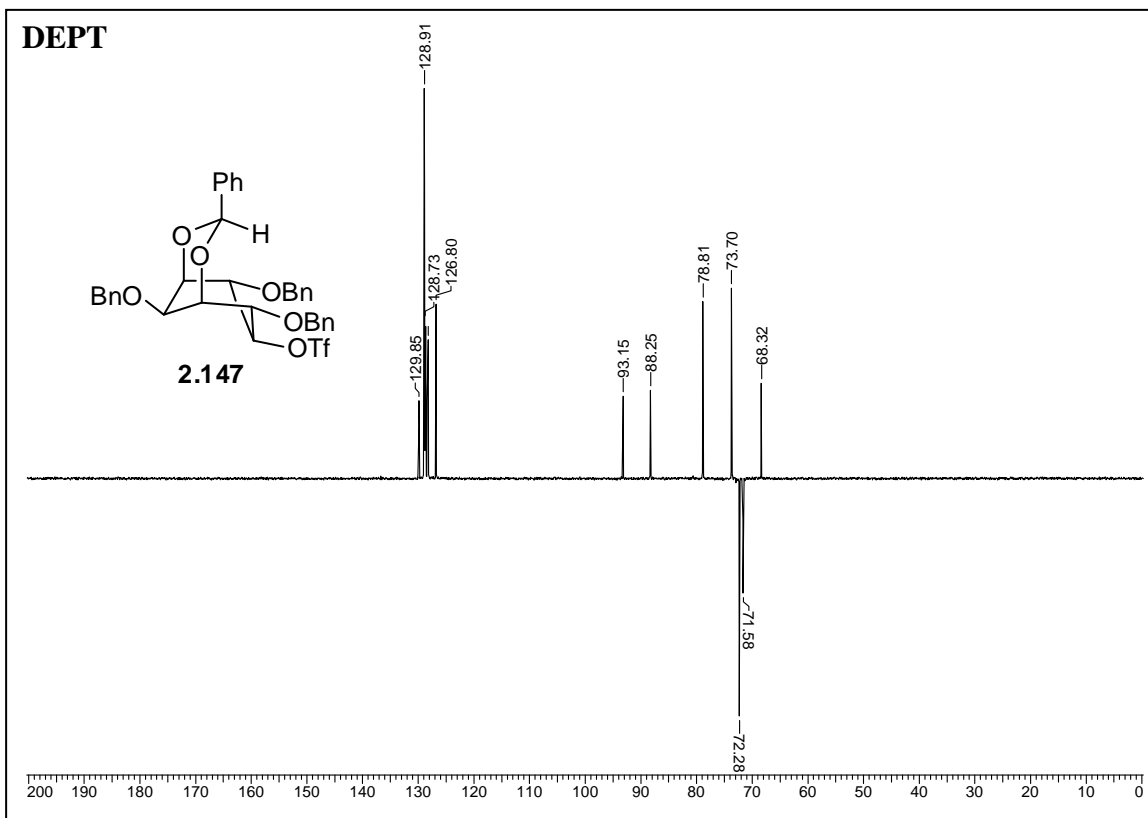


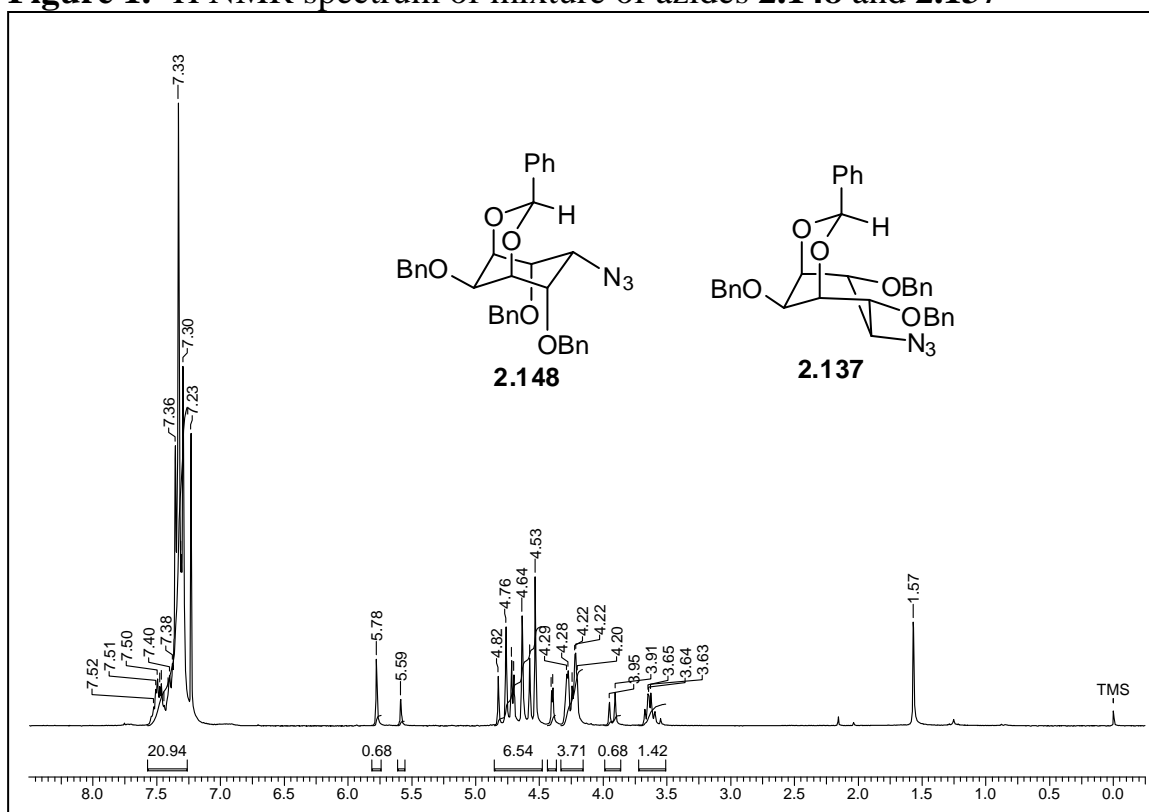
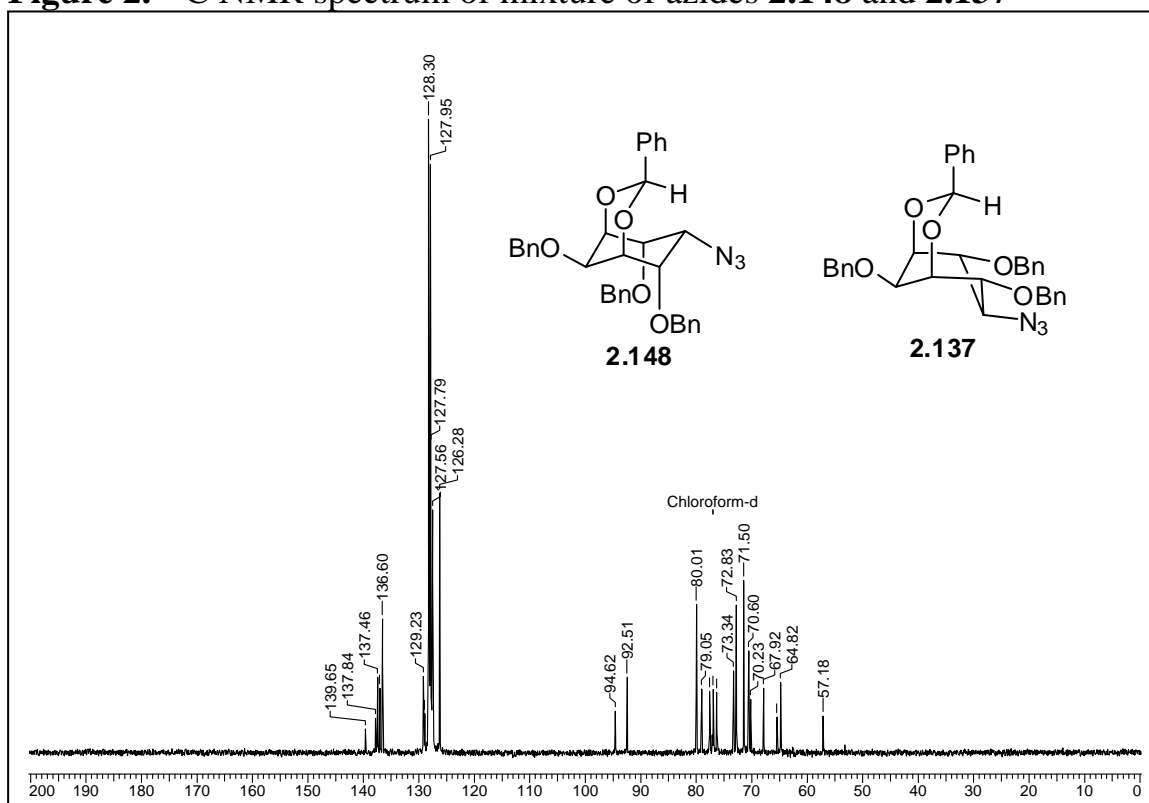
Figure 1. ^1H NMR spectrum of mixture of azides **2.148** and **2.137****Figure 2.** ^{13}C NMR spectrum of mixture of azides **2.148** and **2.137**

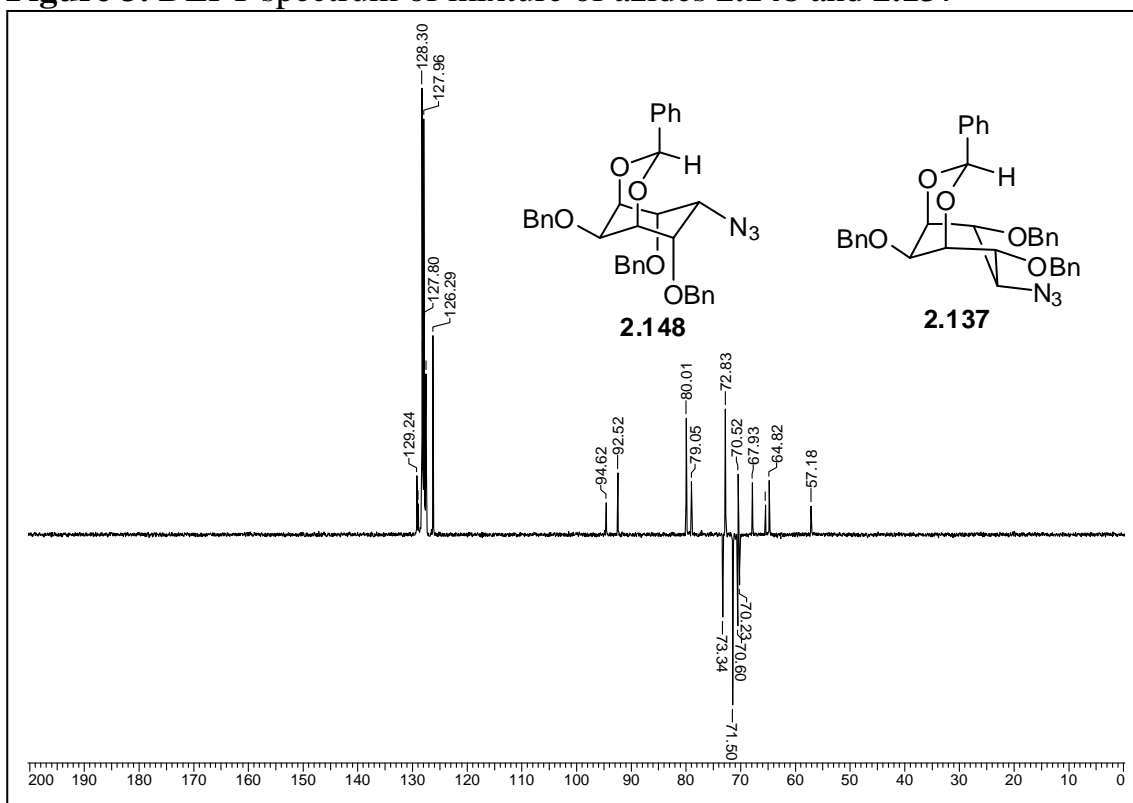
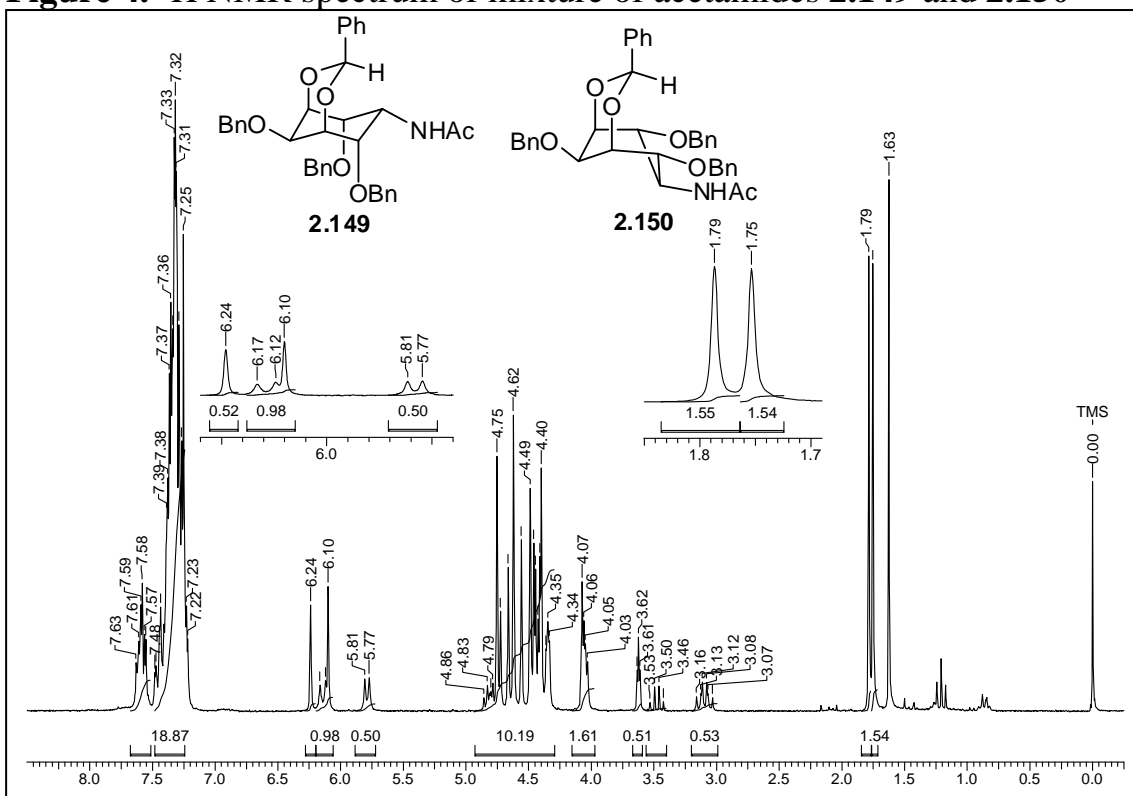
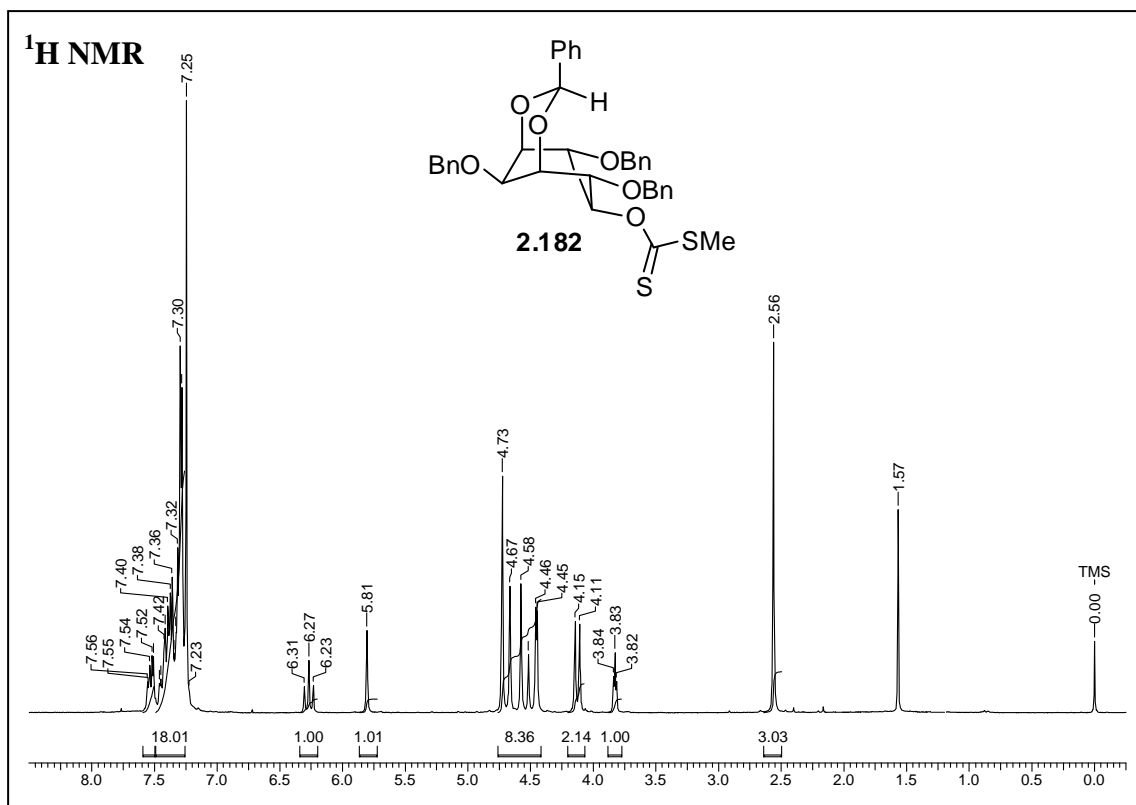
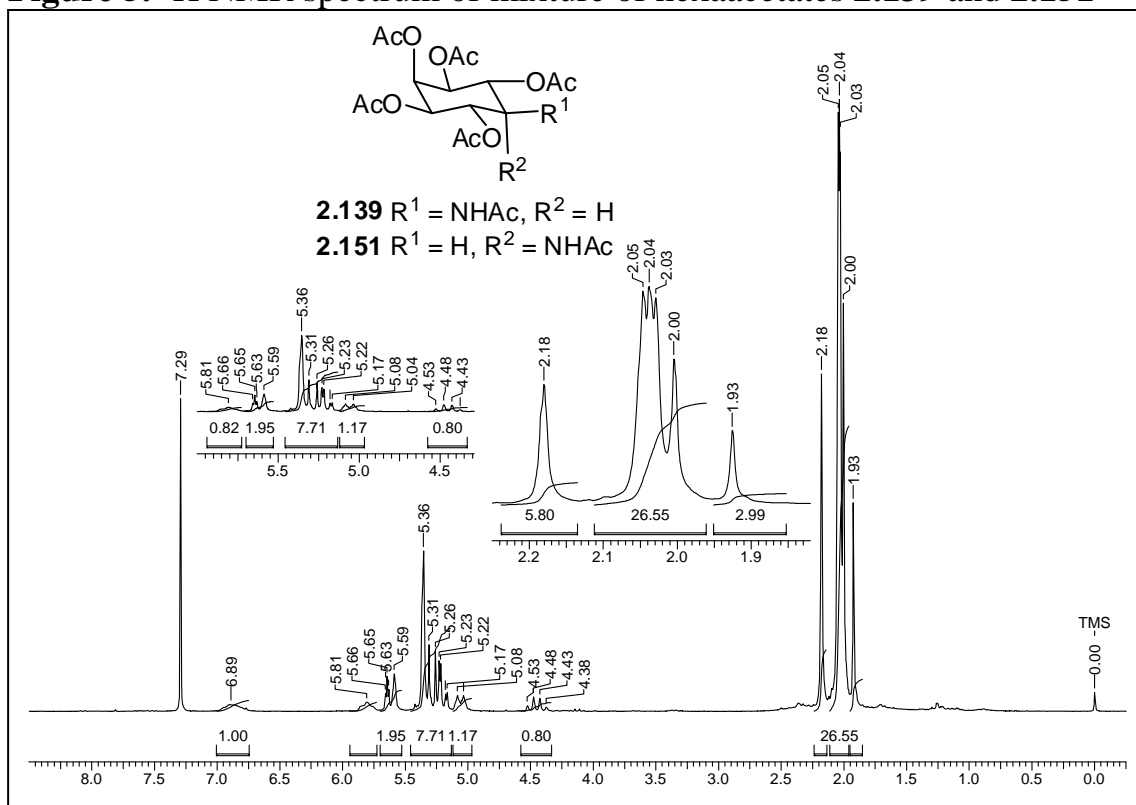
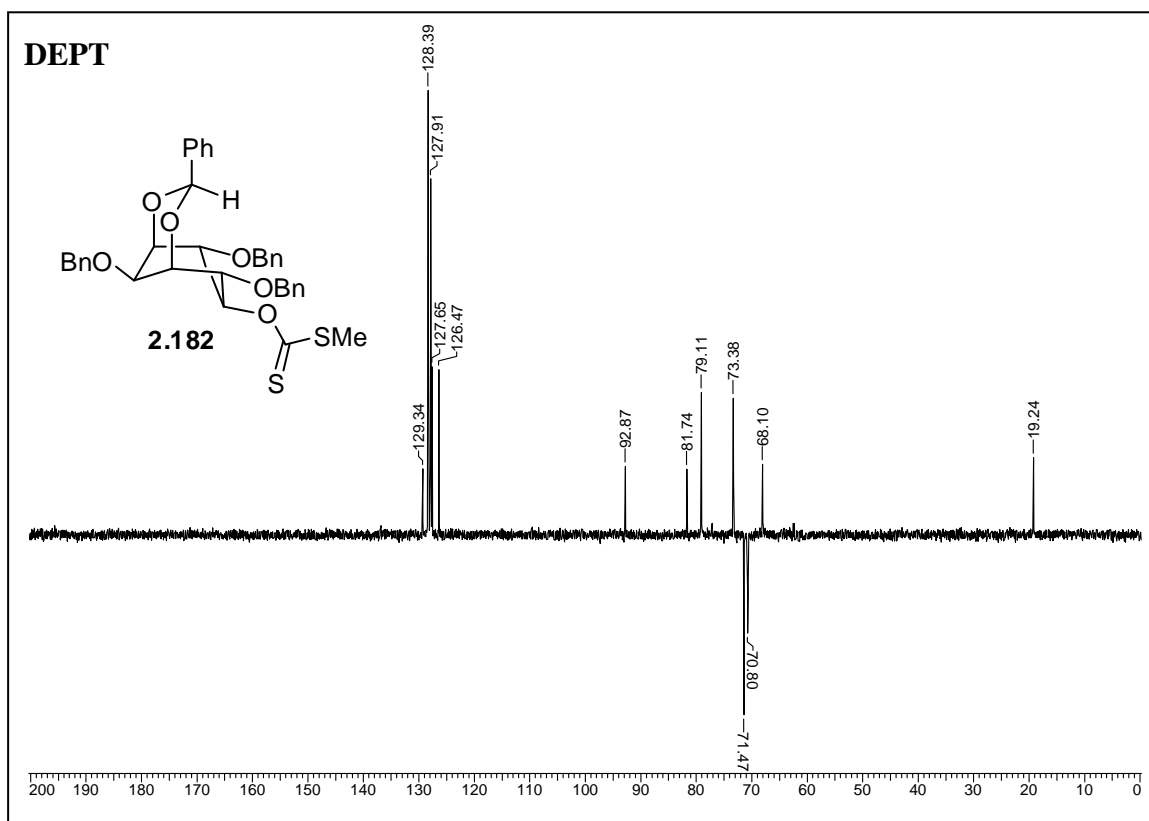
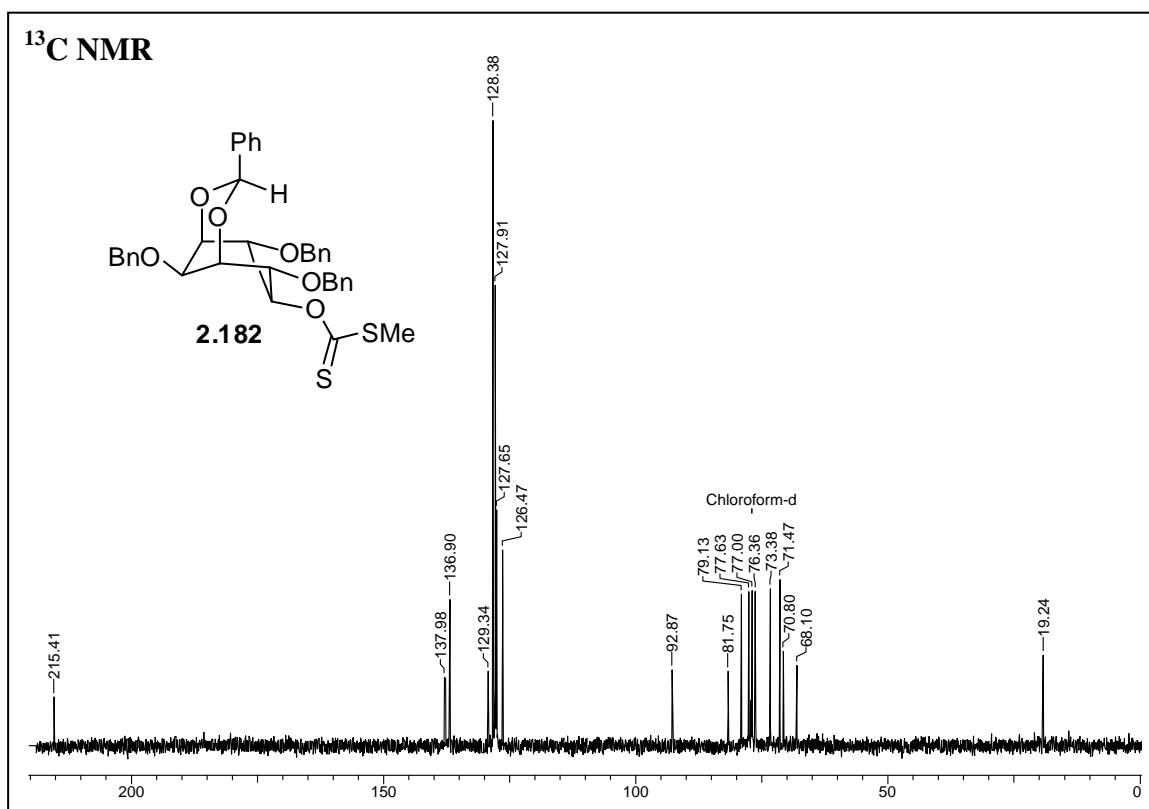
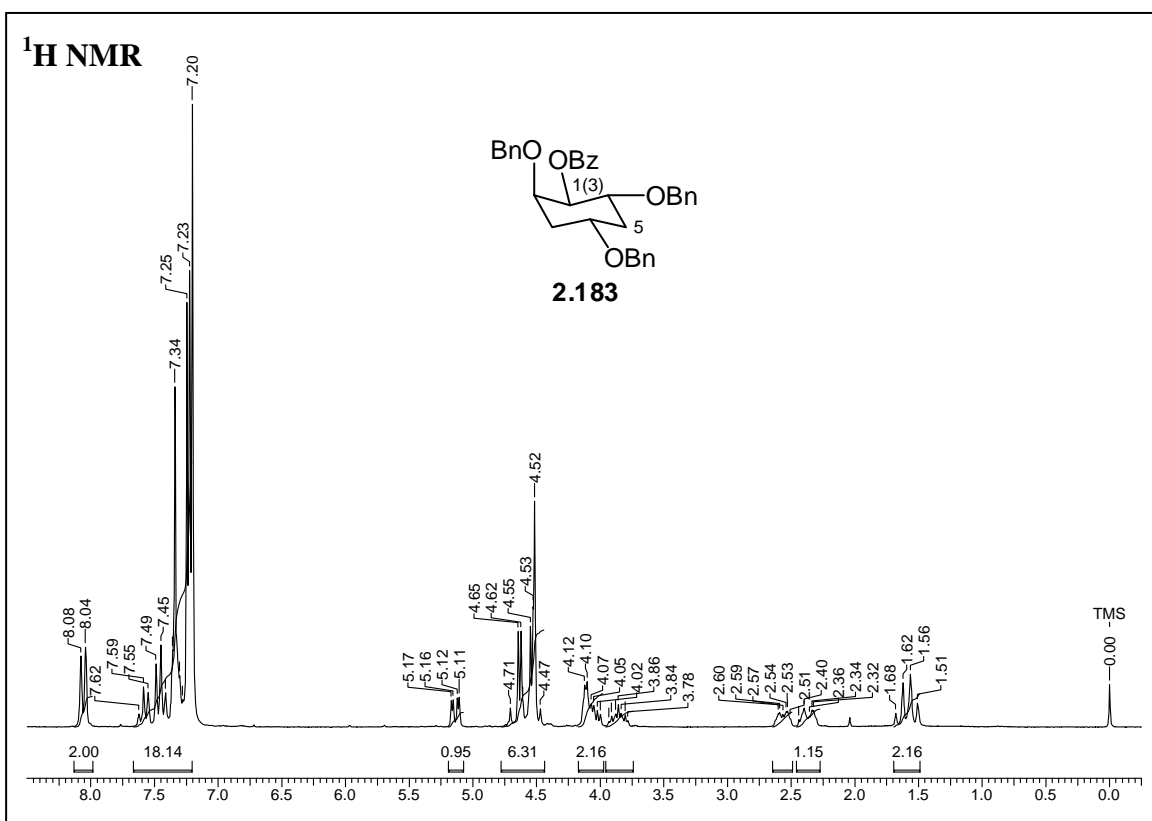
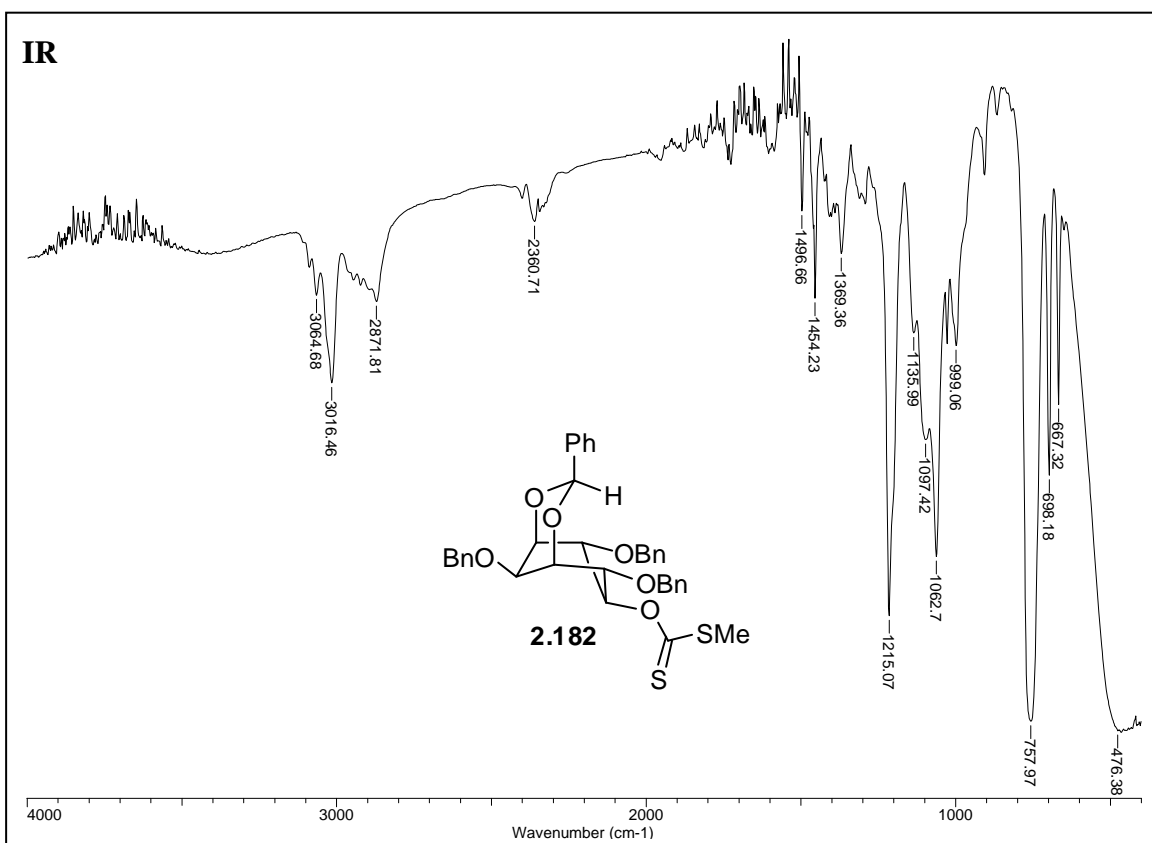
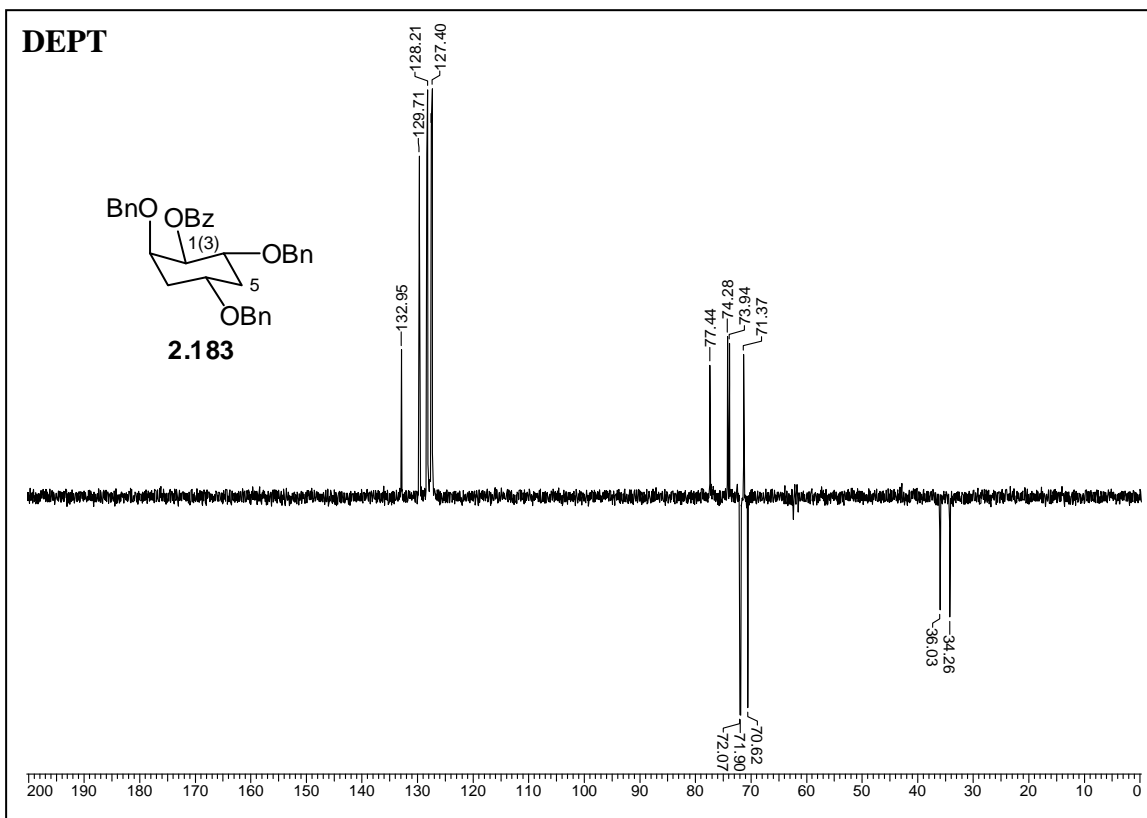
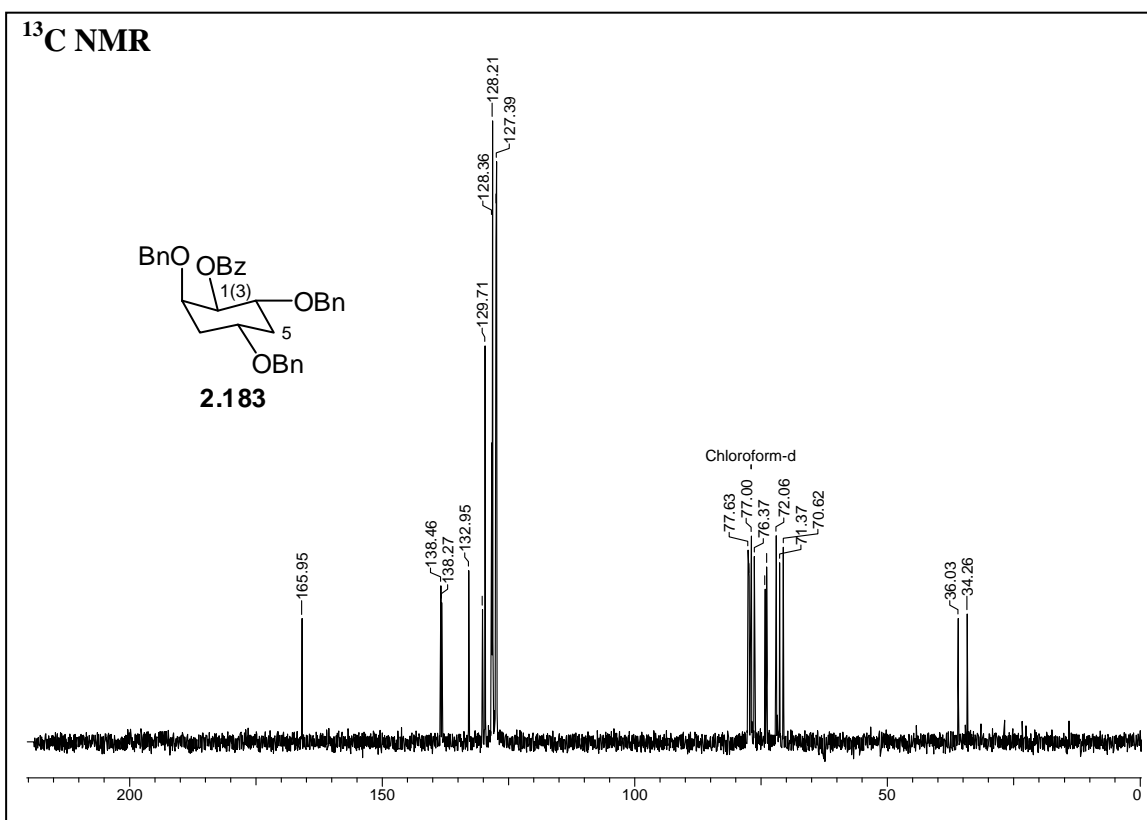
Figure 3. DEPT spectrum of mixture of azides **2.148** and **2.137**Figure 4. ^1H NMR spectrum of mixture of acetamides **2.149** and **2.150**

Figure 5. ^1H NMR spectrum of mixture of hexaacetates **2.139** and **2.151**

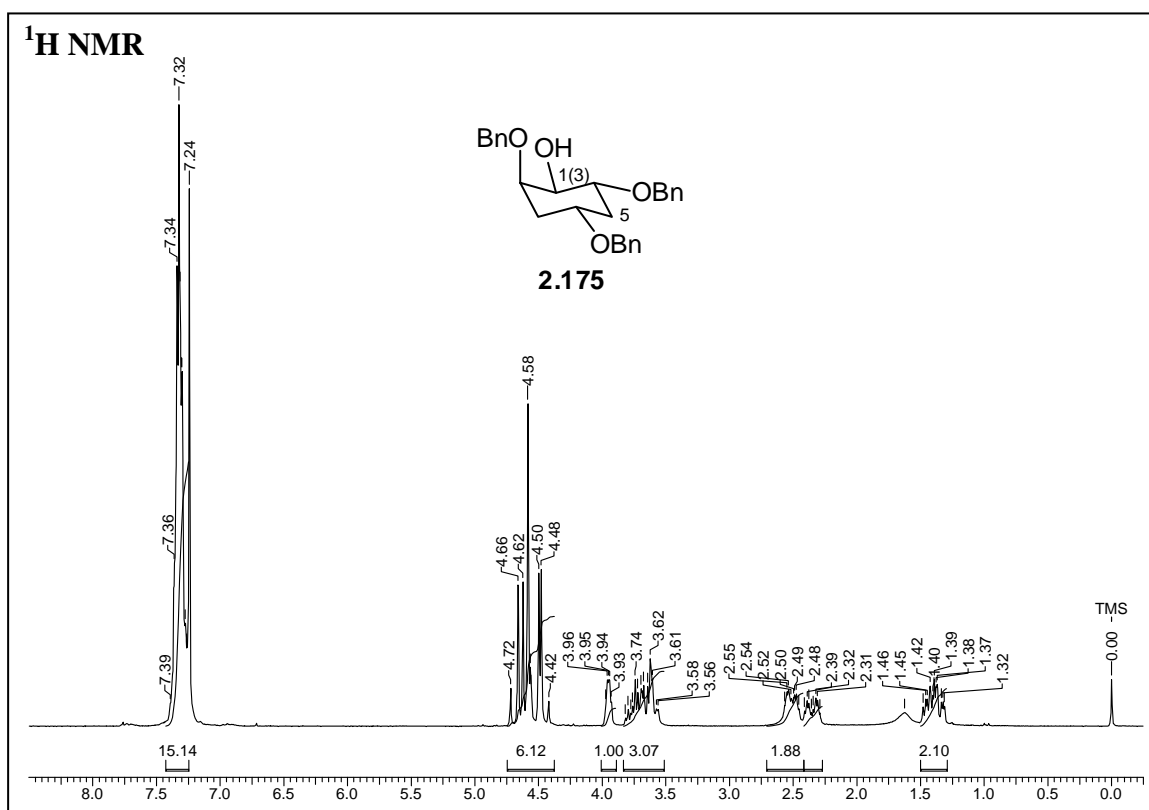
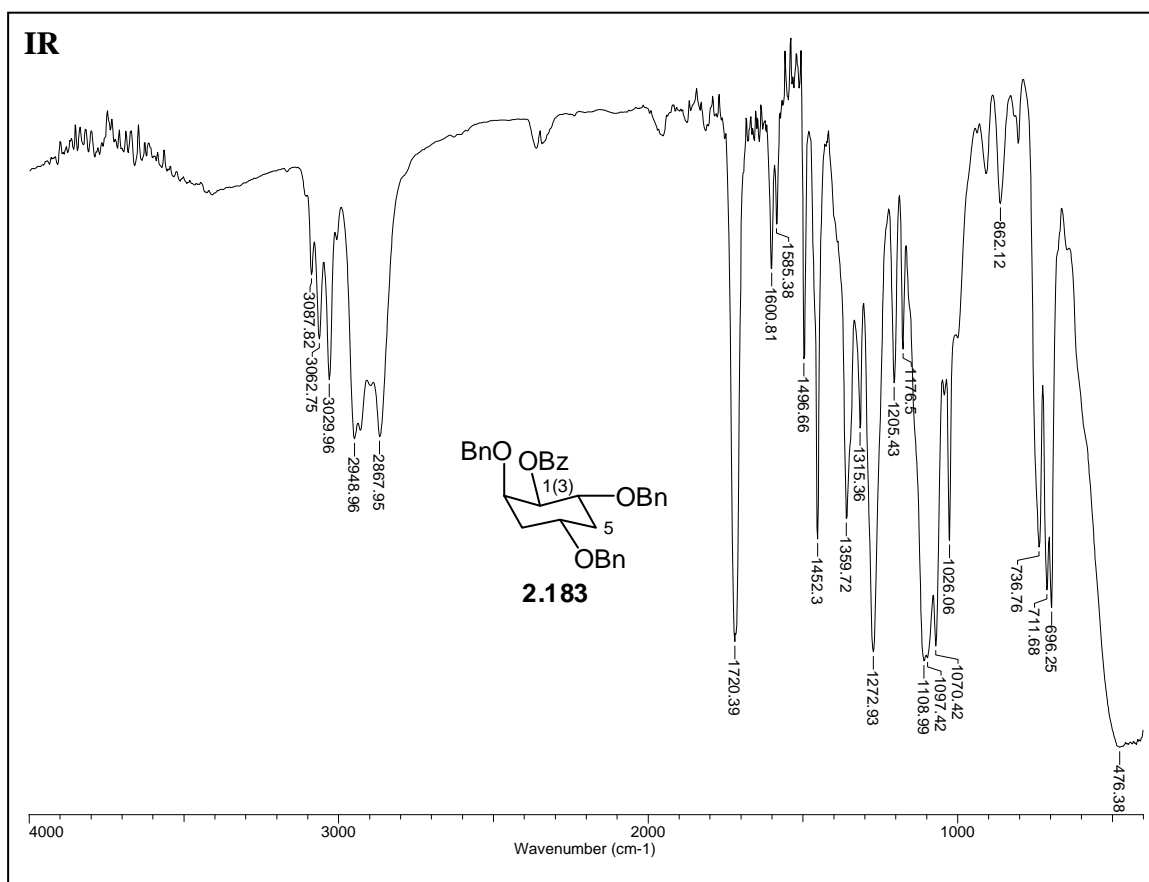


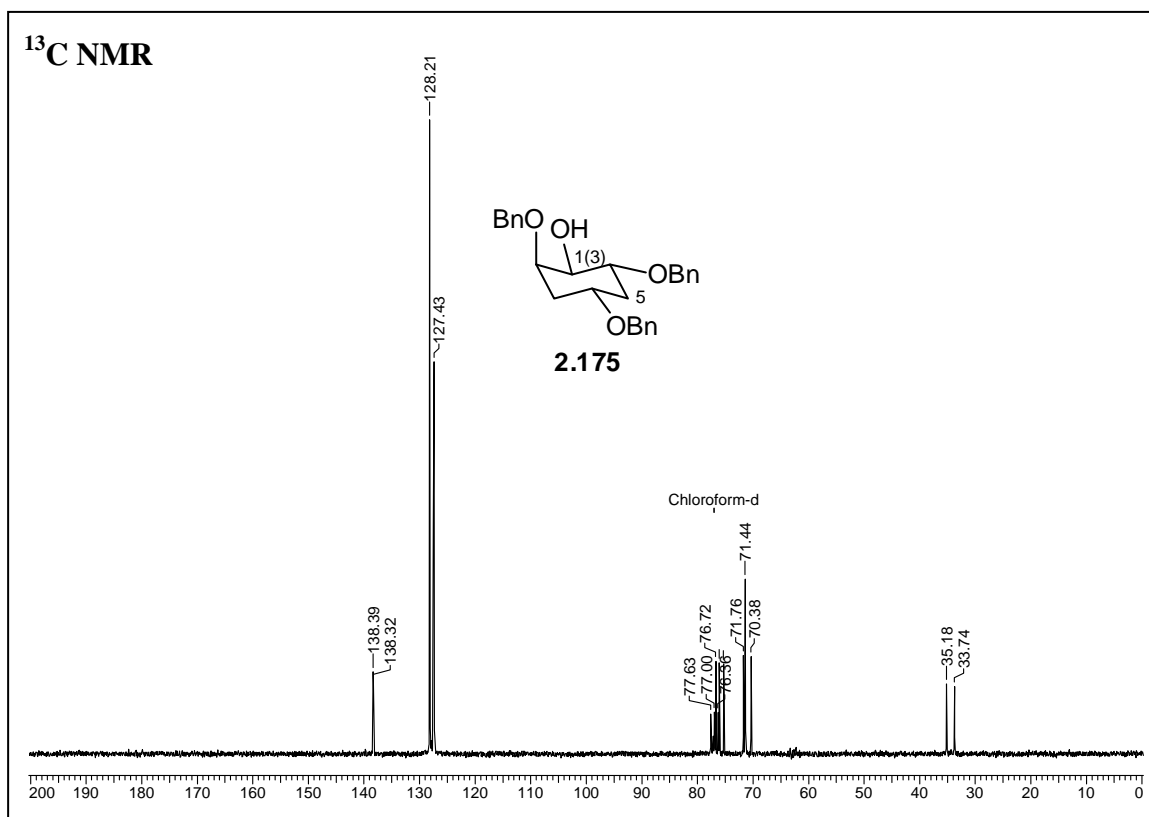
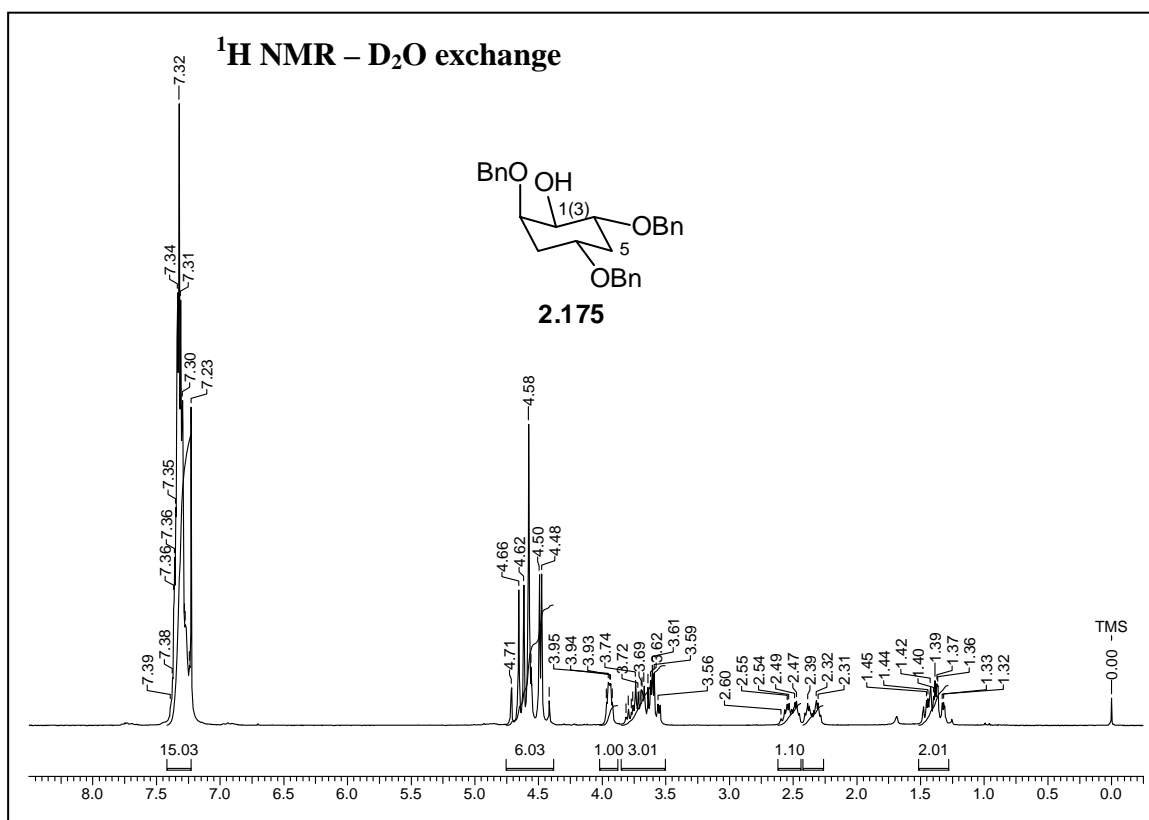
Chapter 2

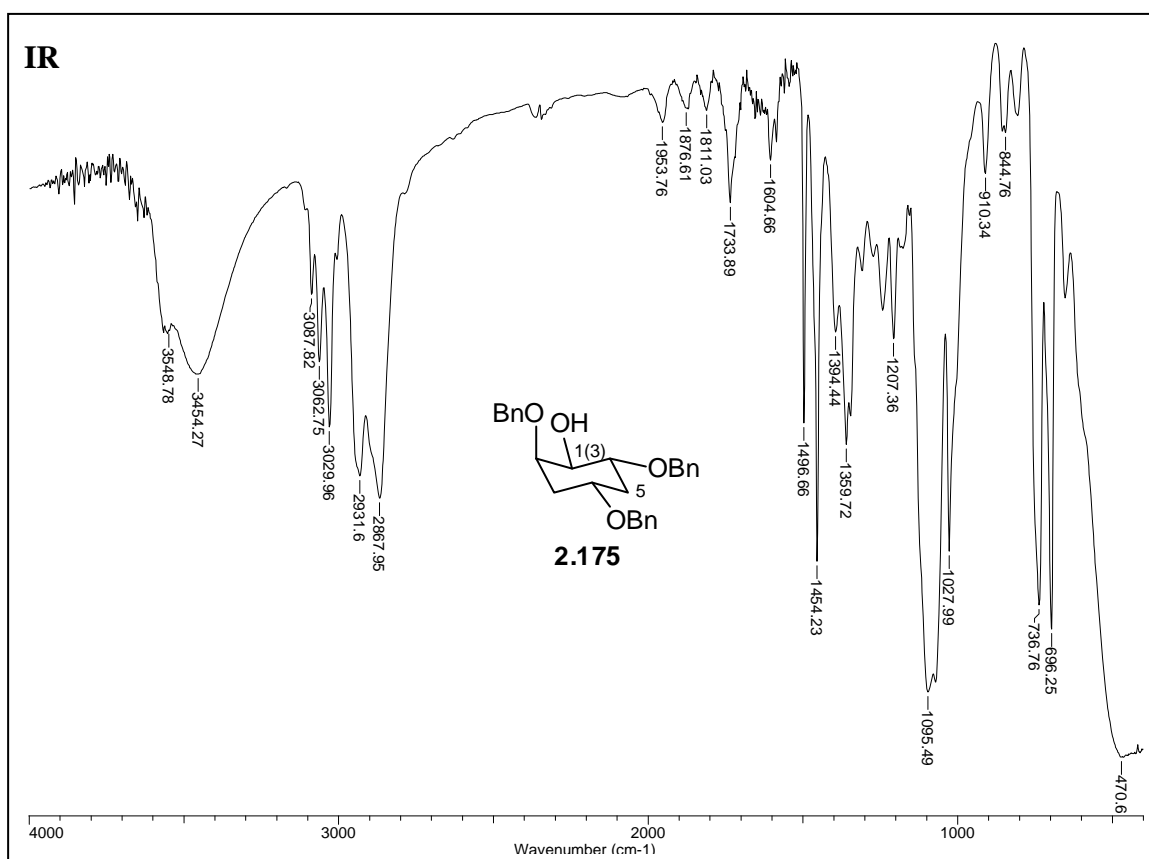
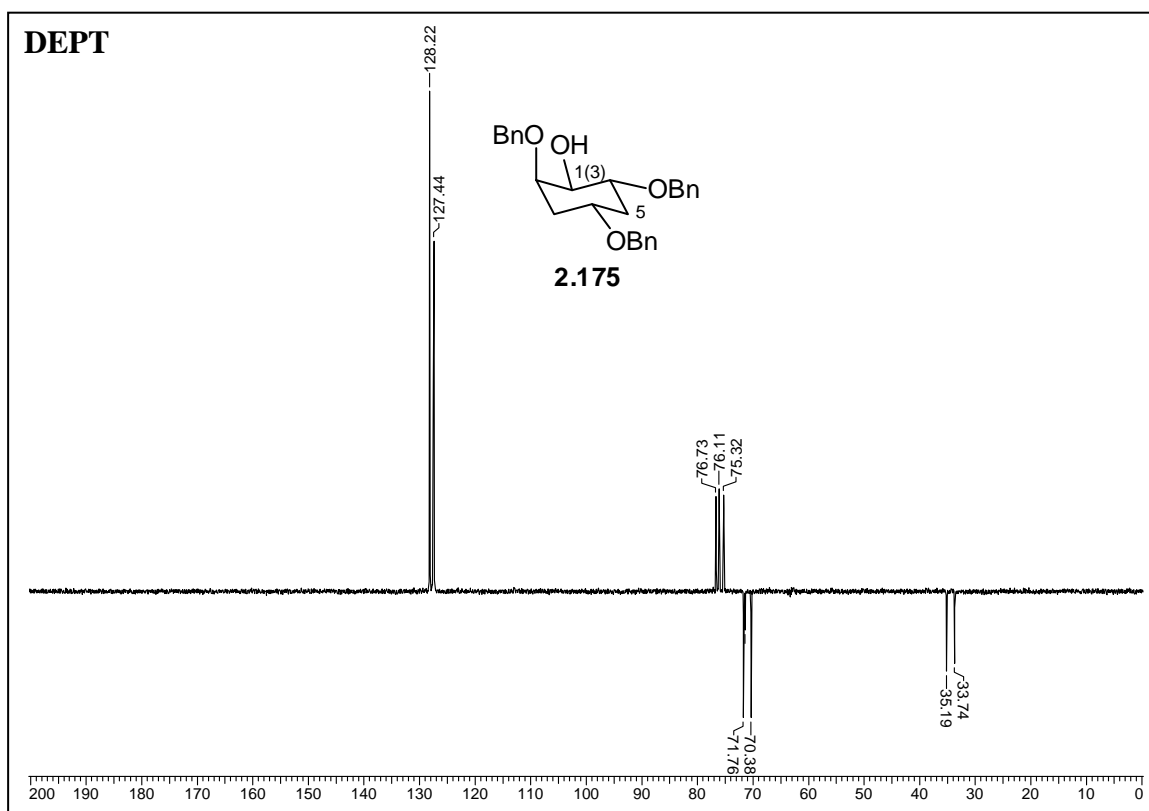




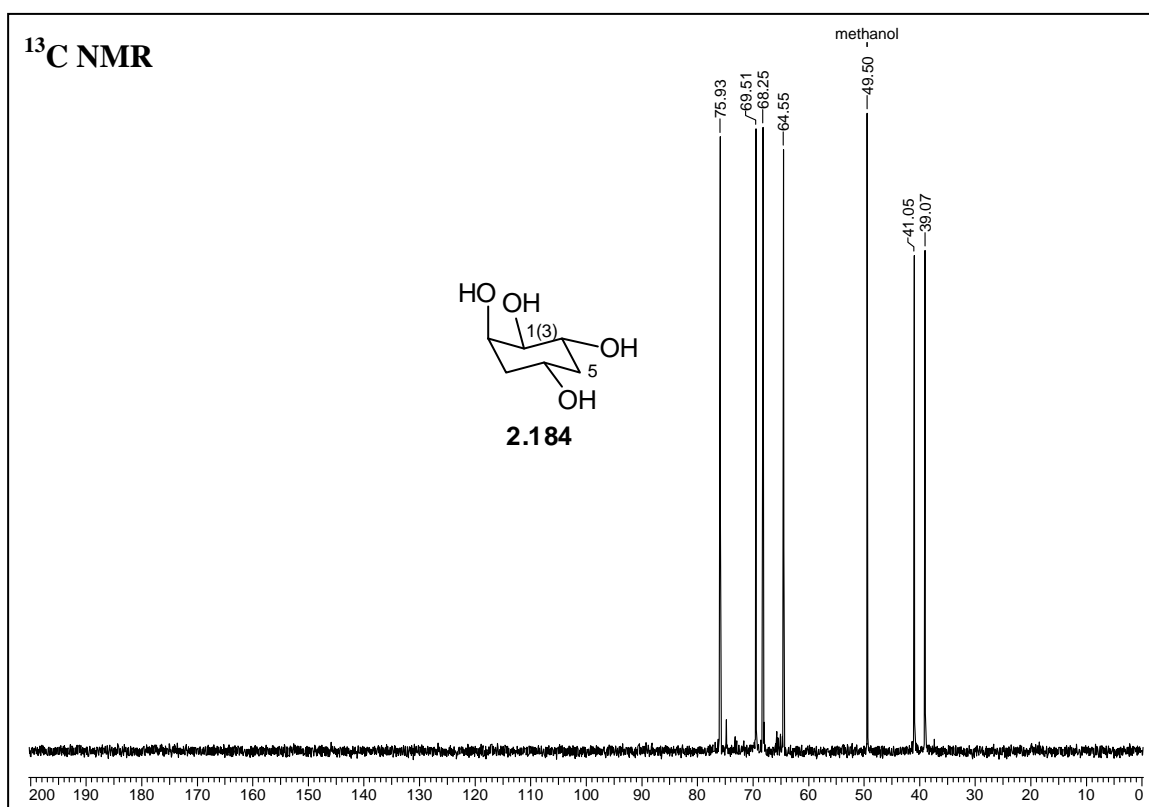
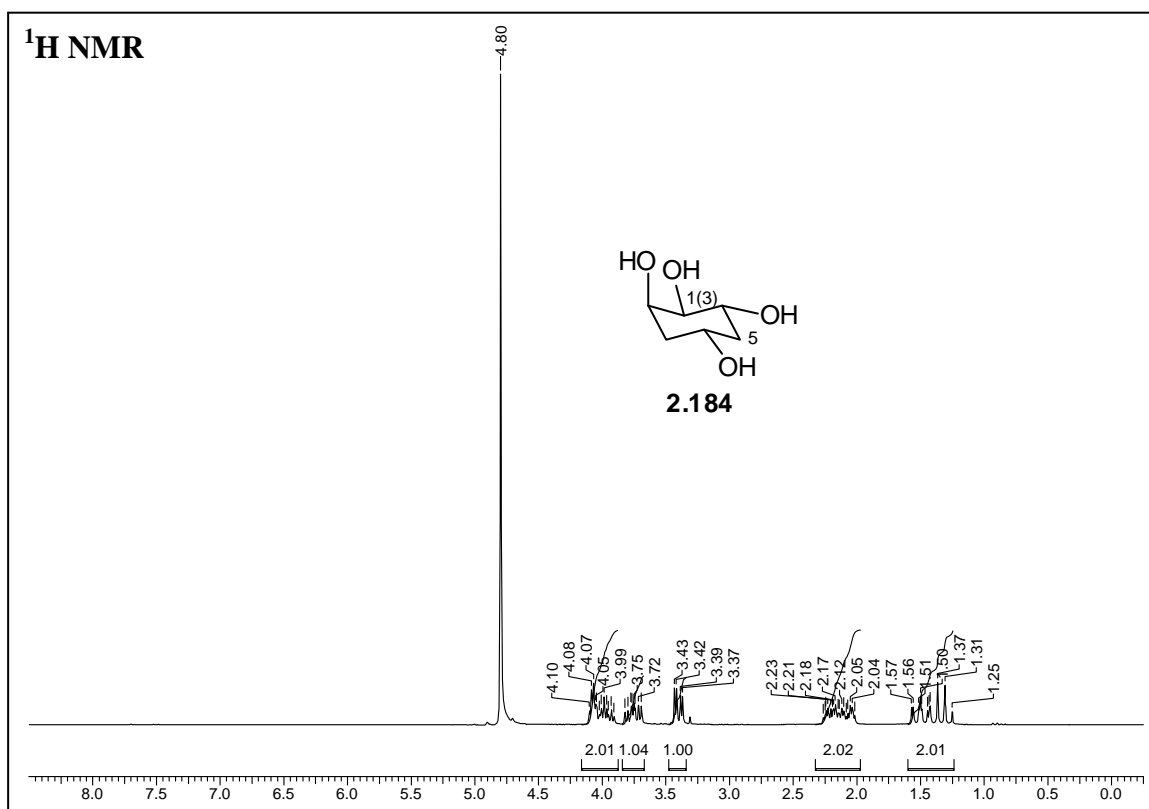
Chapter 2

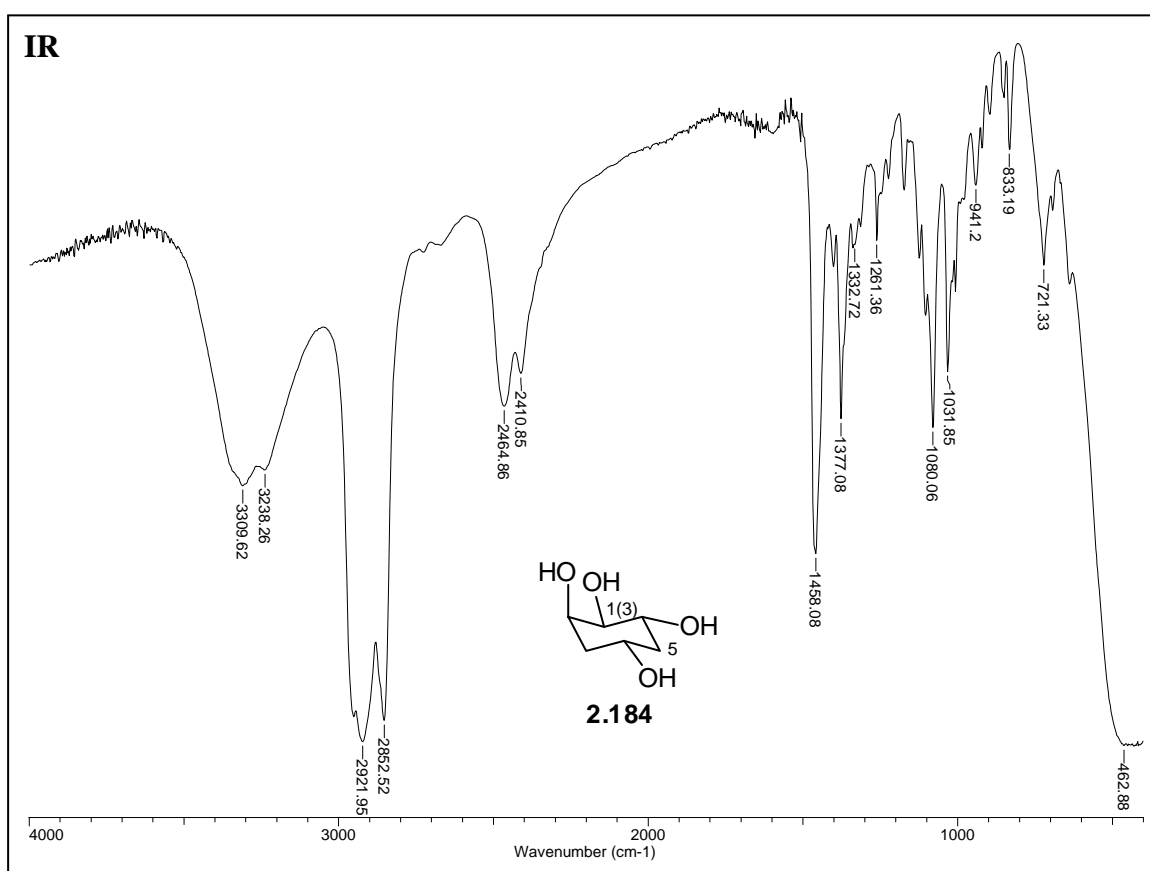
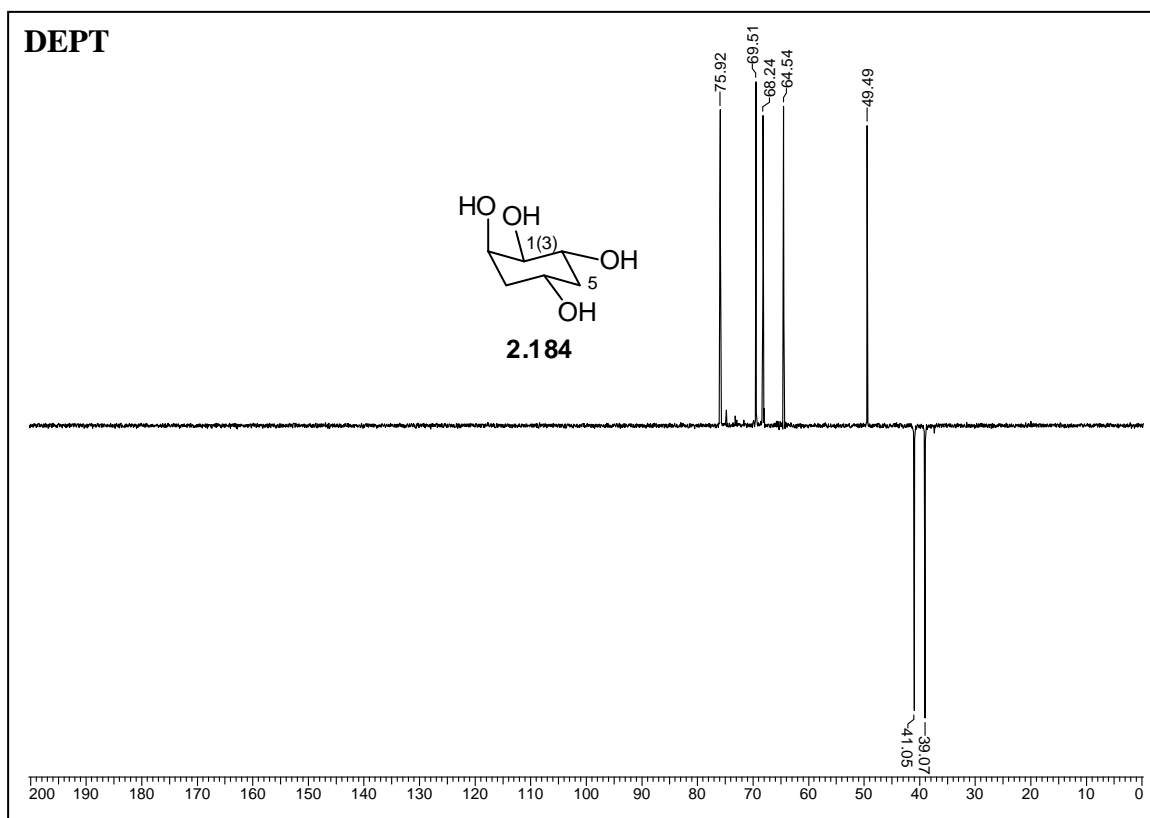


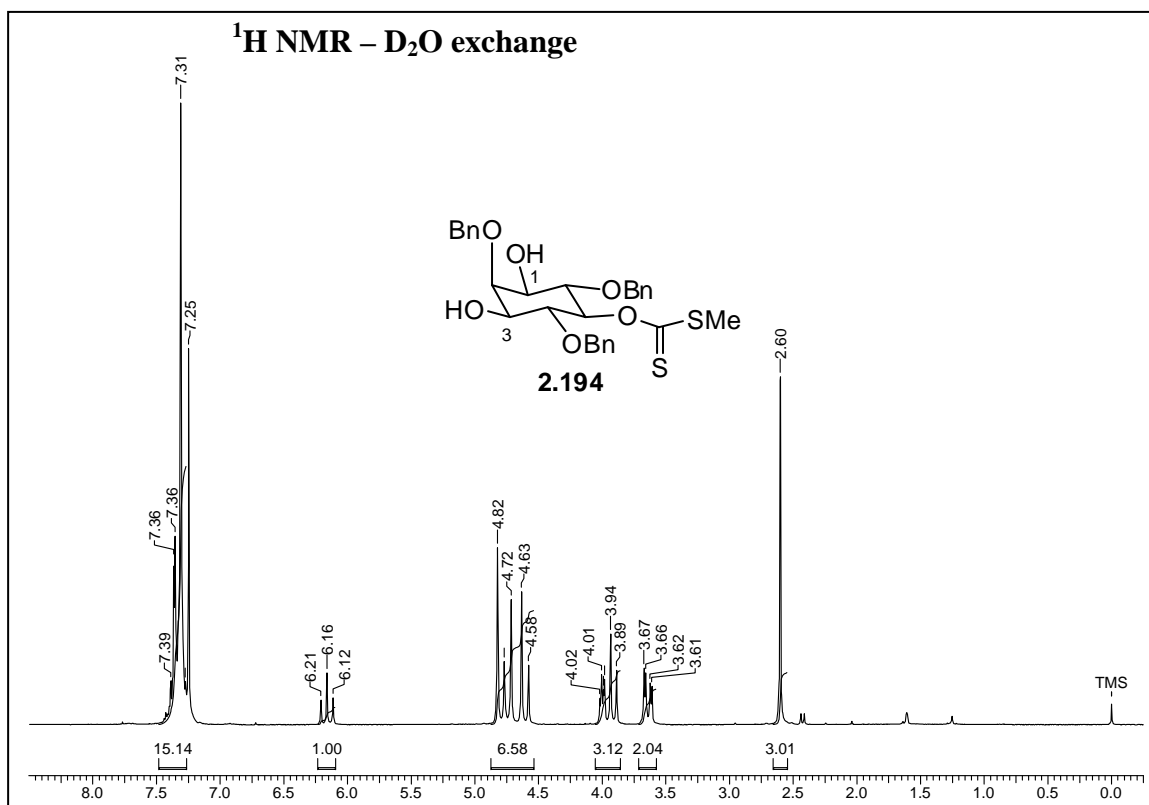
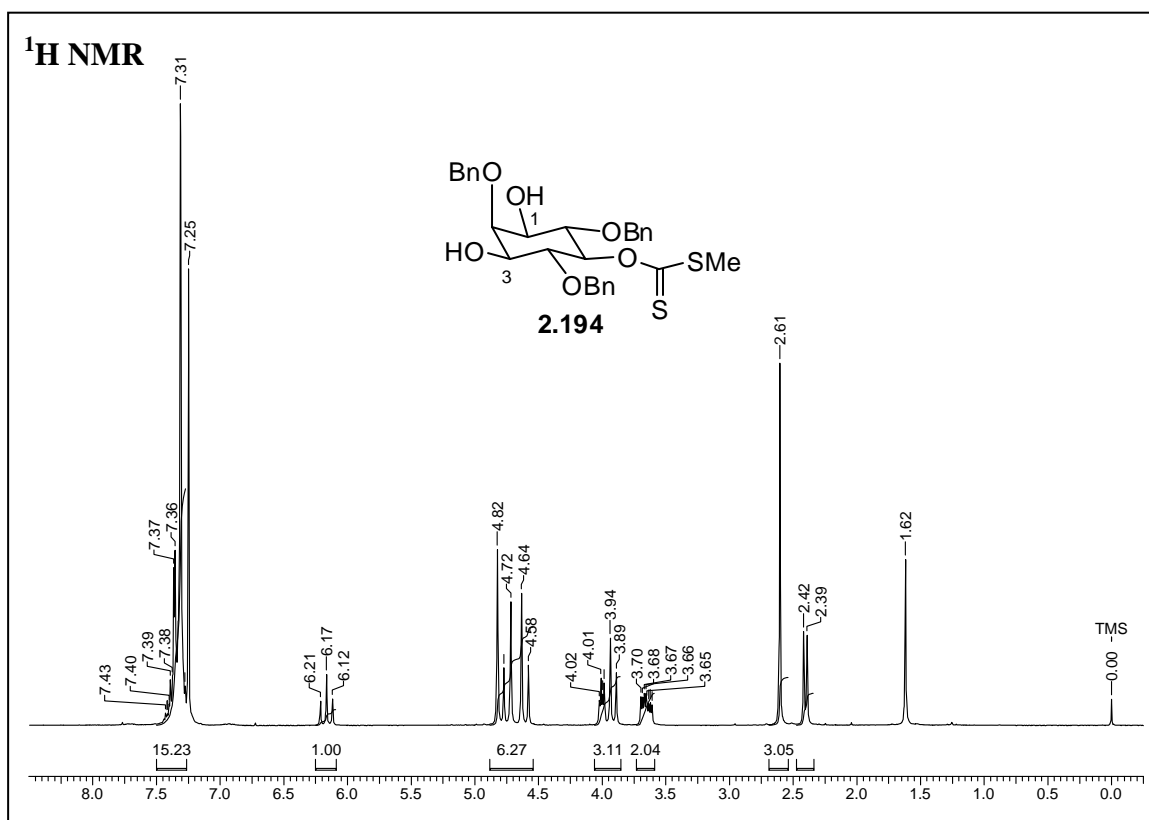


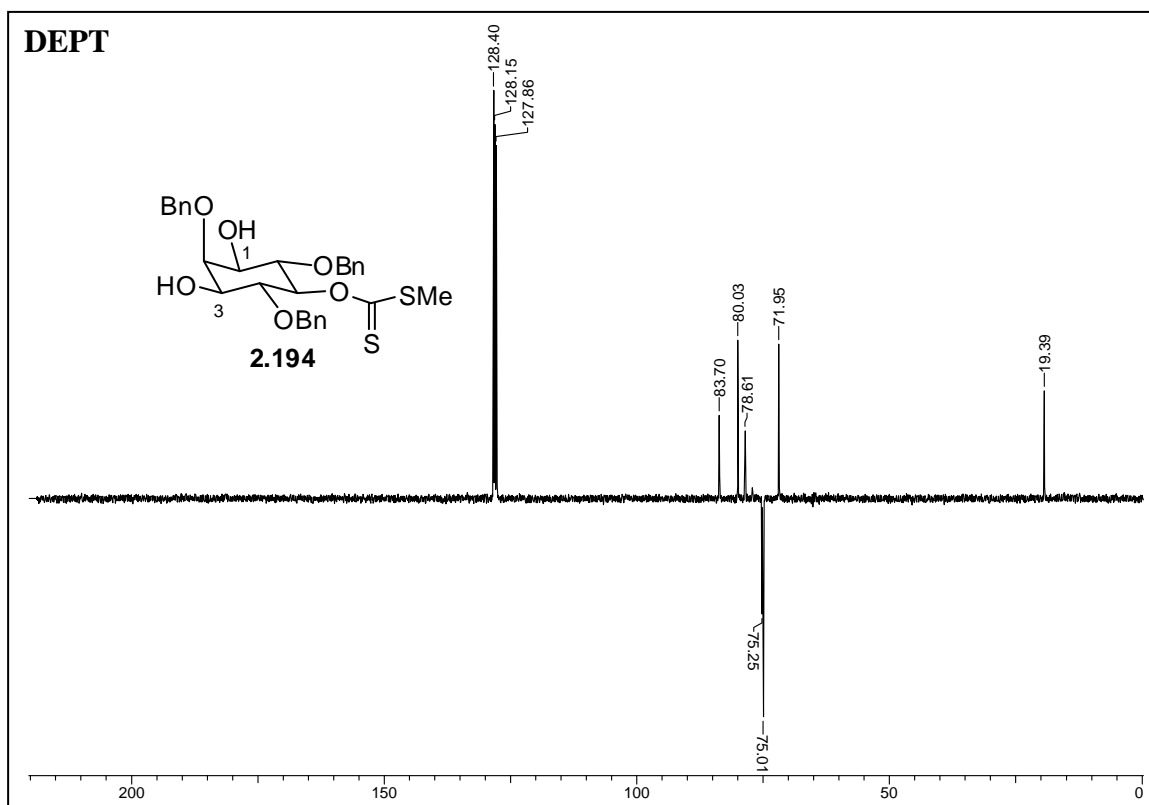
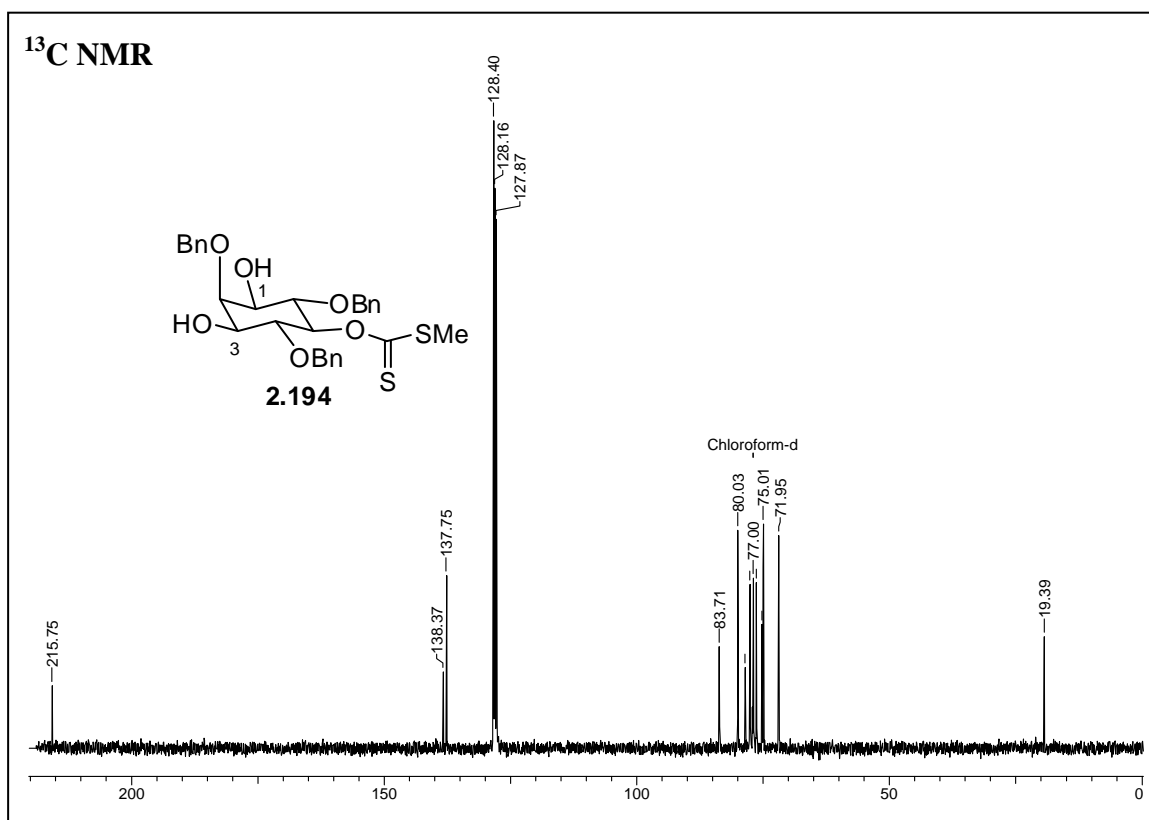


Chapter 2

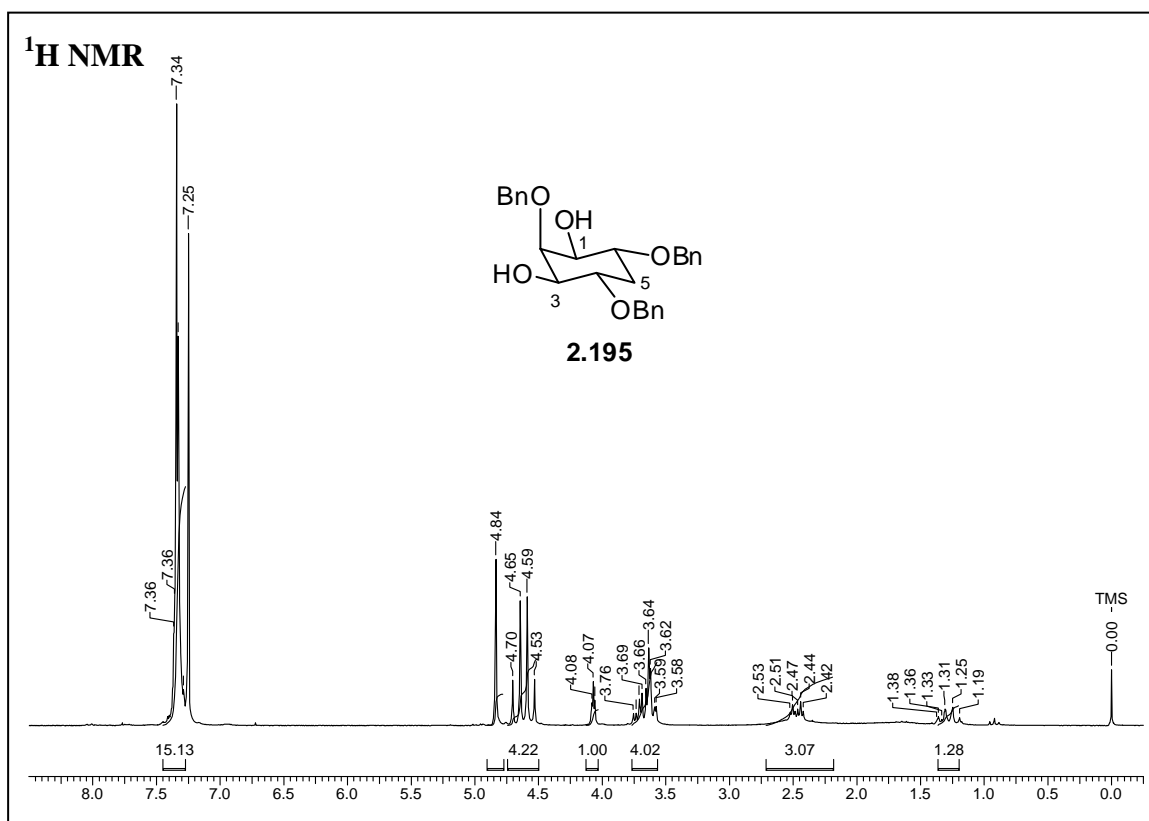
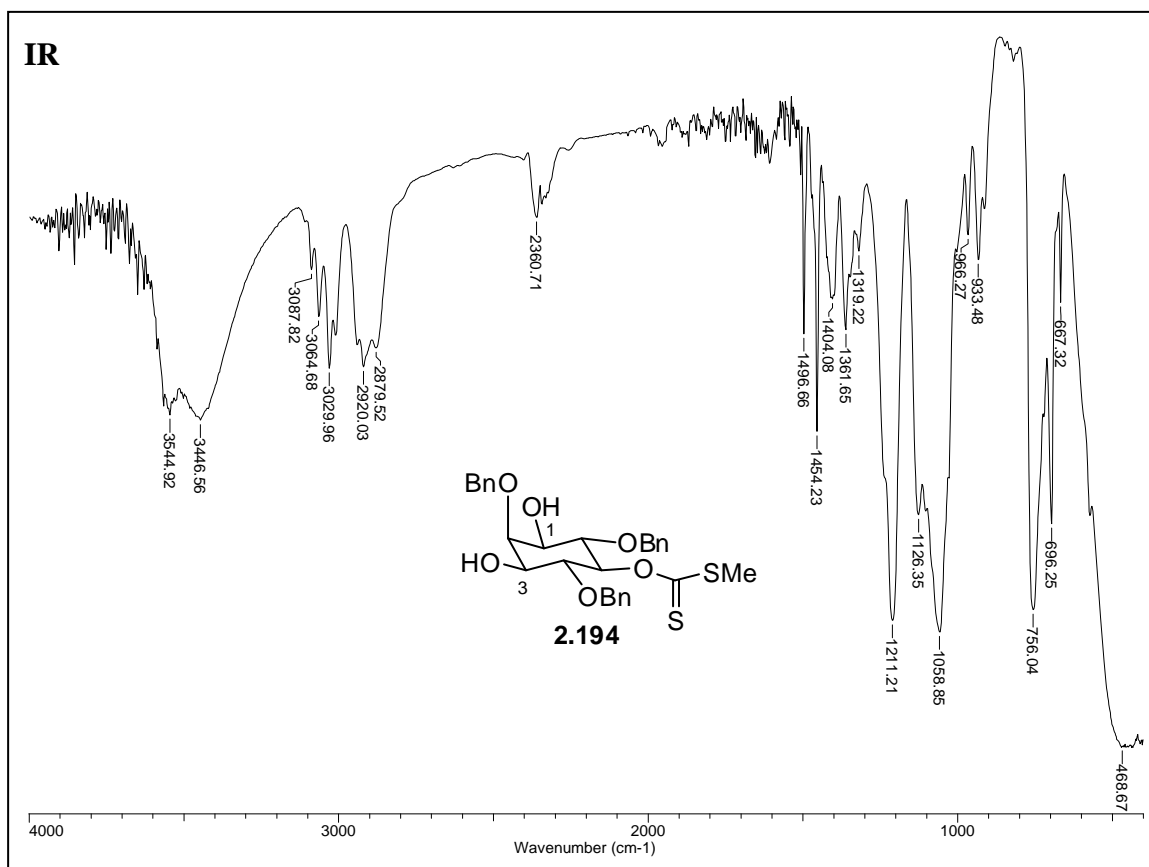


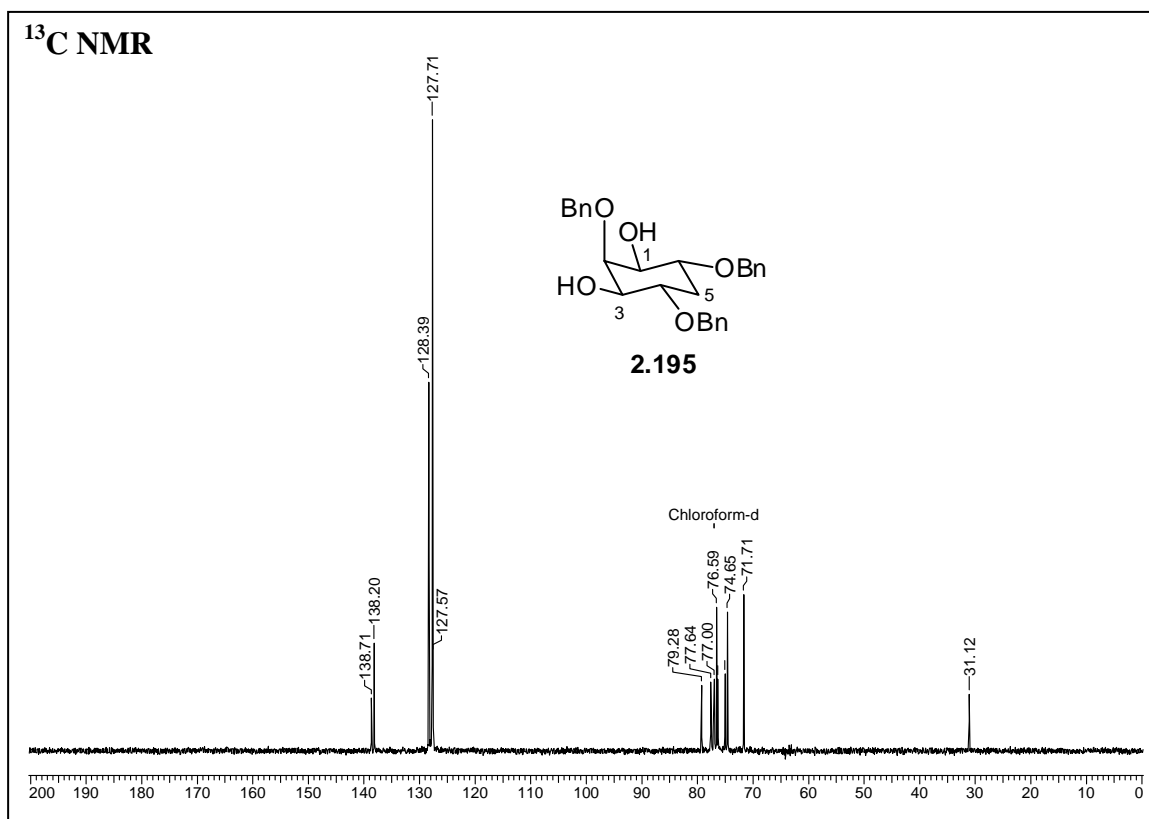
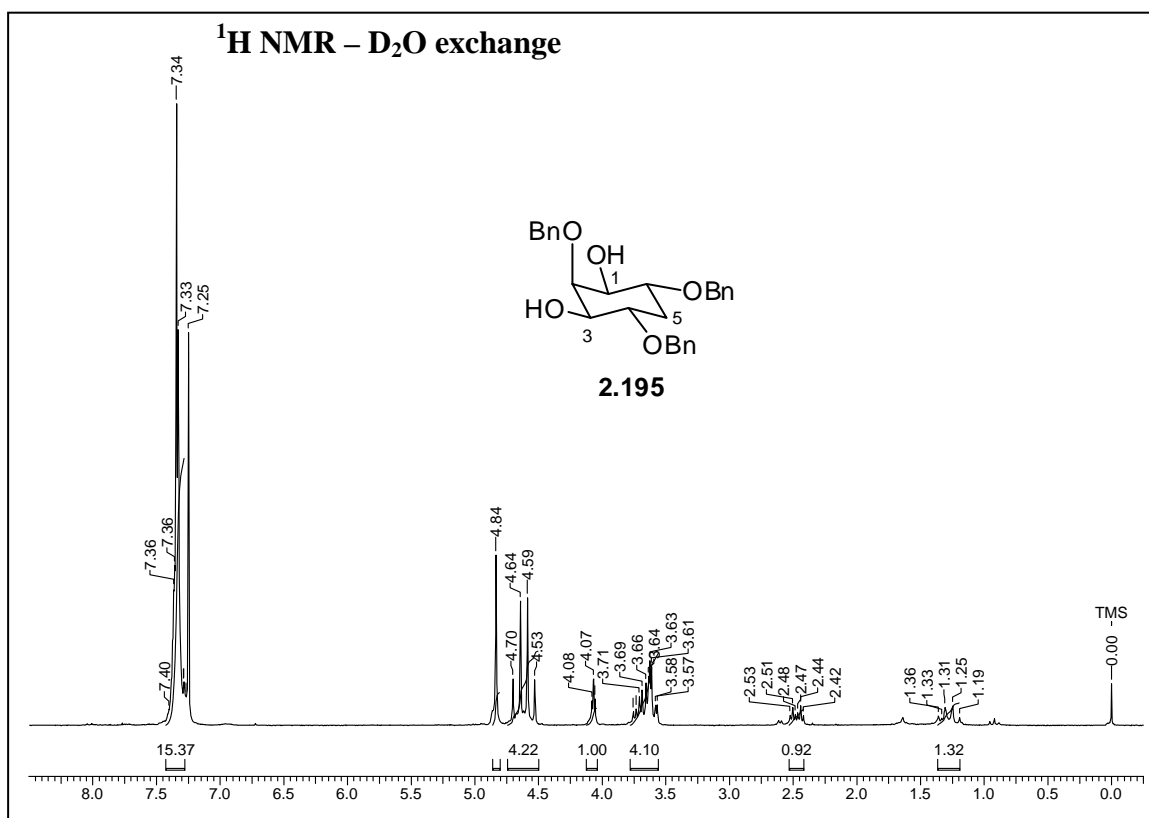


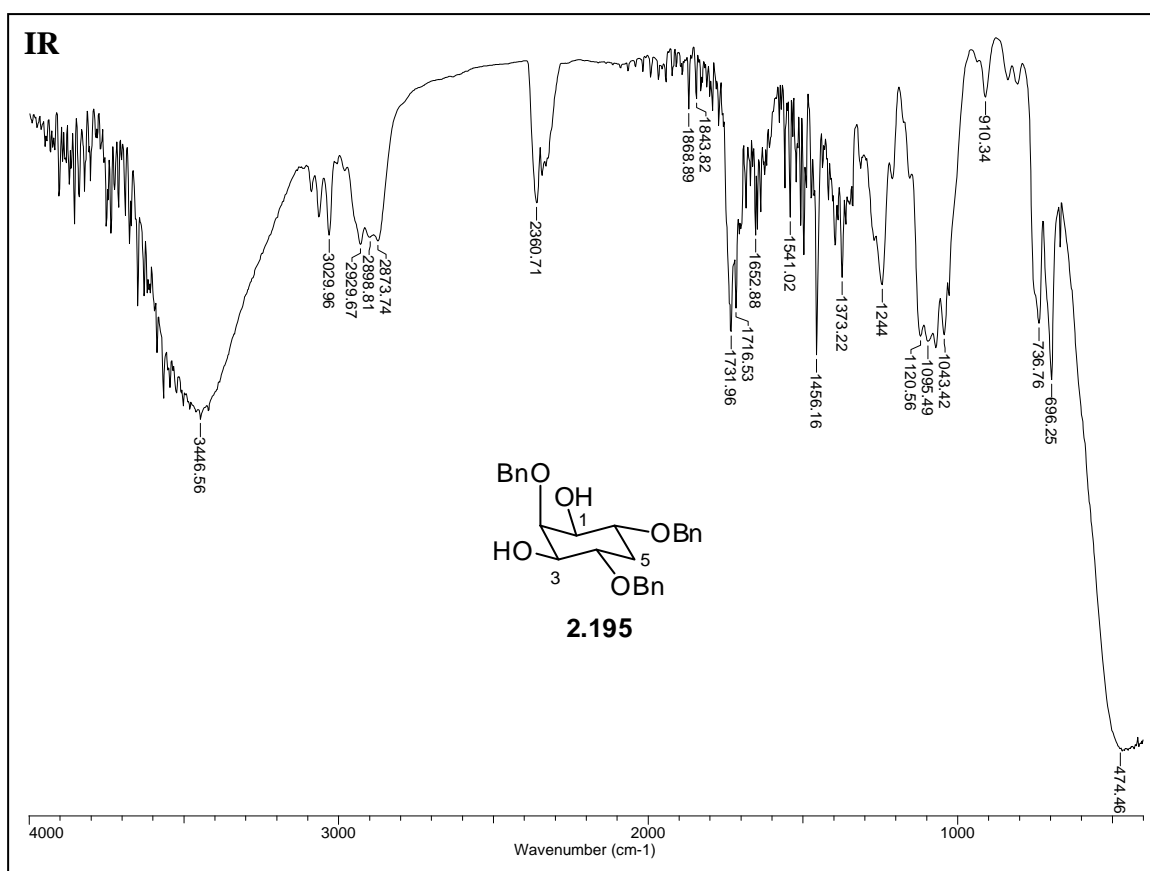
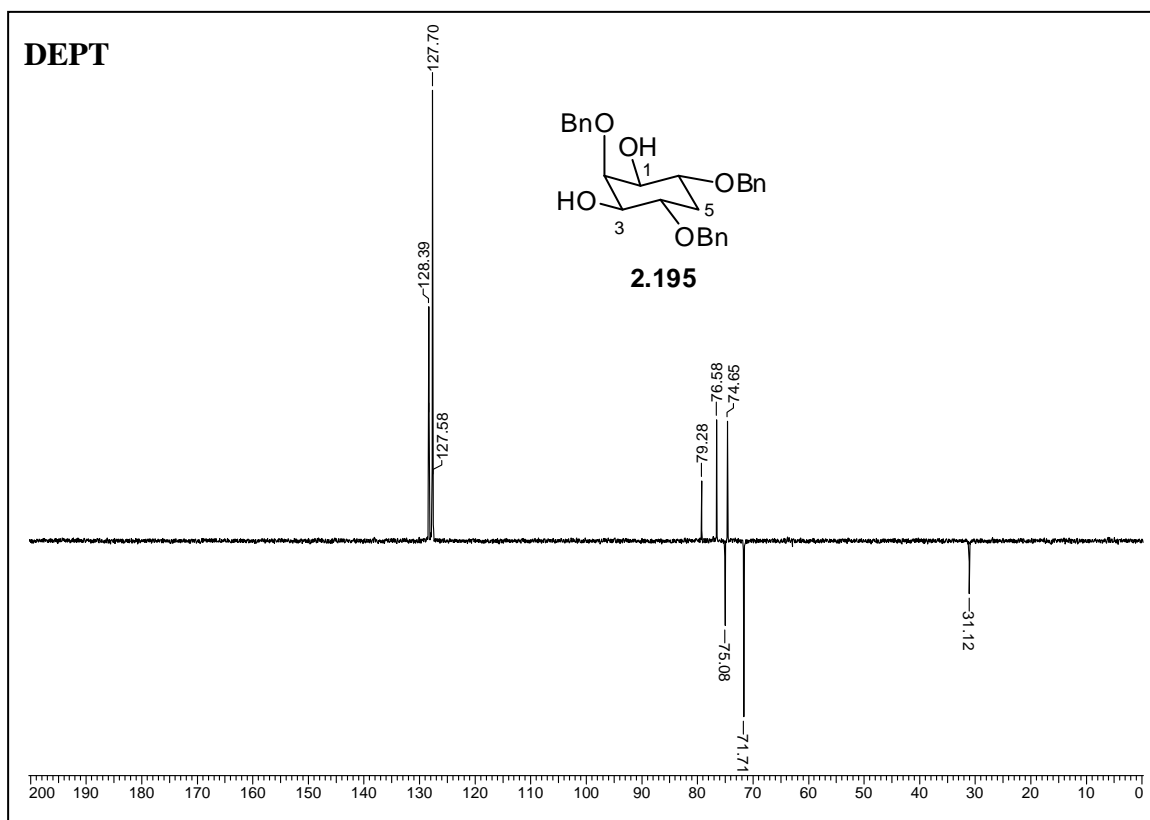




Chapter 2

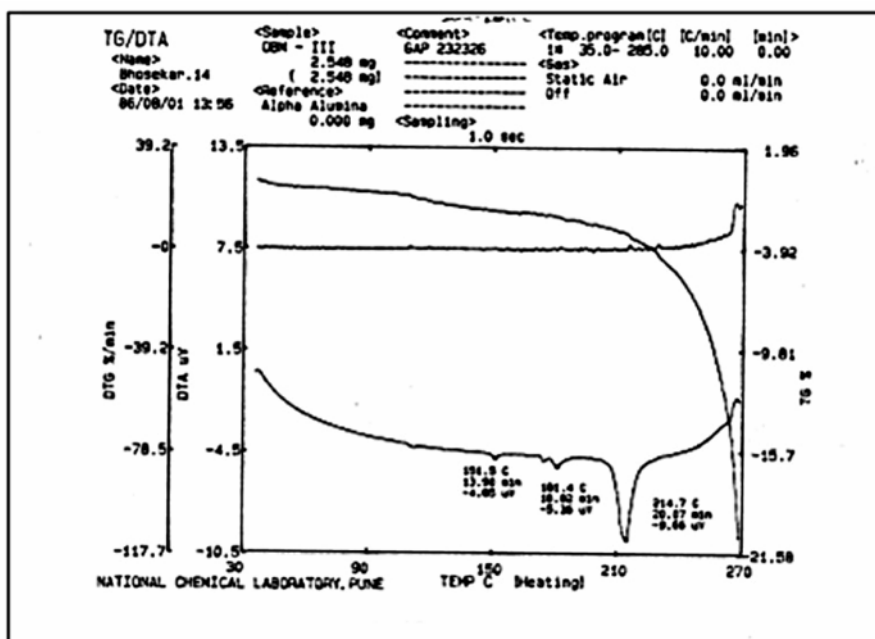




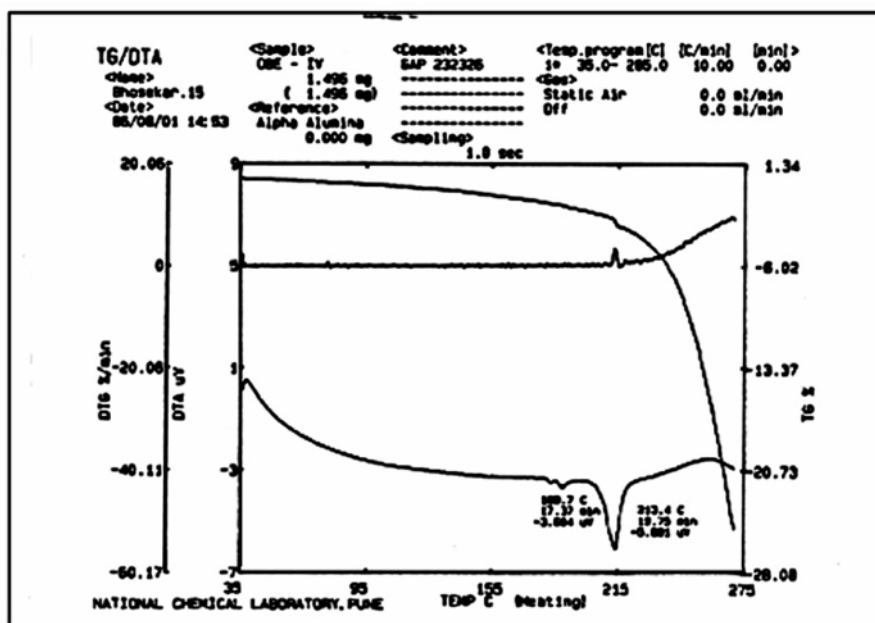


Crystal data table of **Form-I** and **Form-II** of **1.17**

	Form I of 1.17	Form II of 1.17
chemical formula	C ₁₃ H ₁₄ O ₆	C ₁₃ H ₁₄ O ₆
<i>M_r</i>	266.24	266.24
temperature/K	293(2)	293(2)
morphology	Long plate	needle
crystal Size	0.51 × 0.28 × 0.21	0.92 × 0.23 × 0.11
crystal system	Monoclinic	monoclinic
space group	<i>P</i> 2 ₁ / <i>n</i>	<i>P</i> 2 ₁ / <i>c</i>
<i>a</i> (Å)	6.2323 (9)	17.080 (4)
<i>b</i> (Å)	33.014 (5)	6.3196 (14)
<i>c</i> (Å)	6.4077 (9)	11.361 (3)
α (°)	90	90
β (°)	115.897 (2)	108.087 (4)
γ (°)	90	90
volume (Å ³)	1186.0 (3)	1165.7 (4)
<i>Z</i>	4	4
<i>D</i> _{calc} (g cm ⁻³)	1.491	1.517
μ (mm ⁻¹)	0.12	0.12
θ _{max} (°)	25.5	25.0
<i>h</i> , <i>k</i> , <i>l</i> (min, max)	(-7,7), (-38,39), (-6,7)	(-20,18), (-7,7), (-13,11)
reflns collected	8778	5607
unique reflns	2203	2055
observed reflns	2078	1776
no. of parameters	228	228
GOF	1.15	1.05
R1 (all)	0.046	0.040
R1 (all)	0.044	0.034
wR ₂ (all)	0.105	0.096



TGA / DTA of Form I crystals of the orthobenzoate 1.17



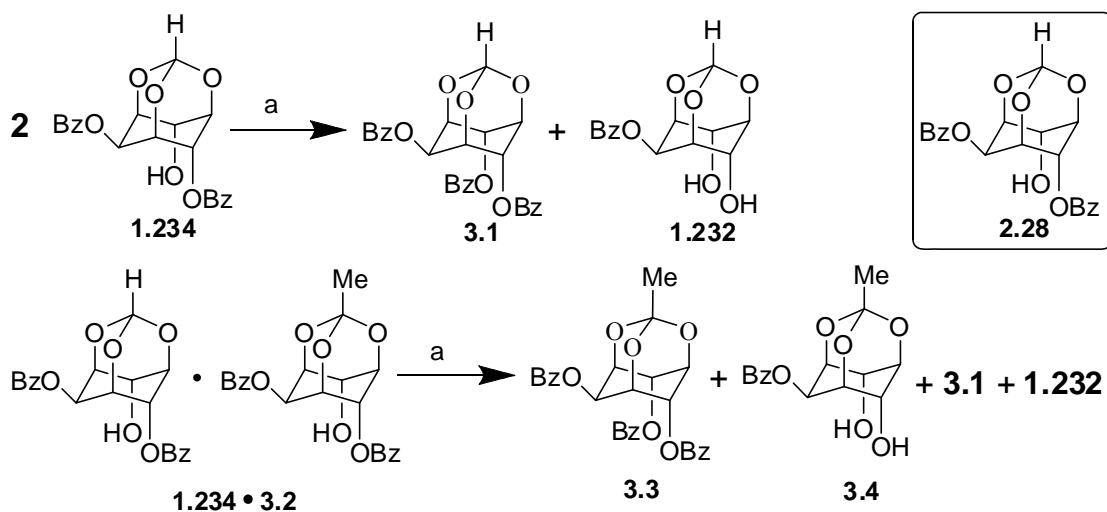
TGA / DTA of Form II crystals of the orthobenzoate 1.17

Chapter 3

Transesterification reaction of *myo*-inositol-1,3,5-orthoester derivatives in the solid state: effect of molecular packing in crystals on acyl transfer reactivity.

3.1. Introduction.

Migration of acyl groups among the hydroxyl groups in polyhydroxy organic compounds, especially carbohydrates and their derivatives have interested organic chemists for several decades.¹ Transesterification reactions among the hydroxyl groups of partially acylated inositol derivatives in solution occur frequently² and this has been exploited for the preparation of several biologically relevant phosphorylated inositol derivatives.³ Most of these acyl migration reactions however result in the formation of a mixture of isomeric hydroxy esters and consequently result in poor isolated yield of the required *O*-protected inositol derivative. Also, isolation of each individual isomer resulting from indiscriminate acyl migration reactions requires efficient and laborious methods of separation. First examples of facile acyl transfer reactions of inositol derivatives (**1.234** and its co-crystal with **3.2**) in the crystalline state (Scheme 3.1) have earlier been reported from our laboratory.⁴



Scheme 3.1: (a) Na₂CO₃, heat.

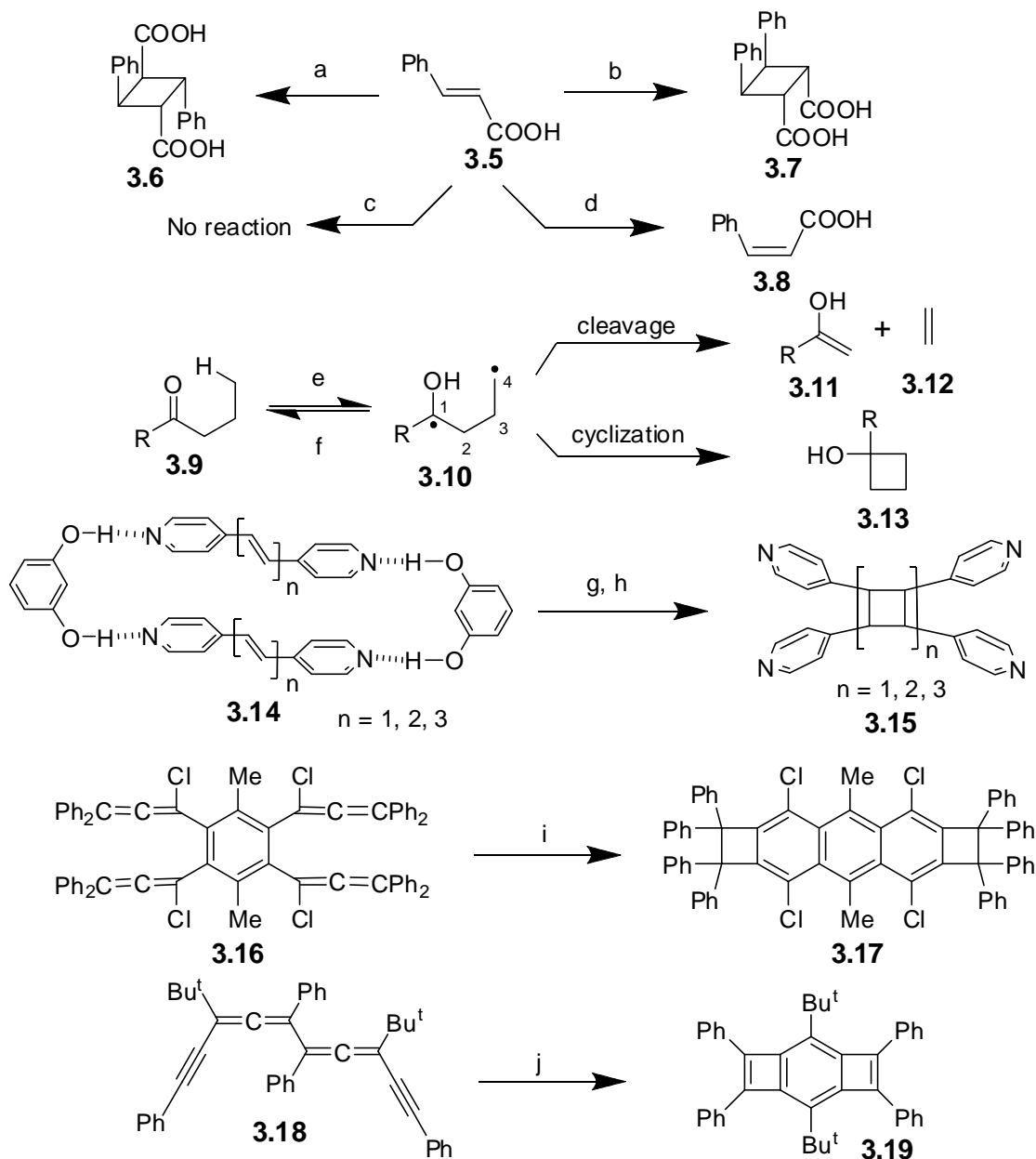
During the course of the work presented in the previous chapter, we realized that crystals of the dibenzoyl orthobenzoate **2.28** had structure similar to that of the analogous orthoformate **1.234** (as well as to the co-crystals of **1.234** • **3.2**. (see pages 222, 232 / Figure 3.2A and 3.7B). Hence we wondered whether this could lead to an efficient

transesterification reaction in crystals of di-benzoyl orthobenzoate **2.28** as we had observed in crystals and co-crystals of **1.234**. As expected, the crystals of **2.28** did exhibit facile acyl transfer reactivity in their crystals. Investigation of this acyl transfer reaction in the crystalline state and comparison of similar reactions of a few analogous *myo*-inositol orthoester derivatives (in the crystalline state as well as in solution) forms the subject of this chapter. The results obtained indicate that the transesterification reaction of *myo*-inositol orthoester derivatives **2.28**, the mono-benzoate **3.48** (Scheme 3.5) and the orthoformate **1.232** are facilitated in the crystalline state as compared to the same reaction in solution. The crystal structure - reactivity correlations presented here support our earlier proposition^{4b} that helical molecular pre-organization with favorable weak intermolecular interactions in the crystal lattice aid these transesterification reactions. Before proceeding to present the details of this work, a brief introduction to reaction of organic compounds in the solid state is given below.

There is an upsurge in interest in the study of solvent free organic reactions,⁵ including the use of ionic liquids⁶ and reactions in aqueous media⁷ due to environment related reasons. Among these methods, reactions in molecular solids are of interest from synthetic as well as mechanistic points of view.^{5, 8} Often reactions in crystals proceed with high facility, regio- and stereo-selectivity due to topochemical control in molecular crystals, as compared to their solution state reactions.^{4a, 8} Since determination of conformation, relative orientation and non-covalent interactions of reacting molecules with their neighbors in crystals is possible by X-ray diffraction analysis, the crystal structure analysis of reactants could provide information on the mechanism and course of organic reactions in the solid state. The reaction mechanisms can also be established by analyzing molecular dynamics in the solid state reactions since the dynamic behavior can be studied by spectral data and X-ray analysis.⁹

Only a few types of reactions occurring in crystals such as addition reactions to carbon-carbon multiple bonds,¹⁰ photolytic carbon-carbon bond cleavage in carbonyl

compounds,¹¹ certain radical forming reactions¹² have been studied in detail and these have provided great insight into the mechanisms of these reactions. Illustrative examples of organic reactions in the solid state are given in Scheme 3.2.¹³

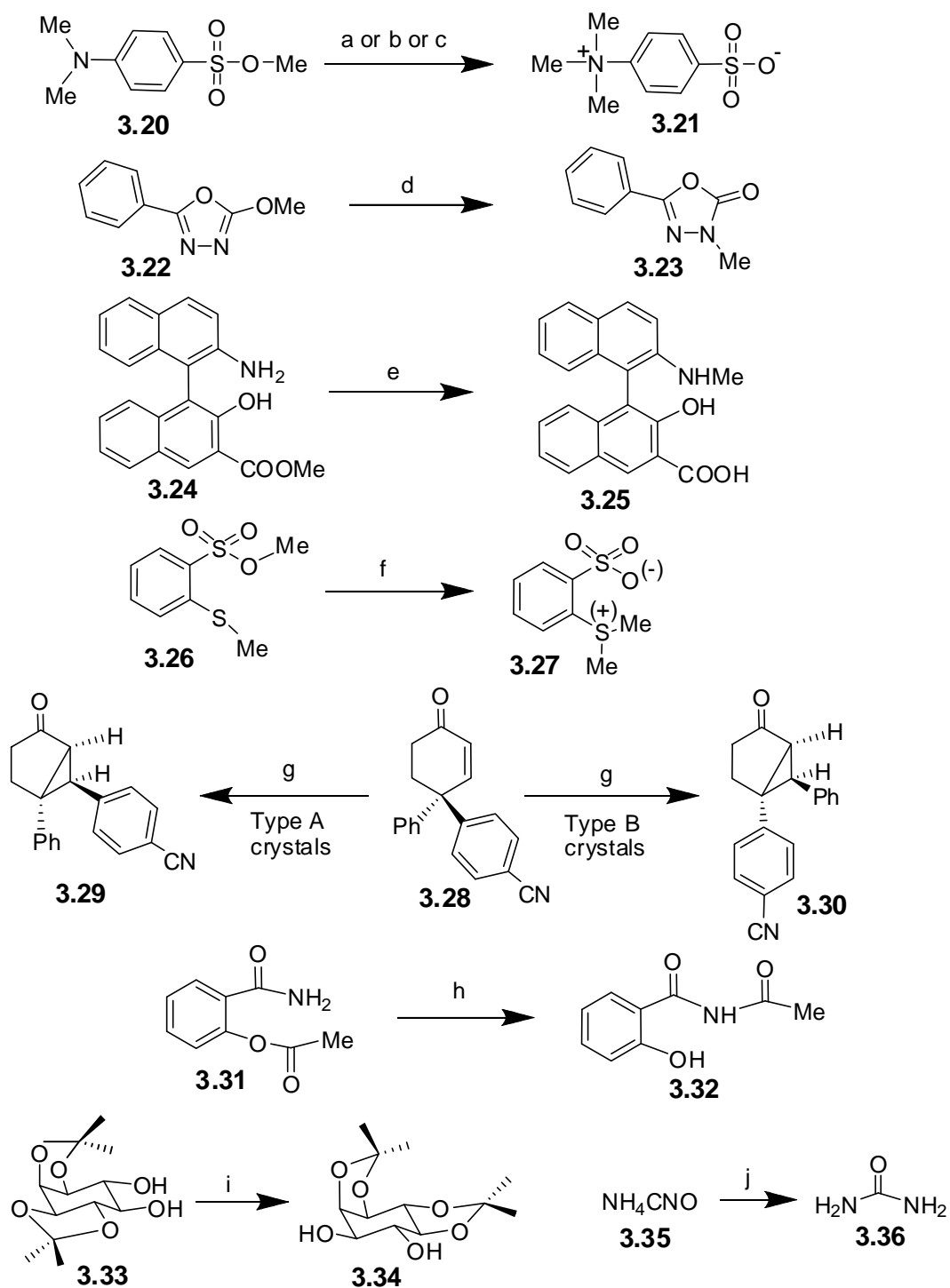


Scheme 3.2: (a) $h\nu$, α - crystals; (b) $h\nu$, β - crystals; (c) $h\nu$, γ - crystals; (d) $h\nu$, solution; (e) $h\nu$; (f) RHT (Reverse Hydrogen Transfer); (g) $h\nu$, solid; (h) removal of template; (i) 180 °C, 1 h; (j) 140 °C

It is pertinent to mention that since the facility of covalent bond formation in the solid state is dependent on the relative orientation of the molecules involved in a

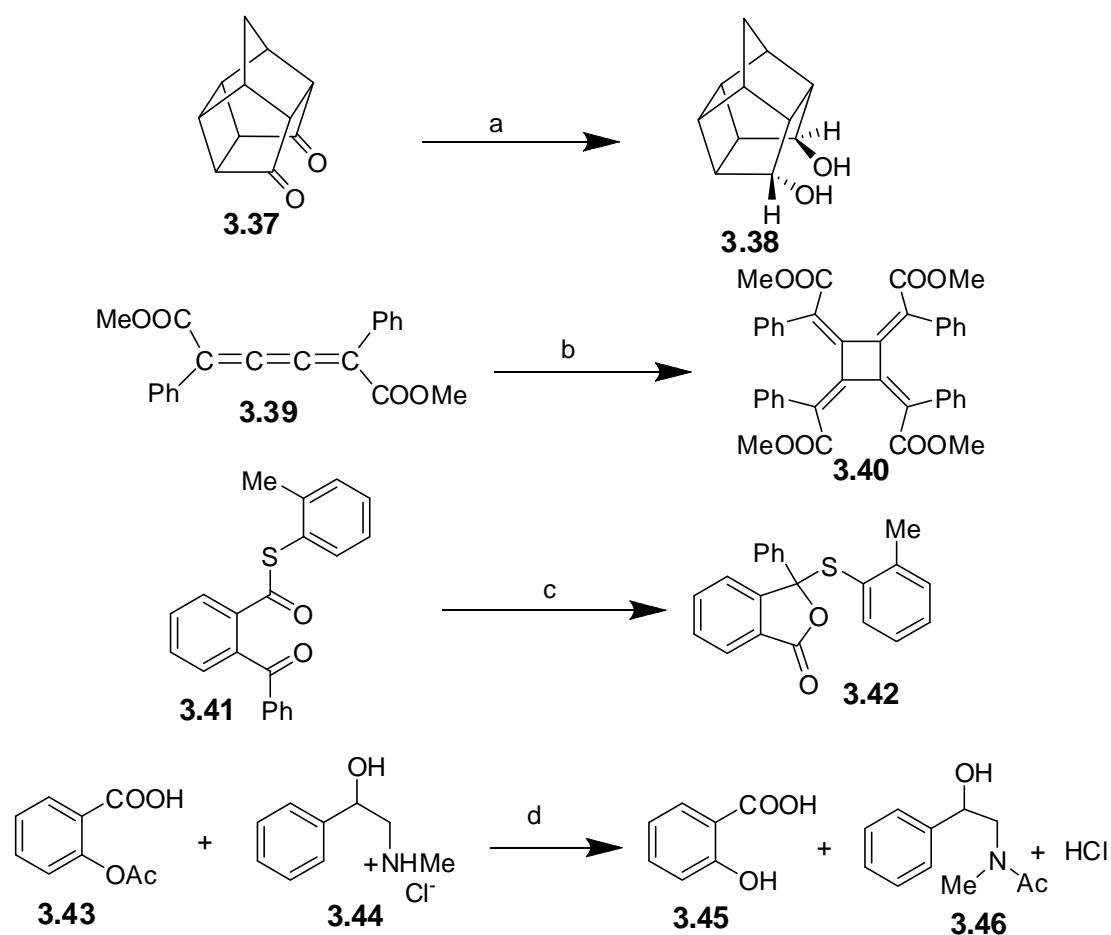
chemical reaction, the observed facility of the reaction could vary from one solid form (phase) to another solid form (phase) consisting of the same molecules. Also polymorphic modifications of crystal forms can have profoundly different reactivity (as illustrated by the solid state reactivity of cinnamic acid **3.5**). Hence tracking thermal changes in molecular solids becomes more or less mandatory during the study of chemical reactions in the solid state.

Other types of reactions occurring in the solid state that have been studied systematically are (Scheme 3.3) rearrangement of methyl *p*-dimethylaminobenzenesulfonate (**3.20**) to the zwitterionic product, *p*-trimethylammoniumbenzenesulfonate (**3.21**, Scheme 3.3);¹⁴ Chapman-like thermal rearrangements (1,3-O to *N* methyl transfer) in 5-methoxy-2-phenyl-1,3,4-oxadiazole (**3.22**) to give the corresponding *N*-methyl amide **3.23**,¹⁵ O → *N* – methyl group transfer reaction in binaphthol derivative **3.24**,¹⁶ non-topochemical methyl transfer reaction in **3.26**,¹⁷ photochemical rearrangement of the enone **3.28**¹⁸ involving transfer of a phenyl group; O → *N*– acyl migration in salicyl amide, **3.31**,¹⁹ transketalization reaction in an inositol derivative **3.33**,²⁰ and thermal transformation of ammonium cyanate to urea.²¹



Scheme 3.3: (a) Crystals, 81- 88 °C, 20-120 min, 49-90 %; (b) Crystals, rt, 17 d, 79 %; (c) Melt, 95 °C, 500 min, 53%; (d) 120-140 °C; (e) 150 °C, 15 min.; (f) 40 °C, 7 days; (g) hv, solid, -20 °C; (h) solid, 100 °C; (i) solid, 110 °C, 10 min, 92-95%; (j) crystals, heat.

Although, the topochemical criteria for double bond juxtaposition has been well recognized for the [2 + 2] dimerization and polymerization reactions in the crystalline state¹⁰ such detailed analysis for other types of reactions has not been carried out. However, there are reports on solid-state organic reactions⁵ which have potential for applications in synthesis, but most of these have not been investigated systematically.²² Illustrative examples of these reactions are given in Scheme 3.4. It is even possible that some of these reactions may be occurring in the molten state which could result due to mixing of several reactants and reagents.

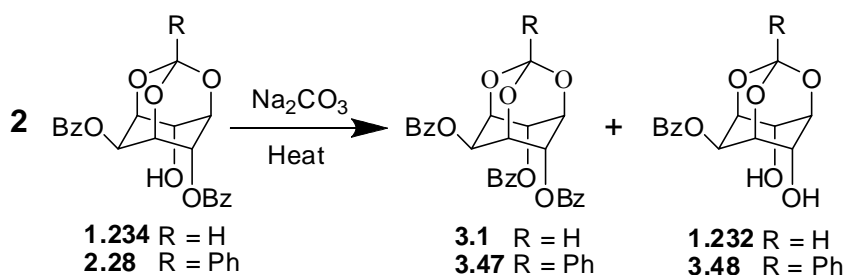


Scheme 3.4: (a) NaBH₄, 100%; (b) solid, 100 °C, 76%; (c) solid, hv, 30% ee, 65%; (d) 70 °C, 34 days.

3.2. Results and Discussion.

3.2.1. Benzoyl Transfer Reaction in crystals.

Crystals of racemic dibenzoyl-orthobenzoate (**2.28**), when heated with solid sodium carbonate underwent transesterification with facility to give the tri-benzoyl-orthobenzoate (**3.47**) and the 2- benzoyl-orthobenzoate (**3.48**) in almost quantitative yield (Scheme 3.5 and Table 3.1).



Scheme 3.5: (a) See Table 1 for reaction conditions.

Table 3.1: Summary of results of transesterification of the dibenzoates **2.28** and **1.234** under different conditions.

Entry	Reactant	Solvent / base / Temp (°C) / time (h)	Yield (%) ^a	
			3.47	3.48
1	2.28	None / Na ₂ CO ₃ / 140 / 62	3.47 (49)	3.48 (48)
2	2.28	None / Na ₂ CO ₃ / 120 / 62	3.47 (33)	3.48 (32)
3 ^b	1.234	None / Na ₂ CO ₃ / 140 / 60	3.1 (47)	1.232 (49)
4 ^b	1.234	None / Na ₂ CO ₃ / 120 / 60	3.1 (31)	1.232 (30)
5	2.28	DMF / DIPEA ^c / 130 / 72	3.47 (16)	3.48 (14)
6	2.28	DMF / DIPEA / rt ^d / 72	3.47 (0)	3.48 (0)
7	1.234	DMF / DIPEA / 130 / 60	3.1 (29)	1.232 (27)
8	1.234	DMF / DIPEA / rt ^d / 120	3.1 (10)	1.232 (8)
9	2.28	None ^e / Na ₂ CO ₃ / 195 / 12 ^f
10	2.28	None ^e / Na ₂ CO ₃ / 180 / 36 ^f

^a This reaction being a disproportionation reaction, the maximum yields possible for **3.47**, **3.48**, **3.1**, **1.232** is 50 % each. ^b From reference 4a; ^c Diisopropylethylamine; ^d Ambient

temperature; ^e Reaction in melt; ^f Mixture of several products was obtained; see experimental section for details.

At lower temperatures, the reaction proceeded smoothly but the conversion was slower, as expected. The DSC curve of di-benzoyl-orthobenzoate (**2.28**) consisted of only a single endotherm (melting, Figure 3.1) and did not show any phase changes in the temperature range over which the reactions in the crystalline state were carried out.

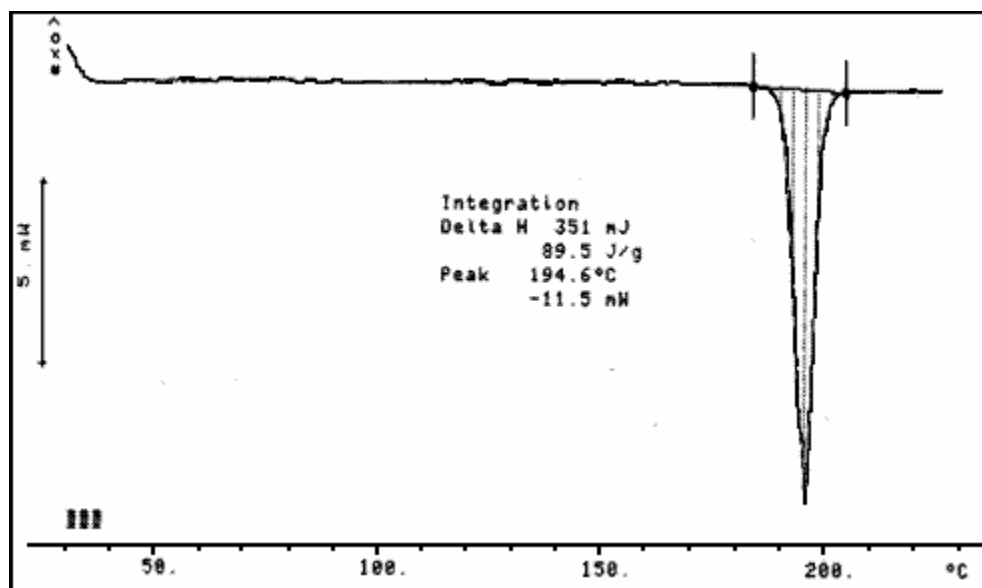


Figure 3.1. DSC profile of crystals of **2.28**.

Interestingly, base catalyzed transesterification reaction of the same dibenzoate **2.28** in solution (at comparable temperature) was less facile and did not react at all, at ambient temperature (25-30 °C). Reaction of dibenzoate **2.28** in the molten state afforded a mixture of several products and was not as clean as the reaction in crystalline and solution states. We also carried out the transesterification reaction of the dibenzoate **1.234** under comparable conditions (Scheme 3.5 and Table 3.1).

A comparison of the results of transesterification (Table 3.1) shows that although transesterification of the dibenzoates **2.28** and **1.234**^{4a} are equally facile in their crystals, they are not so in the solution state; reactivity of the orthobenzoate **2.28** in solution is less

than that of the orthoformate **1.234**. These results strongly suggest the significant role of molecular packing in crystals on the benzoyl transfer reactivity of the orthobenzoate **2.28** and the orthoformate **1.234**.

3.2.2. Correlation of Molecular Pre-Organization and intermolecular interactions with Acyl transfer reactivities.

Crystal structure analysis of the dibenzoates **2.28**, **1.234** and 1:1 molecular complex **1.234•3.2**^{4b} was carried out with the aim of correlating their solid-state reactivities with crystal structures. Earlier work⁴ in our laboratory, pertaining to the solid-state transesterification reaction of the orthoformate **1.234** and its co-crystals with dibenzoyl orthoacetate (**1.234•3.2**), had shown that the facility of intermolecular benzoyl group transfer in crystals was dependent on the relative orientation of the reactive C4(6)-hydroxyl group (nucleophile-Nu) and the C6(4)-acyl carbonyl group (electrophile-EI) in terms of distance (d) and the angle (α) between them (Figure 3.2).

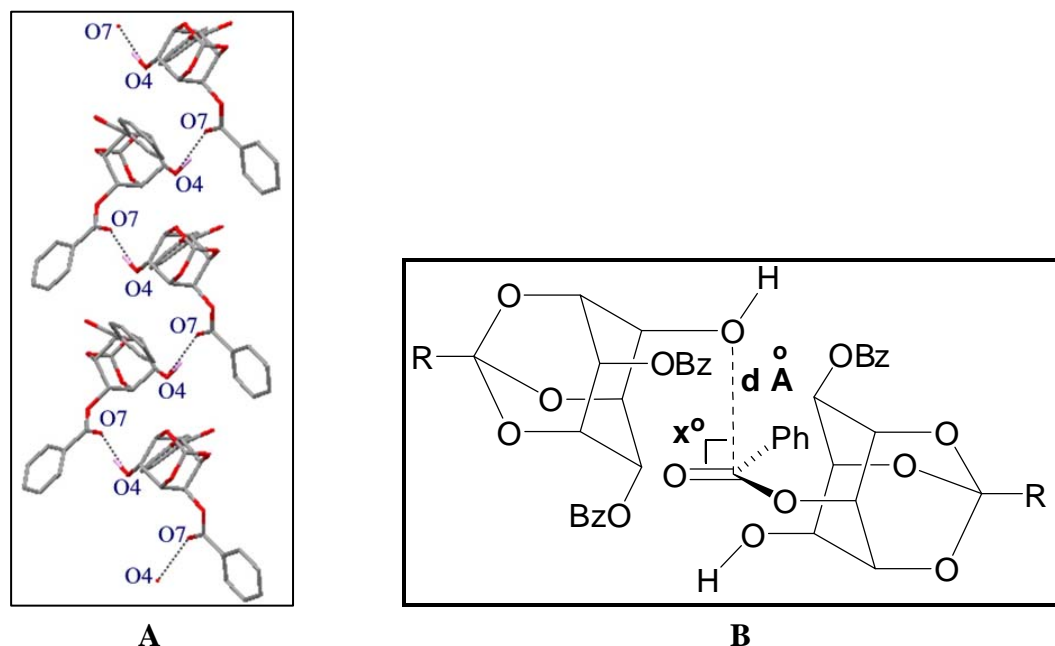


Figure 3.2: Geometrical parameters that determine the facility of intermolecular acyl group transfer in crystals: (A) helical molecular packing in crystals of **1.234** and (B) relative orientation of the reacting molecules.

The corresponding distance (d) and the angle (x) conducive for the intermolecular benzoyl transfer reaction being about 3.2 Å and 80-120°^{4a} El...Nu interactions had earlier been observed in crystals of simple organic compounds^{4a, 23} as well as in macromolecules²⁴ although there was no observable chemical reaction. Hence crystal structure of the orthobenzoate **2.28** was analyzed for these parameters to explain the facility of benzoyl transfer reaction in its crystals.

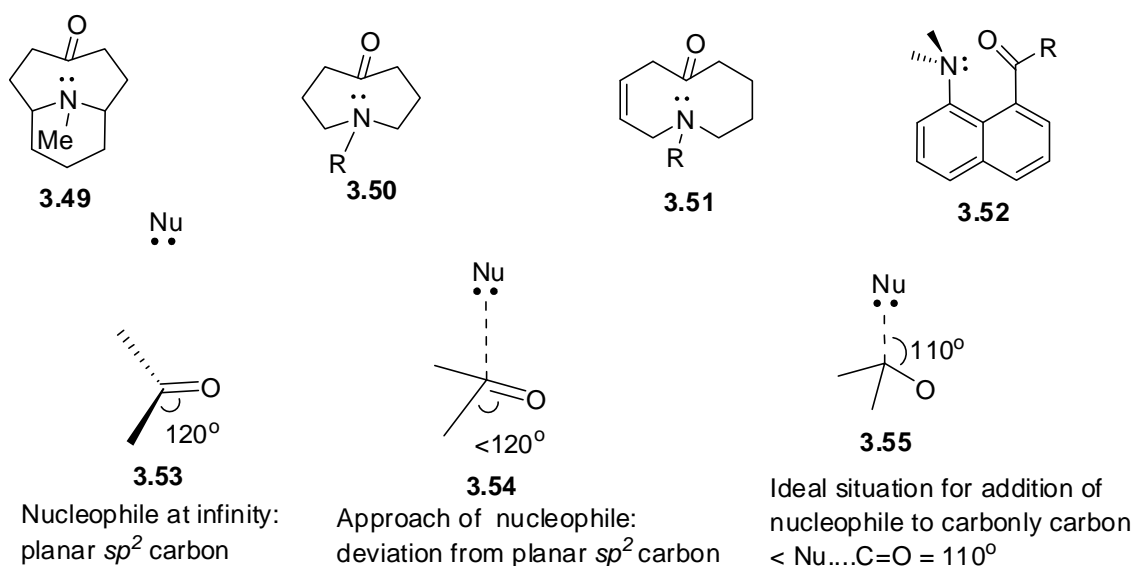


Figure 3.3: Molecular systems that were used to arrive at the geometry of attack of a nucleophile on a carbonyl group by structure correlation.²³

Crystals of the dibenzoate **2.28** belong to the monoclinic space group $P2_1/c$. Molecules in crystals of **2.28** are arranged helically around a crystallographic two-fold screw axis *via* O–H...O hydrogen bonding, very similar to the arrangement of molecules in crystals of the corresponding orthoformate **1.234**.^{4b} The OH group at the C-4 position in the orthobenzoate **2.28** donates its H atom to the carbonyl oxygen O7 of the C2-O-acyl group forming a helical assembly along the b-axis. It is interesting to note that this helical architecture is retained (Figure 3.4A and Table 3.2) despite the large difference on substituting the orthoformate ‘H’ (in the orthoformate, **1.234**)^{4b} with a phenyl group (in the orthobenzoate **2.28**). This ‘reactive’ helical pre-organization shows two striking geometrical similarities – first the electrophile (El)...nucleophile (Nu) (Figure 3.4B and

Table 3.2) and secondly the C–H $\cdots\pi$ ²⁵ interaction that the leaving benzoyl group makes with the C–H group of the reacting partner molecule along the helix (Figure 3.4B and Table 3.2).

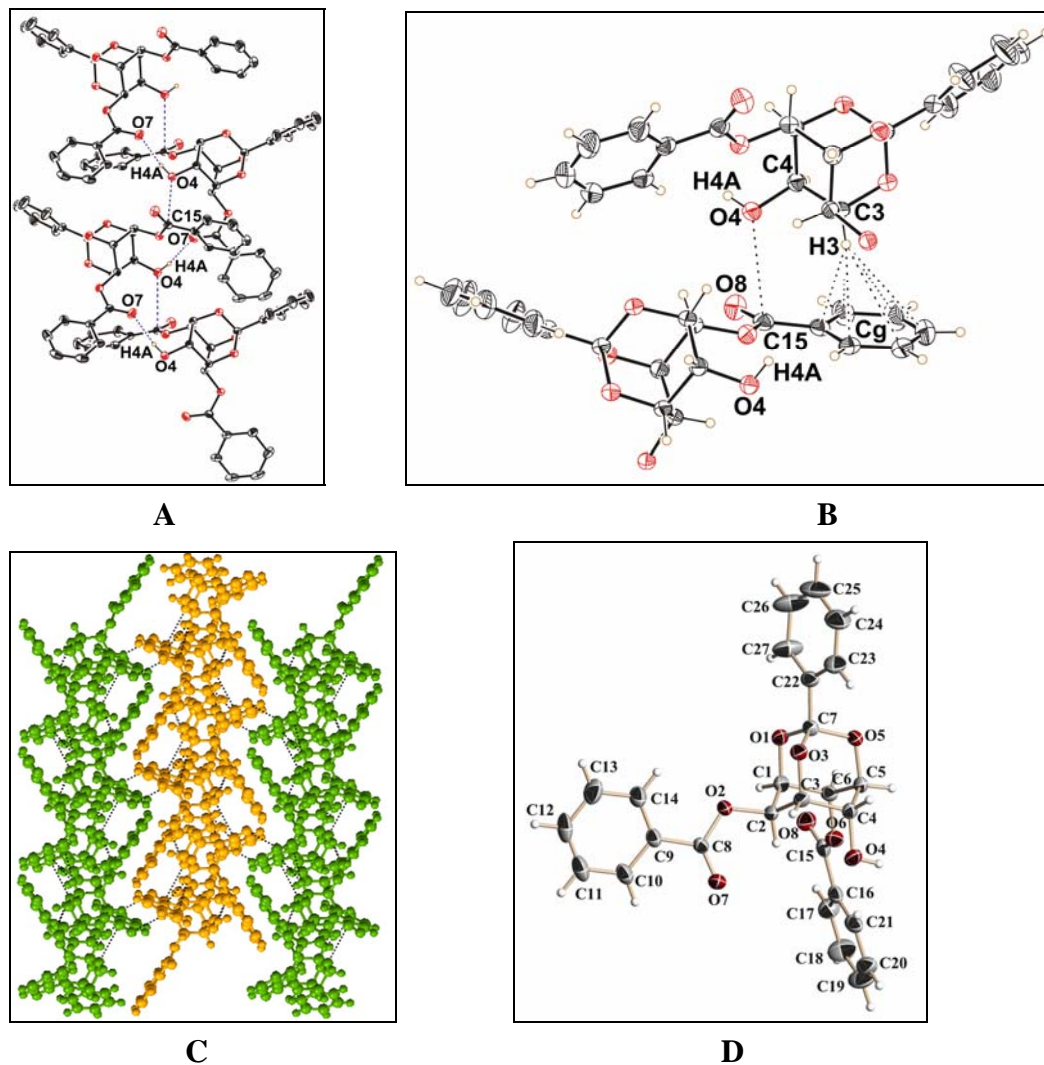


Figure 3.4. (A) Helical self-assembly of molecules in crystals of **2.28** via O–H \cdots O hydrogen bonding; (B) relative orientation of the reacting molecules in crystals of **2.28** (the 2-*O*-benzoyl group is not shown for clarity) and (C) packing of helices in crystals of **2.28**; (D) ORTEP of **2.28**.

Table 3.2. Geometrical parameters for intermolecular hydrogen bonding and C–H $\cdots\pi$ interactions (see Figure 3.4) in crystals of **2.28**. The corresponding geometrical parameters in crystals of **1.234**^{4b} is given for comparison.

Compound	D–H \cdots A	H \cdots A (Å)	D \cdots A (Å)	D–H \cdots A (°)
2.28	O(4)–H(4A) \cdots O(7) ^[a]	1.97(2)	2.795(2)	168(2)
	C(3)–H(3) \cdots Cg(2) ^[b]	2.83	3.805	166
1.234	O(4)–H(4A) \cdots O(7) ^[c]	1.94	2.871(7)	158
	O(4')–H(4'A) \cdots O(7') ^[d]	1.91	2.853(7)	166
	C(3)–H(3) \cdots Cg	2.52	3.520	162.9
	C(3')–H(3') \cdots Cg'	2.62	3.582	155.4

Cg = Ring Centre-of-Gravity (centroid), Cg1 = C9–C14, Cg2 = C16–C21

Symmetry code: [a] $-x, -1/2+y, 1/2-z$; [b] $-x, 1/2 + y, 1/2-z$.; [c] $1-x, -0.5+y, 0.5-z$; [d] $2-x, 0.5 + y, 0.5-z$.

Also, the O6–C15 bond length (see Figure 3.4D) of the C6-axial benzoate group is longer (1.347(2) Å) compared to the chemically equivalent O2–C8 bond of the C2-equatorial benzoate group (1.334 (2) Å), a feature noted in the reactive crystals of the orthoformate **1.234**.^{4b} In fact, the El \cdots Nu geometrical parameters are better in crystals of orthobenzoate **2.28** (Table 3.3) than those observed in crystals of orthoformate **1.234**.⁴

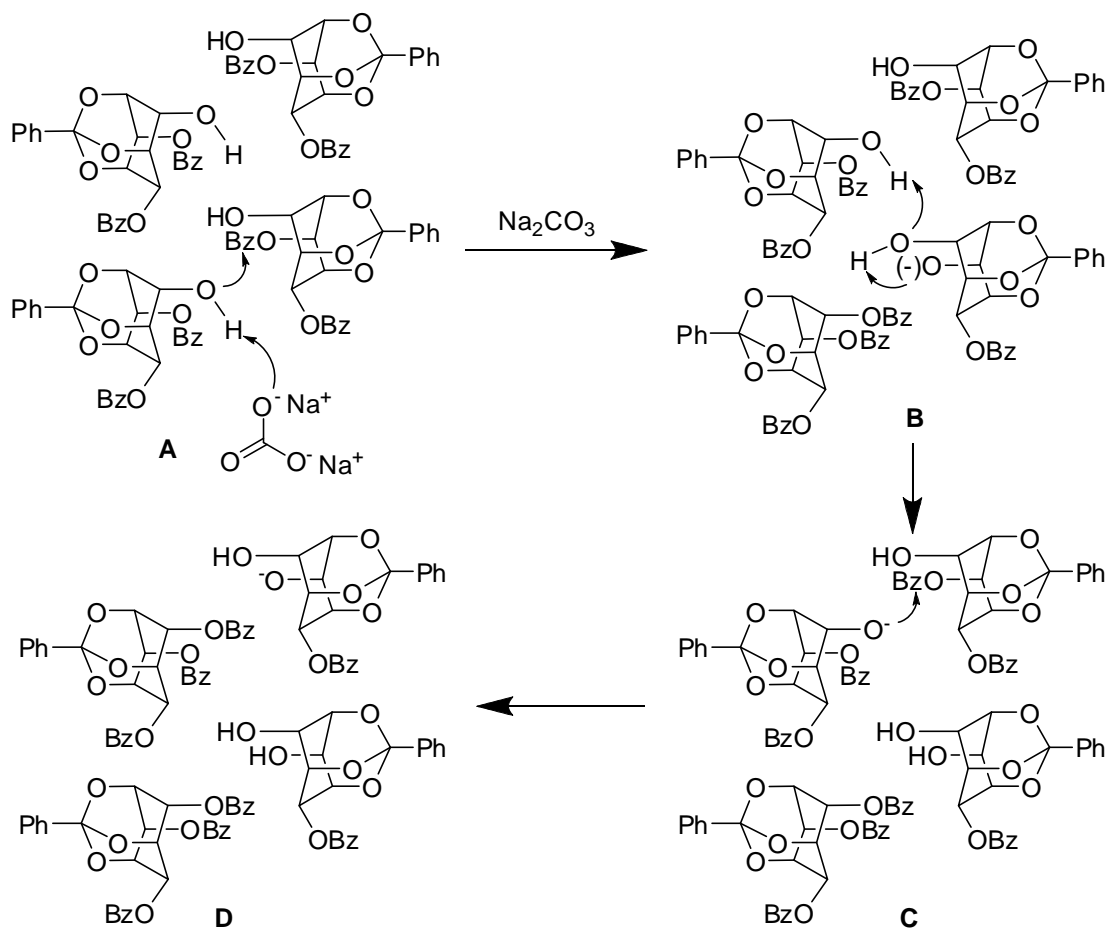
Table 3.3. Geometry of the reacting groups (El \cdots Nu, see Figure 3.4B) in crystals of **2.28**. The corresponding geometrical parameters in crystals of orthoformate **1.234**^{4b} is given for comparison.

Distance (Å) / Angle (°)	2.28	1.234
C15(C8) \cdots O4 (C15' \cdots O4')	3.144(2) ^[a]	3.226 ^[b] (3.249) ^[c]
\angle O4 \cdots C15–O8 (\angle O4' \cdots C15'–O8')	85.6(1)	88.1, ^[b] (89.9) ^[c]
\angle C4–O4 \cdots C15 (\angle C4'–O4' \cdots C15')	111.1(1)	117.6, (113.1)
\angle H4A–O4 \cdots C15 (\angle H4'A–O4' \cdots C15')	113(1)	113.1, (110.0)

Symmetry code: [a] $-x, -0.5+y, 0.5-z$; [b] $1-x, -0.5+y, 0.5-z$.; [c] $2-x, 0.5+y, 0.5-z$.

It is also important to note the packing of individual helices in crystals of orthobenzoate **2.28** (Figure 3.4C). In crystals of **2.28**, the helices linked to each other by C–H···O interactions between the C–H group of the inositol ring with carbonyl oxygen of the C6-O-benzoyl group. Additionally, the aromatic C–H group of C6-O-benzoyl group also makes C–H···O contact with the C2-O-oxygen. (See Appendix, page 270). This pattern of weak interactions keeps the reactive C6-O-benzoyl group in proper orientation with respect to the C4-hydroxyl group during the benzoyl transfer reaction.

The helices thus assembled (Figure 3.4C) are thought to provide ‘reaction tunnels’ throughout the crystal with the intermolecular benzoyl transfer going in a ‘domino’ fashion within each helix.^{4b} A plausible mechanism of the benzoyl transfer reaction in each helix in a domino fashion is shown in Scheme 3.6.



Scheme 3.6: A plausible mechanism for the benzoyl group transfer in crystals of **2.28**

It appears the nucleophilic attack by the hydroxyl group on the benzoate carbonyl carbon is initiated by the base (sodium carbonate) at the surface of the crystal. Subsequently the reaction progresses by a series of alternate proton transfers and nucleophilic attacks.

3.2.3. Attempted preparation of co-crystals of unsymmetrical dibenzoates of *myo*-inositol orthoesters leads to a reactive polymorph of racemic 2,4-dibenzoyl-*myo*-inositol 1,3,5-orthoacetate (3.2).

Earlier work in our laboratory^{4b} had revealed that the dibenzoates **3.2** and **1.234** together form 1:1 co-crystals, in which intermolecular migration of the benzoyl group took place efficiently.^{4b} The solid state reactivity of the molecular complex **1.234**•**3.2** in the presence of solid sodium carbonate afforded the expected tribenzoates **3.1** and **3.3** as well as the diols **1.232** and **3.4** as anticipated from its crystal structure (Scheme 3.1, page 214). The arrangement of molecules in these co-crystals was almost identical to that found in the crystals of the orthoformate **1.234** and the orthobenzoate **2.28** (Figure 3.4; page 224). In these co-crystals, each helical assembly resulted due to the aggregation of orthoacetate **3.2** and orthoformate **1.234** molecules alternately as shown in the Figure 3.5. Geometrical parameters of $\text{E}1 \cdots \text{N}u$ interaction were conducive for the transesterification reaction (Table 3.4).

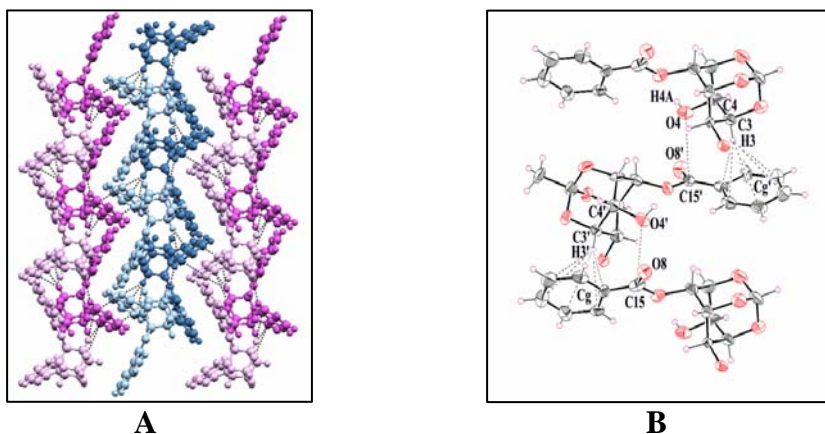


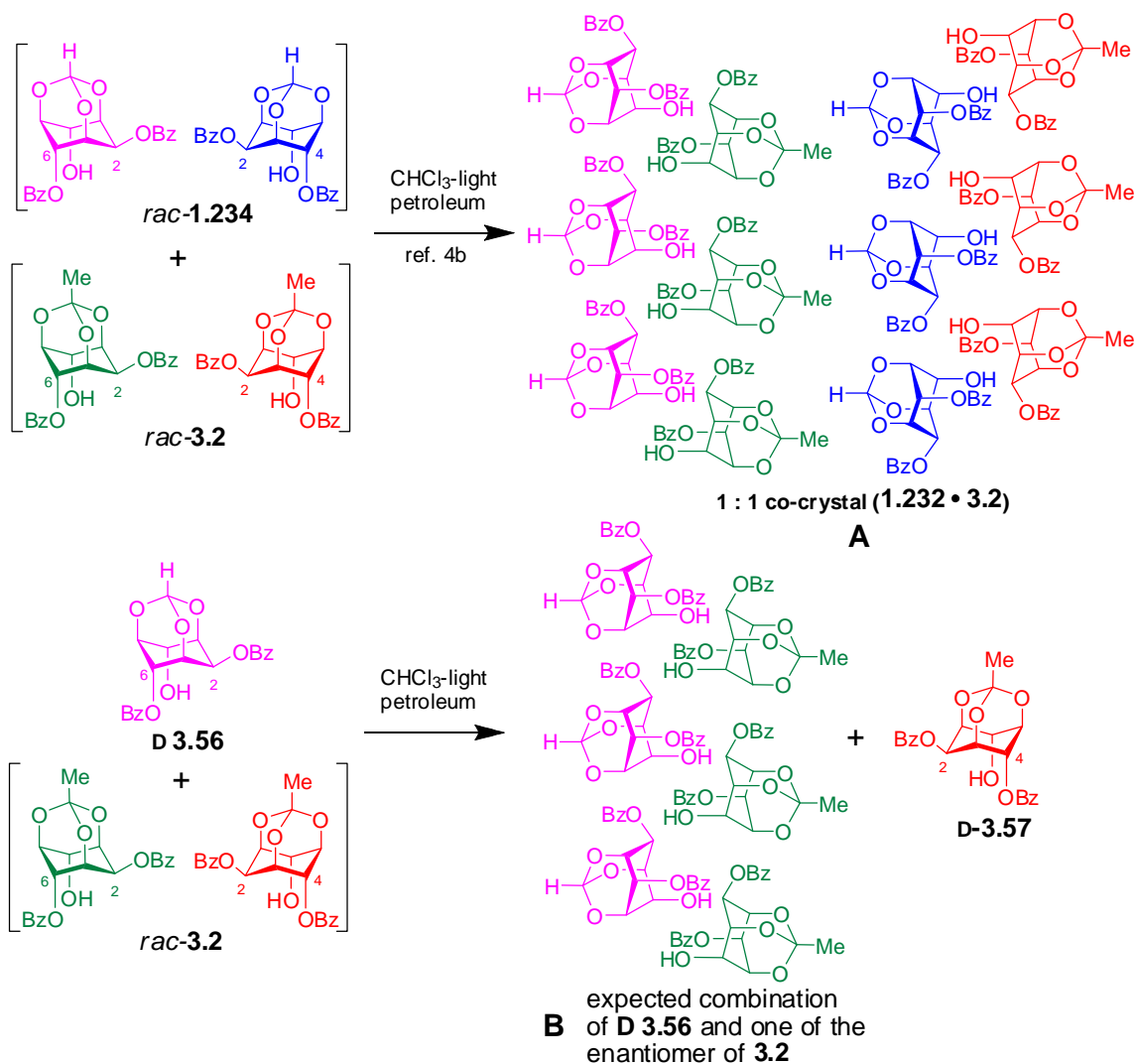
Figure 3.5. Packing of helices (A) and relative orientation (B) of the reacting molecules in co-crystals **1.234** • **3.2** (the 2-*O*-benzoyl group is not shown for clarity).

Table 3.4: Geometrical parameters of the reacting molecules in co-crystals **1.234 • 3.2**.

SL. No.	Distance (Å) / Angle (°)	formate.acetate
1	C15(C13)···O4	3.170 ^[a] , 3.155 ^[b]
2	∠O4···C15(C13)–O8	85.9 ^[a] , 88.4 ^[b]
3	∠C4–O4···C15(C13)	117.6 ^[a] , 116.1 ^[b]
4	∠H4A–O4···C15(C13)	107.9 ^[a] , 119.8 ^[b]

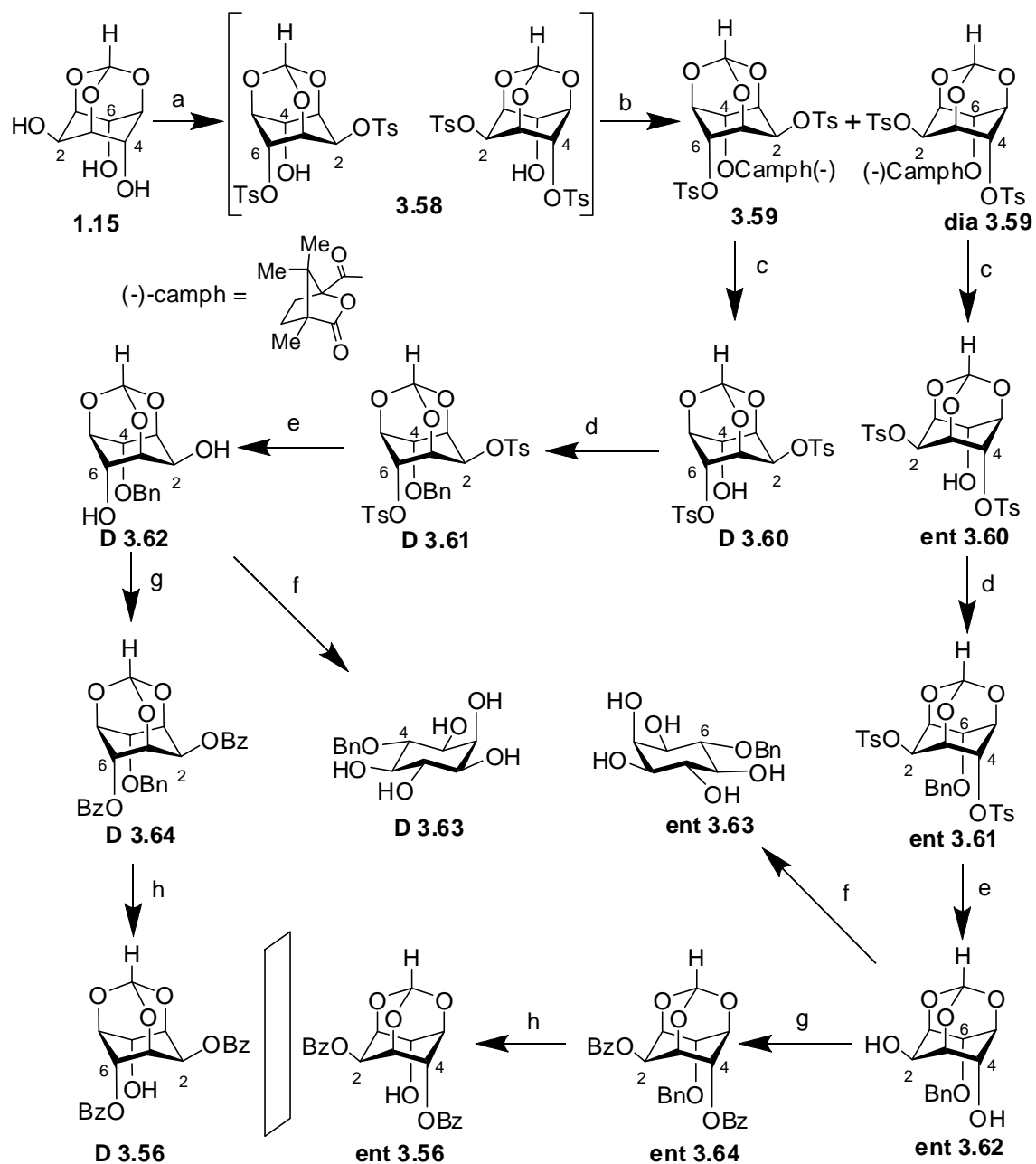
Symmetry code: [a] x, y, z.; [b] 1.5–x, –0.5+y, 0.5–z

Furthermore, a comparison of the packing of molecules in crystals obtained from dibenzoates **1.234**, **3.2** and **2.28** revealed that (a) crystals of **1.234**, **2.28** and **3.2** consisted of helices; (b) each helix was formed by the aggregation of the molecules of a unique configuration [either D (D-2,4-) or L (D-2,6-)]; (c) each helix is surrounded by the helices formed by the molecules of the opposite configuration (either D or L, Figure 3.4); (d) co-crystals **1.234 • 3.2** consisted of only two diastereomeric pairs [D, D; L, L; OR L, D; D, L] of molecules instead of the statistically expected four diastereomeric pairs [(a) D, D; (b) L, L; (c) L, D; (d) D, L]. Hence we attempted the co-crystallization of orthobenzoate **2.28** with orthoformate **1.234**, orthoacetate **3.2** as well as enantiomeric dibenzoates **D 3.56** with **2.28** and **3.2**. It was interesting to see whether crystallization of *rac*-orthoacetate **3.2** (or *rac*-orthobenzoate **2.28**) with optically active dibenzoyl-orthoformate (either **D 3.56** or **ent 3.56**) would result in co-crystals (B, Scheme 3.7) consisting of enantiomeric dibenzoyl-orthoformate and enantiomeric dibenzoyl orthoacetate (or orthobenzoate) leaving the other enantiomer of the orthoacetate (or the orthobenzoate) either in solution or as separate crystalline form (Scheme 3.7).



Scheme 3.7

The optically active dibenzoates **D 3.56** and **ent 3.56** were prepared from *myo*-inositol-1,3,5-orthoformate (**1.15**, Scheme 3.8). The ditosylate **3.58** was resolved as (–)-camphanate esters **3.59** and **dia 3.59**. Enantiomeric mono-benzyl ethers **D 3.63** and **ent 3.63**²⁶ were prepared from the diastereomeric ditosylates **D 3.60** and **ent 3.60** to confirm the configuration of the enantiomeric dibenzoates **D 3.56** and **ent 3.56**. Mono benzyl ethers **D 3.63** and **ent 3.63** are also suitable precursors for the synthesis of *D*-*myo*-Inositol-1,2,3,5,6-pentakisphosphate and *D*-*myo*-inositol-1,2,3,4,5-pentakisphosphates.²⁶



Scheme 3.8: (a) TsCl, Py, 80 °C, 48 h; (b) 1*S*-(-)camphanoyl chloride, Py, DMAP, 90 °C, 10 h; (c) *i*-BuNH₂, DCM-MeOH, reflux, 8 h; (d) BnBr, DMF, NaH, 30 min., rt.; (e) NaOMe, MeOH, reflux, 12 h; (f) TFA - H₂O, rt, 24 h; (g) BzCl, Py, rt, 20 h; (h) H₂ (55 psi), Pd(OH)₂-C, MeOH - EtOAc, rt, 6 h.

The enantiomeric dibenzoates (**D 3.56** and **ent 3.56**) were crystallized by slow diffusion of light petroleum (40-60 °C) into a chloroform solution in a closed vessel. The crystal structures of both D-2,4- (**ent 3.56**) and D-2,6-(**D 3.56**)- dibenzoates were found to

be isostructural to each other, but not isostructural with the corresponding dibenzoate **1.234**.

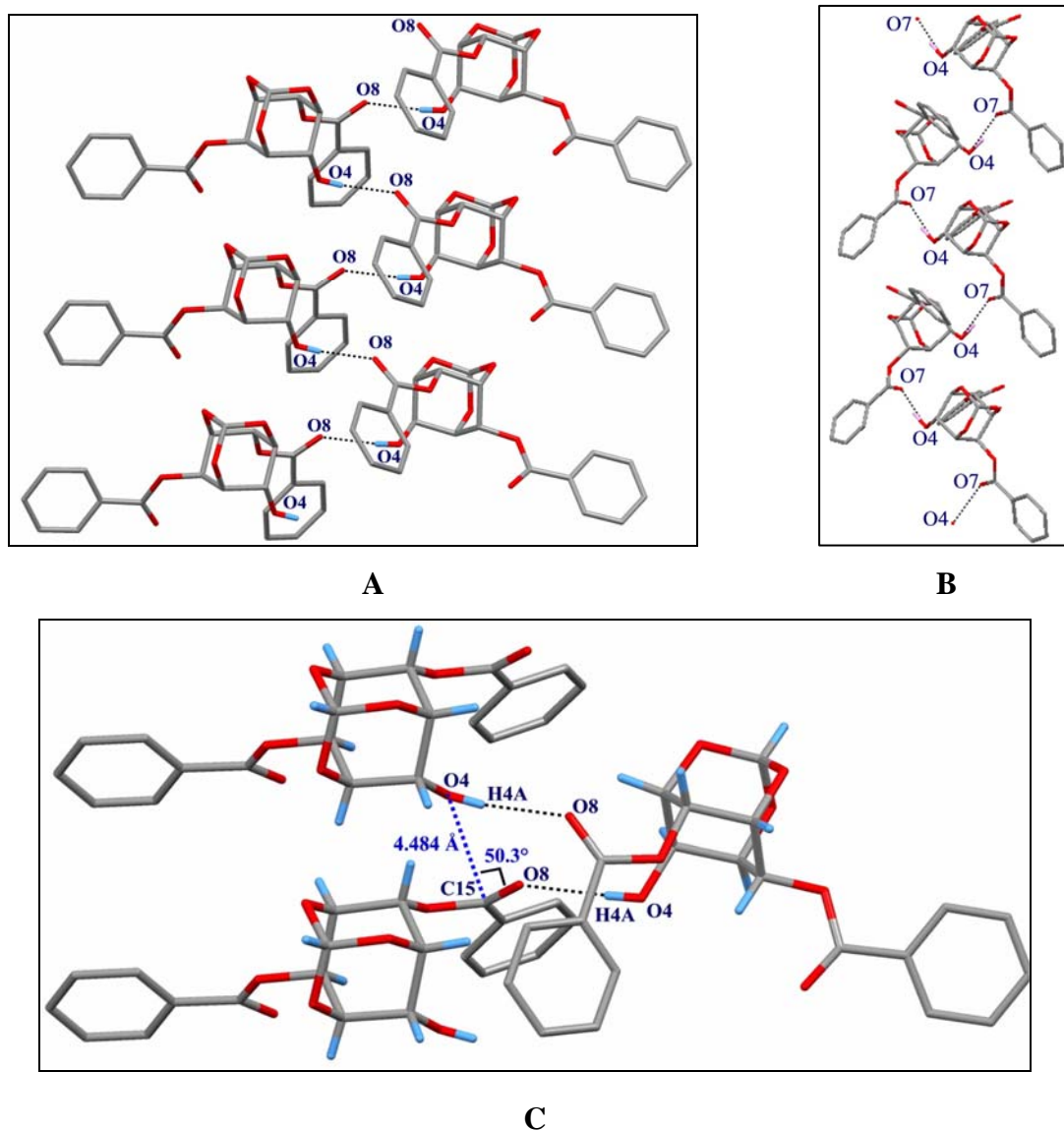


Figure 3.6 (A) Packing of molecules of D-2,6-dibenzoate **D 3.56** in its crystal; (B) packing of molecules in *rac*-dibenzoate **1.234** is shown for comparison; (C) relative orientation of neighboring molecules of D-2,6-dibenzoate **D 3.56** showing El...Nu geometry.

There is a striking difference in the arrangement of molecules in crystals of the optically active dibenzoate **D 3.56** or **ent 3.56** and the corresponding *rac*-di-benzoyl-orthoformate **1.234**. The molecules in the crystals of *rac*-**1.234** are arranged in helical

fashion *via* hydrogen bonding between the C4(6)–OH of one molecule and the ‘equatorial’ benzoate carbonyl group of another molecule (O4H···O7) where as in the case of optically active dibenzoates **D 3.56** and **ent 3.56** the helical assembly is formed *via* hydrogen bonding between the C6–OH (or C4–OH) of one molecule and the ‘axial’ C4-benzoate (or the C6-benzoate) carbonyl group of another molecule (O6–H6A···O8 or O4–H4A···O8, see figure 3.6 and 3.7).

Table 3.5. Intermolecular hydrogen bonding and C–H··· π interactions in crystals of enantiomeric dibenzoate **D 3.56**. See Table 3.2 for a comparison of corresponding parameters in crystals of the *rac*-dibenzoate **1.234**.

	D–H···A	H···A (Å)	D···A (Å)	D–H···A (°)
D 3.56	O(4)–H(4A)···O(8) ^[a]	2.02(2)	2.788(2)	172(2)
	C(5)–H(5)···Cg(1)	3.265	4.086	139

Cg = Ring Centre-of-Gravity (centroid), Cg1 = C9–C14, Cg2 = C16–C21
Symmetry code: [a] $x-1/2, -y-1/2, -z$.

The difference in the packing of the molecules in the crystals of D-2,6-di-benzoyl-*myo*-inositol-1,3,5-orthoformate (**D 3.56**) and the corresponding *rac*-dibenzoate **1.234** is evident from the ball and stick model (Figure 3.7).

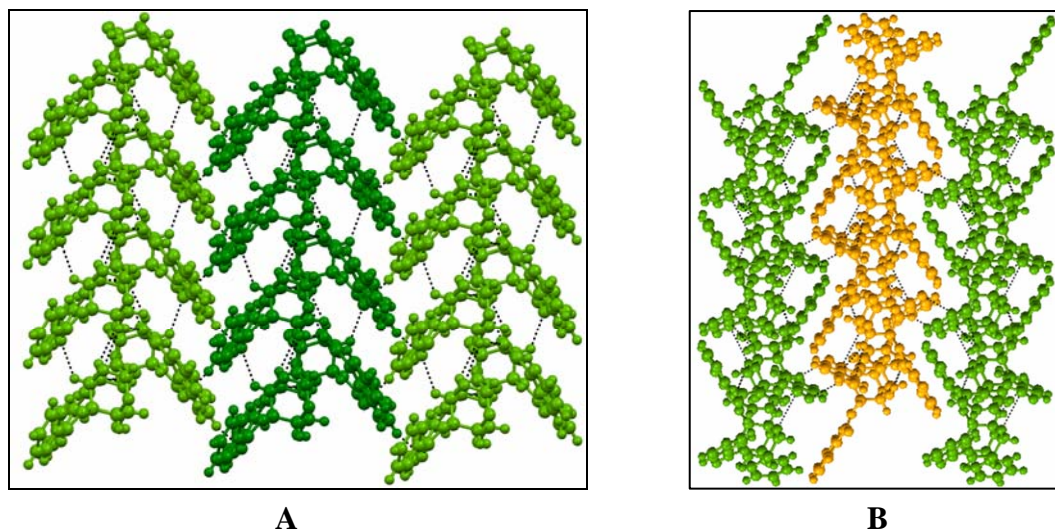
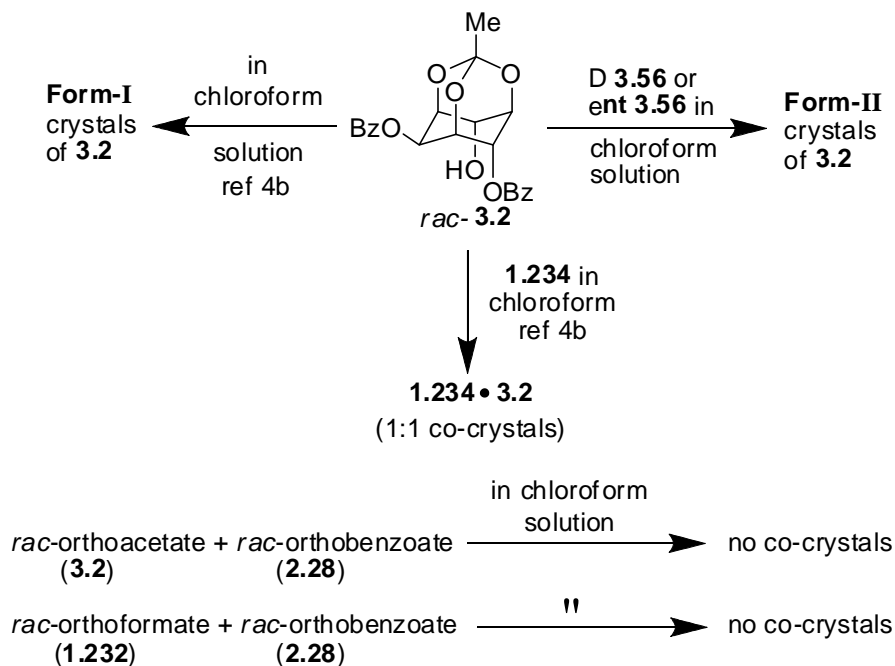


Figure 3.7: Packing of molecules in crystals of (A) **D 3.56**; (B) *rac*- **1.234**.

The solid-state transesterification reaction in crystals of the optically active dibenzoate **D 3.56** in the presence of solid sodium carbonate at 140 °C for 36 h afforded a mixture of products. No attempt was made to separate these products. This was as expected from the crystal structure since the distance between electrophile and nucleophile (O4...C15, Figure 3.6) was found to be too long (4.484 Å) unlike in the reactive crystals of the *rac*-orthoformate **1.234** (3.144 Å) and the *rac*-orthobenzoate **2.28** (3.226 Å). In addition to the interactions between the molecules in individual helices (Figure 3.4 and Tables 3.2 and 3.3), the non-covalent interactions among the helices may also play a role in the formation and alignment of the helical assembly of the molecules. This fact could also be a reason why optically active dibenzoates **D 3.56** and **ent 3.56** could not form proper helical assembly conducive for benzoyl transfer reaction (similar to those present in *rac*-dibenzoates **1.234** and **3.28** in their crystals).

Attempts to obtain co-crystals of racemic orthoformate–orthobenzoate (**1.234–2.28**) and racemic orthoacetate–orthobenzoate (**3.2 - 2.28**) from chloroform (Scheme 3.9) failed. In both cases, either precipitation or formation of amorphous solid was observed. Crystallization from an equimolar solution (in chloroform) containing any one of the enantiomeric of dibenzoate (either **D 3.56** or **ent 3.56**) and *rac*-dibenzoate **3.2** yielded needle shaped crystals. Similar results were obtained on reducing the relative amount of **D 3.56** (or **ent 3.56**) in solution. The minimum amount of the optically active active dibenzoate required to obtain the needle shaped crystals of *rac*-orthoacetate **3.2** was about 10%. Analysis of these needle shaped crystals by single crystal X-ray diffraction established them to be a hitherto unknown polymorph of the *rac*-dibenzoate **3.2**. The needle shaped crystals of **3.2** obtained in these experiments is designated as ‘Form-II’ crystals in the subsequent pages of this thesis. The crystals of **3.2** reported earlier^{4b} from our laboratory is designated as ‘Form I’ crystals. Crystallization of *rac*-orthoacetate **3.2** in the presence of less than 5% of **D 3.56** (or **ent 3.56**) resulted in the formation of concomitant polymorphic forms (Form-I and Form-II crystals) of **3.2**. Thus,

crystallization of **3.2** alone from chloroform solution leads to one form (Form-I crystals) while its crystallization in the presence of **D 3.56** or **ent 3.56** led to the formation of a different crystal form (Form-II). The exact role of the optically active dibenzoates during



Scheme 3.9: Results of co-crystallization experiments with **1.234**, **2.28** and **3.2**.

the formation of Form-II crystals of **3.2** is not known. The presence of enantiomers **D 3.56** or **ent 3.56** might be either preventing the formation of Form-I crystals or aiding in the formation of Form-II crystals.²⁸ No co-crystals consisting of an enantiomeric **D 3.56** or **ent 3.56** and *rac*-dibenzoate **3.2** could be obtained in any of these experiments. These results are schematically summarized in Scheme 3.9.

Form-I crystals of the *rac*-orthoacetate **3.2** were bulky crystals where as Form-II crystals were bunches of sharp needles (Figure 3.8). ¹H NMR spectrum (in solution) of manually separated crystals of Form-II (Figure C) showed the presence of **3.2** and the enantiomeric dibenzoate **D 3.56** in the ratio 20:1. Also, similar analysis of Form-II crystals obtained and separated from different crystallization experiments indicated that the ratio of **3.2** to **D 3.56** present varied. These results suggested that the enantiomeric **D**

3.56 present in these Form-II crystals of **3.2** are not incorporated in the crystals but perhaps was just adhering to the Form-II crystals.

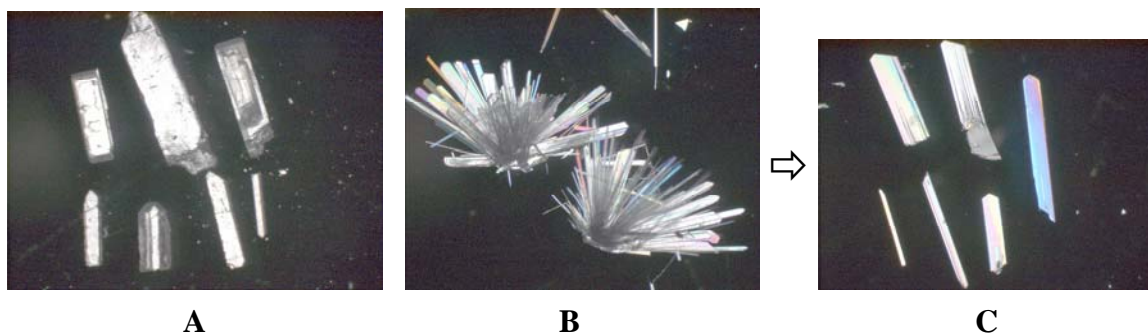


Figure 3.8. Crystals of **3.2**; (A) Form-I crystals: Crystallized from chloroform-light-petroleum; (B) Form-II crystals: Crystallized from chloroform-light-petroleum in the presence of either **D 3.56** or **ent 3.56** and (C) manually separated Form-II crystals from the bunch shown in (B).

The possibility of the formation of co-crystal of **D 3.56** and **3.2** was ruled out on the basis of the space group ($C2/c$) of Form-II crystals, which belongs to an achiral space group. This is because incorporation of chiral molecules in crystals must necessarily result in the formation of crystals belonging to chiral space groups.

DSC analysis of Form-II crystals of **3.2** suggested a phase change around 145-150 °C before its melting (Figure 3.9). Analysis of the crystals (by X-ray diffraction) obtained by heating the Form-II crystals at 145 °C showed them to be Form-I crystals. Hence it was clear that Form-II crystals underwent crystal to crystal transformation to form Form-I crystals around 145 °C. This showed that Form-I crystals are thermodynamically stable while Form-II crystals are meta-stable. ^1H NMR spectrum of the crystals of **3.2** was recorded after the conversion of Form-II to Form-I crystals, which showed no change in the ratio of *rac*-orthoacetate **3.2** to optically active orthoformate **D 3.56**.

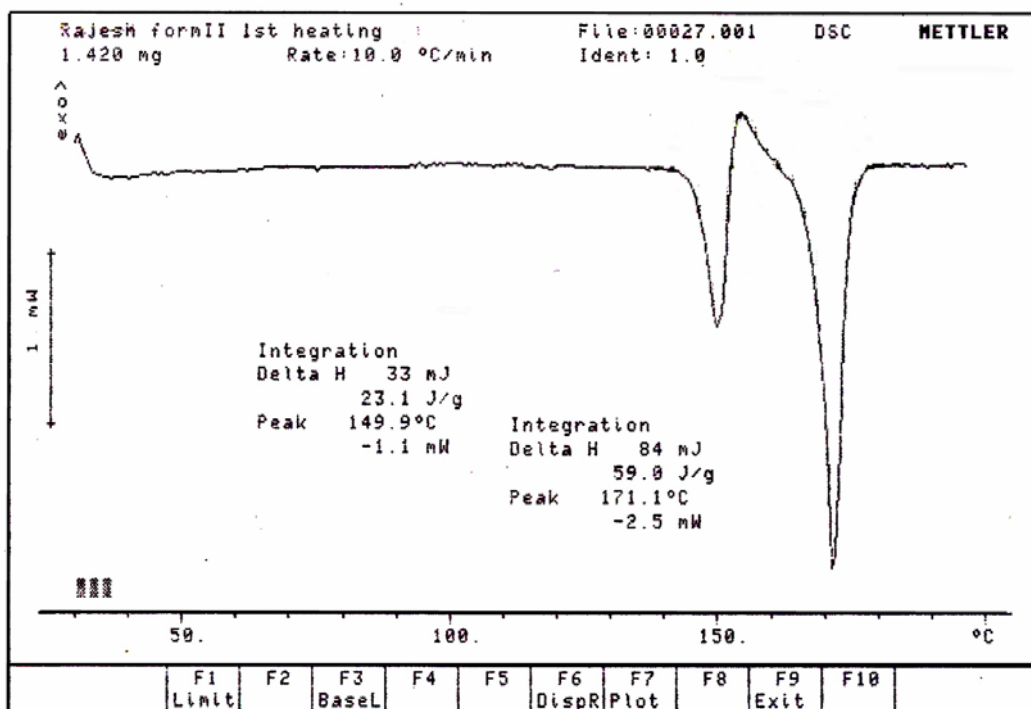


Figure 3.9: DSC analysis of Form-II crystals of *rac*-orthoacetate 3.2.

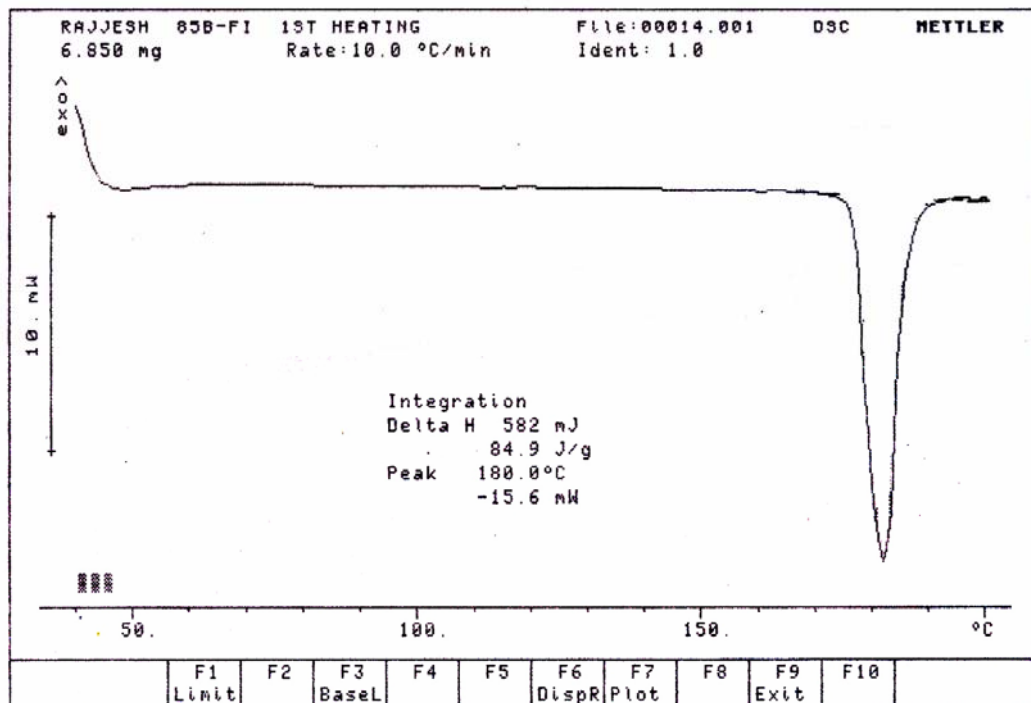


Figure 3.10: DSC analysis of Form-I of 3.2.

Analysis of the Form-II crystal structure (of **3.2**) showed that they were isostructural (Figure 3.11D) with crystals of *rac*- dibenzoate **1.234** (Figure 3.2A) and *rac*- orthobenzoate **2.28** (Figure 3.4A) both of which exhibited very good acyl transfer reactivity. Similarities were observed in terms of O–H···O, C–H··· π and E1···Nu interactions (Tables 3.2, 3.3, 3.6 and 3.7) and the helical assembly of molecules (which is favorable for transesterification reaction in crystals).

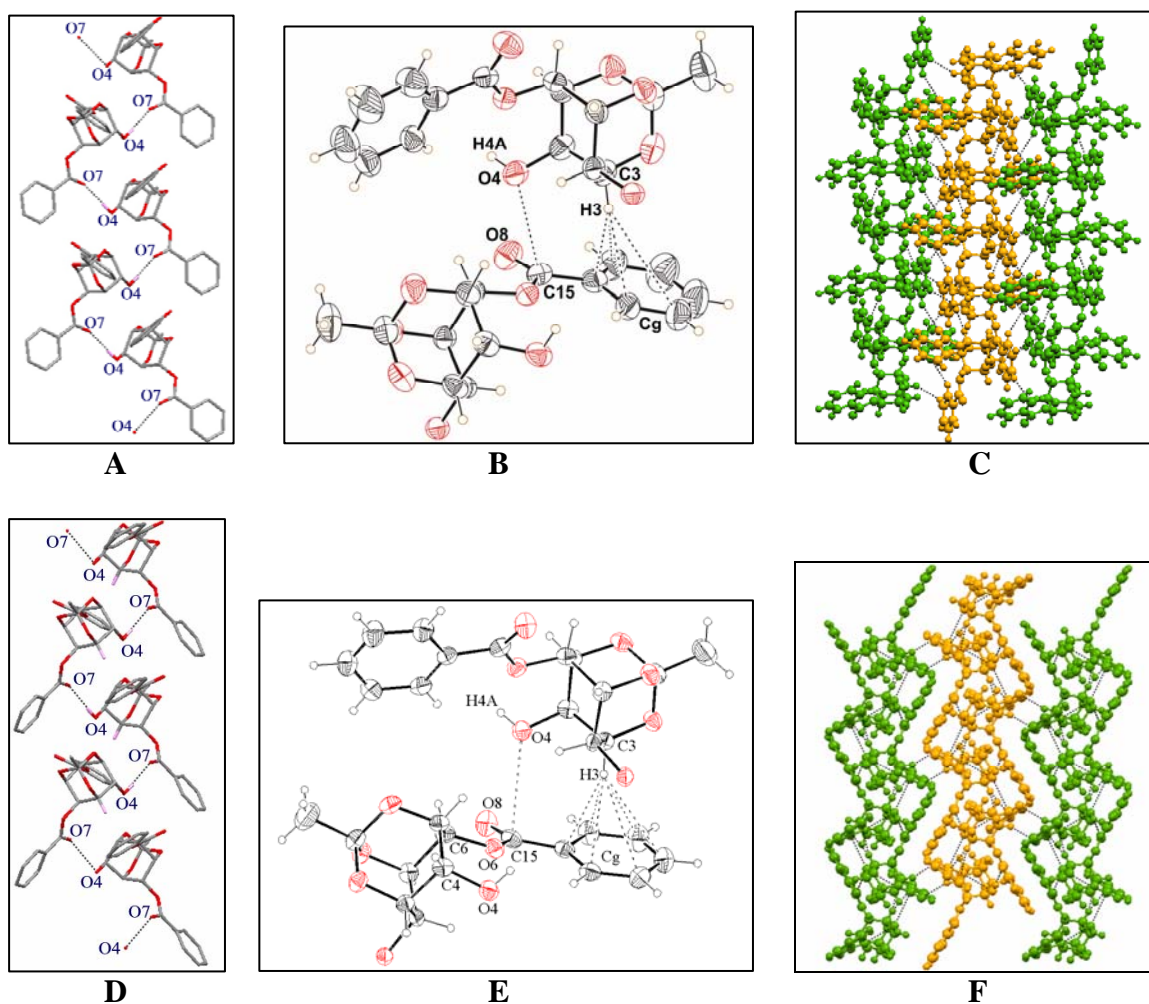


Figure 3.11. A comparison of the crystal structure of Form-I and Form-II crystals of **3.2**. Arrangement of molecules in a helix (A and D); A pair of reacting molecules (B and E); Packing of helices (C and F). Figures A, B, C are reproduced from ref. 4b for comparison.

Table 3.6. Intermolecular hydrogen bonding and C–H $\cdots\pi$ interactions in Form-I and Form-II crystals of *rac*-orthoacetate **3.2**. See Tables 3.2 and 3.3 for a comparison of corresponding parameters in crystals of orthobenzoate **2.28** and orthoformate **1.234**.

	D–H \cdots A	H \cdots A (Å)	D \cdots A (Å)	D–H \cdots A (°)
Form I	O(4)–H(4A) \cdots O(7) ^[a]	1.93	2.775(2)	175
	C(3)–H(3) \cdots Cg(1) ^[b]	3.67	4.472	142
Form II	O(4)–H(4A) \cdots O(7) ^[c]	2.00	2.822(3)	176
	C(3)–H(3) \cdots Cg(1) ^[d]	2.62	3.582	167

Cg = Ring Centre-of-Gravity (centroid), Cg1 = C9–C14.

Symmetry code: [a] 1.5–x, –0.5+y, 0.5–z. [b] 1.5–x, 0.5+y, 0.5–z [c] 0.5–x, –0.5+y, 0.5–z; [d]] 0.5–x, 0.5+y, 0.5–z.

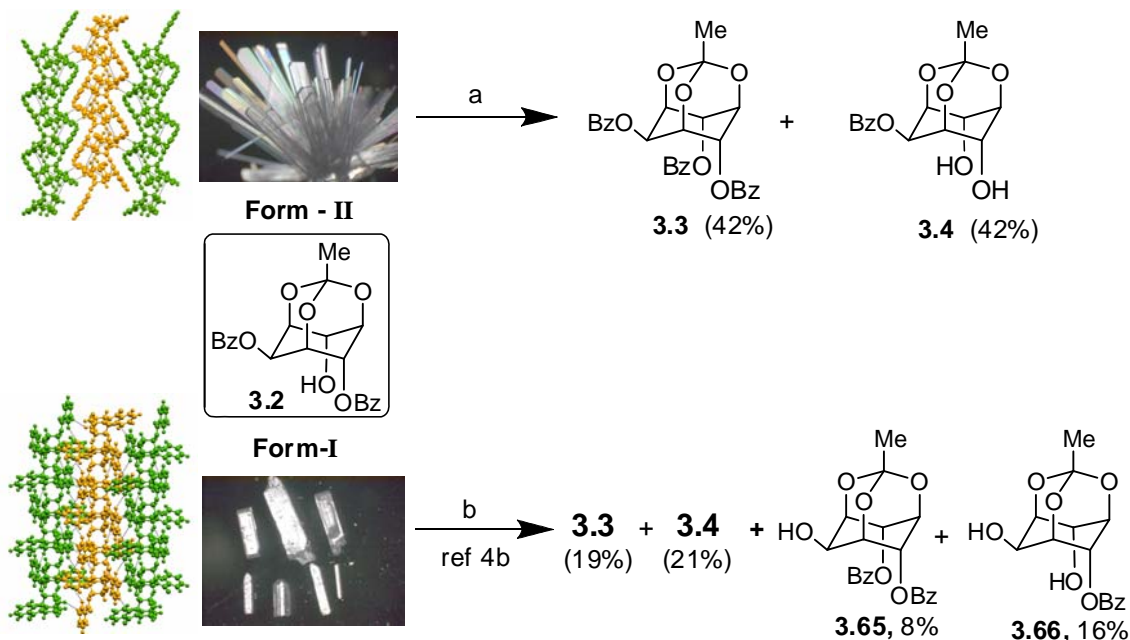
Table 3.7. Geometry of the reacting groups (El \cdots Nu) in Form-I and Form-II crystals of **3.2**. See Tables 3.2 and 3.3 for a comparison of corresponding parameters in crystals of the orthobenzoate **2.28** and the orthoformate **1.234**.

Distance (Å) / Angle (°)	Form-I	Form-II
C15 \cdots O4	3.299 ^[a]	3.135
\angle O4 \cdots C15–O8	84.01 ^[a]	87.6
\angle C4–O4 \cdots C15	97.20 ^[a]	116.5
\angle H4A–O4 \cdots C15	105.8 ^[a]	114

Symmetry code: [a] 1.5–x, –0.5+y, 0.5–z. [b] 0.5–x, –0.5+y, 0.5–z.

These geometrical parameters (Tables 3.6, 3.7 and Figure 3.11) indicated the possibility of a facile intermolecular benzoyl group transfer in Form-II crystals of the *rac*-orthoacetate **3.2**. Heating the Form-II crystals of **3.2** at 115 °C (well below the phase transition temperature of 145 °C) with anhydrous solid sodium carbonate gave very good yield of the corresponding tribenzoate **3.3** and the diol **3.4** (Scheme 3.10). Similar reaction of Form-I crystals at 115 °C did not proceed well (see experimental for details) and most of the starting material was recovered. Prior work in our laboratory^{4b} had shown

that benzoyl group transfer in Form-I crystals of *rac*-orthoacetate **3.2** was inefficient at higher temperatures (unlike in the case of *rac*-orthoformate **1.234** and *rac*-orthobenzoate **2.28** crystals) and gave rise to a mixture of several products.

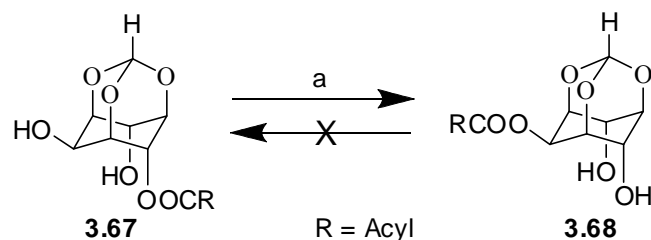


Scheme 3.10: (a) Anhy. Na₂CO₃, 115°C, 190 h; (b) Anhy. Na₂CO₃ 140 °C, 162 h

A comparison of the crystal structures of Form-I and Form-II crystals of **3.2** and the observed differences in facility of benzoyl transfer reaction in these polymorphic crystals clearly reveals the importance of weaker intermolecular interactions for benzoyl group transfer in crystals. These results also show that the facility of acyl transfer reaction in crystals can be predicted from their structure.

3.2.4. Benzoyl group transfer reactivity in monobenzoates of *myo*-inositol orthoesters.

The sodium hydride assisted facile intermolecular acyl migration in *rac*-4-*O*-acyl-*myo*-inositol-1,3,5-orthoesters **3.67** (Scheme 3.11) to the corresponding 2-*O*-acyl derivatives **3.68** in excellent yields (> 90%), in the solution state had earlier been reported^{2b} from our laboratory.



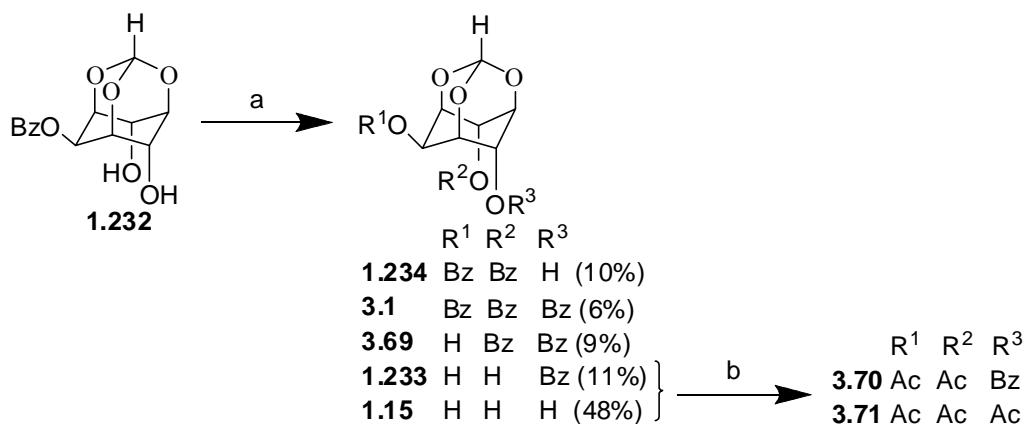
Scheme 3.11: (a) DMF, NaH or *t*-BuOK.

This reaction in solution was irreversible and the 2-*O*-acyl-*myo*-inositol-1,3,5-orthoesters **3.68** were completely stable both in the presence of strong bases (sodium hydride and potassium *t*-butoxide) and at higher temperatures. Encouraged by the results obtained with crystals of *rac*-2,4-di-*O*-benzoyl-*myo*-inositol-1,3,5-orthoesters (**1.234**, **3.2**, **2.28**), we wondered whether the 2-*O*-benzoyl-*myo*-inositol-1,3,5-orthoesters (**1.232** and **3.48**) would undergo transesterification reaction in the crystalline state.

The benzoates **3.48** and **1.232** were crystallized from chloroform-light petroleum mixture by diffusion method. The orthobenzoate **3.48** on crystallization spontaneously yielded chiral crystals (orthorhombic, space group $P2_12_12_1$) irrespective of the solvent used. Our attempts to obtain an achiral polymorph of **3.48** were not successful. Cases where *meso* compounds like **3.48** produce chiral crystals are intriguing, having significance both in understanding the fundamental process of crystallization²⁹ as well as in their applications as NLO materials.

Analysis of the crystal structures of the benzoates **3.48** and **1.232** revealed a relative orientation of molecules that appeared conducive for exhibiting the solid state acyl transfer reactivity, although the $E1 \cdots Nu$ interaction parameters (see tables 3.8-3.10) were not as good as those in crystals of *rac*-dibenzoate **2.28** and **1.234**. This implied that even if the benzoyl group transfer occurred in crystals of benzoates **3.48** and **1.232**, the facility of the reaction would be perhaps less as compared to similar reaction in crystals of *rac*-dibenzoates **2.28** and **1.234**. In order to verify our speculation based on the crystal structures, we subjected crystals of the benzoates **3.48** and **1.232** to transesterification

conditions in the presence of solid sodium carbonate. Although this reaction proceeded to give transesterified products, as expected, it was not a clean reaction. The various products obtained from **1.232** are shown in the Scheme 3.12. Transesterification of crystalline **3.48** also yielded a mixture of products similar to that observed in the case of **1.232**. Analysis of the mixture of products by TLC indicated the presence of several products including the tribenzoate **3.47**, the dibenzoate **2.28**, the triol **1.17** along with two unidentified products; no attempt was made to separate these products.



Scheme 3.12: (a) Na_2CO_3 , 140 °C, 60 h; (b) Ac_2O , Py.

However, it is interesting to note that although both these mono-benzoates (**3.48** and **1.232**) failed to undergo transesterification in solution (See Scheme 3.11), they did undergo the same reaction in the crystalline state owing to the relatively ‘frozen’ assembly of molecules favorable for the transesterification reaction. However, facility and specificity of transesterification in crystals of **3.48** and **1.232** are not as good as those compared to the reaction in crystals of *rac*-dibenzoates **2.28** and **1.234** due to differences in the packing of the molecules in their crystals as discussed below.

3.2.5. Correlation of Molecular Pre-Organization and intermolecular interactions with Acyl transfer reactivities.

Although the benzoates **3.48** and **1.232** have two hydroxyl groups at C4 and C6 positions, these molecules do not assemble by forming intermolecular O–H···O hydrogen

bond in their crystals, from either of these with the O=C of the C2-benzoate group (as observed in crystals of the dibenzoates **2.28** and **1.234**). In both **3.48** and **1.232**, intermolecular O–H \cdots O bonding is formed between the OH group at the C4 and C6 position and the oxygen O1 and O3 of the orthoformate (Figure 3.12 and 3.13, Table 3.8).

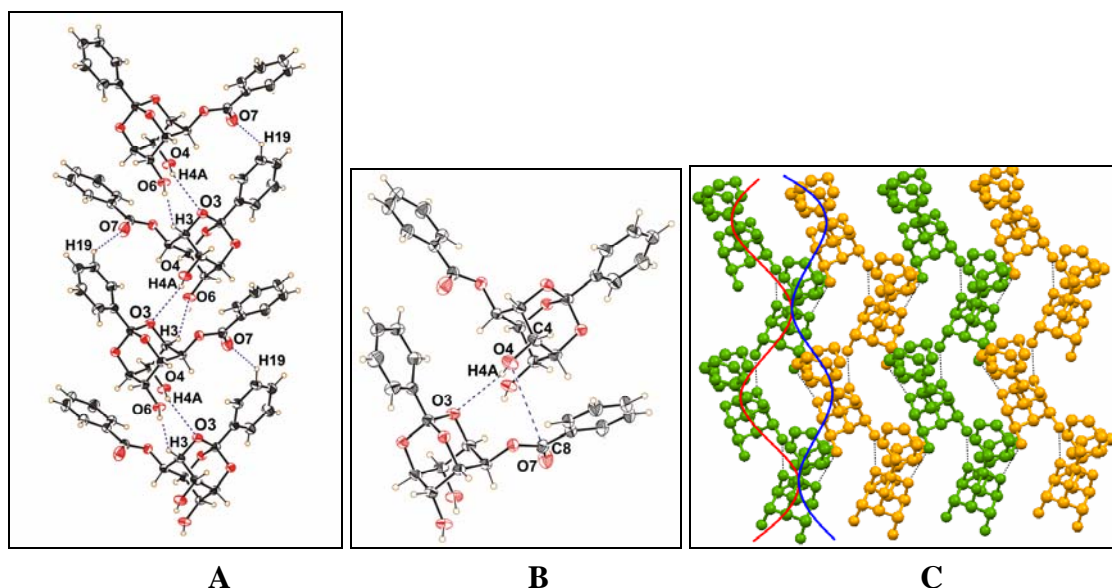


Figure 3.12. (A) Helical self-assembly via O4–H4A \cdots O3 hydrogen bonding in crystals of **3.48**; (B) relative orientation of the reacting molecules in crystals of **3.48** and (C) intersecting helices (O4–H4A \cdots O3, red curved line and O6–H6A \cdots O1, blue curved line) forming two dimensional sheet in crystals of **3.48**.

Table 3.8. Intermolecular hydrogen bonding and C–H \cdots π interactions in crystals of **3.48** and **1.232**.

	D–H \cdots A	H \cdots A (Å)	D \cdots A (Å)	D–H \cdots A (°)
3.48	O(4)–H(4A) \cdots O(3) ^[a]	2.56(3)	3.018(2)	117(2)
	O(6)–H(6A) \cdots O(1) ^[b]	2.11(3)	2.861(2)	156(3)
	C(5)–H(5) \cdots Cg(1) ^[a]	3.91	4.720	139
1.232	O(4)–H(4A) \cdots O(1) ^[c]	1.90(3)	2.656(2)	159(3)
	O(6)–H(6A) \cdots O(3) ^[d]	2.53(3)	3.063(3)	123(2)
	C(5)–H(5) \cdots Cg(1) ^[c]	2.64	3.561	162

Cg = Ring Centre-of-Gravity (centroid), Cg1 = C9–C14, Cg2 = C16–C21

Symmetry code: [a] $1 - x, -1/2 + y, 1/2 - z$; [b] $-x, -1/2 + y, 1/2 - z$; [c] $1/2 + x, 1/2 - y, -1/2 + z$; [d] $-1/2 + x, 1/2 - y, -1/2 + z$.

Intramolecular O–H \cdots O bond exists with the C4–OH donating its proton to the oxygen of the C6–OH group in both benzoates **3.48** and **1.232**. Detailed molecular organization in crystals of these benzoates **3.48** and **1.232** is described below.

The helical assembly in crystals of **3.48** is formed by the O4–H4A \cdots O3 interaction around 2_1 -screw axis (Figure 3.12A). However, one can also imagine another helix that is formed *via* O6–H6A \cdots O1 hydrogen bonding, again along b-axis (Table 3.8). Actually, these two helices are part of an extended two dimensional sheet created by crystallographic 2_1 screw axis along b-axis. The first helix brings the two reacting groups C2–O-benzoyl group (El) and the C4-hydroxyl group (Nu) of the adjacent molecule closer along the helix axis (Figure 3.12B), but the El \cdots Nu distance (C8 \cdots O4 = 3.532 (2) Å, Table 3.9) is somewhat longer than that seen in crystals of *rac*-dibenzoates **2.28** and **1.234**. However, the angle of approach of Nu to El (O4 \cdots C8–O7 = 106.1°, Table 3.9) is closer to the tetrahedral value. The phenyl ring of the C2–O-benzoyl group is not engaged with any C–H group of the inositol ring in the formation of C–H \cdots π contacts (Table 3.8). The second helical assembly with O6–H6A \cdots O1 interactions makes very long and unfavourable El \cdots Nu contacts (Table 3.8). Furthermore, the entire sheet structure (Figure 3.12C) does not leave a ‘modular’ reaction channel in the crystal lattice for the reaction to proceed. This is in contrast to that observed in crystals of the *rac*-dibenzoate **2.28** (Figure 3.4).

Table 3.9. Geometry of the reacting groups (El \cdots Nu; El = PhC=O; Nu = C4–OH) in crystals of **3.48** and **1.232**

Distance (Å) / Angle (°)	3.48	1.232
C15(C8)⋯O4	3.532(2) ^[a]	3.628(2) ^[b]
∠O4⋯C15(C8)–O8(O7)	106.1(2)	105.6(2)
∠C4–O4⋯C15(C8)	112.1(2)	110.3(2)
∠H4A–O4⋯C15(C8)	77(1)	73(1)

Symmetry code: [a] 1–x, 1/2+y, 1/2–z; [b] –1/2+x, 1/2–y, 1/2+z

In crystals of the orthoformate **1.232**, the one-dimensional assembly although appears to be ‘helical’ (Figure 3.13A), the molecules along the string are actually related by n-glide of the space group symmetry. The O4–H4A⋯O1 hydrogen bonded glide related molecules self-assemble to bring the electrophile and the nucleophile together (Figure 3.13B) with an angle close to the tetrahedral value ($\angle\text{O4}\cdots\text{C8}\text{--}\text{O7} = 105.6^\circ$, Table 3.9) but again with somewhat longer El⋯Nu (C8⋯O4) distance (3.628 Å) as compared to crystals of the *rac*-dibenzoate **2.28** or *rac*-dibenzoate **1.234**.

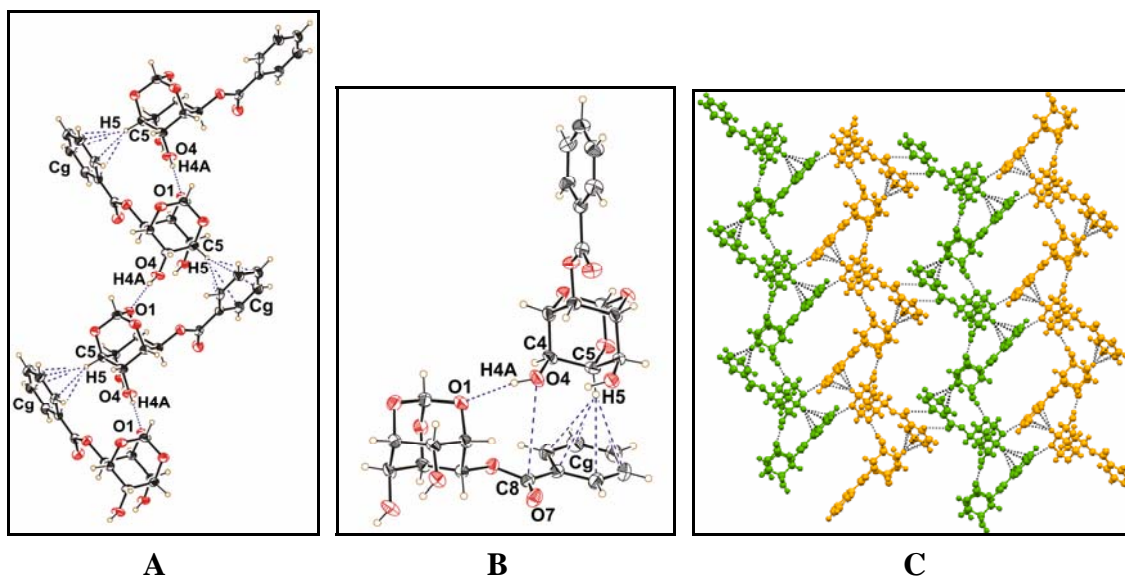


Figure 3.13. (A) Association of molecules in crystals of 2-benzoyl-orthoformate **1.232** via O4–H4A⋯O1 hydrogen bonding interaction, (B) relative orientation of the reacting molecules in crystals of 2-benzoyl-orthoformate **1.232** and (C) linking of helices via C–H⋯O contact forming two dimensional sheet.

However, the geometry of C–H $\cdots\pi$ contacts made by the C5–H5 of the inositol ring with the phenyl ring of the C2–O-benzoyl group from the next molecule is significantly better as compared to that in crystals of **2.28** (Table 3.8).

The self-assembled (diagonal glide related) chains make centrosymmetric inter-chain contacts (essentially of C–H \cdots O type, Figure 3.13C). In addition to O4–H4A \cdots O1 contact, the molecules of **1.232** also form another chain via O6–H6A \cdots O3 bonding as well as via C14–H14 \cdots O6 contact (Figure 3.14) along the diagonal glide related molecules. But along this direction, the reactive groups C6–OH and C2–OBz are not at all in close proximity; the El \cdots Nu distance is 4.452 Å (O6 \cdots C8) and angle O6 \cdots C8–O7 = 154.2° (Table 3.10).

Table 3.10. Geometry of the reacting groups (El \cdots Nu; El = PhC=O; Nu = C6–OH) in crystals of **3.48** and **1.232** along 2_1 -screw and diagonal glide related molecule respectively.

Distance (Å) / Angle (°)	3.48	1.232
C8 \cdots O6	4.599(3) ^[a] , 4.128(3) ^[b]	4.452(3) ^[c]
\angle O6 \cdots C8–O7	149.6(2), 64.9(2)°	154.2(2)°
\angle C6–O6 \cdots C8	77.8(3), 109.2(3)°	140.3(2)°
\angle H6A–O6 \cdots C8	48(1), 104(1)°	101(1)°

Symmetry code: [a] $-x, -1/2+y, 1/2-z$; [b] $1-x, 1/2+y, 1/2-z$; [c] $-1/2+x, 1/2-y, -1/2+z$.

Further, there is no C–H $\cdots\pi$ interaction along these chains. These chains are linked with each other along b-axis by C–H \cdots O contact between the C–H groups of the C2–O-benzoyl group and with one of the orthoformate oxygen (Figure 3.15). Unfavorable approach geometry of the Nu with respect to El and lack of a reaction channel (as in crystals of *rac*-dibenzoate **2.28**) in crystals of **3.48** and **1.232** might well explain the low facility of the acyl transfer reaction as compared to the reactivity in crystals of **2.28** and **1.234**.

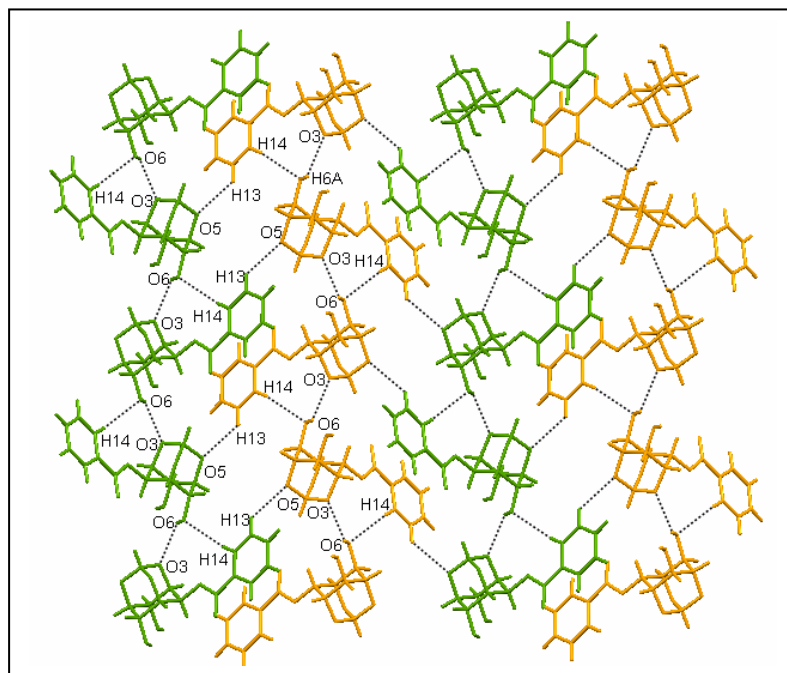


Figure 3.14. Helical assembly formed by $O6-H6A \cdots O3$ and $C14-H14 \cdots O6$ interactions in crystals of **1.232**, which are linked via $C13-H13 \cdots O5$ interhelical contact.

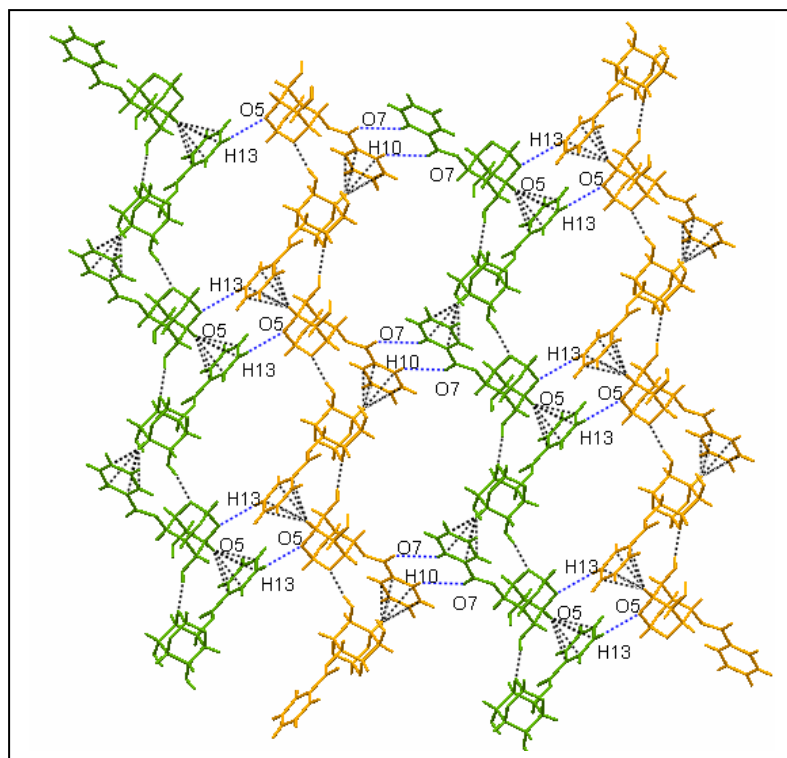


Figure 3.15. Linking of helices in crystals of **1.232** via $C13-H13 \cdots O5$ and $C10-H10 \cdots O7$ contacts forming two dimensional sheet.

3.3. Conclusions.

A comparative study on the intermolecular acyl transfer reactivity in crystals of benzoated inositol derivatives **2.28**, **1.234** **3.2**, **3.48** and **1.232** as well as in solution and an analysis of their crystal structures show that (a) acyl transfer reactivity in crystals is controlled by the relative geometry and juxtaposition of the hydroxyl and ester carbonyl groups; (b) weak intermolecular interactions²⁵ between the reacting molecules in the crystal lattice and (c) packing of molecules in crystals that provide ‘reaction channels’ for the propagation of the reaction. A comparison of the reactivity of mono-benzoates **3.48** and **1.232** in solution and crystals show that molecules that are un-reactive in solution can be coaxed to react in crystals due to proximity of the reacting groups and crystal packing parameters. The crystal structure reactivity correlation described for crystals of the dibenzoate **2.28** is the third example that we have encountered in our laboratory (for first two examples see reference 4. Hence, this spontaneously assembled ‘reactive’ molecular pre-organization in crystals of the dibenzoate **2.28** promises to be valuable while designing reactive crystals that facilitate intermolecular acyl transfer reactions.

Reactions in the solid state and single crystals are attractive as ‘green reactions’ since no solvent is necessary to carry out reactions and also because the possibility of obtaining a single (crystalline?) product starting from a (single crystalline?) starting material cannot be ruled out. Hence solid state reactions can be referred to as a class of potential green futuristic reactions. However, realization of such objectives requires the availability of various types of efficient chemical reactions - those that proceed with ease in the crystalline state. An understanding of polymorphic modifications (of related systems) which could have profound control on reactivity in the crystalline state is also needed to enable engineering of reactive crystals of either a single molecular entity or co-crystals constituted by more than one molecular entities. A survey of the literature pertaining to reactions in crystals shows that there are very few reactions involving group

transfers in crystals. Hence, results presented in this chapter are a valuable addition to the list of well defined group transfer reaction in crystals.

3.4. Experimental.

3.4.1 General methods: General experimental methods are same as in the **section 2.4** (Chapter 2).

3.4.2. X-ray Crystallographic structure determination.

Single crystals of the dibenzoate **2.28**, the monobenzoate **3.48** and **1.232** were obtained from chloroform and light petroleum mixture and good quality crystals were selected using Leica Polarizing microscope. X-ray intensity data were collected on a Bruker SMART APEX CCD diffractometer with omega and phi scan mode, $\lambda_{\text{MoK}\alpha} = 0.71073 \text{ \AA}$ at $T = 297(2) \text{ K}$. All the data were corrected for Lorentzian, polarization and absorption effects using Bruker's SAINT and SADABS programs. SHELX-97³⁰ was used for structure solution and full matrix least squares refinement on F^2 . Hydrogen atoms of the inositol ring and hydroxyl group of **2.28** were located in the difference Fourier map and the rest were included in the refinement as per the riding model, whereas for the 2-benzoate **3.48**, all the H-atoms were located in the difference Fourier map and refined isotropically. Crystal data and details of data collection, structure solution and refinements for **2.28**, **3.48**, and **1.232** are summarized in a Table (see Appendix). All the weak interaction calculations were carried out using PLATON.³¹

Racemic-2,6-di-O-benzoyl-myoinositol-1,3,5-orthobenzoate (2.28): To a solution of *myo*-inositol 1,3,5-orthobenzoate (**1.17**)³² (2.130 g, 8.0 mmol) in dry pyridine (24 mL), freshly prepared benzoyl chloride (2.470 g, 17.6 mmol) was added drop-wise over a

period of 30 min at 0 °C. The reaction mixture was allowed to warm up to room temperature and stirring was continued for 18 h. Solvents were removed under reduced pressure and the residue worked up with ethyl acetate. The crude product was chromatographed (Eluent: ethylacetate: dichloromethane: petroleum ether 1 : 2 : 7) to get the tribenzoate **3.47** (0.385 g, 8%), *rac*-dibenzoate **2.28** (3.130 g, 82%) and the diol **3.48** (0.095 g, 3%).

Data for 2.28:

Mp. = 187-189°C; **IR** (CHCl₃) ν = 1722 (C=O), 3450-3620 (OH) cm⁻¹; **¹H NMR** (CDCl₃, 200 MHz): δ 8.03-8.22 (m, 4H, Ar H), 7.66-7.80 (m, 2H, Ar H), 7.53-7.66 (m, 2H, Ar H), 7.35-7.53 (m, 7H, Ar H), 5.92-6.02 (m, 1H, Ins H), 5.74 (t, 1H, J = 1.6 Hz, Ins H), 4.73-4.92 (m, 3H, Ins H), 4.64-4.71 (m, 1H, Ins H), 2.60 (d, 1H, J = 5.8 Hz, OH) ppm; **¹³C NMR** (CDCl₃, 50.3 MHz): δ 166.3 (C=O), 165.3 (C=O), 136.6 (C_{arom}), 133.6 (C_{arom}), 133.5 (C_{arom}), 129.9 (C_{arom}), 129.8 (C_{arom}), 129.7 (C_{arom}), 129.4 (C_{arom}), 128.9 (C_{arom}), 128.6 (C_{arom}), 128.5 (C_{arom}), 128.1 (C_{arom}), 125.3 (C_{arom}), 107.7 (PhCO₃), 73.1 (Ins C), 71.0 (Ins C), 69.4 (Ins C), 68.5 (Ins C), 67.2 (Ins C), 63.0 (Ins C) ppm.;

Elemental analysis calcd. for C₂₇H₂₂O₈: C 68.35, H 4.67; Found C 68.53; H 4.68 %.

Data for 3.47:

Mp. = 225-226 °C; **IR** (CHCl₃) ν : 1728 (C=O) cm⁻¹; **¹H NMR** (CDCl₃, 200 MHz): δ 8.14-8.22 (m, 2H, Ar H), 7.85-7.94 (m, 4H, Ar H), 7.73-7.83 (m, 2H, Ar H), 7.40-7.66 (m, 8H, Ar H), 7.15-7.25 (m, 4H, Ar H), 5.95-6.05 (t, 2H, J = 4 Hz, Ins H), 5.75-5.81 (t, 1H, J = 1.8 Hz, Ins H), 5.09-5.18 (m, 1H, Ins H), 4.85-4.93 (2H, m, Ins H) ppm; **¹³C NMR** (CDCl₃, 50.3 MHz): δ 166.2 (C=O), 165.2 (C=O), 136.4 (C_{arom}), 133.5 (C_{arom}), 129.9 (C_{arom}), 129.4 (C_{arom}), 128.5 (C_{arom}), 128.4 (C_{arom}), 128.1 (C_{arom}), 125.5 (C_{arom}),

108.2 (PhCO₃), 70.8 (Ins C), 68.5 (Ins C), 67.8 (Ins C), 63.1 (Ins C) ppm; **Elemental analysis** calcd. for C₃₄H₂₆O₉: C 70.58, H 4.53; Found C 70.40, H 4.83 %.

Data for **3.48**:

Mp. = 185-187 °C; **IR** (Nujol) ν : 1715 (C=O), 3350-3600 (OH) cm⁻¹; **¹H NMR** (CDCl₃, 200 MHz): δ 8.10-8.21 (m, 2H, Ar H), 7.55-7.72 (m, 3H, Ar H), 7.33-7.53 (m, 5H, Ar H), 5.64 (t, 1H, J = 1.8 Hz, Ins H), 4.73-4.85 (m, 2H, Ins H), 4.61-4.70 (m, 2H, Ins H), 4.45-4.56 (m, 1H, Ins H), 4.00-4.10 (d, 2H, J = 4.8Hz, 2 OH) ppm; **¹³C NMR** (Acetone-d₆, 50.3 MHz): δ 166.4 (C=O), 138.9 (C_{arom}), 134.2 (C_{arom}), 131.0 (C_{arom}), 130.5 (C_{arom}), 130.0 (C_{arom}), 129.5 (C_{arom}), 128.6 (C_{arom}), 126.5 (C_{arom}), 107.9 (PhCO₃), 74.5 (Ins C), 70.9 (Ins C), 68.7 (Ins C), 64.0 (Ins C) ppm; **Elemental analysis** calcd. for C₂₀H₁₈O₇: C 64.86, H 4.89; Found C 64.52, H 4.59 %.

Reaction of racemic-2,6-di-O-benzoyl-myoinositol-1,3,5-orthobenzoate (2.28) in the solid-state^{4a}: Crystals of dibenzoate **2.28** (0.119 g, 0.25 mmol) and sodium carbonate (0.213 g, 2.0 mmol) were ground together using mortar and pestle and heated in a sealed tube under argon atmosphere at 140 °C for 62 h. The reaction mixture was cooled to room temperature and extracted with chloroform - methanol mixture. The residue obtained from this extract was chromatographed to isolate tribenzoate **3.47** (0.071 g, 49%) and diol **3.48** (0.044 g, 48%).

Reaction of racemic-2,6-di-O-benzoyl-myoinositol-1,3,5-orthobenzoate (2.28) in the molten state: Racemic dibenzoate **2.28** (0.119 g, 0.25 mmol) was melted and heated (190-195 °C) in a sealed tube under argon atmosphere for 30 min. TLC analysis showed the presence of only the dibenzoate (**2.28**). Finely powdered anhydrous sodium carbonate

(0.213 g, 2 mmol) was then added and heating continued for 12 h. TLC analysis of the reaction mixture showed the presence of several products including dibenzoate **2.28**, tribenzoate **3.47**, 2-benzoate diol **3.48** and triol **1.17**. No attempt was made to separate these products.

Reaction of racemic-2,4-di-O-benzoyl-myoinositol-1,3,5-orthobenzoate (2.28) in

solution: A mixture of dibenzoate **2.28** (0.119 g, 0.25 mmol) and diisopropylethylamine (0.259 g, 2.0 mmol) in dry DMF (3 mL) was stirred at room temperature for 72 h. No reaction was observed. The same reaction when carried out at 130°C for 72 h afforded the tribenzoate **3.47** (0.023 g, 16%) and the diol **3.48** (0.013 g, 14%) along with the unreacted dibenzoate **2.28** (68%).

Reaction of racemic-2,6-di-O-benzoyl-myoinositol-1,3,5-orthoformate³³ (1.234) in

solution: A mixture of di-benzoyl-orthoformate **1.234** (0.2 g, 0.5 mmol) and diisopropylethylamine (0.519 g, 4 mmol) in dry DMF (3 mL) was stirred at room temperature for 120 h. (No products could be detected by TLC at the end of 60 h). The solvents were removed under reduced pressure and the products were isolated by column chromatography (eluent = ethyl acetate: dichloromethane: petroleum ether, 1:1:8) to obtain tribenzoate **3.1** (0.025 g, 10%) and 2-benzoate **1.232** (0.012 g, 8%) as white solids along with the unreacted starting material **1.234** (0.151 g, 76%)

Transesterification of 2-O-benzoyl-myoinositol-1, 3, 5-orthobenzoate (3.48) in the

solid-state: Crystals of 2-benzoyl-orthoformate **1.232** (0.185 g, 0.5 mmol) and sodium carbonate (0.424 g, 4.0 mmol) were ground together to a fine powder and heated at 140 °C under argon atmosphere for 62 h. TLC analysis of the reaction mixture showed the

presence of several products including *rac*-dibenzoate **2.28**, tribenzoate **3.47**, 2-benzoate **3.48** and triol **1.17**. No attempt was made to separate these products.

Transesterification of 2-*O*-benzoyl-*myo*-inositol-1,3,5-orthoformate (1.232**)^{2b} in the solid-state:** Crystals of 2-benzoyl-orthoformate **1.232** (0.196 g, 0.66 mmol) and anhydrous sodium carbonate (0.565 g, 5.33 mmol) were ground together to a fine powder and heated at 140 °C under argon atmosphere for 60 h. The reaction mixture was cooled to room temperature and extracted with chloroform-methanol mixture (1:1, 2 × 10 mL). The residue obtained from this extract was chromatographed using 10% ethyl acetate in petroleum ether to get dibenzoate **1.234** (10%), **Mp.** = 163-165 °C (Lit.³³ **Mp.** = 163-165 °C), tribenzoate **3.1** (6%), **Mp.** = 215-217°C (Lit.³⁴ **Mp.** = 216-218 °C), **9** (9%), **Mp.** = 208-211 °C (Lit.³⁵ **Mp.** = 210-213 °C), axial mono-benzoate **1.233** (11%), orthoformate triol **1.15** (48%) and recovered starting material 2-benzoyl-orthoformate **1.232** (10 %).

Structures of **1.233** and **1.15** were established as their acetate derivatives **3.70** and **3.71**: To a mixture of **1.233** and **1.15** (0.086 g) in dry pyridine (2 mL), acetic anhydride (0.5 mL, 5.18 mmol) was added drop wise at 0 °C over a period of 30 min and the mixture was stirred for 8 h at room temperature. Solvents were removed under reduced pressure and the residue worked up with ethyl acetate. The crude product was chromatographed (eluent: 20% ethyl acetate in petroleum ether) to obtain **3.70** (0.028 g) and **3.71** (0.102 g), **Mp.** = 172-174°C (Lit.³⁶ **Mp.** = 173-174°C).

Data for **3.70**:

Mp. = 167-169 °C; **IR** (CHCl₃): ν = 1738 (C=O) cm⁻¹; **¹H NMR** (CDCl₃, 200 MHz): δ 7.98-8.10 (m, 2H, Ar H), 7.55-7.68 (m, 1H, Ar H), 7.40-7.53 (m, 2H, Ar H), 5.72-5.78 (m, 1H, Ins H), 5.55-5.67 (m, 2H, Ins H), 5.33-5.40 (m, 1H, HCO₃), 4.68-4.78 (m, 1H,

Ins H), 4.45-4.52 (m, 1H, Ins H), 4.35-4.43 (m, 1H, Ins H), 2.24 (s, 3H, CH₃), 1.79 (s, 3H, CH₃) ppm; ¹³C NMR (CDCl₃, 50.3 MHz): δ 170.5 (C=O), 169.0 (C=O), 164.7 (C=O), 133.8 (C_{arom}), 129.7 (C_{arom}), 128.7 (C_{arom}), 128.6 (C_{arom}), 103.0 (HCO₃), 69.2 (Ins C), 69.0 (Ins C), 67.7 (Ins C), 67.5 (Ins C), 66.3 (Ins C), 63.2 (Ins C), 21.0 (CH₃), 20.3 (CH₃) ppm; **Elemental analysis** calcd. for C₁₈H₁₈O₉: C 57.15, H 4.79; Found C 56.79, H 4.68 %.

Racemic-2,4-di-O-tosyl-myo-inositol-1,3,5-orthoformate (3.58): To a solution of the triol **1.15** (2.090g, 10.991 mmol) in dry pyridine (55 mL) tosyl chloride (4.603g, 24.144 mmol) was added and heated at 80 °C for 48 h. Reaction mixture was cooled to room temperature and pyridine was removed by evaporation under reduced pressure. The crude reaction mixture was worked with in dichloromethane and dried over anhydrous sodium sulfate to get gummy compound which was purified by column chromatography (eluent: 30 % ethyl acetate in light petroleum) to afforded *rac*-2,4-di-O-tosyl-myo-inositol-1,3,5-orthoformate (**3.58**) as a white solid (4.681g, 85 %).

Mp. = 112-114 °C (Lit.³⁷ Mp. = 114-115 °C).

D-2,4- and D-2,6-di-O-tosyl-4(6)-O-[-(-)-*ω*-camphanoyl]-myo-inositol-1,3,5-orthoformates (2.59 and dia 2.59): To a solution of *rac*-2,4-di-O-tosyl-myo-inositol 1,3,5-orthoformate (**3.58**) (2.780g, 5.576 mmol) and DMAP (0.05 g) in dry pyridine (30 mL), freshly prepared 1*S*-(-)-camphanoyl chloride (1.812g, 8.363 mmol) was added and heated at 90 °C for 10 h. The reaction mixture was cooled to room temperature and the solvents were removed under reduced pressure. The residue obtained was worked up with dichloromethane to get gummy product. The mixture of diastereomers was isolated by

flash column chromatography (eluent: light petroleum, dichloromethane, ethylacetate mixture (7: 2.7: 0.3) to get D-2,4-di-*O*-tosyl-6-*O*-[(-)- ω -camphanoyl]-*myo*-inositol-1,3,5-orthoformate (**dia 2.59**) (1.678 g, 44 %); **Mp.** = 183-185 °C (Lit.³⁸ **Mp.** = 184-185 °C)

$[\alpha]_{\text{D}}^{27} = -25.44$, C = 1, CDCl₃ (Lit.³⁸ $[\alpha]_{\text{D}}^{25} = -25.4$, C = 1, CHCl₃)

and D-2,6-di-*O*-tosyl-4-*O*-[(-)- ω -camphanoyl]-*myo*-inositol-1,3,5-orthoformate (**2.59**) (1.56 g, 41 %); **Mp.** = 222-224 °C (Lit.³⁸ **Mp.** = 222-225 °C)

$[\alpha]_{\text{D}}^{29} = -7.71$, C = 1, CDCl₃ (Lit.³⁸ $[\alpha]_{\text{D}}^{26} = -7.7$, C = 1, CDCl₃)

and a mixture of both diastereomers (0.31 g, 8 %).

D-2,4-di-*O*-tosyl-*myo*-inositol-1,3,5-orthoformate (ent 3.60): A mixture of D-2,4-di-*O*-tosyl-6-*O*-[(-)- ω -camphanoyl]-*myo*-inositol-1,3,5-orthoformate (**dia 2.59**) (1.402 g, 2.065 mmol) and isobutyl amine (5 mL) in dichloromethane (10 mL) and methanol (10 mL) was refluxed for 8 h. The reaction mixture was cooled to ambient temperature and the solvents were evaporated under reduced pressure. The residue worked up with dichloromethane and dried over anhydrous sodium sulfate. The crude product obtained was purified by column chromatography (eluent: 30% ethylacetate in light petroleum to get D-2,4-di-*O*-tosyl-*myo*-inositol-1,3,5-orthoformate (**ent 3.60**), 0.967 g, 94 %).

Mp. = 111-113 °C (Lit.²⁷ **Mp.** = 112-114 °C).

$[\alpha]_{\text{D}}^{27} = -9.08$ C = 1, CHCl₃

D-2,4-di-*O*-tosyl-6-*O*-benzyl-*myo*-inositol-1,3,5-orthoformate (ent 3.61): To an ice cooled solution of D-2,4-di-*O*-tosyl-*myo*-inositol-1,3,5-orthoformate (**ent 3.60**) (0.951 g, 1.907 mmol) and benzyl bromide (0.34 mL, 2.861 mmol) in dry DMF (10 mL), sodium hydride (0.087 g, 2.175 mmol) was added and stirred at ambient temperature for 30 min.

Excess of sodium hydride was quenched with ice and solvent was removed under reduced pressure. Usual work up with dichloromethane followed by drying over anhyd. sodium sulfate afforded a gummy residue which was purified by column chromatography using 25% ethyl acetate in light petroleum as eluent to get D-2,4-di-*O*-tosyl-6-*O*-benzyl-*myo*-inositol-1,3,5-orthoformate (**ent 3.61**) as a white solid (1.077g, 96 %).

Data for **ent 3.61**:

Mp. = 76-78 °C; $[\alpha]_D^{29} = -8.85$ C = 1, CHCl₃; **¹H NMR** (CDCl₃, 200 MHz): δ 7.67-7.84 (m, 4H, Ar H), 7.21-7.38 (m, 9H, Ar H), 5.43 (d, 1H, $J = 1.3$ Hz, HCO₃), 5.08 (dt, 1H, $J = 4.1$ and 1.7 Hz, Ins H), 4.92 (dt, 1H, $J = 3.27, 1.76$ Hz, Ins H), 4.42-4.64 (q, 2H, $J = 11.6$ Hz, CH₂), 4.33-4.41 (m, 1H, Ins H), 4.24 (dt, 1H, $J = 4.2$ and 1.6 Hz, Ins H), 4.12-4.20 (m, 1H, Ins H), 4.01-4.11 (m, 1H, Ins H), 2.47 (s, 3H, Me), 2.43 (s, 3H, Me) ppm; **¹³CNMR** (CDCl₃, 50.3 MHz): δ 145.6 (C_{arom}), 145.3 (C_{arom}), 136.7 (C_{arom}), 132.7 (C_{arom}), 132.2 (C_{arom}), 130.0 (C_{arom}), 129.9 (C_{arom}), 128.3 (C_{arom}), 127.8 (C_{arom}), 127.7 (C_{arom}), 127.3 (C_{arom}), 102.4 (HCO₃), 72.2 (Ins C), 72.0 (Ins C), 71.2 (CH₂), 69.8 (Ins C), 69.6 (Ins C), 68.6 (Ins C), 67.0 (Ins C), 21.5 (CH₃), 21.4 (CH₃) ppm; **Elemental analysis** calcd. for C₂₈H₂₈O₁₀S₂: C, 57.13; H, 4.79; S, 10.89; Found: C, 57.20; H, 4.88; S, 10.55 %.

D-6-*O*-benzyl-*myo*-inositol-1,3,5-orthoformate (ent 3.62): A mixture of D-2,4-di-*O*-tosyl-6-*O*-benzyl-*myo*-inositol-1,3,5-orthoformate (**ent 3.61**) (1.015 g, 1.724 mmol) and sodium methoxide (0.931 g, 17.234 mmol) in dry methanol (10 mL) was refluxed for 12 h. The reaction mixture was allowed to cool to ambient temperature and methanol was removed under reduced pressure to get a gummy product which was purified by column chromatography (eluent: 1:2 ethyl acetate and light petroleum) to obtain D-6-*O*-benzyl-*myo*-inositol-1,3,5-orthoformate (**ent 3.62**) as a gummy compound (0.445 g, 92 %).

Data for **ent 3.62**:

$[\alpha]_{\text{D}}^{27} = -14.9$, C = 1, Ethanol. Lit.^{27c} $[\alpha]_{\text{D}}^{25} = -16.6$, C = 1, Ethanol; **IR** (neat) $\nu = 3300$ - 3650 cm^{-1} ; **¹H NMR** (CDCl₃, 200 MHz): δ 7.28-7.45 (m, 5H, Ar H), 5.44 (d, 1H, $J = 1.3$ Hz, HCO₃), 4.61-4.73 (q, 2H, $J = 11.6$ Hz, CH₂), 3.39-4.45 (m, 2H, Ins H), 4.18-4.32 (m, 3H, Ins H), 4.09 (d, 1H, $J = 9.5$ Hz, Ins H), 3.74 (d, 1H, $J = 10.2$ Hz, OH), 3.21 (d, 1H, $J = 11.2$ Hz, OH) ppm; **¹³C NMR** (CDCl₃, 50.3 MHz): δ 135.8 (C_{arom}), 128.7 (C_{arom}), 128.6 (C_{arom}), 127.9 (C_{arom}), 102.5 (HCO₃), 74.6 (Ins C), 74.0 (Ins C), 72.8 (CH₂), 72.1 (Ins C), 67.7 (Ins C), 67.1 (Ins C), 60.4 (Ins C) ppm; **Elemental analysis** calcd. for C₁₄H₁₆O₆: C, 59.99; H, 5.75; Found: C, 59.84; H, 5.84%.

D-6-O-benzyl-myoinositol (ent 3.63): A mixture of D-6-O-benzyl-myoinositol-1,3,5-orthoformate (**ent 3.62**) (0.07g, 0.249 mmol), trifluoroacetic acid (0.8 mL) and water (0.1 mL) was stirred at room temperature for 24 h. The solvents were removed under reduced pressure and residue co-evaporated with dry toluene. The residue obtained was crystallized from methanol - dichloromethane mixture (1:4) at 0°C to obtain D-4-O-benzyl-myoinositol (**ent 3.63**) as white needle type crystals (0.059 g, 87 %).

Mp. = 175-176 °C (Lit.³⁹ Mp. = 176-178 °C),

$[\alpha]_{\text{D}}^{29} = -6.38$, C=1, Methanol. Lit.³⁹ $[\alpha]_{\text{D}}^{22} = -6^{\circ}$, C = 1, Methanol).

D-2,4-di-O-benzoyl-6-O-benzyl-myoinositol-1,3,5-orthoformate (ent 3.64): To an ice-cooled solution of D-6-O-benzyl-myoinositol-1,3,5-orthoformate (**ent 3.62**) (0.350 g, 1.249 mmol) and DMAP (0.02 g) in dry pyridine (6 mL), benzoyl chloride (1.053 g, 7.491 mmol) was added drop-wise over a period of 10 min. The reaction mixture was stirred for 20 h at ambient temperature and pyridine was removed under reduced

pressure. The residue was worked up with dichloromethane and dried over anhydrous sodium sulfate. The gummy product obtained was purified by column chromatography (eluent: 20 % ethyl acetate in light petroleum) to afford D-2,4-di-*O*-benzoyl-6-*O*-benzyl-*myo*-inositol-1,3,5-orthoformate (**ent 3.64**) as a white solid (0.596 g, 98 %).

Data for **ent 3.64**:

Mp. = 140-143 °C; $[\alpha]_D^{25} = +25.6$, $C=1$, CHCl_3 ; **IR** (CHCl_3) $\nu = 1724 \text{ cm}^{-1}$; **$^1\text{H NMR}$** (CDCl_3 , 200 MHz): 8.13-8.22 (m, 2H, Ar H), 7.87-7.96 (m, 2H, Ar H), 7.43-7.65 (m, 4H, Ar H), 7.21-7.32 (m, 7H, Ar H), 5.80 (dt, 1H, $J = 3.9, 1.6 \text{ Hz}$, Ins H), 5.64-5.70 (m, 2H, Ins H, HCO_3), 4.70-4.75 (m, 1H, Ins H), 4.52-4.69 (m, 4H, CH_2 and Ins H), 4.48 (dt, 1H, $J = 3.8$ and 1.7 Hz) ppm; **$^{13}\text{C NMR}$** (CDCl_3 , 50.3 MHz): δ 166.1 (C=O), 165.3 (C=O), 136.7 (C_{arom}), 133.4 (C_{arom}), 133.3 (C_{arom}), 129.9 (C_{arom}), 129.5 (C_{arom}), 128.9 (C_{arom}), 128.43 (C_{arom}), 128.37 (C_{arom}), 128.0 (C_{arom}), 127.9 (C_{arom}), 103.2 (HCO_3), 73.4 (Ins C), 72.1 (CH_2), 69.9 (Ins C), 69.6 (Ins C), 68.1 (Ins C), 67.4 (Ins C), 64.2 (Ins C) ppm; **Elemental analysis** calcd. for $\text{C}_{28}\text{H}_{24}\text{O}_8$: C, 68.84; H, 4.95; Found: C, 68.93; H, 4.89 %.

D-2,4-di-*O*-benzoyl-*myo*-inositol-1,3,5-orthoformate (ent 3.56): A solution of D-2,4-di-*O*-benzoyl-6-*O*-benzyl-*myo*-inositol-1,3,5-orthoformate (**ent 3.64**) (0.489 g, 1.001 mmol) in methanol (3 mL) and ethyl acetate (3 mL) was hydrogenolyzed in the presence of 20% $\text{Pd}(\text{OH})_2\text{-C}$ (0.040 g) at 50 psi. After 6 h, the reaction mixture was filtered over a short bed of Celite and the Celite was washed with ethyl acetate (10 mL). Removal of the solvents from filtrate and washings under reduced pressure followed by column chromatography (eluent: 1:3 ethyl acetate and light petroleum) afforded D-2,4-di-*O*-benzoyl-*myo*-inositol-1,3,5-orthoformate (**ent 3.56**) as a white solid (0.380 g, 95 %).

Daa for **ent 3.56**:

Mp. = 162-164 °C (crystal obtained from chloroform and light petroleum); $[\alpha]_D^{22} = +66.0$, C = 1, CHCl₃; **IR** (CHCl₃): $\nu = 3540 - 3240, 1701, 1728 \text{ cm}^{-1}$; **¹H NMR** (CDCl₃, 200 MHz): 8.02-8.20 (m, 4H, Ar H), 7.55- 7.70 (m, 2H, Ar H), 7.39-7.54 (m, 4H, Ar H), 5.83 (dt, 1H, $J = \text{Hz}, 3.7, 1.6 \text{ Hz}$, Ins H), 5.62-5.75 (m, 2H, Ins H and HCO₃), 4.70-4.82 (m, 1H, Ins H), 4.56-4.67 (m, 2H, Ins H), 4.45-4.55 (m, 1H, Ins H), 2.69 (d, 1H, $J = 5.8 \text{ Hz}$, OH) ppm; **¹³C NMR** (CDCl₃, 50.3 MHz): δ 166.3 (C=O), 165.3 (C=O), 133.6 (C_{arom}), 129.9 (C_{arom}), 129.8 (C_{arom}), 129.3 (C_{arom}), 128.8 (C_{arom}), 128.6 (C_{arom}), 128.5 (C_{arom}), 102.9 (HCO₃), 71.7 (Ins C), 69.6 (Ins C), 68.5 (Ins C), 68.4 (Ins C), 67.2 (Ins C), 63.8 (Ins C) ppm; **Elemental analysis** calcd. for C₂₁H₁₈O₈: C, 63.31; H, 4.55; Found: C, 63.21; H, 4.29 %.

D-2,6-di-O-tosyl-myo-inositol-1,3,5-orthoformate (D 3.60): A mixture of D-2,6-di-O-tosyl-4-O-[-(-)- ω -camphanoyl]-myo-inositol-1,3,5-orthoformate (**3.59**) (1.004 g, 1.479 mmol), isobutyl amine (4 mL), dichloromethane (8 mL) and methanol (8 mL) was refluxed for 8 h. The reaction mixture was cooled to ambient temperature and the solvents were evaporated under reduced pressure. The residue was worked up with dichloromethane, and dried over anhydrous sodium sulfate and the solvent evaporated under reduced pressure. The crude product obtained was purified by column chromatography (eluent: 30 % ethyl acetate in light petroleum) to obtain D-2,6-di-O-tosyl-myo-inositol-1,3,5-orthoformate (**D 3.60**) (0.708 g, 96 %).

Mp. = 111-113 °C (Lit.³⁸ Mp. = 112-113 °C).

$[\alpha]_D^{26} = +9.13$ (C=1, CHCl₃)

D-2,6-di-*O*-tosyl-4-*O*-benzyl-*myo*-inositol-1,3,5-orthoformate (D 3.61): To an ice cold solution of D-2,6-di-*O*-tosyl-*myo*-inositol-1,3,5-orthoformate (**D 3.60**) (0.701 g, 1.41 mmol) and benzyl bromide (0.25 mL, 2.102 mmol) in dry DMF (8 mL), sodium hydride (0.068 g, 1.7 mmol) was added and stirred at ambient temperature for 30 min. Excess of sodium hydride was quenched with ice and solvent was removed under reduced pressure. Usual work up with dichloromethane followed by drying over anhydrous sodium sulfate and evaporation of the solvent afforded a gummy residue which was purified by column chromatography (eluent: 20% ethyl acetate in light petroleum) to obtain D-2,6-di-*O*-tosyl-4-*O*-benzyl-*myo*-inositol-1,3,5-orthoformate as a white solid (**D 3.61**) (0.778 g, 94 %).

Data for **D 3.61**:

Mp. = 75-78 °C; $[\alpha]_D^{25} = + 8.8$ (C = 1, CHCl₃); **¹H NMR** (CDCl₃, 200 MHz): δ 7.68-7.83 (m, 4H, Ar H), 7.21-7.40 (m, 9H, Ar H), 5.43 (d, 1H, *J* = 1.3 Hz, HCO₃), 5.08 (dt, 1H, *J* = 3.9, 1.64 Hz, Ins H), 4.89-4.96 (m, 1H, Ins H), 4.42-4.65 (q, 2H, *J* = 11.6 Hz, CH₂), 4.35-4.41 (m, 1H, Ins H), 4.24 (dt, 1H, *J* = 4.1, 1.65 Hz, Ins H), 4.12-4.20 (m, 1H, Ins H), 4.01-4.10 (m, 1H, Ins H), 2.47 (s, 3H, CH₃), 2.43 (s, 3H, CH₃) ppm; **¹³C NMR** (CDCl₃, 50.3 MHz): δ 145.6 (C_{arom}), 145.3 (C_{arom}), 136.7 (C_{arom}), 132.9 (C_{arom}), 132.3 (C_{arom}), 130.0 (C_{arom}), 129.9 (C_{arom}), 128.4 (C_{arom}), 127.9 (C_{arom}), 127.8 (C_{arom}), 127.4 (C_{arom}), 126.8 (C_{arom}), 102.5 (HCO₃), 72.3 (Ins C), 72.1 (Ins C), 71.3 (CH₂), 69.9 (Ins C), 69.6 (Ins C), 68.7 (Ins C), 67.1 (Ins C), 21.6 (CH₃), 21.5 (CH₃) ppm; **Elemental analysis** calcd. for C₂₈H₂₈O₁₀S₂: C, 57.13; H, 4.79; S, 10.89; Found: C, 57.4; H, 4.53; S, 11.03 %.

D-4-*O*-benzyl-*myo*-inositol-1,3,5-orthoformate (D 3.62): A mixture of D-2,6-di-*O*-tosyl-4-*O*-benzyl-*myo*-inositol-1,3,5-orthoformate (**D 3.61**) (0.589 g, 1.00 mmol) and sodium methoxide (0.541 g, 10.015 mmol) in dry methanol (8 mL) was refluxed at 12 h. The

reaction mixture was allowed to cool to ambient temperature and methanol was removed under reduced pressure to get a gummy product which was purified by column chromatography (eluent: 1:2 ethyl acetate and light petroleum) to obtain D-4-*O*-benzyl-*myo*-inositol-1,3,5-orthoformate (**D 3.62**) as a gum (0.275 g, 98 %).

Data for **D 3.62**:

$[\alpha]_D^{27} = +15.3$, $C = 1$, Ethsnol; **IR** (neat): $\nu = 3200-3550 \text{ cm}^{-1}$; **$^1\text{H NMR}$** (CDCl_3 , 200 MHz): δ 7.23-7.50 (m, 5H, Ar H), 5.44 (d, 1H, $J = 1.3 \text{ Hz}$, HCO_3), 4.67 (q, 2H, $J = 11.6 \text{ Hz}$, CH_2), 4.38-4.55 (m, 2H, Ins H), 4.18-4.35 (m, 3H, Ins H), 4.09 (s, 1H, Ins H), 3.75 (d, 1H, $J = 10.2 \text{ Hz}$, OH), 3.23 (s, 1H, OH) ppm; **$^{13}\text{CNMR}$** (CDCl_3 , 75.48 MHz): δ 135.8 (C_{arom}), 128.9 (C_{arom}), 128.8 (C_{arom}), 128.0 (C_{arom}), 102.7 (HCO_3), 74.7 (Ins C), 74.2 (Ins C), 73.0 (CH_2), 72.2 (Ins C), 67.8 (Ins C), 67.3 (Ins C), 60.6 (Ins C) ppm; **Elemental analysis** calcd. for $\text{C}_{14}\text{H}_{16}\text{O}_6$: C, 59.99; H, 5.75; Found: C, 60.11; H, 5.70 %.

D-4-*O*-benzyl-*myo*-inositol (D 3.63): A mixture of D-4-*O*-benzyl-*myo*-inositol-1,3,5-orthoformate (**D 3.62**) (0.021 g, 0.075 mmol) in trifluoroacetic acid and water (0.4 mL + 0.1 mL) was stirred at room temperature for 24 h. The solvents were removed under reduced pressure and co-evaporated with dry toluene. The residue obtained was crystallized from methanol - dichloromethane mixture (1:4) at 0°C to obtain D-4-*O*-benzyl-*myo*-inositol (**D 3.63**) as white needle type crystals (0.017 g, 84 %).

Mp. = 175-176 $^\circ\text{C}$ (Lit.³⁹ Mp. = 175-177 $^\circ\text{C}$).

$[\alpha]_D^{30} = +6.41$, $C=1$, Methanol. Lit.³⁹ $[\alpha]_D^{22} = +6^\circ$, $C = 1$, Methanol.

D-2,6-di-*O*-benzoyl-4-*O*-benzyl-*myo*-inositol-1,3,5-orthoformate (D 3.64): To a cold solution of D-4-*O*-benzyl-*myo*-inositol-1,3,5-orthoformate (**D 3.62**) (0.25 g, 0.89 mmol)

and DMAP (0.01 g) in dry pyridine (4 mL), benzoyl chloride (0.75 g, 0.62 mL, 5.33 mmol) was added drop-wise over a period of 10 min. Stirring was continued for 20 h at ambient temperature and pyridine was removed under reduced pressure. The residue was worked up with dichloromethane and dried over anhydrous sodium sulfate. The gummy product obtained was purified by column chromatography (eluent: 20 % ethyl acetate in light petroleum) to afford D-2,6-di-*O*-benzoyl-4-*O*-benzyl-*myo*-inositol-1,3,5-orthoformate (**D 3.64**) as a white solid (0.418 g, 96 %).

Data for **D 3.64**:

Mp. = 140-142 °C; $[\alpha]_D^{27} = -25.02$, $C = 1$, CHCl_3 ; **IR** (CHCl_3) $\nu = 1722 \text{ cm}^{-1}$; **$^1\text{H NMR}$** (CDCl_3 , 200 MHz): 8.13-8.21 (m, 2H, Ar H), 7.87-7.97 (m, 2H, Ar H), 7.43- 7.68 (m, 4H, Ar H), 7.20-7.33 (m, 7H, Ar H), 5.80 (dt, $J = 4.0, 1.8 \text{ Hz}$ 1H, Ins H), 5.64-5.70 (m, 2H, Ins H, HCO_3), 4.69-4.76 (m, 1H, Ins H), 4.52-4.68 (m, 4H, Ins H), 4.48 (dt, 1H, $J = 3.8, 1.6 \text{ Ins H}$) ppm; **$^{13}\text{C NMR}$** (CDCl_3 , 50.3 MHz): δ 166.1 (C=O), 165.3 (C=O), 136.7 (C_{arom}), 133.4 (C_{arom}), 133.3 (C_{arom}), 129.9 (C_{arom}), 129.5 (C_{arom}), 128.9 (C_{arom}), 128.4 (C_{arom}), 128.3 (C_{arom}), 128.0 (C_{arom}), 127.9 (C_{arom}), 103.2 (HCO_3), 73.4 (Ins C), 72.1 (CH_2), 69.9 (Ins C), 69.6 (Ins C), 68.1 (Ins C), 67.4 (Ins C), 64.2 (Ins C) ppm; **Elemental analysis** calcd. for $\text{C}_{28}\text{H}_{24}\text{O}_8$: C, 68.84; H, 4.95; Found: C, 68.57; H, 4.61 %.

D-2,6-di-*O*-benzoyl-*myo*-inositol-1,3,5-orthoformate (D 3.56**):** A solution of D-2,6-di-*O*-benzoyl-4-*O*-benzyl-*myo*-inositol-1,3,5-orthoformate (**D 3.64**) (0.3 g, 0.61 mmol) in methanol (2 mL) and ethyl acetate (3 mL) was hydrogenolyzed in the presence of 20% $\text{Pd}(\text{OH})_2\text{-C}$ (0.025 g) at 50 psi. After 6 h, the reaction mixture was filtered over a short bed of Celite and the Celite was washed with ethyl acetate ($2 \times 5 \text{ mL}$). Removal of the solvents from combined filtrate and washings under reduced pressure followed by

column chromatography (eluent: 1:3 ethyl acetate and light petroleum) afforded D-2,6-di-*O*-benzoyl-*myo*-inositol 1,3,5-orthoformate (**D 3.64**) as white solid (0.234 g, 96 %); it was crystallized by slow diffusion of light petroleum vapor into a chloroform solution of the dibenzoate (**D 3.64**) in a closed container at rt.

Data for **D 3.64**:

Mp. = 163-165 °C; $[\alpha]_D^{27} = -65.9$, $C = 1$, CHCl_3 ; **IR** (CHCl_3): $\nu = 3412, 1722, 1703 \text{ cm}^{-1}$
 $^1\text{H NMR}$ (CDCl_3 , 200 MHz): δ 8.10-8.20 (m, 2H, Ar H), 7.99-8.09 (m, 2H, Ar H), 7.54-7.66 (m, 2H, Ar H), 7.40-7.52 (m, 4H, Ar H), 5.84 (dt, 1H, $J = 4.0, 1.8 \text{ Hz}$, Ins H), 5.63-5.70 (m, 2H, Ins H, HCO_3), 4.69-4.81 (m, 1H, Ins H), 4.56-4.67 (m, 2H, Ins H), 4.45-4.54 (m, 1H, Ins H), 2.65 (d, 1H, $J = 5.4 \text{ Hz}$, OH) ppm; **$^{13}\text{C NMR}$** (CDCl_3 , 50.3 MHz): δ 166.3 (C=O), 165.3 (C=O), 133.7 (C_{arom}), 133.5 (C_{arom}), 129.9 (C_{arom}), 129.8 (C_{arom}), 129.3 (C_{arom}), 128.8 (C_{arom}), 128.6 (C_{arom}), 128.5 (C_{arom}), 102.9 (HCO_3), 71.7 (Ins C), 69.6 (Ins C), 68.5 (Ins C), 68.4 (Ins C), 67.3 (Ins C), 63.8 (Ins C) ppm; **Elemental analysis** calcd. for $\text{C}_{21}\text{H}_{18}\text{O}_8$: C, 63.31; H, 4.55; Found: C, 63.01; H, 4.41 %.

Solid state reaction of D-2,4-di-*O*-benzoyl-*myo*-inositol-1,3,5-orthoformate. A mixture of crystals of D-2,4-di-*O*-benzoyl-*myo*-inositol-1,3,5-orthoformate (0.04 g) and anhydrous sodium carbonate (0.085) was ground together in to a fine powder using a mortar and a pestle. The resultant contents were heated in a sealed tube under argon atmosphere for 36 h. TLC analysis of the reaction mixture showed the presence of mixture of products and no attempt was made to separate these products.

Crystallization of *rac*-2,4-di-*O*-benzoyl-*myo*-inositol-1,3,5-orthoacetate in the presence of D-2,6-di-*O*-benzoyl *myo*-inositol-1,3,5-orthoformate in chloroform

solvent: Racemic 2,4-di-*O*-benzoyl *myo*-inositol 1,3,5-orthoacetate (0.052 g) and D-2,6-di-*O*-benzoyl *myo*-inositol-1,3,5-orthoformate (0.005 g) were dissolved in chloroform (3 mL). Light petroleum was diffused into this solution in a closed container over 4-5 days at rt. Bunches of sharp needles were obtained (0.044 g) as shown in the Figure 3.8B. The sharp needles (Figure 3.8C) were separated manually and collected (0.037 g). ¹H NMR spectrum of these needles showed that they contained *rac*-2,4-di-*O*-benzoyl *myo*-inositol 1,3,5-orthoacetate and D-2,4-di-*O*-benzoyl *myo*-inositol 1,3,5-orthoformate in the ratio 20 : 1.

Transesterification reaction of Form-II crystals of *rac*-2,4-di-*O*-benzoyl-*myo*-inositol-1,3,5-orthoacetate in solid state: Form-II crystals of the orthoacetate (0.032 g) and anhydrous sodium carbonate (0.07 g) were ground together as a fine powder and heated at 115°C under argon atmosphere for 195 h. The reaction mixture was cooled to room temperature and the products were extracted with chloroform- methanol mixture (10 mL, 1:1). The crude products were separated by preparative TLC to obtain 2,4,6-tri-*O*-benzoyl *myo*-inositol-1,3,5-orthoacetate (**3.3**) (0.017 g, 42 %); **Mp.** = 153-155 °C; Lit.⁴⁰ **Mp.** = 154-155 °C and 2-*O*-benzoyl-*myo*-inositol-1,3,5-orthoacetate (**3.4**) (0.01 g, 42 %). **Mp.** = 156-159 °C; Lit.^{2b} **Mp.** = 160 °C as white solids.

Transesterification reaction of Form-I crystals of *rac*-2,4-di-*O*-benzoyl-*myo*-inositol 1,3,5-orthoacetate (3.2) in solid-state. The reaction was carried out as above using Form-I crystals of the orthoacetate **3.2** (0.103 g, 0.25 mmol) and anhydrous sodium carbonate (0.212 g) at 115°C for 195 h. TLC analysis of the products obtained showed the presence of tribenzoate **3.3**, 2-benzoate **3.4** along with the starting material **3.2** and

two unidentified products. The tribenzoate **3.3** (0.017 g, 13%) and the starting material **3.2** (0.024 g, 23%) were separated by column chromatography using a mixture of ethyl acetate-dichloromethane-petroleum ether (1:1:8) as the eluent.

3.5. References:

1. (a) Wolfrom, M. L.; Thompson, A.; Inatome, M. *J. Amer. Chem. Soc.* **1957**, *79*, 3869-3871; (b) Tejima, S.; Fletcher Jr., H. G. *J. Amer. Chem. Soc.* **1963**, *28*, 2999-3004; (c) Reese, C. B.; Trentham, D. R. *Tetrahedron Lett.* **1965**, *29*, 2467-2472; (d) Tsuda, Y.; Yoshimoto, K. *Carbohydr. Res.* **1981**, *87*, C1-C4; (e) Nicholls, A. W.; Akira, K.; Lindon, J. C.; Farrant, R. D.; Wilson, I. D.; Harding, J.; Killick, D. A.; Nicholson, J. K. *Chem. Res. Toxicol.* **1996**, *9*, 1414-1424; (f) Akira, K.; Uchijima, T.; Hashimoto, T. *Chem. Res. Toxicol.* **2002**, *15*, 765-772.
2. (a) Chung, S-K.; Chang, Y-T. *J. Chem. Commun.* **1995**, 13-14.; (b) Sureshan, K. M.; Shashidhar, M. S. *Tetrahedron Lett.* **2000**, *41*, 4185-4188; (c) Ahm, Y-H.; Chang, Y-T. *Journal of Combinatorial Chem.* **2004**, *6*, 293-296.
3. (a) Chung, S-K.; Chang, Y-T.; Lee, E. J.; Shin, B-G.; Kwon, Y-U.; Kim, K-C; Lee, D. H.; Kim, M-J. *Bioorg. Med. Chem. Lett.* **1998**, *8*, 1503-1506; (b) Chung, S-K.; Kwon, Y-U.; Chang, Y-T.; Sohn, K-H; Shin, J-H; Park, K-H; Hong, B-J.; Chung, I-H. *Bioorg. Med. Chem. Lett.* **1999**, *7*, 2577-2589; (c) Godage, H. Y.; Riley, A. M.; Woodman, T. J.; Potter, B. V. L. *Chem. Commun.* **2006**, 2989-2991.
4. (a) Praveen, T.; Samanta, U.; Das, T.; Shashidhar, M. S.; Charkrabarti, P. *J. Am. Chem. Soc.* **1998**, *120*, 3842-3845; (b) Sarmah, M. P.; Gonnade, R. G.; Shashidhar, M. S.; Bhadbhade, M. M. *Chem. Eur. J.* **2005**, *11*, 2103-2110.
5. Tanaka, K.; Toda, F. *Chem. Rev.* **2000**, *100*, 1025-1074.
6. (a) Welton, T. *Chem. Rev.* **1999**, *99*, 2071-2084; (b) Wasserscheid, P.; Keim, W. *Angew. Chem. Int. Ed. Engl.* **2000**, *39*, 3772-3789; (c) Gholap, A. R.; Venkatesan,

- K.; Pasricha, R.; Daniel, T.; Lahoti, R. J.; Srinivasan, K. V. *J. Org. Chem.* **2005**, *70*, 4869-4872.
7. (a) Kobayashi, S.; Manabe, K.; *Acc. Chem. Res.* **2002**, *35*, 209-217; (b) Lindström, U. M. *Chem. Rev.* **2002**, *102*, 2751-2772; (c) Li, C-J.; Chen, L. *Chem. Soc. Rev.* **2006**, *35*, 68-82.
8. (a) Ohashi, Y.; Yanagi, K.; Kurihara, T.; Sasada, Y.; Ohgo, Y. *J. Am. Chem. Soc.* **1982**, *104*, 6353-6359; (b) Kim, J. H.; Hubig, S. M.; Lindeman, S. V.; Kochi, J. K. *J. Am. Chem. Soc.* **2001**, *123*, 87-95; (c) Garcia-Garibay, M. A. *Acc. Chem. Res.* **2003**, *36*, 491-498; (d) Braga, D.; Grepioni, F. *Angew. Chem. Int. Ed. Engl.* **2004**, *43*, 4002-4011.
9. *Topics in Current Chemistry*, 254, Ed. Fumio Toda, Springer-Verlag Berlin Heidelberg 2005.
10. (a) Cohen, M. D.; Schmidt, G. M. J. *J. Chem. Soc.* **1964**, 1996-2000; (b) Cohen, M. D.; Schmidt, G. M. J.; Sonntag, F. I. *J. Chem. Soc.* **1964**, 2000-2014; (c) Schmidt, G. M. J. *J. Chem. Soc.* **1964**, 2014-2021.
11. (a) Cheung, E.; Netherton, M. R.; Scheffer, J. R.; Trotter, J. *Org. Lett.* **2000**, *2*, 77-80; (b) Braga, D.; Chen, S.; Filson, H.; Maini, L.; Netherton, M. R.; Patrick, B. O.; Scheffer, J. R.; Scott, C.; Xia, W. *J. Am. Chem. Soc.* **2004**, *126*, 3511-3520.
12. Ramamurthy, V.; Venkatesan, K. *Chem. Rev.* **1987**, *87*, 433-481.
13. (a) Boese, R.; Benet-Buchholz, J.; Stanger, A.; Tanaka, K.; Toda, F. *Chem. Commun.* **1999**, 319-320; (b) Toda, F. *Eur. J. Org. Chem.* **2000**, 1377-1386; (c) Tanaka, K.; Takamoto, N.; Tezuka, Y.; Kato, M.; Toda, F. *Tetrahedron* **2001**, *57*, 3761-3767; (d) Friščić, T.; MacGillivray, L. R. *Croatica Chemica Acta* **2006**, *79*, 327-333 and references cited therein.
14. (a) Kuhn, R.; Ruelius, H. W. *Chem. Ber.*, **1950**, *83*, 420-431; (b) Brand, J. C. D.; Rutherford, A. *J. Chem. Soc.*, **1952**, 3927.

Chapter-3

15. (a) Lander, G. D.; *J. Chem. Soc.*, **1903**, 83, 406.; (b) Schulenburg, J. W.; Archer, S.; *Org. React.*, **1965**, 14, 24; (c) Dessolin, M.; Golfier, M. *J. Chem. Soc., Chem. Commun.*, **1986**, 38-39; (d) Dessolin, M.; Eisenstein, O.; Golfier, M.; Prangé, T.; Sautet, P. *J. Chem. Soc., Chem. Commun.* **1992**, 132-134.
16. Smrčina, M.; Vyskočil, Š.; Hanuš, V.; Poláček, M.; Langer, V.; Chew, B. G. M.; Zax, D. B.; Verrier, H.; Harper, K.; Claxton, T. A.; Kočovský, P. *J. Am. Chem. Soc.*, **1996**, 118, 487-488.
17. Venugopalan, P.; Venkatesan, K.; Klausen, J.; Novotny-Bregger, E.; Leumann, C.; Eschenmoser, A.; Dunitz, J. D. *Helv. Chim. Acta.*, **1991**, 74, 662-669.
18. (a) Zimmerman, H. E.; Wilson, J. W. *J. Am. Chem. Soc.*, **1964**, 86, 4036-4042; (b) Zimmerman, H. E.; Hancock, K. G. *J. Am. Chem. Soc.*, **1968**, 90, 3749-3760.
19. Vyas, K.; Manohar, H.; Venkateshan, K. *J. Phys. Chem.*, **1990**, 94, 6069-6073.
20. Sureshan, K. M.; Murakami, T.; Miyasou, T.; Watanabe, Y. *J. Am. Chem. Soc.*, **2004**, 126, 9174-9175.
21. (a) Wöhler, F. Ueber Künstliche Bildung des Harnstoffes. *Ann. Phys. Chem.* **1828**, 12, 253-256. (b) Dunitz, J. D.; Harris, K. D. M.; Johnston, R. L.; Kariudki, B. M.; MacLean, E. J.; Psallidas, K.; Schweizer, W. B.; Tykwinski, R. R. *J. Am. Chem. Soc.* **1998**, 120, 13274-13275.
22. (a) Troup, A. E.; Mitchner, H. *J. Pharm. Sci.* **1964**, 53, 375-379; (b) Jacobs, A. L.; Dilatush, A. E.; Weinstein, S.; Windheuser, J. J. *J. Pharm. Sci.* **1966**, 55, 893-895; (c) Koshy, K. T.; Troup, A. E.; Duvall, R. N.; Conwell, R. N.; Shankle, L. L. *J. Pharm. Sci.* **1967**, 56, 1117-1121.
23. (a) Bürgi, H. B.; Dunitz, J. D.; Shefter, E. *J. Am. Chem. Soc.*, **1973**, 95, 5065-5067; (b) Bürgi, H. B.; Dunitz, J. D.; Shefter, E. *Acta Crystallogr.*, **1974**, B30, 15171527; (c) Bürgi, H. B.; Lehn, J. M.; Wipff, G. J. *J. Am. Chem. Soc.*, **1974**, 96, 1956-1957; (d) Bürgi, H. B.; Dunitz, J. D. *Acc. Chem. Res.*, **1983**, 16, 153-161.

24. (a) Chakrabarti, P.; Pal, D. *Protein Sci.*, **1997**, *6*, 851-859; (b) Marquart, M.; Walter, J.; Deisenhofer, J.; Bode, W.; Huber, R. *Acta Crystallogr.*, **1983**, *B39*, 480-490.
25. (a) Nishio, M.; Hirota, M.; Umezawa, Y. *The CH/ π Interaction: Evidence, Nature and Consequences*, Wiley-VCH, **1998**; (b) Boese, R.; Clark, T.; Gavezzotti, A. *Helv. Chim. Acta* **2003**, *86*, 1085-1100; (c) Nishio, M. *Cryst. Engg. Comm.* **2004**, *6*, 130-158.
26. Garegg, P.J.; Lindberg, B. *Carbohydr. Res.* **1985**, *139*, 209-215.
27. (a) Vacca, J. P.; deSolms, S. J.; Huff, J. R. *J. Am. Chem. Soc.* **1987**, *109*, 3478-3479; (b) Ozaki, S.; Kondo, Y.; Nakahira, H.; Yamaoka, S.; Watanabe, Y. *Tetrahedron Lett.* **1987**, *28*, 4691-4694; (c) Baudin, G.; Glänzer, B. I.; Swaminathan, K. S.; Vasella, A. *Helv. Chim. Acta.* **1988**, *71*, 1367-1378; (d) Gou, D-M.; Liu, Y-C.; Chen, C-S. *Carbohydr. Res.* **1992**, *234*, 51-64; (e) Rudolf, M. T.; Kaiser, T.; Guse, A. H.; Mayr, G. W.; Schultz, C. *Liebigs Ann./Recueil* **1997**, 1861-1869; (f) Leung, L.W.; Bittman, R. *Carbohydr. Res.* **1998**, *305*, 171-179.
28. Huang, J.; Chen, S.; Guze, I. A.; Yu, L. *J. Amer. Chem. Soc.* **2006**, *128*, 11985-11992.
29. Gonnade, R. G.; Bhadbhade, M. M.; Shashidhar, M. S. *Chem. Commun.* **2004**, 2530-2531.
30. Sheldrick, G. M. SHELX97, Program for crystal structure solution and refinement, University of Göttingen (Germany) **1997**.
31. Spek, A. L.; PLATON, Bijvoet Centre for Biomedical Research, Vakgroep Kristal-en Structure-Chemie, University of Utrecht (The Netherlands) **1990**.
32. Bhosekar, G.; Murali, C.; Gonnade, R. G.; Shashidhar, M. S.; Bhadbhade, M. M. *Cryst. Growth Des.* **2005**, *5*, 1977-1982.
33. Benarjee, T.; Shashidhar, M. S. *Tetrahedron Lett.* **1994**, *43*, 8053-8056.
34. Das, T.; Shashidhar, M. S. *Carbohydr. Res.* **1997**, *297*, 243-249.

Chapter-3

35. Das, T.; Shashidhar, M. S. *Carbohydr. Res.* **1998**, *308*, 165-168.
36. Lee, H. W.; Kishi, Y. *J. Org. Chem.* **1985**, *50*, 4402-4404.
37. Sureshan, K. M.; Shashidhar, M. S.; Praveen, T.; Gonnade, R. G.; Bhadbhade, M. M. *Carbohydr. Res.* **2002**, *337*, 2399-2410.
38. Sarmah, M. P.; Shashidhar, M. S.; Sureshan, K. M.; Gonnade, R. G.; Bhadbhde, M. M. *Tetrahedron* **2005**, *61*, 4437-4446.
39. Garreg, P. J.; Svensson, S. C. T. *Carbohydr. Res.* **1985**, *139*, 209-215.
40. Praveen, T.; Shashidhar, M. S. *Carbohydr. Res.* **2001**, *330*, 409-411.

3.6. Appendix.**Appendix index.**

Sl. No.	Spectrum / Diagram / Table / Compound No.	Page No.
1.	Packing of helices in crystals of 2.28	270
2.	Crystal data table of 2.28 , 3.48 and 1.232 .	271
3.	ORTEP and crystal data table of D-3.56	272
4.	Crystal data table of ent-3.56	273
5.	Crystal data table of Form-II of 3.2	274
6.	¹ H NMR and ¹ H NMR- D ₂ O exchange spectra of 2.28	275
7.	¹³ C NMR and DEPT spectra of 2.28	276
8.	IR spectrum of 2.28	277
9.	¹ H NMR spectrum of 3.47	277
10.	¹³ C NMR and DEPT spectra of 3.47	278
11.	IR spectrum of 3.47	279
12.	¹ H NMR spectrum of 3.48	279
13.	¹ H NMR- D ₂ O exchange and ¹³ C NMR spectra of 3.48	280
14.	DEPT and IR spectra of 3.48	281
15.	¹ H NMR and ¹³ C NMR spectra of 3.70	282
16.	DEPT and IR spectra of 3.70	283
17.	¹ H NMR and ¹³ C NMR spectra of ent 3.61	284
18.	DEPT spectrum of ent 3.61	285
19.	¹ H NMR spectrum of ent 3.62	285
20.	¹ H NMR- D ₂ O exchange and ¹³ C NMR spectra of ent 3.62	286
21.	DEPT and IR spectra of ent 3.62	287
22.	¹ H NMR and ¹³ C NMR spectra of ent 3.64	288
23.	DEPT and IR spectra of ent 3.64	289
24.	¹ H NMR and ¹ H NMR- D ₂ O exchange spectra of ent 3.56	290
25.	¹³ C NMR and DEPT spectra of ent 3.56	291

26	IR spectrum of ent 3.56	292
27	^1H NMR spectrum of D 3.61	292
28	^{13}C NMR and DEPT spectra of D 3.61	293
29	IR spectrum of D 3.61	294
30	^1H NMR spectrum of D 3.62	294
31	^1H NMR- D_2O exchange and ^{13}C NMR spectra of D 3.62	295
32	DEPT and IR spectra of D 3.62	296
33	^1H NMR and ^{13}C NMR spectra of D 3.64	297
34	DEPT and IR spectra of D 3.64	298
35	^1H NMR and ^1H NMR- D_2O exchange spectra of D 3.56	299
36	^{13}C NMR and DEPT spectra of D 3.56	300
37	IR spectrum of D 3.56	301

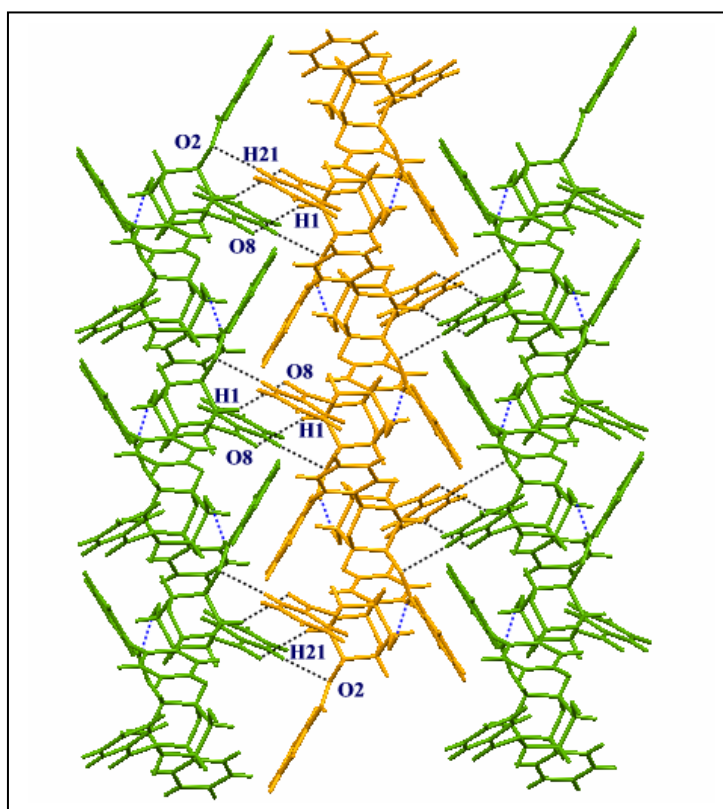
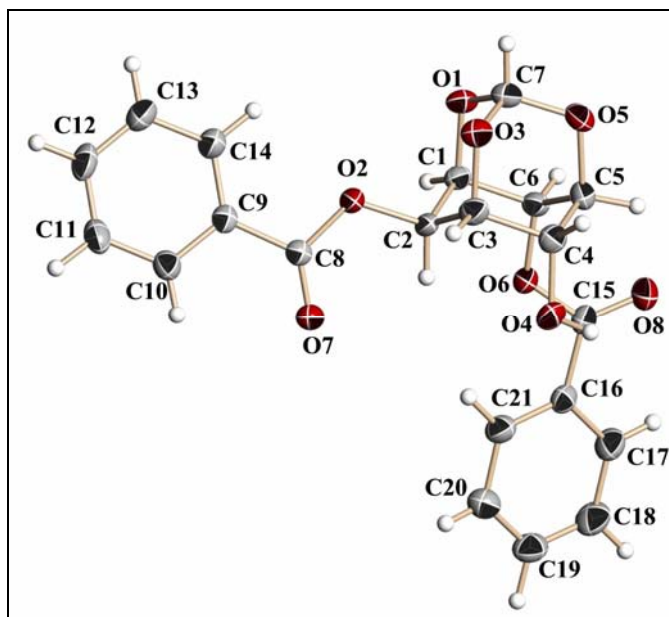


Figure 3.16. Packing of helices in crystals of orthobenzoate **2.28** showing interhelical contacts.

Crystal data table of dibenzoate **2.28**, and monobenzoates **3.48** and **1.232**.

Crystal data	2.28	3.48	1.232
Formula	C ₂₇ H ₂₂ O ₈	C ₂₀ H ₁₈ O ₇	C ₁₄ H ₁₄ O ₇
<i>M_r</i>	474.45	370.34	294.25
Crystal size, mm	0.38 x 0.33 x 0.28	0.41x0.15x0.13	0.51x0.23x0.22
Temp. (K)	297(2)	297(2)	297(2)
Crystal system	monoclinic	orthorhombic	monoclinic
space group	<i>P</i> 2 ₁ / <i>c</i>	<i>P</i> 2 ₁ 2 ₁ 2 ₁	<i>P</i> 2 ₁ / <i>n</i>
A [Å]	14.819(2)	6.2886(17)	6.198(3)
B [Å]	9.4652(14)	11.361(3)	17.764(10)
C [Å]	16.977(3)	23.481(6)	11.748(7)
β [°]	103.908(3)	90	91.599(14)
V [Å ³]	2311.5(6)	1677.6(8)	1293.0(13)
Z	4	4	4
F(000)	992	776	616
D calc [g cm ⁻³]	1.363	1.466	1.512
μ [mm ⁻¹]	0.101	0.112	0.123
absorption correction	multi-scan	multi-scan	multi-scan
T _{min}	0.9628	0.9552	0.9400
T _{max}	0.9726	0.9851	0.9733
reflns. collected	11265	12068	6204
Unique reflns.	4053	2963	2263
Observed reflns.	3254	2498	1989
index range	-16⇒h⇒17, -9⇒k⇒11, -15⇒l⇒20	-7⇒h⇒7, -13⇒k⇒8, -27⇒l⇒26	-5⇒h⇒7, -21⇒k⇒19, -7⇒l⇒13
R ₁ [I>2σ(I)]	0.0384	0.0396	0.0464
wR ₂	0.0953	0.0757	0.1071
R ₁ (all data)	0.0509	0.0501	0.0539
WR ₂ (all data)	0.1032	0.0788	0.1110
goodness-of-fit	1.037	1.048	1.128
Δ ρ _{max} , Δ ρ _{min} (eÅ ⁻³)	-0.174, 0.157	-0.126, 0.143	-0.173, 0.153
CCDC number	617709	617710	617711

ORTEP diagram of **D 3.56**Crystal data table of **D 3.56**

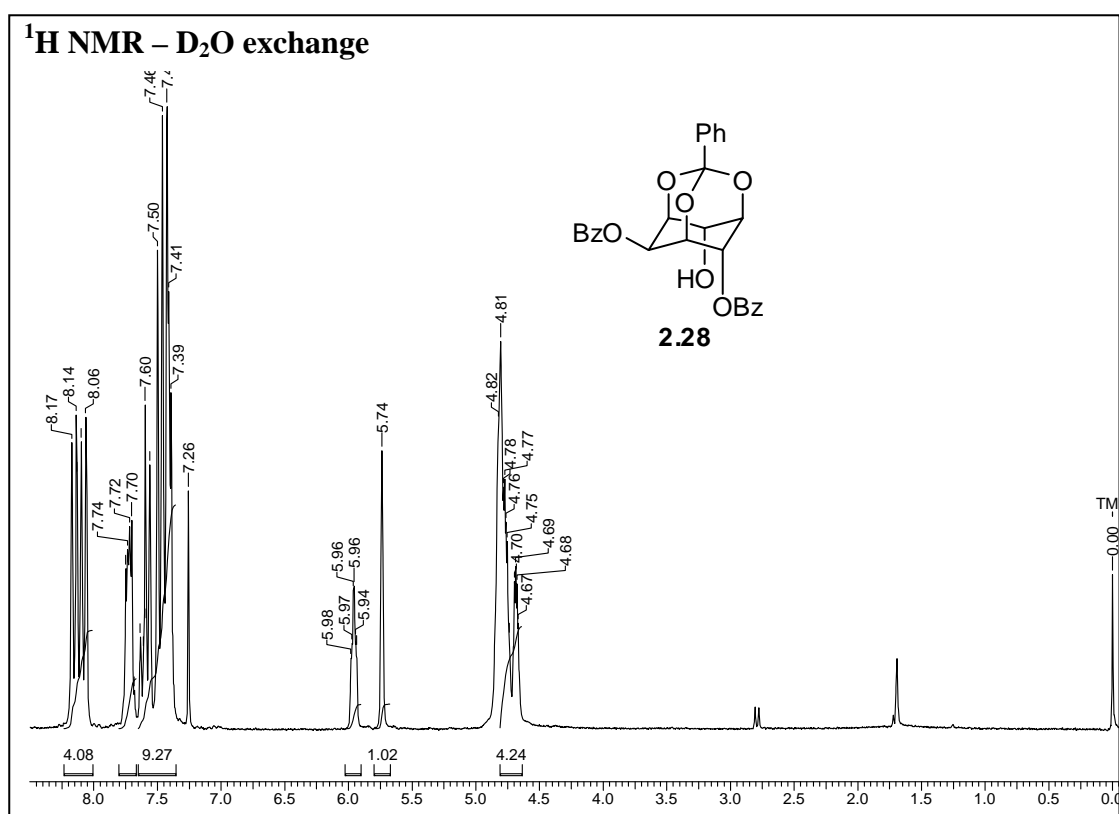
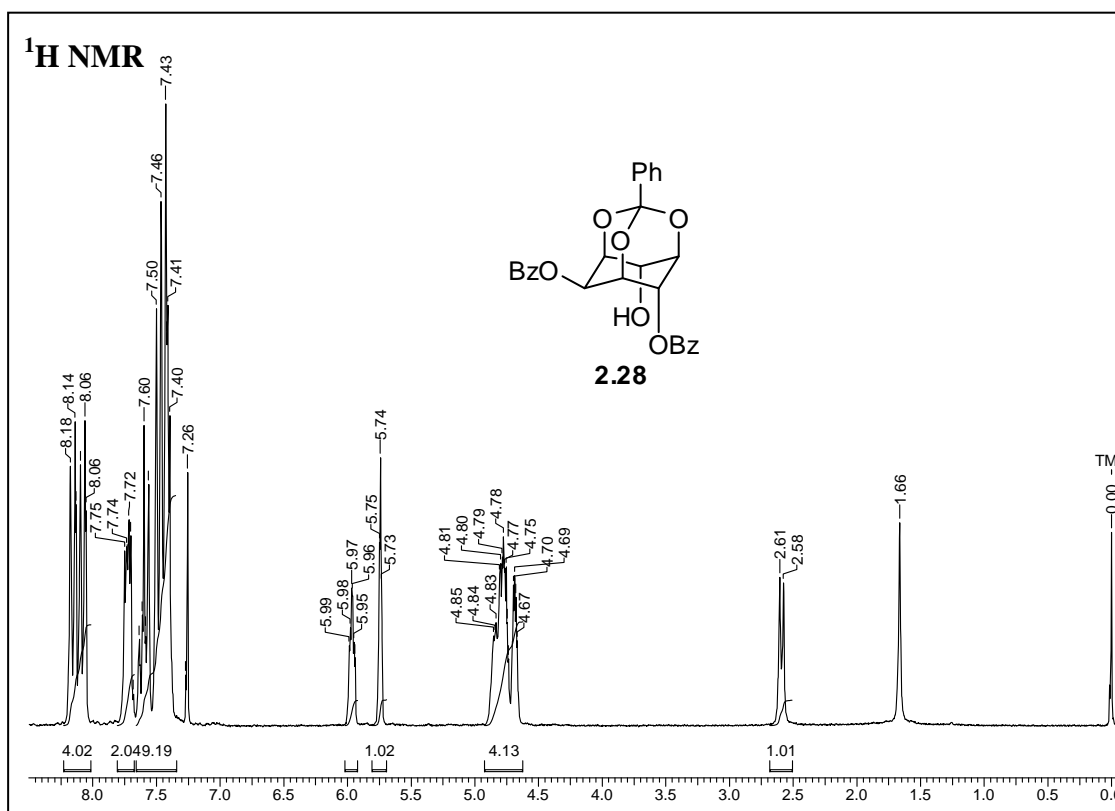
Identification code	D 3.56 crystals from CHCl ₃ -light petroleum
Empirical formula	C ₂₁ H ₁₈ O ₈
Formula weight	398.35
Temperature	297(2) K
Wavelength	0.71073 Å
Crystal system, space group	Orthorhombic, P 212121
Unit cell dimensions	a = 5.914(2) Å b = 16.229(6) Å c = 18.957(7) Å
Volume	1819.3(12) Å ³
Z, Calculated density	4, 1.454 Mg/m ³
Absorption coefficient	0.113 mm ⁻¹
F(000)	832
Crystal size	0.69 x 0.19 x 0.12 mm
θ range for data collection	2.15 to 25.00°
Limiting indices	-6 ≤ h ≤ 7, -19 ≤ k ≤ 19, -22 ≤ l ≤ 22
Reflections collected / unique	11640 / 3200 [R(int) = 0.0290]
Completeness to θ = 25.00	99.8 %
Absorption correction	Semi-empirical from equivalents
Max. and min. transmission	0.9862 and 0.9265
Refinement method	Full-matrix least-squares on F ²
Data / restraints / parameters	3200 / 0 / 334
Goodness-of-fit on F ²	1.099
Final R indices [I > 2σ (I)]	R1 = 0.0344, wR2 = 0.0779
R indices (all data)	R1 = 0.0379, wR2 = 0.0797
Absolute structure parameter	-0.2(9)
Largest diff. peak and hole (ρ _{max} & ρ _{min})	0.127 and -0.119 e.Å ⁻³

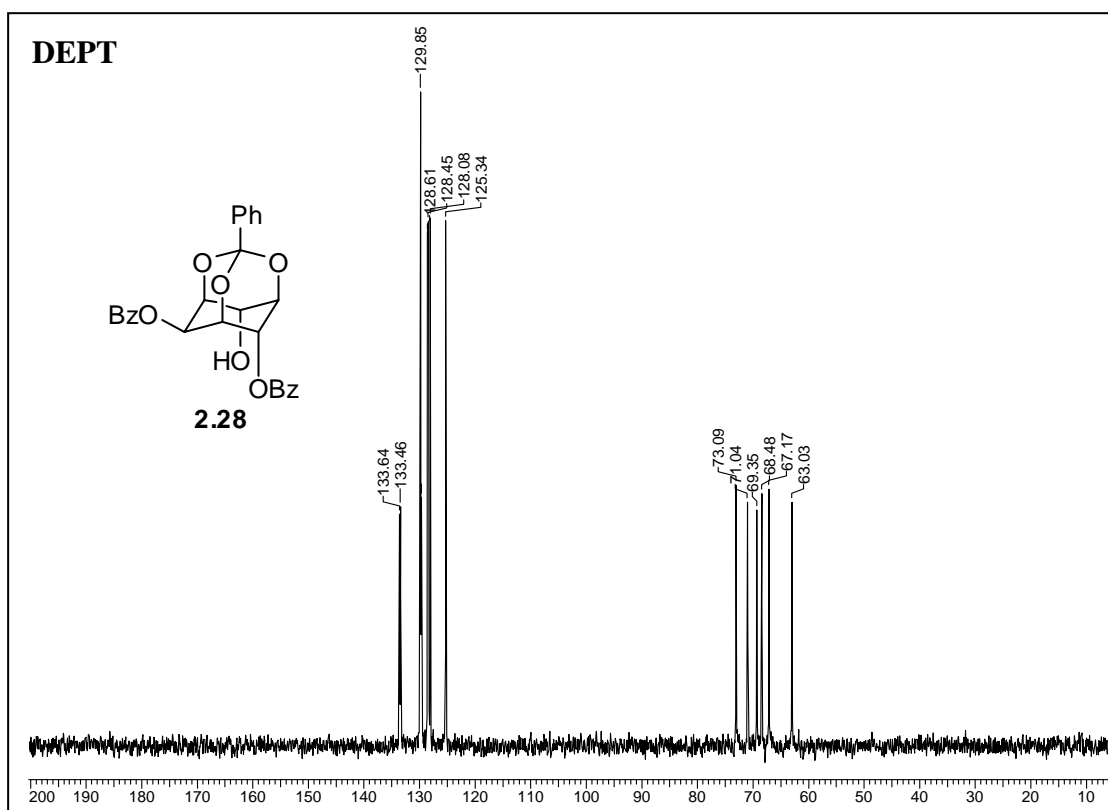
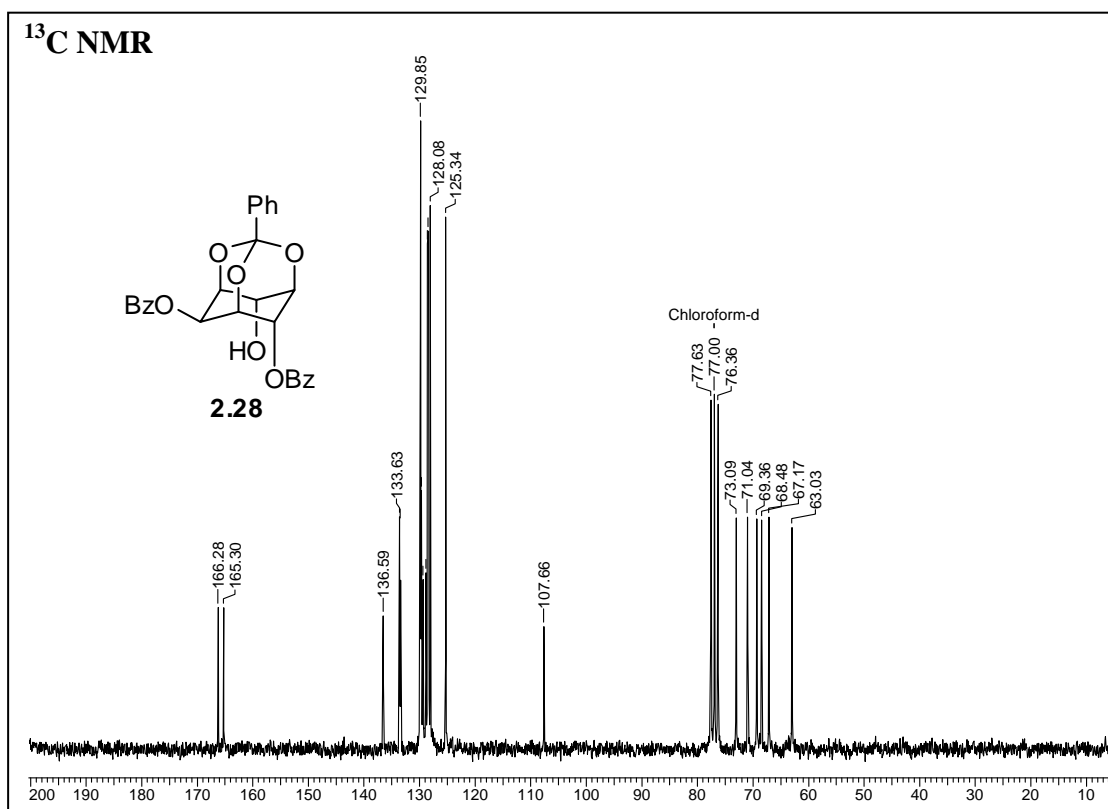
Crystal data table of **ent 3.56**

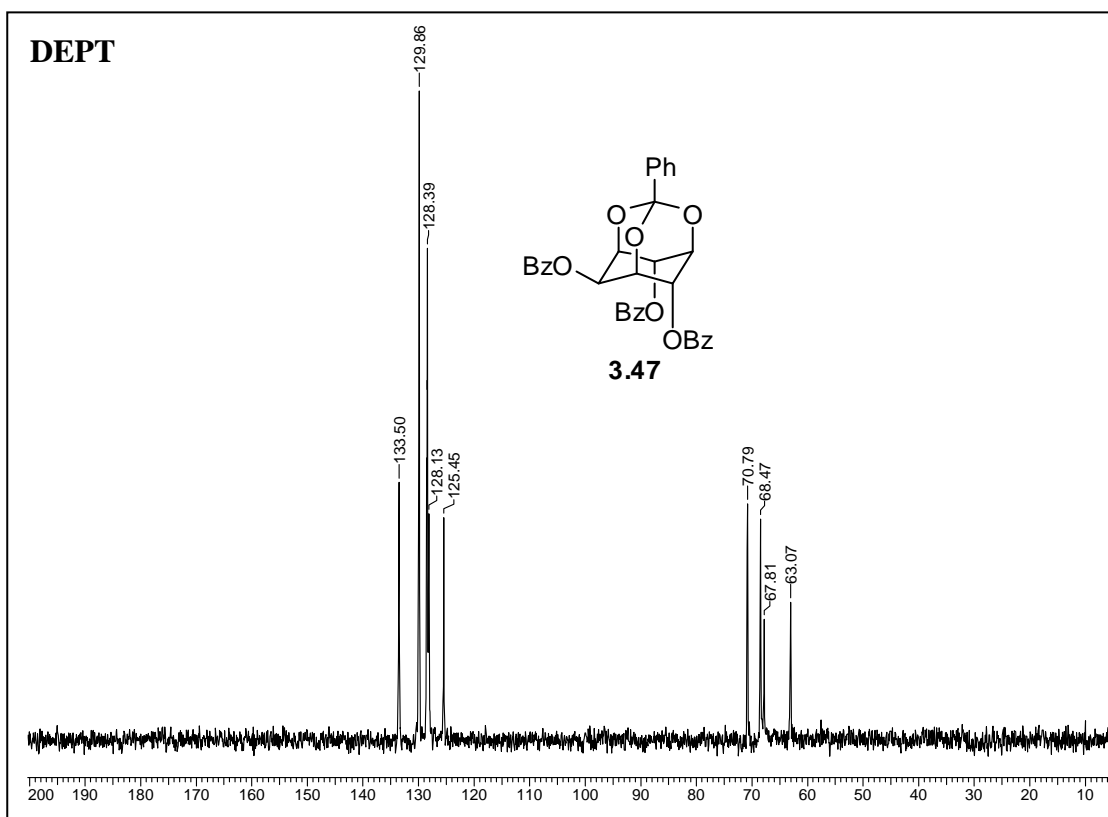
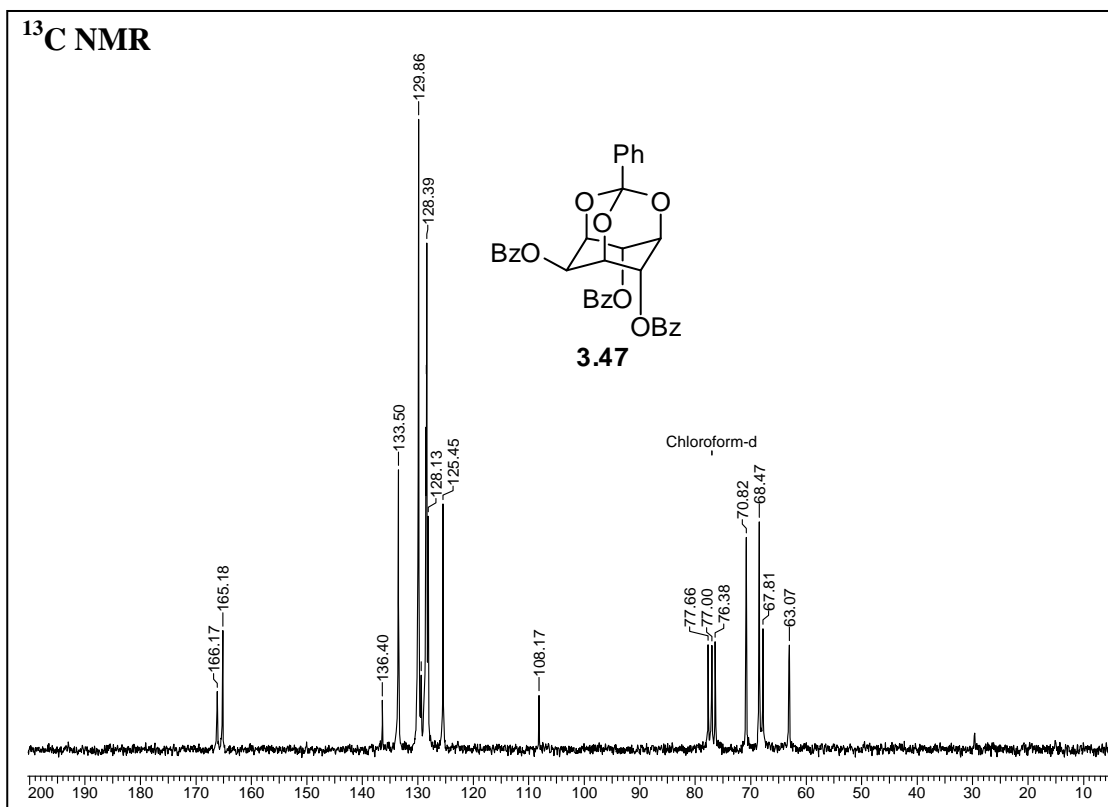
Identification code	ent 3.56 crystals from CHCl ₃ -light petroleum
Empirical formula	C ₂₁ H ₁₈ O ₈
Formula weight	398.35
Temperature	297(2) K
Wavelength	0.71073 Å
Crystal system, space group	Orthorhombic, P 2 ₁ 2 ₁ 2 ₁
Unit cell dimensions	a = 5.9105(17) Å b = 16.200(4) Å c = 18.861(5) Å
Volume	1805.9(9) Å ³
Z, Calculated density	4, 1.465 Mg/m ³
Absorption coefficient	0.114 mm ⁻¹
F(000)	832
Crystal size	0.50 x 0.12 x 0.11 mm
θ range for data collection	1.66 to 25.00°
Limiting indices	-7<=h<=7, -16<=k<=19, -18<=l<=22
Reflections collected / unique	8909 / 3161 [R(int) = 0.0334]
Completeness to θ = 25.00	99.9 %
Absorption correction	Semi-empirical from equivalents
Max. and min. transmission	0.9876 and 0.9454
Refinement method	Full-matrix least-squares on F ²
Data / restraints / parameters	3161 / 0 / 266
Goodness-of-fit on F ²	1.176
Final R indices [I>2σ (I)]	R1 = 0.0520, wR2 = 0.0838
R indices (all data)	R1 = 0.0654, wR2 = 0.0872
Absolute structure parameter	-0.6(14)
Largest diff. peak and hole (ρ _{max} & ρ _{min})	0.150 and -0.174 e. Å ⁻³

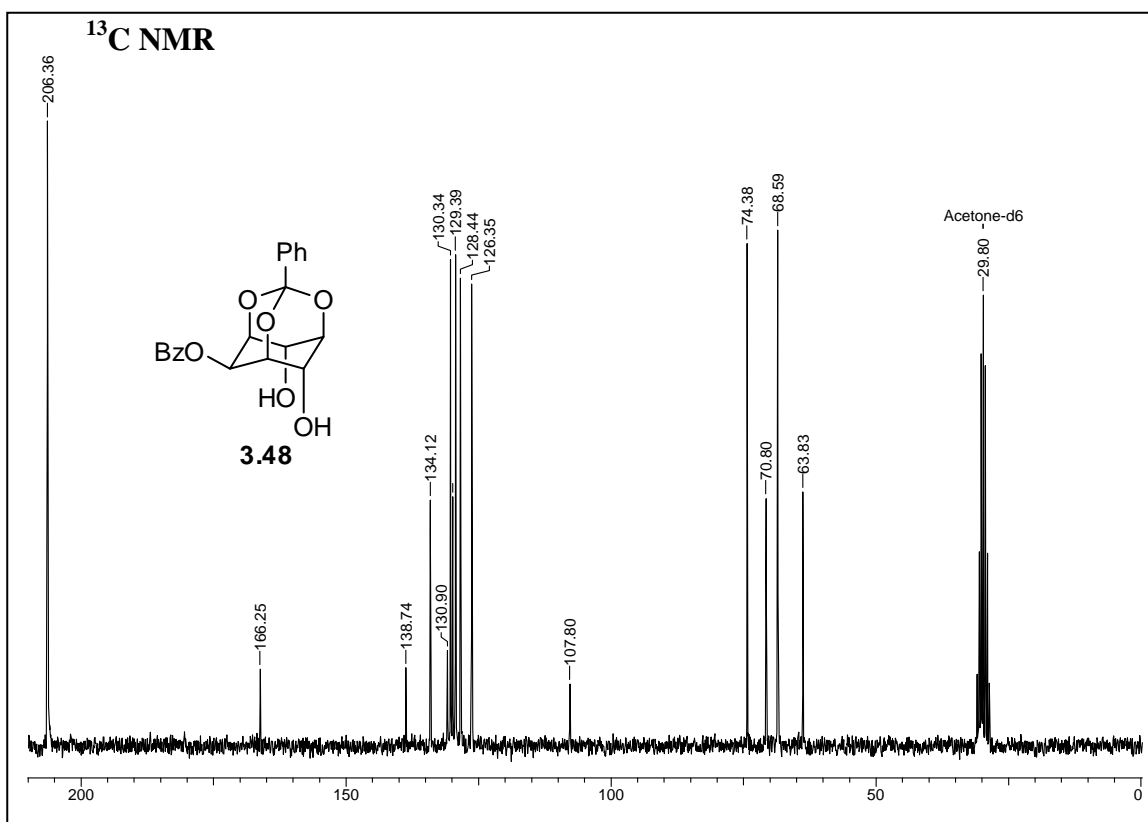
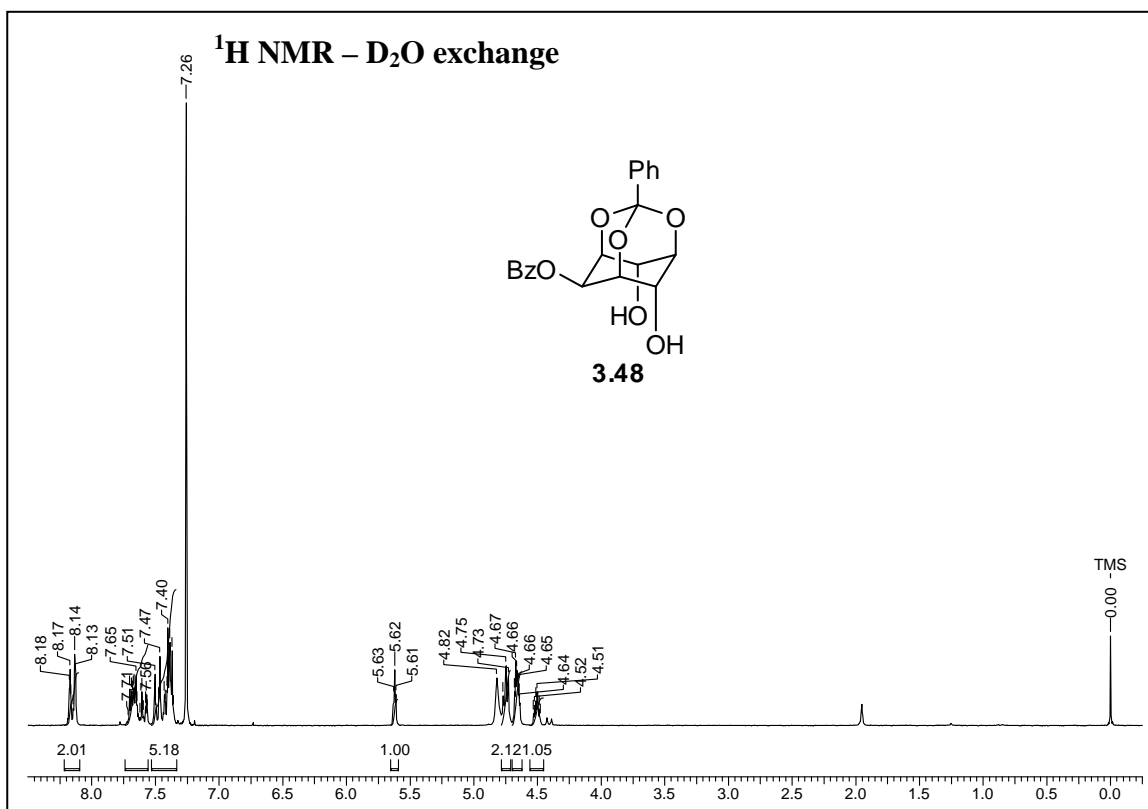
Crystal data table of Form-II of **3.2**:

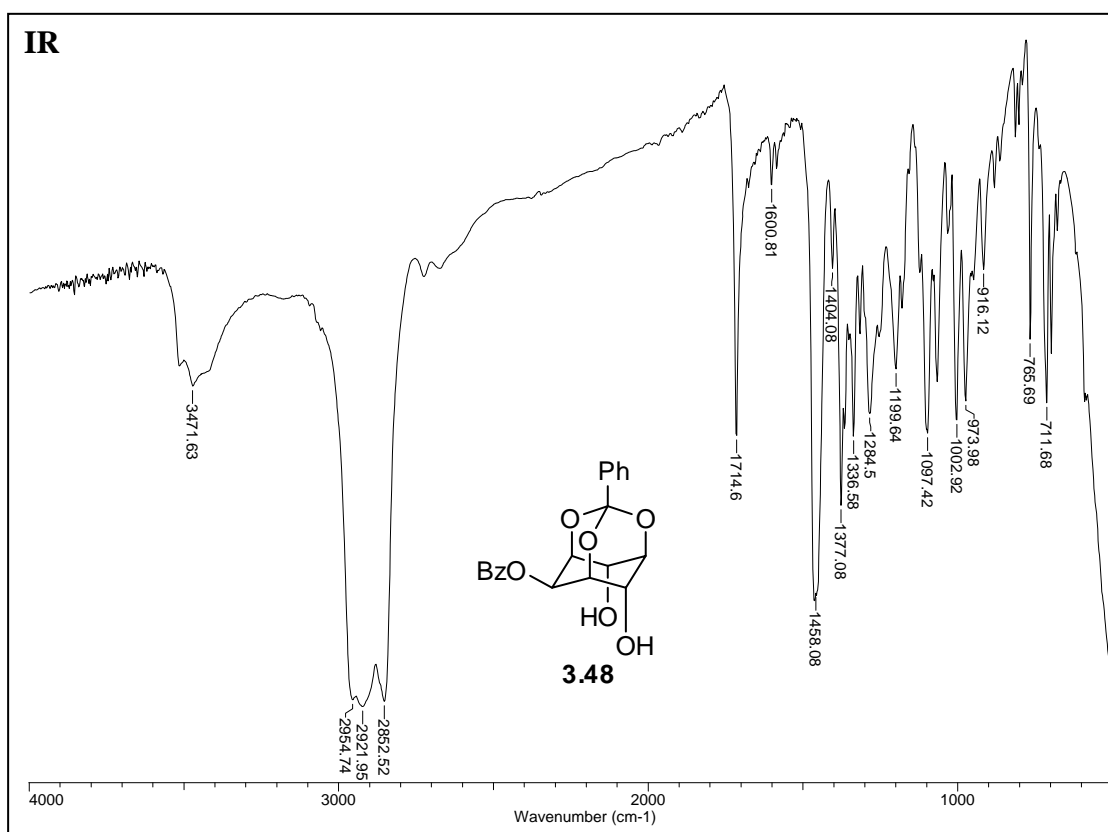
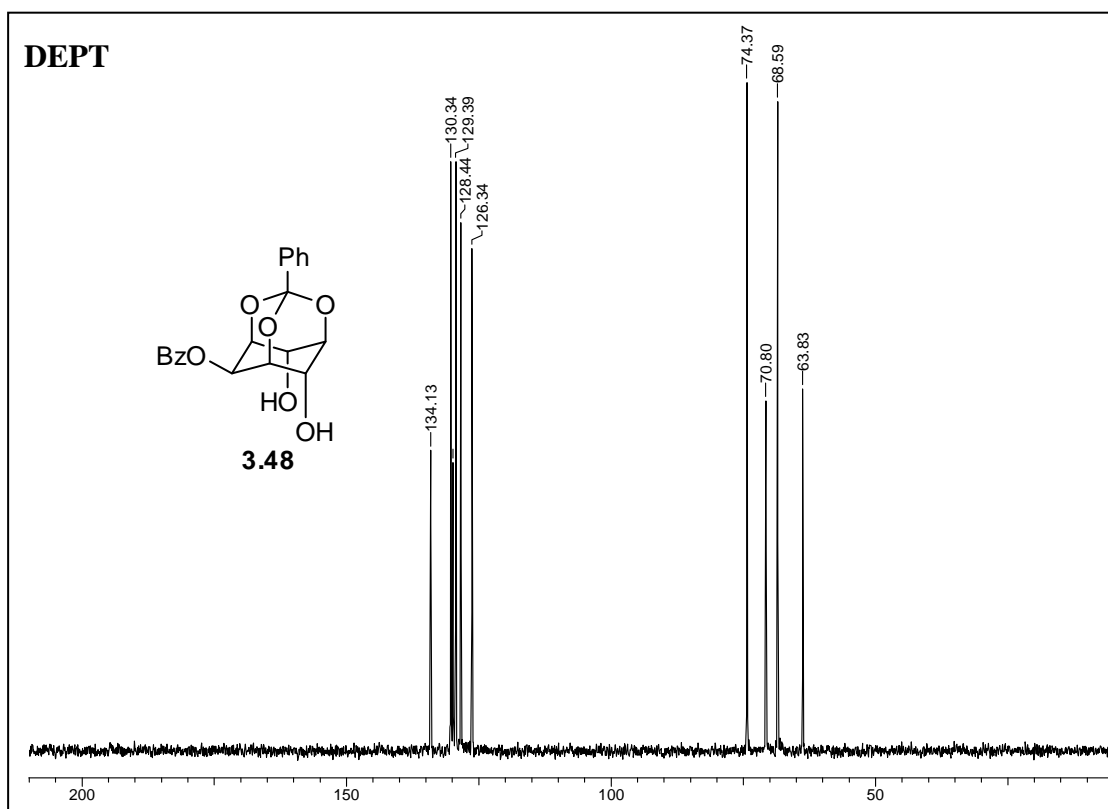
Identification code	Form-II crystals from CHCl ₃ -light petroleum
Formula	C ₂₂ H ₂₀ O ₈
M_r	412.38
Crystal size, mm	0.78 x 0.10 x 0.08
Temp. (K)	297(2)
Crystal system	monoclinic
space group	<i>C2/c</i>
A [Å]	27.591(7)
B [Å]	9.383(3)
C [Å]	16.938(4)
β [°]	117.346(4)
V [Å ³]	3895.0(18)
Z	8
F(000)	1728
D calc [g cm ⁻³]	1.406
μ [mm ⁻¹]	0.108
absorption correction	multi-scan
T_{\min}	0.9205
T_{\max}	0.9912
Reflections collected	13715
Unique reflections	3422
Observed reflections	2857
index range	-32 \Rightarrow h \Rightarrow 32, -11 \Rightarrow k \Rightarrow 11, -20 \Rightarrow l \Rightarrow 19
R ₁ [I>2 σ (I)]	0.0693
wR ₂	0.1468
R ₁ (all data)	0.0834
WR ₂ (all data)	0.1534
goodness-of-fit	1.214
$\Delta \rho_{\max}, \Delta \rho_{\min}$ (eÅ ⁻³)	-0.259, 0.178

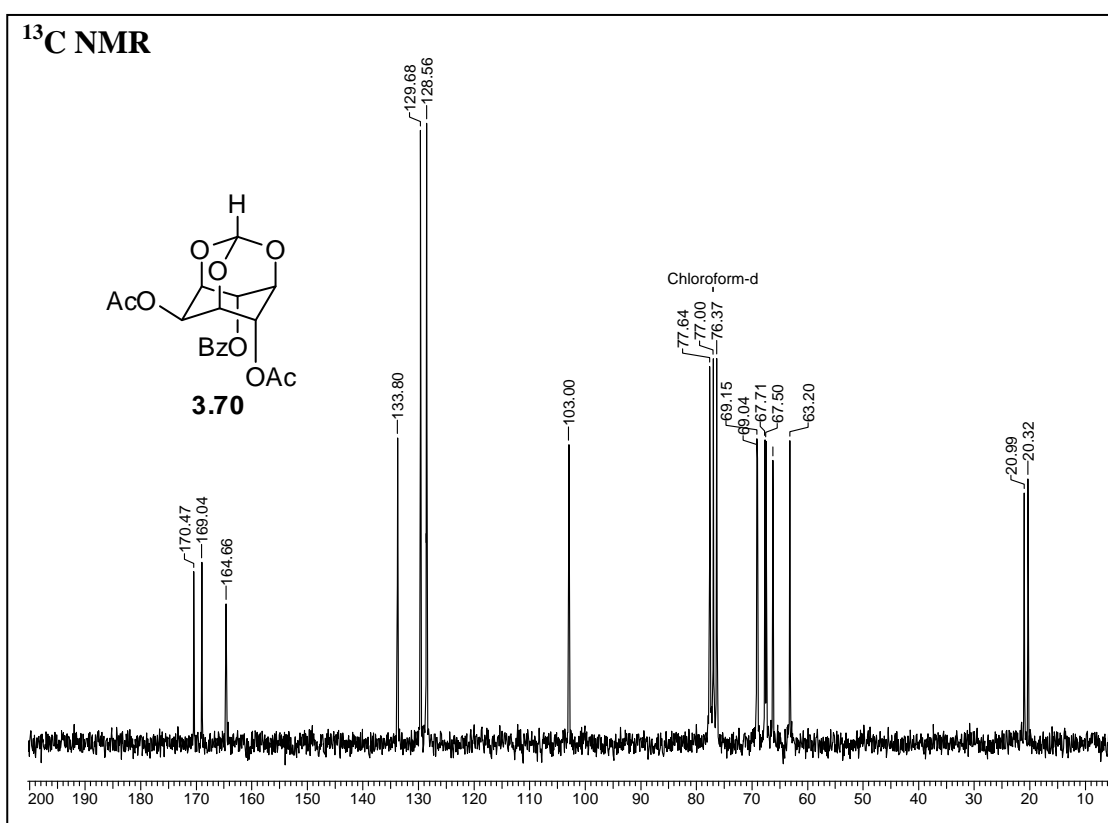
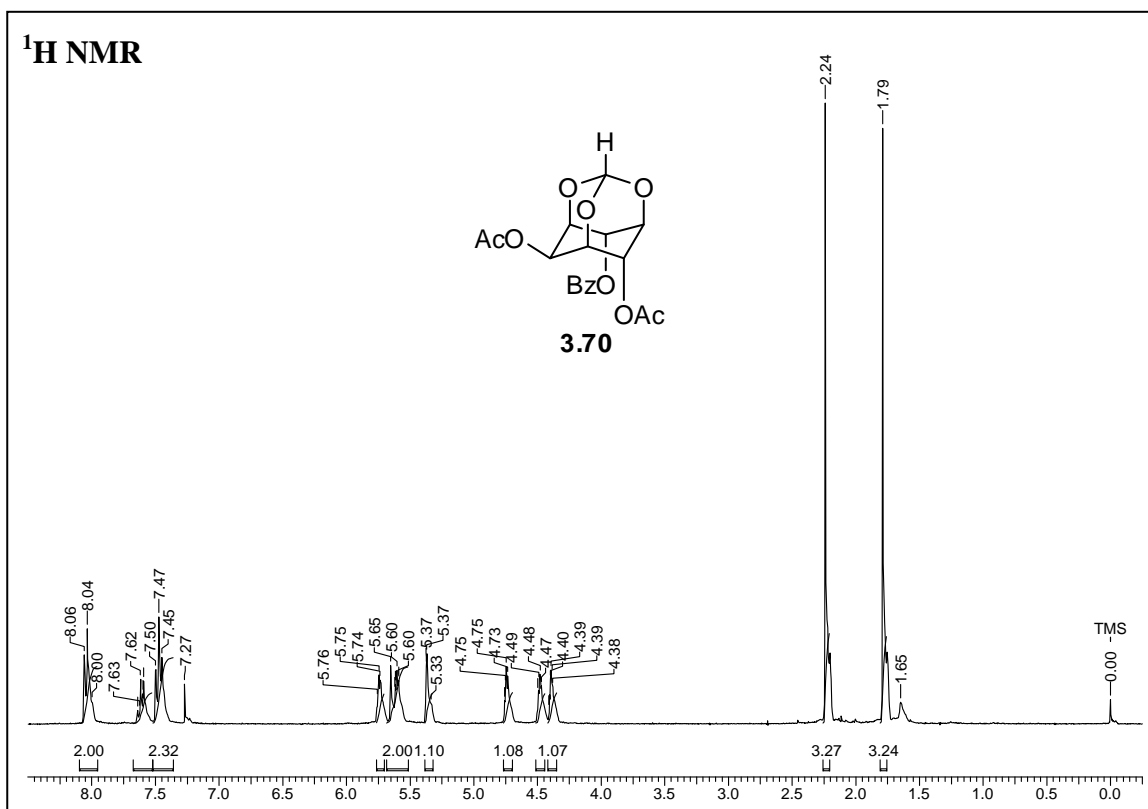


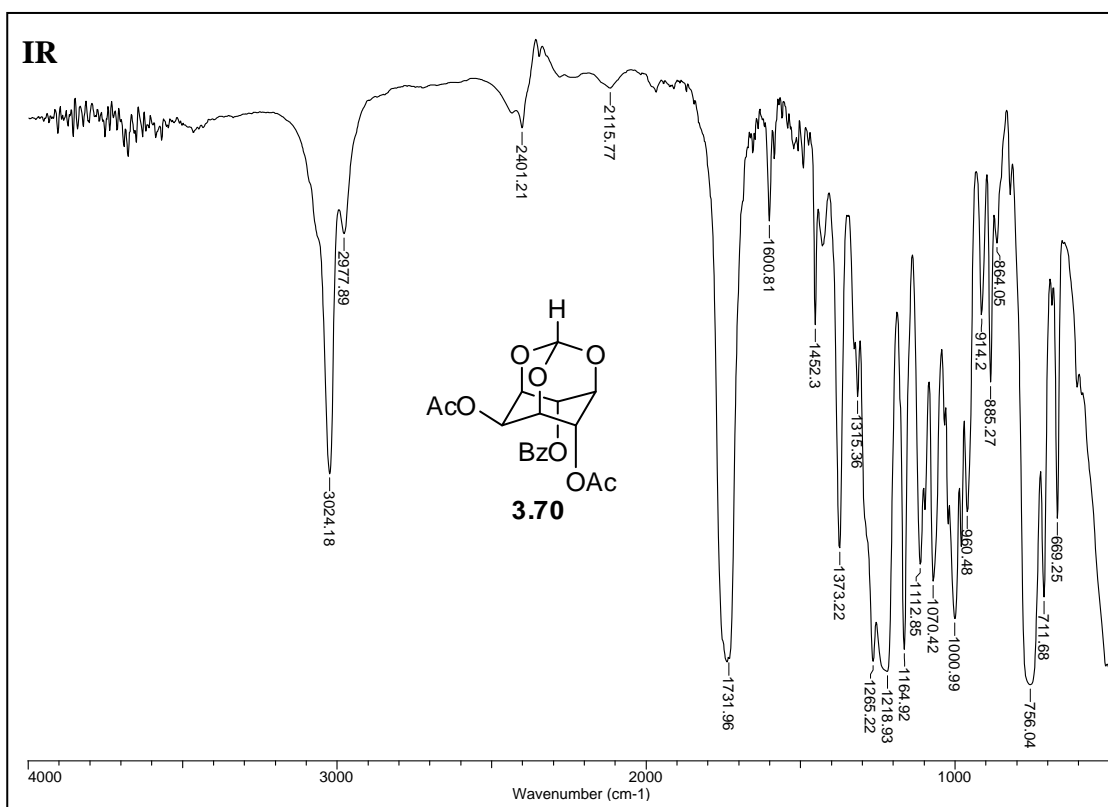
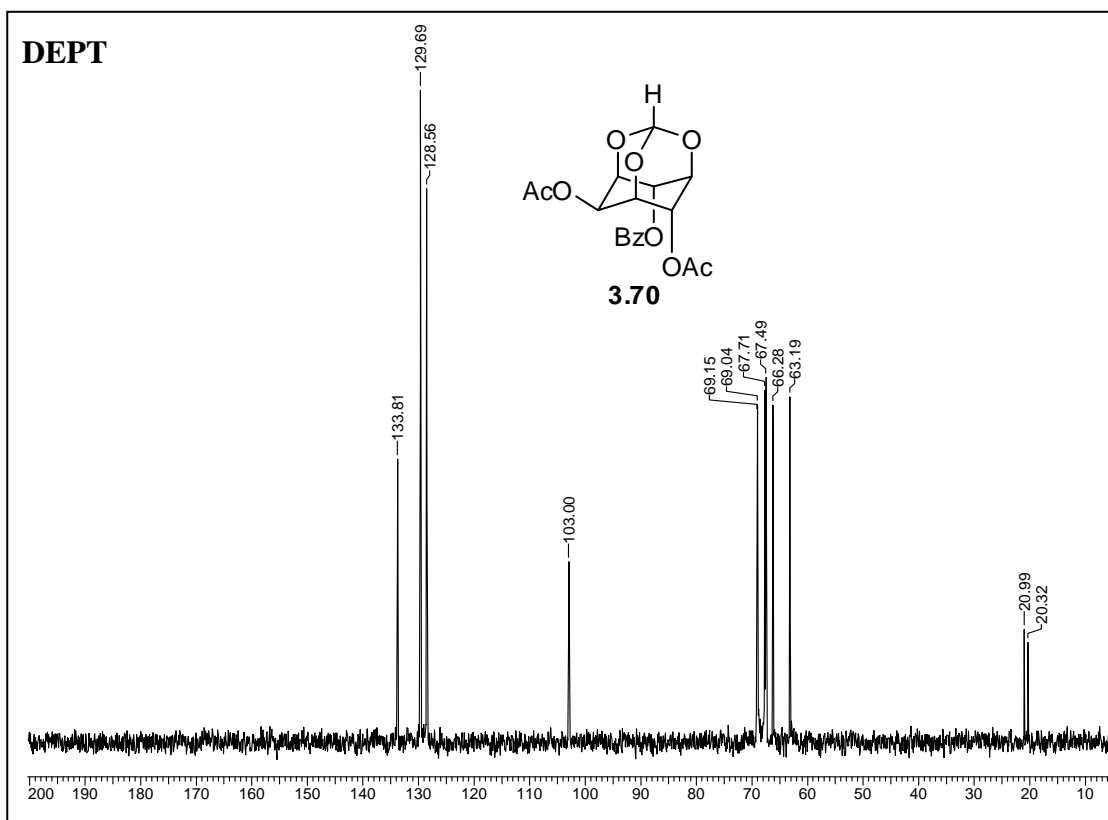




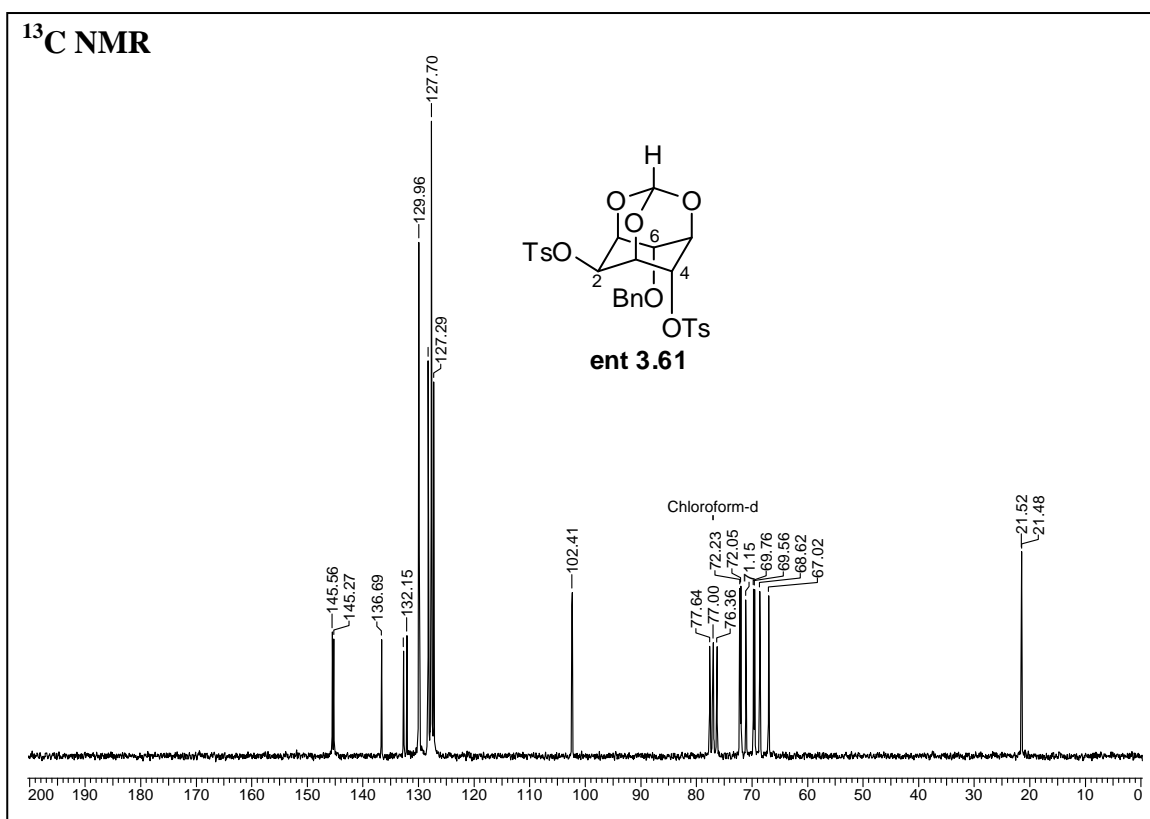
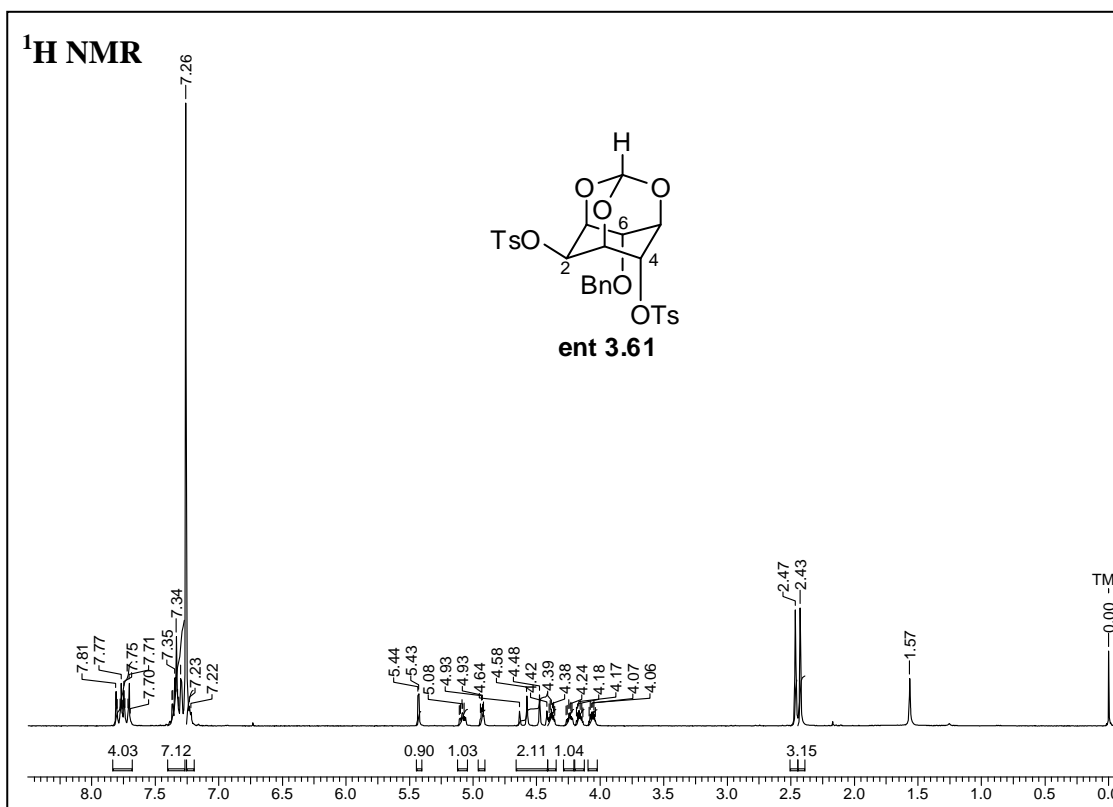


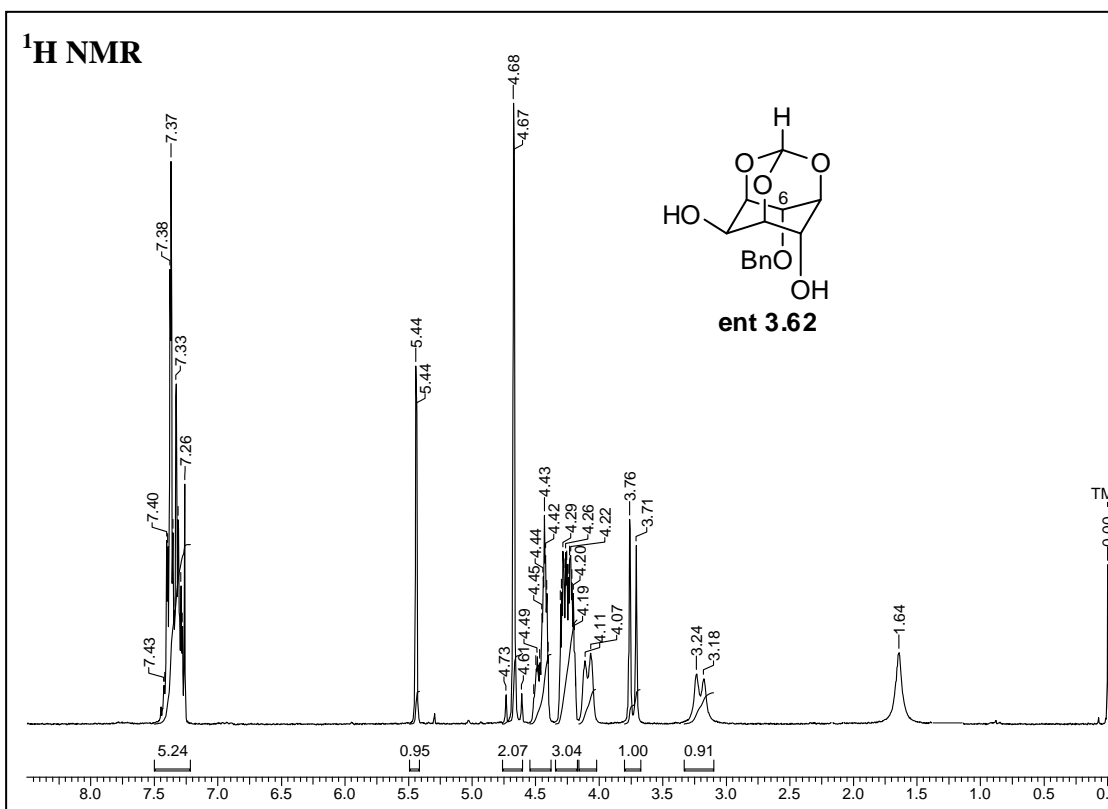
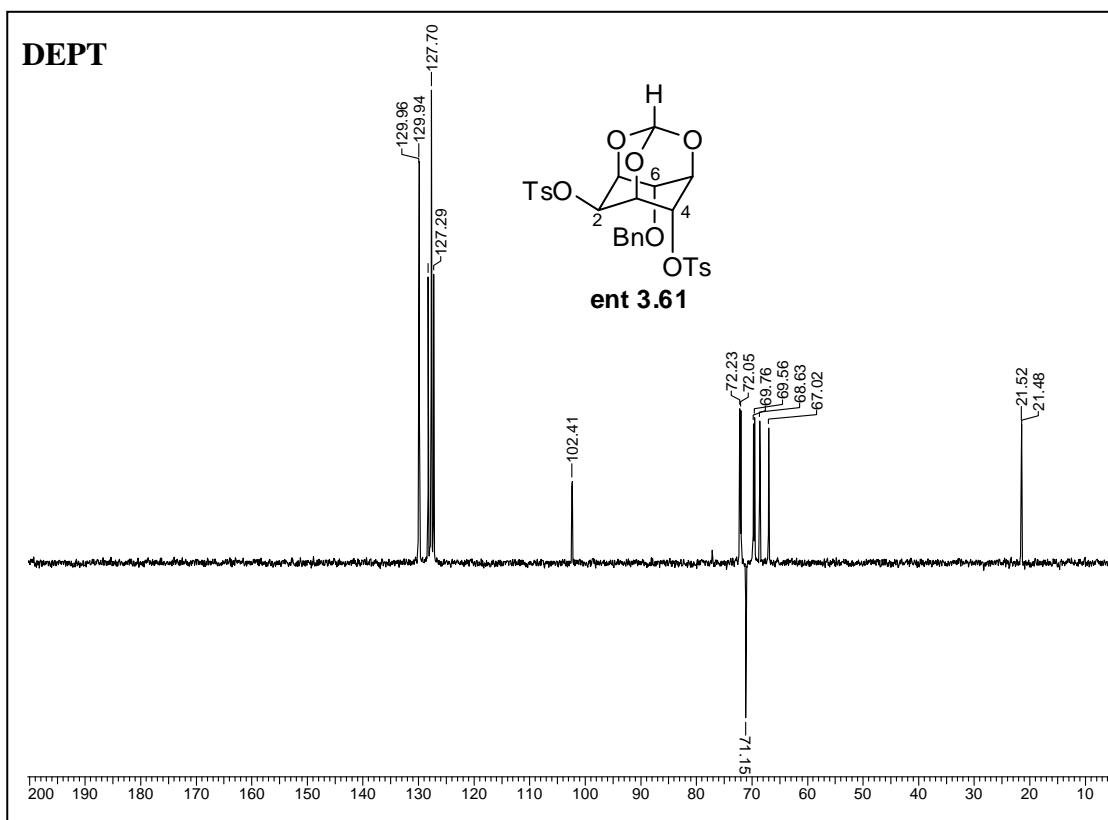


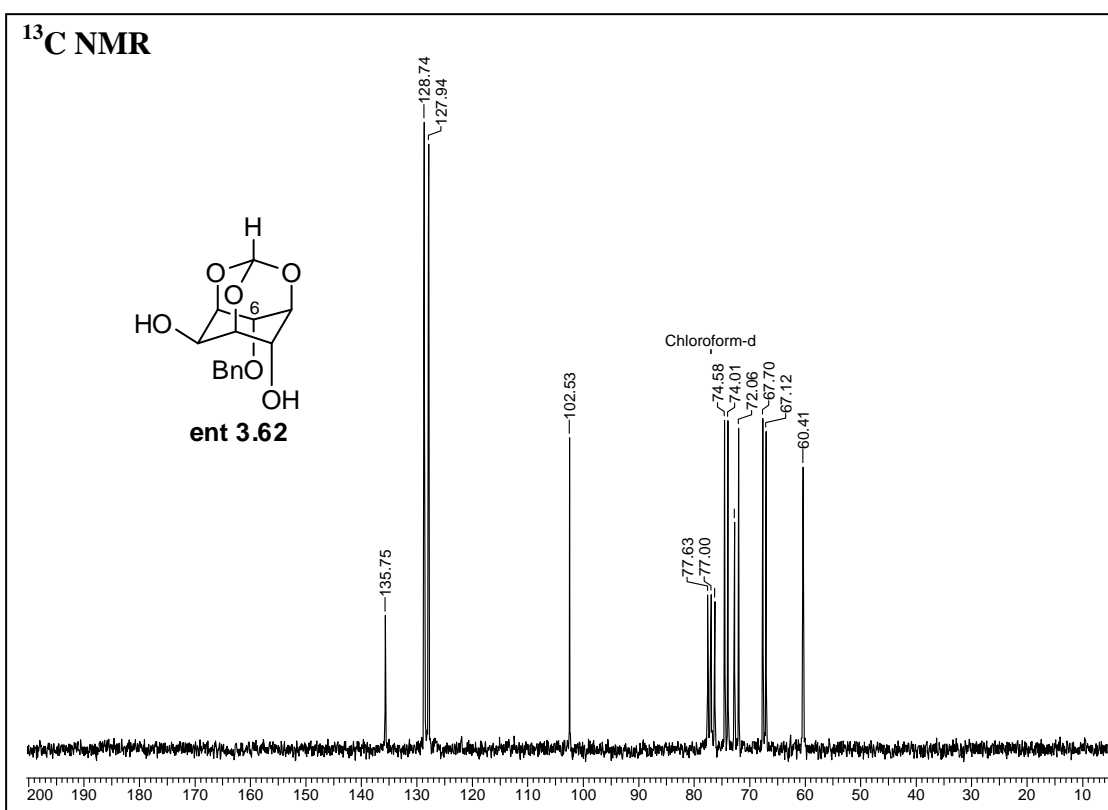
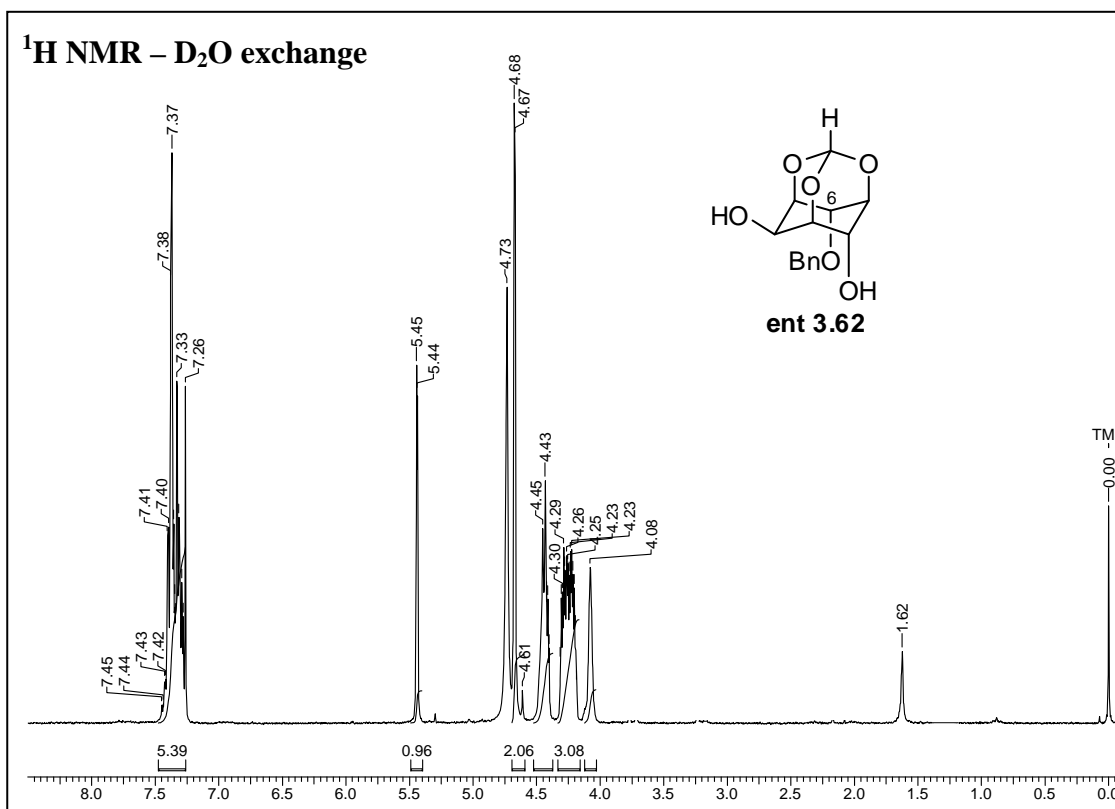


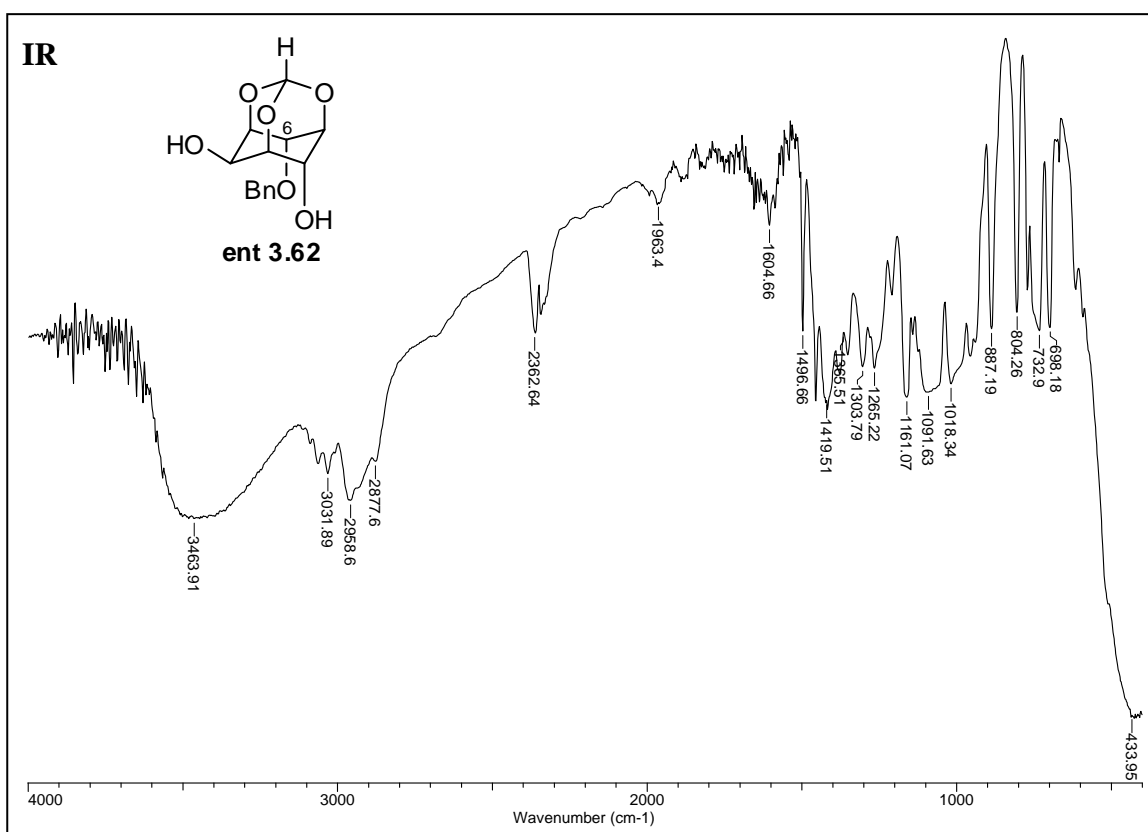
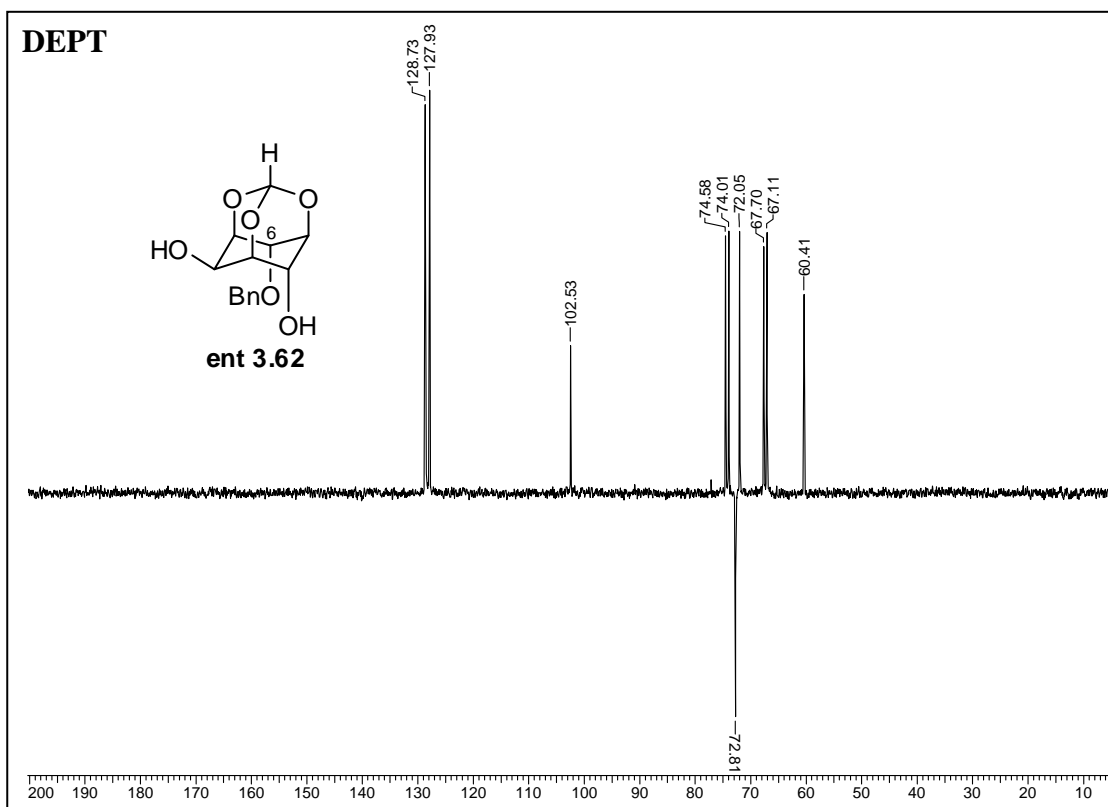


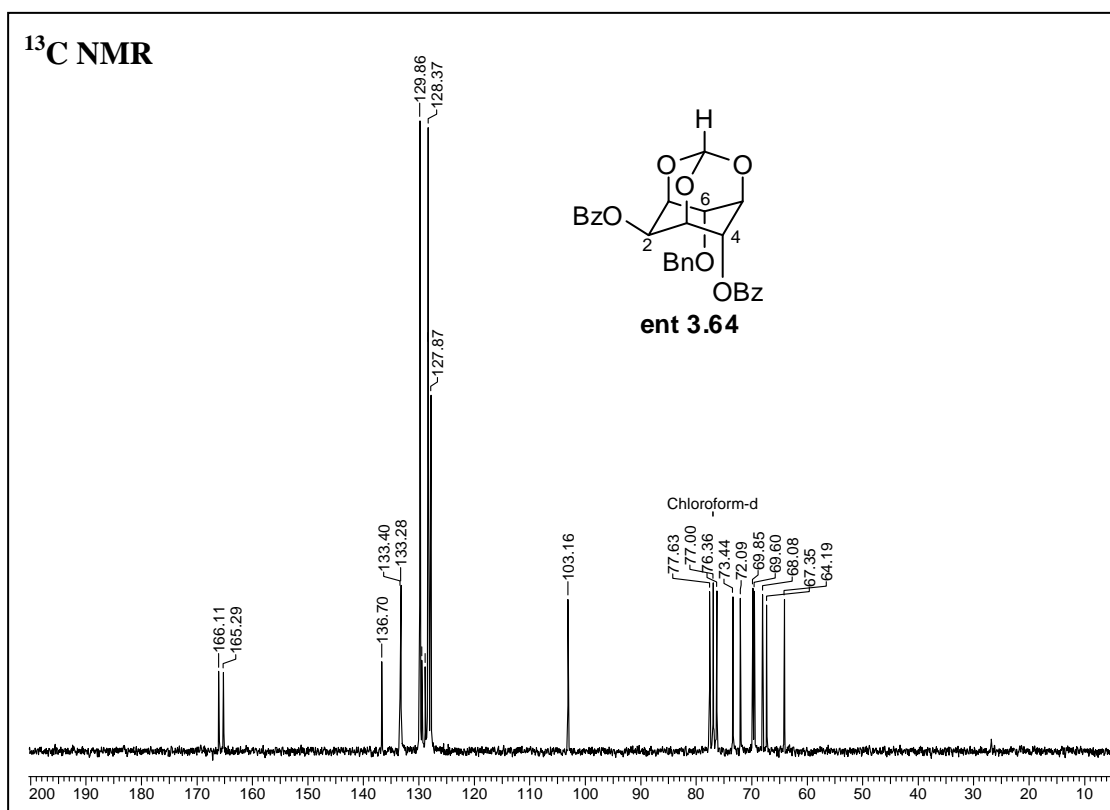
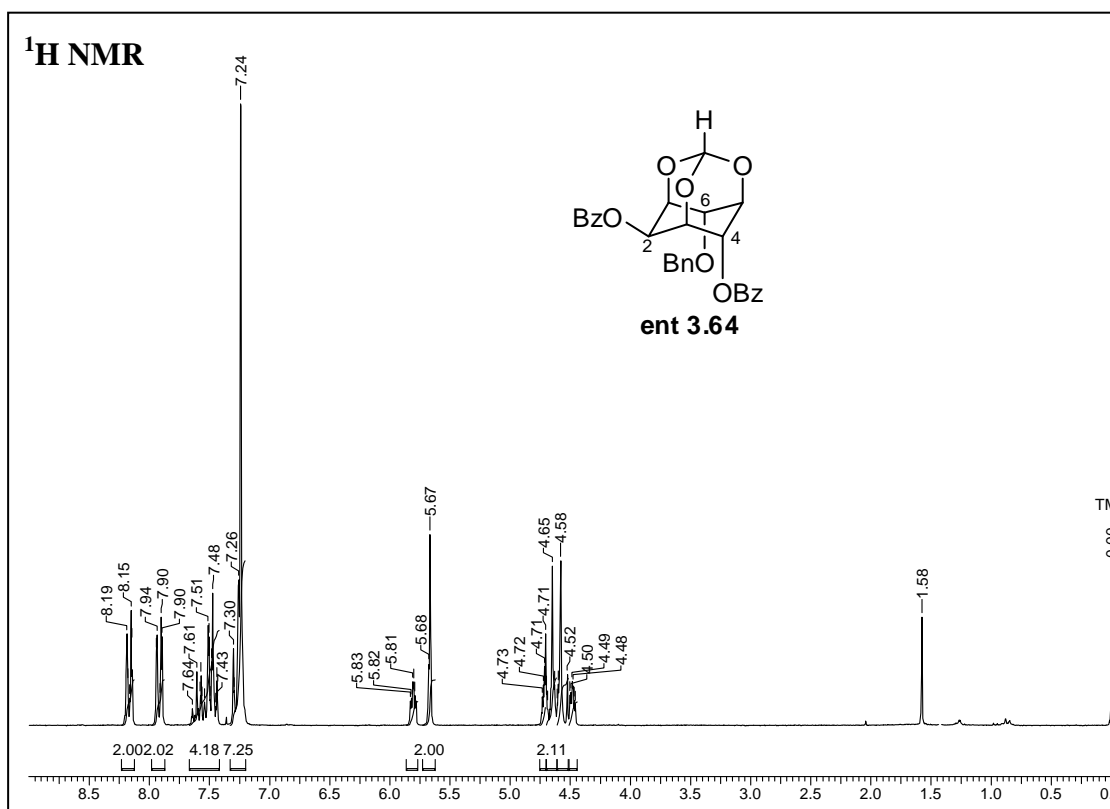
Chapter-3

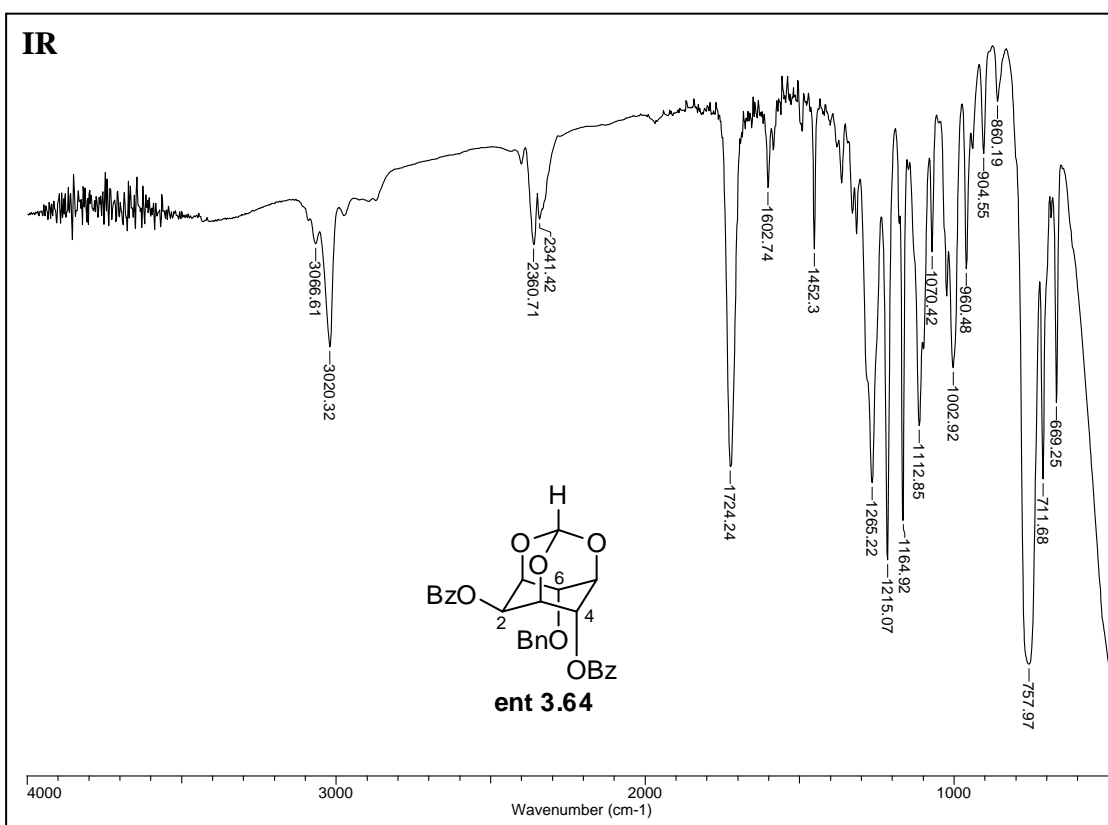
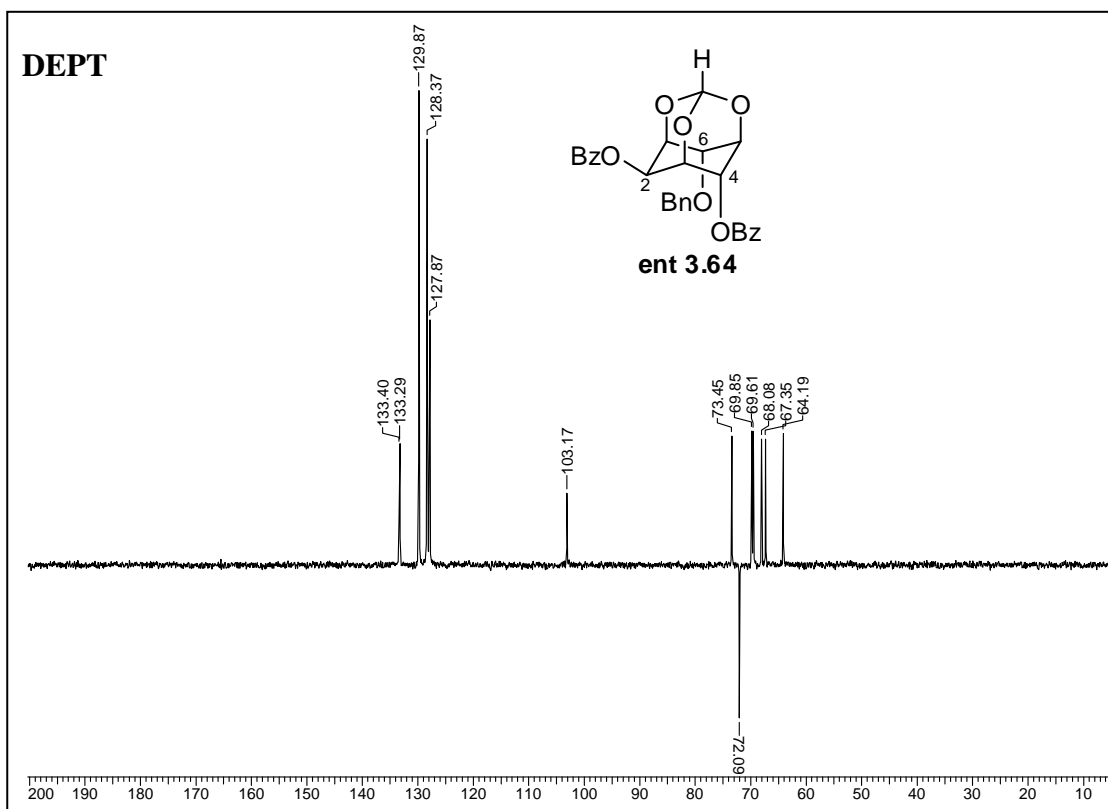


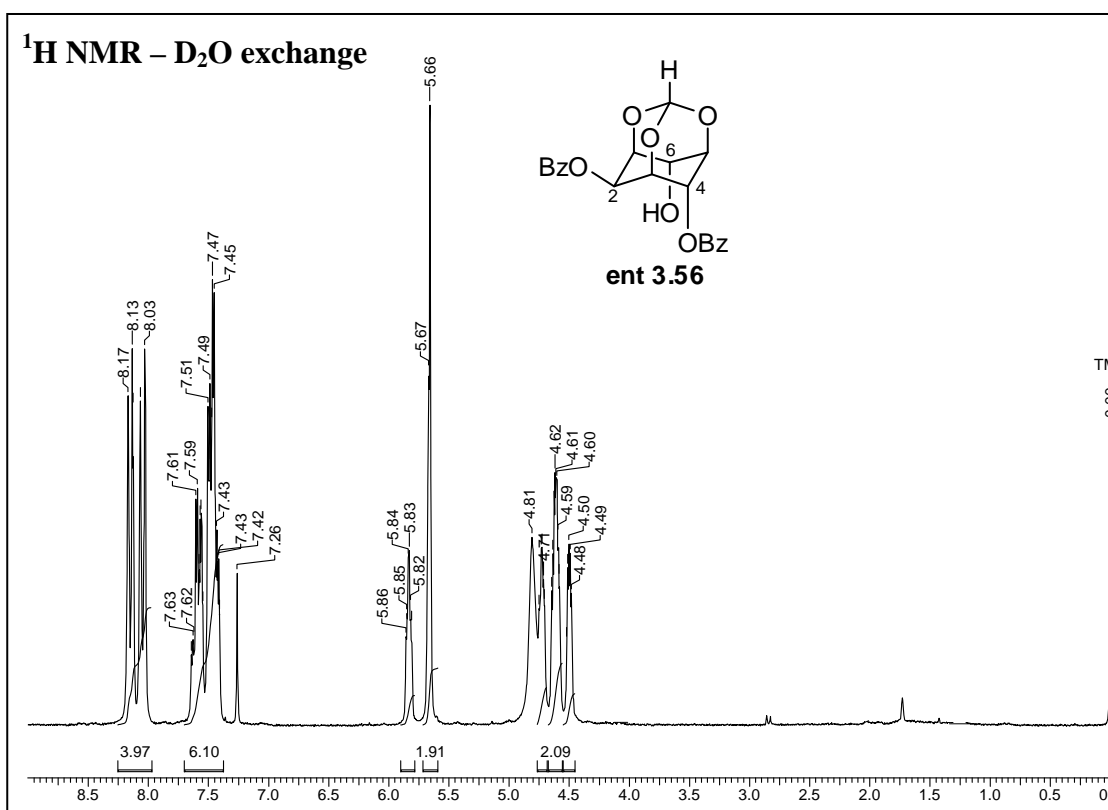
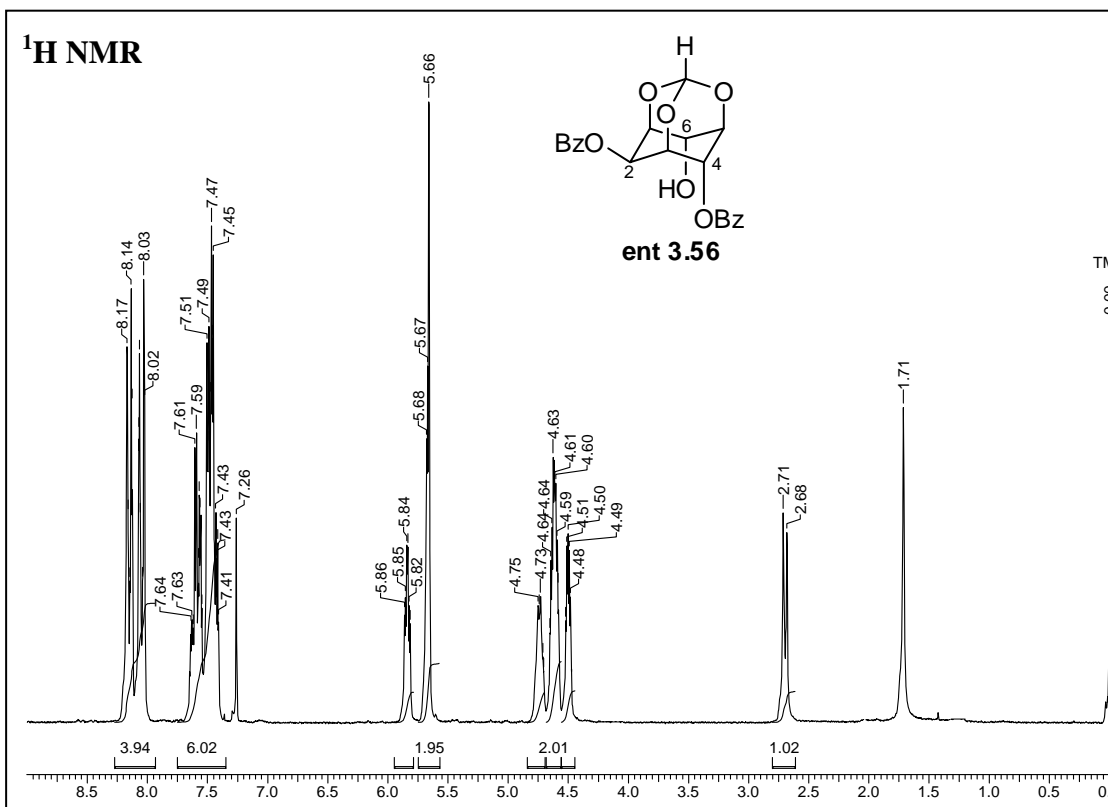


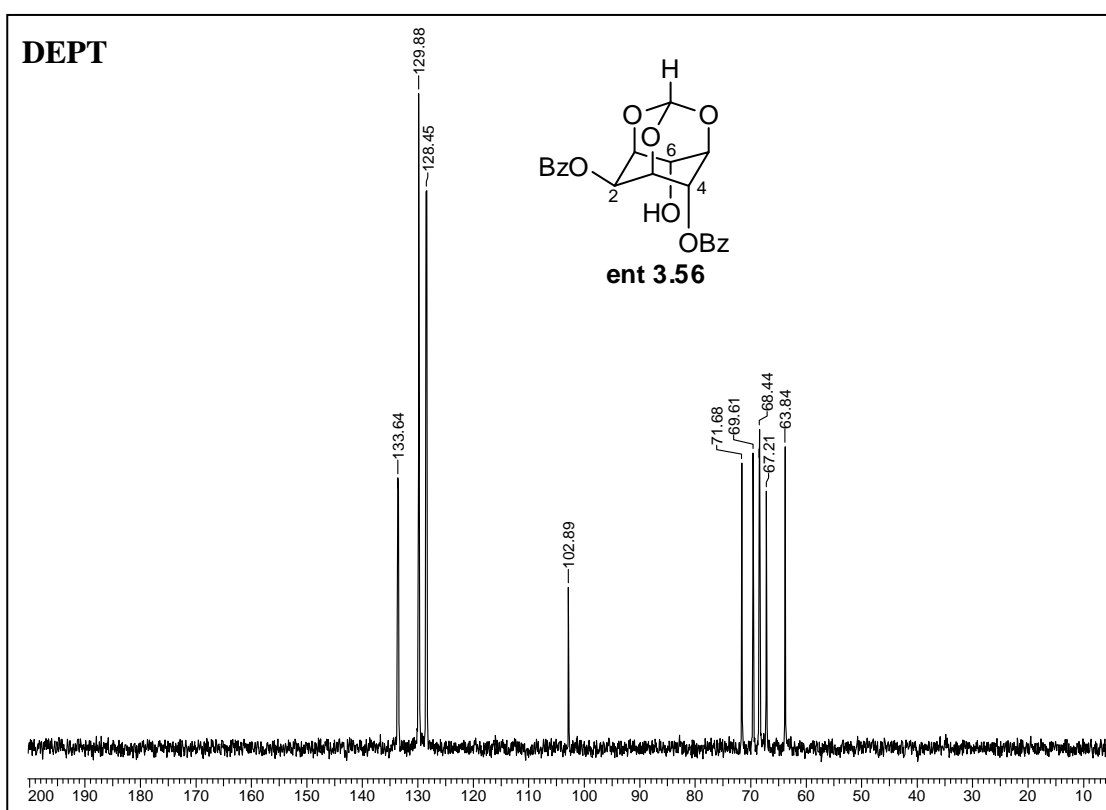
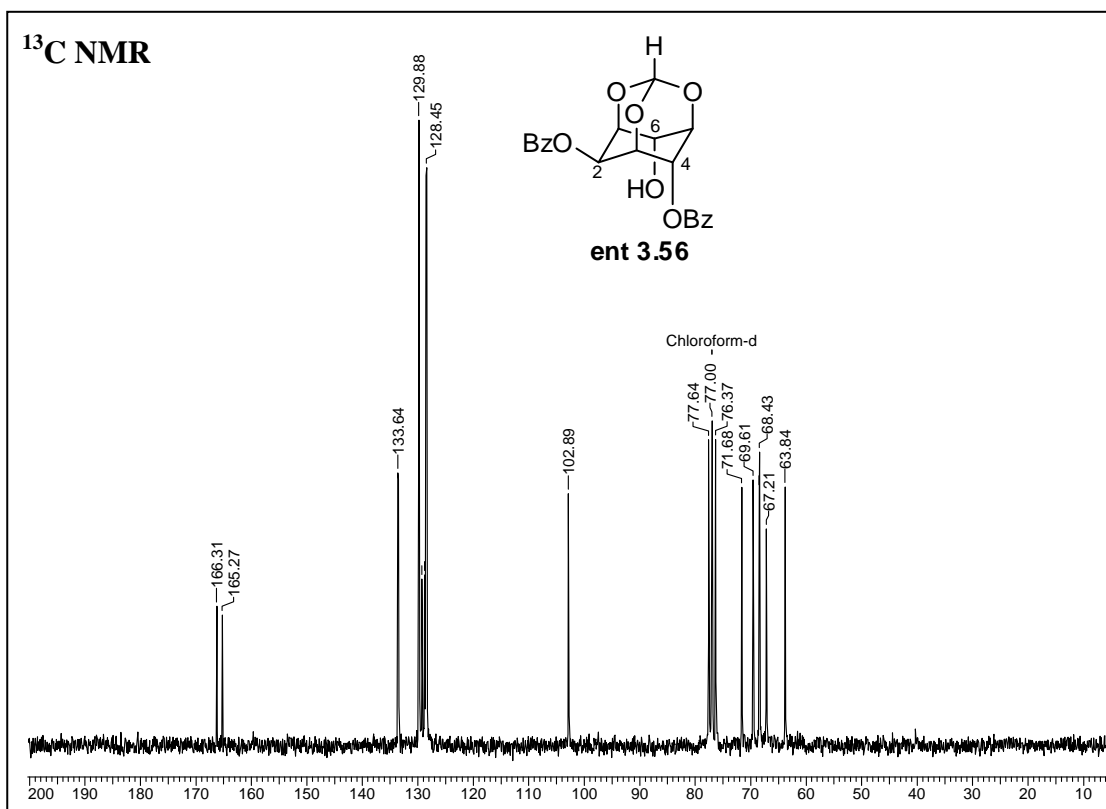


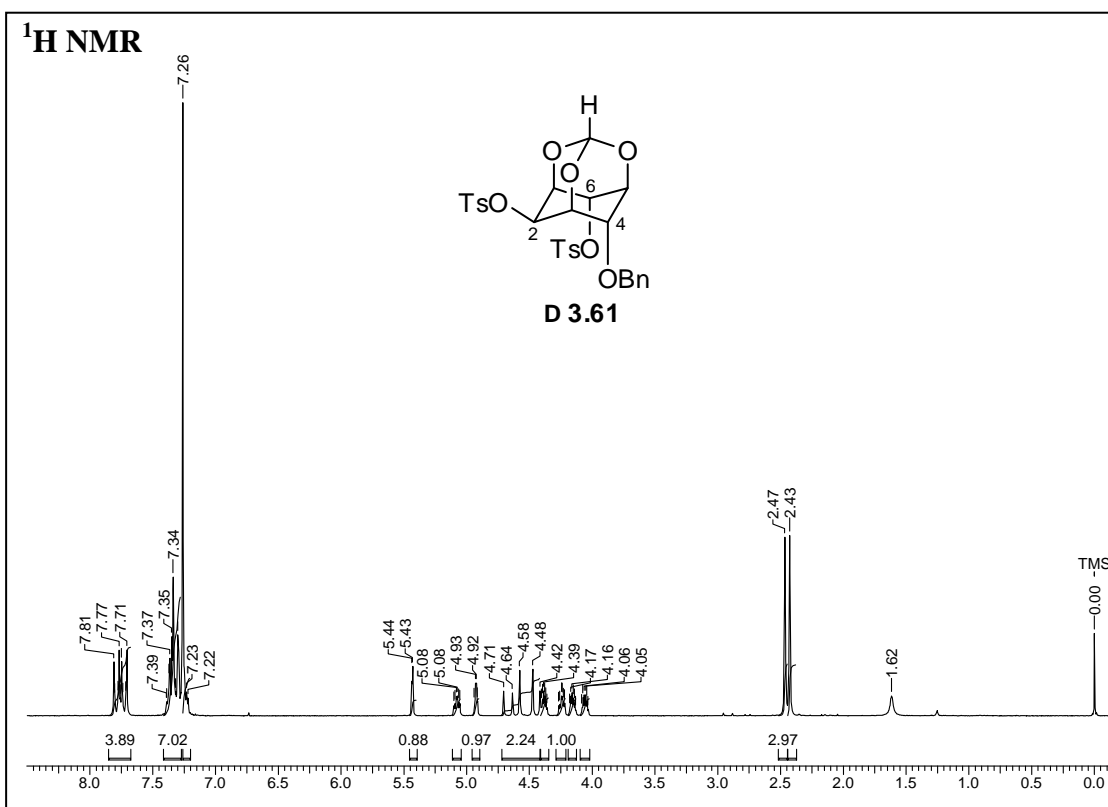
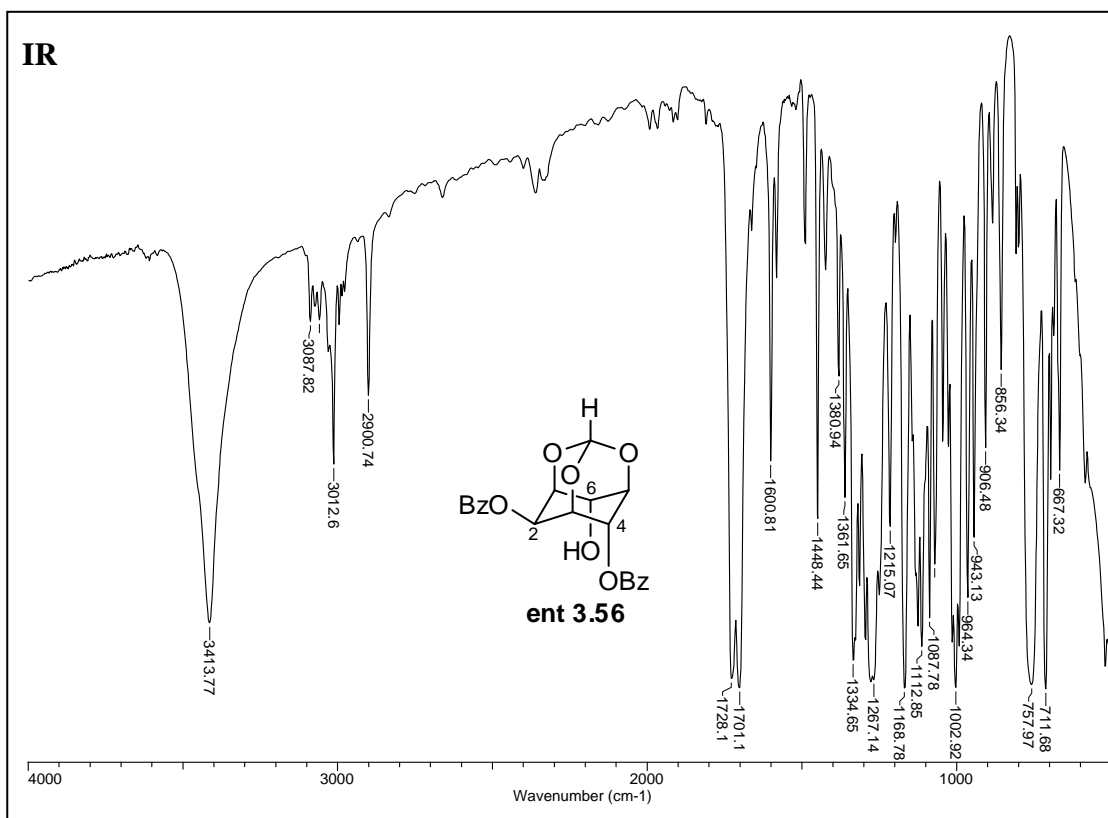


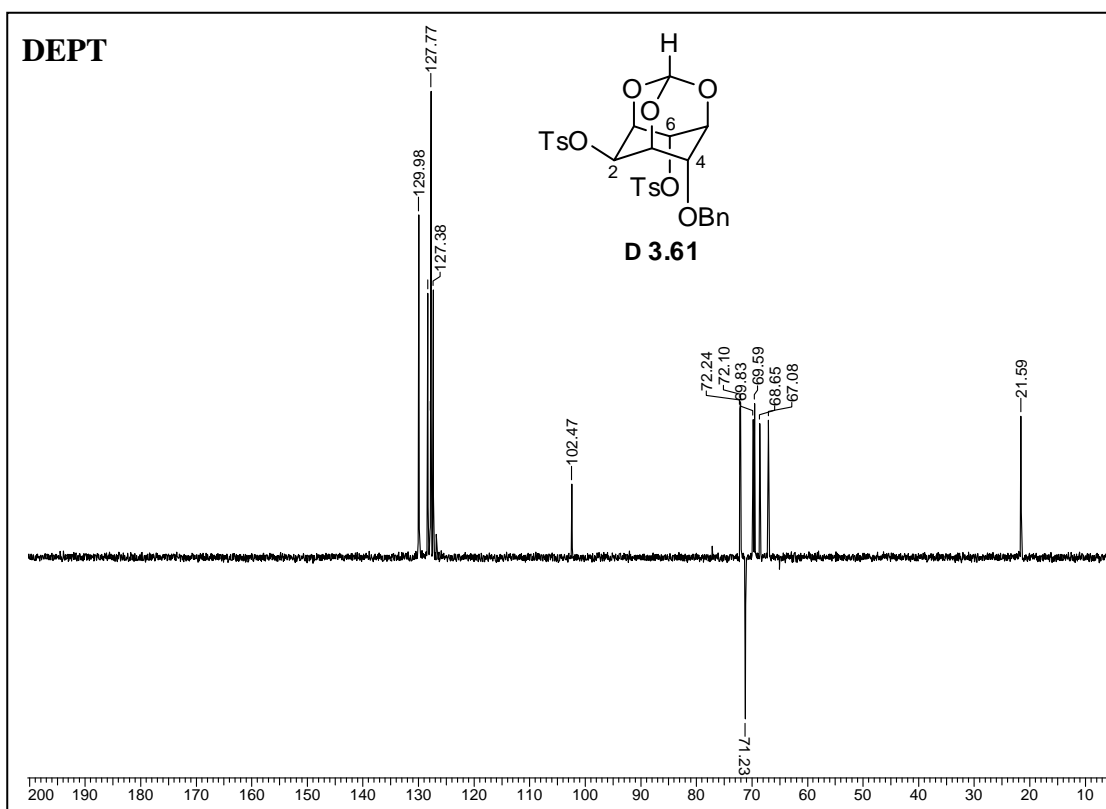
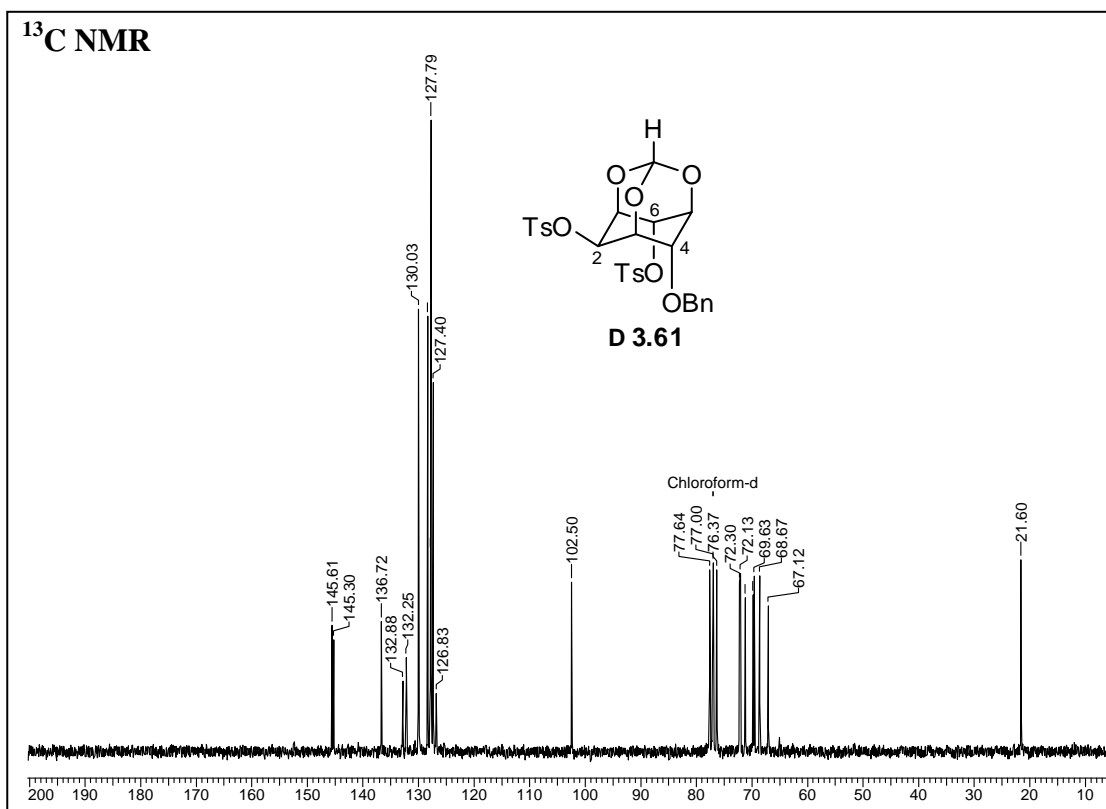


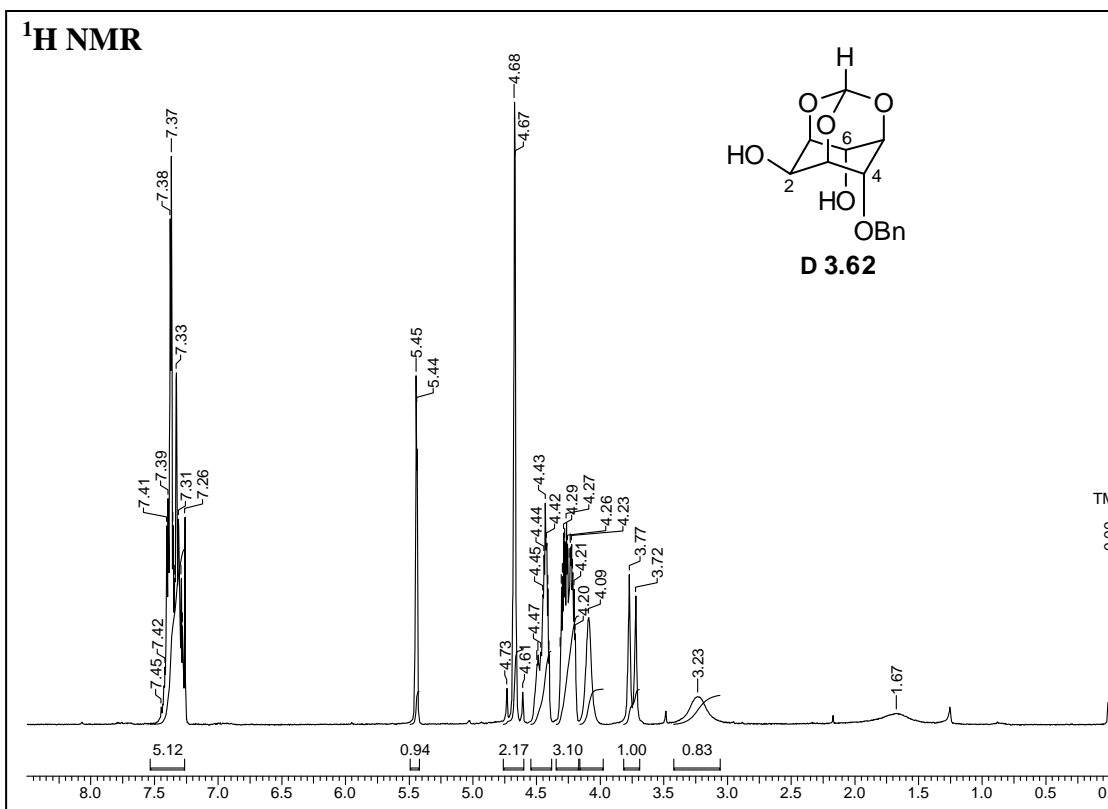
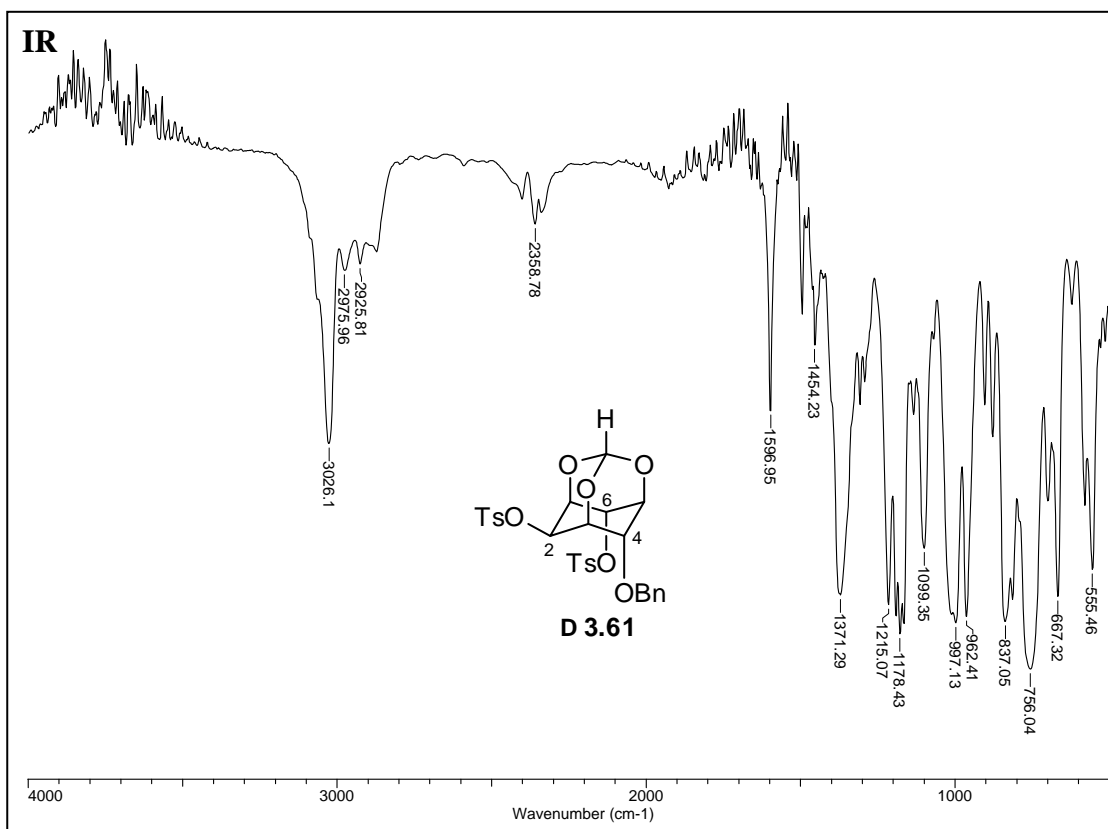


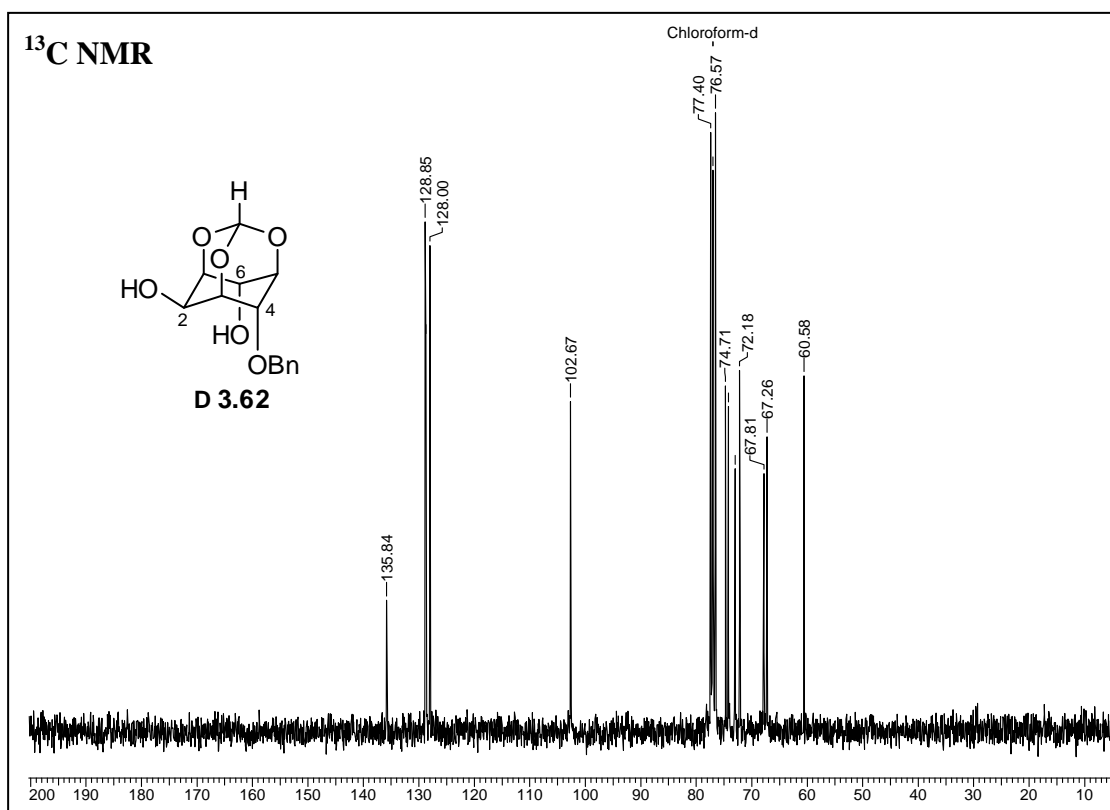
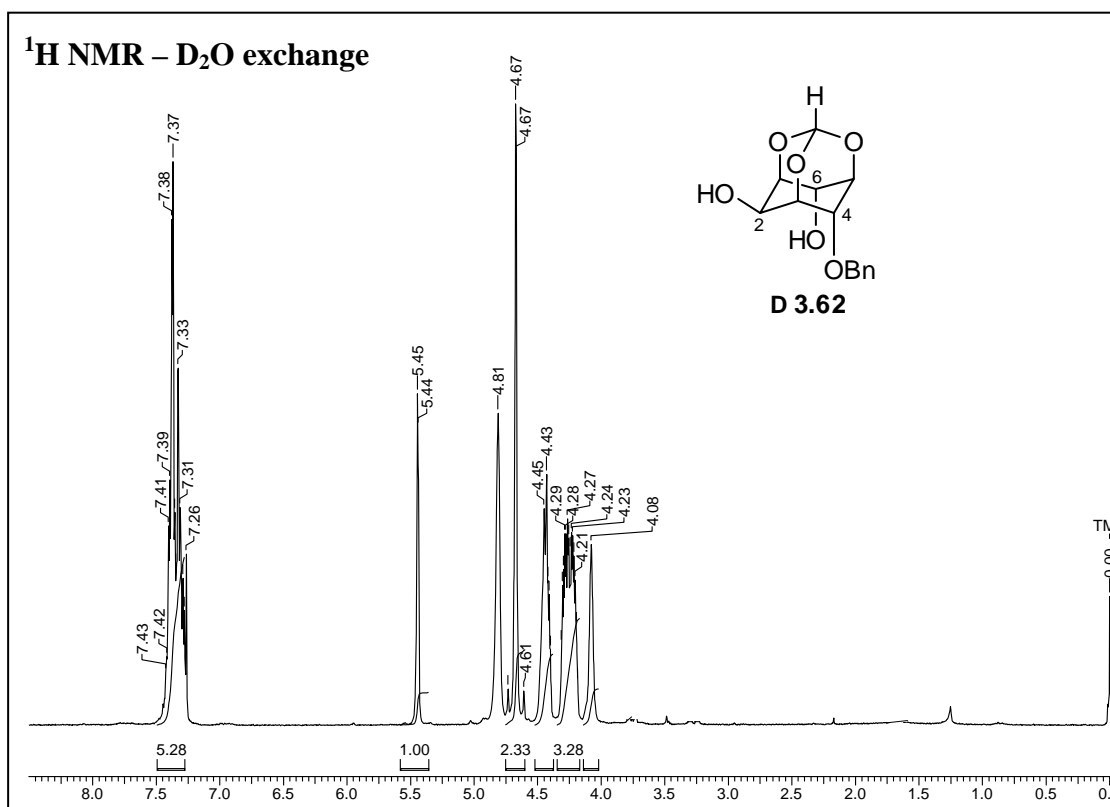


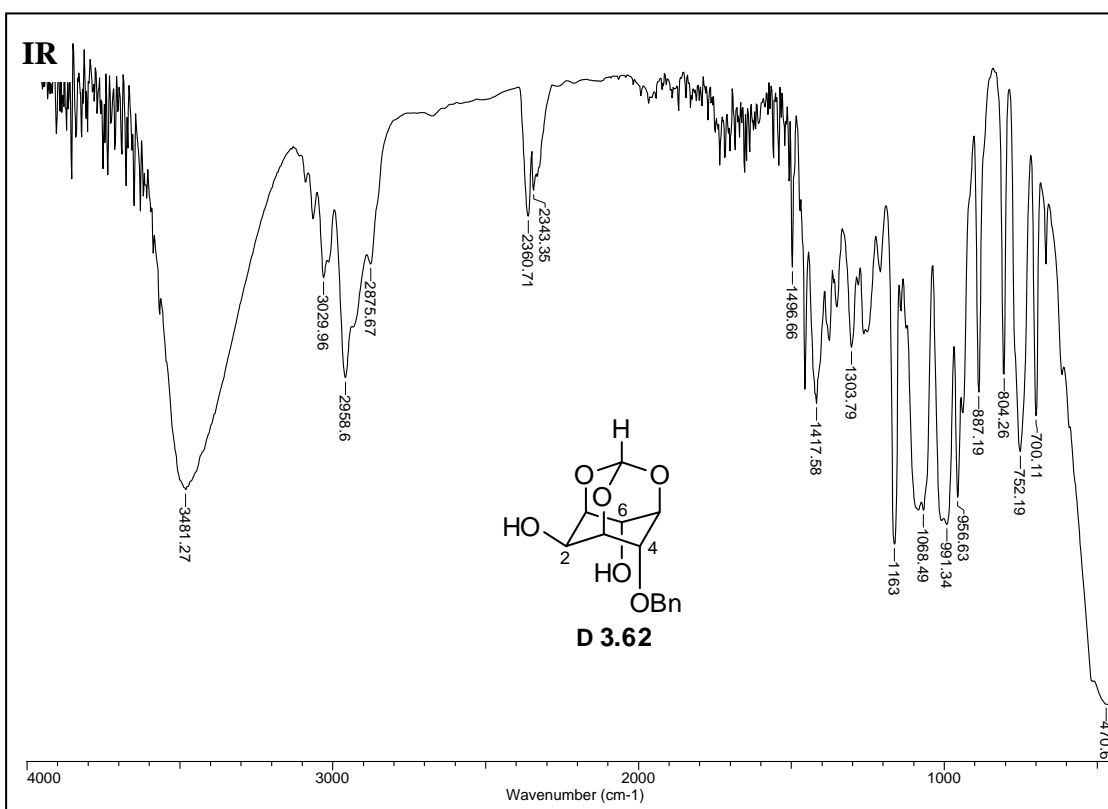
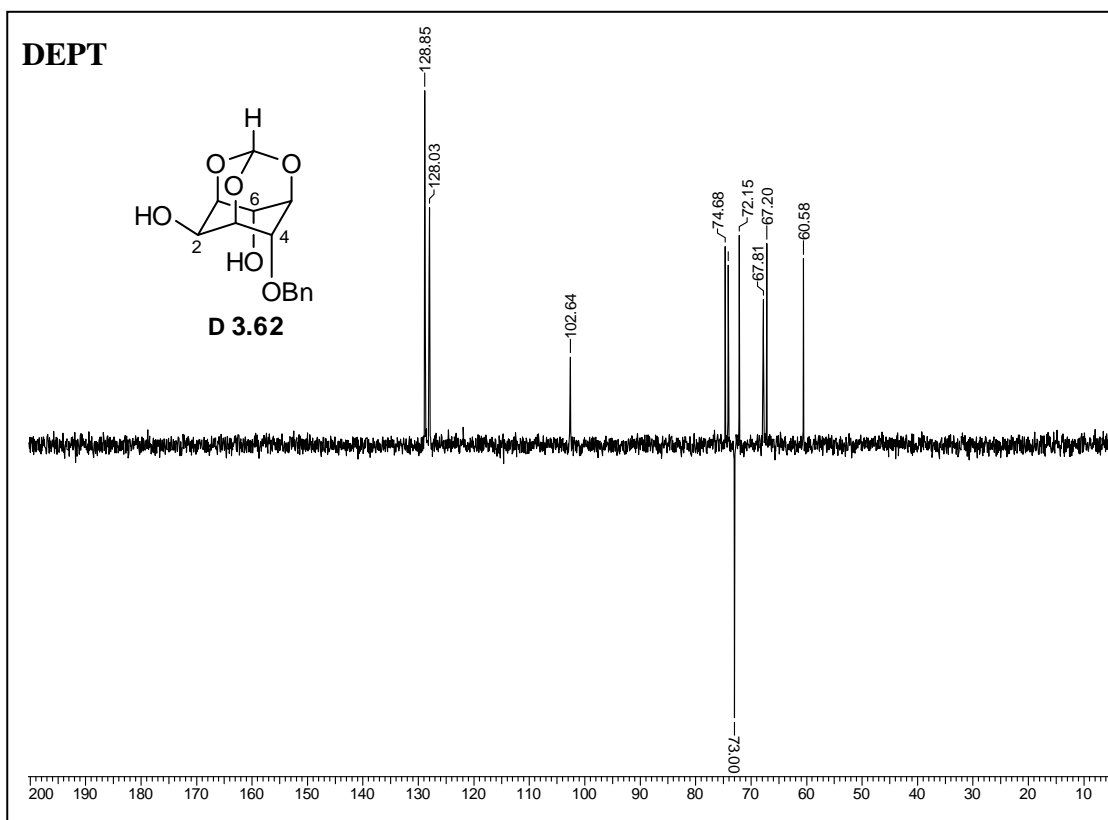












Chapter-3

